Synthetic sulfated saccharides in cell signalling

by

Daniel Sheppard

A thesis submitted to Victoria University of Wellington in fulfilment of the requirements for degree of Doctor of Philosophy in Chemistry

Victoria University of Wellington

2021

Ferrier Research Institute
Te Kāuru

i. Abstract

Access to heparan sulfate-like oligosaccharides, displaying a specific sulfation pattern, is chemically challenging but highly desirable for further insight into the relationship between structure (including sulfation pattern) and function of heparan sulfates. One of the difficulties encountered in heparan sulfate oligosaccharide synthesis is the incorporation of uronic acids, due to reduced reactivity of these saccharides. Another difficulty is the design of a protecting group strategy to give selective access to sites for sulfation.

To investigate the use of uronic acids as donors in oligosaccharide synthesis, a series of comparative glycosylation reactions was carried out using both hexose and uronate, donor and acceptor disaccharides. An orthogonally protected disaccharide was synthesised to access these donors and acceptors. It was found that acetimidate donor systems performed very well in the hexose case, whereas using a uronate acetimidate donor significantly reduced yields of the reaction. A thioglycoside donor performed similarly in both cases but was overall significantly lower yielding than the hexose acetimidate reaction.

Later, two fully protected octasaccharide targets were synthesised. The compounds were designed to investigate the structural requirements for FGF/FGF2 binding. Considering the previous results, the synthesis of these octasaccharides was carried out using hexose donors, necessitating an oxidation step following chain assembly. Firstly, two monosaccharide starting materials, incorporating a novel protecting group allowing orthogonal access to the 3-*O*-position of glucosamine residues, were synthesised. The monosaccharides were then glycosylated to produce disaccharide building blocks, from which the octasaccharide chains were assembled.

Considerable difficulty was encountered in oligosaccharide assembly reactions using tetrasaccharide and especially hexasaccharide acceptors. This difficulty may have arisen from the novel protecting group, which is proximal to the reaction site. Some optimisation was achieved by changing the donor system used, but ultimately a revised glycosylation strategy was used to overcome this difficulty.

In future work, the fully protected octasaccharides will be oxidised, deprotected and sulfated in sequence to produce an octasaccharide heparan sulfate mimetic with a specific sulfation pattern.

ii. Acknowledgements

I would like to take this opportunity to offer my thanks to all the people who have helped me in the years of work which have gone into this thesis. When I first travelled to New Zealand in late 2016, I could not begin to imagine all that I would experience, the opportunities I would have and the warm welcome I would receive. There have been a few challenges in this time, most notably the laboratory fire of late 2018, a significant head injury of late 2019 and the global pandemic of early 2020.

Firstly, I would like to thank my supervisors, Prof. Peter Tyler and Dr. Ralf Schwoerer. They have always been there to answer my incessant questions from day one and have taught me so much.

I would also like to thank Dr Karl Shaffer, who was instrumental in the synthesis contained within this document, and Dr Farah Lamiable-Oulaidi, who has been especially helpful in both synthetic and analytic matters. In addition, my thanks to Dr Herbert Wong and Dr Andrew Lewis for their assistance in all matters NMR, and to Dr Yinrong Lu for his assistance in all matters MS.

Funding for this work comes from a Marsden Fund research grant, so my thanks also to them for enabling these studies, and thanks to the Ferrier Research Institute for providing extended funding during the most turbulent times of the last few years.

Furthermore, I would like to thank all members of the Ferrier Research Institute. This group has been incredibly warm and welcoming, and a thoroughly enjoyable place to work in. Thanks to Prof. Richard Furneaux, Rachael Odlin, and Chris Dixson for their outstanding support. Thanks also to all of my fellow PhD students and post-docs - Elizabeth, Hannah, Taylor, Juby, Roselis, Rinu, Emily, Cara, Mike, Sam, Nick, James, Tom, Josh, and Ed. Thanks also to Li and Andreas, who had to endure the sharing of a fume cupboard with me for a time.

Perhaps most importantly, I would like to thank my family for their support throughout this journey. Although we have been separated by distance, they have been by my side every step of the way.

Contents

iii. List of Figures

iv. List of Schemes

v. List of Tables

vi. List of abbreviations

Ac – Acetate group

Bn – Benzyl group

Bz- Benzoyl group

AMB – 2-(Acetoxymethyl)benzoate

AD – Alzheimer's disease

AT – Antithrombin

BACE1 – Beta-site APP cleaving enzyme 1

BAIB – Bis(acetoxy)iodobenzene

BSP – 1-(Phenylsulfinyl)piperidine

CAN - Ceric ammonium nitrate

ClAc – Chloroacetyl group

CS – Chondroitin sulfate

CXCL – Chemokine (C-X-C motif) ligand

DCC – Dicyclohexylcarbodiimide

DCU – Dicyclohexylurea

DIDMH – 1,3-Diiodo-5,5-dimethylhydantoin

DMDS – Dimethyl disulfide

DS – Dermatan sulfate

Fmoc - Fluorenylmethoxycarbonyl group

HS – Heparan sulfate

FGF – Fibroblast growth factor

FGFR – Fibroblast growth factor receptor

GAG – Glycosaminoglycan

HSBP – Heparan sulfate binding protein

HCII – Heparan co-factor II

HRMS – High resolution mass spectrometry

HSPG – Heparan sulfate proteoglycan

HIV – Human immunodeficiency virus

HA – Hyaluronic acid

HIC-HRMS – Hydrophilic interaction chromatography–high-resolution mass spectrometry

LMWH – Low molecular weight heparin

MS – Mass spectrometry

N-PTFA - *N*-Phenyl trifluoroacetimidate

NMR – Nuclear magnetic resonance

Ph – Phenyl group

PMP – *p*-Methoxyphenyl

RADS – Reciprocal Donor Acceptor Selectivity

RT – Room temperature

SAR – Structure activity relationship

TBAB – Tetrabutylammonium bromide

TBDMS – *tert*-Butyldimethylsilyl group

TCA – Trichloroacetimidate

TEMPO – 2,2,6,6-Tetramethyl-1-piperidinyloxy

TMS – Trimethylsilyl group

Tol – Toluene group

TTBP – 2,4,6-Tri-tert-butylpyrimidne

1. Chapter 1

1.1 Introduction

1.1.1 Cell signalling

Cell signalling is a term encompassing a wide range of inter- and intra-cell communication processes, which influence a range of cellular functions.[1-3] Signalling is generally carried out by the extracellular release of small signalling molecules, and their subsequent binding to receptors on the cell surface. This binding may then lead to conformational changes of the membrane-bound receptor, in both the extracellular and intracellular components. Conformational changes in the intracellular component of a receptor can then trigger conformational changes in other proteins within the cell, or the release of molecules within the cell. The cell signalling process may eventually result in the corresponding release from the cell of another signalling molecule or hormone. The process may also trigger the beginning or end of a cellular activity, such as protein transcription. A series of such linked cell signalling processes is known as a 'signalling cascade'.

Well known examples of cell signalling include the release of the neurotransmitter acetylcholine at the synapses,[4] which is triggered by the arrival of an impulse. The neurotransmitter 'transmits' this impulse by diffusing across the junction between the cells. Acetylcholine binds to receptors on the cell surface of the adjacent neuron, triggering depolarisation by rapid ion gradient change and thus a new impulse in the adjacent cell. Another example is the release of the hormones insulin and glucagon from the pancreas,[5] which lowers and raises blood sugar levels respectively by activating processes in liver cells, such as glycogenesis, glycogenolysis, and gluconeogenesis. In both cases, there are further cell signalling pathways operating in both the transmitting and receiving cells, activating as the hormone or neurotransmitter binds to receptors on the target cell (Figure 1).

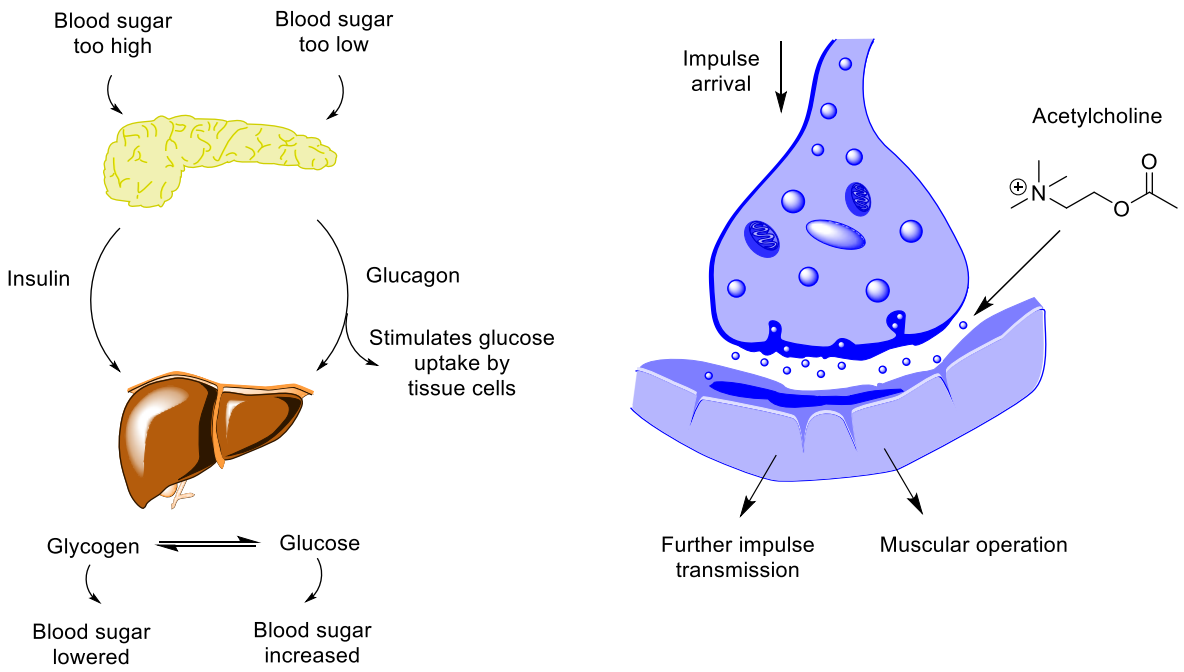

Figure 1 - Diagrams representing common cell signalling examples.
The action of the hormones insulin and glucagon to lower and raise blood sugar respectively (left) and the action of the neurotransmitter acetylcholine at the synaptic junction (right) are well known examples of part of a cell signalling cascade.[4,5]

However, these are relatively simple intercellular signalling pathways with a significant research history, while many complex intra- and intercellular signalling pathways remain poorly understood. This is compounded by signalling molecules and receptors often having multiple functions or acting in several different pathways. For example in the case of insulin, there is significant recent evidence of other functions of the hormone, including roles in immune response[6] and neurological diseases.[7,8] One relatively unexplored class of cell signalling interactions is the interaction between heparan sulfates and proteins.

1.1.2 What are Heparan sulfates?

The class of compounds known as heparan sulfates (HS) are glycosaminoglycans (GAG) with a wide variety of functions in many cell types.[9-14] HS is composed of a heterogenous mixture of sulfated oligosaccharides, with a large variation in chain length and degree of sulfation between molecules. Additionally, the degree and location of sulfation varies across regions of each individual oligosaccharide chain.

Oligosaccharides are short polymers of carbohydrates, made up of monosaccharides linked by glycosidic bonds. An individual monosaccharide within an oligosaccharide is often described as a 'residue'. Within an oligosaccharide, the terminal residue with a free anomeric centre is known as the 'reducing end', whilst the opposite terminal is known as the 'non-reducing end'.

HS is found in virtually all types of mammalian cell matrices as heparan sulfate proteoglycans (HSPGs),[11,13,15] which are HS sequences attached to proteins. The presence of patterns of sulfation leads to a variety of complex, polyanionic structural motifs in the polysaccharide. HSPGs can be placed into several categories: syndecans and glypicans, which are associated within cell membranes; perlecan and agrin which are secreted HSPGs; and serglycins, which feature in intracellular storage. HS, heparin, and other GAGs including chondroitin sulfate (CS) and dermatan sulfate (DS) are usually synthesised in the endoplasmic reticulum and Golgi apparatus of a eukaryotic cell, with further modification occurring both inside and outside the cell.[16-20] The biosynthetic pathway has been reviewed by Li and Kusche-Gullberg,[21] and Annaval et al.[22]

First, within the Golgi, a series of monosaccharide glycosylation reactions occur to generate a tetrasaccharide, which is anchored to a serine residue on a protein (Figure 2). The subsequent glycosylation determines if this tetrasaccharide starting unit will generate a heparin/HS-type polysaccharide chain or a CS/DS-type polysaccharide chain, by extension with either *N*-acetylgalactosamine (leading to CS/DS) or *N*-acetylglucosamine (leading to HS/heparin). For HS, this step is followed by stepwise chain extension of alternating glucuronic acid and *N*-acetylglucosamine monosaccharides, generating the precursor polysaccharide chain. Chain termination occurs by the incorporation of a 2-*O*-phosphorylated xylose monosaccharide, which results in a terminal region that is not a substrate for the transferase enzymes.

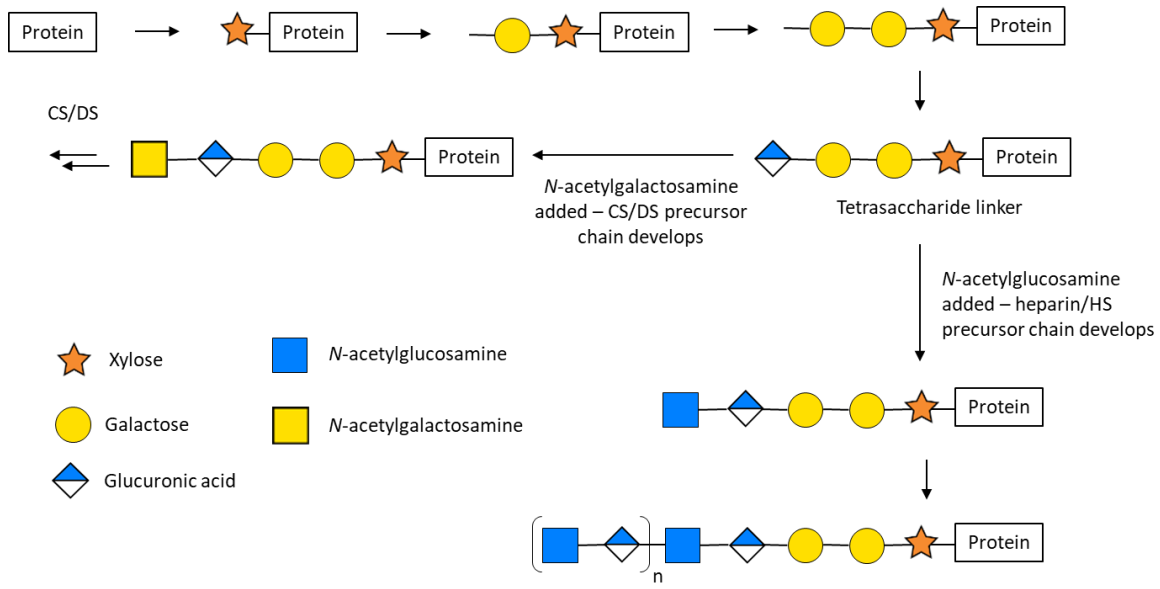

Figure 2 - A representation of the initial stage of GAG biosynthesis. A short tetrasaccharide chain is assembled on a serine residue, onto which an N-acetylglucosamine monosaccharide is added to begin HS/heparin oligosaccharide chain synthesis. Based on a review by Li and Kusche-Gullberg,[21] in symbol nomenclature.[23,24]

Once the polysaccharide is formed, modifications are carried out by enzymes bound to the Golgi membrane. *N*-Acetyl groups are removed from *N*-acetylglucosamine residues, and these amino groups are rapidly sulfated by *N*-deacetylase/*N*-sulfotransferases. *N*-Sulfation is thought to be a key step that triggers further modification in that region of the polysaccharide, both by providing substrate recognition for later modifications, and promoting further action of the *N*-deacetylase/*N*-sulfotransferases along the chain (Figure 3).

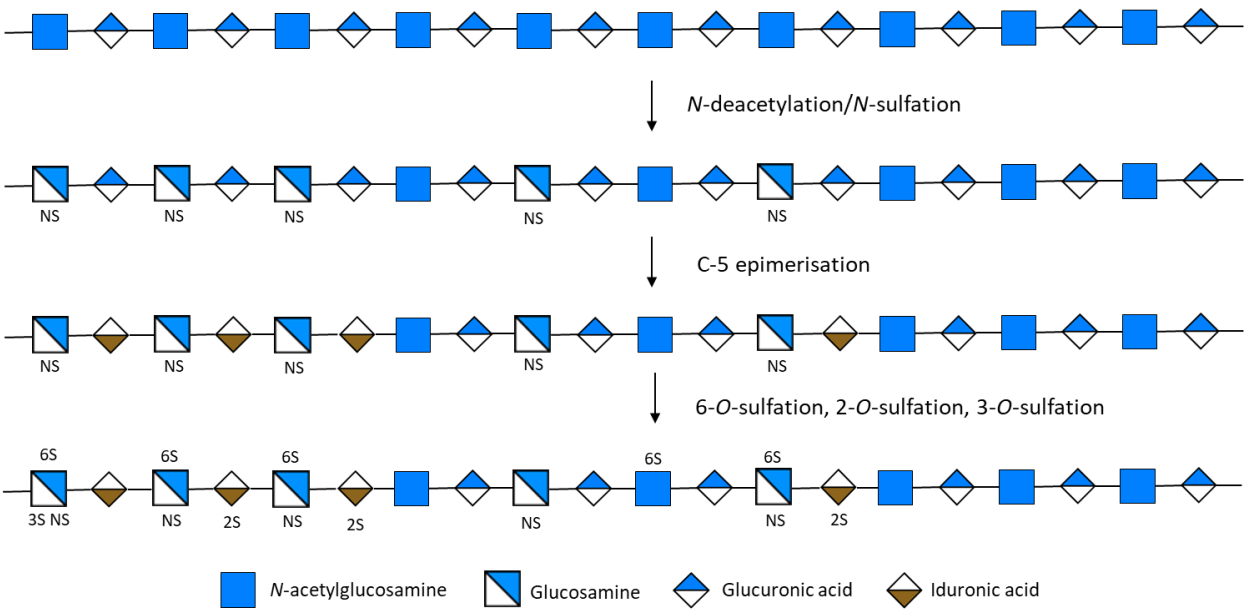

Figure 3 - A representation of the modification of the sugar backbone in heparin/HS biosynthesis.

A series of enzyme-catalysed reactions occur to transform the homogenous repeating chain into a heterogeneous product. Based on a review by Li and Kusche-Gullberg,[21] in symbol nomenclature.[23,24]

Following this, glucuronic acid residues are converted to iduronic acid by a C-5 epimerase. This epimerisation enzyme requires an adjacent *N*-sulfate for recognition, and so iduronic acids are only found adjacent to *N*-sulfated glucosamine. Subsequently, a variety of positions on the sugar residues are sulfated by sulfotransferase enzymes. Uronic acid 2-*O*-sulfation is carried out by a uronyl-2-*O*-sulfotransferase, which works on both D-glucuronic and L-iduronic acids but has a significant preference for the iduronic substrate. Glucosamine 6-*O*-sulfation is carried out by three types of glucosaminyl 6-*O*-sulfotransferases, with no specific requirement for activation. However, once a random 6-*O*-sulfate is installed on the oligosaccharide chain, the glucosaminyl 6-*O*-sulfotransferases prefer installing 6-*O*-sulfates on adjacent glucosamines, leading to distinct regions of sulfation. Six types of glucosaminyl 3-*O*-sulfotransferases can install 3-*O*-sulfates on *N*-sulfate-α-D-glucosamine, and the specifics of 3-*O*-sulfates are less understood. Although considered a rare modification in natural HS,[25] 3-*O*-sulfates have been implicated in a variety of biological processes.[26] However, the natural occurrence of 3-*O*-sulfation in HS may in fact be more common than thought. 3-*O*-Sulfated residues are susceptible to a selective peeling reaction, which occurs during the enzymatic degradation of HS chains. Therefore, 3-*O*-sulfates may go undetected during analysis of HS.[27]

The various sulfotransferases do not generally act on every available site and therefore contribute significantly to the heterogeneity of the product polysaccharide. Post synthesis modifications may occur in the extracellular matrix, by action of heparanase and 6-*O*-sulfatase enzymes. The product of these enzymes is exceptionally heterogeneous HS oligosaccharide chains. Whilst the synthesis of HS appears chaotic, the presence of consistent patterns of HS modification within a specific type of cell or organism implies well-regulated control of the biosynthesis. The mechanisms of such control remain poorly understood.

The genes encoding the various enzymes involved in GAG synthesis have been established by assessment of gene knockout models.[28] Glycosyltransferase enzymes responsible for assembling the HS sugar backbone are encoded by the exostosin genes, EXT1, EXT2 and EXT3. Additionally, three EXTL genes (EXT-like) encode similar protein structures with roles in HS biosynthesis, but their specific roles are not yet understood. EXT gene deficiencies can cause bone growth defects.[29-31] The spectrum of genes encoding sulfotransferase enzymes is much broader in reflection of the complex nature of post-assembly modifications.[28] The genes NDST1, NDST2, NDST3 and NDST4 encode *N*-deacetylase/*N*-sulfotransferase enzymes. The genes HS2ST, HS3ST and HS6ST encode heparan sulfate 2-*O*-, 3-*O*-, and 6-*O*-sulfotransferase enzymes respectively, and each of these genes has other family members. Furthermore, a single glucuronyl C5-epimerase enzyme is encoded by the gene GLCE, which

introduces iduronic acids to the sugar backbone. Beyond the organelles, modifications to HS may take place elsewhere in the cell or outside of it. An example of this is the action of heparanase, which specifically cleaves HS by hydrolysing the glycosidic bond between *N*-sulfated glucosamine and glucuronic acid residues, and the extracellular sulfatase enzymes, which remove 6-*O*-sulfates. The sulfatase enzymes are found on the cell membrane and encoded by Sulf1 and Sulf2 genes.[32-34]

To aid in the understanding of complex HS sequences, the pattern of modifications within an oligosaccharide can be divided into broad groupings. The modified oligosaccharide chain can be divided into disaccharide residues, mirroring the original alternating *N*-acetylglucosamine and glucuronic acid residues of the pre-modification HS oligosaccharide (Figure 4). Around 50% of disaccharide residues in a HS oligosaccharide are the non-sulfated *N*-acetyl-α-D-glucosamine (1→4) linked to β-D-glucuronic acid, whereas around 80% of disaccharide residues in heparin are highly sulfated, featuring an α-D-glucosamine 2-*N*-6-*O*-disulfate (1→4) linked to α-L-iduronic acid 2-*O*-sulfate.

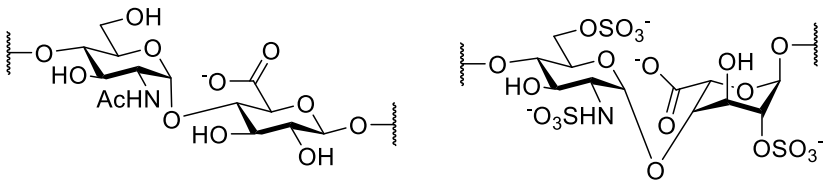

Figure 4 - The most common disaccharide constituents of HS and heparin. N-acetyl-α-D-glucosamine (1→4) linked to β-D-glucuronic acid (left) is the most common by far in HS, at around 50% of residues, whereas in heparin, α-D-glucosamine 2-N-6-O-disulfate (1→4) linked to α-L-iduronic acid 2-O-sulfate (right) is the most common at around 80% of residues.[9] Bond lengths of the (1→4) linkage are extended to display the conformation of the idose sugar.

The arrangement of modifications in the HS oligosaccharide sequence gives rise to regions of differing average compositions, called domains (Figure 5).[21] However, no domain is entirely homogenous. These domains are termed NA domains if they are mostly composed of non-sulfated disaccharide residues, and NS domains if they are mostly composed of the highly sulfated disaccharide residues. Transition between the domains occurs through mixed regions known as NA/NS domains, which feature more equal amounts of sulfated and non-sulfated disaccharide residues.

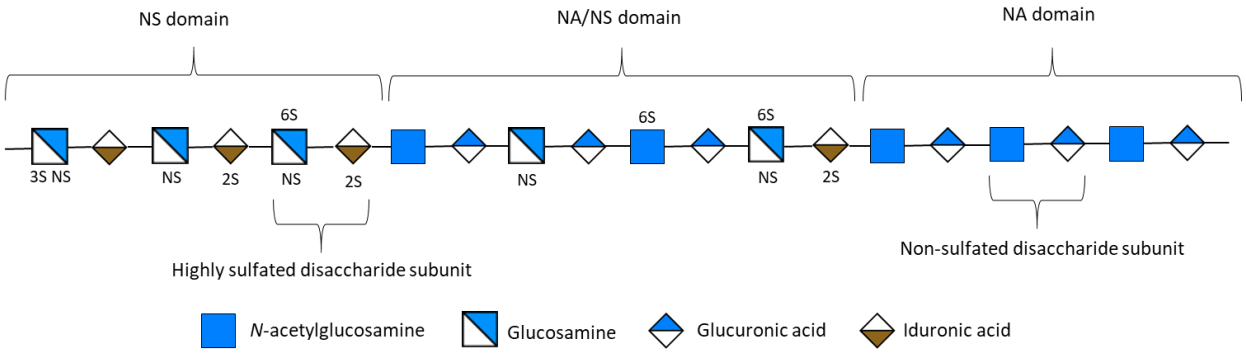

Figure 5 - A representation of the domains of a HS/heparin oligosaccharide. This representation is for illustrative purposes only, as no domain in HS/heparin is homogenous. Rather, the domain designation reflects the average composition of each domain. Based on a review by Li and Kusche-Gullberg,[21] in symbol nomenclature.[23,24]

As previously discussed, the most common disaccharide repeating unit in HS oligosaccharides is *N*-acetyl-α-D-glucosamine (1→4) β-D-glucuronic acid, at around 50% of disaccharide residues. Therefore, HS, somewhat counterintuitively for a material with sulfate in the name, is predominantly formed of non-sulfated NA domains.[12] In HS, the pattern of sulfation commonly occurs as short (8-mer or below) NS domains bordered by NA domains.

HS is distinguished from heparin, a structurally similar highly sulfated GAG, by differences in the composition and degree of sulfation of the oligosaccharide chains. As previously discussed, the most common disaccharide residue in heparin, at around 80% of disaccharide residues, is 2-*N*-6-*O*-disulfate α-D-glucosamine (1→4) 2-*O*-sulfate-α-L-iduronic acid. Therefore, the vast majority of typical heparin sequences are filled by highly sulfated NS domains.[12]

High degrees of sulfation across these molecules means they carry a significant and distributed negative charge at physiological pH. These polyanionic motifs can interact with proteins as part of a cell signalling pathway, functioning as regulators in a range of cellular processes.[35] A large number of distinct HSPGs, and proteoglycans presenting other GAG functionalities, have been reported and characterised, which indicates the prevalence and importance of these structures.[36] HS-binding proteins are involved in cell functions such as movement, proliferation, and recognition, and are also implicated in a variety of diseases.[9] Bacteria and viruses also display proteins capable of interacting with HSPGs, which is thought to be a mechanism for recognition and cell invasion.[37]

There is considerable interest in the synthesis of HS sequences, both for the purposes of further exploring the function of HS in cells, and for novel therapeutic purposes. However, production of longer sequences of HS, with defined sulfation patterns, remains challenging despite recent advances. In the following sections, a comprehensive exploration of HS function and synthesis will be detailed.

1.2 Background

1.2.1 The roles of HS in an organism

HS sequences have been shown to be involved in a variety of interactions with proteins, regulating a wide range of cell processes and cell signalling pathways (Figure 6).[37-40] HS-binding proteins are involved in signalling pathways governing inflammation, blood coagulation, and cell movement, have been shown to have roles in viral and bacterial invasion, and are also involved in the development of cancer, Parkinson's and Alzheimer's diseases. This makes such sequences both potential targets and potential pharmaceuticals.[9,41-47]

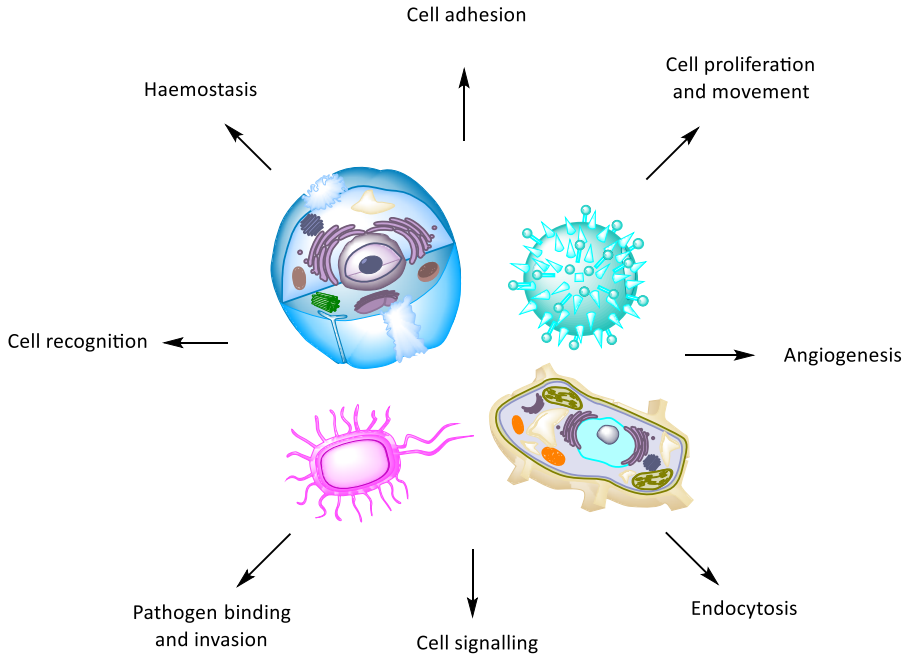

Figure 6 - A representation of some of many functions of HS and HS-binding proteins in organisms. HS and HSBPs are present on the cell surface and in the extracellular space, and have functions which include roles in cell movement, recognition and signalling. [37-40]

The actual dynamics of an HS sequence binding with a protein are complex,[37,48-51] and have been comprehensively reviewed by Xu and Esko.[49] Such proteins are often labelled 'heparan sulfate binding proteins' (HSBPs). In some cases, binding is largely an electrostatic interaction between negatively charged, highly sulfated subunits of HS and positively charged components of the HSBP, often involving lysine and arginine residues. In other cases, a true 'lock and key' binding model is observed, where the interactions are mediated by hydrogen bonding between the oligosaccharide sequence of HS and the complimentary peptide tertiary structure within the HSBP.[14] In this mode of binding, the HSBP has a binding pocket containing residues or spaces that can accommodate one or more sulfate groups, and multiple separate binding pockets may be present across the protein binding site, to allow binding to different combinations of sulfates. Other amino acid residues such as asparagine, glutamine

and histidine develop non-specific hydrogen bonding interactions elsewhere on the sequence. In many cases a mixture of these two binding modes is observed, and the degree of random electrostatic versus lock-and-key binding character can vary between different HS-HSBP interactions.

Furthermore, owing to their structural diversity, HS sequences are often capable of binding to more than one HSBP, and are also capable of mediating binding between several peptide sub-units to create an oligomer, the formation of which leads to a new biological effect.[49,50] One of the roles of HS is to act as tether on the cell surface for large numbers of HSBPs, drawing them from solution in high affinity, providing a flexible scaffold, protection from digestion and therefore extending half-life, and potentially mediating allosteric changes in the HSBP when binding. Allosteric changes are peptide conformational changes induced by a molecule binding at a site other than the active site.

HSBPs themselves are structurally diverse, with many binding more than one HS sequence, and appear to have evolved separately from each other, as an example of convergent evolution. In addition, HSBPs are often able to bind other sulfated GAGs that are structurally similar to HS, such as CS and DS. However, the binding affinity of a HSBP for CS and DS is usually several orders of magnitude weaker than HS, although in some cases DS affinity can approach or even exceed HSBP affinity for HS.[49]

1.2.2 Analysis methods for assessing GAGs

One of the major difficulties encountered in any assessment of GAGs is their characterisation. This difficulty is due to the high degree of heterogeneity of HS sequences produced by organisms. HS sequences vary in terms of length and degree of sulfation due to factors such as the varied action of biosynthetic enzymes, material availability and the movement of materials through the Golgi apparatus.[49] This heterogeneity is in remarkable contrast to other biopolymers such as polypeptides and oligonucleotides, which are generally well defined because they are synthesised from a template. Nature has evolved to operate in this way, so this seemingly random process is most likely a poorly understood but complex and finely balanced system - a demonstration of the power of nature, and an enigma to solve in modern cell biology.

Heterogeneity of GAGs in organisms means the same is true of samples isolated from biological sources, and there is significant difficulty in purifying said samples to the degree that even a small number of sequences are present.[9] Therefore, there is a need to develop methods for the analysis of complex GAG mixtures. The powerful analytical tools of NMR, and especially MS, are used in many of these methods.

NMR spectra of oligosaccharides such as isolated GAGs are phenomenally complicated. There are many protons and carbons in similar chemical environments in the molecule, leading to significant

overlap of signals in ^{1}H and ^{13}C spectra. Proton couplings, which provide information on the stereochemistry of sugar ring protons, is likewise generally obscured by this overlap.[52] Analysis by NMR methods can give an approximate gauge of chain length by integration of the number of sugar ring or anomeric protons, the degree of sulfation by chemical shift of the protons adjacent to the sulfate, acetylation by the presence of well-separated *N*-acetate methyl peaks, and the purity of the sample. However, NMR analysis struggles to define the specific sequence of an oligosaccharide, or its components.[53] The heterogeneous composition of naturally sourced GAG species significantly further complicates the NMR analysis method.

Further progress in the analysis of complex oligosaccharide mixtures using existing and novel NMR techniques continues to be made. In a report concerning the analysis of honey,[52] a material composed of a mixture of mono-, di- and oligosaccharides, an NMR technique was developed using highly specific chemical shift filters followed by TOCSY experiments. By using this method, spectra for each sugar ring without background signals could be acquired, allowing the identification of the ring system. Each sugar ring forms an isolated spin system separated by glycosidic bonds. Such a technique could prove useful in other oligosaccharides such as HS.

Methods using high performance liquid chromatography (HPLC) or high performance anion exchange chromatography (HPAEC), coupled with mass spectrometry (MS) have become commonplace in the analysis of HS and other GAG samples.[54] Mass spectra of such materials are often complicated by the functionally similar but structurally diverse nature of the material, leading to multiple charge states and the potential for several, different counter ions, but good progress has been made in using this strategy. One such recently reported method is the use of activated electron dissociation tandem mass spectrometry to produce mass spectra, which is then analysed with an algorithm to determine, with reasonable accuracy, the HS sequence present.[55] Another recent report details the method of 'shotgun ion' mass spectrometry, in which a whole HS oligosaccharide is dissociated and the collision cross section fragments are compared against a library of known standards, allowing the determination of the specific sequence.[56]

Samples can also be partially digested by enzymes, acting at known cleavage sites, to yield shorter length chains, which can be easier to separate and analyse for structural features.[50,57,58] Furthermore, chemical modification of analysis samples can be carried out to promote separation by HPLC and sequencing by MS. A recent report using acid hydrolysis of chains from natural sources is one example.[59] Commonly used modifications include methylation, acetylation, and the addition of propionyl groups.[60] This chemical modification can be general, or targeted at a specific functional

group. Future analytical methods may include a focus towards the single-molecule level, using single-molecule force spectroscopy or fluorescence.[61]

A very recent report for interrogating binding sequences involves the enzymatic fragmentation of GAG chains in the protein-bound state. The protein-bound fragments are then separated from non-bound fragments by size exclusion chromatography and assessed with online MS analysis. This allows the identification of the length and degree of sulfation or acetylation of the bound chains, which have been protected from enzymatic cleavage.[62]

1.2.3 HS as a target

HS-protein interactions can be viewed as a potential target for therapies, generally by inhibiting or preventing the interaction, which should then curtail the associated signalling cascade. HS sequences and HS-binding proteins are presented on the surface of many types of eukaryotic cell. HS can therefore be prevented from interacting with HS-binding proteins on the cell surface, or in the extracellular space, by the use of heparanase[63] and endosulfatase enzymes.[64] Several types of heparanase enzymes can cleave sites in the HS repeating unit, and endosulfatases can selectively remove 6-*O*-sulfates, both of which disrupt the structure of the HS sequence and negate, to some degree, its ability to bind to proteins. Thus, treatment with such enzymes in the extracellular space could inhibit binding of pathogens relying on HS interactions, or prevent tumour growth and movement, as these processes also involve HS interactions (Figure 7). However, various clinical trials did not prove fruitful, as getting these enzymes to selectively disrupt these targets whilst allowing normal cell function has proven challenging.[37] While, for example, an invading pathogen has adapted to utilise these HS sequences for initial binding, the sequence will also serve a necessary biological role. Any loss of structure or charge on a cell surface HS sequence will therefore also likely impede vital cell functions or signalling.

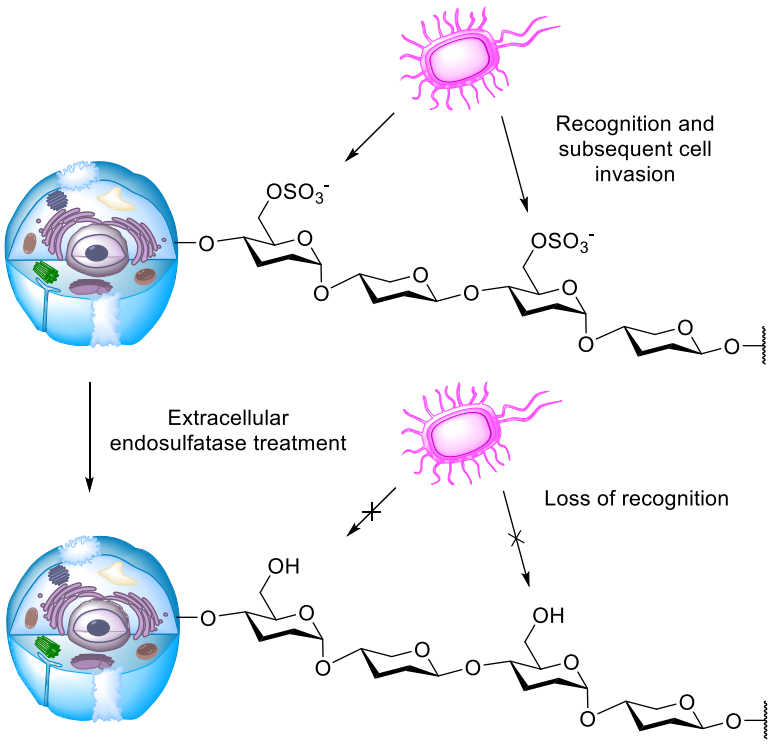

Figure 7 - A representation of the intended action of extracellular endosulfatase treatment. Here, the enzyme in the extracellular space removes structural features from HS on the surface of the cell, leading to a loss of recognition by pathogens and subsequently preventing invasion. However, this also inhibits the intended function of this motif on the cell, which could have consequences for cell function.[37,64]

Furthermore, HS has been shown to bind with several enveloped viruses such as herpes simplex viruses[65], hepatitis viruses[66], human immunodeficiency virus (HIV)[67] and dengue virus (DENV).[68] The HS binding action is involved with the travel of the virus through the extracellular matrix, initial contact with and subsequent binding with the membrane of cells, and their entry to the cell leading to infection. The initial contact is often made up of several relatively weak interactions between different HSPGs, which act to bring the virus closer to the cell membrane. Therefore, the blocking of HS binding sites on the cell surface could be a broad method of targeting common and resistant strains of viruses. Research in this area has identified the chemokines CXCL9 and CXCL12 as having antiviral activity against the aforementioned targets.[69] Chemokines are involved in the proper functioning of the immune system. CXCL9 and CXCL12, which have a substantial positively charged region, have been reported to demonstrate high binding affinity for HS. Chemokine-derived peptides could therefore be potential lead compounds for new antiviral therapeutics.

1.2.4 HS use as pharmaceuticals

The use of GAGs as pharmaceuticals is well established from using heparin as an anticoagulant. Although they have differences, heparin and HS are structurally related, and much of the early work

in the GAG space was carried out with or on heparin. HS - although not identified as such until later - was often isolated during this work on heparin and passed over as a side-product.

Heparin was first purified in 1916 in Baltimore, USA, by then-student, Jay McLean, in the group of Professor William Henry Howell[70], and the discovery of the material itself and its anticoagulant properties is often attributed to them. While McLean did indeed conduct several in vitro experiments to prove the anticoagulant effect, there are earlier references in the literature to the anticoagulant effects of heparin by Maurice Doyon in a 1912 summary of his previous years of work.[40,71] Many other groups and scientists, including Charles Best and David Scott, contributed to expanding the knowledge of heparin and its isolation in the early years, and later controversy surrounding the distribution of credit for the discovery was somewhat amicably resolved. Heparin was first put into trials in 1935 and is still in common clinical use today as an anticoagulant. The term 'heparin' originates from the Greek 'hepar', or liver, from which it was first isolated. It is typically obtained from animal tissue for commercial pharmaceutical use, but this has caused problems with purity[72] and variable effectiveness clinically.[73]

Heparin's interaction with antithrombin III is well documented and establishes the potential of GAGs to interact with proteins.[74-76] The signalling cascade of coagulation is very complex, with two different pathways in effect - intrinsic which is triggered by contact with collagen, and the extrinsic which is triggered by exposure to tissue factor, a glycoprotein found outside the blood vessels (Figure 8). Cofactors including calcium ions and phospholipids are also required during the cascade. The cascade occurs secondary to the binding of platelets at the wound site and serves to generate fibrin. Fibrin can then polymerise to form a clot. The action of heparin is to bind with and inhibit various activated serine-protease factors within the pathway (factors XIIa, XIa, IXa, and Xa), or to activate antithrombin which is a serine-protease inhibitor. [77]

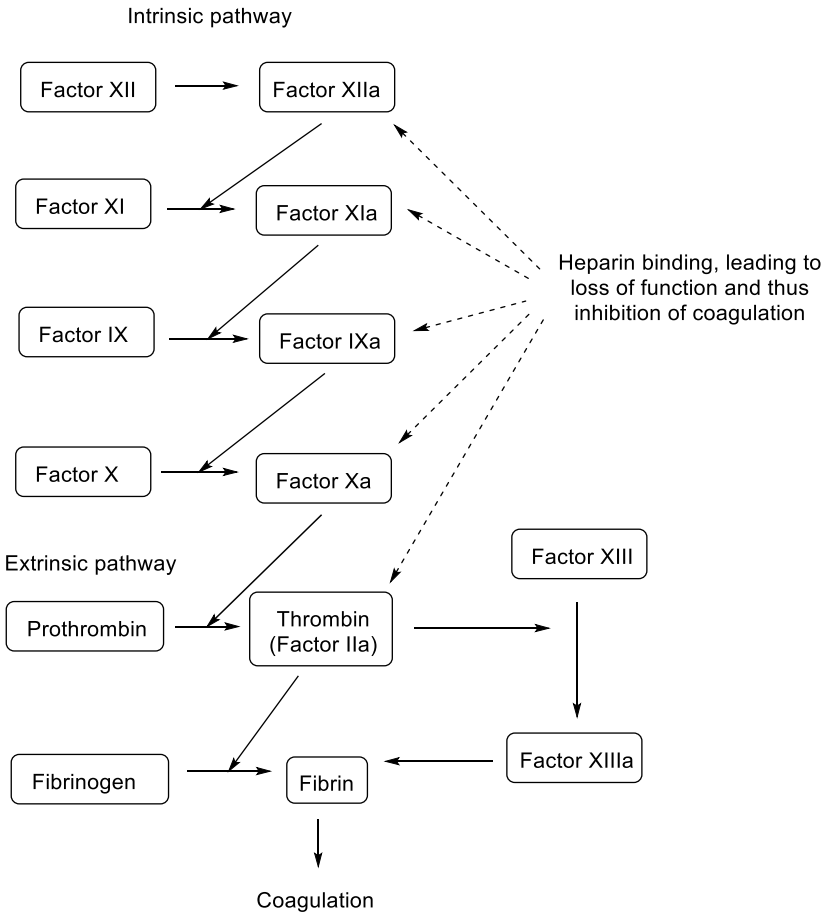

Figure 8 - A map of the coagulation cascade pathway, showing the interconversion of various factors. In addition to the well-known thrombin interaction, heparin also has an inhibitory effect in several activated serine-protease factors leading to the inhibition of fibrin generation, and therefore inhibiting clotting.[77]

Alternative anticoagulant therapies have become available. These include the use of low molecular weight heparin (LMWH)[78,79] such as the semi-synthetic LMWH enoxaparin,[80,81] and purely synthetic compounds such as fondaparinux[82] and idraparinux[83] (Figure 9). The structures of fondaparinux and idraparinux were based on the specific pentasaccharide antithrombin binding region of heparin.[9]

The synthesis of fondaparinux and similar molecules has been carried out on a large scale and continues to be optimised.[84-86] These alternatives to heparin have been used with good success clinically, with ongoing development of their administration.[87,88] However, these synthetic alternatives were generally observed to have weaker anticoagulant activity than unfractioned heparin. Furthermore, these alternatives cannot be neutralised by protamine sulfate when an overdose or substantial bleeding is present.[89] Protamine sulfate is a polypeptide with multiple positive charges, which binds to the substantial distributed negative charges present in heparin. Binding reverses the anticoagulant effect of heparin, although the mechanism is poorly understood. Rapid clearance of the resulting complex may contribute to neutralisation of activity. There is some research towards the use

of cationic small molecules to neutralise the anticoagulant effects of heparin. These compounds may be more effective when used to neutralise synthetic heparin alternatives, and have the advantages of easier manufacture, formulation, delivery, and greater shelf life.[37] Other possible treatments such as heparin-binding co-polymers, which can also reverse the effects of synthetic derivatives such as fondaparinux, have been reported.[90]

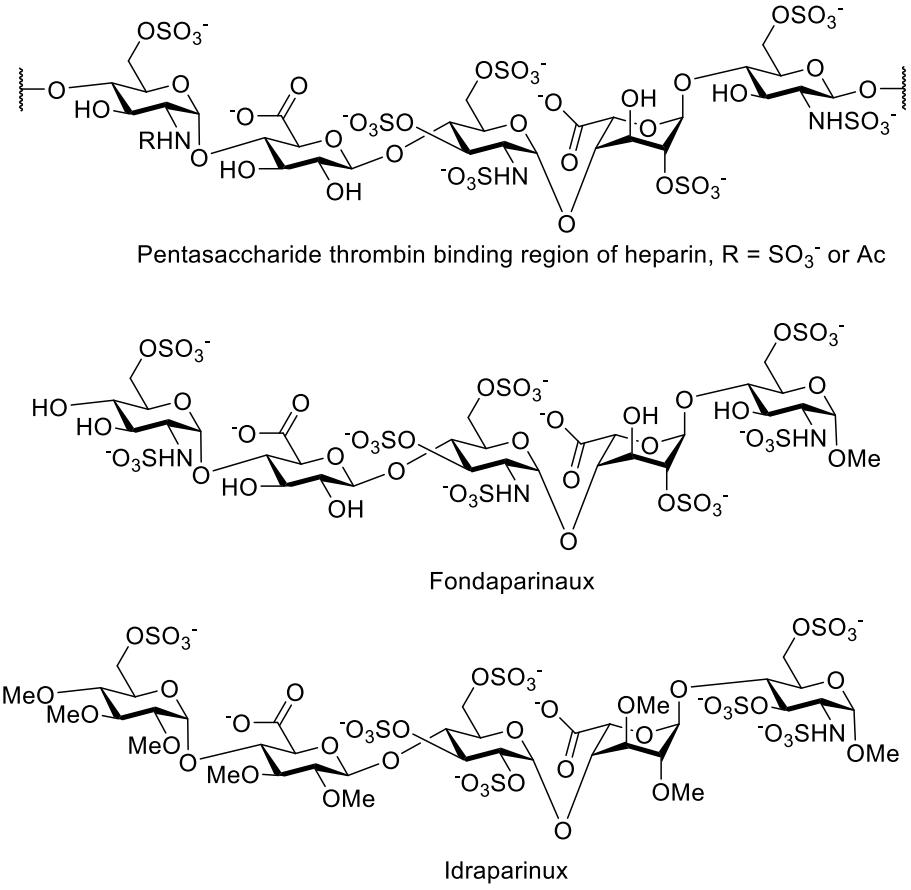

Figure 9 - The minimal thrombin binding pentasaccharide motif discovered in heparin. This motif has been used as the basis of several synthetic anticoagulants such as fondaparinux and idraparinux.[9,80,82]

Synthetic oligosaccharide heparin alternatives continue to be developed and improved, and will likely remain at the cutting edge of anticoagulant therapies for the foreseeable future.[91] Even for well-known sulfated GAGs, research continues to be carried out on their role in the blood coagulation pathway over 100 years since the first discovery of heparin, with a recent report indicating that heparin of sufficient chain length will facilitate an AT/Factor Xa interaction in a bidentate manner.[92]

Following this long history of clinical use as an anticoagulant, heparin was also identified as an inhibitor of β-secretase (BACE1) enzyme.[93] BACE1 catalyses the cleavage of amyloid-β peptide fragments from the amyloid precursor protein. As part of the theory of the amyloid cascade,[94] an excess of free amyloid-β peptide fragments are able to aggregate and form insoluble deposits of amyloid-β peptide

in brain cells, commonly referred to as plaques. There is evidence[94] that this deposition contributes towards the progression of Alzheimer's disease (AD), although there is not necessarily a linear correlation between the emergence and development of amyloid plaques and disease progression. There is however an apparent linear correlation between the deposition of hyperphosphorylated tau protein into neurofibrillary tangles in neurons and AD progression. The tau proteins bind to, and subsequently stabilise, microtubules in cells and are abundant in neurons. Tangle formation appears to occur downstream of amyloid plaque formation and may be catalysed by it. The overall effect of these aggregates is a loss of neuron function, and therefore disruption of signal transmission in the brain leading to dementia.

Various hypotheses have been put forward to describe the role of amyloid plaques in AD progression, such as the trigger or threshold scenarios.[94] In the trigger scenario, a level of amyloid plaque deposition in the brain is reached which triggers the progression of tau neurofibrillary tangle formation. The tau pathology then accelerates independently of any further changes in amyloid plaque formation. In this case, a therapeutic inhibiting amyloid plaque formation would only be effective if given before the trigger point is reached, which may be well before the onset of symptoms. In the threshold scenario, tau pathology is similarly accelerated by a certain level of amyloid plaque deposition. However, if the level of amyloid plaque deposition is reduced, the progression of tau pathology is likewise reduced. In this case, a therapeutic inhibiting amyloid plaque formation could provide benefit by stopping further progression of AD after symptoms develop.

It follows that inhibiting the BACE1 enzyme could prevent the deposition of amyloid-β protein aggregates, and therefore prevent the progression of AD depending on the nature of the role played by amyloid plaques. The ability of heparin to provide this inhibition has already been remarked upon. However, the anticoagulant properties of heparin would be undesirable for its use as a medication for AD patients, due to the typical demographics of this patient group.[95] This has led to interest in synthetic HS sequences that demonstrate BACE1 inhibition, but with reduced or without anticoagulant effects. Efforts to synthesise oligosaccharides for this purpose, by our group, will be discussed in a later section.

Research continues into the roles of HS interactions in amyloid protein pathology, including investigations of propagation and cell uptake of protein aggregates, and the interactions of HS in the guise of HSPGs with this process.[96,97] Indeed, further research into the disease itself continues and new discoveries about the pathology of AD continue to be made.[98] Separate research has suggested particular sulfation patterns in heparin and HS that may be contributing, via HSPGs in the case of HS, to the formation and stability of amyloid-β protein aggregates.[99] Additionally, HSPGs can have a similar

role in the formation of other aggregates implicated in the progression of neurodegenerative diseases, such as Parkinson's disease.[100] These interactions representing another possible mechanism to target with HS based therapies.

HS sequences, in addition to sequences of other GAGs, have also been shown to interact with fibroblast growth factors (FGFs).[57,58,101-103] FGFs are a diverse family of signalling proteins with 19 separate FGFs and four highly conserved fibroblast growth factor receptors (FGFRs) identified in vertebrates. FGFs act as a co-receptor by interacting with FGFRs and HSPGs on the cell surface to form a signalling complex. Complex formation leads to a conformational change in kinase domains, which may then carry out their function of catalysing the phosphorylation of target proteins within the cell. This acts as a molecular switch that begins a cell signalling pathway.[48,104] FGF interactions regulate many fundamental pathways throughout development,[105] and are further involved in the physiology of an adult organism.

The role of heparin and HS as active components in the FGF/FGFR signalling complex has been demonstrated by a *Drosophila* development model.[106] Mutations in enzymes involved in the biosynthesis of HS led to failures in FGF signalling. Subsequently, this signalling failure led to developmental abnormalities. Additionally, the role of HS as a mediator of FGF2 activity in the proliferation of satellite cells in has been explored.[103] Satellite cells are human skeletal muscle stem cells residing in healthy muscle fibres. These cells activate in response to muscle injury, differentiating and fusing to existing muscle to generate new fibres. Treatment of cells extracted from mice with highly sulfated HS analogues inhibits FGF2 signalling and promotes satellite cell activity. In contrast, treatment with N-acetylated HS analogues promotes FGF2 signalling and inhibits satellite cell activity.

The structural features of FGF1 and FGF2 have been reviewed by Faham et al.[107] The various FGFs are globular proteins which share a highly conserved 28 residue core region, and range in mass from 17-24 kDa in vertebrates. The tertiary structure of FGF2 contains a β barrel of 12 antiparallel β sheets, which can be further distinguished as four-stranded β sheets arranged in a triangular array. One of the loops between β sheets carries multiple basic amino acid residues that form the primary heparin/HS binding site. Comparison of the residues in this binding site across the FGF family show that it is not fully conserved, suggesting that the various FGFs will have specificity for different heparin/HS sequences. Other distinct loops between β sheets, separate from the heparin/HS binding site, are thought to be involved in receptor binding. The structural features of FGFRs include 3 immunoglobulin-like regions. A separate heparin/HS binding site with a highly conserved 18 residue sequence is also present, and is essential for receptor activity.[104] When forming a complex in the

absence of heparin/HS, the heparin/HS binding sites of the both the FGF and FGFR are contiguous, further supporting a heparin/HS bridged FGF/FGFR complex model.

FGF2 itself is of interest in clinical applications, for example as a component of wound healing constructs, but has significant stability issues when isolated.[108] In the cell environment, the high affinity interaction between FGFs and heparin/HS acts to stabilise the FGF from proteolysis and thermal denaturation, while also limiting the travel of FGFs away from the cell.[104]

FGF/FGFR complex formation occurs via an initial 1:1 FGF/FGFR complex, to which a further FGFR is recruited, leading to a weakly bound minimal complex. This weak complex binding is possible even in the absence of HS. This minimal complex is further stabilised and activated by the presence and binding of appropriate HS molecules, leading to a minimal active complex that can induce signalling. Additionally, HS involvement significantly increases the affinity of FGF for the FGFRs, such that the minimal active complex (1:2 FGF/FGFR with HS) may immediately form without weak FGF/FGFR association. A further molecule of FGF may subsequently bind, leading to a 2:2 FGF/FGFR signalling complex with HS involvement, which is more stable. This stabilised complex enables stronger and much longer lasting signalling activation.[104]

Heparin chains have been observed interacting with FGF2 and FGFR1 in a 2:2:2 complex. A single crystal X-ray structure was obtained, and it was found that heparin has a role in both the binding of FGF2 to FGFR1, and the coalescence of two of these units into a dimer (Figure 10, reproduced from the Protein Data Bank, entry 1FQ9). This binding is accomplished by a variety of hydrogen bonding interactions, with participation from the sulfates as might be expected, but also with carboxylate oxygens, glycosidic bond oxygens, and sugar ring oxygens of the heparin chain, demonstrating the importance of the underlying sugar backbone. Of the sulfates, bonding to the protein primarily occurs through the glucosamine *N*-sulfate and iduronic acid 2-*O*-sulfate groups on the heparin chain, with minor contributions from occasional glucosamine 6-*O*-sulfate interactions. The component of the two heparin chains involved directly in binding is well-resolved, but the full chain is not shown as the sections of each chain not involved in binding were too mobile to resolve.[109]

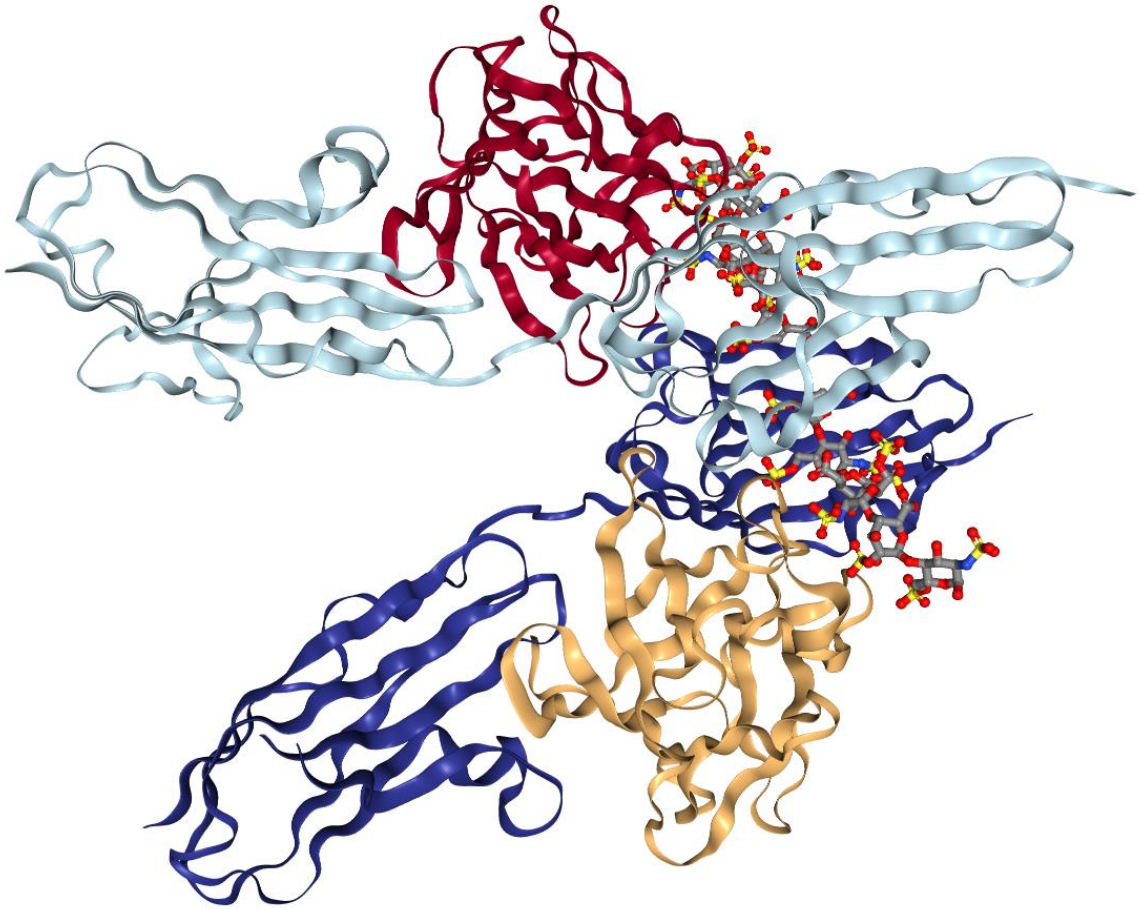

Figure 10 - A representation of a single crystal of an FGF-FGFR-heparin complex. This crystal shows two units of FGF2 (red and gold) and two units of FGFR1 (teal and dark blue) in a 2:2:2 complex with binding mediated by the non-reducing ends of two heparin chains shown as ball and stick models. Reproduced from the Protein Data Bank (PDB), entry 1FQ9, as submitted by Schlessinger et al. [109]

In theory, HS sequences could be synthesised which selectively regulate FGF/FGFR complex formation, and therefore allow specific cell signalling pathways to be up- or down-regulated. This suggests a potential future role for HS pharmaceuticals in diverse areas such as combating cancer development,[110] enhancing wound healing,[111] and influencing stem cell development.[112] Our own interest in FGF/FGFR interactions is to establish some of the structural features of HS that modulate binding affinity. The octasaccharide targets presented, and discussed later, in this work were designed to investigate the structural features of HS which are important for FGF2/FGFR1 interaction, based on the studies of our collaborators.

The prevalence of FGFs and their role in cell multiplication and survival mean that FGFs have multiple roles in many cancers.[44,113] A deregulation of FGF signalling pathways is thought to have a pathogenic role in the development of tumours, including migration and proliferation of tumour cells. However,

they may also have tumour suppressive roles through interaction with the immune system and pathway regulation. Although not all of these pathways are fully understood and tend to be specific to the tumour type, there exists the possibility that HS pharmaceuticals can be developed against cancers in which FGF-FGFR interactions are driving tumour development.[39,114]

For example, in a recent report, an octasaccharide HS mimetic was prepared based on an HS sequence previously identified as having a strong affinity for various FGFs and heparanase inhibitors, both of which are highly expressed on the extracellular surface of tumours (Figure 11).[115] The sequence is therefore expected to be a potent inhibitor of angiogenesis and metastasis mediated by these proteins. Firstly, an octasaccharide chain was assembled from a repeating disaccharide unit and two capping monosaccharides, with an alkyne functional group on a short carbon chain at the reducing end. This mimetic was then conjugated to a fluorine-18 radiolabel, with good decay-corrected radiochemical yields of 15 to 24%.

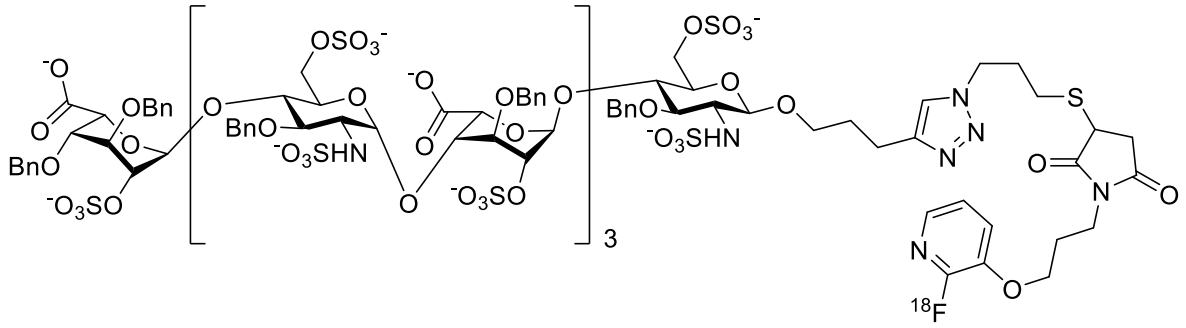

Figure 11 - The structure of an octasaccharide HS mimetic attached by a linker to a ^{18}F radiolabel. This mimetic has been designed as an inhibitor of angiogenesis in tumours and displayed favourable pharmacological properties in a healthy rat model. Benzyl protecting groups were not removed in this synthesis.

The *in vivo* pharmacological characteristics of the mimetic were studied by positron emission tomography (PET) in a healthy rat model. This model showed favourable *in vivo* pharmacological properties in healthy rats, with long residence time in the vascular system and elimination by the liver and kidneys. These results are encouraging for the future use of this HS mimetic in cancer treatment, and the authors intend to evaluate the ^{18}F-labelled HS mimetic in a rat tumour model.

HS sequences have been shown to interact with chemokines, leading to the regulation of inflammation and angiogenesis.[116] Chemokines, a type of cytokine, are short polypeptides with a well conserved tertiary structure. They promote the migration of leukocytes towards sites of infection, with the cells moving towards sites of increased concentration of chemokines. This process is known as chemotaxis, and the cells move along a concentration gradient. Other chemokine structures can have roles in cell survival, proliferation, infection and development, and the development of tumours.[117]

Chemokines are categorised by differences in the pattern of cysteine residues near the amino terminus of the protein, and divided into families: CXC, CC, C and CX_3C.[118] Chemokines of the CXC, CC and C families are known to be soluble and mobile. These chemokines can interact with proteoglycans, which performs several functions, such as localising the chemokines in the right areas, stabilising and orienting the directional concentration gradient, promoting or inhibiting chemokine oligomer formation, and regulating chemokine activity.[116] The latter family, CX_3C, is rather exceptional - it has only a single member, and differs significantly from the other families of chemokines. CX_3C features an additional long 'stalk' that terminates in a short hydrophobic region of 18 residues, which suggests that this chemokine is anchored to the cell membrane. This chemokine is highly expressed by endothelial cells, and may be of importance for recruiting leukocytes from the blood.[119]

Although the specific HS sequences responsible for chemokine interaction are not known, various features that lead to regulation have been explored. It has been reported that the addition of a single, site-specific 6-sulfate on a glucosamine residue, in an otherwise homogenous dodecasaccharide, could switch the inhibitive effect of this compound from the chemokine CXC8 to CXC12. This identifies the glucosamine 6-*O*-sulfate moiety as a feature of importance for this chemokine interaction, and suggests that such site-specific modifications will be good targets for future biological applications.[120] In addition, many other interactions between cytokines and HS have been documented, and knowledge of their many roles and functions continues to be expanded upon.[121]

A recent report utilised *in silico* modelling and analysis of a hexasaccharide library to predict hexasaccharide HS sequences that would selectively target heparin co-factor II (HCII).[122] HCII is a serine protease inhibitor found in high levels in blood plasma, and is known to selectively inhibit thrombin in much the same way as antithrombin, although the full physiological role remains unclear.[123,124] HCII and antithrombin have considerable similarity in primary, secondary, and tertiary structure. A selective GAG activator of HCII had not previously been identified. Hexasaccharides were then synthesised and their HCII and antithrombin activation properties tested. Several of these hexasaccharide HS sequences, containing a 2-*O*-sulfate on two glucuronic acid residues within two consecutive disaccharide motifs, can induce HCII activation. However, some of these hexasaccharide sequences are also good activators of antithrombin, which appears to arise from the presence of 3-*O*-sulfated glucosamine residues in these structures. Notably, in all tested hexasaccharides, the glucosamine residues are always *N*-sulfated and a subset are 6-*O*-sulfated. The most promising example (Figure 12) induced HCII activation by around 250-fold, whilst being a poor activator of antithrombin.[122]

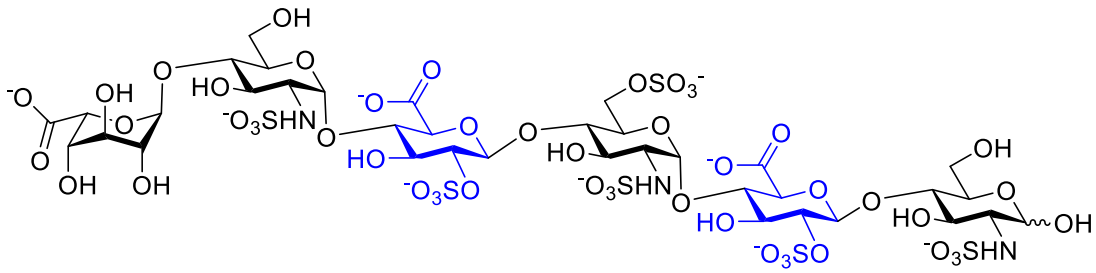

Figure 12 - The structure of a hexasaccharide HS mimetic, which is a selective HCII activator. The 2-O-sulfated glucuronic acid residues are highlighted in blue. This pattern of two consecutive disaccharide subunits containing a 2-O-sulfated glucuronic acid residue is necessary for HCII activation.

The unique structures of these hexasaccharides may explain why a selective GAG activator of HCII has not been found previously. None of the hexasaccharides are heparin-like, as heparin has high proportions of iduronic acid. As previously discussed, natural HS has high proportions of *N*-acetylated glucosamine residues and low proportions of 2-*O*-sulfated glucuronic acid residues. Two consecutive disaccharide motifs containing 2-*O*-sulfated glucuronic acid residues is therefore a rare motif in natural HS, and this research shows that specifically this type of arrangement is required for activation of HCII. It also demonstrates that 3-*O*-sulfated glucosamine residues led to antithrombin activation. A HS sequence made to specifically inhibit HCII should therefore not contain 3-*O*-sulfated glucosamine residues to prevent antithrombin activation, and feature two consecutive disaccharide motifs containing 2-*O*-sulfated glucuronic acid residues to achieve HCII activation. No conclusion is drawn on any requirement for the presence of 6-*O*-sulfated and/or *N*-sulfated glucosamine residues for HCII or antithrombin activation. However, the most effective hexasaccharide notably contained one 6-*O*-sulfated glucosamine residue, and all glucosamine residues were *N*-sulfated.

1.2.5 Discovering the biological effect of an HS sequence

Whilst HS and HS-based pharmaceuticals have great promise, there are several challenges that remain to be overcome. Conclusively establishing a specific sequence of heparin, or HS, as the structure within a sample which produces a biological effect is very difficult, and therefore the initial determination of which HS sequences can interact with a certain protein can be a long process. This is due to the structural complexity of HS, the multitude of protein-binding features present in a single HS sequence, and the wide range of HS-HSBP interactions in an organism. Furthermore, even once a potential HS sequence of interest has been established, developing a compound based on this to specifically target only one interaction, without other side effects, may be difficult. However, good progress has been made in establishing which chemical features (for example, the location and degree of sulfation) of heparin and HS are responsible for causing a specific biological effect, based on synthetic products.[10,125]

A common approach to assessing HS function has been by the production of 'semi-synthetic' HS fragments. In this method, the heterogeneous heparin or HS is cleaved into fragments by the action of enzymes, and these smaller fragments are chemically modified (hence semi-synthetic).[10,39,57,58,126] These fragments can then be purified into a more homogeneous mixture in a variety of ways and used in binding assays to develop a map of the structural features required for interaction. Identification of these fragments and their structural features is much easier than long and complex natural HS sequences. Furthermore, an analysis of the quantity of each type of fragment can inform the approximate composition of the original heterogeneous mixture. There is also interest in the further chemical modification of these semi-synthetic chains, in which some of the anionic moieties are replaced with uncharged, structurally diverse groups.[126] Such changes will significantly alter and perhaps improve the physical properties of these fragments, and provide further avenues for interaction investigations.

As an example, a recent study identified HS structures with affinity for the receptor Robo1 which indicated specific structural changes are key in up- and down-regulating binding.[127] Robo1 is involved in axon guidance and cell migration. To establish which interaction was causing the biological effect, short HS sequences were produced by the action of enzymes on natural HS, and these short sequences were then purified and enriched using an immobilised target protein. The structures of these HS sequences were identified by a hydrophilic interaction chromatography–high-resolution mass spectrometry (HIC-HRMS) method. This information was used to direct the chemical synthesis of a small library of well-defined HS oligosaccharides, with relatively simple sulfation patterns, for structure-activity relationship (SAR) studies. This strategy was thus able to determine some of the possible sequences which influence HS binding to Robo1, but further refinement is required. This research serves to highlight the challenging process of establishing the specific features of a HS sequence which affect a specific target.

1.2.6 Biological and chemo-enzymatic synthesis of HS sequences or analogues

The main source of heparin and other GAGs worldwide has been animal tissue from food animals, with China being the leading exporter, but this has led to issues of vulnerability of supply due to an inability to scale up, variable quality of the product, contamination with viruses or prions, seasonal variations, or trade disruption.[128] The risks associated with mammalian animal sources have been acknowledged and alternatives, such as sourcing from invertebrate or marine organisms, are under investigation.[129] However, the GAGs from these alternatives can exhibit different structures and may require further modification or development to be used.

Perhaps the most unfortunate, and most public demonstration of this vulnerability was in 2008, when there was a global recall of heparin products after numerous deaths (81 reported by the US Food and Drug Administration) and adverse events.[72] It was later established that adulteration of heparin samples with over-sulfated chondroitin sulfate was responsible for the problems. In some cases, the chondroitin sulfate made up over half of the crude material. This was almost certainly done intentionally, before the crude heparin entered processing at a facility with robust good manufacturing practice (GMP) procedures, as this GAG is not found in nature and required synthesis. It would have been difficult to ascertain that the adulteration had taken place during the typical quality control testing used at the time. Thus, there is substantial interest in alternative, non-animal, large scale, safe and reliable production methods of heparin and HS.

The first and perhaps most obvious method of producing heparin, HS and related analogues industrially would be leveraging the existing cellular machinery used to produce HS in organisms on a large scale. Our understanding of the biosynthesis of HS has already been discussed in detail. As a brief summary, several types of sulfated GAGs are synthesised by the action of glycosyltransferases and sulfotransferase enzymes, primarily in the Golgi apparatus[130] and endoplasmic reticulum, of eukaryotic cells.[16-18] They can then be excreted from the cell in vesicles, transported to the cell membrane, or to other organelles for further modification, such as the nucleus.[131] Overexpression of genes related to GAG biosynthesis could allow for increased HS production. However, the output of biological synthesis of GAGs is very heterogeneous – chains of HS are often of different length and sulfation pattern, due to the presence of many enzymes of different functionalities in the Golgi, availability of materials, and material flow. Therefore, simply over-expressing HS and other GAGs in the natural state would be useful for supply but not an optimal solution for generating specific sequences.

A further development of this strategy would be to co-opt elements of the cellular machinery to produce our own desired sequences. There is a significant breadth of work in the area of bioengineering as a source of GAGs.[128,132-136] The cellular machinery of the Golgi also contributes to the synthesis of other oligosaccharides, proteoglycans, and glycolipids. These molecules have a huge variety of roles in the cell, have potential therapeutic and pharmaceutical applications, and are ongoing targets for synthesis.[137,138] As the mechanisms of the cellular machinery continue to be investigated, new protein structures involved in chain assembly and post assembly have been characterised.[139]

An example of using bioengineering to produce GAGs is the synthesis of hyaluronic acid (HA), which has been reviewed by Kogan et al.[140] HA is a heterogeneous mixture of differing lengths of a high molar

mass, linear, non-sulfated polysaccharide. It is comprised entirely of alternating (1→3) linked *N*-acetyl-β-D-glucosamine and (1→4) linked β-D-glucuronic acid monosaccharides, forming repeating disaccharide units (Figure 13). HA is present throughout the human body with high concentrations in the extracellular matrix, synovial fluid, and skin. It has functions such as providing lubrication, influencing dermis tissue repair, and providing a space-filling matrix in tissues. Because of these functions, HA has several industrial and medical applications, for example in dermatology and plastic surgery, ophthalmologic surgery, and orthopaedic surgery.

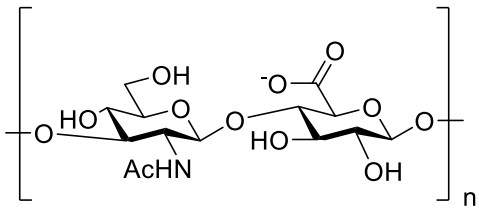

Figure 13 - The disaccharide repeating unit of hyaluronic acid (HA).
Note the absence of any sulfation, and the (1→3) linkage between N-acetyl-β-D-glucosamine and β-D-glucuronic acid.

HA was initially isolated for clinical applications primarily from rooster combs, but is now commercially synthesised through a 'fermentative' process in bacteria by several companies.[140] However the sequences produced are not of a defined length, and HA is not modified following synthesis of the oligosaccharide chain as are other sulfated GAGs, and thus it is simpler to set up a biosynthetic pathway. Additionally, production by bacteria carries the risk of bacterial strain mutations or co-production of toxins. Progress on this approach using genetically modified bacteria strains is ongoing.

As an example of the specific biosynthesis of more complex GAGs, in a recent study, heparin-like HS was biosynthesised via the recombinant expression of human serglycin, in human cells.[141] The expressed serglycin was further modified in a variety of patterns with chondroitin or dermatan sulfate chains. One of these variants was assessed as having anticoagulant activity one-seventh that of unfractionated heparin from pig sources, demonstrating that clinically effective human heparin-like heparan sulfate could be generated by a bioengineering route. The challenge inherent in a bioengineering pathway, however, is overcoming the heterogeneous nature of the products, as this is very undesirable for the synthesis of pharmaceuticals.

Given the prevalence of GAGs in cells, and the biologically active nature of natural heparin, HS and other sulfated GAG sequences, it is perhaps unsurprising that enzymes responsible for producing such sequences have become targets for research and development.[101,142-144] Many types of enzyme with various roles in biosynthesis, and with applications in bioengineering, are known.[145] Chemo-enzymatic synthesis is a combined approach, making use of naturally sourced or chemically developed starting

materials, and a specific 'toolbox' of enzymes, to produce a target sequence of complete or high homogeneity.[129] Assembly of such a toolbox, with specific enzymes to carry out specific transformations in the synthetic pathway, is made possible by knowledge of the structure, specificity, mechanism, optimal conditions, isolation and purification of glycosyltransferases[146,147] and sulfotransferases.[148-150] Additionally, studies of binding affinity and free energy change will help to inform the development of experimental procedures.[151] Armed with this 'toolbox' and robust synthetic procedures, chemical transformations and the use of glycosyltransferases and sulfotransferases can be used to readily produce a small library of relatively well-defined HS sequences, from commonly available starting materials.[152] Such syntheses show a lot of promise, and future development in this area could see a chemo-enzymatic route to access sulfated GAGs become commonplace. However, some challenges concerning the use of enzymes in a synthetic pathway remain.

Enzymes have many attributes that make them attractive for use in synthesis, such as a high efficiency and stability, catalytic nature, substrate selectivity, regio- and stereo-specificity, and that may require only mild conditions and environmentally-friendly solvents.[153,154] They may be further biologically or chemically modified to introduce changes in their tertiary structure and functional group presentation, which may lead to a change in their preferred substrates or products. Furthermore, there is literature describing the role of *O*-sulfotransferases in the biosynthesis of heparin and HS, both *in vivo* and in the laboratory.[155-157]

However, there are some disadvantages. At present, enzymes alone cannot be used to access all possible HS sequences. *O*-Sulfotransferase enzymes can only function on a few substrates, as they are unable to selectively sulfate desired sections of a fully assembled oligosaccharide in the manner which are often required for targets of interest. Native enzymes are sometimes challenging to employ in the synthesis and modification of long chains. These enzymes may prefer to either begin new chains, extend existing chains, or prefer to modify more substituted chains over less substituted chains, and so on. Some enzymes require co-factors to operate, which can greatly complicate the development of a reaction, and purification of the products. Although an enzyme is catalytic, an expensive excess may be needed to drive some synthetic reactions to high conversion. The enzyme itself must be expressed and purified, which is not always a trivial task. Purification of the product material from a mixture containing enzymes can also be challenging, especially in the case of HS synthesis where the targets themselves are of a significant size and charge. Considerable difficulty has also been encountered in attempts to scale up enzymatic processes to the outputs required for industrial applications.[129,152-154] This means a purely synthetic procedure, allowing access to a variety of long-chain, well defined HS sequences, is also an area of active research.

1.2.7 Synthetic HS-like oligosaccharides

There is a desire to chemically access HS-like oligosaccharides. These are small (compared to a true HS chain), synthetic, sulfated, and well-defined analogues of HS. Analogues are often sufficient for investigations into protein binding, whilst being synthetically much more accessible than the long HS sequences found in nature. They do not have all the structural features of a true HS sequence, but present regions of sulfated sugar units that 'mimic' the function of a HS sequence. These can be biologically sourced from other types of GAG such as chitosan sulfates, and diversified by chemical or chemo-enzymatic modification, or synthesised in the laboratory.[158]

There are many factors to consider in the design of a HS-like oligosaccharide. The full synthesis of a significant HS chain would be incredibly challenging, but a short sequence, containing the relevant functional sulfate groups, is a much more achievable target. It is known that well-defined short sequences can be assembled with specific features that are thought to influence protein interaction.[159] Such features may include, for example, specific patterns of glucosamine 6-*O*-sulfation or iduronic acid 2-*O*-sulfation, as well as the pattern of monosaccharide residues in the sequence. The size or molecular weight of HS-like oligosaccharides has shown correlation to the efficacy of binding, such that a minimum chain length is often required, and short mimetics such as disaccharides show very low potency. The precise pattern and level of sulfation will highly influence the effect on the intended target, but it has been demonstrated that this effect is not simply the result of greater or lesser degree of sulfation - the position of the sulfates in the chain can also have a significant effect. The conformation of glycosidic linkages and the degree of flexibility in the oligosaccharide will also play a significant role.[71]

One novel chemical route, reported in recent literature, has suggested that the assembly of HS-like oligosaccharides using amide linkages between sugar units, rather than glycosidic bonds, can be used to more quickly and easily investigate protein interactions.[160] Although the reported binding affinities were relatively low, the observation of a binding interaction can be diagnostic in establishing targets for conventional synthesis. Indeed, HS-like oligosaccharides may need not be a chain at all, as shown by the synthesis of small, low molecular weight clusters displaying multiple sulfated GAGs with biological effects.[161] However, a 'true' HS-like oligosaccharides, with the correct sugar backbone, would most closely represent the natural binding motif and therefore should give the best results.

Some of the types of monosaccharides required for HS mimetic oligosaccharide chain assembly are not commercially available and require synthesis. Specifically, in the case of assembling HS-like structures, idose monosaccharides are often required. Our own group accesses idose monosaccharides via a route from 1,2:5,6-di-*O*-isopropylidene-α-D-glucofuranose (Scheme 1 – Access

to orthogonally protected idosaccharide residues from 1,2:5,6-di-O-isopropylidene-α-D-glucofuranose.Scheme 1).[162]

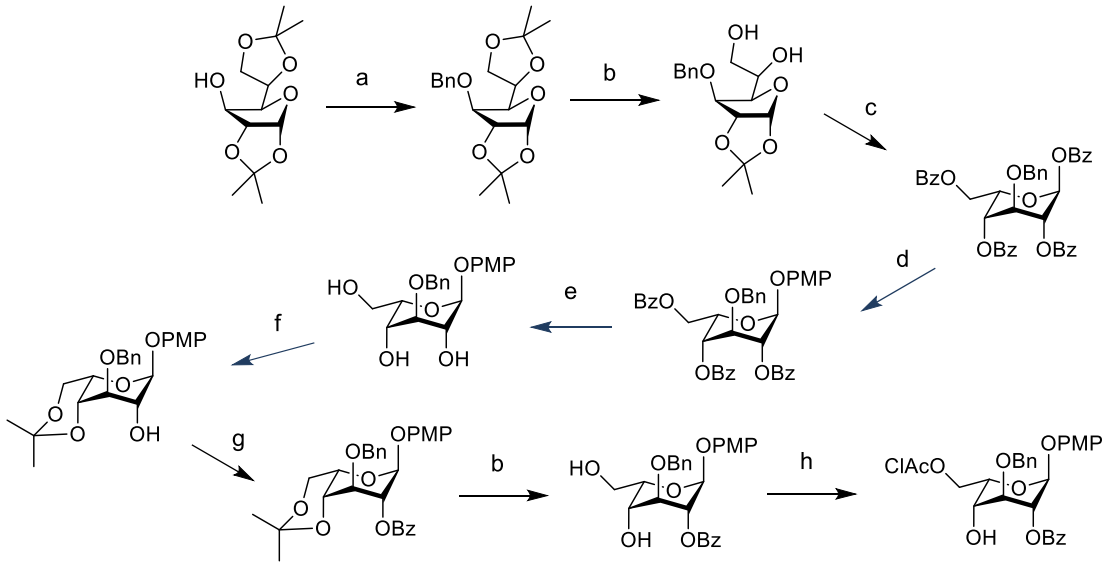

a) BnBr, NaH, DMF, RT; b) aq. HOAc, 80 °C; c) H_2SO_4, dioxane, 80 °C then BzCl, py, DCM, 0 °C; d) p-methoxyphenol, $BF_3.Et_2O$; e) NaOMe; f) $Me_2C(OMe)_2$, TsOH; g) BzCl, py; h) ClAcCl, py, DCM, -78 °C

Scheme 1 – Access to orthogonally protected idosaccharide residues from 1,2:5,6-di-O-isopropylidene-α-D-glucofuranose.

In this synthetic route, the starting material is first 3-*O*-benzylated, and then selectively 5,6-*O*-deprotected. Treatment with acid to convert to the idose sugar and remove the 1,2-*O*-acetal was followed by benzoylation on all available positions. Glycosylation with p-methoxyphenol and subsequent de-benzylation was followed by selective 4,6-*O*-protection. The remaining 2-OH was benzoylated, followed by 4,6-*O*-deprotection and subsequent selective 6-OH protection to give an orthogonally protected idose sugar.

Other groups access these idosaccharide residues in other ways. For example, access to uncommon L-idose and L-iduronic building blocks from the cheap and available D-glucuronolactone has been reported.[163]

1.2.8 Considerations in the chemical synthesis of oligosaccharides

The chemical synthesis of oligosaccharides is carried out by a series of glycosylation reactions. A glycosylation reaction is the name given to a reaction in which a sugar becomes chemically linked through C1 to another molecule with a new covalent bond. The reaction involves the nucleophilic attack of another molecule at the anomeric centre of a sugar. It is common to describe the sugar species with the reacting anomeric centre as the glycosyl donor (or just 'donor') and the species carrying out nucleophilic attack as the glycosyl acceptor (or just 'acceptor'). The nucleophile is usually

an alcohol, which could be on another sugar, or other molecules such as simple alcohols. The overall reaction is a nucleophilic substitution, but the exact mechanism of a chemical glycosylation reaction is a matter of some debate.[164]

Classical nucleophilic substitution reactions are broadly distinguished as having either a unimolecular or bimolecular process occurring in the rate determining step, which is abbreviated as S_N1 or S_N2 respectively (Scheme 2).[165]

In the classical S_N1 mechanism, a bond is broken between a leaving group and the carbon of the reaction centre, leading to a positive charge on the carbon. This is known as a carbocation, which generally has a trigonal planar sp_2 hybridised structure with an unfilled p orbital. A nucleophilic species then donates electrons to the carbocation to form a bond. The rate limiting step in the classical S_N1 mechanism is bond breaking, which is a unimolecular process. As attack can occur on either face of the trigonal planar carbocation, the classical S_N1 mechanism leads to a racemic mixture of products. However, other conditions such as the groups attached to the carbocation or reaction conditions can favour one product over the other.

In the classical S_N2 mechanism, bond breaking, and bond formation with the nucleophile occur at the same time. The transition state for this mechanism is trigonal bipyramidal, with the attacking and leaving species on opposite sides of a pentacoordinate carbon at the reaction centre. The rate limiting step in this mechanism is both breaking and forming bonds, involving two separate molecules. As attack occurs rigidly, the S_N2 mechanism always leads to an inversion of the original stereochemistry.

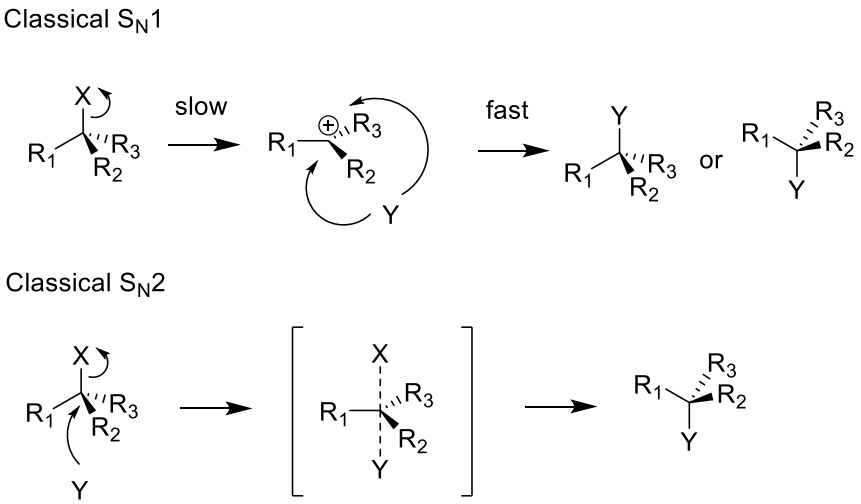

Scheme 2 - A representation of the classical S_N1 and S_N2 reaction mechanisms.

Nucleophilic substitution reactions may display classical S_N1 or S_N2 behaviour, have characteristics of one or both of these mechanisms (S_N1-like or S_N2-like), or even proceed by either mechanism under

different conditions.[165] Distinction between mechanisms can be made by studies of reaction kinetics, using methods such as varying the concentration of reactants and kinetic isotope effects. The degree of S_N1 vs. S_N2 character in a glycosylation reaction is a matter of debate, and may depend upon the conditions of the reaction.[164,166,167]

A common mechanism proposed for the glycosylation reaction proceeds through the formation of an oxacarbenium ion (Scheme 3).[168,169] In this mechanism, promoter-activated loss a leaving group attached to C1 on a sugar ring occurs, and a lone pair of electrons from the ring oxygen is donated to generate a double bond between the ring oxygen and the anomeric carbon. This structure is called an oxacarbenium ion. The sugar ring adopts a flattened half-chair structure as the oxacarbenium ion forms. Contact ion pairs, either closely associated with the oxocarbenium ion or solvent-separated, may also form with the counterion on one of the two faces of the oxocarbenium ion, further extending the spectrum of reactive intermediates.

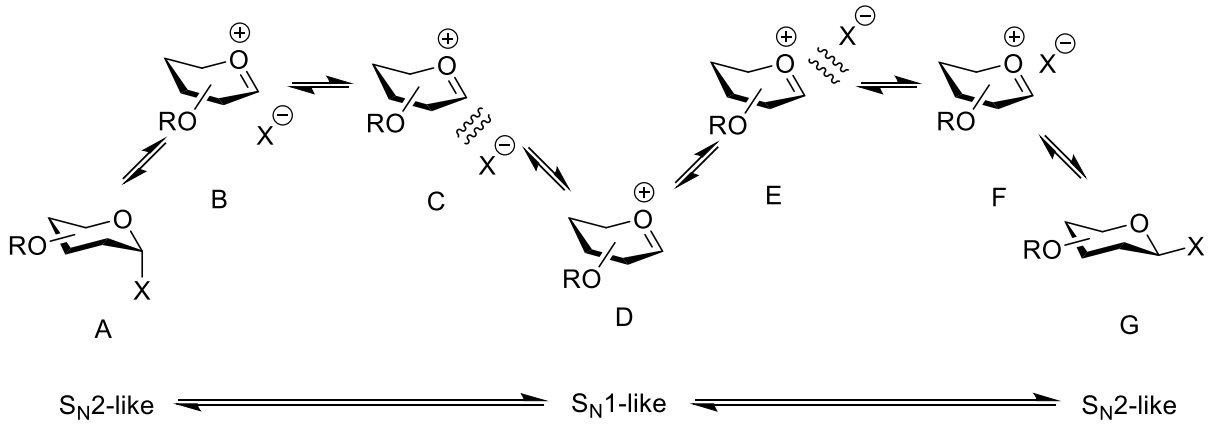

Scheme 3 - The series of possible reactive intermediates of the glycosylation reaction. Structures A and G are the α- and β-configurations of activated donor that would react in an S_N2-like manner, and structure D is an oxocarbenium ion that would react in an S_N1-like manner. Structures B and F are the α- and β-configurations of close ion pairs, and structures C and E are the α- and β-configurations of solvent-separated contact ion parts.

The overall formal oxocarbenium ion glycosylation mechanism is described as S_N1-like, with a two-step process, formation of positive charge on the carbon at the reaction centre, and a mixture of stereochemical products. Nucleophilic attack by a hydroxyl group of another nearby sugar can occur at C1 either above or below the plane of the $C=O^+$ bond, leading to the generation of either 1,2-*cis* or 1,2-*trans* linked glycosides (Scheme 4).[169] Recent investigation into the S_N1 character of glycosylation reactions has provided further insight into the influence that the degree of S_N1/ S_N2 character in the reaction mechanism has on reaction outcomes, including the stereochemistry of the products.[166]

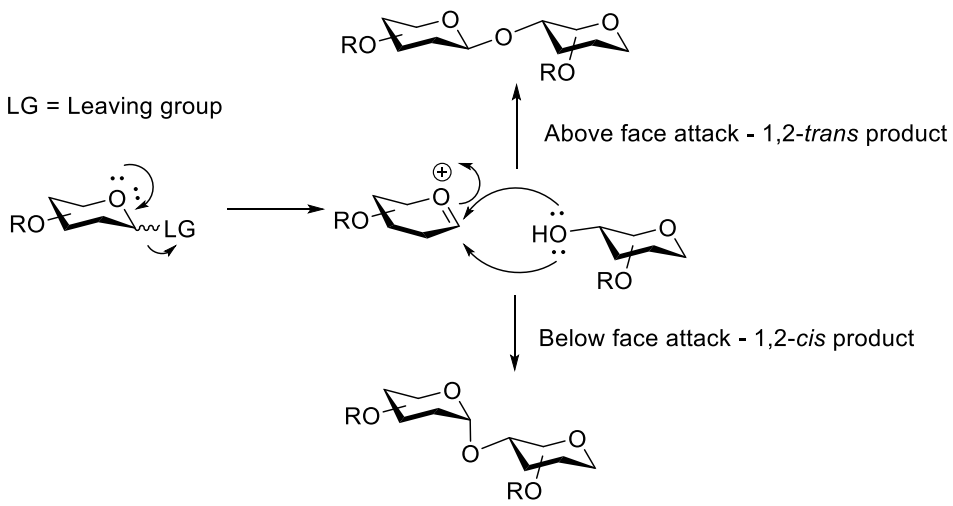

Scheme 4 - A generalised glycosylation mechanism through an oxacarbenium ion. The promoter-activated expulsion of an anomeric leaving group generates an oxacarbenium ion intermediate, which can then be attacked at either face by the hydroxyl group of another sugar to produce two products of different stereochemistry, although the alpha product is favoured by the anomeric effect.[169]

The 1,2-*cis* linked (α-linked) product of a glycosylation with glucose residues is often observed to be the major product. This outcome, in contrast to the assumed steric preference for equatorial substituents on a hexose ring, is caused by the anomeric affect. Outcomes in other systems, such as mannose, may also follow this 'unexpected' pattern. In many synthetic routes, glycosylation conditions are tuned to either make use of or overcome the anomeric effect, and so a brief discussion of this effect would be prudent.

The anomeric effect is the observed tendency of an group attached to the C1 carbon of a hexose ring to adopt an axial orientation, as opposed to the equatorial orientation that would be expected from a purely stereo-chemical argument.[170] It was originally known as the Edward-Lemieux effect and was first proposed by J. T. Edward in 1955, the same year in which R. U. Lemieux reported a stereoelectronic contribution to the anomeric equilibrium of pyranoses. The phenomenon became known as the anomeric effect in 1958.[171] It was theorised that the effect arises in part from an antiperiplanar hyper-conjugation interaction of filled, non-hybridised p orbitals from the ring oxygen and the sigma antibonding orbital in the bond between C1 and an electronegative substituent. There was also thought to be polar repulsion in the equatorial conformation. In addition, by the same hyper-conjugation argument, an exo-anomeric effect can be caused by an interaction between the filled p orbitals on an oxygen atom bonded at C1 with the sigma antibonding orbital between C1 and the ring oxygen. However, the exo-anomeric effect applies for both axial and equatorial substituents.[170]

These hyper-conjugation models account for the observed lengthening of the C-X bond and shortening of the C-O bond in the case of the electronegative C1 substituent. However, these models do not

account for observations of the equatorial position being favoured in certain solvents. Other studies have suggested the anomeric effect is dominated by electrostatic and steric considerations. As such, there is no current consensus in regard to the definitive cause of the effect, although investigations into its nature are ongoing.[172,173]

There are four common postulated mechanisms for the anomeric affect (Scheme 5). The first is the dipole moment argument, in which the overall dipole moment of the molecule is lesser in the axial conformation and greater in the equatorial conformation. The second is the Coulombic interaction argument, where there is favourable interaction between partial charges on anomeric substituent X and C5, or repulsion between partial charges of the ring oxygen and X. The third is the non-classical CH-X hydrogen bond argument, in which a non-classical bonding interaction may form between the axial hydrogen attached to C5 and X when the anomeric substituent is in the axial conformation but not when it is in the equatorial conformation. The fourth and perhaps most common explanation is the hyperconjugation argument, in which a stabilising interaction occurs as a lone pair of electrons from an sp^3 hybridised orbital on the ring oxygen donates electron density to the adjacent antibonding σ* orbital of the bond between C1 and X. This is favourable in the axial configuration of X, as the lone pair occupied sp^3 hybridised orbital on the ring oxygen and the σ* orbital of the X-C1 bond are then antiperiplanar.

Recent research and computational modelling of energy changes suggest the truth of the matter may be some combination of these modes of action, with no single mode being the definitive cause. This is postulated by Wiberg et al.[174] in their particularly aptly named publication, 'The Anomeric Effect: It's Complicated'.

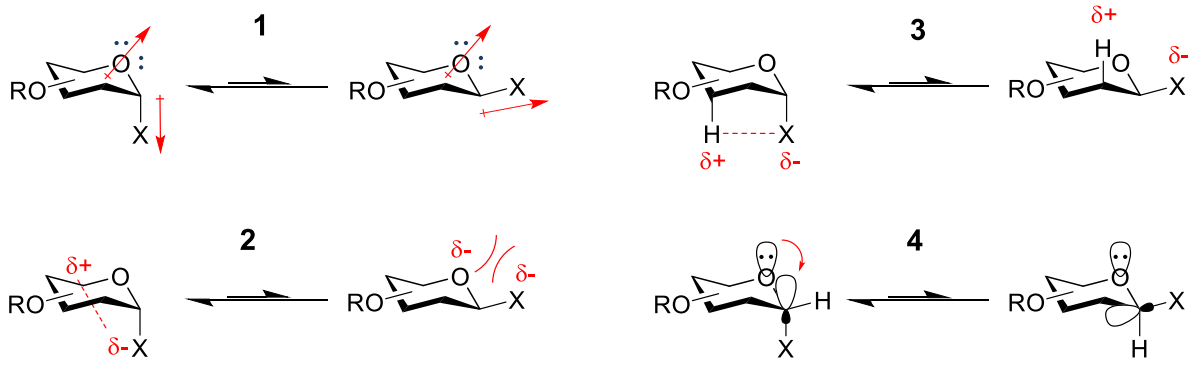

Scheme 5 - Four postulated mechanisms of the anomeric effect with an anomeric heteroatom. These are: 1, the dipole moment argument; 2, the Coulombic interaction argument; 3, the non-classical CH-X hydrogen bond argument; and 4, the perhaps more well-known hyperconjugation argument. It is likely that all these effects are active for the appropriate substituent and no one effect is truly responsible for the anomeric effect.[174]

The specificity of the stereochemistry achieved in glycosylation reactions is also influenced by the protecting group strategy employed across the remaining positions of the donor and acceptor species.[175,176] Particularly relevant is the protecting group at 2-position on the glycosyl donor, where groups can readily influence the glycosylation.[177-179] An acetate or benzoate protecting group at C2 can participate through donation of electrons from the carbonyl oxygen to the carbon of the oxocarbenium ion, forming a bicyclic system and moving the positive charge to a relatively stable tertiary carbocation centre (Scheme 6). This prevents nucleophilic attack at C1 from the 'below' face of the sugar, leaving attack from the 'above' face as the favoured outcome and in theory giving exclusively the 1,2-*trans* product, although there are well documented exceptions.[180-182] However, another outcome is possible - nucleophilic attack at the participating group carbonyl carbon, which generates an ortho-ester. Depending on the species in question, ortho-esters may be relatively stable and can be isolated. Common outcomes of ortho-ester formation are a collapse to the intended product over time, or hydrolysis back to the acceptor and hemiacetal of the donor on work-up. In the case that a stable ortho-ester is isolated, simply stirring the material with further Lewis acid promoter may enable rearrangement to the desired glycoside.

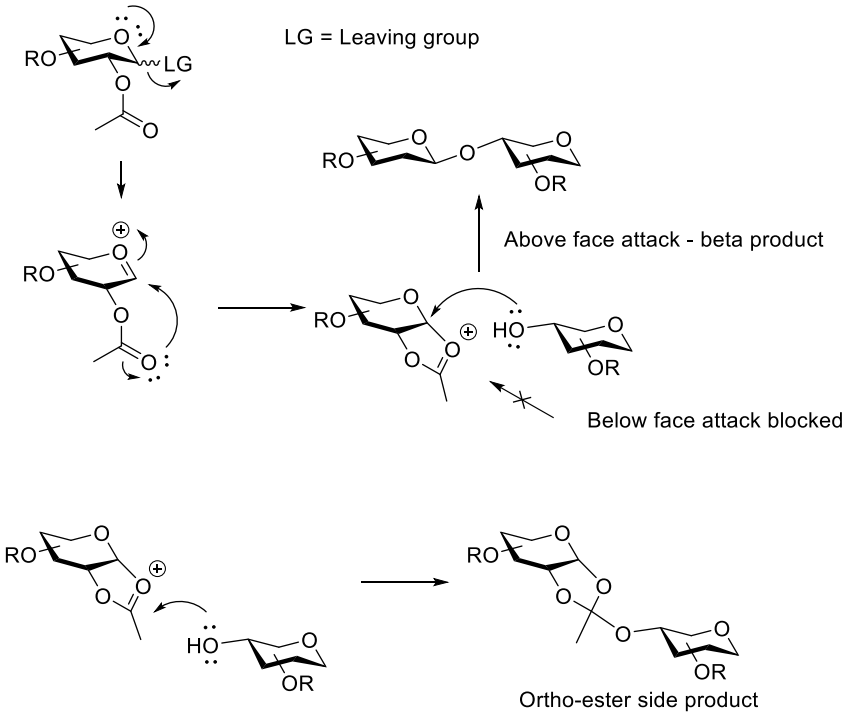

Scheme 6 - The action of a 2-O-acyl substituent of the mechanism of a chemical glycosylation. Upon oxocarbenium ion formation, a bond is formed between the carbonyl oxygen and C1, producing a more stable bicyclic system. This blocks nucleophilic attack from the below face of the ring, leading to a stereoselective product. However, this can also lead to the formation of an ortho-ester side-product depending on the species involved. [177-179]

Further effects on stereochemistry can come from reaction conditions such as the solvent used, temperature, promoter system and order of addition of the reactants.[183-185] The influence of protecting groups on stereochemical outcome of glycosylation reactions continues to be investigated and novel synthetic strategies developed to yield specific products.

An additional consideration in oligosaccharides is the conformation of the sugar rings. Sugar ring structures drawn in this work will be drawn in their expected low energy conformer. For example, glucosamine will be drawn in the $^4C_1$ conformation. However, it should be recognised that six-membered rings are able to adopt several possible conformations that may be energetically favourable.[186] Conformational changes to the sugar rings of both mono- and oligosaccharides have been previously reported.[187,188] Therefore in biologically active oligosaccharides, other conformers, such a $^1C_4$ or skew-boat, may exist. It may be the case that binding to a protein, or chemical reaction of a sugar may only occur through these other conformers, as reviewed by Mulloy and Forster.[189] Additionally, binding of a sugar residue to a protein may adjust or require adjustment of the conformation of the sugar, as discussed in a study investigating the effect of single molecule force microscopy on the conformations of heparin.[190]

1.2.9 Methods for accessing specific oligosaccharides

Generating a specific oligosaccharide through chemical synthesis is a difficult process. An efficient glycosyl donor system, and a well-tuned orthogonal protecting group strategy, must be employed. The synthesis of a specific oligosaccharide requires the selective formation of various anomeric linkages, as reviewed by Codée et all.[191] Orthogonal and semi-orthogonal protecting group strategies, with selective activation of leaving groups, are key to fast and efficient production of complex carbohydrates. Many groups have developed methods for reliable and convenient synthesis of such oligosaccharides, and these methods have been discussed at length in reviews by Kaeothip and Demchenko,[192] Wang and Demchenko,[193] and a review of chemical *O*-glycosylation reactions by Das and Mukhopadhyay.[169]

The protecting group strategy used by our group[194] includes the acetate (Ac), azide (N_3), benzoate (Bz), benzyl (Bn), chloroacetate (AcCl), 9-fluorenylmethyloxycarbonyl (Fmoc) and *p*-methoxyphenyl (PMP) groups (Figure 14). These groups are strategically placed to allow access to both glycosyl donors and acceptors from fully protected saccharides.

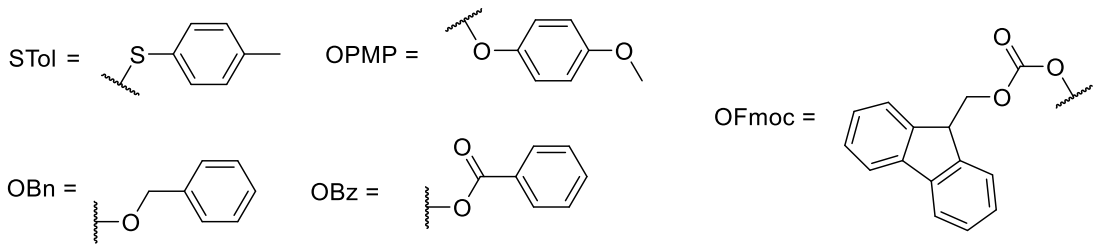

Figure 14 – Several of the protecting groups used in our orthogonal protecting group strategy. Additionally, well-known acetate (OAc) and azide (N_3) protecting groups are also used.

A variety of other orthogonal protecting groups, such as the (2-nitrophenyl)acetyl group,[195] the levulinoyl ester, and 1-naphthylmethyl ether groups,[196,197] have been used in oligosaccharide synthesis. These alternatives and others have been used in orthogonal protecting group strategies of several groups, as reviewed by Ágoston et al.[198] A specific example of the use of these protecting groups in the synthesis of HS-like oligosaccharides is in the previous work of the Reichardt group.[199] In this synthesis, a core trisaccharide structure is assembled using a short and high-yielding synthetic approach.

Some saccharides, such as uronic acids, have proven challenging to use in glycosylation reactions. Previous work in which a uronic acid has been used in a glycosylation features a uronic acid protected as an alkyl ester, such as the methyl or *tert*-butyl ester. Several groups have used a combination of electron-donating protecting groups at the 2-*O*- and 4-*O*- positions of a uronic acid,[200] or cyclic lactone protecting groups,[201] to 'arm' or 'disarm' the molecule for glycosylation reactions. Electron donating effects from these groups increase the stability of formed oxocarbenium ion, overcoming the electron withdrawing effects of the uronic acid group. The concept of 'armed/disarmed' glycosylation reaction partners was developed by Fraser-Reid.[202]

Concepts of 'armed/disarmed' glycosylation reaction partners have developed alongside the concept of matched and mismatched glycosyl donor-acceptor combinations.[203] It has been observed that the reactivity of the glycosyl donor and acceptor should be matched for a glycosylation to proceed. Significant differences in the reactivity of the two components can lead to poor glycosylation outcomes.

A recent development in this space is the theory of Reciprocal Donor Acceptor Selectivity (RADS) by Fraser-Reid.[204] This is an extension of the matched and mismatched donor concept towards regioselectivity. In this specific case, Fraser-Reid and co-workers reacted an acceptor diol with equivalent amounts of two different donors. A double differential glycosylation, the regioselective assembly of a single trisaccharide from four possible outcomes, was demonstrated.

The precise mechanism of RADS is poorly understood, but the theory uses principles of increased or decreased reactivity arising from electron donating or withdrawing protecting groups. RADS is used by various groups to explain differences in the regioselectivity of sugars in glycosylation reactions. Furthermore, this regioselectivity can be utilised to generate specific glycosylation products in the presence of multiple alcohols of differing nucleophilicity. In contrast, certain glycosyl donor and acceptor combinations are too mismatched for the reaction to proceed.[167,205] The impact of the relative reactivates of the two components of the glycosylation reaction has been well explored by Wong and co-workers,[206-210] with work ongoing in this area.[168]

Work continues to further develop glycosylation strategies, with different approaches. One approach is the use of temporary protecting groups generated immediately prior to, or during, glycosylation reactions. An example is a report of temporary *N*-acetyl glucosamine *N*-protection with methyl or ethyl triflate on an acceptor, allowing 4-*O* glycosylation (Scheme 7).[211] The temporary *N*-protection was readily removed under mild conditions (AcOH/Ac_2O at 55 °C) following glycosylation, yielding an *N*-acetyl glucosamine residue.

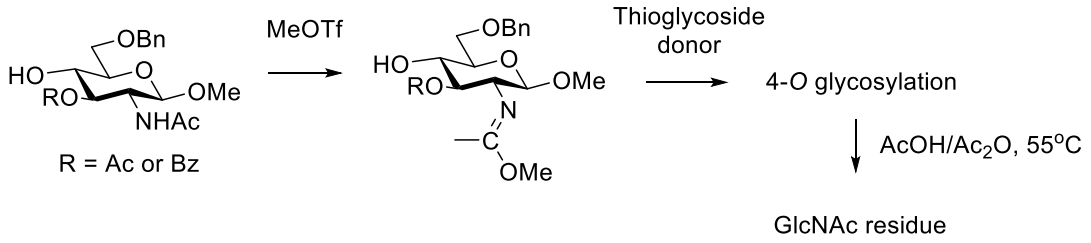

Scheme 7 – Temporary NHAc protection of a GlcNAc acceptor using MeOTf. In this report, a N-acetyl glucosamine acceptor is temporarily N-protected as an imidate using MeOTf, before the addition of a thioglycoside donor, leading to MeOTf-promoted glycosylation. The imidate protecting group is readily removed following glycosylation using mild conditions, returning the GlcNAc residue.[211]

The choice of glycosyl donor is often key to the outcome of a chemical glycosylation reaction. There are a variety of glycosyl donors used by different carbohydrate chemistry groups,[212] including trichloroacetimidates (TCA) used by our own group and others,[194,213,214] *N*-phenyl trifluoroacetimidates (*N*-PTFA),[215-217] thioglycosides also used by our group and others,[194,213,218-221] and glycosyl halides.[222,223]

The development of new glycosyl donors is a very active field of investigation, and glycosylation reactions using recent developments such as *O*-Box and *O*-Fox imidates,[224] thio-click chemistry approaches,[225] and gold-catalysed glycosylations using thioglycoside donors,[226] continue to be reported (Figure 15). Another alternative is a recent report of oxidative glycosylation with a glycosyl stannane donor, which requires a free hydroxyl group adjacent to the anomeric position.[227] While

interesting, this method requires the specific synthesis of a 2-hydroxy donor, and this group may require protection following glycosylation to be suitable for further synthetic steps.

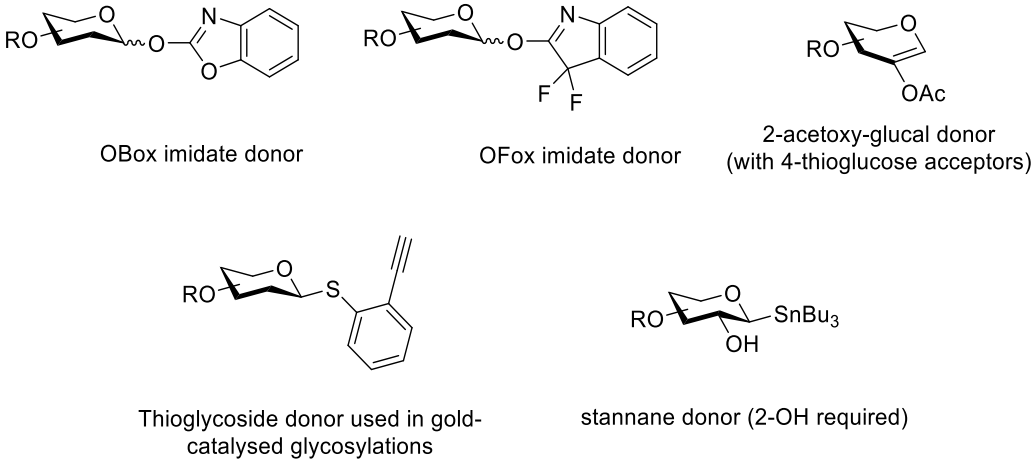

Figure 15 – Several recently reported glycosyl donor systems.
Each of these donors has been reported to perform well in glycosylation reactions.[224-227]

A further consideration is that various different glycosyl donors may undergo side reactions that can lead to the formation of undesired by-products, which must be removed during purification.[228,229] TCA donors are the one of the most common glycosyl donors used, but are susceptible to a specific side reaction in which the TCA donor rearranges to a more stable trichloroacetamide. This side reaction is often observed if the glycosyl donor is used in excess but can lead to reduced yields if the glycosyl acceptor is a poor nucleophile. The *N*-PTFA donor was developed to address this issue.[228,230] This donor is much less likely to rearrange to an acetamide form due to the presence of the *N*-phenyl group (Figure 16). The phenyl group is election withdrawing, which consequently reduces the nucleophilicity of the nitrogen and thus inhibits the formation of the acetamide.

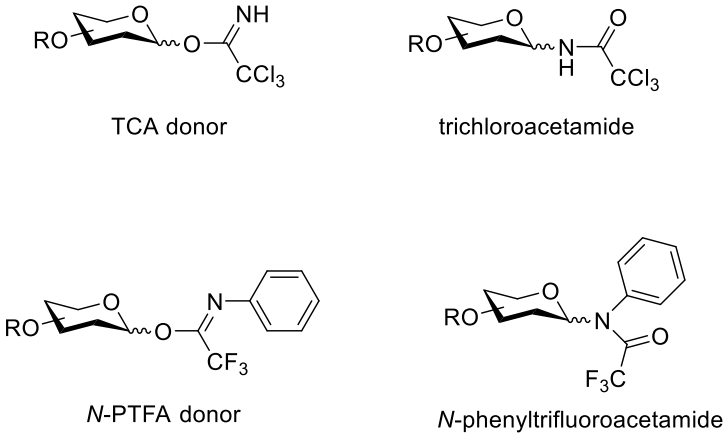

Figure 16 – Possible rearrangement by-products of TCA and N-PTFA donors.
TCA donor rearrangement is a common by-product of using these donors, whereas N-PTFA donor rearrangement is not generally observed.

The use of an orthogonal protecting group strategy allows selective access to specific sites on the oligosaccharide chain for further modification. In the synthesis of HS-related oligosaccharides, these modifications may include oxidation, and will include sulfation, post-chain assembly.[194] Other modifications to oligosaccharides, if desired, can be accomplished in a variety of ways, such as using Wittig reactions[231], Mitsunobu conditions to carry out regioselective monochlorination[232] or copper-catalysed *O*-arylation[233] to give recent examples. Compounds of interest that could be generated with these methods include glycopeptides, as demonstrated in a recent report of the successful synthesis of a complex, highly branched *N*-linked glycan.[234]

Using state-of-the-art glycosylation chemistry, many groups have reported the synthesis of specific, complex oligosaccharide target fragments by use of an orthogonal protecting group strategy.[180,214,235-244] Further development continues on other sugar systems beyond the commonly encountered glucose and idose, such as in the area of 2,6-dideoxy and 2,3,6-trideoxy sugars.[245] Significant progress has been made from early experiments in chemical oligosaccharide synthesis.[246]

1.2.10 The building block strategy

The design of a total synthesis of a HS mimetic sequence is not trivial. For large oligosaccharides, which are desirable targets, a significant multistep synthesis is required. Multistep synthesis of such large molecules is generally time-consuming, and features low overall yields, despite high yields from the individual steps if this is achievable. The length of the oligosaccharide chain required for effective HS mimetics, often at least hexasaccharide or above, mean that a linear sequence of single monosaccharide glycosylations is not economical for these reasons.[194] Also, glycosylation reactions in general have proven to be somewhat temperamental, and generating the correct stereochemistry at each linkage and the purification at each stage would also contribute to a difficult synthesis. Because of this, different strategies for oligosaccharide chain assembly have been reported.

The idea of a modular synthetic approach, in which the target oligosaccharide is assembled from closely related building blocks, has been detailed in a review by Codée, Overkleeft, van der Marel, and van Boeckel.[247] The terminology applied to the chemical assembly of oligosaccharide chains by the building block method is often described in terms of the length of sugar subunits which are glycosylated. For example, an iterative [n+1] synthesis would involve assembling a chain in single sugar increments, whereas a [n+2] synthesis would assemble a chain from disaccharide increments, [n+3] being a trisaccharide increment and [n+4] being a tetrasaccharide increment, and so on. There is much variability in the approach, and even for small chains, variations in the assembly strategy can improve results.[248]

The disaccharide repeating unit of HS sequences has become a convenient intermediate for synthetic chemists.[175,221,240,249-251] Quantities of a HS-like disaccharide subunit, which can later be glycosylated to produce longer oligosaccharides, can be quickly and easily assembled. The coupling of these disaccharide subunits in [n+2] glycosylation reactions to form the oligosaccharide chain is more efficient compared to an iterative [n+1] synthesis of the same oligosaccharide.

When considering HS-like disaccharide building blocks, there are two different approaches. These are generating a disaccharide building block with the uronic acid component monosaccharide at the reducing end, or with the glucosamine component monosaccharide at the reducing end (Figure 17). The two arrangements vary in both the stereochemistry between the monosaccharides, and the stereochemistry which is desired in the subsequent [n+2] glycosylation.

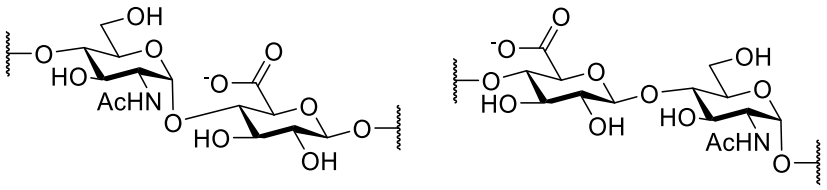

Figure 17 – The two possible HS-like disaccharide repeating unit structures. One approach is to have the uronic acid residue at the reducing end. The other approach is to have the glucosamine residue at the reducing end. Different groups have used each approach in the synthesis of HS mimetics.

Some groups choose to take the approach of having the glucosamine component at the reducing end. Often in this approach, azido protecting groups are used to mask the glucosamine amine, and high yields of the desired 1,2-*cis* linked glycosylation product are reported.[115,122] However, in our hands, these reactions do not appear to be stereospecific. Unwanted 1,2-*trans* linked products were observed, and these products do not follow the pattern of linkages required for a HS-like oligosaccharide. These side-products would be progressively harder to remove as the chain length increases and further reduce the yield of the specific desired product.

The other approach to is to use HS-like disaccharide building blocks with the uronic acid component at the reducing end. At the disaccharide stage, it is relatively easy to separate the two anomers of the glycosidic linkage between the two monosaccharides in the disaccharide subunit, which is of great convenience in forming the synthetically more challenging anomeric α-linkage, or 1,2-*cis* glycosidic bond.[177,214,252] Optimised conditions for our [1+1] glycosylation have been developed. Under these conditions little to none of the unwanted 1,2-*trans* product is observed, although any by-product can be readily separated by column chromatography.

Anomeric β-linkages, or 1,2-*trans* glycosidic bonds, are generally easily accessed by use of a participating acyl or benzoyl group at the 2-*O* position of the glycosyl donor, as previously discussed.[177] Previously a benzoyl protecting group has been utilised at the 2-*O* position of the uronic acid residue (although oxidation does not take place until following oligosaccharide chain assembly) to generate a selective 1,2-*trans* glycosidic bond in the subsequent [n+2] glycosylation reactions (Scheme 8). This disaccharide building block strategy has been employed in previous HS sequence synthesis by our group and others, of hexa- to dodecasaccharide in length, and will be employed in this work.[194,213,253]

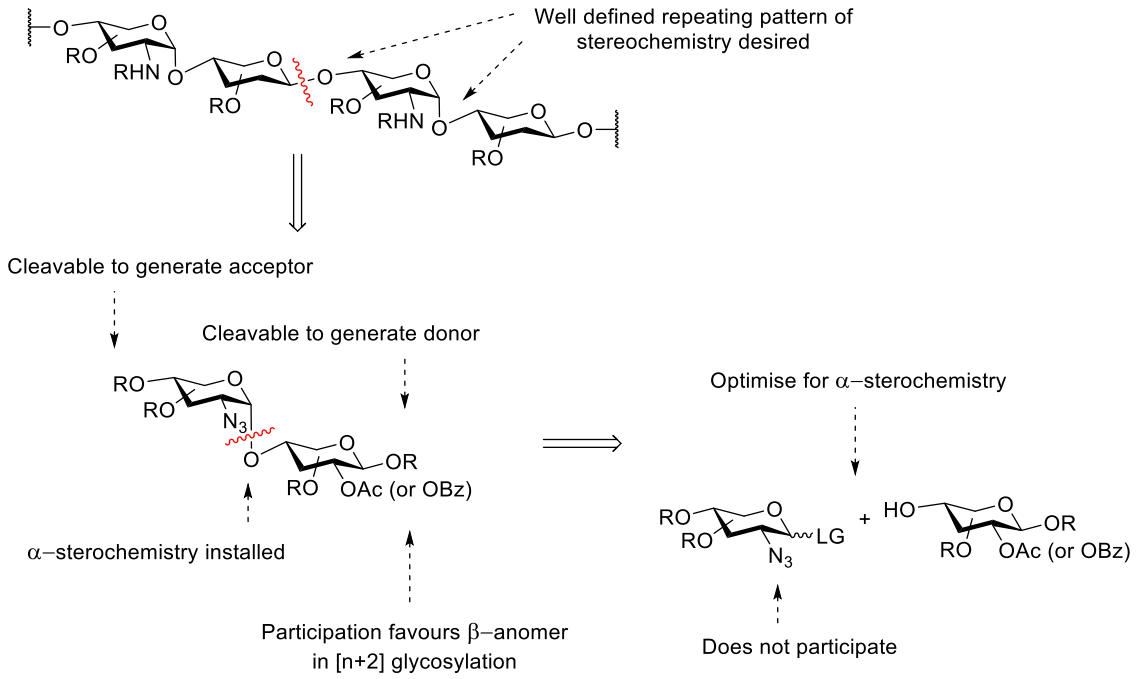

Scheme 8 - A retrosynthetic representation of a disaccharide building block pathway to produce oligosaccharides with a defined, repeating stereochemical pattern. Optimising a [1+1] glycosylation for α-stereochemistry and purifying the product is relatively easy and installs this stereochemistry early. Later disaccharide coupling steps can use participating OAc or OBz protecting groups at the 2-O position of the glycosyl donor to generate selective β-linkages. Using orthogonal protecting groups allows access to both donor and acceptor disaccharides from the same molecule.[194]

Other groups have reported success in making large branched oligosaccharides using a building block approach, such as in a report of a hexasaccharide produced by a [3+3] or a [4+2] glycosylation.[180] Despite the difficulty in synthesis of well-defined oligosaccharides greater than 10mer in length, methodology has been reported that allows the chemical assembly of much longer, specific sequences of up to 40mer in length.[238] The process makes use of a tetrasaccharide building block and [n+4] glycosylation reactions, in much the same way as the previously described disaccharide building blocks.[239] Tetrasaccharide building blocks might well be suitable for the synthesis of larger molecules, but are more expensive (in both time and resources) to produce, and the need for excess glycosyl donor equivalents means significant quantities are necessary. Even larger well-defined

polysaccharides, though not sulfated, have been reported in the literature, such as the successful synthesis of a 92-mer oligosaccharide by Wu and co-workers.[254] This synthesis notably features multiple, pre-activation based, six-component, one-pot glycosylation reactions to generate hexasaccharide building blocks. The final step is an impressive [31+31+30] double glycosylation. Chemical synthesis can deliver quantities of large, well-defined HS sequences and mimetics, but this remains a resource and time expensive endeavour.

1.2.11 Recent efforts towards HS-like oligosaccharides

Our group has previously completed the synthesis of a library of HS-like oligosaccharide compounds. Several compounds in this library of targets have proven effective as selective inhibitors of BACE1 (Figure 18).[194] The methodology developed for the synthesis of these compounds was used as the starting point for the synthetic strategy that will be reported in subsequent chapters of this work.

The structures of mono-, di- and oligosaccharides presented in relation to this synthesis specifically will be shown using the Haworth representation. This drawing method greatly simplifies the representation of residues which may be either glucuronic or iduronic acids, of which there are several in the following targets. This also aligns with the representation of structures used in the publication itself.

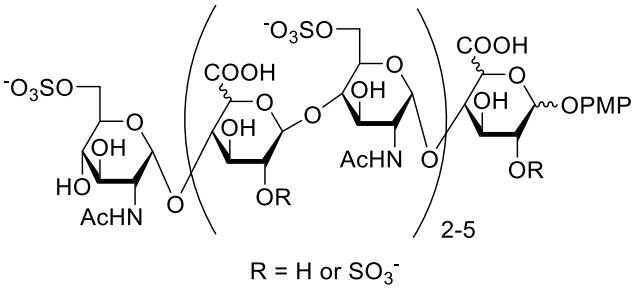

Figure 18 - A library of HS-like hexa- to dodecasaccharides targeted at BACE1 inhibition. Synthesis of these 16 targets was accomplished and several proved to be potent, non-anticoagulant BACE1 inhibitors.[194]

Synthesis of these targets was carried out using the disaccharide building block strategy discussed in the previous section. To access suitable disaccharide donors and acceptors, orthogonally protected monosaccharides were synthesised from starting materials available in our laboratory (Scheme 9). Methyl 2-azido-2-deoxy-1-thio-β-D-glucopyranoside was used as a starting point for glycosyl donor synthesis. Glucose monosaccharide acceptors were accessed from commercially available 1,2:5,6-di-*O*-isopropylidene-α-D-glucofuranose. Idose monosaccharide acceptors were also accessed from this material, using the synthetic method shown in Scheme 1 (Section 1.2.7). Yields for all reactions were good, in the range of 60 – 80%.

Orthogonal protecting groups, including some of those described in the previous section, are installed on the monosaccharides. This allows later access to specific positions on the eventual oligosaccharide for modification.

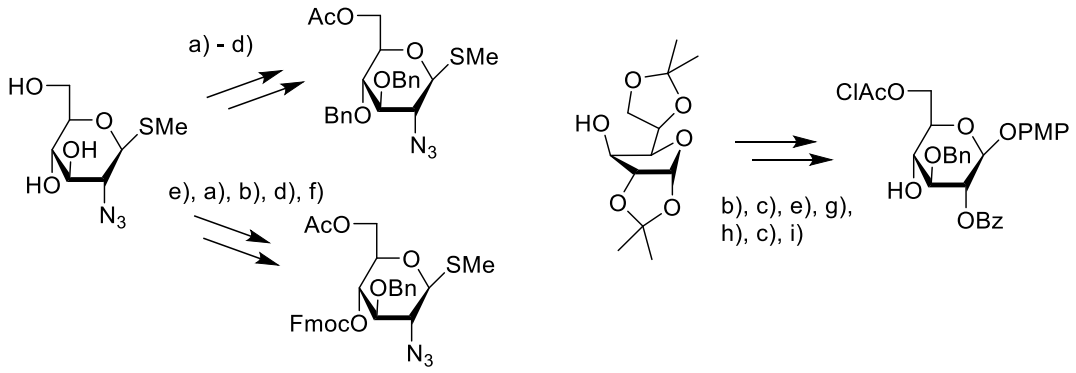

a) TrCl, py; b) BnBr, NaH, DMF, RT; c) aq. HOAc, 80 °C; d) Ac_2O, py;
e) $PhCH(OMe)_2$, TsOH, DMF, 60 °C; f) FmocCl, py;
g) BzCl, py, DCM; h) p-methoxyphenol, $BF_3.Et_2O$; i) ClAcCl, py, DCM, -78 °C

Scheme 9 – Previously established synthesis of monosaccharide acceptors and donors.

From these orthogonally protected monosaccharides, disaccharide building blocks were produced (Scheme 10). Highly optimised glycosylation reaction conditions, using SMe donors, were used to afford almost exclusively the 1,2-*cis* linked (α-linked) disaccharide product in 80-90% yields.

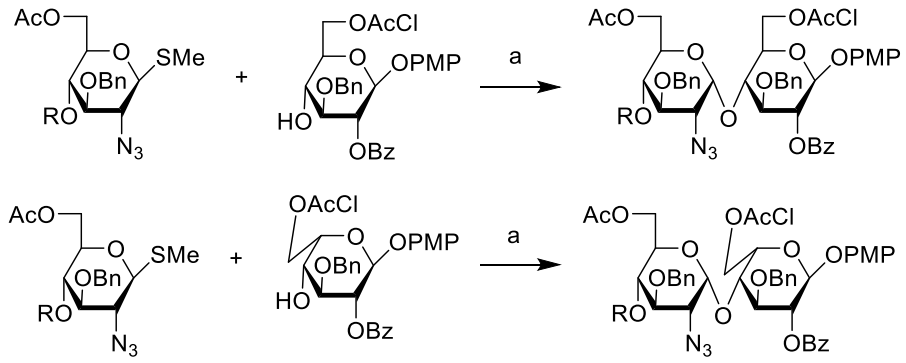

R = Fmoc or Bn, a) NIS, AgOTf, toluene, DCM, -15 °C

Scheme 10 – Previously established synthesis of disaccharide building blocks.

From these disaccharides, both glycosyl donors and acceptors could be synthesised (Scheme 11). The p-methoxyphenyl group may be selectively deprotected using cerium ammonium nitrate (CAN) to expose the hemiacetal, which can be further reacted to a trichloroacetimidate glycosyl donor using trichloroacetonitile and NaH. Separately, the Fmoc group at the non-reducing end of the dissachairde may be selectively deprotected using basic conditions to synthesise a disaccharide glycosyl acceptor. Yields varied from 80-90%.

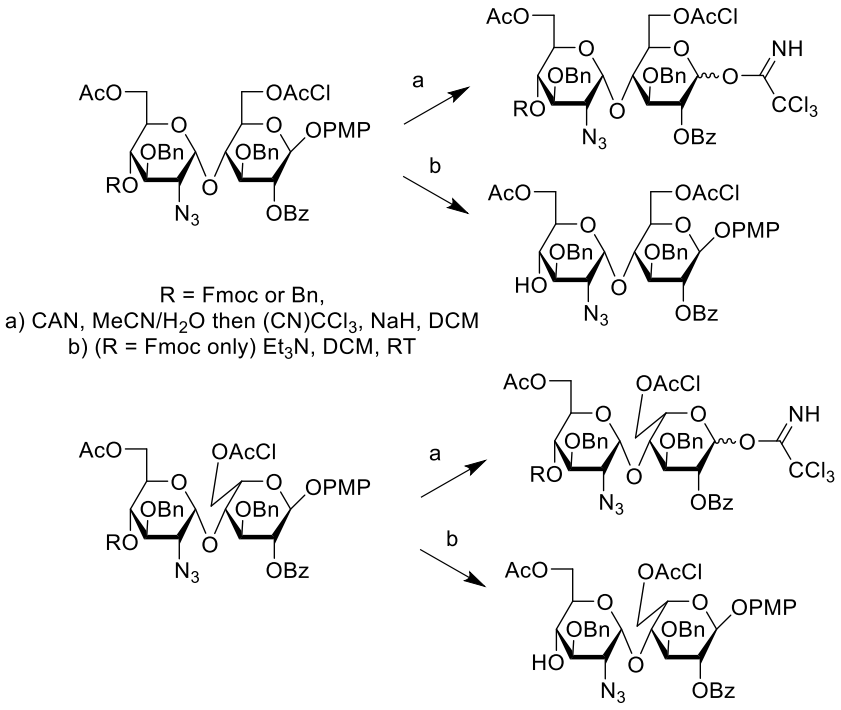

Scheme 11 – Previously established synthesis of disaccharide building blocks for oligosaccharide chain assembly.

These disaccharide building blocks could then be assembled into oligosaccharide chains (Scheme 12). The glycosylation of a donor and acceptor disaccharide, using TMSOTf as a promoter, produces a tetrasaccharide. This tetrasaccharide can then be selectively Fmoc-deprotected to expose the non-reducing end, becoming the acceptor for the following glycosylation reaction. Yields for the glycosylation reaction raged from 70-90%, and Fmoc deprotection yields ranged from 70-80%. Using several cycles of chain extension and deprotection, and either gluco- or ido-containing disaccharides, a library of fully protected oligosaccharides was synthesised.

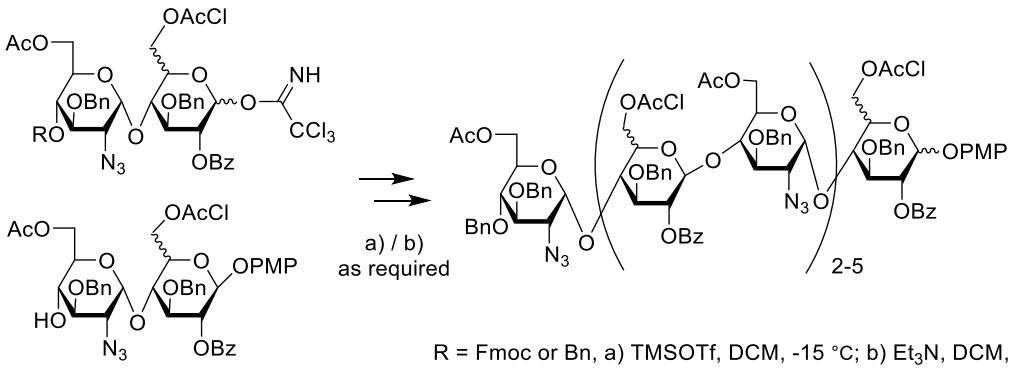

Scheme 12 – Synthesis of a library of fully protected octasaccharides.
By varying the starting acceptor and the donor used, many oligosaccharides with different configurations were produced.

Finally, the fully protected oligosaccharides were processed through a series of deprotections and sulfations to yield the final HS-like sulfated oligosaccharide targets shown in Figure 18. First, the chloroacetate groups were selectively removed by treatment with DABCO. The exposed positions were oxidised using TEMO-BAIB and the methyl ester is formed using diazomethane. Subsequently, the azide groups were transformed to N-acetylated amine groups with thioacetate.

Following these modifications, the primary acetate groups were removed under acidic conditions. These positions were then sulfated. The next step was saponification to remove the benzoyl protecting groups. At this point, the synthesis diverged depending on if the 2-*O* positions were then sulfated or remained unmodified. A final global debenzylation using reductive conditions yielded the desired HS-like oligosaccharide targets (Figure 18). Yields across the processing steps ranged from 60-90%.

Other groups have also carried out work in this area. A recent publication by the Boons group[255] details the synthesis of HS-like hexasaccharides with varying sulfation patterns. An example of the hexasaccharide structures produced, in both fully protected and sulfated/deprotected forms, is shown in Scheme 13. It is noted that from this point, compounds will once again be drawn using the chair representation. Processing of the fully protected hexasaccharides is conducted in a similar manner, in which sites are accessed in a sequence by removal of orthogonal protecting groups.

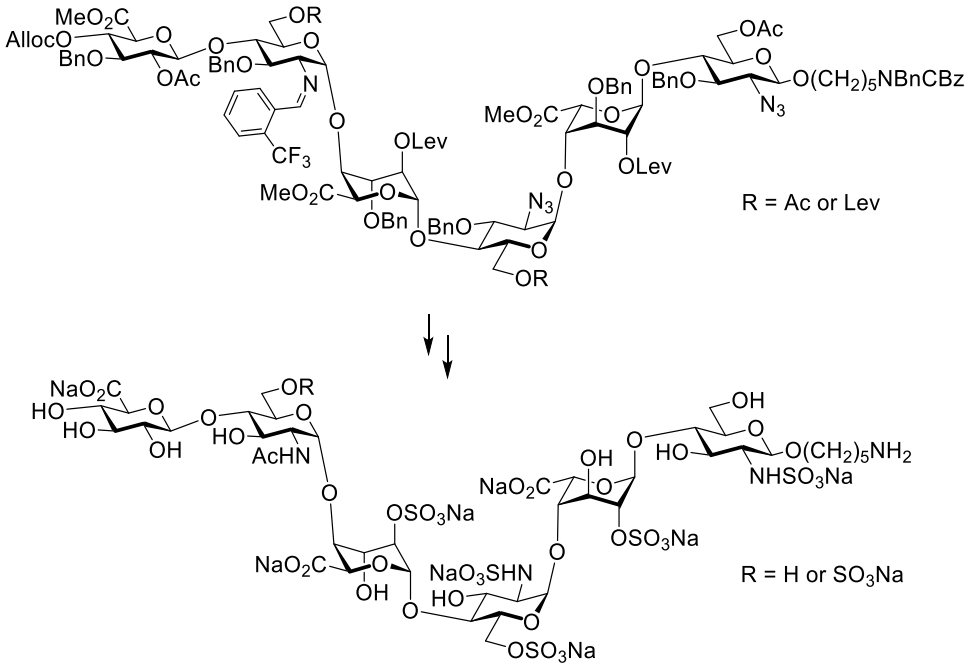

Scheme 13 – An example of the HS-like hexasaccharides synthesised by the Boons group.

This synthesis notably features the trifluoromethylphenyl-methanimine moiety at a 2-*O* position, which allows selective access for later *N*-acetylation. This synthetic route also used a disaccharide building block strategy (Figure 19), and features the alternative orthogonal hydroxyl protecting groups levulinic (Lev) ester, thexyldimethylsilyl (TDS) ether, and allyloxycarbonate (Alloc). Furthermore, an *N*-phenyl trifluoroacetimidate glycosyl donor was used. This method features the glucosamine residue at the reducing end of the disaccharide building block and forms a 1,2-*cis* linkage between building blocks. This contrasts with our approach, in which a 1,2-*trans* linkage is formed selectively with the expected participation of a 2-*O*-acetyl or benzoyl group.

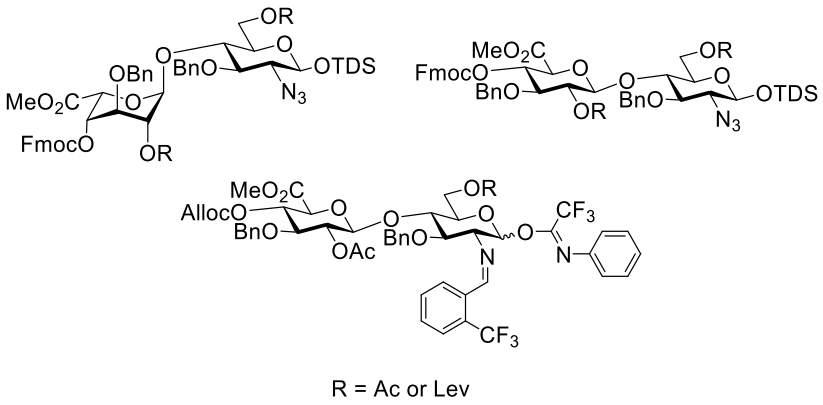

Figure 19 – Modular building blocks used by the Boons group in the synthesis of HS-like hexasaccharides.

Although the details of the approach differ, the overall synthetic strategy is like that previously used by our group. These two examples are representative of the conventional state-of-the-art methods used to access HS-like oligosaccharides.

1.2.12 Solid phase synthesis and automation – methods of the future?

Solid-phase oligosaccharide synthesis is a rapidly developing space. An automated, solid-phase approach similar to that of polypeptide and polynucleotide synthesis has been developed and described for polysaccharides. Prominent work in this field in relation to HS-like oligosaccharides has been carried out by Seeberger and co-workers,[256-260] leading to the development of the Glyconeer® instrument. The Reichardt group has also carried out work in this area.[261,262] Furthermore, Codée and coworkers report several oligosaccharide syntheses via an automated route.[263,264]

In this method, a small saccharide starting unit is affixed to a solid resin, often polystyrene, using a cleavable linker. Deprotection and chain extension steps are then carried out in an alternating manner by washing the support with the appropriate mixture of reactants and reagents, with the deprotection being orthogonal to the linker cleavage. The assembled oligosaccharide can then be conveniently

purified with further washes and cleaved from the resin.[265] A schematic of this strategy using the Glyconeer® instrument is illustrated below (Scheme 14).

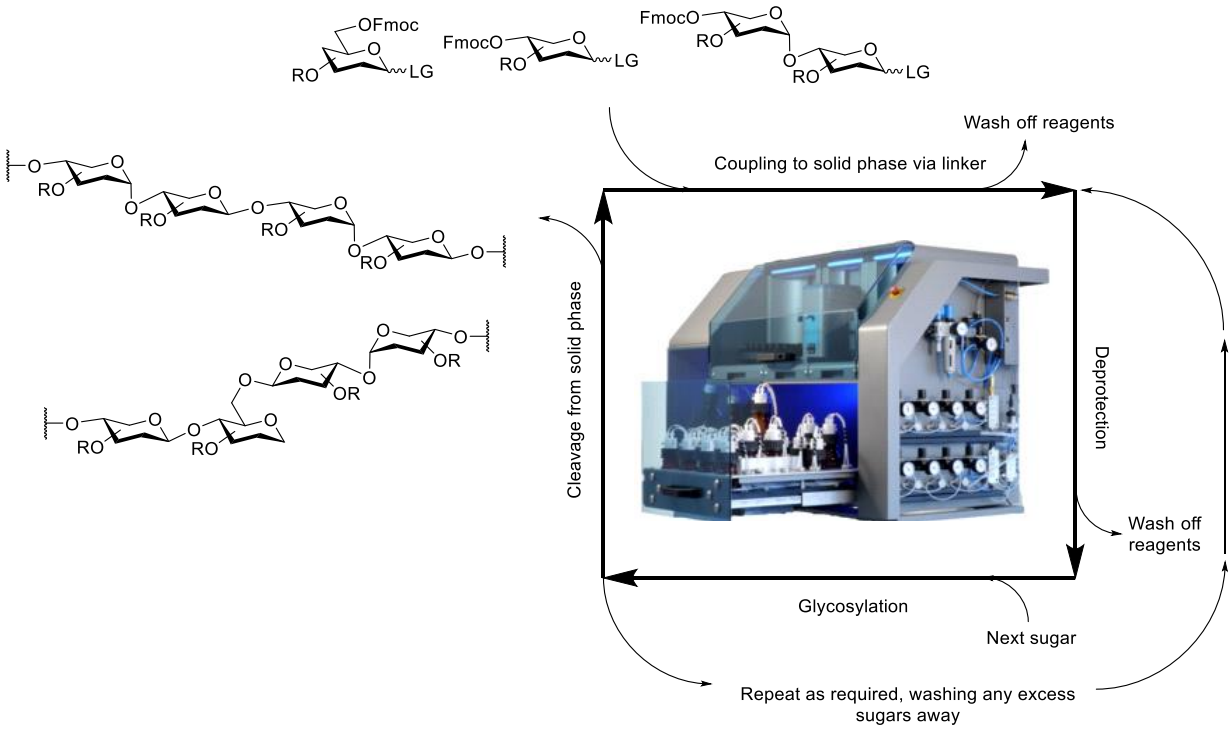

Scheme 14 - A map of the cycle of oligosaccharide synthesis using a Glyconeer® instrument. In this example, mono- and disaccharide building blocks use the UV-detectable Fmoc protecting group. A sugar is first coupled to the solid phase via linker, and then deprotected and further reacted with another sugar to extend the chain. Cycles of deprotection and glycosylation continue until the product is formed, at which point linker cleavage occurs and the oligosaccharide is recovered.[265]

This strategy has the advantage of easy removal of reagents between extensions and deprotection, as they are simply washed away, and the potential for automation of said washes would make the assembly process quite time efficient.

Polypeptides are linearly linked by the formation of amide bonds and polynucelotides are linearly linked by the formation of phosphate diester bonds. Both biopolymers lend themselves well to synthesis by the automated solid phase method, and this is how these molecules are generally synthesised in the laboratory setting. There are no stereoselective requirements for the bonds formed between monomers in either of these biopolymers, and the coupling reactions themselves have been optimised to be high yielding.

In contrast, conventional *O*-linked oligosaccharides are assembled by glycosylation reactions, the S_N1-like mechanism of which has been discussed previously. These couplings are known to give quite variable yields, depending on the system in question, and two possible stereochemical outcomes. Overcoming these challenges might require unconventional saccharide coupling methods, such as

those reported by Revuelta and colleagues,[160] in which monosaccharides are functionalised with amino acids and coupled by amide bonds. Coupling methods such as these could prove useful in overcoming the difficulty of synthesising oligosaccharides by an automated route. However, these methods introduce structural changes to the oligosaccharide backbone that might impact the functionality of the final products.

There are also significant regioselective requirements for the synthesis of oligosaccharides, due to the much greater number of potential glycosylation sites, and so a protecting group strategy and stereospecific glycosylation methods are required. Furthermore, the inability to analyse the growing chain at each step leads to a need for high coupling yields, along with a high level of regio- and stereo-control. Errors in the assembly will be carried forward and only realised once the oligosaccharide is cleaved from the resin, isolated and characterised.

This method is extremely promising for the synthesis of oligosaccharide chains, but has current limitations - it encounters aforementioned issues with controlling the stereochemistry of the product, on which development continues, and the quantities of oligosaccharide capable of being synthesised.[166,167] As previously discussed, the stereochemical outcomes of glycosylation reactions used to assemble to the chain will vary with solvent, temperature, and the protecting group strategy, and this needs to be optimised for every new reaction. Chemical transformations, such as oxidation and sulfation, that may be required after oligosaccharide chain assembly to produce a HS sequence such as our own targets are nontrivial and require a significant quantity of oligosaccharide material to be produced. This is not generally a quantity that is easily produced on a solid support, and would require even larger excesses of building blocks, given that such systems often make use of 10 equivalents or more of building block donor per chain extension. The synthesis of these building blocks may itself be time consuming and expensive depending on the functionality and protecting group strategy required.

During our group's own experience with the Glyconeer® instrument, through a collaboration with the University of York, it proved particularly challenging to couple a basic disaccharide unit featuring our orthogonal protecting group strategy to the resin. Further challenges were found in the assembly of oligosaccharides longer than hexasaccharide, and the hexasaccharides themselves required significant quantities of precursor disaccharide reagents to assemble.[266]

Therefore, the coupling of sugars to a resin, the first step of automated oligosaccharide synthesis, may also need to be modified for each reaction. Different linker designs and coupling chemistry could be considered. Linker design remains an active area of research,[267] moving beyond established methods used in polypeptide and oligonucleotide synthesis. One recent advance is the use of geminal

difluorines placed adjacent to the acceptor hydroxyl group in a photocleavable linker (Figure 20). This design is shown to promote exclusive 1,2-cis linkage to the sugar without affecting subsequent immobilisation.[268]

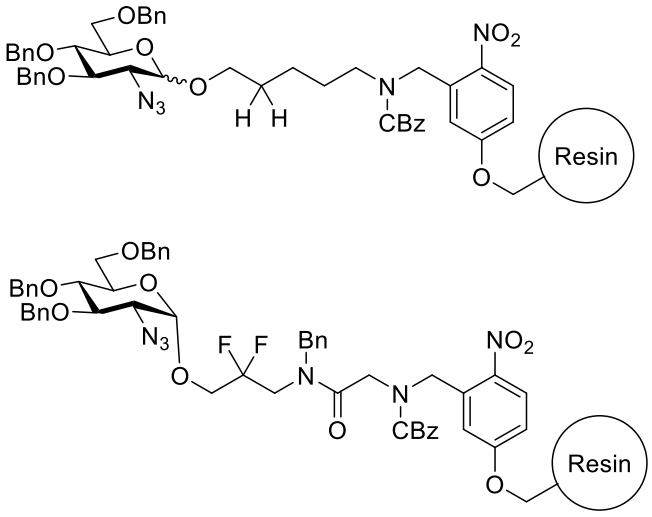

Figure 20 – Differing linker designs used when coupling sugars to a solid support. In this report, modification of the linker to include geminal difluorines was able to induce a stereoselective outcome when coupled with the same monosaccharide thioglycoside.[268]

Other types of automated oligosaccharide synthesis have been investigated. Automated solution-phase synthesis in a batch reactor has been reported by Saliba, Pohl and co-workers, by adapting their manual glycosylation procedure to automated use, combined with fluorous solid-phase extraction.[269] Furthermore, continuous flow reaction systems, which are a developing area, have been developed to produce semi-protected building blocks from levoglucosan, which are accessed more quickly and efficiently, and can then be used in further synthesis.[270,271] However, these methods also suffer from similar limitations in scope and scale.

Progress in this area may in the future lead to a reliable, automated synthetic route to well-defined polysaccharide chains with complex functionality, but at present such synthesis remains the task of the synthetic organic chemist, and the humble round bottom flask.

1.3 Research aims

As discussed, the synthesis of heparan sulfate mimetics with a specific sulfation pattern is difficult, but highly desirable. This work is intended to establish effective routes to mimetic targets of interest, by investigation of some of the challenges presented by such a synthesis.

One of the challenges in heparan sulfate mimetic synthesis is the incorporation of uronic acids. Using uronic acid building blocks in the oligosaccharide chain assembly would be more efficient, but these molecules are thought to give poorer glycosylation results.[250,272] Oxidation following chain assembly, meanwhile, might give better glycosylation yields, but adds extra steps to oligosaccharide processing following the chain assembly. Therefore, initially investigations will focus on the effect of uronic acids and their hexose equivalents on glycosylation outcome, using comparable [2+2] glycosylation reactions. Both hexose and uronate disaccharide acceptors and donors will be assessed. The disaccharides will feature our orthogonal protecting group strategy, allowing access to each analogue of the molecule from a single starting material. Several varieties of donor will be tested, and the results will inform the synthetic strategy used for later oligosaccharide assembly.

Another challenge is the design of an orthogonal and robust protecting group strategy to give selective access to sites for sulfation, whilst giving good glycosylation yields and the formation of the correct stereochemistry at the anomeric position. Glucosamine 3-*O*-sulfation, which is less often observed in nature, has been identified by our collaborator, Prof. Turnbull of the University of Liverpool, as a modification of interest in the development of an effective mediator of FGF2-FGFR1 binding. In this work, the 2-(acetoxymethyl)benzoate (AMB) protecting group[273,274] will be used for glucosamine 3-*O* protection in our disaccharide building blocks, which will then allow selective access to the glucosamine 3-*O* position for sulfation. The AMB groups features a primary acetate, which, when removed, triggers a favourable ring closure leading to deprotection. This occurs at the same time as glucosamine 6-*O*-deprotection of Ac and sulfation, and iduronic acid 2-*O*-deprotection of AMB and sulfation, elsewhere in the oligosaccharide. All these locations feature primary acetates, which are more reactive than secondary acetates, and primary and secondary benzoates, and therefore can be selectively deprotected in the presence of other protecting groups in the oligosaccharide.

This work encompasses progress towards the total chemical synthesis of two selectively sulfated octasaccharide targets **1** and **2**, which are heparan sulfate mimetics (Figure 21). The structure of the targets has been designed in collaboration with Professor Jeremy Turnbull and his group at the University of Liverpool. Prof. Turnbull leads a group with world-leading expertise in HS biology. Specifically, these HS mimetic structures are predicted by Prof. Turnbull's research to mediate FGF2 interaction with its FGFR1 receptor.[275]

These targets have been designed to allow investigation of the relationship between the sulfation pattern of heparan sulfate mimetics and their biological function. Separate synthesis by colleagues will provide the equivalent octasaccharides that lack glucosamine 3-*O*-sulfation for comparison in eventual testing. The variance of glucosamine 6-*O*-sulfation and iduronic acid 2-*O*-sulfation between the two targets will provide further insight into the importance of these modifications. The structure of the targets, with a highly sulfated core region bordered on both sides by a non-sulfated region, is reminiscent of natural HS, which as previously discussed features short NS domains surrounded by NA domains.

This work is part of a broader collaborative effort between this research group and the Turnbull group, which seeks to address two problems discussed in the previous section: the general lack of understanding of which HS sequences regulate a biological process, and the difficulty in synthesising such well-defined sequences. With the combination of the Turnbull group's HS biology expertise and the synthetic ability of our own group, it is anticipated that great progress can be made in this area. Previous research from the Turnbull group identified structures of interest that have been synthesised by our group and assessed to have potent BACE1 inhibitory effects, demonstrating the potential of this combined approach.[93,194]

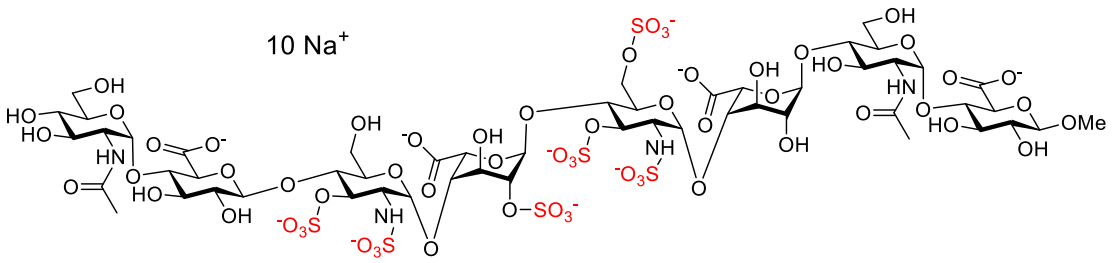

1

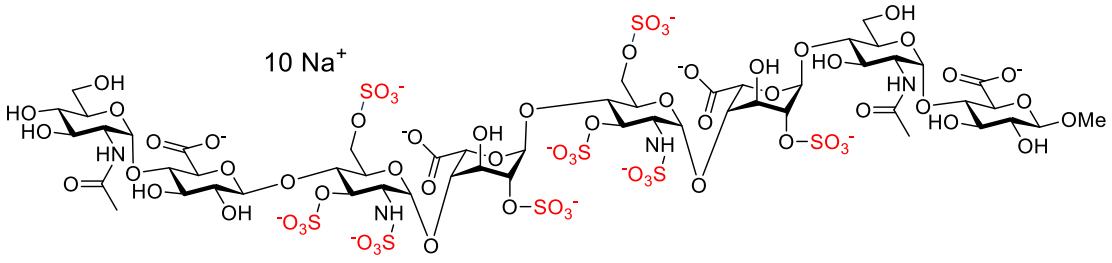

2

Figure 21 - The two sulfated octasaccharide targets, which are heparan sulfate mimetics. Sulfate groups are highlighted in red.

To access targets **1** and **2**, two fully protected octasaccharides **3** and **4** will be synthesised (Figure 22). These octasaccharides have the necessary orthogonal protecting groups, based on the slight modification of our existing strategy with the AMB group, to allow the production of **1** and **2** by a series of selective deprotections, oxidation, and sulfations. Establishing selective access to the glucosamine 3-*O*-position and iduronic acid 2-*O* position by use of the AMB group would set a valuable precedent for accessing this position in routes to other oligosaccharides of interest.

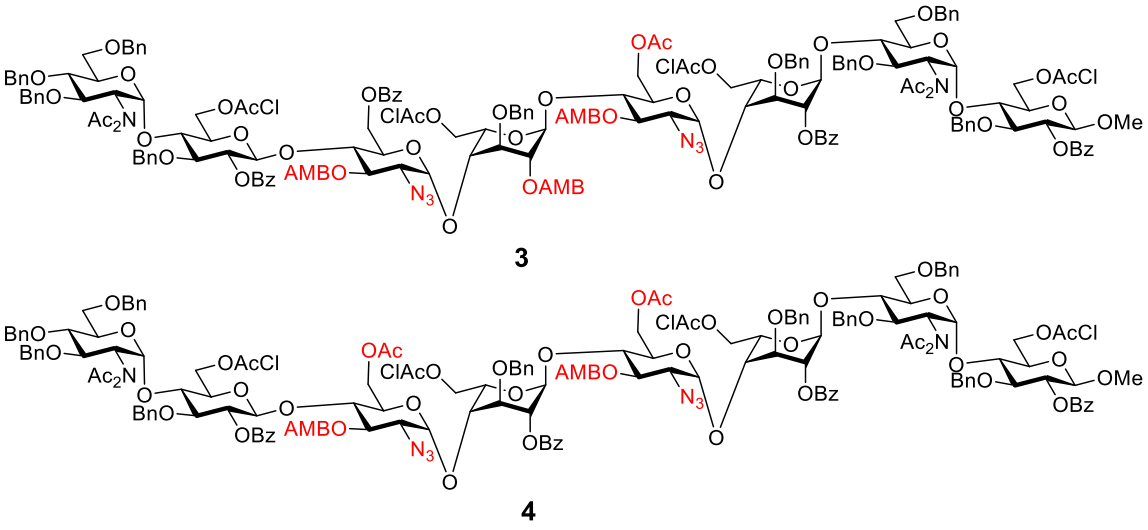

*Figure 22 - Fully protected octasaccharides required to access the sulfated targets **1** and **2**. Protecting groups in locations that will become sulfated are highlighted in red.*

The octasaccharides themselves will be assembled using a [n+2] disaccharide building block strategy, with the disaccharides **5**, **6**, **7** and **8** required (Figure 23). The merits of the disaccharide building block method have been discussed earlier, and in our case represent a means to install the challenging 1,2-*cis* (α-linkage) stereochemistry early in the synthesis. Octasaccharide **3** will be assembled with one unit each of disaccharide **6** and **7**, whereas octasaccharide **4** will utilise two units of disaccharide **6**. Disaccharides **5** and **8** are common to both targets.

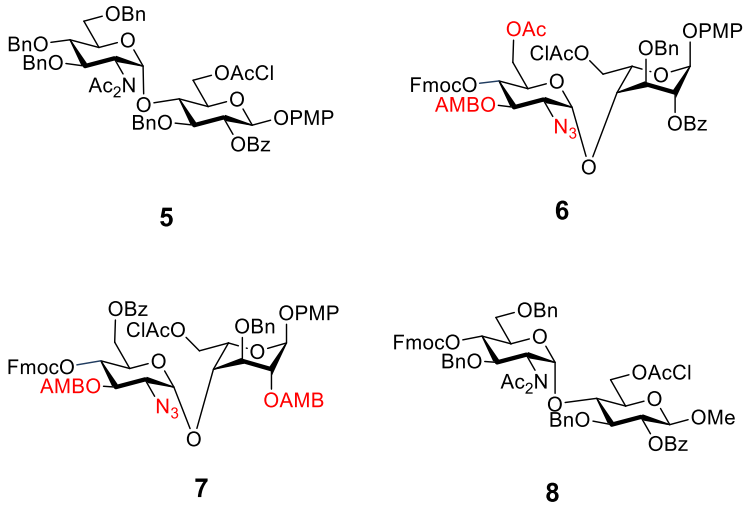

*Figure 23 - The four disaccharide units required for chain assembly. These disaccharides will be glycosylated to form the fully protected octasaccharide targets **3** (using one each of disaccharide **6** and **7**) and **4** (using two equivalents of disaccharide **7**). Protecting groups in locations that will become sulfated are highlighted in red. **5-7** will be selectively PMP-deprotected and transformed to form donors for glycosylation.*

Depending on the results of our investigation into the incorporation of uronic acids into an oligosaccharide, it might be possible to produce disaccharides **5**-**8** directly as their uronic acid counterparts. This would take the form of methyl-ester protected iduronic or glucuronic acid residues at the reducing end of each disaccharide, rather than the existing idose and glucose residues with a 6-*O*-chloroacetate protecting group. The uronic acid versions of disaccharides **5**-**8** would feature the same protecting group strategy at all other positions. This would improve the synthesis by removing a step from the post assembly processing of precious octasaccharides.

There are two approaches to access the uronic acid counterparts of disaccharides **5**-**8**. The first is assembling our disaccharide building blocks with a suitably protected uronic acid monosaccharide acceptor. However, the [1+1] glycosylation to produce the disaccharide building blocks, which would then use monosaccharide uronic acid acceptors, could be more challenging and may give a poorer stereochemical outcome of the glycosylation. Another approach would be to assemble disaccharides **5**-**8** as planned, and then selectively deprotect the glucose and idose 6-*O*-chloroacetate protecting groups and oxidise the disaccharides before oligosaccharide assembly. This mirrors our plan to access uronic acid variations of donors and acceptors for comparative glycosylation reactions. However, using this method may then make the subsequent [n+2] chain assembly for challenging.

2. Chapter 2

2.1 Comparison of hexose and uronate disaccharides in glycosylation reactions

One of the challenges in the synthesis of single entity HS mimetic sequences is the incorporation of uronic acids. As previously mentioned, uronic acids are commonly known to act as relatively poor glycosyl donors and acceptors, when compared to their hexose counterparts.[250,272] It is thought that this is due in part to the strong inductive effect of the carboxylic acid ester group. The presence of this group on the sugar ring destabilises the formation of positive charge elsewhere in the uronic acid residue, such as the charge present when an oxocarbenium ion is generated (Figure 24). Similar inductive effects also may weaken the nucleophilicity of hydroxyl groups on the uronic acid ring, contributing to reduced acceptor reactivity.[276,277]

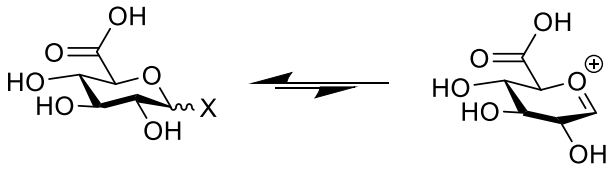

Figure 24 - A simple electronic rationalisation of the lowered glycosyl donor reactivity of uronic acids. The label X represents a leaving group. The inductive draw of the carboxylic acid affects reactivity by disfavouring the formation of an oxocarbenium ion. [199,200]

The ability to use uronic acids directly in a glycosylation, in good yield, would be of immense benefit to the complex synthetic process of producing novel HS-like compounds. In some synthetic routes, glycosylation reactions are carried out with 6-*O*-protected hexose derivatives, which are subsequently selectively 6-*O*-deprotected and oxidised in further steps.[272,278] This is less efficient than glycosylating the acids directly.[276] In contrast, the syntheses of effective uronate donor systems has been reported.[279] Several groups have carried out the synthesis of oligosaccharides using uronic acids as glycosyl donors and acceptors, with various leaving and protecting group combinations.[240,249,280]

However, unpublished attempts to use uronic acids directly in oligosaccharide assembly in our group have been met with limited success. Glycosylation reactions were attempted using our standard protecting group strategy and trichloroacetimidate donors. In these experiments, glycosylation reactions using uronate donors and acceptors generated an unexpected mixture of anomers of the product oligosaccharide. The uronic acid used as a glycosyl donor featured a participating benzoate group at the 2-*O*-position, and so would be expected to yield only the 1,2-*trans* (β-linked) product.

This work seeks to compare several currently used glycosylation strategies when applied to both hexoses and uronic acids. The efficiencies of both hexose and uronic acid analogues of several glycosyl donors will be compared. For this investigation, the disaccharide **9** was designed with a system of orthogonal protecting groups. Derivatisation of **9** allows access to both hexose and uronic acid analogues. Further derivatisation of each analogue allows access to different glycosyl donors and acceptors.[177,194] Our protecting group strategy is well established for later transformations following oligosaccharide chain assembly, based on previous efforts.[194] Therefore, this work will only investigate different glycosyl donors. This protecting group strategy will then be used, with slight modification, in the synthesis of octasaccharides **3** and **4** in the following chapters.

The synthesis of disaccharide **9** requires the monosaccharide glycosyl donor **10** and acceptor **11**.[194] These will be synthesised using the starting materials thioglycoside **12**, which was bought commercially, and *p*-methoxyphenyl glycoside **13**, which was available in our laboratory from previous projects (Scheme 15). Monosaccharides **12** and **13** could be accessed from the simple, commercially available starting materials D-glucosamine hydrochloride and 1,2:5,6-di-*O*-isopropylidene-α-D-glucofuranose respectively, if required, using literature methods.[162,281]

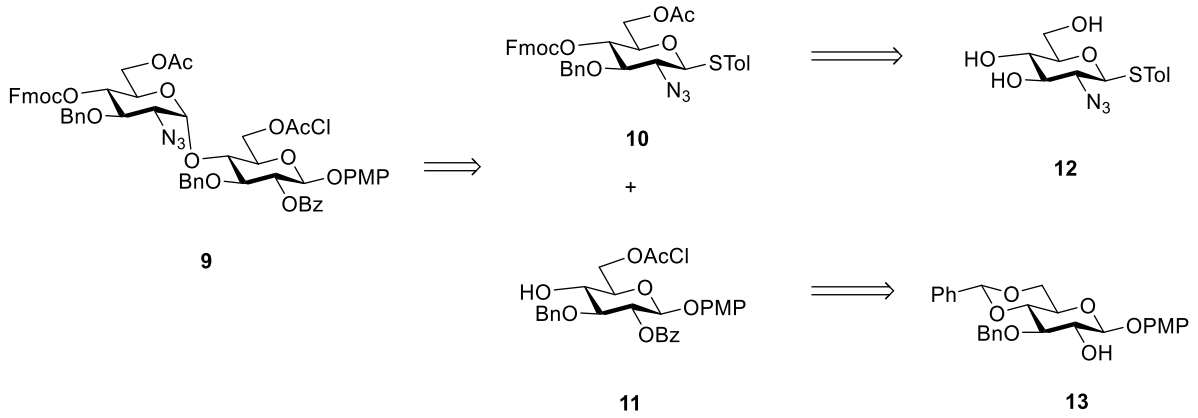

*Scheme 15 - A retrosynthetic analysis of the requirements for disaccharide **9.** This can be produced by glycosylation of monosaccharides **10** and **11**. Starting materials **12** and **13** are available in our laboratory from previous projects and will be used to begin the synthesis.*

Disaccharide **9** can then undergo selective 6-*O*-chloroacetate removal on the reducing end residue, and subsequently be oxidised to a glucuronic acid. Hemiacetals of the hexose and uronate analogues may be generated by selective 1-*O*-PMP hydrolysis using ceric ammonium nitrate (CAN). Further derivatisation of the hemiacetals would yield both hexose and uronate analogues of glycosyl donors. Separately, glycosyl acceptors can be produced from disaccharide **9**. In the hexose analogue, a glycosyl acceptor is accessed by selective removal of the 4-*O*-Fmoc protecting group from the non-reducing end. In the uronic acid analogue, both the 4-*O*-Fmoc from the non-reducing end and the 6-*O*-chloroacetate group from the reducing end residue are removed in one step. Subsequent selective

oxidation of the primary hydroxyl group on the reducing end residue gives access to the uronate acceptor. These donors and acceptors can then be glycosylated to synthesise tetrasaccharides **14** and **15** (Scheme 16).

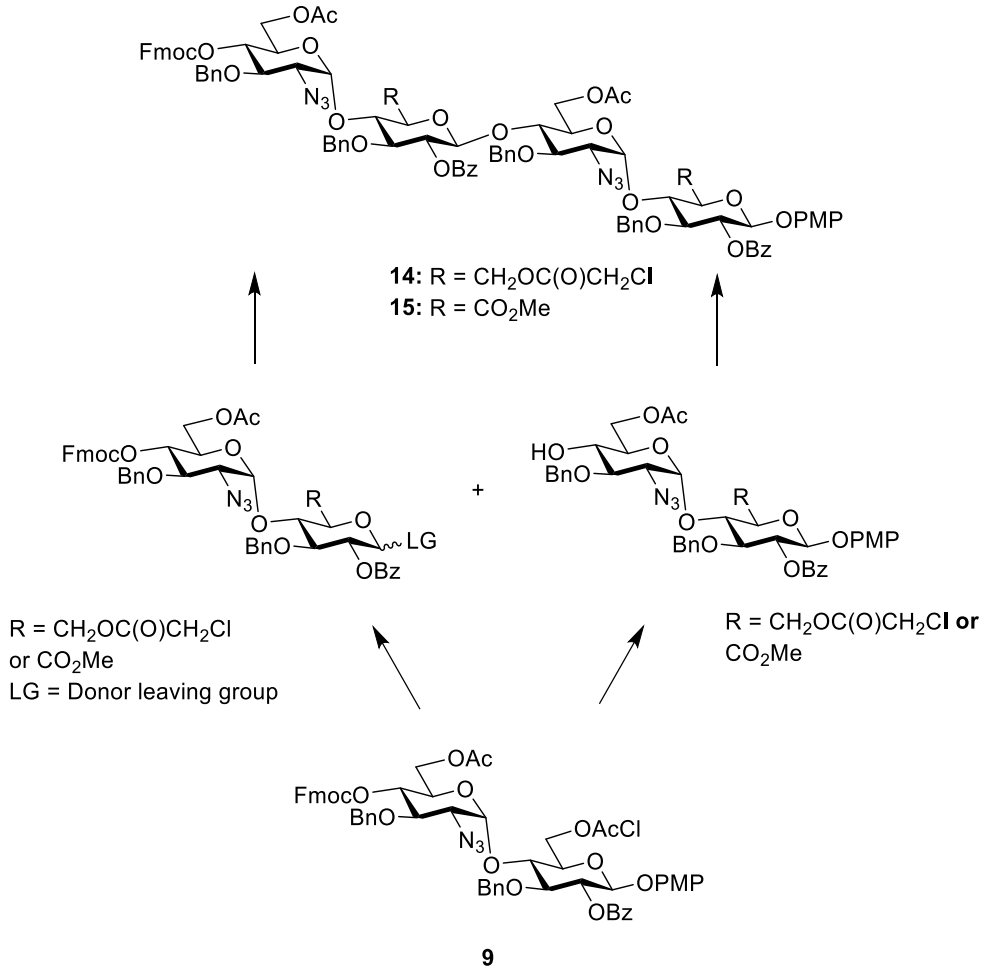

*Scheme 16 - A plan for the synthesis of tetrasaccharides **14** and **15**.*
*These may be assembled by the glycosylation of various disaccharide donors in both uronic acid and hexose forms, and the corresponding acceptors. All of these can be generated from disaccharide **9**.*

Comparison of the yields of each glycosylation reaction will provide a measure of the effectiveness of the various donors in both hexose and uronic acid form. Additionally, these glycosylation reactions will allow a direct comparison of the effectiveness of several glycosyl donors. For this work, it was decided to limit the comparison to TCA, *N*-PTFA, thioglycoside, and glycosyl chloride disaccharide donors.

2.2 Results

The synthesis of the monosaccharide donor **10** and acceptor **11**, and subsequently the assembly of disaccharide **9** has been carried out using our existing procedures (Scheme 17).[194] The starting monosaccharides **12** and **13** were available in multi-gram quantities in our laboratory, and so made ideal starting materials.

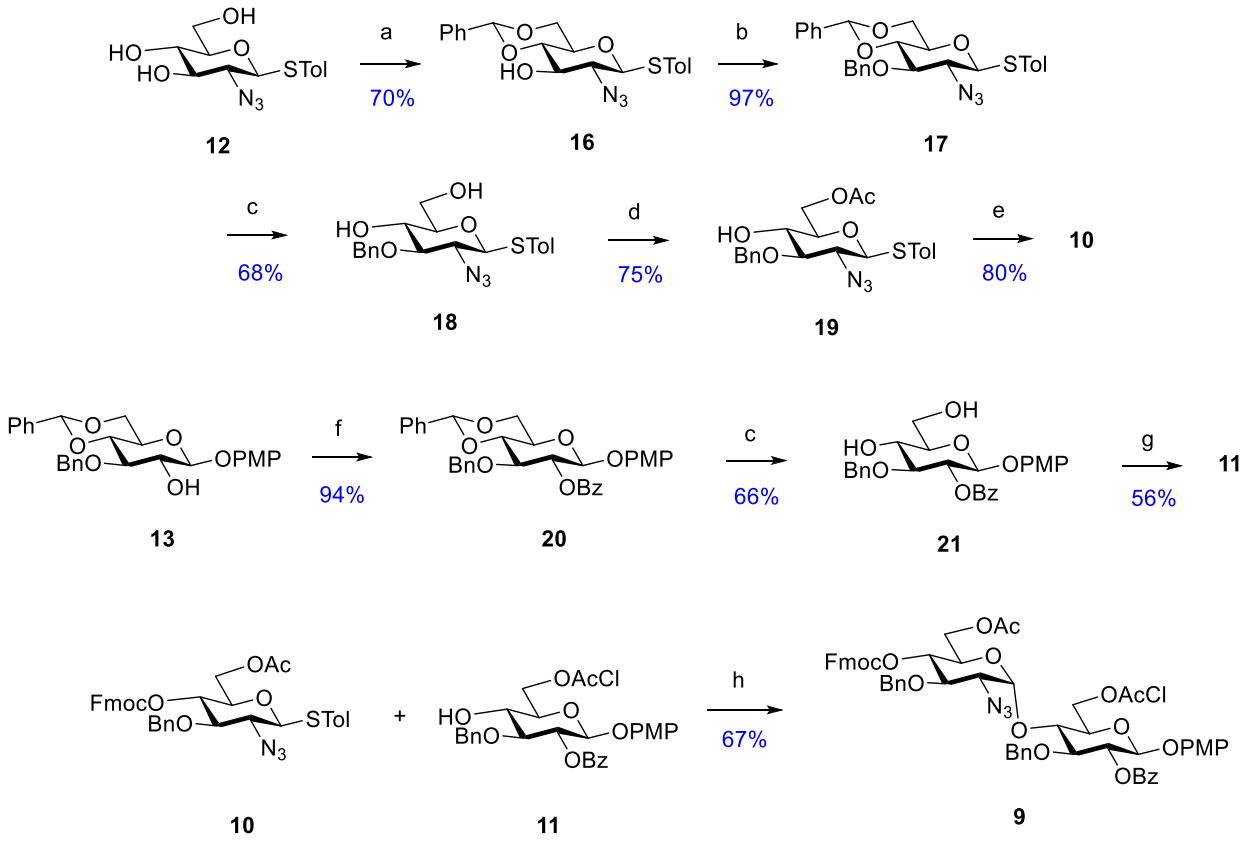

a) $PhCH(OMe)_2$, CSA, DMF, 60 °C; b) BnBr, NaH, DMF, RT; c) AcCl, MeOH, dioxane, 0 °C then RT; d) AcCl, pyridine, DCM, -78 °C; e) Fmoc-Cl, DMAP, DCM, pyridine, 0 °C then RT; f) BzCl, pyridine, DCM, 0 °C; g) ClAcCl, pyridine, DCM, -78 °C; h) NIS, AgOTf, DCM, toluene, -20 °C.

*Scheme 17 - Synthesis of the disaccharide building block **9**.*

Monosaccharide **12** was selectively 4,6-OH protected as the benzylidene acetal to give **16**, and subsequently the 3-OH was protected as the benzyl ether to give **17**. The benzylidene acetal protecting group was removed to give **18**, and the 6-OH position selectively acetylated to give **19**. The remaining 4-OH position was protected with an Fmoc group to give the monosaccharide glycosyl donor **10**. Monosaccharide **13** was protected as the benzoyl ester at the 2-OH position to give **20**, and then the benzylidene acetal protecting group was removed to give **21**. Finally, the 6-OH position was selectively reacted with 1-chloroacetyl chloride to give the glycosyl acceptor **11**. The donor **10** and acceptor **11** were then glycosylated to yield the disaccharide **9**, using optimised conditions from our previous

work.[194] This reaction gave a near complete 1,2-*cis* (α-linked) stereoselective glycosylation outcome. The 1,2-*trans* (β-linked) anomer of the product was not isolated.

Following the successful synthesis of disaccharide **9**, further reactions were carried out to produce the hexose glycosyl acceptor disaccharide **22** and hemiacetal **23** (Scheme 18). To obtain acceptor **22**, disaccharide **9** was stirred with triethylamine to selectively remove the 4-*O*-Fmoc from the non-reducing end. Separately, disaccharide **9** was subjected to selective CAN mediated 1-*O*-PMP deprotection conditions to yield hemiacetal **23**.

The glucuronic acid analogues of **22** and **23**, namely glycosyl acceptor **24** and hemiacetal **26**, were also synthesised (Scheme 18). Disaccharide **9** was stirred with DABCO in EtOH/MeCN to remove both the 4-*O*-Fmoc protecting group from the non-reducing end, and the 6-*O*-chloroacetyl protecting group from the residue at the reducing end. Selective 6-OH oxidation with TEMPO/BAIB followed by treatment with trimethylsilyldiazomethane afforded the glycosyl acceptor uronate ester **24**.

Separately, disaccharide **9** was treated with thiourea to selectively remove the 6-*O*-chloroacetyl protecting group from the residue at the reducing end. Use of the previously described oxidation and esterification protocol yielded glucuronic ester disaccharide **25**. CAN mediated 1-*O*-PMP deprotection of **25** yielded the uronate hemiacetal **26**.

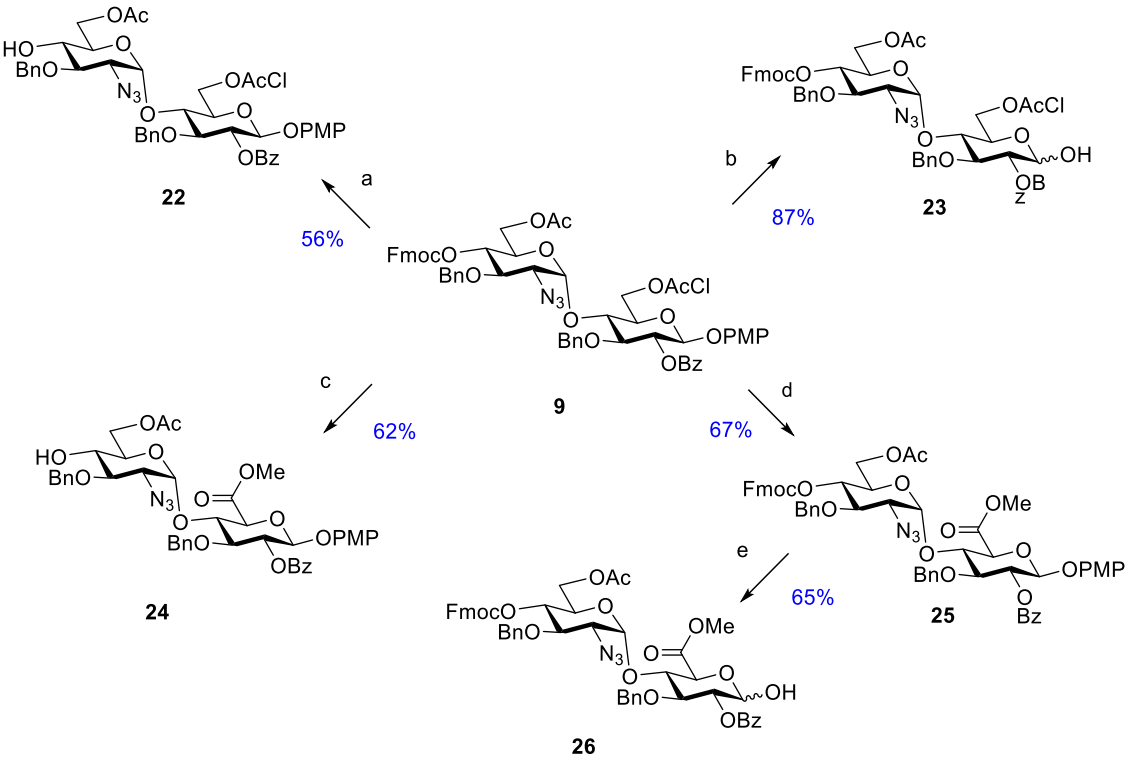

a) 4:1 DCM/Et_3N, RT; b) CAN, MeCN, H_2O, RT; c) i) DABCO, EtOH, MeCN, 70 °C; ii) iodobenzene diacetate, TEMPO, MeCN, H_2O, RT; iii) $(Me)_3SiCN_2$, MeOH, Et_2O, RT; d) i) Thiourea, EtOH, MeCN, 70 °C; ii) iodobenzene diacetate, TEMPO, MeCN, H_2O, RT; iii) $(Me)_3SiCHN_2$, MeOH, Et_2O, RT; e) CAN, MeCN, H_2O, RT.

*Scheme 18 - Reactions of disaccharide building block **9** to produce glycosyl acceptors and hemiacetals.*

A sample of the uronate glycosyl acceptor **24** was found to crystallise after being dissolved in a small amount of EtOAc and diluted with MeOH, and then evaporating solvents slowly from a partially covered vial over several days. From a crystalline sample of **24** recovered from this solution, a single crystal X-ray structure was successfully obtained (Figure 25). This confirmed the presence of the 1,2-*cis* (α-linked) anomeric (1→4) linkage in the disaccharide, the installation of which is key for our later synthesis of oligosaccharide HS mimetics. The crystal was formed of pi-stacked dimers, which themselves were formed from hydrogen bonding interactions between the 4-OH hydroxyl group and the 6-*O*-Ac protecting group on the non-reducing residue of two adjacent molecules.

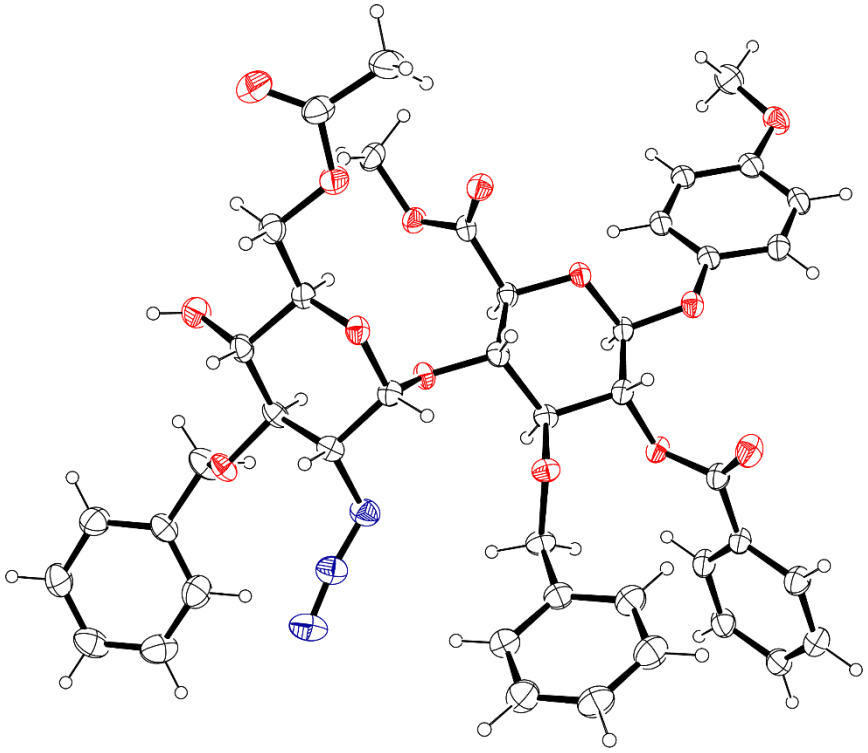

*Figure 25 - The ORTEP plot of the single crystal structure of **24**.*
Shown with 30% probability ellipsoids. This disaccharide forms a single crystal featuring pi-stacked dimers, with hydrogen bonding between the 4-OH and 6-O-Ac of adjacent molecules, which is not shown.

However, despite extensive efforts, application of the same method to the hexose glycosyl acceptor **22** did not produce crystals suitable for structural analysis. Fully protected uronate disaccharide **25** also failed to crystallise by this method. Disaccharide **25** cannot form the dimers observed in the single crystal X-ray structure of **24**, as the 4-*O* position is protected with Fmoc. However, a single crystal X-ray structure of disaccharide **9** has been previously reported, suggesting that dimer formation is not a requirement for these disaccharides to crystallise.[282]

Following the synthesis of hemiacetals **23** and **26**, a set of anomeric leaving groups was installed on each, to produce a series of comparable glycosyl donors (Scheme 19). The TCA glycosyl donors **27** and **28**, *N*-PTFA glycosyl donors **29** and **30**, and thioglycoside donors **33** and **34** proved to be obtainable in moderate to high yields using both hemiacetal starting materials. Experimental procedures to form the trifluoroacetimidate and thioglycoside donors were first optimised using the hexoses, before being applied to the uronates. A procedure to form the trichloroacetimidate donors has previously been reported and was used successfully, without further modification, on both starting materials.[194]

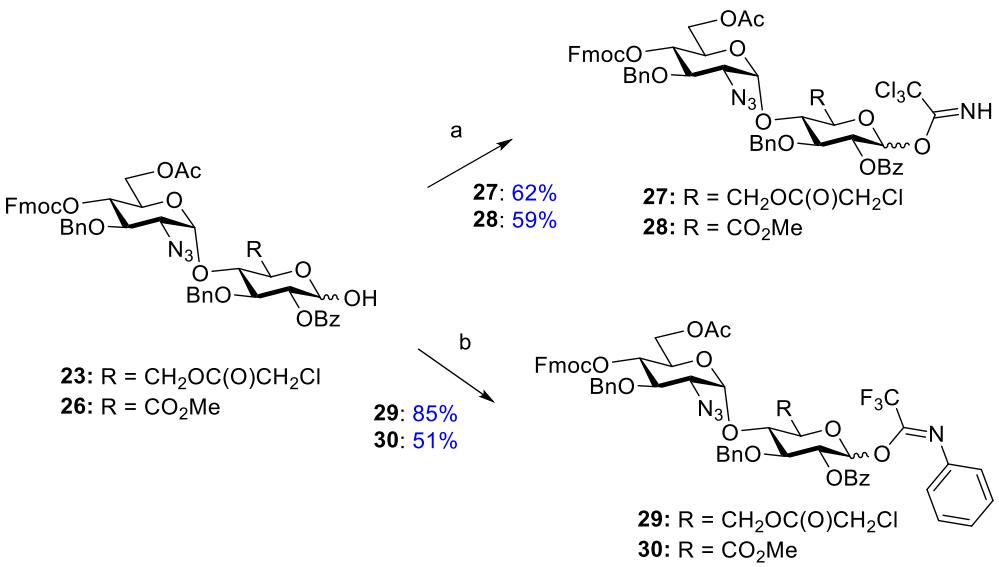

*Scheme 19 – Reactions carried out on hemiacetals **23** and **26** to access a series of glycosyl donors.*

To form the hexose trifluoroacetimidate glycosyl donor **29**, the hemiacetal **23** was reacted with four equivalents of 2,2,2-trifluoro-*N*-phenylacetimidoyl chloride and a single equivalent of NaH (Scheme 20).[215,216] This reaction proceeded in a high yield of 85% following purification by column chromatography. Glycosyl donor **29** was stable for 3-4 days when stored under argon at -20 °C. Uronate donor **30** was synthesised by the same protocol using the uronate hemiacetal **26**, although with a lower yield of 51%.

Purification of glycosyl donors **29** and **30** by column chromatography, using a hexanes/EtOAc solvent system, was initially challenging. Significant quantities of hemiacetal were isolated, indicating that hydrolysis of the glycosyl donor was occurring during purification. The chromatography method was optimised by using a triethylamine additive to neutralise column acidity, affording higher isolated yields of the product. However, this purification method required additional work to neutralise the eluted solvent. Further refinement of chromatography conditions, to use a dichloromethane/acetonitrile solvent system without a triethylamine additive, and either isocratic or relatively fast gradients, allowed successful purification of the glycosyl donors. Larger scale synthesis of the *N*-PTFA donors **29** and **30** was carried out and purified using this method.

The thioglycoside donors were accessed through the anomeric acetate. This is not the optimal method for the synthesis of these disaccharide donors but was sufficient for the purposes of our investigation. The hexose hemiacetal **23** was first acetylated to produce **31** (Scheme 20). Several procedures reported for anomeric acetylation were considered.[283,284] Many methods of sugar acetylation involve the use of bases such as pyridine, which could cause the loss of the base-labile 4-*O*-Fmoc protecting

group on the non-reducing end of disaccharide **9**. To avoid this, in our approach, the acetylation was carried out using multiple equivalents of anhydrous sodium acetate and acetic anhydride.

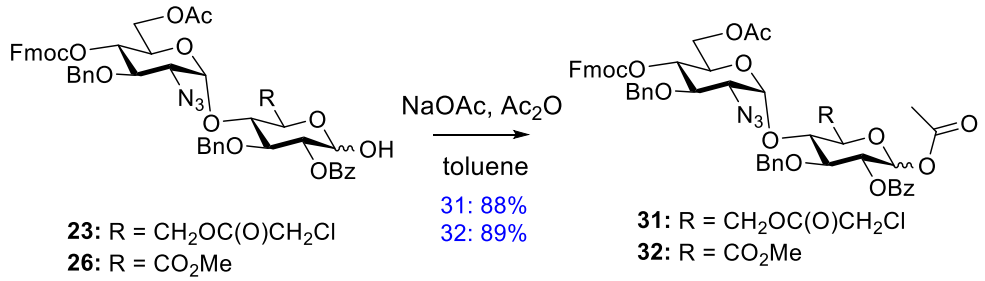

*Scheme 20 – Synthesis of anomeric mixtures of acetates **31** and **32**.*

The initial reaction produced the acetate in good yield. However, analysis by NMR confirmed that the anomeric ratio of acetate **31** was α/β : 2/1. This was determined by comparing the $J_{1,2}$ coupling of the reducing end anomeric proton to the sugar ring proton at C2 in the two distinct anomers. It was known that the subsequent formation of the thioglycoside donor would proceed five-fold faster using the β-acetate.[285,286] Having a thiol present in a prolonged reaction might lead to unwanted side products, as thiols can carry out nucleophilic substitution to displace the chloride from the 6-*O*-chloroacetate. A similar mechanism is operating during the selective deprotection of a chloroacetate by thiourea. Therefore, a series of test reactions, on a 50 mg scale, were carried out to attempt to improve the proportion of β-anomer present in the acetylation product mixture (Table 1).

Entry	Reagents	Solvent	Temperature [°C]	Yield [%]	α/β
1	4 equiv. NaOAc	Ac_2O	RT	65	2:1
2	4 equiv. NaOAc	Ac_2O	-15	80	2:1
3	4 equiv. NaOAc	Ac_2O	70	84	3:2
4	4 equiv. NaOAc	Ac_2O	140	52	1:1
5	4 equiv. Ac_2O, 4 equiv. NaOAc	Xylene	140	92	1:2
6	4 equiv. Ac_2O, 4 equiv. NaOAc	DMF	140	-	-
7	4 equiv. Ac_2O, 4 equiv. NaOAc	Toluene	110	84	3:7

*Table 1 - Optimisation of acetylation conditions for generating the desired β-anomer of acetate **31**. All reactions were carried out on the 50 mg (0.05 mmol) scale, with 2 mL of solvent.*

There are two processes to consider in the acetylation reaction - the anomerisation of the hemiacetal, and the subsequent acetylation of the hemiacetal. Changing the conditions of the reaction to affect these processes should change the ratio of acetate anomers produced.

The first modification to the acetylation procedure attempted was to change the reaction temperature. It was established that higher temperatures appeared to favour the formation of greater proportions of the β-acetate, improving the α/β ratio of the acetylation product **31** from 2:1 at RT to

1:1 at reflux (140 °C) in neat acetic anhydride. It is postulated that increased temperature led to an increased rate of anomerisation, overcoming the preference of the hemiacetal for the α-anomer due to the anomeric effect, to give a closer to 1:1 ratio of the anomers of the hemiacetal.[287] Subsequent acetylation of this hemiacetal would yield closer to equal proportions of each anomer of the acetate, as there would be a greater proportion of the β-anomer of the hemiacetal present as the substrate for the acetylation.

The next modification was to reduce the rate of acetylation. Anomerisation is a unimolecular process but the acetylation reaction is bimolecular. It follows that reducing the number of equivalents of acetic anhydride used and diluting the acetic anhydride with another solvent, should affect the rate of acetylation. It was anticipated that the β-anomer of the hemiacetal would acetylate faster than the α-anomer, and so reducing the rate of acetylation should promote formation of the desired β-acetate.

Xylene (Entry 5 in Table 1) and DMF (Entry 6 in Table 1) were initially selected as solvents for the acetylation reaction, as they both had boiling points close to acetic anhydride. Reactions using the conditions described in Entry 5 produced a good improvement in the anomeric ratio, improving the α:β ratio of the acetylation product **31** from 1:1 to 1:2. The β-anomer of acetate **31** was now the major product, compared to the original reaction were the α-anomer of acetate **31** was the major product. Reactions using the conditions described in Entry 6, however, failed to produce acetate **31**. Subsequent NMR analysis indicated degradation.

Next, the reaction was attempted using toluene as the solvent, at the lower refluxing temperature of this solvent (110 °C). This acetylation reaction resulted in a slightly improved α:β ratio in the product **31** of 3:7, compared to the 1:2 previously achieved using xylene solvent at reflux, and in acceptable yield. There is potentially scope to further optimise this reaction, although in the interests of time, it was decided that the toluene solvent method (Entry 7 in Table 1) was acceptable to produce hexose acetate **31** for this work. The same method was used to generate the uronate acetate **32** in good yields**,** although with a slightly lower α:β ratio in acetate **32** of 2:3 (Scheme 20).

The mixture of hexose acetate anomers **31** was then treated with *p*-toluenethiol and boron trifluoride diethyl etherate[218-220] to form the thioglycoside donor **33** (Scheme 21). Initial reactions afforded a low yield (20%) of the thioglycoside **33**. However, these reactions were carried out using batches of acetate **31** which had an α/β ratio of acetate anomers of 3:2. TLC analysis during the reaction indicated that the β-acetate was rapidly consumed, whilst the α-acetate appeared to react very slowly and eventually degradation was observed. During chromatography, starting material was isolated in a mostly α-acetate form. Later experiments, using batches of acetate **31** with an improved α/β ratio of 3:7, gave an improved yield of 64% as expected.[286] In all attempts, the reaction to form thioglycoside

donor **33** produced exclusively the β-anomer of the product. The same procedure was then successfully applied to uronate acetate **32** to produce uronate thioglycoside 3**4** (Scheme 21) in a very similar yield of 62%. However, the starting material **32** featured an α/β ratio of acetate anomers of 2:3.

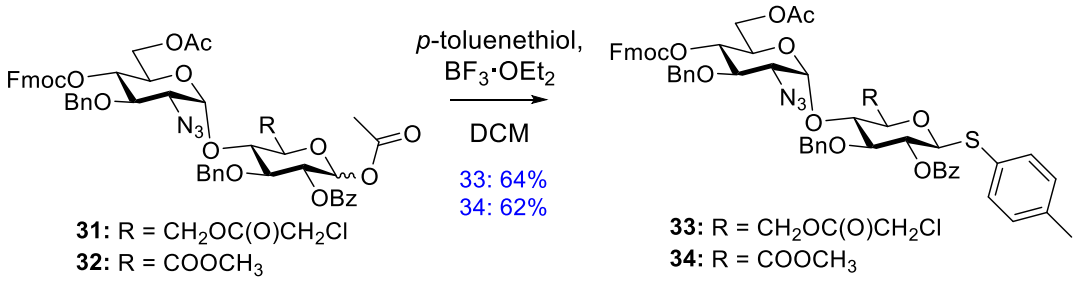

*Scheme 21 – Synthesis of thioglycoside donors **33** and **34** from acetates **31** and **32**.*

Crystals of thioglycoside **33** suitable for structural analysis were developed using the method previously described for glycosyl acceptor **24**. A single crystal X-ray structure was successfully obtained (Figure 26). This crystal composition showed similar crystal packing to the previously solved **9**, including a similar level of disorder in the non-reducing end of the disaccharide.[282] Figure 26 shows the observed disorder. The crystal contained a 1:1 sequential array of molecules of each non-reducing end conformation, with no formation of dimers or specific interactions as observed in the crystal structure of uronate acceptor **24**. Unfortunately, when the same method was applied to uronate thioglycoside **34**, this did not generate any suitable crystals.

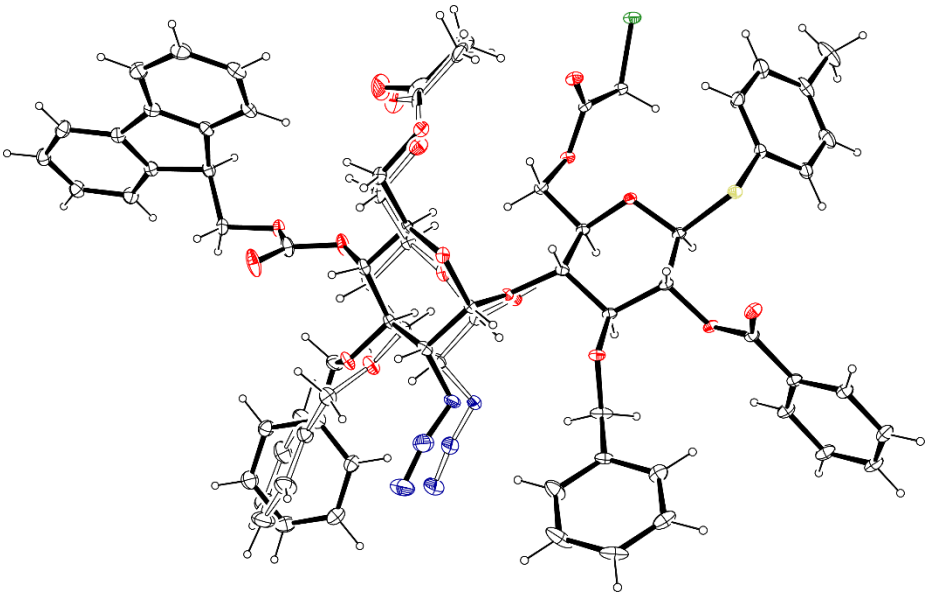

*Figure 26 - The ORTEP plot of the single crystal structure of **33**.*
*Shown with 30% probability ellipsoids. Here some disorder is observed at the non-reducing end of the sugar, especially around C3 where the benzyl protecting groups exists in a 1:1 mixture of conformations in the crystal. Similar disorder is observed in the crystal structure of **9**.*

It was initially thought that leftover anomeric acetate from the reaction to form the thioglycosides, mainly comprised of the unreacted α-acetate, would be unable to be further used. Up to five-fold longer reaction times would be problematic as previously discussed, and any method to remove the anomeric acetate could also affect the primary 6-*O*-acetate on the sugar residue at the non-reducing end of the molecule.

However, a report documenting a method of selectively deprotecting anomeric acetate using zinc acetate as a catalyst was found, demonstrating the feasibility of the strategy.[288] In this report, the authors used this system on per-acetylated mono- and disaccharides, affording hemiacetals in moderate to high yields. Therefore, this system should leave our primary 6-*O*-acetate on the sugar residue at the non-reducing end of the disaccharide untouched. This method was applied to a sample of mostly α-acetate **32** and the uronate hemiacetal **26** was isolated in 73% yield (Scheme 22). This hemiacetal was then re-acetylated using our optimised conditions to generate further useful β-acetate, allowing recovered α-acetate from the thioglycoside formation to be recycled. The same strategy was not attempted on the hexose acetate **31**, as reworking of unreacted acetate material was not required in the hexose case.

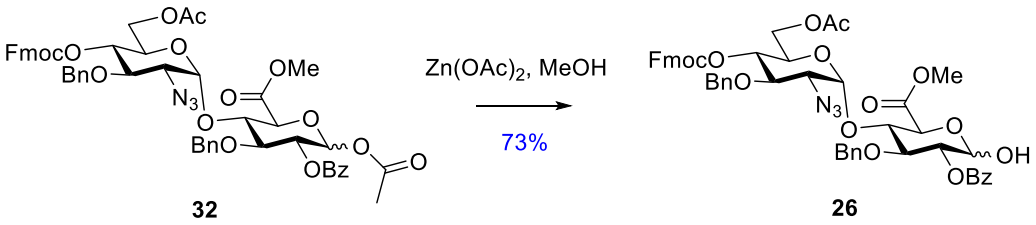

Scheme 22 - The selective removal of an anomeric acetate.
*Acetate **32**, predominantly the α-anomer recovered from the synthesis of thioglycoside **34**, was treated with zinc acetate to selectively remove the anomeric acetate, returning the hemiacetal **26** and leaving the 6-O-Ac of the non-reducing end residue unmodified.*

Having developed a robust methodology to access disaccharide donors **27**, **29**, and **33** from hemiacetal **23**, these reactions where scaled up to produce enough of each of these three donors for the comparative [2+2] glycosylation experiments. The corresponding uronic acid donors **28**, **30** and **34** were accessed in quantities by similar methodology from the hemiacetal **26**, although with slightly lower yields for all reactions. This consistent pattern of reduced yields using uronates matches our expectations of these systems.

2.2.1 Attempts to form the chloride donor system

Glycosyl chloride **35** and uronyl chloride **36** were also desired as donors for comparative studies in glycosylation reactions. The chloride donors could also be accessed from the glycosyl acetate, using tin tetrachloride and thionyl chloride (Scheme 23).[186,199] This procedure should selectively generate the α-glycosyl chloride in good yield, and would not require a specific anomer of the glycosyl acetates as was the case in forming the thioglycosides. Using this strategy therefore provided another potential use for the otherwise unused disaccharide acetate, which was now predominantly the α-acetate, recovered from the reaction mixtures of experiments to form thioglycoside donors **33** and **34**.

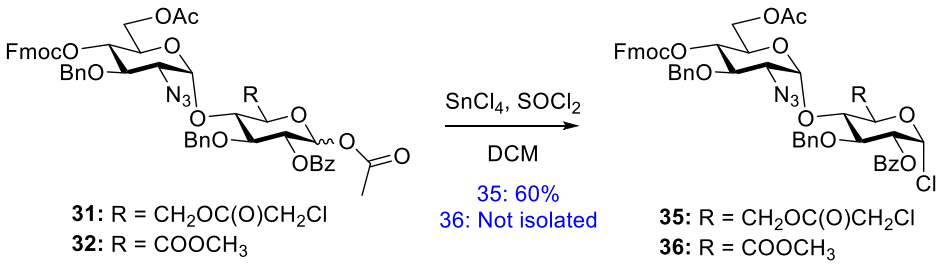

*Scheme 23 - The proposed synthesis of glycosyl chloride **35** and uronyl chloride **36**. This route used acetates **31** and **32** as starting materials, and both acetate anomers appeared to react equally well. This allowed use of recovered mostly α-acetate from the thioglycoside reactions.*

Disaccharide acetate **31** was dissolved in anhydrous dichloromethane and treated with thionyl chloride and tin tetrachloride to produce the glycosyl chloride **35**.[222] Whilst TLC analysis of the reaction mixture indicated high levels of conversion, the initial isolated yield of chloride donor **33** was low (25%). Purification by chromatography proved challenging, and a large amount of hemiacetal was isolated. The same optimisations that were used in chromatography of *N*-PTFA glycosyl donors **29** and **30** were attempted. However, use of a triethylamine additive to neutralise column acidity afforded even lower isolated yields (10%) of chloride glycosyl donor **35**. The use of a dichloromethane/acetonitrile solvent system, and either isocratic or relatively fast gradients, appeared to limit hydrolysis of the glycosyl chloride donor during purification, resulting in a 60% isolated yield.

Following the successful synthesis of glycosyl chloride **35**, the same reaction conditions were used to attempt to synthesise uronyl chloride **36** from uronate acetate **32**. Whilst this reaction did produce **36**, it also failed to consume all the acetate over the same reaction time and produced several other species of a lower R_f on the TLC plates. The resulting mixture comprised five compounds in approximately equal proportions.

It was postulated that this outcome was a result of side reactions of tin tetrachloride, the possibility of which has been previously reported.[289] Separation of the mixture by column chromatography was proving difficult, despite separation on TLC analysis in the same solvent systems. LC-MS analysis of the crude mixture was used to identify the major side-products. This yielded the molecular ion mass for each of the five species (Table 2).

Peak	Retention time [min]	Molecular ion peak, Na^+ adduct [*m*/*z*]	Molecular ion peak [*m*/*z*]
1	6.04	918	895
2	6.11	918	895
3	6.25	960	937
4	6.33	1008	985
5	6.58	984	961

*Table 2 - The retention times and the corresponding molecular ion mass of 5 major species observed in the reaction mixture of uronyl chloride **36**.*
Peak 5 corresponds to the intended product and peak 4 to the starting material, but the other peaks appear to represent deprotected side-products. Only the MS peak of 5 displays a chloride isotope pattern.

The $[M+Na]^+$ masses of 984 *m*/*z* and 1008 *m*/*z* where identified as the molecular ion masses of the product uronate chloride **36** and the unreacted uronate acetate **32** respectively. Crucially, only the peak of the intended product, with a retention time of 6.58 minutes, produced a characteristic chloride isotope pattern in the mass spectrum (Figure 27).

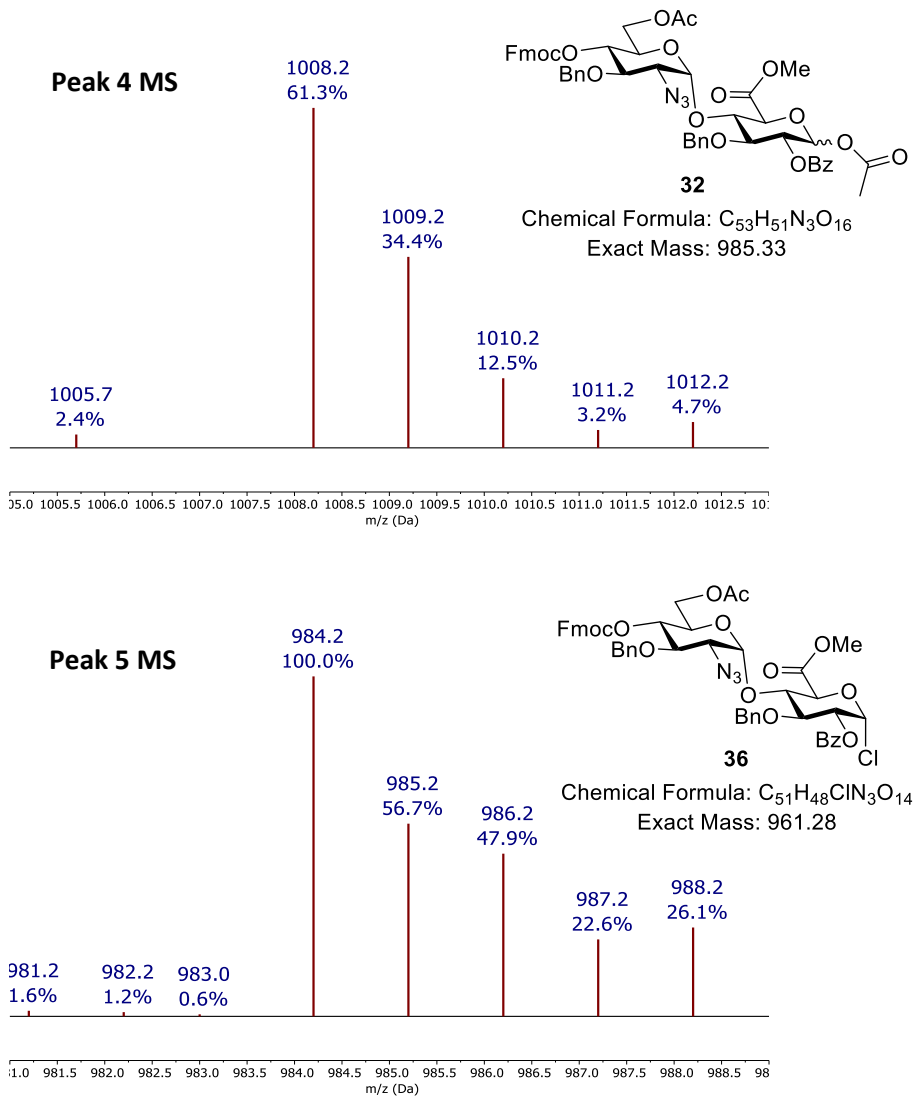

*Figure 27 – Mass spectra of compounds detected by LCMS analysis of the reaction mixture of **36.** The mass spectra are displayed with the proposed identities of each compound adjacent. The starting material, mixed acetate **32**, corresponds to peak 4 in Table 1, while the product uronyl chloride **36** corresponds to peak 5.*

The masses present in peaks 1 and 2 are the result of the loss of a benzyl group. This is consistent with a $[M+Na]^+$ molecular ion mass of 918 *m/z*, which corresponds to the uronate acetate **32** with one benzyl group removed (Figure 28). There are two distinct peaks with this mass, which could be due to separation of the two anomers of this compound, or due to the loss of either one of the two benzyl groups in the disaccharide. Here the disaccharide acetate **37** is suggested as the side-product, with a deprotected 3-OH on the sugar residue at the reducing end of the disaccharide. The mass of the other side-product could arise from the replacement of the benzyl protecting group with an acetate protecting group, giving the fully protected disaccharide **38** (Figure 28). This is consistent with a $[M+Na]^+$ molecular ion mass of 960 *m/z*, but it was unclear how this transformation occurred.

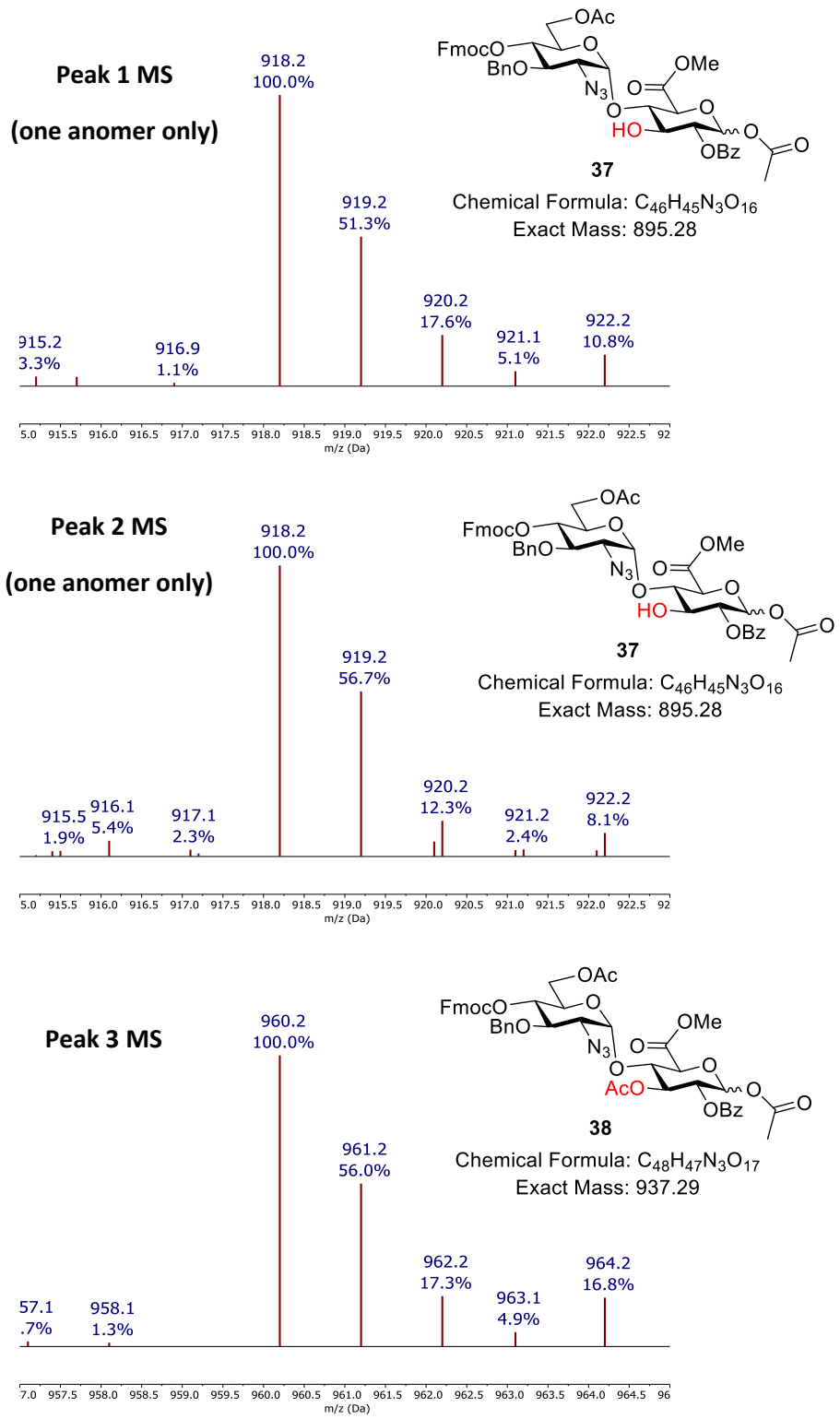

*Figure 28 - Mass spectra of side-products detected by LCMS analysis of the reaction mixture of **36.** The mass spectra are displayed with the proposed identities of each compound adjacent. The de-O-benzylated side-product **37** corresponds to peaks 1 and 2 in Table 1. The acetylated side -product **38** corresponds to peak 3.*

Previous literature around tin reactivity in nucleosides,[290] tin-mediated selective deprotection[291] and particularly selective de-*O*-benzylation[292] leads to the suggestion that these side-products are the result of the formation of a tin complex leading to the elimination of benzyl chloride. A postulated mechanism for the benzyl loss in the uronate disaccharide is shown (Scheme 24), based on a report from Hori and co-workers.[292] Here, the tetrahedral tin tetrachloride forms an octahedral complex with two oxygen atoms in the molecule, before displacement of a chloride by the 3-*O*-Bn oxygen of the reducing end residue. Then, breaking of the C-O bond and forming a Sn-O bond occurs, producing benzyl chloride. Metal-oxygen bond formation is driven by the oxygenophilicity of the metal atom, and the stability of the benzyl carbonium ion.

Our experiments appear to indicate that the presence of the ester is necessary for the mechanism of production of these side-products, which could assist in providing a favourable binding site for the tin-sugar complex. The tin complex could form above the sugar ring, interacting with the carboxylate group and another oxygen elsewhere in the disaccharide, in addition to the benzyl ether oxygen. The other oxygen may be one of several, but here the ring oxygen of the non-reducing end residue is suggested. Despite the electron-withdrawing effect of the uronic acid, this oxygen could provide a binding site for the complex to carry out de-*O*-benzylation. It is also possible that a tin dimer-sugar complex may be forming, with the size of the tin dimer allowing interaction with the various protecting groups on the disaccharide. It is suggested here that the benzyl group lost is the benzyl group at the 3-*O*-position on the reducing end residue of the disaccharide, although this was not confirmed. The 3-*O*-acetylated side-product **38** could be forming during the reaction by reaction with acetate liberated from the anomeric position when the glycosyl chloride product is generated. The 3-OH side-product **37** could be forming by hydrolysis during the reaction, although anhydrous conditions were used. Side-product **37** could also be formed during the work-up, which involves a quench with ice-cold saturated aqueous sodium bicarbonate, or by hydrolysis occurring during subsequent chromatography.

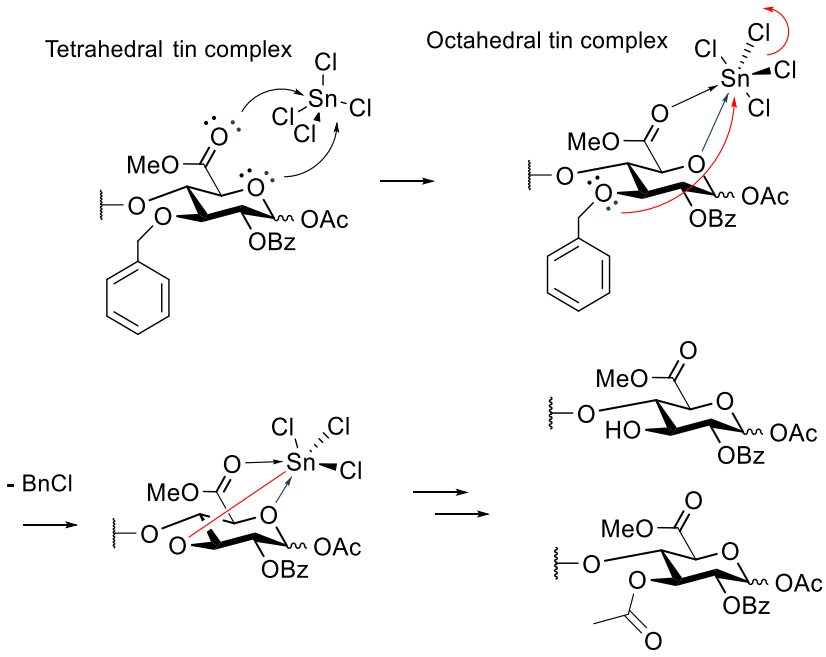

*Scheme 24 - The elimination of a benzyl cation during the reaction to make uronyl chloride **36**. Based on the work of Hori and co-workers, it is proposed that a tin-mediated de-O-benzylation occurs during this reaction by formation of a tin-sugar complex.[292] It is thought to occur at the reducing end of the disaccharide as this side-product was not observed in the hexose equivalent reaction after several days, suggesting involvement of the methyl ester.*

These side-products where not observed in the synthesis of glycosyl chloride **35** by this method. A reaction that was carried out for 3 days did not generate analogous side-products, suggesting that the ester was responsible for the de-*O*-benzylation outcome. In the synthesis of **35**, the 6-*O*-position on the reducing end residue of the disaccharide is protected as the chloroacetate. While the chloroacetate still features a carbonyl group, the carbonyl oxygen is two bonds further away from the sugar ring. In the interests of time no further assessment of this reaction was undertaken to establish the true mechanism. Furthermore, as separation of these five compounds was challenging, NMR analysis of the various species present in the reaction mixture was not carried out and only tentative assignments could be made.

Due to these issues, a new method was required to access the uronyl chloride donor **36** from acetate **32**. Several other methods were briefly assessed. One of these methods was treatment with zinc chloride and 1,1-dichloromethyl methyl ether,[243,293] and another was treatment with thionyl chloride and bismuth (III) chloride.[223,294]. Neither of these methods produced identifiable amounts of the expected product. Due to these results and time constraints, the chloride donor system was not assessed for the comparative series of glycosylation reactions. Other methods are reported in the literature which could be attempted if more time was available, including synthesis from other starting materials, such as the thioglycoside analogue.[295] Glycosyl chlorides, or indeed several of the glycosyl

halides, could also be synthesised from the hemiacetal directly by a variety of methods, including the use of tetramethyl-α-haloenamines[296], or the trichlorotriazine (TCT) and DMF system.[297]

2.2.2 Comparison of [2+2] glycosylation reactions

To compare, and contrast, the effectiveness of the hexose and uronate glycosyl donor and acceptor combinations, it was decided to carry out [2+2] glycosylation reactions on a consistent 200 mg scale. Each experiment was repeated several times. Similar conditions for each glycosylation were used with the hexose and uronate versions of each donor, allowing for the direct comparison of their performance. The tetrasaccharide product, either as the hexose or the uronate, was the same for all three reactions (Scheme 25).

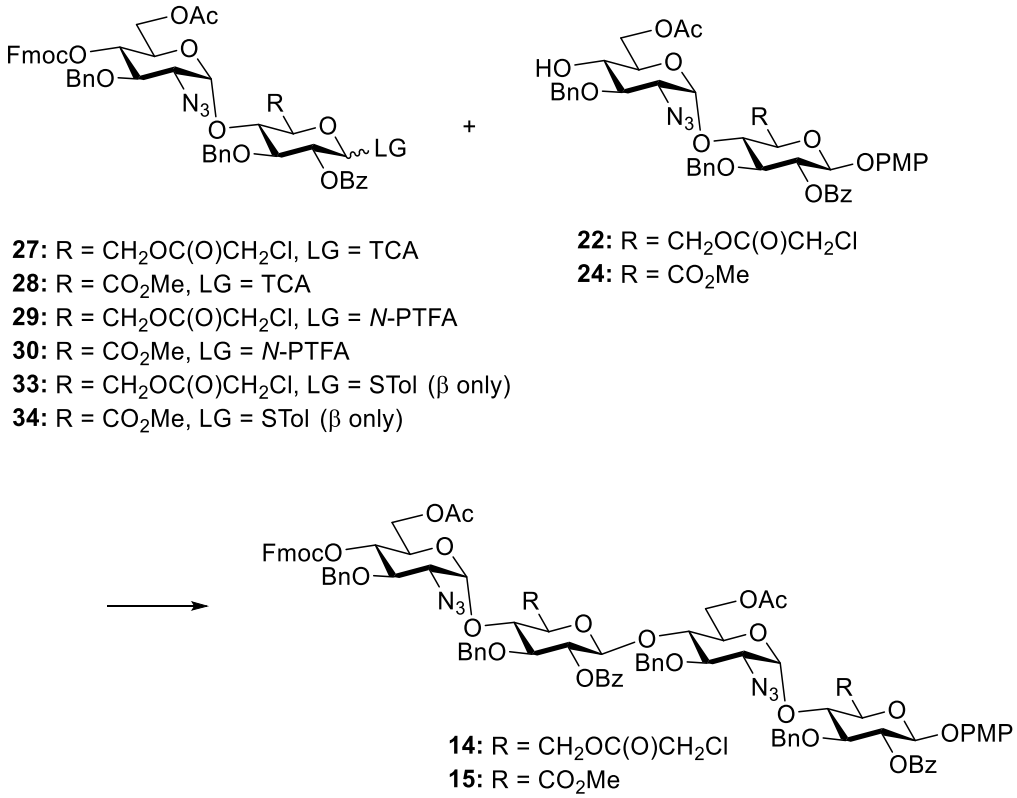

Scheme 25 – An overview of the comparable [2+2] glycosylation reactions.

The results of the set of glycosylation reactions using donors **27**, **28**, **29**, **30**, **33** and **34**, and their respective acceptors **22** or **24,** is summarised below (Table 3). Each of these experiments were repeated several times, and the average yield of at least three successful reactions is presented. However, as will be detailed below, the precise number of experiments conducted with each system varied, based on the difficulties encountered in each case. Additionally, when experiments were successful using one analogue but not the other, different conditions were explored.

Entry	Donor	Acceptor	Analogue	Donor type	Promoter	Product	Yield [%]
1	**27**	**22**	Hexose	TCA	TMSOTf	**14**	90
2	**28**	**24**	Uronate	TCA	TMSOTf	**15**	47
3	**29**	**22**	Hexose	*N*-PTFA	TMSOTf	**14**	87
4	**30**	**24**	Uronate	*N*-PTFA	TMSOTf	**15**	5
5	**33**	**22**	Hexose	STol	NIS/AgOTf	**14**	53
6	**34**	**24**	Uronate	STol	NIS/AgOTf	**15**	56

Table 3 - The results of a comparative series of glycosylation reactions, showing an average yield of all the repeats of each reaction.

The glycosylation of TCA donor **27** and acceptor **22**, producing tetrasaccharide **14**, proceeded in high yield (90%, Scheme 26). This result is in line with yields previously achieved using this chemistry in our group. Analysis of the product indicated that only the specific 1,2-*trans* linkage stereochemistry of our desired target tetrasaccharide **14** was produced, again as expected. Several repetitions of the experiment produced consistent results.

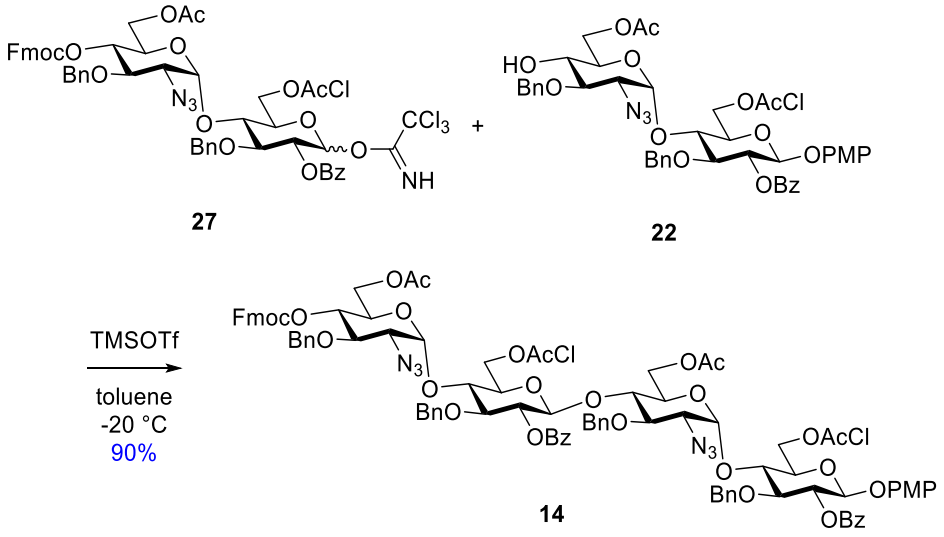

*Scheme 26 – Synthesis of tetrasaccharide **14** using glycosyl donor **27**.*

However, under the same conditions, glycosylation of donor **28** and acceptor **24,** producing tetrasaccharide **15**, appeared to stall during the reaction (Scheme 27). Attempts to drive the reaction further, by treatment with TMSOTf and warming to room temperature, were made. However, this did not appear (by TLC analysis) to lead to completion. Two major tetrasaccharide products were eventually isolated by chromatography. Unreacted acceptor **24** and hemiacetal **26** were also isolated. Purification of the two major products proved challenging and required multiple chromatography attempts. Identification of the two major products was carried out using the highest purity fractions available, although small impurities remained.

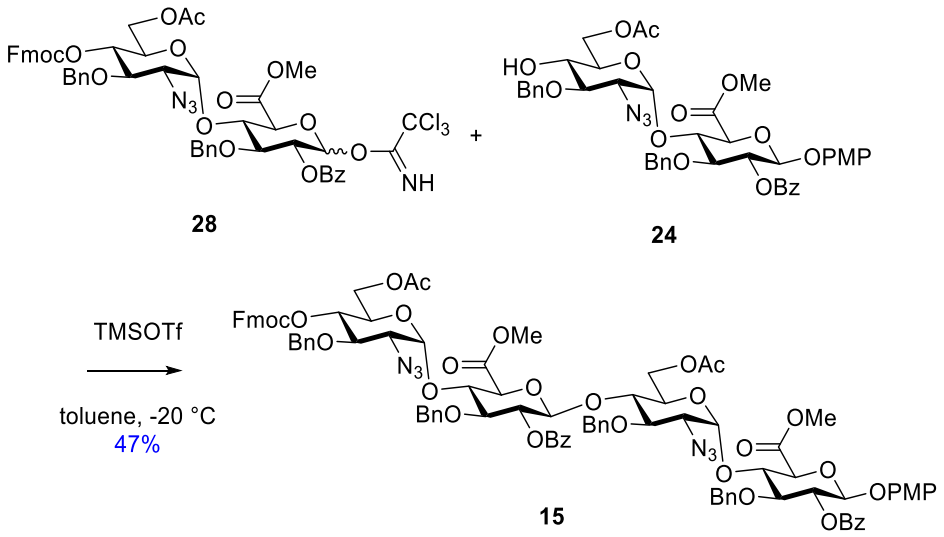

*Scheme 27 – Synthesis of tetrasaccharide **15** using glycosyl donor **28.***

Mass spectrometry of the two tetrasaccharide products showed that they have the same molecular mass, which was the expected mass of the tetrasaccharide **15**. However, analysis of the ^{1}H, ^{13}C and 2D NMR spectra of these products identified one as most likely the target product **15**, which featured two α (presenting as a resolved doublet with a small *J* value) and two β (presenting as a resolved doublet with a large *J* value) anomeric hydrogens. Target product **15** was isolated in 47% yield. The NMR spectra of the side-product indicated the presence of three α-anomeric hydrogens and one β anomeric hydrogen. Two of the anomeric proton peaks were broad and poorly resolved. The anomeric proton peaks that were resolved are doublets with large coupling constants. This side-product was isolated in 30% yield.

It was thought initially that this side-product could be a stable orthoester **39**. Orthoesters are a well-documented intermediates of some glycosylation reactions with a participating group at the 2-*O*-position of the reducing end of the donor (Figure 29).[181,178] However, exposing this material again to the reaction conditions of TMSOTf in anhydrous dichloromethane did not lead to the expected collapse of the orthoester to give the product.[298]

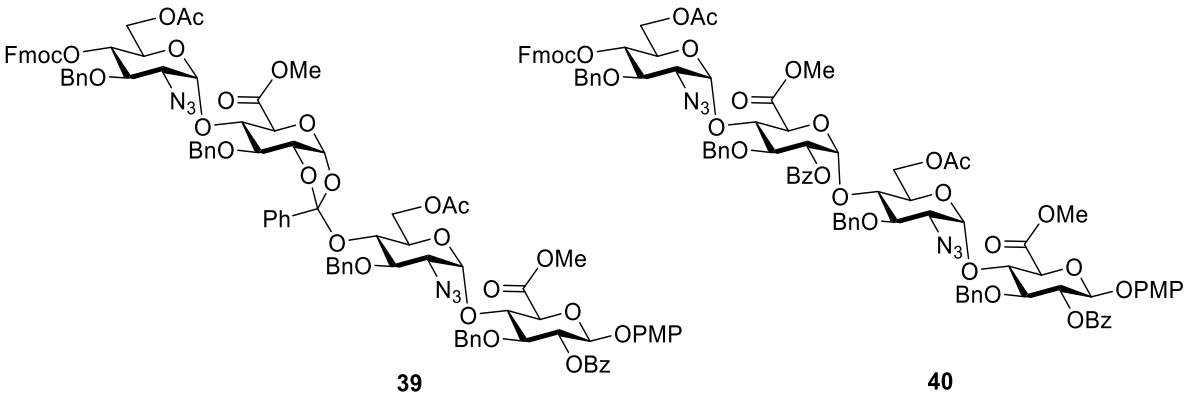

*Figure 29 - The orthoester product **39** and unexpected 1,2-cis (α-anomeric) linkage product **40** of the reaction of uronate TCA donor **28** and uronate acceptor 2**4**.*

Therefore, based on NMR analysis, the second tetrasaccharide product in this case was **40**. This tetrasaccharide has an unexpected 1,2-*cis* (α-anomeric) linkage at the newly formed centre, despite the presence of a 2-*O*-benzoyl group in the donor disaccharide, which should participate to give the 1,2-*trans* linked product exclusively (Figure 29). Other groups have experienced unexpected stereochemical outcomes from glycosylation reactions with a carbonyl containing group at the 2-*O*-position of the reducing end of the donor, and remarked upon possible causes.[180-182,299] The unexpected 1,2-*cis* (α-linked) tetrasaccharide side-product **40** appeared to have formed in significant yield.

HSQC NMR spectra of tetrasaccharides **15** and **40** are displayed below (Figure 30) and show significant differences between the two molecules. As previously discussed, the *J* couplings of the anomeric proton signals is diagnostic for the presence of an α- or β- anomeric linkage. This figure highlights the difficulty sometimes encountered in calculating these coupling constants, due to overlap between anomeric and non-anomeric proton signals.

The HSQC NMR spectrum is presented for this comparison as it provides a distinct visual separation of the anomeric proton signals. These are found in the region described by ^{1}H chemical shifts of 4.5-6.0 ppm and between ^{13}C chemical shifts of 90-110 ppm. The four signals representing the anomeric protons of each residue within the tetrasaccharide are distinctly different. In the case of **15**, two of the anomeric proton signals closely overlap with each other and another proton signal from a benzyl CH_2. In the case of **40**, this also occurs for the anomeric proton at approximately ^{1}H chemical shift 5.5 ppm.

The signals representing the protons on each sugar ring also show a distinctly different pattern. These are found in the region described by ^{1}H chemical shifts of 3.0-5.5 ppm and between ^{13}C chemical shifts of 40-90 ppm. An example is seen in the two doublet of doublets signals between ^{1}H chemical shifts

of 3.0-3.5 ppm, which represent the proton at C2 in two of the sugar rings adjacent to the azide group. These two signals are well resolved in the spectra of **15** but overlap in the spectra of **40**. This may suggest that the conformation of the two tetrasaccharides is different, leading to slight differences in the chemical environments of many sugar ring protons.

There is no significant difference in the methyl (^{1}H chemical shifts around 2.0 ppm) and aromatic (^{1}H chemical shifts of 6.5-8.5 ppm) regions. The protons in these regions are in remote chemical environments and would not be expected to vary significantly with sugar ring conformation.

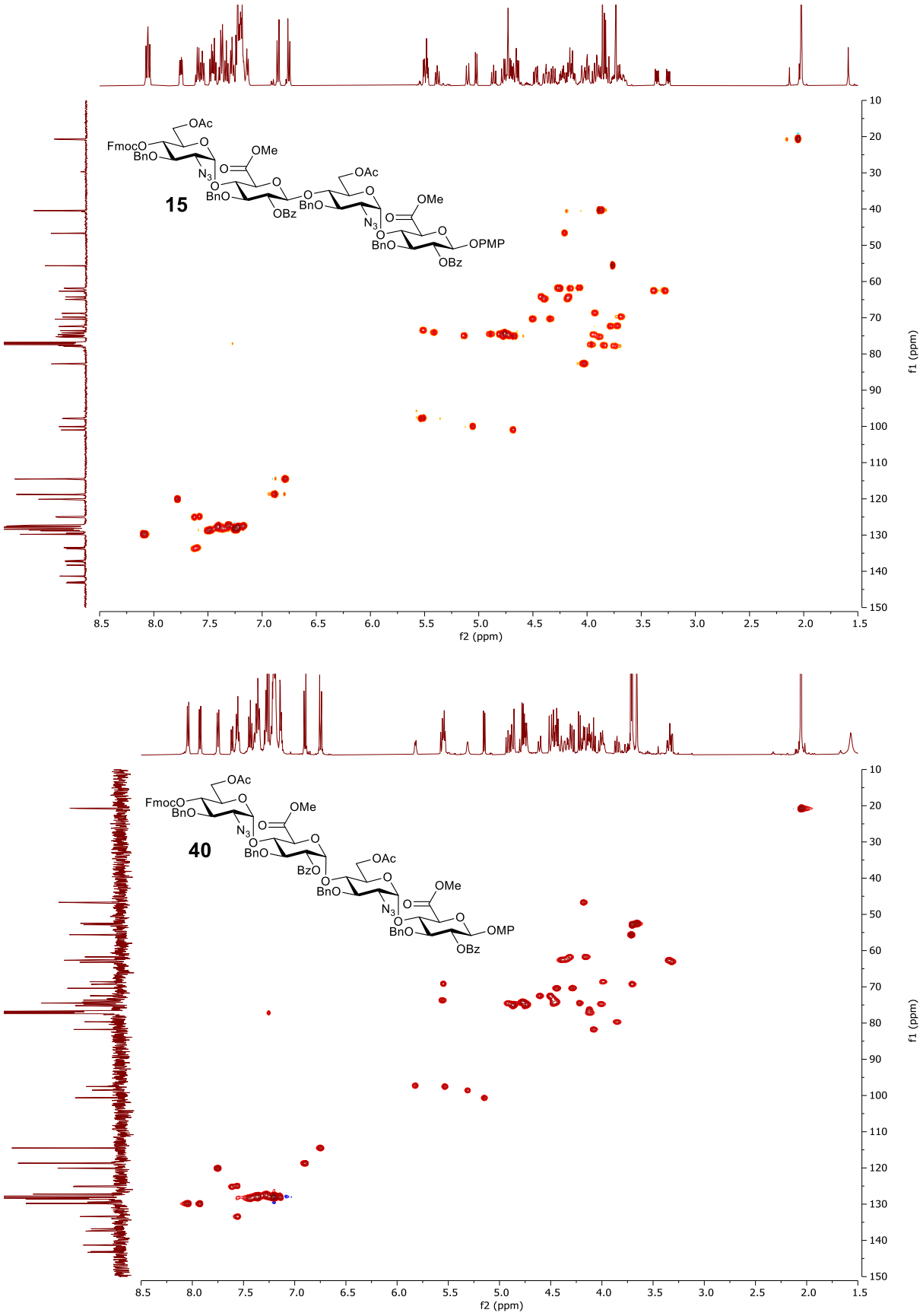

*Figure 30 – HSQC NMR spectra of the tetrasaccharide product **15** and unexpected product **38**. These spectra show significant differences between the two compounds.*

The glycosylation of donor **28** and acceptor **24** was repeated several times, and the same proportion of products was formed consistently. Additionally, modifications to the reaction conditions, by changing the solvent and temperature, did not reduce the formation of the unwanted side-product, but did reduce the overall yield. Similarly, an attempt using TBDMSOTf as the promoter in place of TMSOTf produced only a slightly lower yield, with unwanted side-product still forming. The side-product **40** was stable when stored in air for 2 years.

Glycosylation of *N*-PTFA donor **29** and acceptor **22,** producing tetrasaccharide **14**, also proceeded in a high yield (87%, Scheme 28). *N*-PTFA donors have similar reactivity to the TCA donors, and are less likely to rearrange to the amide side-product than TCA donors,[228] so this reaction was expected to work well. The initial experiment was conducted at the same temperature as the TCA equivalent, -20 °C. In this experiment the *N*-PTFA donor was observed to react rapidly following the addition of promoter, with TLC analysis indicating full progression of the reaction within minutes. A further experiment was conducted at the lower temperature of -78 °C, in which the *N*-PTFA donor fully reacted over 30 minutes by TLC analysis, and gave a slightly improved yield of the product compared to the experiment conducted at -20 °C. This is consistent with our expectation that the *N*-PTFA donor would perform similarly to, or better than, the TCA donor in our hexose system.

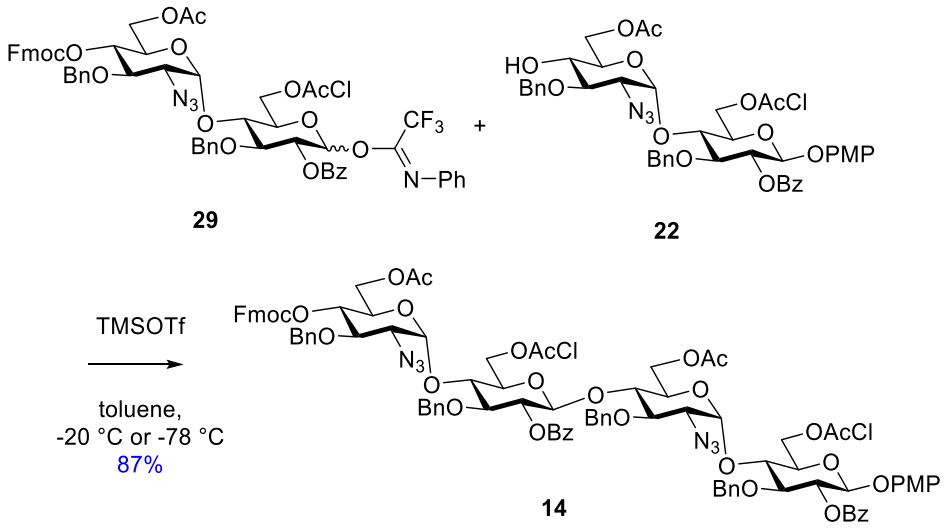

*Scheme 28 – Synthesis of tetrasaccharide **14** using glycosyl donor **29.***

However, the glycosylation of uronate *N*-PTFA donor **30** with acceptor **24** was very low yielding (5%) over several attempts (Scheme 29). All reactions appeared to stall, despite the addition of additional TMSOTf promoter and warming from -78 °C to higher temperatures of -20 °C, 0 °C and RT. Several changes to the reaction solvent, and an attempt using TBDMSOTf rather than TMSOTf as the promoter, gave no improvement. A small amount of product was observable by LC-MS in the reaction

mixture, but most of the material isolated following work-up was hemiacetal **26**, and unreacted acceptor **24**.

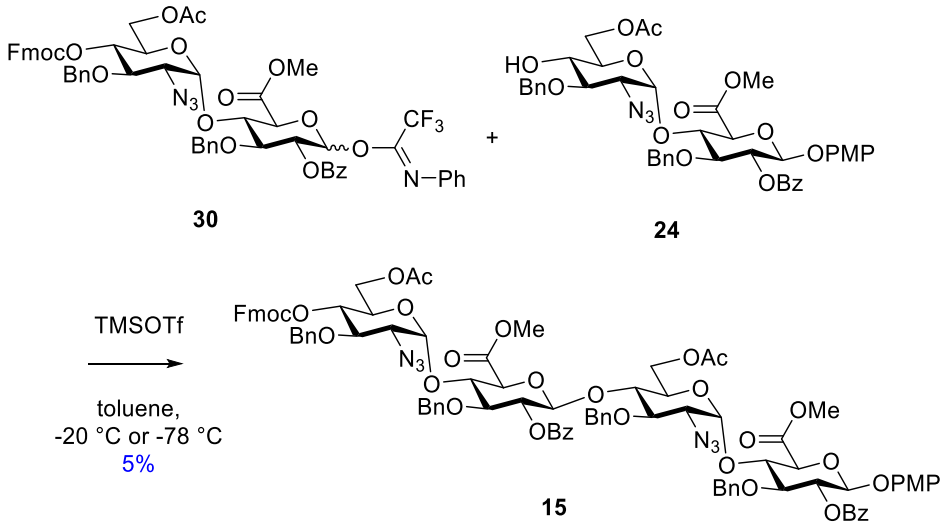

*Scheme 29 – Synthesis of tetrasaccharide **15** using glycosyl donor **30.***

Other activator systems for acetimidates have been reported in the literature, including recent reports of MeOTf and TBSOTf in significantly complex systems.[234,300] However due to time constraints, no other promoter systems beyond TMSOTf and TBDMSOTf were assessed for the acetimidate donors **27**, **28**, **29** and **30**.

Glycosylation of hexose thioglycoside donor **33** and hexose acceptor **22**, producing tetrasaccharide **14**, was successful but lower yielding (53%) than the equivalent acetimidate donor reactions (Scheme 30). Separate experiments with modifications to the reaction temperature and solvents all gave the product with a similar reduction in yield.

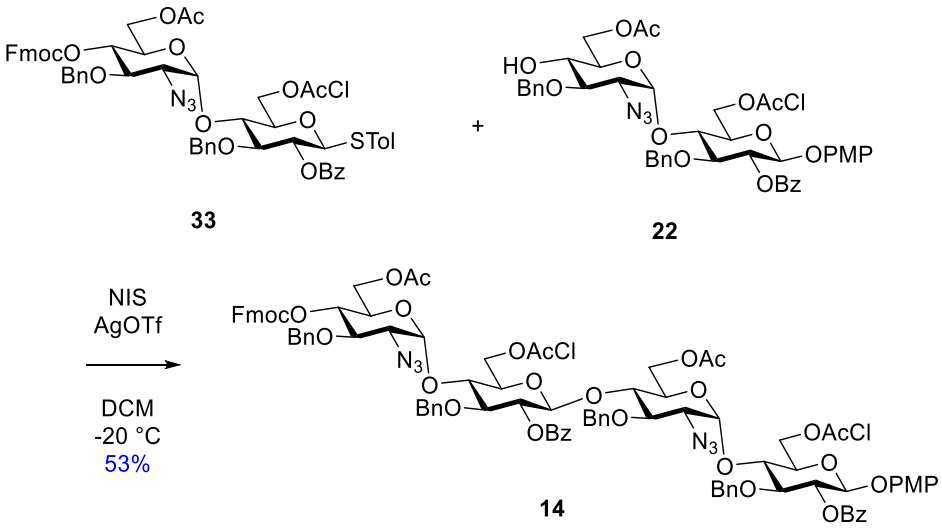

*Scheme 30 – Synthesis of tetrasaccharide **14** using glycosyl donor **33.***

Returning to the original solvent and temperature conditions, the reaction was attempted with variety of donor activation methods. In addition to the NIS/AgOTf promoter system familiar to our group,[194] the 1-(phenylsulfinyl)piperidine (BSP) / Tf_2O promoter system[301] and the dimethyl disulfide (DMDS) / Tf_2O promoter system were also assessed (Table 4).[302] In the BSP system, the donor **33**, BSP, 2,4,6-tri-tert-butylpyrimidne (TTBP) and 3Å molecular sieves were dissolved in dichloromethane and cooled to -60 °C. The reaction was then treated with trifluoromethanesulfonic anhydride and stirred for 5 minutes to form an activated leaving group, before the addition of acceptor **22** and stirring for 30 minutes before work up. In the DMDS system, a 1 M promoter solution was first made by adding trifluoromethanesulfonic anhydride (0.17 mL, 1 mmol) to a solution of dimethyl disulfide (0.10 mL, 1.1 mmol) in anhydrous dichloromethane (0.75 ml) at 0 °C and stirring the mixture for 30 min at the same temperature before use. Then, a solution of the donor **33** and acceptor **22** in dichloromethane at -40 °C was treated with a small amount of the promoter solution, stirring for a short time before work up. The results of these two promoter systems in our hands was poor and gave lower yields of product than the NIS/AgOTf promoter system.

Entry	Activation system	Yield [%]
1	**NIS/AgOTf**	53
2	**BSP/TTBP/Tf_2O**	47
3	**DMDS/Tf_2O**	31

*Table 4 - Yields of the glycosylation of donor **33** and acceptor **22** using multiple activation systems.*

Additionally, in the case of the BSP/TTBP/Tf_2O promoter system, a test was carried out to determine that the activation system was functioning, using existing thioglycoside materials that had been synthesised during this work. Use of the BSP system in the glycosylation of the original monosaccharide thioglycoside donor **10** and monosaccharide acceptor **11** to produce disaccharide **9** proceeded in high yields of 85% (Scheme 31). This was comparable to results from the NIS/AgOTf system. This result indicates that the activating system was working as expected.

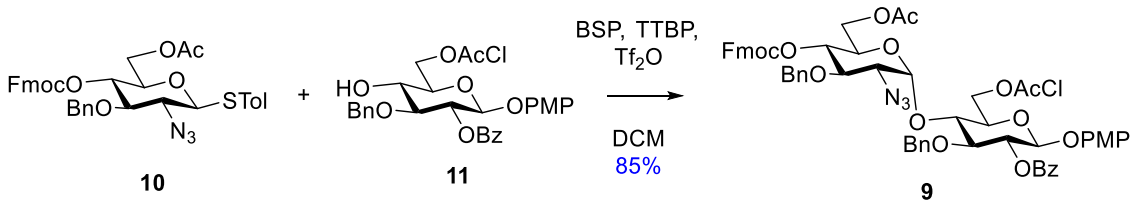

*Scheme 31 - A re-synthesis of disaccharide **9** using the BSP/TTBP thioglycoside activation system. The success of this test indicates that the activation system is working as expected.*

Glycosylation of uronate thioglycoside donor **34** and uronate acceptor **24** was, somewhat surprisingly, as effective as the corresponding hexose thioglycoside glycosylation, giving an average yield of 56% across three reactions with the same conditions (Scheme 32). Whilst moderately more challenging to

purify using column chromatography, tetrasaccharide **15** was isolated. This mirrors the experience of other groups who have reported favourable glycosylation yields using uronate thioglycoside donor systems.[201,238-240] However, this reaction was still substantially lower yielding than the equivalent hexose acetimidate glycosylation reactions. Only the NIS/AgOTf activating system was tried for the reaction of **34** and **24**, as the experience of the hexose analogue suggested that neither of the other activation systems tried would produce a better result.

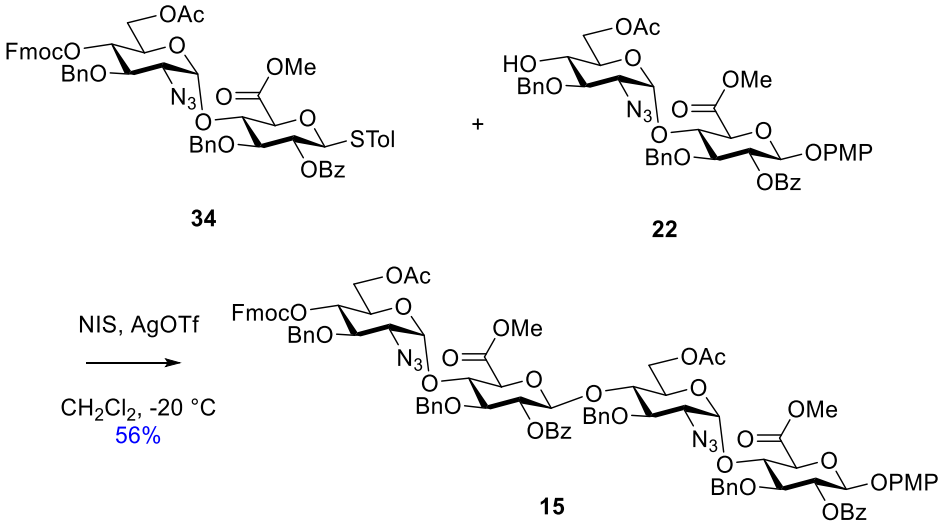

*Scheme 32 – Synthesis of tetrasaccharide **15** using glycosyl donor **34**.*

Other activation methods for thioglycosides have been reported, such as the Ph_2SO/Tf_2O system,[303,304] the *p*-nitrobenzenesulfenyl chloride/AgOTf system,[305] MeOTf activation,[306] or the recently reported DIDMH/TfOH system.[307] These promoter systems could be tested in our glycosylation reactions in future work.

2.3 Conclusions

The synthesis of the disaccharide **9** was successfully carried out on a large scale. Hexose and uronic acid analogues of disaccharide **9** were then accessed. Glycosyl acceptors and hemiacetals of each analogue were synthesised. The hemiacetals were then used to form TCA, *N*-PTFA and thioglycoside glycosyl donors. Each of these donors was accessed in moderate to high yields, and the uronate donors accessed using the same procedures. Glycosylation reactions using these combinations of donors and acceptors were carried out to determine the relative effectiveness of each. This investigation has compared both hexoses and uronic acid glycosyl donors, and the donors themselves. The synthesis of the glycosyl chloride donor was successful. However, despite several alternative methods that were tried, the synthesis of the uronyl chloride was unsuccessful in the timeframe of this work. Because of this problem, the chlorides were not used as a donor system in the comparative [2+2] glycosylation reactions.

From this work, it can be concluded that the direct use of uronic acids as donors and acceptors, in systems using our protecting group strategy and the glycosylation methods assessed, does not appear to be preferable. The yields of [2+2] glycosylation reactions using the TCA donor system were as good as previously reported by our group[194] using the hexose species (average yields of 90%). However, this glycosyl donor performed poorly using the uronate analogue (average yields of 47%) and generated a significant quantity of side-product that was not trivial to separate from the target material. This side-product has the same mass as the target product by MS, and NMR analysis showed this was a tetrasaccharide with an unexpected 1,2-*cis* linkage formed in the [2+2] glycosylation. The yields of [2+2] glycosylation reactions using the *N*-PTFA system were also very good for glycosylation reactions using the hexose species (average yields of 85%). However, the yields using the uronate analogue were extremely poor (average yields of ~5%) and the product was difficult to isolate. The thioglycoside donor system gave moderate yields for glycosylation reactions of the hexose analogues, with the best yields using the NIS/AgOTf promoter system (average yields of 53%). However, these yields compare poorly to the acetimidate equivalents. Several alternative activating methods were tested, but none of these promoter systems led to improved yields. The uronate thioglycoside analogue performed similarly to the hexose analogue (average yields of 56%), which was impressive given the yields obtained using the previous two uronate donors.

Ultimately, these results were not enough to suggest a change in strategy for later oligosaccharide synthesis. The moderate yield and selectivity of the uronate thioglycoside donor compared to the uronate imidates suggests this glycosylation strategy could be further explored. However, the overall yield of a high yielding [2+2] glycosylation using hexose imidate donors, followed by selective 6-*O*-

deprotection and oxidation of the product, would likely be comparable. Furthermore, it is expected from prior experience in this group that the glycosylation yields for extension of longer oligosaccharides will get progressively worse. Therefore, starting from an average yield of 56%, subsequent chain extensions using tetrasaccharide and hexasaccharide acceptors may become very poor yielding. This would compare badly to assembling a hexose chain followed by late oxidation. The safest option for the synthesis of a complex oligosaccharide would therefore be to use our existing methodology.

Our comparison of donor systems could be further extended to look at other types of glycosyl donor and assess if they change the effectiveness of uronic acids in glycosylation reactions. Other sugar systems, such as idose and iduronic acid donors and acceptors, could also be assessed. In addition, the issue of forming a uronyl α-chloride could be revisited, and a procedure to access this species developed. This work has been published.[308]

3. Chapter 3

3.1 Towards the synthesis of octasaccharide targets

As previously discussed, the heparan sulfate mimetic targets **1** and **2** were identified by collaborator, Prof. J. Turnbull of the University of Liverpool,[275] as potential pharmaceutical targets with expected high activity as a mediator of FGF2-FGFR1 binding. Access to quantities of these single chemical entities, as opposed to isolated mixtures of natural HS, are desired for further investigation of the sulfation pattern required for FGF2-FGFR1 interaction. To this end, a synthetic strategy was developed from known chemistry within our group to access these targets.[194] In the last chapter, it was determined that directly glycosylating uronic acids was not possible with our existing protecting group strategy and the three types of glycosyl donor assessed. Therefore, a total synthesis begun using the established method of oxidation following chain assembly.

A feature of note in this synthesis is the incorporation of the 2-acetoxymethylbenzoate (AMB) protecting group.[273,274] AMB is used in the protection of the 3-*O*-position in the glucosamine residues of two disaccharide building blocks. AMB is also used in one instance at the 2-*O*-position of the iduronic acid component. The AMB group is cleavable under the same conditions as primary acetates, whilst primary and secondary benzoates elsewhere in the molecule remain stable (Scheme 33). Under these conditions, the primary acetate present on the AMB group is removed, exposing the 2-hydroxymethyl group, which then may attack the adjacent carbonyl group, leading re-cyclisation and deprotection. This is driven by the extremely favourable formation (via cyclisation) of phthalide.

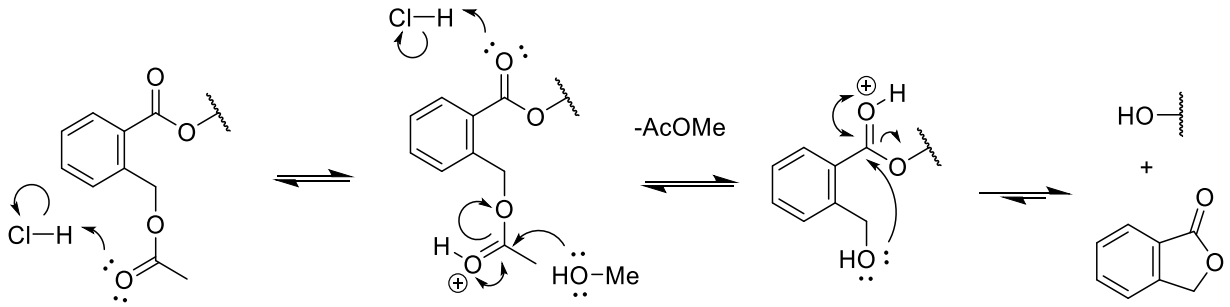

Scheme 33 - The acid promoted deprotection of an AMB group using anhydrous HCl. Here, protonation of the carbonyl oxygen and subsequent nucleophilic attack by the chloride ion leads to the ejection of acetyl chloride, leaving the negatively charged oxygen to quickly attack the also protonated linker carbonyl, cleaving the bond to the hydroxyl group and reforming phthalide. The favourable formation of phthalide drives the reaction.

This method is preferential to simply protecting the 3-*O*-position of the glucosamine residues with an acetate directly. Such a motif would be a secondary acetate and is therefore more challenging to selectively deprotect with respect to the secondary benzoate protecting groups elsewhere in the

molecule. 3-*O*-AMB protection allows selective access to sulfate the glucosamine 3-*O*-position at the same time as glucosamine 6-*O*-positions protected by primary acetates. Additionally, AMB installed in a 2-*O*-position should still be able to participate in glycosylation in the same manner as a benzoate or acetate, which our group has used in this position in previous work. When installed at the iduronic acid 2-*O*-position in disaccharide building block **6**, AMB should allow stereochemical control of the [n+2] glycosylation using this disaccharide donor to achieve the 1,2-*trans* linked product.

Other groups have used a variety of variations on a selectively activated, ring-closing driven protecting group, including 2-(azidomethyl) benzoate,[309,310] 2-(chloroacetoxymethyl) benzoate,[311] and (2-nitrophenyl) acetyl.[195] These protecting groups have been used effectively in other synthesis, but would not be suitable for our purposes. The required deprotection conditions do not fit within our orthogonal protecting group strategy.

There is evidence that the presence of 3-*O*-sulfation in synthetic sulfated oligosaccharides may have a specific biological effect.[25,312] Therefore, while these two specific targets are highly desirable, it is also extremely worthwhile to develop the methodology to selectively access the 3-*O*-position for sulfation within our existing protecting group strategy.

3.1.1 Synthesis of 2-(acetoxymethyl) benzoic acid

The AMB protecting group is installed using 2-(acetoxymethyl) benzoic acid. This reagent is commercially unavailable, although our group has synthesised and characterised the material previously.[313] A synthetic pathway was established to produce AMB from the cheap reagent phthalide, based on previous literature (Scheme 34).[311] In this pathway, phthalide is first saponified using excess NaOH in water, and then precipitated as the protonated 2-(hydroxymethyl) benzoic acid **41** by the addition of concentrated HCl. This material is then filtered off, washed, and dried on a rotary evaporator to remove water. Following this, the hydroxyl group of the acid is then acetylated by the slow addition of AcCl into a dilute solution of the acid in DMF, in the presence of the base 2-chloropyridine. Following a period of stirring, the reaction mixture is diluted and washed to remove DMF and then placed on the rotary evaporator, evaporating to near dryness. 2-(Acetoxymethyl) benzoic acid **42** is then rapidly precipitated on the addition of EtOAc followed by a large volume of hexanes. It is crucial to filter off the precipitate which forms in the first few minutes, as leaving the solution to precipitate further leads to the formation of phthalide and the loss of the product.

The choice of base was critical to the success of the reaction and was made based on the rationale of pKa, as detailed in the work of Ziegler and Pantkowski.[311] The use of species with higher basicity, such as pyridine, would quickly lead back to the starting material phthalide through a mixed anhydride intermediate. Furthermore, weak bases gave no reaction, as was the case when sodium hydrogen

carbonate was used. In our case, the base 2-chloropyridine was chosen as the pKa of the conjugate acid, 0.72, was much lower than the pKa of 2-hydroxymethylbenzoic acid at 3.84. Therefore, this base was several orders of magnitude from deprotonating the carboxylic acid group. Initial experiments had used the base 2-methoxypyridine, with a conjugate acid pKa of 3.28, which may have been able to deprotonate our carboxylic acid and lead to the return of starting material.

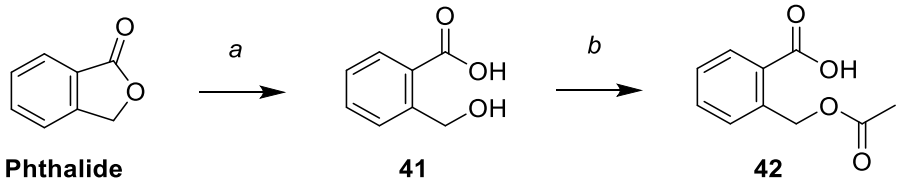

a) NaOH, H_2O; b) AcCl, 2-chloropyridine, DMF

*Scheme 34 - The two-step synthesis of 2-(acetoxymethyl) benzoic acid **42** from phthalide via 2-(hydroxymethyl) benzoic acid **41**. See Table 5 for yields.*

This synthesis proved to be challenging. Initial attempts failed to produce the product. It was later recognised that this failure was due to procedural errors. In the saponification, it is important to filter the precipitated acid directly after addition of HCl and whilst still hot. Allowing the reaction mixture to cool, as is generally standard practice for the precipitation of a product, caused the material to re-cyclise and form phthalide. Furthermore, a substantial period of rotary evaporator time was required for the solid material to dry following filtering. Several hours of exposure on the rotary evaporator was sufficient to achieve a constant mass of the acid **41**. A yield of approximately 60% was consistently achieved over several batches.

In the acetylation step, other problems were encountered. The precipitate formed within the first minute following the addition of hexanes had to be filtered and dried quickly. Leaving the mixture for any greater length of time led again to the reformation of phthalide. Attempts to evaporate down the mother liquor and re-crystallise the leftover material also led to the reformation of phthalide. Despite TLC analysis showing majority conversion, this step consistently yielded around 20%, with the rest of the material recoverable only as starting material phthalide. 2-(Acetoxymethyl) benzoic acid has been previously described as too unstable to be isolated,[314] so this yield was considered acceptable. The results of several experiments to optimise the procedure are detailed below (Table 5).

Entry	Saponification yield (reaction a) [%]	Isolated mass of **41** [g]	Acetylation yield (reaction b) [%]	Isolated mass of **42** [g]
1	45	52	0	0
2	76	87	0	0
3			0	0
4			6	3
5	85	97	0	0
6			0	0
7			2	1
8			21	5
9	61	70	22	10
10			20	9
11	65	84	25	11.5
12			18	11
13	56	71.5	22	10
14			25	11.5

*Table 5 - Results of various attempts to synthesise 2-(acetoxymethyl) benzoic acid **42**. Saponification yields are spread across several attempts as the material from each saponification was split into several smaller batches to attempt the acetylation, due to the dilution required in the second step. See Scheme 34 for reaction conditions.*

The product was also only isolated in around 95% purity, with the impurity appearing as phthalide starting material by ^{1}H NMR analysis. Subsequent recrystallisation attempts could not entirely remove the impurity, and it was suspected some re-cyclization occurred each time the product was dissolved. For this reason, later batches of **42** were only recrystallised once and used with the minor impurity present. Phthalide did not appear to interfere with the subsequent chemistry and was easily removed following the reaction.

With a robust synthetic protocol to access **42** established, the reaction was scaled up. A typical full-scale reaction process began with the saponification of 100g of phthalide, and following acetylation, around 20g of **42** was recovered. The second step of the reaction was carried out in two equal batches, which limited the volume of DMF solvent that had to be handled at any one time. Using this method, a large amount (approximately 80g over all reactions) of 2-acetoxymethyl benzoic acid, with a purity of 95% by NMR, was synthesised. The material was able to be stored under Ar in a freezer for over 2 years with little evidence of degradation by NMR.

3.1.2 Synthesis of disaccharide building blocks

The starting and terminal disaccharides of the octasaccharide chain, disaccharides **5** and **8**, were kindly provided by Dr. Karl Shaffer, as they had already been produced for a related synthesis. However, the disaccharides **6** and **7** needed to be produced from starting materials available in our laboratory. These disaccharides contain a 3-*O*-AMB protecting group on the glucosamine residue and form the core of each octasaccharide target.

The initial synthesis of monosaccharide donors was carried out with procedures described in the previous chapter (Scheme 35). The starting material **12** was protected as the 4,6-*O*-benzylidene acetal to give **16** in high yield of 82%. This gives selective access to the monosaccharide 3-*O*-position, which was then protected as AMB using dicyclohexylcarbodiimide (DCC) coupling to give monosaccharide **43** in high yield of 85%. Following this step, the 4,6-*O*-protecting group is removed to **44** in 71% yield, and the 6-*O*-position selectively protected by treatment with benzoyl chloride or acetyl chloride to give **45** in 72% yield or **46** in 86% yield respectively. The monosaccharide 4-*O*-position could then be finally protected with Fmoc, by stirring in a concentrated base/Fmoc-Cl slurry to give the fully protected monosaccharides **47** in 75% yield and **48** in 88% yield.

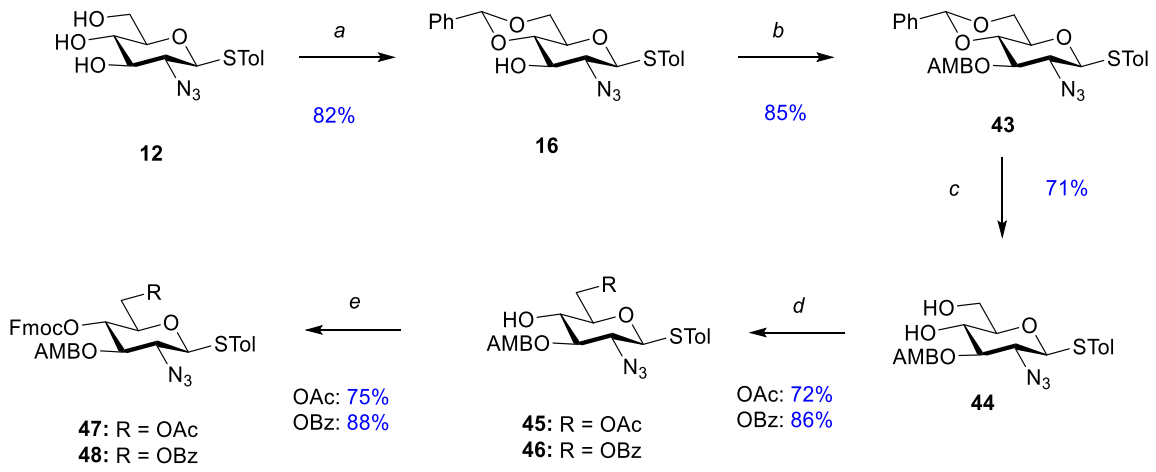

a) benzaldehyde dimethy acetal, CSA, DMF, 60 °C; b) 2-(acetoxymethyl) benzoic acid, DCC, DMAP, DCM, RT;
c) AcOH 60% in water, RT; d) AcCl or BzCl, pyridine, DCM, -78 °C;
e) FmocCl, pyridine, RT

Scheme 35 - The synthesis of two monosaccharide building blocks with an AMB group at the 3-O-position.

DCC is a cheap reagent and the coupling in our hands was high yielding. However, DCC is converted to insoluble dicyclohexylurea (DCU) during the reaction, which can cause purification issues. DCU was removed by dissolving the concentrated crude reaction mixture in toluene following work up, which caused DCU to precipitate out of solution at RT overnight. Filtering through a thick silica pad removed the insoluble precipitate, and then the product was isolated from any remaining impurities by chromatography.

Monosaccharide **43** was found to precipitate from a mixture of EtOAc and hexanes. Subsequently, **43** was dissolved in EtOAc and petroleum ether was added with stirring until just prior to the mixture turning opaque. The mixture was then left standing in a fridge over 2 days, leading to the formation of crystals suitable for structural analysis. A single crystal x-ray structure was able to be acquired (Figure 31), confirmed the successful installation of the AMB protecting group at the 3-*O*-position.

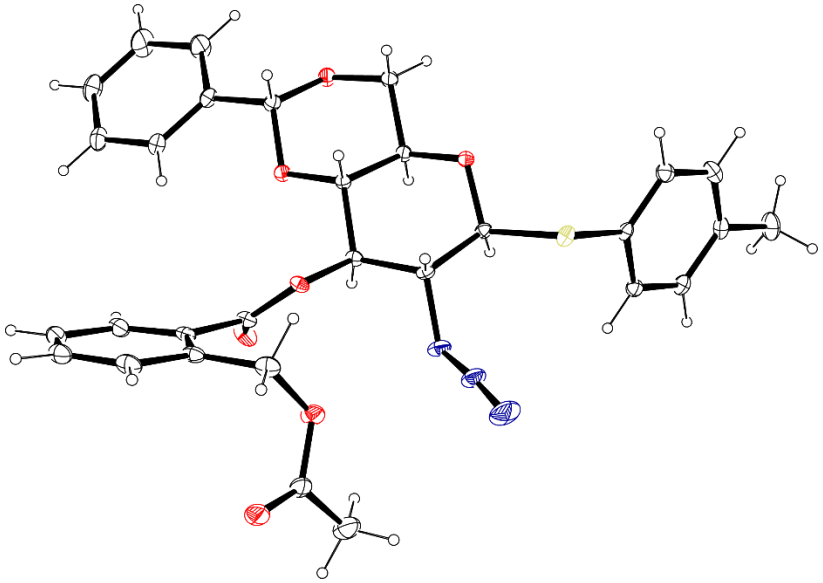

*Figure 31 - The ORTEP plot of the single crystal structure of monosaccharide **43.***
Shown as 30% probability ellipsoids. The 3-O-AMB group is correctly installed. This material was readily crystalline, greatly aiding purification.

In later batches, this synthetic pathway was optimised to carry out the selective monosaccharide 6-*O*-Ac or 6-*O*-Bz protection and subsequent 4-*O*-Fmoc protection in a one pot two step manner. This afforded **47** in 67% yield and **48** in 86% yield directly from **44** (Scheme 36).

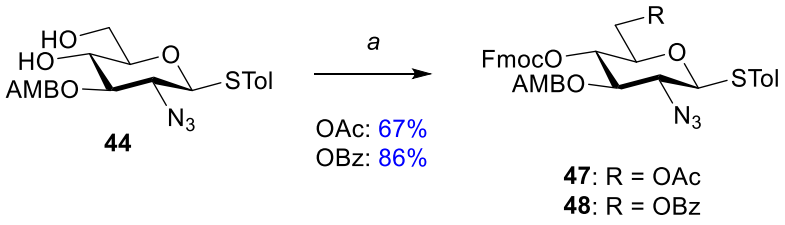

a) AcCl or BzCl, pyridine, DCM, then FmocCl

*Scheme 36 - Optimised synthesis of monosaccharides **47** and **48** from **44**.*
Acquisition of a new batch of Fmoc-Cl reagent allowed the one pot two step 6-O-Ac or 6-O-Bz protection followed by subsequent 4-O-Fmoc protection, with just 1.2 equivalents of Fmoc as opposed to the large quantities used previously in a slurry.

This one-pot, two-step procedure was carried out with much smaller quantities of Fmoc-Cl than the original 'slurry' method, which made the reaction purification much easier. This was due to the formation of much smaller amounts of insoluble dibenzofulvene-polymer by-product, which previously began to form rapidly following work-up. This by-product can also form when Fmoc groups are deprotected in the presence of base (Scheme 37).[315] By-product formation was exacerbated by the high number of equivalents of Fmoc-Cl used in the original method.

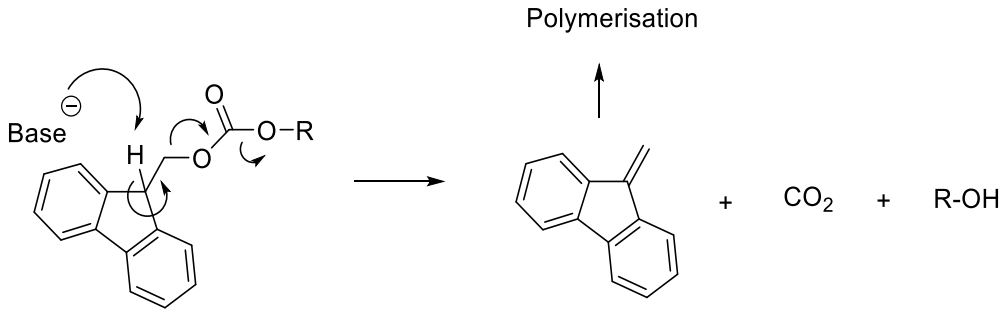

Scheme 37 - The mechanism of base-catalysed Fmoc deprotection.

Earlier attempts to carry out the protections in this dilute manner, which was reported elsewhere,[196,198,200] had met with no success in our hands. It is thought that the quality of the Fmoc-Cl reagent used could be responsible for this change. Our revised synthetic pathway, featuring one-pot two-step 4-*O*- and 6-*O*-protection, was successfully carried out using a fresh batch of Fmoc-Cl. The older batch of Fmoc-Cl was disposed of.

Once the requisite monosaccharides had been accessed, glycosylation of 6-*O*-Ac protected monosaccharide donor **47** and 2-*O*-Bz protected idosaccharide acceptor **49**, or 6-*O*-Bz protected monosaccharide donor **48** and 2-*O*-AMB protected idosaccharide acceptor **50** respectively, produced the corresponding disaccharide building blocks **6** and **7** (Scheme 38). The idose monosaccharide acceptor components **49** and **50** were synthesised and kindly provided by Dr Karl Shaffer. These idose monosaccharides had been synthesised for use in other targets, and an excess was produced for use in this synthesis as well.

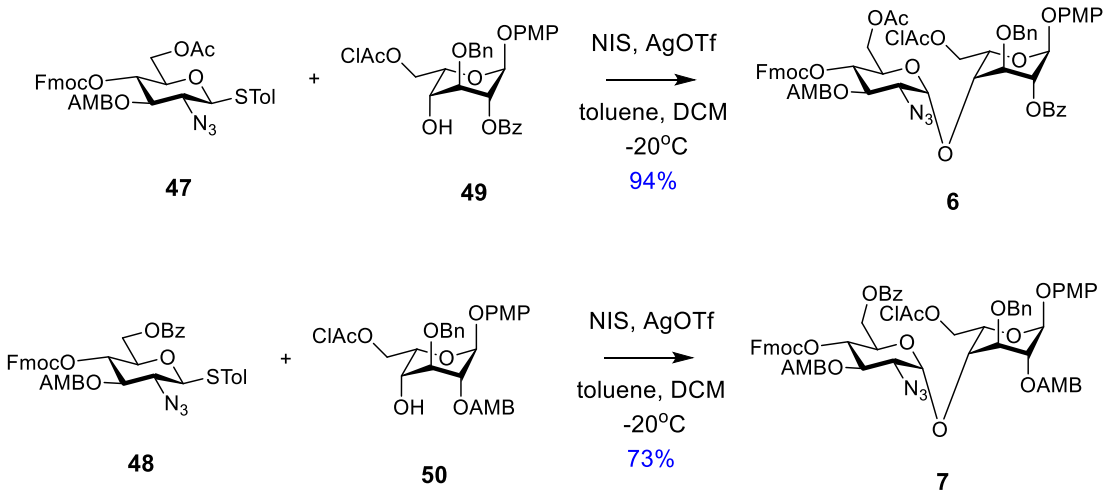

*Scheme 38 - The synthesis of core disaccharides **6** and **7** for octasaccharide assembly.*

Batches of 6'-*O*-Ac protected disaccharide **6** were subjected to selective CAN mediated 1-*O*-PMP deprotection to produce the hemiacetal **51**. From the hemiacetal, TCA disaccharide donor **52** or *N*-PTFA disaccharide donor **53** were obtained using the appropriate reagents. Meanwhile, batches of 6'-

O-Bz protected disaccharide **7** were subjected to selective CAN mediated 1-O-PMP deprotection to produce the hemiacetal **54**. From the hemiacetal, TCA disaccharide donor **55** or *N*-PTFA disaccharide donor **56** were obtained using the appropriate reagents (Scheme 39). The formation of the core disaccharides and their subsequent transformations proceeded in good yields, smoothly, and as expected.

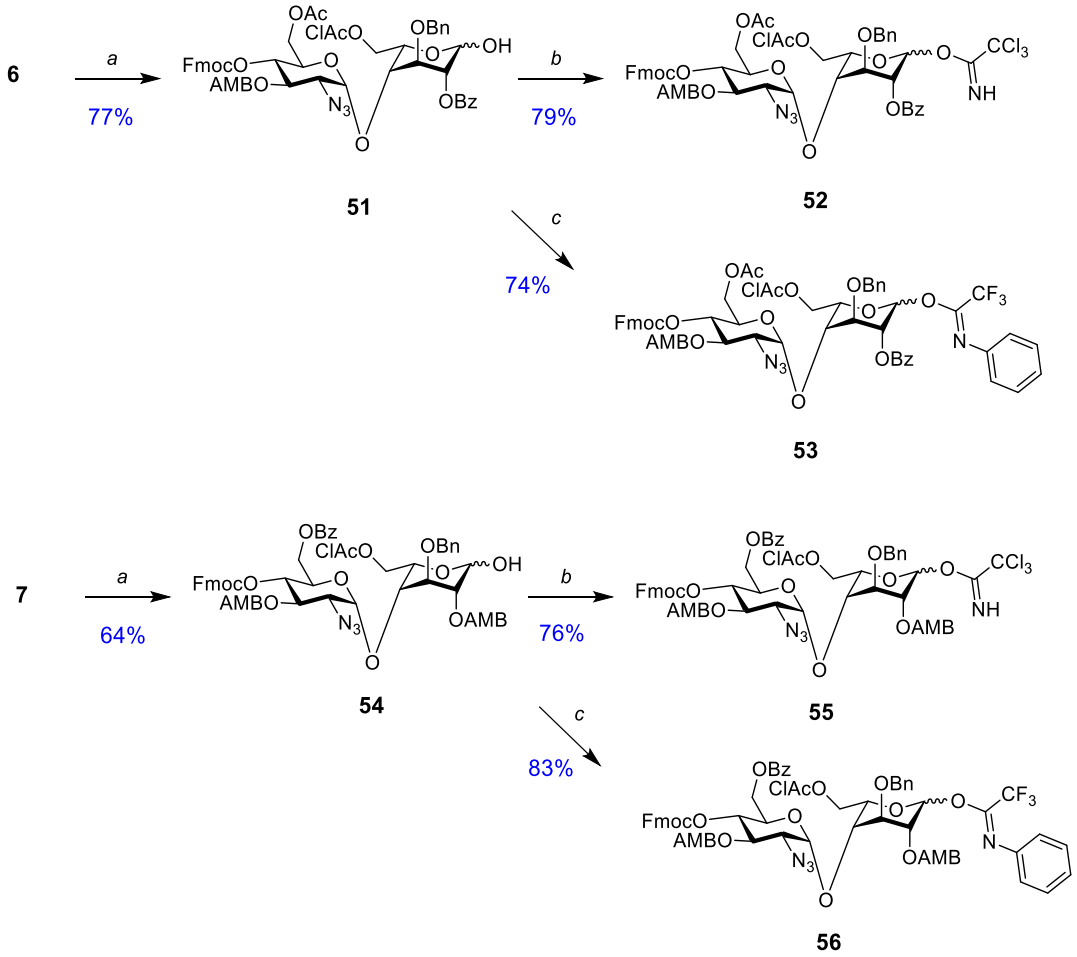

a) CAN, water, MeCN, RT; b) CCl_3CN, NaH, DCM, RT; c) $CF_3CN(Ph)Cl$, NaH, DCM, RT

Scheme 39 - The synthesis of disaccharide donors for octasaccharide assembly.

It appeared that the presence of the 2-*O*-AMB on the idose component of the 6-*O*-Bz disaccharide **7** did not have a significant effect on donor formation. With disaccharide donors **52**, **53**, **55** and **56** accessed, oligosaccharide chain assembly could begin.

3.1.3 Accessing alternative donors for the final glycosylation of octasaccharide assembly

The disaccharide used in the final glycosylation of octasaccharide assembly, which forms the non-reducing end of the octasaccharide, was initially provided as the TCA donor **57**. For reasons that will

be discussed in the following chapter, it was desired to access *N*-PTFA donor **59**. However, this required intentional hydrolysis of TCA donor back to hemiacetal **58** (Scheme 40). This was carried out over several reactions with a THF/water solvent system and TMSOTf as a promoter. Optimised conditions were found with a temperature of 0 °C used to minimise rearrangement to the acetamide by-product. This hydrolysis reaction afforded hemiacetal **58** in 77% yield. Following this, the *N*-PTFA donor **59** was accessed in the same manner as previously shown, in a high yield of 94%.

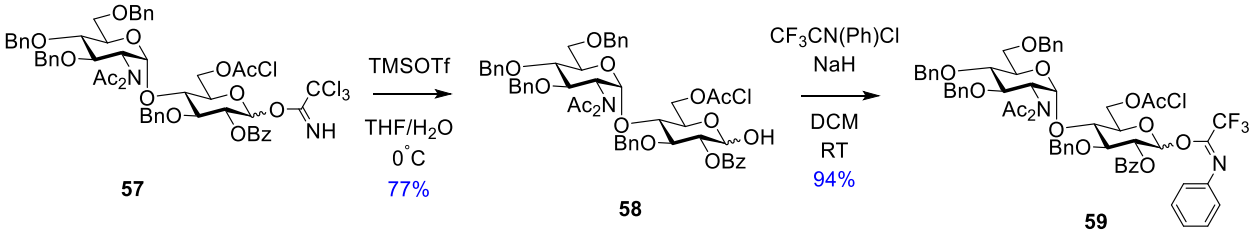

Scheme 40 - Hydrolysis and subsequent N-PTFA donor formation of the terminal disaccharide. This disaccharide was provided in the TCA donor form. Intentional hydrolysis was carried out to generate hemiacetal for transformation into new donors.

Later, multi-gram quantities of the 1-*O*-PMP protected disaccharide **5** were synthesised by colleagues. Disaccharide **5** was then used to generate new batches of glycosyl donors (Scheme 41). CAN mediated 1-*O*-PMP hydrolysis of disaccharide **5** afforded the hemiacetal **58** in 74% yield. TCA donor formation procced in high yield of 82%, whilst *N*-PTFA donor formation proceeded in a slightly lower but still high yield of 73%. Due to the availability of **5**, intentional hydrolysis of **57** was not used to access **58** in later syntheses. Some hemiacetal recovered from attempted octasaccharide glycosylation reactions was also used to generate the donors **57** and **59**. NMR and MS analysis confirmed no difference between the materials acquired through these different methods.

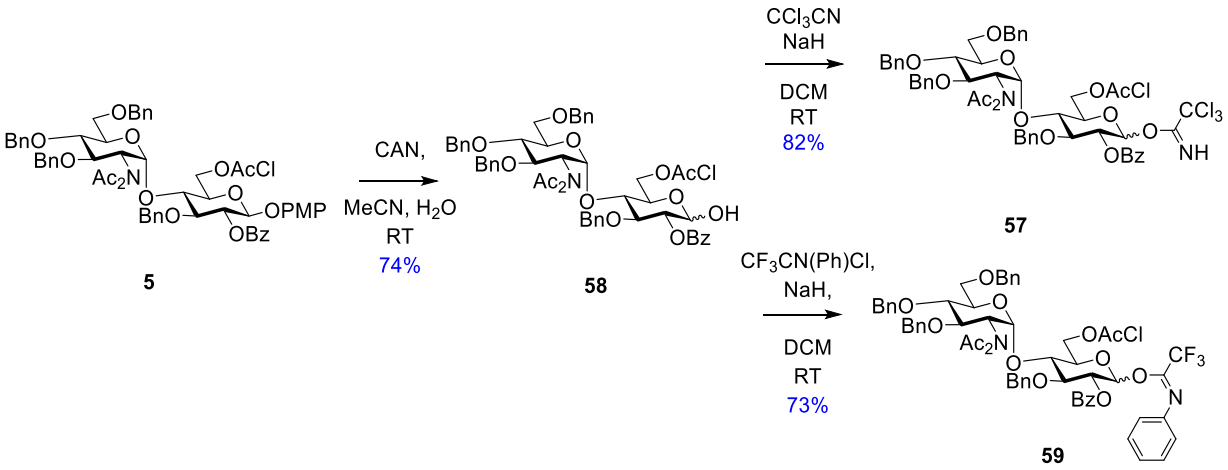

*Scheme 41 - The re-synthesis of terminal disaccharide donors **57** and **59** from the provided disaccharide **5**.*

Furthermore, an attempt was made to synthesise the thioglycoside donor **60** of this disaccharide. As detailed earlier in this work, thioglycosides have been made directly from hemiacetals and have proven to work in difficult glycosylation systems. However, the presence of a *N*-Ac_2 protecting group in this disaccharide, which is known to be easily acid/base labile and thermally unstable, was a cause for concern. In contrast, NHAc is exceptionally stable and requires specific conditions to remove.[316,317]

Firstly, the in situ generation of a bromide using an Appel reaction, and subsequent formation of thioglycoside in a one-pot two step procedure[318] was tested (Scheme 42). The reaction required the use of tetrabutylammonium bromide (TBAB) to catalytically interconvert the α-bromide to the β-bromide, increasing the reaction rate.

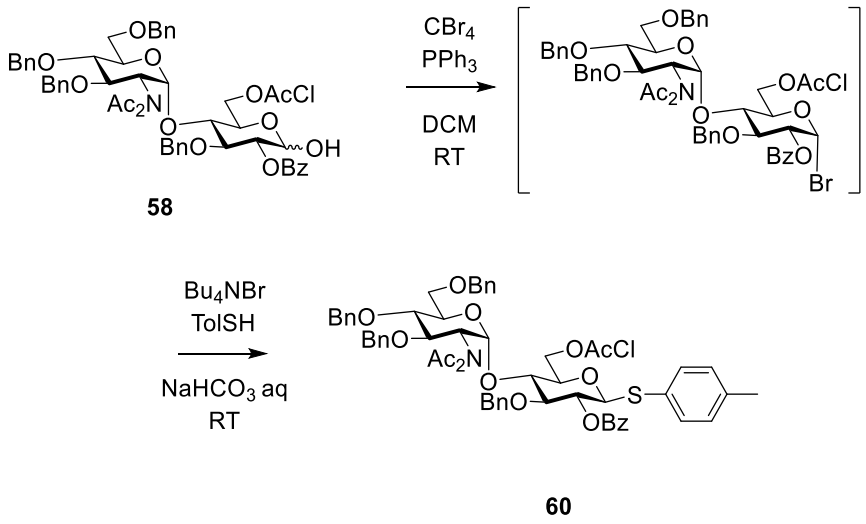

Scheme 42 - The attempted synthesis of a thioglycoside donor through a bromide intermediate. In this reaction, Appel chemistry is used to form a reactive bromide species, which is further reacted to form a thioglycoside without purification.[318] The reaction was ultimately unsuccessful in our hands.

The first step of this reaction appeared to proceed well by TLC analysis. This result was in line with conversion described in the procedure. However, on addition of the reagents for the second step, no further reaction was observed. This reaction yielded only a small amount of the α-bromide and returned mostly the starting material following chromatography. Minor impurities relating to displacement of the 6-*O*-AcCl chloride by the thiol were also observed.

The original procedure utilised a biphasic dichloromethane/aqueous system in which the aqueous phase contains 10% sodium bicarbonate. This acts to quench the HBr formed in the reaction. It was thought that removing the biphasic layer could remove the possibility of hydrolysis of the bromide, so the reaction was modified to use DMF as the solvent and the base replaced with potassium carbonate, which is sparingly soluble in DMF. This would be sufficient to quench the small amount of acid formed. The original procedure reports that bromide formation works nearly as well in DMF, with 85%

conversion to the bromide compared to 90% for dichloromethane. However, these modified conditions produced a very similar poor result.

After reviewing reports featuring the glucosamine residue *N*-Ac_2 protecting group, it appeared that the group would survive in the presence of pyridine[306,319]. Based on this, a further modification was made. With dichloromethane as the solvent, a full equivalent of pyridine was added instead of using biphasic conditions in the second step. However, this produced the same result as previous attempts. It appeared that this procedure could not be used to generate the thioglycoside on this hemiacetal.

To check that the bromide formation was working correctly, a solution of hemiacetal **56** was subjected to the Appel reaction and then isolated. This returned the α-bromide as expected, but in a low yield of around 30%. It appeared that some of the bromide hydrolysed during purification, which is expected as bromides are reactive. Hemiacetal **36** was also recovered. Other side products were observed but could not be identified or isolated.

Alternatively, conditions previously described were used in attempts to access the thioglycoside **60** through the anomeric acetate.[308] The hemiacetal **58** was treated with acetic anhydride and sodium acetate in toluene, conditions that have been previously optimised, to form the acetate **61** (Scheme 43). However, this reaction gave a low yield of the acetate of 25%. The product was mostly the α-acetate, with only trace peaks of the β-acetate observed in the ^{1}H NMR spectrum. Having previously discussed that the desired acetate anomer is the β-acetate for reactivity in the next step,[286] this result was disappointing. Although α-acetate should react in the presence of $BF_3{\cdot}OEt_2$ and a thiol to give the desired product, the reaction time would be significantly longer. This could lead to side reactions involving the chloroacetate. Furthermore, another group have reported that this formation can be carried out in a one pot two step manner using $BF_3{\cdot}OEt_2$ to promote both acetylation and thioglycoside formation,[320] which would remove a chromatography step. However, attempts at this methodology using our hemiacetal resulted in only trace product, with some of the material isolated as the α-acetate **61** (10%) and the remainder as the hemiacetal **58**. Mass recovery was particularly poor in this attempt, with many side products observed.

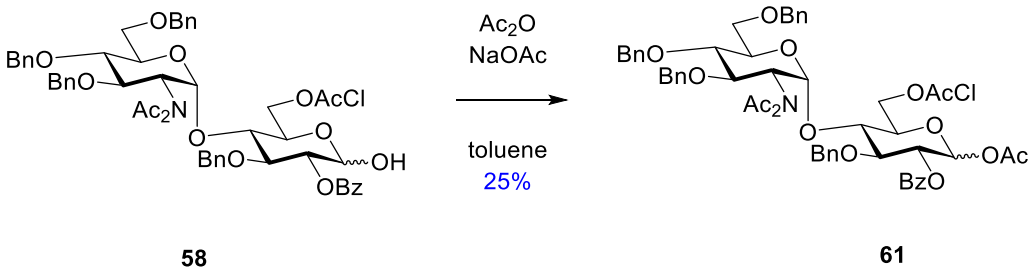

58 **61**

Scheme 43 - Synthesising anomeric acetate of the terminal disaccharide for generating thioglycoside.

This reaction produced only low yields of the α-acetate, in stark contrast to great performance and β-selectivity when used in earlier disaccharide transformations.

Mitsunobu conditions were considered for modifying hemiacetal **58**. Mitsunobu conditions have been used in a variety of reactions with success, as detailed by Hain et al.[321] However, the authors specifically discuss that these conditions cannot be used to generate a thioglycoside from a hemiacetal. The nucleophilicity of a thiol would lead to fast reaction with the reactive intermediate and likely lead to disulfide or polymeric by-products.[322] A set of small test reactions confirmed this in our system, with TLC analysis showing degradation. No improvement was produced by varying the order of reagent addition or other reaction conditions. Hain and co-workers observed that Mitsunobu conditions can be used to modify an existing thioglycoside, wherein the thiol acts as a nucleophile. Recent research has highlighted the scope of Mitsunobu reactions when applied to sugars, including the mechanisms involved and solvent effects.[323] However, a lack of time prevented further investigation.

However, a similar reaction using a disulfide species has also been reported[244,324], which would give the S-Ph thioglycoside **62** (Scheme 44). Such a reaction generates an extra equivalent of the thiol, which could lead to side products. It was reasoned that if the reaction proceeded quickly, side reactions could be avoided or generate only minor impurities. Practically, this experiment produced the correct product **62**, but in low yields of 10%. The mechanism is similar to the Mitsunobu reaction, with the disulfide species functioning in a similar manner to DEAD.[325] The only suitable disulfide reagent available was diphenyl disulfide, but the same chemistry has been reported with other versions of this reagent.[236]

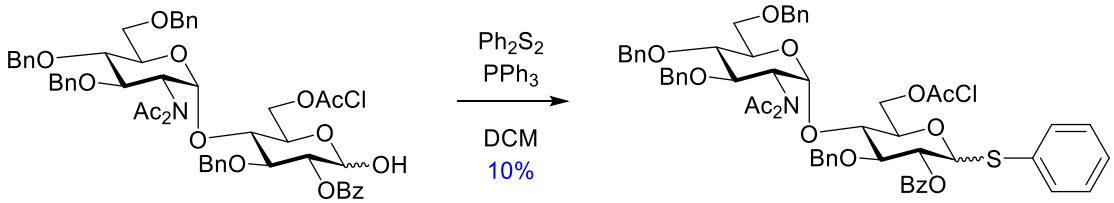

58 **62**

Scheme 44 – Attempted synthesis of a thioglycoside donor using diphenyl disulfide. Interestingly the only product isolated from this reaction was in the α-anomeric conformation by NMR analysis.

The thioglycoside **62** was almost exclusively isolated in the α-thiophenol configuration, with only trace peaks in the NMR which might indicate the β-product. Our previously reported chemistry had only generated the β-thioglycoside. There as some question as to the reactivity of this α-thioglycoside product should the reaction be optimised for better yields. However, the literature supports moderate

to high reactivity from α-thioglycosides in general.[326,327] Side-products related to chloroacetate attack by thiophenol were also observed in the attempted synthesis of **62**, suggesting that the thiol generated in this reaction was going to cause issues.

Further literature suggests alternative routes to thioglycosides that could be attempted, such as a chloro-1,3-dimethylimidazolinium chloride (DMC), also known as Shoda's reagent, mediated condensation.[328] A recent review of this chemistry has been produced which showcases the wide scope of transformations that can be achieved using this reagent.[329] However, a lack of time prevented further investigation.

Transforming the terminal disaccharide hemiacetal **58** into a thioglycoside donor was not successful with the methods attempted. Access to this donor could be obtained by installation of the thioglycoside earlier in the synthesis. A re-synthesis of the terminal disaccharide **5** to have a thioglycoside motif installed would be time-consuming and was not attempted in this work.

3.1.4 Changes during synthesis – swapping 6-*O*-Bn protection for 6-*O*-Bz

During development of our protecting group strategy, benzyl groups, rather than benzoyl groups, were used at the 6-*O*-position of the glucosamine residue of one of the disaccharide building blocks. This protecting group was present on residues at which there would be no 6-*O*-sulfation in the final molecule. A monosaccharide donor with a 6-*O*-Bn protecting group was accessed using a selective opening of the 4,6-*O*-benzylidene acetal protecting group. This resulted in a benzyl group on the 6-*O*-position and an exposed 4-OH. This selective opening was afforded by treatment with triethylsilane and triflic acid. Subsequent 4-*O*-Fmoc protection would give the fully protected monosaccharide glycosyl donor (Scheme 45).

This procedure was first attempted on monosaccharide **17**, synthesised during the pathway to disaccharide **9** (Chapter 2, section 2.2 Results, Scheme 17). Treatment with triethyl silane and trifluoroacetic acid in CH_2Cl_2 gave the 6-*O*-Bn monosaccharide **63** in 70% yield, and 4-*O*-Fmoc protection produced the fully protected monosaccharide **64** in 69% yield. Subsequent application of this method to the 3-*O*-AMB protected monosaccharide **43** proved successful and provided access to the 6-*O*-Bn monosaccharide **65** in a high yield of 90%. 4-*O*-Fmoc protection afforded the fully protected monosaccharide **66** in 80% yield.

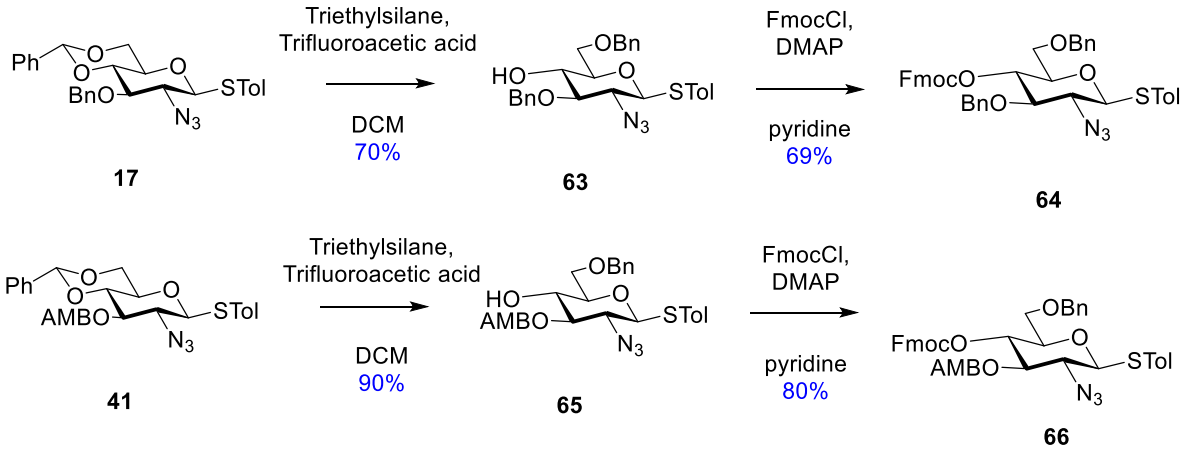

Scheme 45 - Accessing 6-O-Bn protected monosaccharides via selective 4,6-O-benzylidene acetal opening.

However, the [1+1] glycosylation reaction using this material, producing disaccharide **67**, proceeded in a low yield of 39%. The product was isolated in an unfavourable anomeric ratio of α/β : 1/3 (Scheme 46). The two anomers of disaccharide **66** proved difficult to separate. As previously discussed, when synthesising the disaccharide building blocks, α-stereochemistry is desired. Due to these poor results, disaccharide **67** was not a suitable building block for octasaccharide synthesis. An alternative protecting group strategy was required.

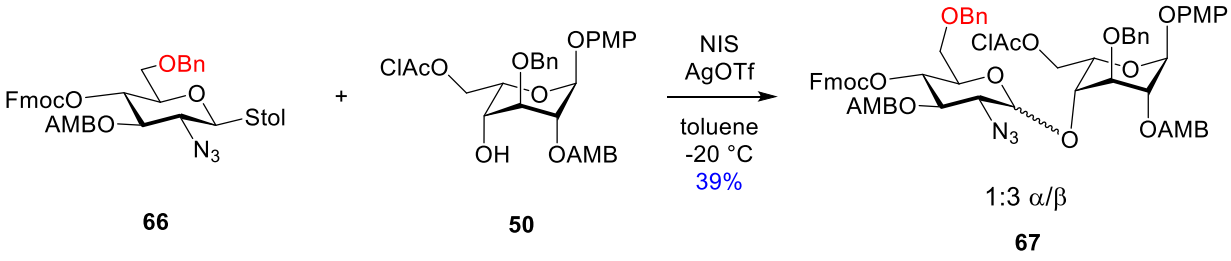

Scheme 46 - The synthesis of the original 6-O-Bn monosaccharide, and subsequent core disaccharide. Time was invested in optimising a selective 4,6-O-benzylidene acetal opening reaction using triethyl silane to generate this monosaccharide, but poor performance in the subsequent glycosylation meant a change in strategy was needed.

This issue was overcome by swapping 6-*O*-Bn for 6-*O*-Bz protection. Previous chemistry within the group had not tested the stability of primary benzoates during primary acetate deprotection, but subsequent experiments have shown that the 6-*O*-Bz survives primary acetate deprotection conditions. This introduced another step which required purification into the synthetic pathway. However, the overall process is more efficient due to a more favourable anomeric ratio of the product, better yields, and easier purification. Later optimisation of the one-pot 6-*O*-benzoyl/acetyl and 4-*O*-Fmoc protection reaction, as detailed previously (Scheme 36), removed this extra purification step as a factor.

3.1.5 Changes during synthesis - identity of core disaccharides

Initially, one of the two octasaccharide targets specified for this project differed from those described earlier in this work. The first target had one glucosamine residue 6-*O*-Ac group (yielding a glucosamine 6-*O*-sulfate following processing), and one glucosamine residue 6-*O*-Bz group (yielding a glucosamine 6-hydroxyl group following processing), which is target octasaccharide **3**. The other target had two 6-*O*-Bz groups (yielding no glucosamine 6-*O*-sulfates), which is target **68** (Scheme 47). This target was to be accessed via fully protected octasaccharide **69**.

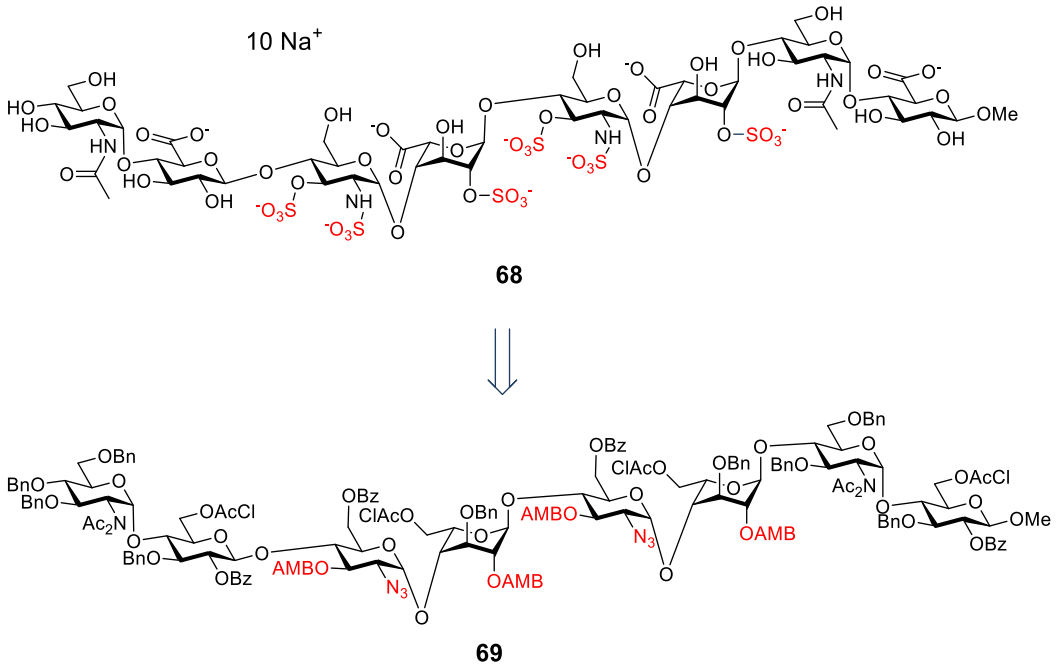

*Scheme 47 - A retrosynthetic analysis of the original target octasaccharide **68**. Access to **68** would have required the fully protected octasaccharide **69**. The synthesis of **69** (and the other octasaccharide target **3**) requires significantly more disaccharide **7** than disaccharide **6**. Synthesis was begun with these quantities in mind, leading to delays when the targets changed.*

However, later discussions with our collaborator Prof. Turnbull resulted in a change of targets. Recent research by his group suggested that the 6-*O*-sulfate was critical for binding in the oligosaccharide/FGF2/FGFR1 complex. Therefore, the ideal octasaccharide targets would include 6-*O*-sulfates. The target with a single glucosamine residue 6-*O*-Ac group, octasaccharide **3**, was already partially assembled at the time of these discussions. It was decided that the second target would be changed from featuring no glucosamine residue 6-*O*-Ac (therefore, no glucosamine 6-*O*-sulfates in the final compound), compound **69**, to featuring two 6-*O*-Ac groups (and therefore two glucosamine 6-*O*-sulfates in the final compound), compound **4**. The changes to the sulfated tetrasaccharide core of the octasaccharide targets are represented below (Figure 32).

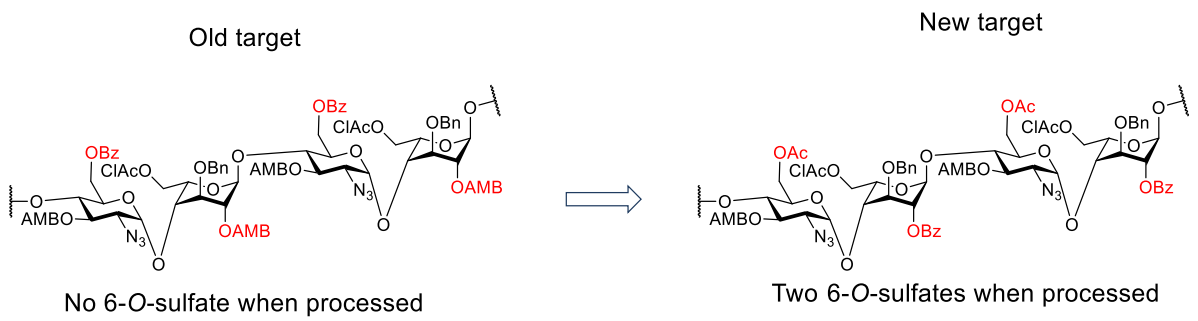

Figure 32 – Changes to the core tetrasaccharide between two sets of octasaccharide targets. One target changed from having two glucosamine residue 6-OBz groups (leading to no 6-O-sulfate) to having two 6-OAc groups (leading to two 6-O-sulfates). The other target remained the same with a single 6-OAc leading to a single 6-O-sulfate.

The original targets had called for a significantly larger amount of the disaccharide building block featuring 6-*O*-Bz protection on the glucosamine residue. These targets also required the synthesis of two different tetrasaccharides during chain assembly. Due to this requirement, a large quantity of the 6-*O*-Bz protected monosaccharide **48**, and subsequent disaccharide **7**, had already been synthesised.

Due to the change in targets, a significantly larger amount 6-*O*-Ac protected monosaccharide **47**, and subsequent disaccharide **6**, was now required. 6-*O*-Bz protected monosaccharide **48**, and subsequent disaccharide **7**, could not be easily converted to 6-*O*-Ac protected analogues. Therefore, further synthesis of disaccharide **6** was required, which caused delays in assembly of the second target. However, the initial tetrasaccharide produced during octasaccharide chain assembly was now the same between both targets.

Chapter 4 - Octasaccharide assembly

4.1.1 n+2 chain assembly

The disaccharide **8** was kindly provided by Dr. Karl Shaffer as a starting point for the assembly of both octasaccharide targets **3** and **4**. Disaccharide **8** was selectively Fmoc-deprotected to give acceptor **70** in 75% yield (Scheme 48).

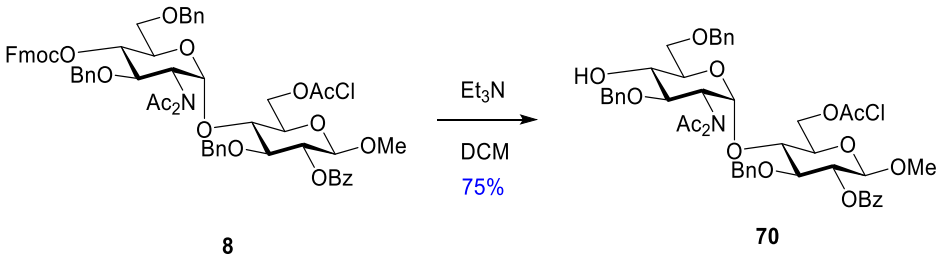

*Scheme 48 - Synthesis of the starting acceptor **70** by deprotection of disaccharide **8**.*

The glycosylation reaction of acceptor **70** with TCA donor **52** gave tetrasaccharide **71** in a high yield (77%) on small scale (Scheme 49). In a later, larger scale batch, two distinct spots were observed on TLC analysis of the reaction mixture, and two separate tetrasaccharide compounds were isolated. NMR and MS analysis confirmed that the first compound was the intended product **71**.

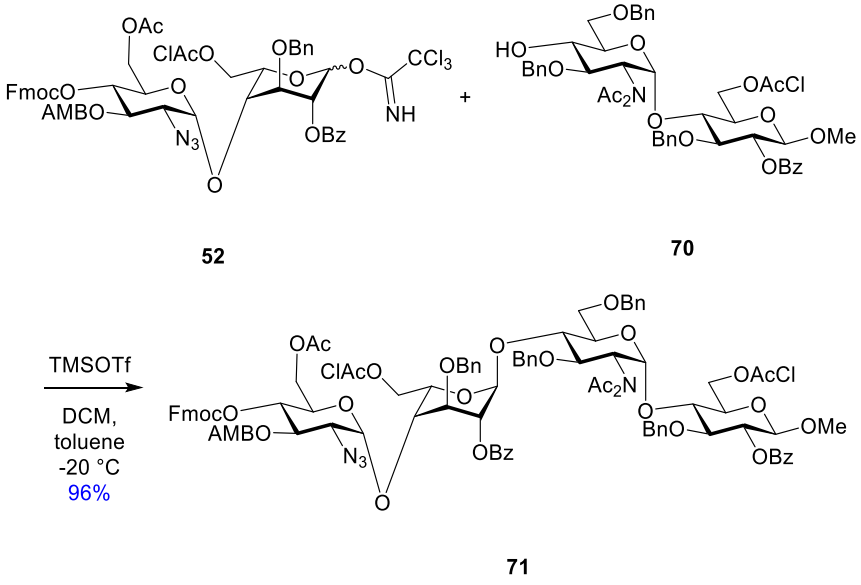

Scheme 49 - Synthesis of the initial tetrasaccharide 71 by [2+2] glycosylation.
*Produced from the initial disaccharide acceptor **70** and disaccharide TCA donor **52**.*
This tetrasaccharide is conserved between both targets and so high quantities were produced.

The second compound, found at lower R_f than **71**, was identified as **71** which had lost single *N*-Ac group. The appearance of an *N*-H peak was noted in the ^{1}H NMR spectra of the side-product. MS

showed a mass for the side-product consistent with the loss of an acetate group. This side-product was re-*N*-acetylated to give the target product **71** using the procedure used in the synthesis of the original *N*-Ac_2 protected monosaccharide, by treatment with isopropenyl acetate.[330] A further synthesis of tetrasaccharide **71** was accomplished on a larger scale without loss of *N*-Ac groups, with an excellent yield of 96%. The glycosylation reaction was quenched by injection of a small volume of saturated sodium bicarbonate solution whilst still at -20 °C, which prevented *N*-Ac loss. This quench method was used in all subsequent glycosylation reactions. Following the change of the identity of the core disaccharides discussed earlier, tetrasaccharide **71** was conserved between the two targets. This synthesis was later repeated in several batches throughout the chain assembly attempts. As the [2+2] glycosylation reaction gave high yields with the TCA donor **52**, no other donor system was tested.

Tetrasaccharide **71** was then treated with base to remove the Fmoc protecting group, affording tetrasaccharide acceptor **72** in 81% yield (Scheme 50). This acceptor was then glycosylated with TCA donor **55** to produce hexasaccharide **73**, in 51% yield. However, this product was impure. Hexasaccharide **73** is a precursor to the octasaccharide target **3**. A significantly higher quantity of the 6'-*O*-Bz protected disaccharide **7** was available, as more of this material was required for the synthesis of the original set of octasaccharide targets. Consequently, larger scale synthesis of this material had been carried out. Therefore, glycosylation reactions to afford hexasaccharide target **73** were used for method development.

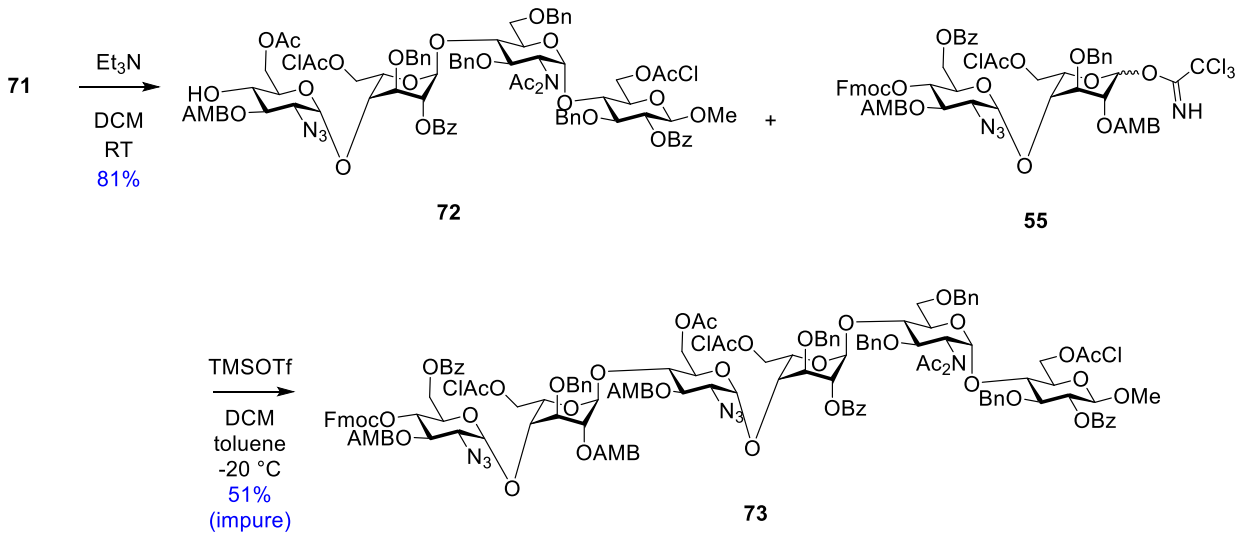

*Scheme 50 - Synthesis of hexasaccharide **73**.*
The yield reported here for hexasaccharide formation includes an inseparable impurity.

Glycosylation of the tetrasaccharide acceptor **72** with disaccharide TCA donor **55** proved to be challenging. The reaction produced the desired product **73** in moderate yields, but also several side-

products, including one very close running impurity. LCMS analysis showed side-products consistent with the loss of AMB groups from either the hydrolysed glycosyl donor, glycosyl acceptor, or product compounds. This led to the suggestion that the presence of AMB groups near to the reaction centre is not favourable for this glycosylation system. In this specific reaction, AMB is present at the reducing end 2-*O*-position of the donor and the 3-*O*-position of the non-reducing end residue of the acceptor, both of which are adjacent to the reaction centre. Additionally, a significant quantity of disaccharide TCA donor **55** underwent rearrangement to the trichloroacetamide.[228] A second, larger scale batch of hexasaccharide **73** was synthesised. This reaction gave a slightly lower yield of **73** (42%) and the product was also difficult to isolate. The impure material was taken forward to the next step, with the aim of removing impurities following further modification.

The impure sample of hexasaccharide **73** was then 4-*O*-Fmoc deprotected to give hexasaccharide acceptor **74** in 65% yield. However, the product remained impure (Scheme 51). A closely running impurity was still visible by TLC analysis, despite the removal of Fmoc, and co-eluted in all chromatography attempts.

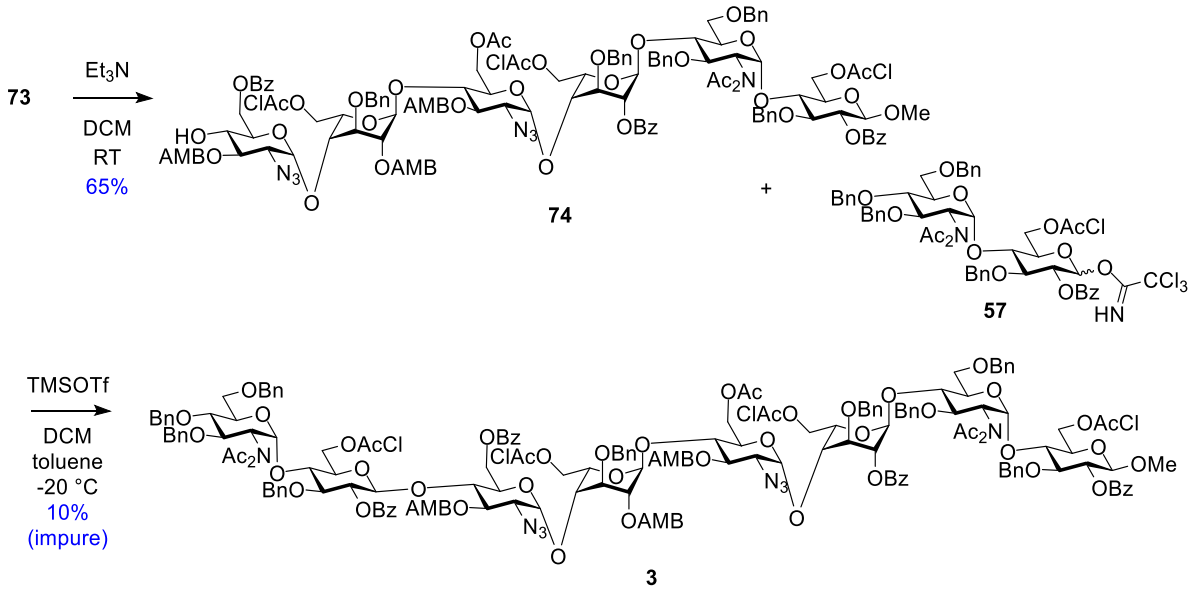

*Scheme 51 - Synthesis of fully protected octasaccharide **3** by a [6+2] method. The glycosylation of donor **57** and acceptor **74** performed extremely poorly, with a low yield of impure octasaccharide material produced.*

The final glycosylation reaction of donor **57**, which was provided by colleagues in the TCA donor form, and hexasaccharide acceptor **74** was then attempted (Scheme 51). A spot suggestive of the product, fully protected octasaccharide **3**, was observed by TLC analysis of the reaction mixture. However, a

close running impurity was also present. The reaction appeared sluggish with the majority of the glycosyl acceptor remaining unreacted. The rearranged TCA donor by-product was also observed.

A second reaction on a larger scale again produced the product and a close running impurity. The yield of this impure product, 10%, was extremely poor. It was postulated that the side reaction was occurring in the synthesis of hexasaccharide **73** was also occurring in this reaction. There are similarities between the acceptor used in both reactions, with a 3-*O*-AMB protecting group at the non-reducing end of the acceptor that was adjacent to the nucleophilic hydroxyl group.

This product could not be isolated at this stage despite extensive effort. Repeats of the reaction with rigorous condition control produced no improvement. Extensive measures were taken to exclude water from the reaction. A low yield of impure material at this stage of the synthesis was a significant problem, and attempts were made to improve this step. The combination of these initial batches of impure **3** was used firstly in tests to identify the impurity. Then, being a relatively small amount after repeated poor yields and purification attempts, used both to test conditions for the subsequent post assembly processing reactions, and to investigate if purification was possible after further reactions.

4.1.2 The identity of the impurity

The close running impurity observed in the synthesis of both hexasaccharide **73** and octasaccharide **3** had proved difficult to separate from the products by common methods.[229] As previously discussed, it was postulated that the impurity could be a modification of the acceptor in both cases, as any donor-related side-products would be disaccharides. These smaller molecules should have different retention times on silica compared to the hexasaccharide or octasaccharide products. It was further reasoned that the impurity was forming due to the same side-reaction in both cases. To separate a sample of the impurity for analysis, a comprehensive series of purification methods was used on the impure hexasaccharide **73** (Table 6).

Multiple normal phase columns using high-grade silica were attempted using different solvent mixtures, in some cases with additives including chloroform or triethylamine. However, neither the product nor the impurity was isolated from these attempts. The use of reverse phase columns did not achieve separation. Other modifications used to attempt separation included dry loading, the use of isocratic gradients, and using large quantities of silica for the sample size. Overall, suitable conditions for a chromatography method to isolate the product were not found.

Entry	NP / RP	Column	Eluting solvents	Modifications	Outcome
1	NP	EcoFlex	Toluene/EtOAc	-	Co-elution
2	NP	EcoFlex	Hexanes/EtOAc	-	Co-elution
3	NP	EcoFlex	CH_2Cl_2/MeCN	-	No separation
4	NP	EcoFlex	CH_2Cl_2/Acetone	-	No separation
5	NP	EcoFlex	Toluene/EtOAc	Low silica loading	Co-elution
6	NP	EcoFlex	Toluene/EtOAc	-	Co-elution
7	NP	EcoFlex	Hexanes/EtOAc	-	Co-elution
8	NP	Standard	Toluene/EtOAc	-	Co-elution
9	NP	Standard	Toluene/EtOAc	20% $CHCl_3$ additive	Co-elution
10	NP	Standard	Toluene/EtOAc	1% Et_3N additive	Co-elution
11	NP	Standard	Toluene/EtOAc	20% $CHCl_3$ additive	Co-elution
12	RP	Standard RP	MeOH/water	-	No separation
13	RP	Standard RP	MeOH/water	1% TFA additive	No separation
14	NP	HP silica	Toluene/EtOAc	Isocratic gradient	Co-elution
15	NP	HP silica	Toluene/EtOAc	20% $CHCl_3$ additive	Co-elution
16	NP	HP silica	Toluene/EtOAc	Isocratic gradient	Co-elution
17	NP	HP silica	CH_2Cl_2/MeCN	-	No separation
18	NP	HP silica	CH_2Cl_2/Acetone	-	No separation
19	NP	HP silica	Toluene/Et_2O	-	Co-elution
20	NP	HP silica	CH_2Cl_2/MeCN	20% $CHCl_3$ additive	No separation
21	NP	HP silica	CH_2Cl_2/MeCN	Isocratic gradient	No separation
22	NP	HP silica	CH_2Cl_2/MeCN	Low silica loading	No separation

*Table 6 - The purification methods used to attempt to remove a close running impurity from **73**. All these attempts were repeated 2-3 times, and none proved successful in allowing proper separation of the product and impurities. Several displayed significant co-elution.*

Other analysis methods were considered to identify the impurity. LCMS analysis provided masses for several of the compounds present, including the product mass and masses of the appropriate hemiacetal and glycosyl acceptor. However, there were several masses present in various quantities that could not be easily attributed to expected products or side-products. It was unclear if the masses were caused by reaction during the MS fragmentation or present beforehand. The use of HPLC was considered, however access to the necessary training, equipment, and instrument time was delayed due to external factors.

Likely identities for an impurity produced during the glycosylation reaction to synthesise hexasaccharide **73** could include an orthoester, a tetrasaccharide acceptor which was modified in some way, or loss or migration of protecting groups in the product. However, stirring a small sample of the impure octasaccharide product material with a small amount of Lewis acid (both TMSOTf and $BF_3.Et_2O$ were tried), which would be expected to convert an ortho-ester to the 1→4 linked product, gave no reaction. Further treatment led to degradation of the material. Furthermore, an attempt to silylate the impurity with TBDMS-Cl and imidazole in DMF, and an attempt to acetylate the impurity with acetic anhydride, were both unsuccessful and no reaction was observed (Table 7). It would be expected, if the impurity was leftover acceptor with a 4-OH group or deprotected product material with a free hydroxyl group, that these reactions would modify the impurity such that separation could be achieved.

Entry	Objective	Conditions	Outcome
1	Glycosylation	TMSOTf, glycosyl donor DCM, -20 °C to RT	No reaction
2	Sialylation	TBDMS-Cl, imidazole, CH_2Cl_2, RT	No reaction
3	Acetylation	$BF_3{\cdot}OEt_2$, Ac_2O, RT	Degradation
4	AMB protection	2-acetoxymethylbenzoic acid, DCC, DMAP, DCM, RT	No reaction
5	Collapse orthoester	TMSOTf, DCM, RT	Degradation
6	Collapse orthoester	$BF_3{\cdot}OEt_2$, DCM, RT	Degradation

Table 7 - Results of exposing the impure mixture to various reaction conditions. The aim of these experiments was to further react the impurity in several ways that should have either converted the material to the correct product or modified it to allow separation. None were successful.

Following these experiments, preparative TLC analysis of the product and impurity from the reaction to make hexasaccharide **73** was carried out on a 40 mg sample of the impure product. This separation used the same 20% EtOAc in toluene elutent as the reaction monitoring TLCs, in which marginal separation was observed. The resulting preparative TLC plate was assessed by UV irradiation and showed poor separation. However, 26 thin strips of silica were cut from the of plate, and then each slice washed with EtOAc to remove the attached compound. This isolated 4 mg of an impurity, and NMR and MS analysis revealed the impurity to be 4-*O*-acetylated acceptor, tetrasaccharide **75** (Figure 33).

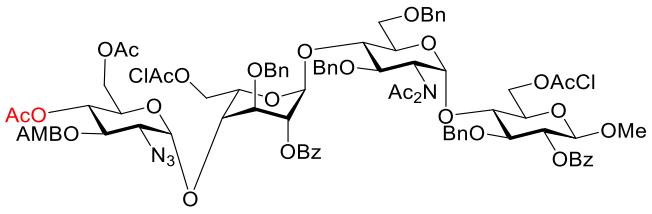

*Figure 33 - The 4-O-acetylated impurity **75** isolated from the synthesis of hexasaccharide **73**. The extra acetate group, highlighted in red, is suggested by both NMR and MS, and this fully protected material would have a similar R_f to the intended product as had been experimentally observed. Note that all other protecting groups are intact.*

This acetylation appears to occur under the glycosylation reaction conditions, as the impurity spot is observed forming during the reaction. It was thought that this acetate could be migrating from within the same molecule, but the MS does not support this as no other groups appear to have been lost on the isolated sample. This suggests the acetate is coming from elsewhere, perhaps another molecule that was separated from the product and not isolated. A likely candidate is the labile second acetate of the *N*-Ac_2 moiety on the glycosyl acceptor. The resultant deprotected tetrasaccharide or hexasaccharide molecule (with a non-reducing end 4-OH and an NHAc at the 2-position of the reducing end) would have a significantly lower R_f than any of the other reaction components. This material could be retained on the column until elution with a high percentage of polar solvent. This would also explain being unable to account for all the mass of acceptor following the reaction. However, analysis of the 100% polar solvent washing fractions of several chromatography attempts did not show any of this postulated side-product.

The formation of this side-product could be related by the presence of the 3-*O*-AMB group. However as shown previously (Figure 33), the 3-*O*-AMB group is still present in the impurity isolated by preparative TLC. Therefore, the acetate of the 3-*O*-AMB has not migrated, which should cause the rapid loss of phthalide in the presence of a Lewis acid. It is plausible that the presence of 3-*O*-AMB disfavours glycosylation to the extent that side reactions are observed, for example by hydrogen bonding to obscure the 4-OH.

Attempts were made to optimise the glycosylation reaction conditions. A variety of modifications were made to the conditions of the glycosylation reaction of disaccharide TCA donor **55** and tetrasaccharide acceptor **72**. This included varying the promoter, solvent, and temperature for glycosylation reactions on the 20 mg scale (Table 8). TLC analysis was used to assess the suitability of each set of conditions. It was established that no improvement could be made using these changes. Furthermore, repeat reactions with inverse addition[331] were carried out for each of these cases, and again no change in outcome was observed. As TLC analysis showed that these test reactions presented either no significant improvement or degradation, the products were not isolated.

Entry	Solvent	Promoter	Temperature [°C]	Outcome
1	Toluene	TMSOTf	-20	No change
2	CH_2Cl_2	BF_3	-20	Degradation
3	CH_2Cl_2	TBDMSOTf	-20	Degradation
4	MeCN	TMSOTf	-20	Degradation
5	Et_2O	TMSOTf	-20	Degradation
6	Toluene	TMSOTf	-78	No change
7	Toluene	TBDMSOTf	-20	No change
8	Toluene	TMSOTf	RT	Degradation

*Table 8 - Attempted optimisation of a hexasaccharide glycosylation reaction. Specifically, these tests were carried out on the hexasaccharide glycosylation of disaccharide TCA donor **53** and tetrasaccharide acceptor **70**. This system was used to carry out optimisation studies as good quantities of both materials were available.*

With the lack of success in the hexasaccharide glycosylation using TCA donor **55**, a change was made to the glycosylation strategy by returning to the use of the *N*-phenyl trifluoroacetamide donor system, disaccharide **56**. It was known, from work detailed earlier in this thesis,[308] that this system is comparatively reactive to the TCA equivalent. As an additional benefit, the reaction of **56** could be carried out at lower temperatures if required, and this system should not be as likely to undergo rearrangement to the amide.[228] It was hoped that this system would lead to less formation of the acetylated acceptor side-product **75**.

The same glycosylation reaction using the *N*-PTFA donor **56** and tetrasaccharide acceptor **72** was tested on the 20mg and 100mg scales (Scheme 52). This reaction outcome was much better than with the TCA system, giving ~60% yields in short reaction times of 10-15 minutes, and forming no noticeable side-product in this timeframe. It was found that longer reaction times may lead to the formation of side-products. Despite further addition of promoter and fresh donor during the reaction, the total amount of acceptor was never fully used up, being mostly recovered unmodified. Success with this donor proved to be robust and repeatable, giving 65% yield in the case of the *N*-PTFA donor **56** to give hexasaccharide **73** and 72% yield in the case of the *N*-PTFA donor **53** to give hexasaccharide **76**.

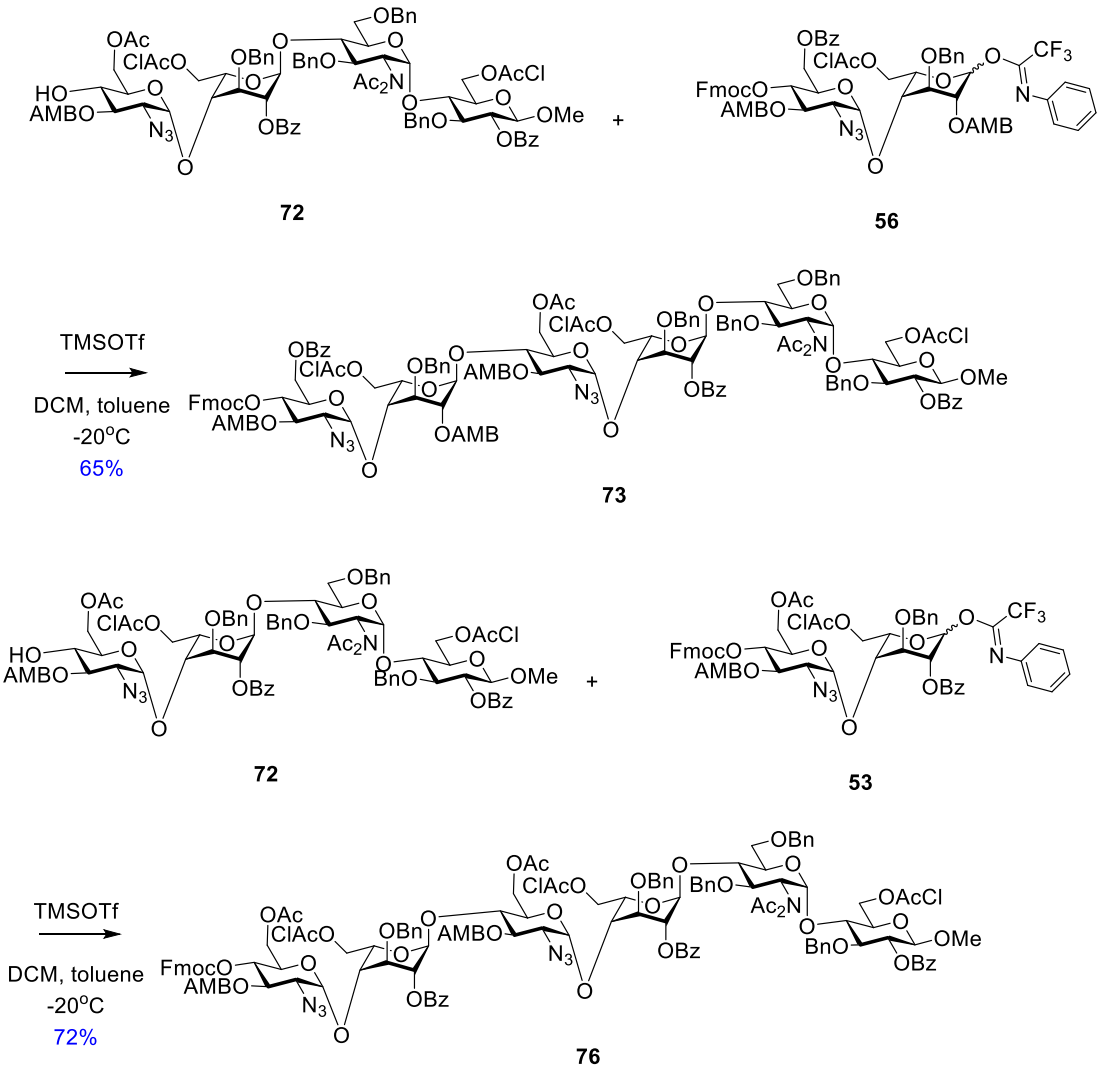

*Scheme 52 - The synthesis of hexasaccharides **73** and **76** using N-PTFA donors **56** and **53**. These donors performed much better than the TCA equivalent with higher yield and minimal impurities, and in a very short reaction time.*

Following optimisation of the hexasaccharide glycosylation reactions, a larger scale batch of hexasaccharide **76** was produced. The corresponding hexasaccharide acceptor **77** then accessed (Scheme 53) by selective 4-*O*-Fmoc deprotection.

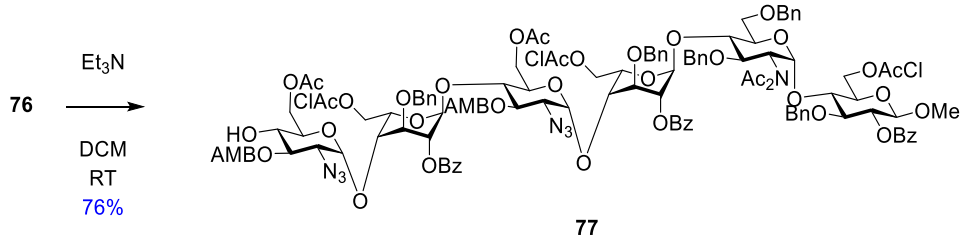

*Scheme 53 - Production of hexasaccharide acceptor **77** by selective Fmoc deprotection of hexasaccharide **76**.*

Later, in a larger scale re-run of the hexasaccharide glycosylation using the *N*-PTFA donor **56**, a large quantity (~180 mg) of a high R_f donor-based by-product was isolated, allowing analysis of the by-product of *N*-PTFA donor activation. A high R_f spot, similar in R_f to the spot produced by TCA donor amide rearrangement, had been observed during previous glycosylation reactions using the *N*-PTFA donors but was not isolated. The *N*-PTFA donor disfavours rearrangement, as previously discussed, and so this by-product was analysed to establish if this was occuring.

NMR and MS analysis of this by-product led to the conclusion that the major by-product is a 2-hydroxyglycal derivative of the donor, disaccharide **78** (Figure 34). [332,333] The most distinct sign of this change was the presence of only one anomeric proton signal in the typical chemical shift range. A sharp, singlet, single proton peak was observed at a high chemical shift, corresponding with the proton at C1 of the reducing end of the disaccharide.

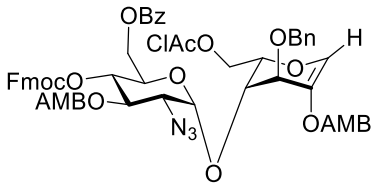

78

*Figure 34 - The glycal by-product **78** based on donor **56**, isolated from a glycosylation reaction. NMR and MS analysis are both suggestive of this by-product, and it appears stable.*

As detailed in the work of Ferrier, glycals are often formed through elimination reactions, with leaving groups including bromides and acetates.[333] In the disaccharide species **78**, the 2-*O*-AMB group at the reducing end is intact by NMR and MS, giving a protected 2-hydroxyglycal. A similar case occurring during an attempted glycosylation with an idose sugar, although in this instance arising from an orthoester starting material and yielding a 2-acetoxylglycal, has been reported.[242] Presumably, in this case the glycal forms first by the Lewis acid promoted loss of the imidate to give an oxocarbenium ion, and loss of the sugar ring proton at C2 of the reducing end, leading to double bond formation. This would also likely result in the forming of *N*-phenyltrifluoroacetamide, which may be the cause of a large UV active peak observed early in the chromatography trace during purification of these reactions. 2-Hydroxyglycals are an active area of research[334] and therefore this side reaction is of reasonable interest. Glycals have been used as donors in some cases.[230] However, any further glycosylation chemistry that this glycal molecule is employed for could lead to a mixed stereochemical product at C2 of the reducing end, and thus may not be of great use for this specific synthesis.

4.1.3 Issues with the octasaccharide glycosylation

The terminal disaccharide, kindly provided by Dr Karl Shaffer, was already in the TCA donor form **57**. The TCA donor system had been shown to perform poorly in the first small scale synthesis of the octasaccharide target. The octasaccharide glycosylation, using disaccharide TCA donor **57** and hexasaccharide acceptor **74** to form the final target **3**, had generated a close running impurity. Considering the preparative TLC analysis of impure hexasaccharide **73**, it was postulated that the impurity could be the hexasaccharide acceptor which had been 4-*O*-acetylated at the non-reducing end. It was further assumed that changing to the *N*-PTFA donor **59** would give higher isolated yields, as had been the case in the hexasaccharide glycosylation reactions.

Following the acquisition of donor **59**, as detailed in the previous chapter (Section 3.1.3, Scheme 41), several subsequent attempts to carry out octasaccharide production were made. These attempts used the new donor and hexasaccharide acceptor **74** to form the final target **3**. However, TLC analysis showed small amounts of product-like spots, unreacted starting materials, and multiple side-products (Scheme 54). Further additions of TMSOTf, addition of $BF_3{\cdot}OEt_2$, addition of extra donor **59**, and warming the reaction from -40 °C to -20 °C, and then to 0 °C to RT, failed to push the reaction further. The product could not be purified from this reaction mixture following workup and chromatography. Additionally, there was significant recovery of unaltered acceptor hexasaccharide **74** and disaccharide hemiacetal **58** resulting from donor hydrolysis.

This was surprising, as the hexasaccharide synthesis using the *N*-PTFA donor **56** and tetrasaccharide acceptor **72** had given higher isolated yields over the TCA donor analogue. It could be the case that the *N*-PTFA donor is poorly matched with the relatively unreactive acceptor in the octasaccharide production.[167,205]

Experiments with the *N*-PTFA donor were mostly carried out using donor **59** and hexasaccharide acceptor **74** to give the octasaccharide **3** as there were greater quantities of this material available. However, the equivalent glycosylation to make the other fully protected octasaccharide target **4,** from hexasaccharide acceptor **77**, was attempted and gave similar results.

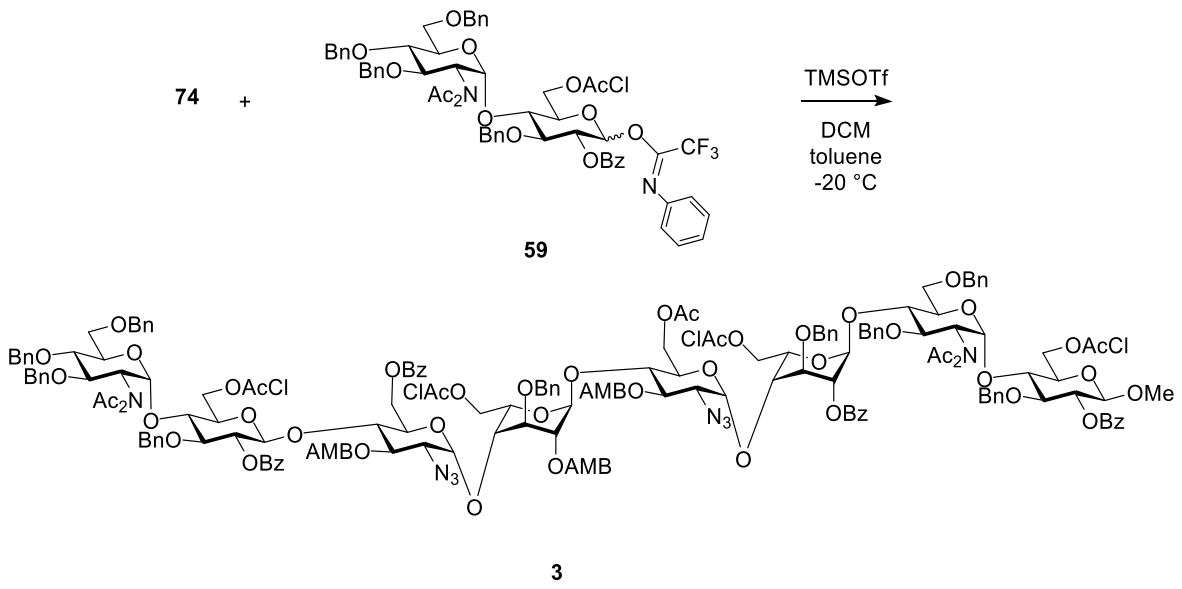

*Scheme 54 - The revised attempted glycosylation reaction to access octasaccharide **3** using donor **59**. This reaction failed to proceed over multiple attempts. Only trace amounts of product were observed on TLC analysis and in LCMS.*

Other attempts to improve the reaction were considered, but changes were limited by the need to keep the current protecting group strategy. Different donor systems or changes to the reaction method, such as inverse addition[331] (which was attempted and produced no change in yield or the formation of side-products), were examined. An alternative report featured the addition of NaH to the glycosyl acceptor, which would deprotonate the hydroxyl group and lead to a more reactive acceptor.[237] While a promising idea, side reactions - especially the observed 4-*O*-acetylation of the acceptor - might also be catalysed by this method. NaH may also act as a base and remove protecting groups.

The stability of hexasaccharide acceptor **74** in the presence of NaH was tested. A solution of hexasaccharide acceptor **74** in anhydrous dichloromethane was treated with 1 equivalent of NaH 60% *w*/*w* dispersion in mineral oil at room temperature and stirred for 30 minutes. TLC analysis of this mixture showed the material remained mostly intact, with 91% recovery. A small quantity of side-product appearing at very low R_f was observed and isolated. The loss of *N*-Ac (from an NAc_2 group) causing a significant R_f drop has been observed previously and fits with the TLC analysis. NMR and MS of this material following chromatography confirmed the presence of this side-product. NaH can act as a base to remove the *N*-Ac. It was reasoned that the low temperature and short time of the glycosylation reaction should keep this deprotection to a minimum. The imidate glycosyl donors are generated in the presence of NaH, and so were expected to be stable towards the reagent during the reaction.

Glycosyl acceptor **74** was treated with NaH 60% *w*/*w* dispersion in mineral oil at the reaction temperature of -20 °C, before the addition of glycosyl donor followed by the addition of TMSOTf promoter. Separately, a solution of the NaH-treated acceptor **74** was treated with of a pre-mixed solution of glycosyl donor and promoter. Unfortunately, this did not improve the results of the glycosylation reaction, with a very similar quantity of impure product produced.

Following these experiments, optimisation of glycosylation reactions using disaccharide TCA donor **57** was attempted. Modified conditions were used, including a short reaction time, the use of toluene as the solvent and a temperature of -30 °C using a dry ice / MeCN bath, which resulted in minor improvement. Glycosylation reactions using these conditions yielded 15% of an impure octasaccharide product. The mass of the product was observed in these fractions by MS analysis, but the mass of the 4-*O*-acetylated acceptor side-product was also observed. NMR spectra of this material were exceptionally complicated, owing to the large molecules involved and overlap between the product and impurity, and was of limited use in identifying the compound. Further attempts at chromatographic separation of the impurity were not successful.

This was the best result achieved with imidate donors, so focus turned to other donor systems. Consideration was given to utilising thioglycoside donor **60** or analogues, the attempted synthesis of which was described in the previous chapter (section 3.1.3, Scheme 42, Scheme 44). Due to the lack of success in producing this donor, this system could not be tested. However, the first step of the first method used to attempt to access **60**, which generated a glycosyl bromide in situ, had appeared to work well.[318] It was reasoned that glycosylation could be attempted with the bromide donor generated in situ, using a traditional bromide activator, silver carbonate, as the promoter.[335]

A solution of the terminal disaccharide hemiacetal **58** in anhydrous dichloromethane was treated as previously described to form the bromide, and then to this solution was added the hexasaccharide acceptor **74** and then silver carbonate. However, this reaction failed to produce any detectable product octasaccharide **3**. Unmodified acceptor and hydrolysed donor were isolated following work up and chromatography.

A TBAB catalyst was used in the attempted synthesis of **60**, but this was not initially used in this octasaccharide glycosylation test. It was thought that the bromide from TBAB would quickly react with the silver carbonate and thus be unable to convert the α-bromide to the β-bromide. The other role of TBAB in the original reaction, as a phase transfer catalyst, was not required in the glycosylation reaction. A further test reaction using the same method but including the addition of TBAB did not change the result of the glycosylation reaction.

Other activation systems for α-bromide donors have been reported, including silver triflate[336] and silver oxide in combination with catalytic TMSOTf.[337] However, limited time prevented any further assessment of this route. Further consideration was given to several published methods in which glycosylation was carried out directly from the hemiacetal **58** using other reactive intermediates generated in situ.[338-340] Several of these strategies where attempted on a test scale. Firstly, the glycosylation was attempted using phthalic anhydride and triflic anhydride as activating agents for hemiacetal **58**. Separately, triflic anhydride and diphenyl sulfoxide were used as activating agents. However, neither of these methods were able to produce a promising result in our hands.

During the extensive testing of methods to develop a viable octasaccharide glycosylation strategy, a significant quantity of precious hexasaccharide acceptor **74** was being lost over the many repeated reactions. Although the tests often returned some 50% or more of the unmodified acceptor, the remainder was not recovered. This led to attempts to optimise glycosylation conditions using a model system, the analogous glycosylation reaction of the terminal disaccharide TCA donor **57** and a disaccharide acceptor **79**. Glycosyl acceptor **79** was accessed from selective 4-*O*-Fmoc deprotection of disaccharide **7** (Scheme 55).

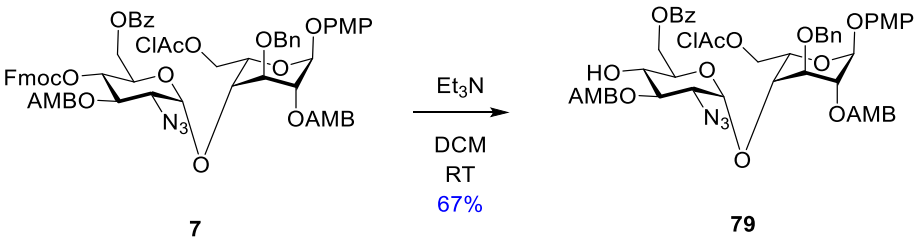

*Scheme 55 - The synthesis of disaccharide acceptor **79** from disaccharide **7**. This acceptor was used as a model system for hexasaccharide acceptor **74** in glycosylation method development.*

A glycosylation reaction of terminal disaccharide TCA donor **57** and disaccharide acceptor **79** would produce tetrasaccharide **80** (Scheme 56). It was reasoned that this system was analogous to the octasaccharide glycosylation of disaccharide TCA donor **57** and hexasaccharide acceptor **74** around the reaction centre. Therefore, a viable glycosylation method here might also yield successful, although lower yielding, results in the octasaccharide glycosylation.

Initial attempts to optimise this smaller system, using both the TCA and *N*-PTFA donors, produced very poor results. Later attempts using the TCA donor proved to be successful in generating this tetrasaccharide **80** in moderate yields (Scheme 56). The best yield achieved was 65%, however this was not consistently achievable. Extensive effort was made to thoroughly dry the materials used in the reaction, as disaccharide acceptor **79** appeared to retain water by NMR analysis even after several

co-evaporations with anhydrous toluene. The NMR solvent used in this analysis was dried over 3 Å molecular sieves before use. Ultimately, high quantities of freshly activated molecular sieves, stirred with the glycosyl donor and acceptor sugars in anhydrous dichloromethane for several hours prior to addition of promoter, allowed the reaction to proceed.

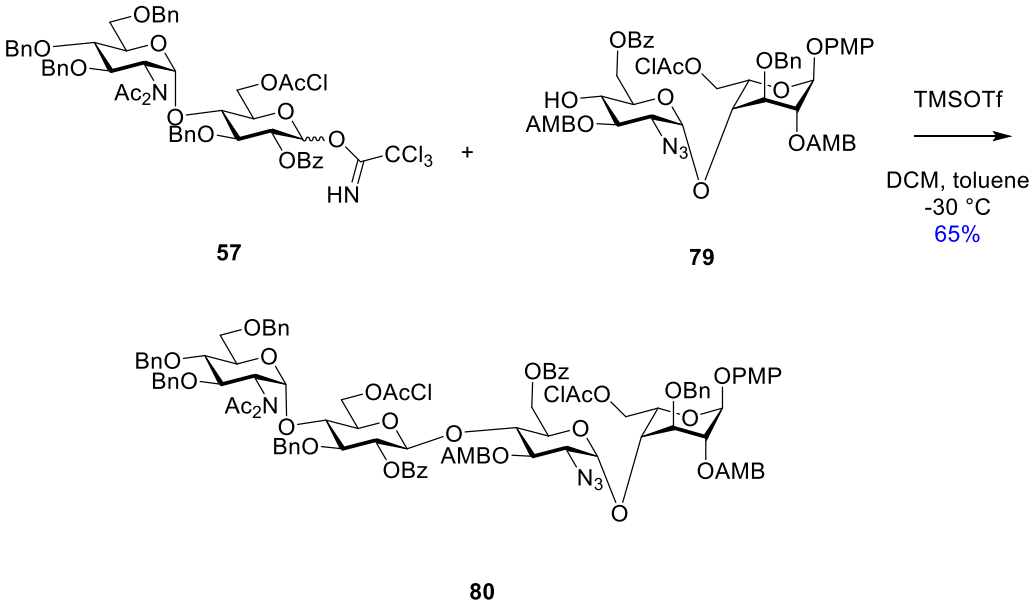

*Scheme 56 - Attempted [2+2] glycosylation of dissacharide TCA donor **57** and dissacharide acceptor **79** to give tetrasaccharide **80**.*
This was initally used as a model system for the establishment of good glycosylation reactions for the analogous [6+2] reaction.

However, these optimised conditions produced poor results when applied to the [6+2] glycosylation, and the hexasaccharides did not appear to retain water to the same extent. No improvement in product yield or a reduction of side-product formation was observed.

4.1.4 Change in strategy - the [4+4] glycosylation method

With access to tetrasaccharide **80**, an alternative route to the original octasaccharide glycosylation method could be attempted (Scheme 57). Tetrasaccharide **80** could be selectively hydrolysed to give hemiacetal **81** and then transformed into a *N*-PTFA donor system **82** (Scheme 58). This tetrasaccharide donor could then be used in a [4+4] glycosylation reaction to produce the octasaccharide target **3**. Tetrasaccharide impurities in the [6+2] glycosylation reaction mixture may be easier to remove than analogous hexasaccharide impurities.

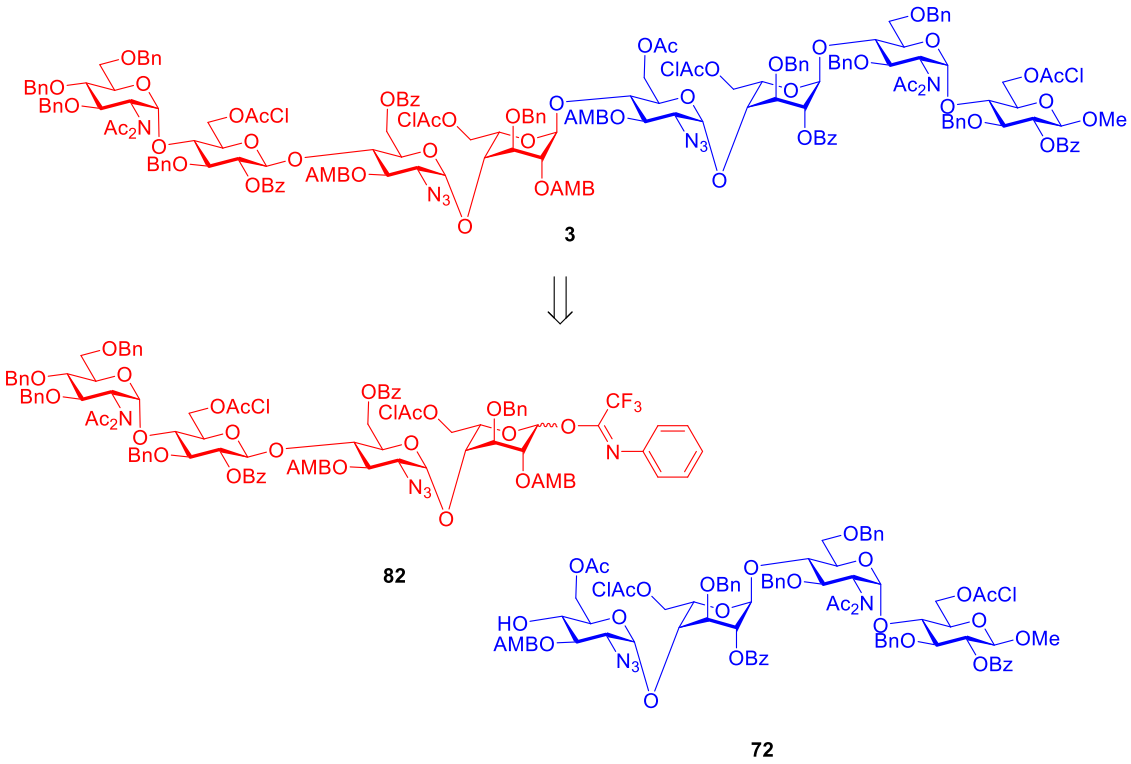

*Scheme 57 - A reterosynthesis of octasaccharide **3** showing a new [4+4] route. Here, a N-PTFA donor, which had been shown to be effective in the analogous [4+2] glycosylation on this tetrasaccharide acceptor, is used.*

Optimised conditions in the analogous [4+2] glycosylation reaction had already given good results. These conditions, using the *N*-PTFA donor, gave a good starting point for this synthesis.

Therefore, the tetrasaccharide **80** was selectively deprotected by CAN mediated 1-*O*-PMP hydrolysis to give hemiacetal **81** in 70% yield. This hemiacetal was readily transformed into *N*-PTFA donor **82** in 82% yields by our established method (Scheme 58).

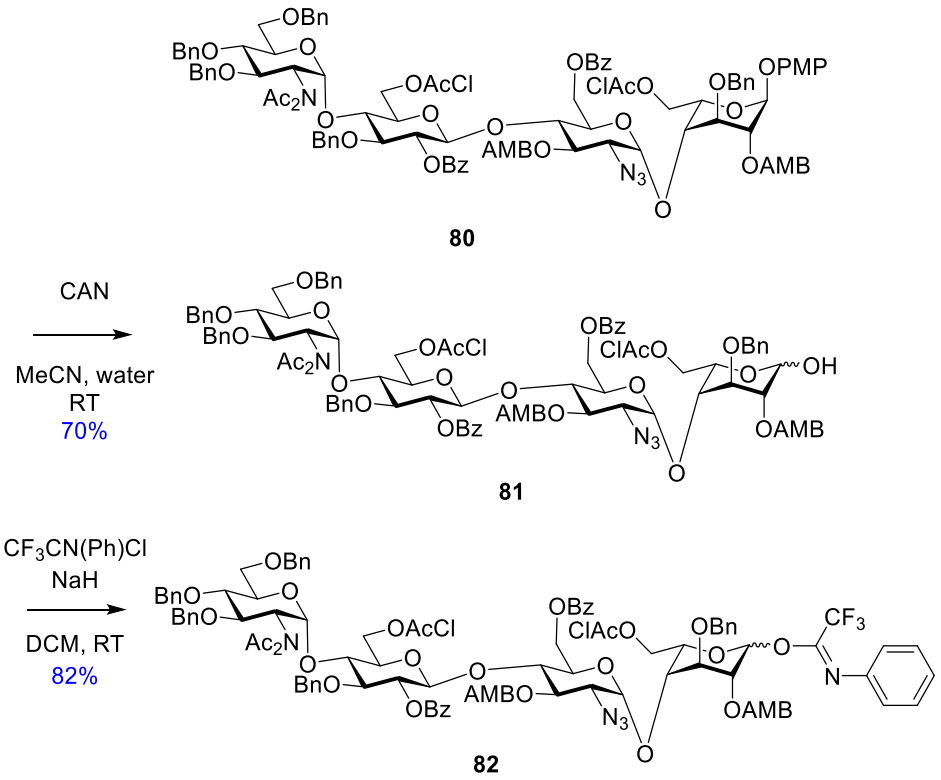

*Scheme 58 - The synthesis of N-PTFA donor **82** from tetrasaccharide **80**.*
Both of these reactions performed very well and the products could be easily isolated in high purity and yield, somewhat in constrast to their dissacharide counterparts.

Glycosylation of tetrasaccharide donor **82** and tetrasaccharide acceptor **72** to produce octasaccharide **3** was tested (Scheme 59). This experiment used tetrasaccharide acceptor **72** from the same batch as previously used in [6+2] glycosylation reactions to ensure consistency. This reaction was observed to only partially proceeded by TLC analysis, with glycosyl acceptor and donor by-products present. However, following work-up, chromatography afforded a pure product in 43% yield. No significant impurities were observed, but some hemiacetal formation was observed. The small scale (65 mg of acceptor) of these reactions meant that small amounts of retained water may have a significant impact on yield. A larger scale attempt will be required in the future for an accurate assessment of yield.

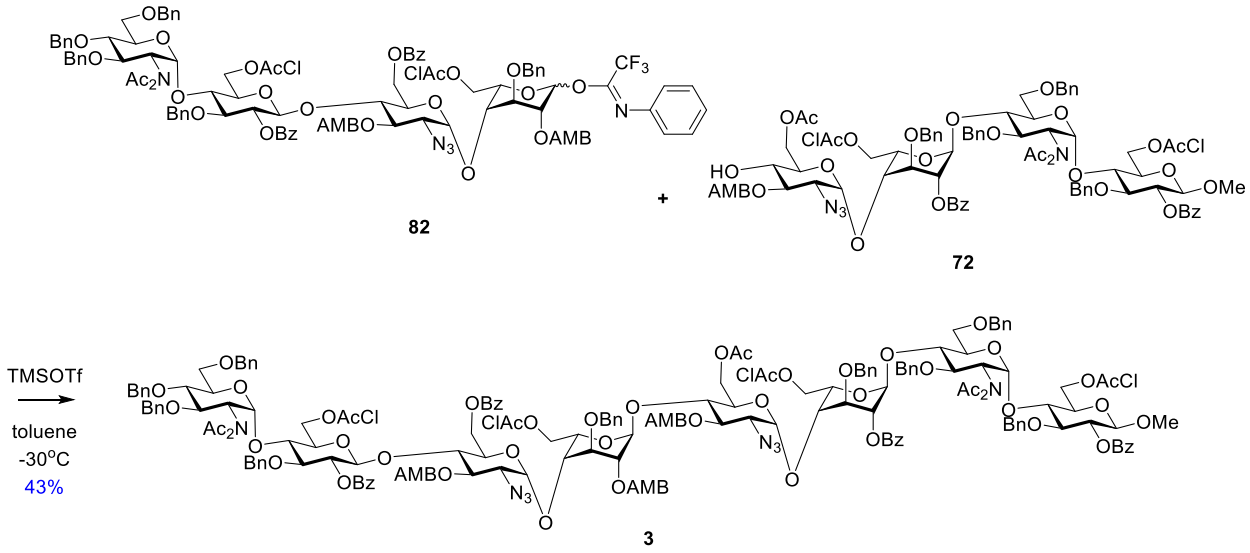

*Scheme 59 - Synthesis of octasaccharide **3** in a [4+4] manner.*

This was an exceptionally pleasing result, showing a way to access the desired octasaccharides without changing the existing protecting group strategy. In addition, a pure sample of a high R_f donor-related impurity was also isolated. This high R_f material was identified using NMR and MS analysis as the glycal version of the tetrasaccharide donor in this glycosylation, tetrasaccharide glycal **83** (Figure 35). This mirrors the by-product observed in the hexasaccharide glycosylation using disaccharide *N*-PTFA donor **59**, in which disaccharide glycal **78** was isolated. The ^{1}H NMR of tetrasaccharide glycal **83** displays differences compared to the spectra of the equivalent donor. These differences are also like those observed in the spectra of **78**. A characteristic singlet proton signal is present at a high chemical shift, and the other three anomeric protons are present in the typical chemical shift range. Both this tetrasaccharide glycal and the disaccharide glycal **78** degraded by TLC analysis when stored as films in air over several days.

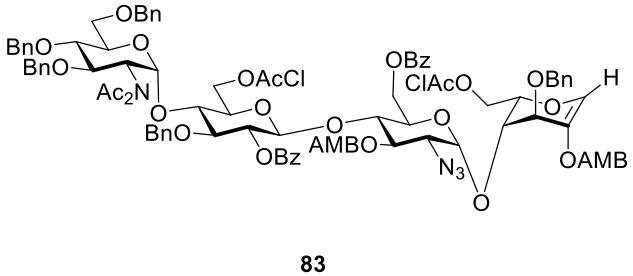

83

*Figure 35 - The tetrasaccharide glycal by-product **83** of a [4+4] glycosylation.*
*This material is related to donor **82** and displays the same changes to NMR spectra as was observed in the isolation of disaccharide glycal **78**.*

The same chemistry was attempted to make the other target, octasaccharide **4**. The selective 4-*O*-Fmoc deprotection of the disaccharide **6** worked very well, giving pure disaccharide acceptor **84** in 92% yield (Scheme 60).

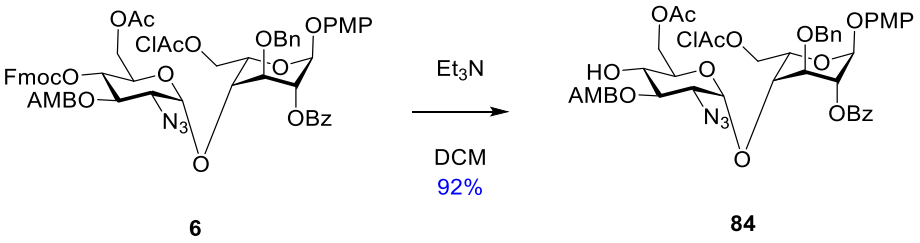

*Scheme 60 - Synthesis of disaccharide acceptor **84** from disaccharide **6**.*

However, significant difficulty was encountered in carrying out the [2+2] glycosylation of disaccharide TCA donor **57** with acceptor **84**, to generate tetrasaccharide **85** (Scheme 61). The same conditions which had worked successfully in the case of acceptor **79** produced only low yields of 5% to 10% in several attempts. The product also had close running impurities.

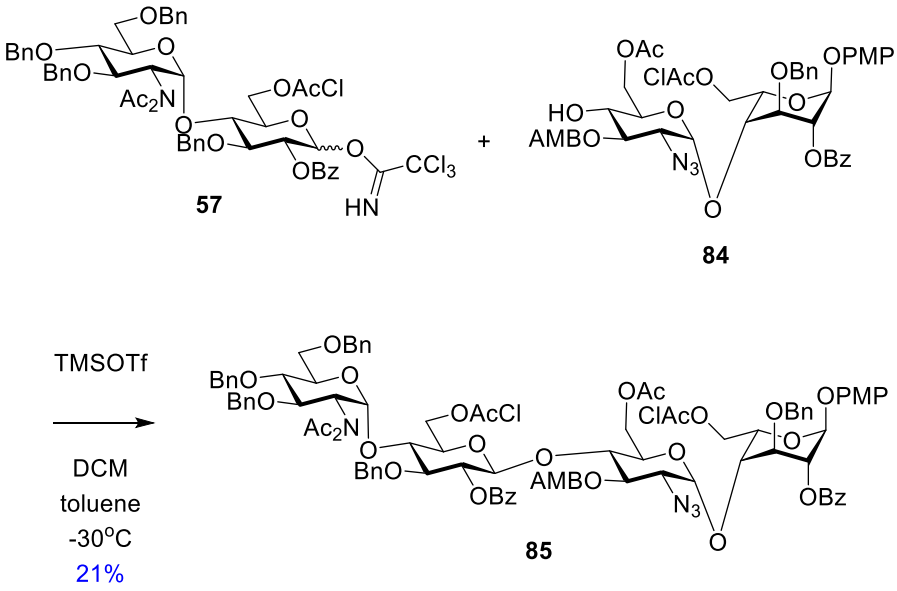

*Scheme 61 - Attempted access to a tetrasaccharide **85** from the glycosylation of TCA donor disaccharide **57** and disaccharide acceptor **84**.*
*This reaction gave low yields over several attempts using our optimised conditions, including attempts with the use of donor **59**. This is in marked contrast to the equivalent [2+2] glycosylation to make tetrasaccharide **80**, which was able to be better optimised.*

Additionally, a [2+2] glycosylation was carried out using *N*-PTFA donor disaccharide **59** with acceptor **84**, but this reaction also produced only trace product. Large quantities of donor hemiacetal **58** and unreacted acceptor **84** were recovered in all three attempts. Separation of **58** and **84**, both of which are disaccharides, proved to be quite challenging but could be achieved. A subsequent glycosylation

attempt, at a lower temperature of -30 °C, gave a higher yield of 30% of the intended tetrasaccharide product **85**, however this product contained impurities. Optimisation of the chromatography method allowed the isolation of pure tetrasaccharide **85** in a low yield (21%).

Following the synthesis of tetrasaccharide **85**, the material was selectively deprotected by CAN mediated 1-*O*-PMP hydrolysis to give hemiacetal **86**, in a yield of 59%. The hemiacetal was converted into *N*-PTFA donor **87** in 71% yield by our established method (Scheme 62).

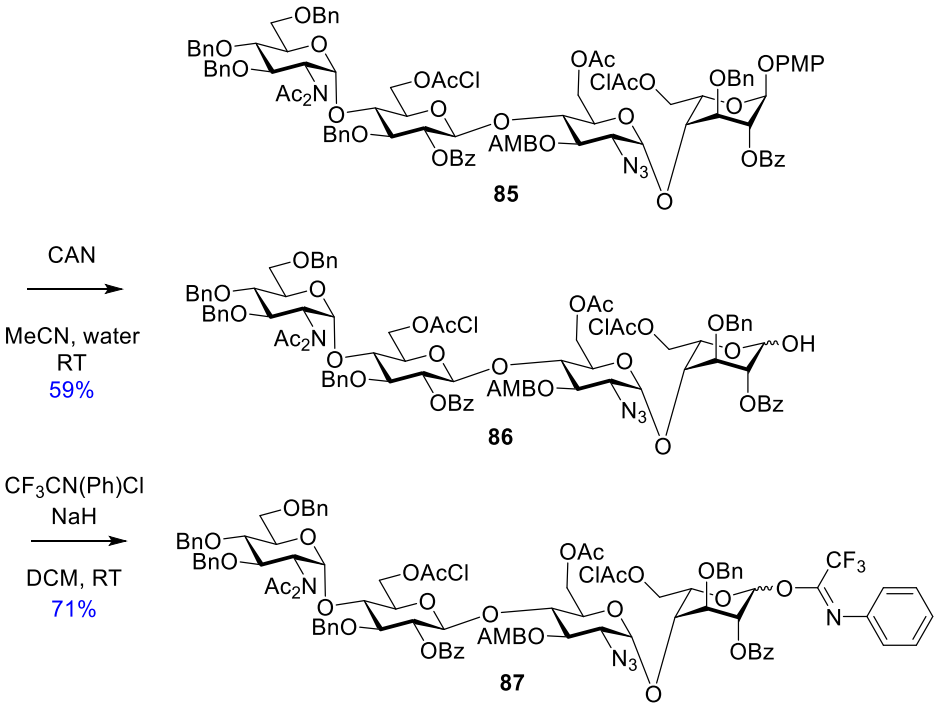

*Scheme 62 - The synthesis of N-PTFA donor **87** from the tetrasaccharide **85**.*
*Both of these reactions performed well as was experienced in the synthesis of N-PTFA donor **82** from tetrasaccharide **80**.*

An attempt was made to synthesise octasaccharide **4** by using a [4+4] glycosylation of tetrasaccharide *N*-PTFA donor **87** and tetrasaccharide acceptor **72**. This was a small-scale reaction owing to the difficulties encountered in the synthesis of tetrasaccharide **85**. The reaction yielded octasaccharide target **4** in a yield of 39% (Scheme 63). This was comparable to the synthesis of octasaccharide **3**. However, formation of hemiacetal was observed on TLC analysis of the reaction mixture, which indicated that some water was present in the reaction.

Due to the small scale of this reaction, only 20 mg of purified octasaccharide **4** was produced. Grease and water were both present in the ^{1}H NMR spectra and were difficult to remove. Acquisition of a suitable ^{13}C spectrum on this small sample proved challenging. Therefore, ^{13}C assignments for this molecule were determined by HSQC.

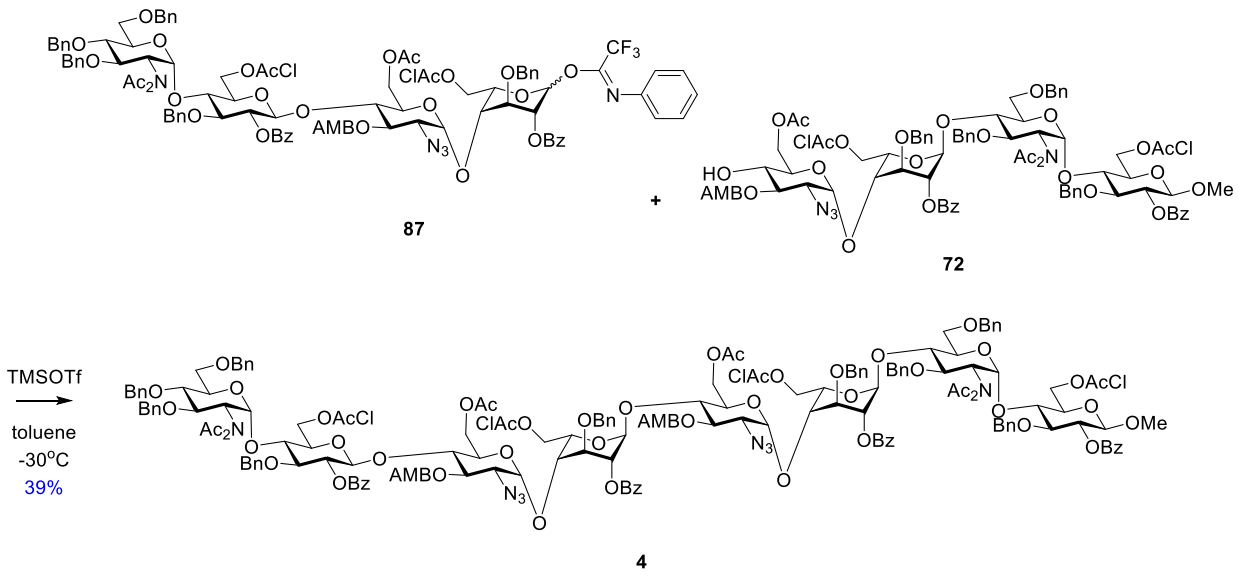

*Scheme 63 - The synthesis of octasaccharide **4** in a [4+4] glycosylation.*

With the successful synthesis of octasaccharide targets **3** and **4** by the [4+4] glycosylation method, a proven route to these fully protected molecules has been established.

4.1.5 Preliminary processing of impure octasaccharide material

The initial batch of impure fully protected octasaccharide **3**, 50 mg, was subjected to DABCO to remove the four chloroacetate groups and give octasaccharide **88**. This reaction gave a moderate yield of 40%, which remained impure. Additionally, a significant side-product appearing further down the TLC plate was observed. This was isolated and it was confirmed that there was loss of one of the *N*-Ac groups in this side-product.

Therefore, this de-*N*-acetylated material was re-*N*-acetylated using previously reported conditions.[330] The sum of the masses of the two sets of material (reaction product and re-*N*-acetylated side-product) gave an acceptable overall yield of 63% for the chloroacetate deprotection. However, impurities remained present in both samples of **88** despite extensive chromatography attempts. Co-elution of impurities was observed in the various column methods tested.

Alternative conditions for selective chloroacetate deprotection were explored. The chloroacetate deprotection of **3** was carried out using thiourea in moderate yields of 62%. No *N*-Ac loss was observed. Thiourea reacts selectively to remove chloroacetates and is less basic than DABCO, which prevents base-catalysed *N*-acetate deprotection. It was also reasoned that over-exposure to acidic Dowex 50WX8-200 resin, used to quench the reaction, could be responsible for *N*-Ac loss. In the initial attempt, the reaction mixture was exposed to resin for 10-15 minutes after slight cooling from the reaction temperature (70 °C). In subsequent attempts at the DABCO deprotection of octasaccharide

3, the reaction mixture was thoroughly cooled to RT before the addition of Dowex 50WX8-200 resin. Furthermore, the mixture was stirred for no more than 5 minutes before filtering off the resin. These attempts were successful in producing octasaccharide **88** with minimal *N*-Ac loss observed.

MS analysis of the impurities present in the sample of octasaccharide **88** indicated the presence of a 4-*O*-acetylated hexasaccharide which had lost three chloroacetate groups. The presence of three unprotected hydroxyl groups on this compound, versus the four of the product octasaccharide, would be expected to aid in separation. However, separation of this impurity was not achieved despite extensive efforts.

The four primary hydroxyl groups of octasaccharide **88** were then oxidised using the previously described TEMPO/BAIB method followed by methyl ester formation. This afforded octasaccharide **89** in a high yield (79%). However, the product was impure, despite multiple chromatography attempts (Scheme 64). MS analysis showed the presence of an oxidised 4-*O*-acetylated hexasaccharide impurity, and multiple other impurities which could not be identified.

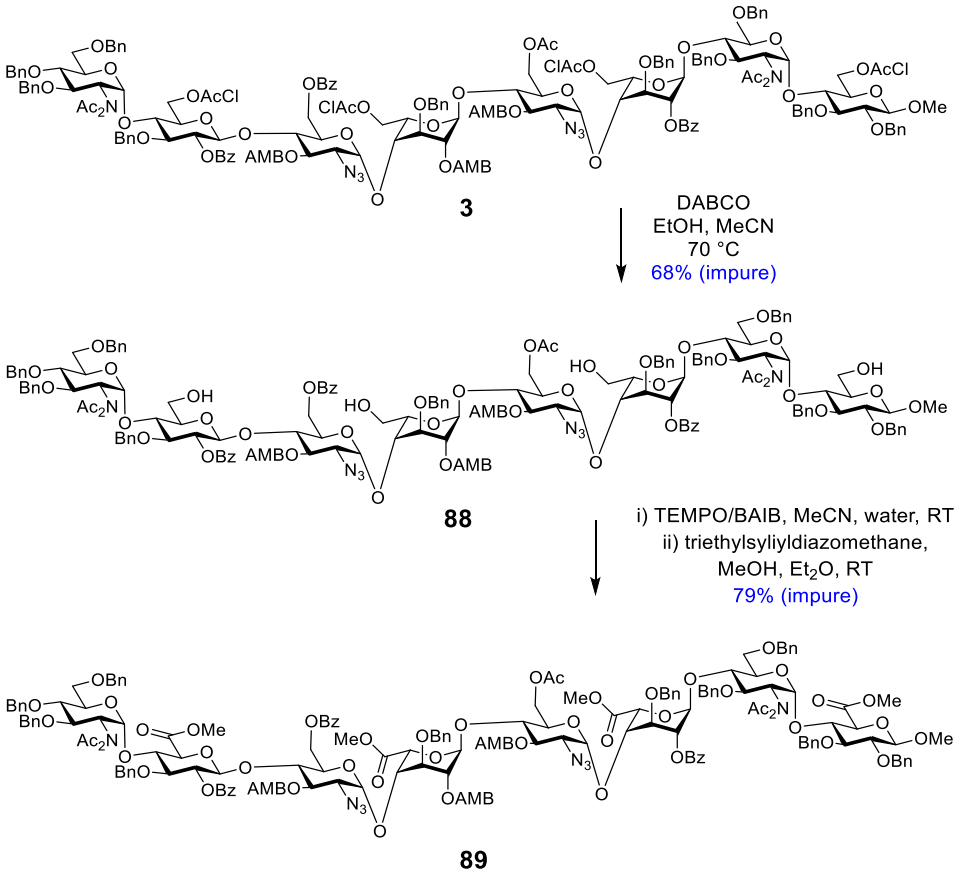

*Scheme 64 - Selective deprotection and subsequent oxidation of the impure octasaccharide **3**.*

Further reactions were not carried out on the impure sample of octasaccharide **89** due to time constraints. However, these investigations showed that purification of impure octasaccharides reaction following the selective deprotection and oxidation steps remained challenging.

4.2 Conclusions

The synthesis of fully protected octasaccharides **3** and **4** has been achieved. The successful synthesis used a strategy featuring a pair of [2+2] glycosylation reactions followed by a [4+4] glycosylation reaction. A robust protecting group strategy and the parallel synthesis of disaccharide building blocks was employed. Significant quantities of monosaccharides, and subsequently disaccharide building blocks, were synthesised. In addition, a large quantity of 2-(acetoxymethyl) benzoic acid was synthesised. Synthetic procedures were developed to install AMB as a protecting group at the glucosamine residue 3-*O*-position. This work establishes a pathway to selectively access the glucosamine 3-*O*-position, or other positions of interest, in future oligosaccharide synthesis using AMB protection. Furthermore, AMB protecting group chemistry could be used to access sites for selective modification in other saccharide molecules, such as in branched rather than linear oligosaccharides, or in dendrimer constructs.

The difficulty of the reactions undertaken to synthesise the fully protected octasaccharide targets showcases the level of fine-tuning of the glycosylation reaction required. Changes to the synthetic pathway were numerous, including using a different donor system and reaction conditions. In this, the work of Chapter 2 was especially helpful, as the synthesis, handing and use of the *N*-PTFA donor system on a similar sugar platform was familiar. The differences between the synthesis of octasaccharide targets without a glucosamine residue 3-*O*-AMB group by colleagues, and this synthesis, further showcases that each glycosylation is different and requires its own development to be carried out successfully.

5. Chapter 5

5.1 Overall conclusions and future work

Regarding the series of comparative hexose and uronate [2+2] glycosylation reactions detailed in Chapter 2, there is scope for further investigation. The work could be extended to investigate more donor systems, some of which were mentioned previously. Additionally, the effectiveness of other sugars, such as idosaccharides, could be assessed under the same conditions. Furthermore, future work could return to the chloride donor and developing a successful synthesis of the uronyl chloride. An alternative method that does not use tin tetrachloride, such as the use of trifluoromethanesulfonic or methanesulfonic anhydride,[341] or perhaps zinc chloride and dichloromethyl methyl ether,[342] could be used. Other orthogonal protecting group strategies could also be considered, as this can have significant effects on glycosylation reaction yields. A large library of comparative glycosylation reactions on a system with multiple orthogonal functionalities could be assembled, which would be a valuable resource for carbohydrate chemists.

The mixed fortunes during the octasaccharide assembly are of interest. Why was the [4+2] glycosylation step able to be optimised with a change from TCA to *N*-PTFA donor systems? Why did this same optimisation fail for the [6+2] glycosylation step?

The main consideration is matched and mismatched donor acceptor combinations.[204] In our case, the [6+2] glycosylation system may have mismatched donors and acceptors when using both the TCA and *N*-PTFA donors. This would lead to the observed poor yields and sluggish reactions. The [4+2] glycosylation system may have a good reactivity match between the *N*-PTFA donor and acceptor, but not a good match with the TCA donor. Recent literature has highlighted the role of the reactivity of the acceptor in the success or failure of a glycosylation.[167,184,205,343] In these studies it was shown that the protecting groups used on the acceptor can have a significant effect on reactivity. Furthermore, in our hands, larger sugars have proven to be poorer glycosyl acceptors.

Another possibility is a steric hinderance between the reaction centres of the two molecules. This may occur in the [6+2] glycosylation between the participating 2-*O*-Bz group on the glycosyl donor and the opposing 3-OAMB group. However steric hinderance might not occur in the [4+2] glycosylation, where the donor is an idose sugar (Figure 36).[203] This would not explain why the [2+2] glycosylation, with a reaction centre analogous to the [6+2] glycosylation, would proceed.

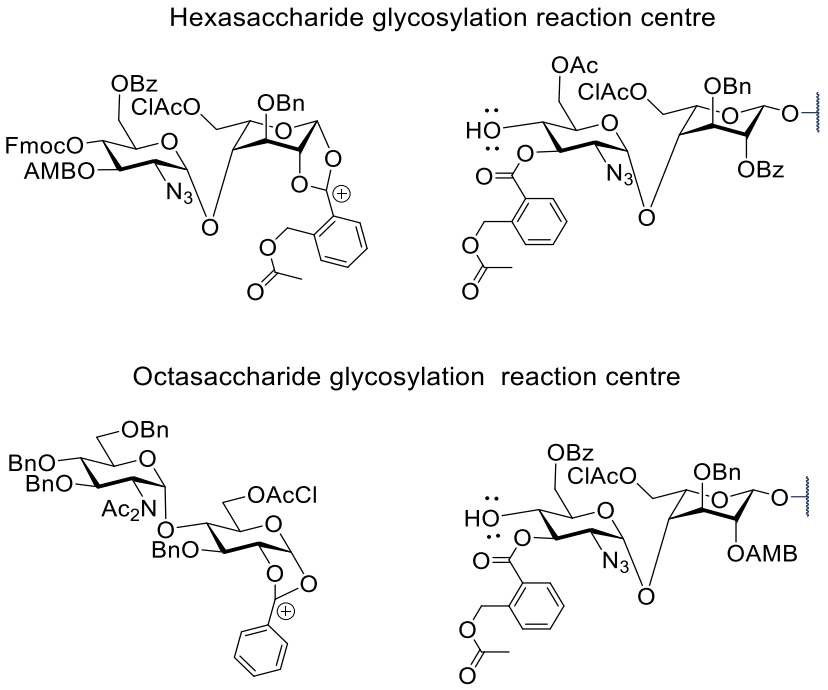

Figure 36 – Structural differences between the octasaccharide and hexasaccharide glycosylation reactions.
In the hexasaccharide glycosylation, the donor has an idosaccharide residue at the reducing end. In contrast, in the octasaccharide glycosylation and analogous [2+2] glycosylation, the donor has a glucose residue at the reducing end.

There is also evidence to suggest that the anomeric configuration of existing linkages in the acceptor may have a remote effect on the outcome of a glycosylation.[344] It is possible that the hexasaccharide acceptor adopts a conformation in solution that disfavours glycosylation by hindering access to the hydroxyl group. This would explain the success found in the analogous [2+2] glycosylation, as the acceptor disaccharide would be less hindered by conformation.

Another cause for the difficult glycosylation could be some level of participation by the 3-*O*-AMB protecting group adjacent to the unprotected alcohol on the acceptor. The acetate group on the 3-*O*-AMB may be able to interact with the hydroxyl group, perhaps through hydrogen bonding. Similar effects have been noted in the work of Crich et al in a thorough investigation of diminished acceptor reactivity in some systems.[345] In this report, a 3-*O*-picolinyl ether was able to hydrogen bond with the nearby 4-hydroxyl group, with devastating results for glycosylation yields using this glycosyl acceptor. Other groups have reported similar participating effects.[184] This could also occur to some degree when AMB is used as a protecting group at C2 on the glycosyl donor in the [4+2] glycosylation reaction, however this reaction was successful.

In the presence of a Lewis acid, it is conceivable that the acetate group on the AMB group could migrate to an exposed hydroxyl group. However, the resulting 2-(hydroxymethyl) benzoate ester

should then readily cyclise to phthalide. The product of AMB deprotection was not detected in MS of crude glycosylation reaction mixtures. A possible remedy for issues caused by this protecting group is to change part of our protecting group strategy. Other groups have synthesised oligosaccharides with 3-*O*-sulfation using alternative combinations which could be adopted,[241,342] and beyond this, new protecting group strategies continue to be developed.[346-348]

There is now a significant quantity of hexasaccharide material in our laboratory. 2 g of the hexasaccharide acceptor **74** and 1 g of the hexasaccharide acceptor **77** have been synthesised. This material represents a large synthetic effort, and it would be gratifying to see the challenge of the [6+2] glycosylation overcome. A new synthesis of disaccharide thioglycoside donor **60** or other thioglycoside motifs could be carried out. This thioglycoside donor could then be used in the [6+2] glycosylation. Furthermore, there are many other donor systems,[230] including varieties of thioglycosides,[349,350] sulfoxides,[235] fluorides,[336] iodides[351-353] or phosphates[354-357] that could be trialled to make this octasaccharide glycosylation work. Within each of these groups of donor systems, there are also different promoters and catalysts that could be tested.

Overall, this work is a good example of the variety of problems encountered during the synthesis of complex oligosaccharides. It was famously observed by Paulsen that "*Although we have now learned to synthesise oligosaccharides, each oligosaccharide synthesis remains an independent problem, whose resolution requires considerable systematic research and a good deal of know-how. There are no universal reaction conditions for oligosaccharide syntheses*".[246] Certainly this has proven to be the case in this synthesis.

There is scope for further work based on our octasaccharide targets. Discussions with our collaborators has highlighted interest in other targets, which have a single glucosamine 3-*O*-sulfate group, rather than two. This could readily be achieved using the chemistry already for developed in this project. Exchanging one of the disaccharides used in this synthesis for an analogue lacking 3-*O*-AMB protection of the glucosamine residue would afford a mono-3-*O*-sulfated product.

5.2 Planned octasaccharide processing to final sulfated targets

Originally, it was planned to access the octasaccharides **1** and **2** during this project. Due to the difficulties encountered in the synthesis of **3** and **4**, there was not enough time available to accomplish this. In future work, gram-scale quantities of octasaccharides **3** and **4** can be synthesised by the proven [4+4] route. The fully protected octasaccharides **3** and **4** can then be processed through a series of selective deprotections and modifications to give the final octasaccharide heparan sulfate mimetics **1** and **2**.

The first two of these modifications, selective chloroacetate deprotection followed by oxidation and methylation, have been detailed in the previous section. However, they will be briefly included here for completeness. The below examples will all follow the planned pathway from fully protected octasaccharide **3** to final target octasaccharide **1** for consistency. The fully protected octasaccharide is first selectively deprotected to remove the four chloroacetate groups. The exposed primary hydroxyl groups are then oxidised and subsequently methylated (Scheme 65).

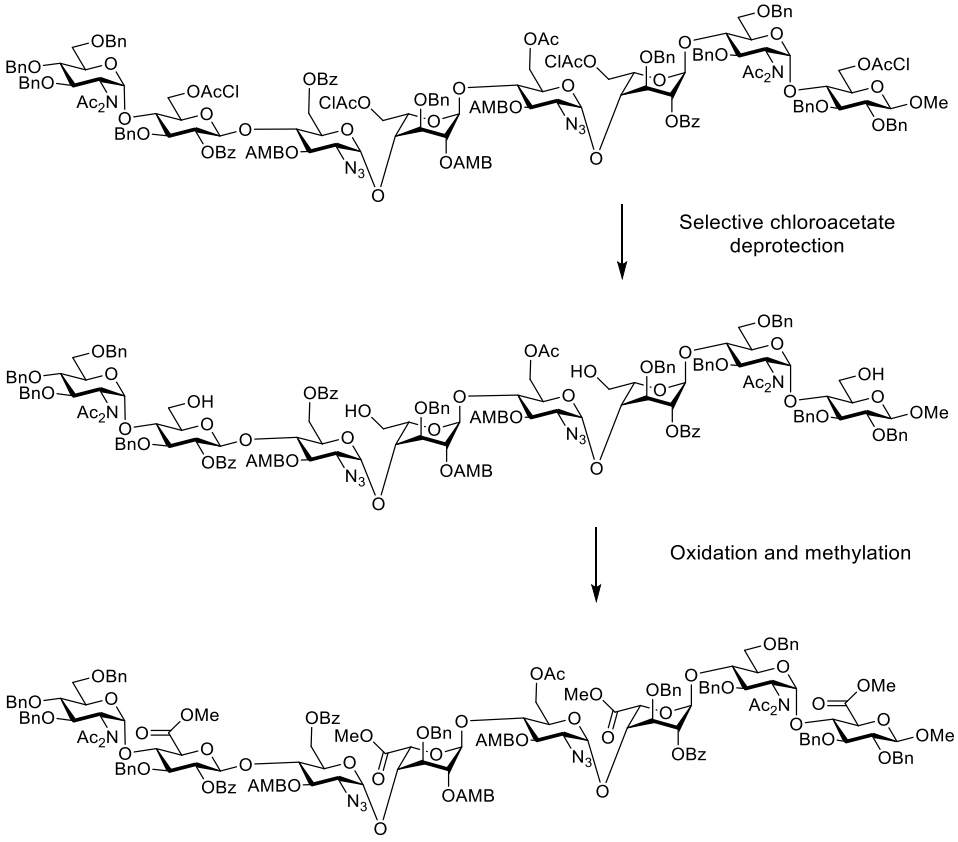

Scheme 65 - Selective deprotection and subsequent oxidation of the octasaccharide.

The octasaccharide can then undergo selective deprotection of primary acetates, including the 3-*O*-AMB groups as detailed in a previous chapter, which exposes sites for selective O-sulfation (Scheme 66). Primary and secondary benzoates present elsewhere in the molecule should remain stable.

Sulfation can then be carried out on the exposed hydroxyl groups. Glucosamine residue 6-*O*-sulfation and iduronic acid 2-*O*-sulfation has been demonstrated previously.[194] Glucosamine 3-*O*-sulfation has not been carried out by our group previously. The stability and handling of these 3-*O*-sulfated oligosaccharides, particularly in subsequent modifications, will require investigation.

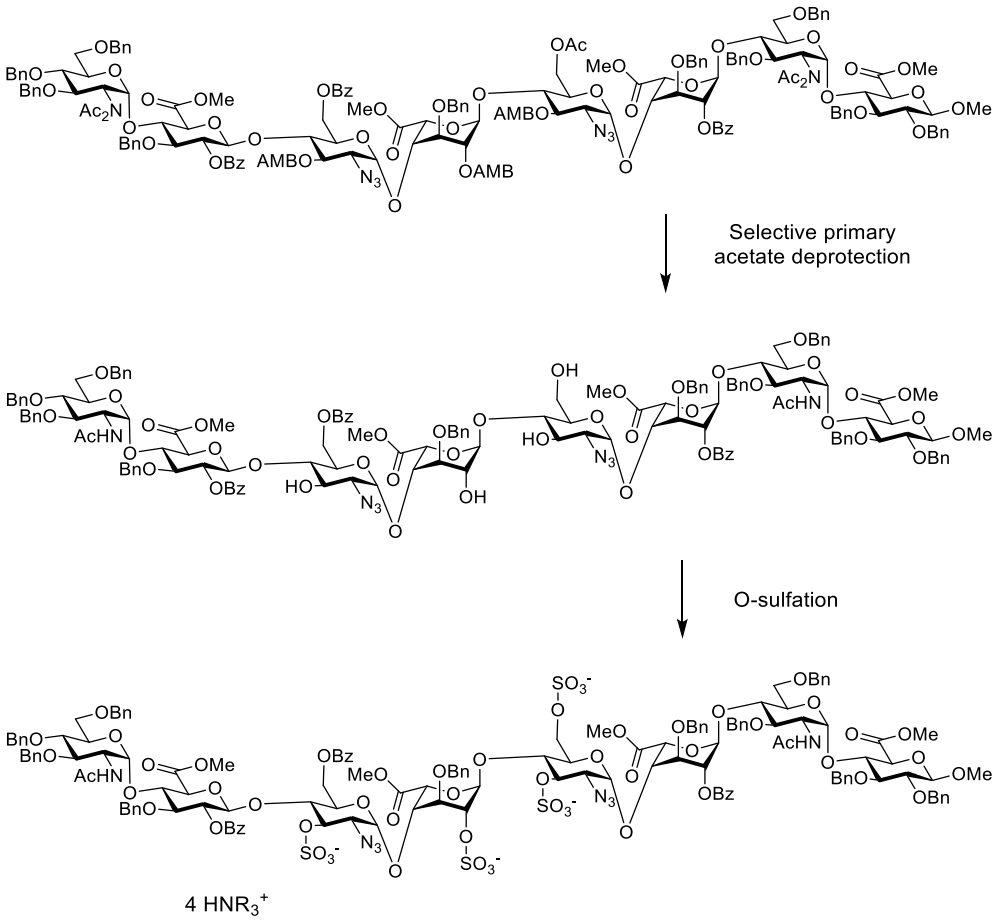

Scheme 66 - Further selective deprotection and O-sulfation of the octasaccharide

Following the sulfation step, the octasaccharide can then be subjected to saponification conditions. These conditions will remove benzoyl protecting groups and hydrolyse the methyl esters to the corresponding acids. These compounds can then be reduced to remove benzyl groups and reduce the azides to the corresponding amines. Finally, the now deprotected octasaccharide can be subjected to *N*-sulfation conditions to give the final product, octasaccharide **3** (Scheme 67).

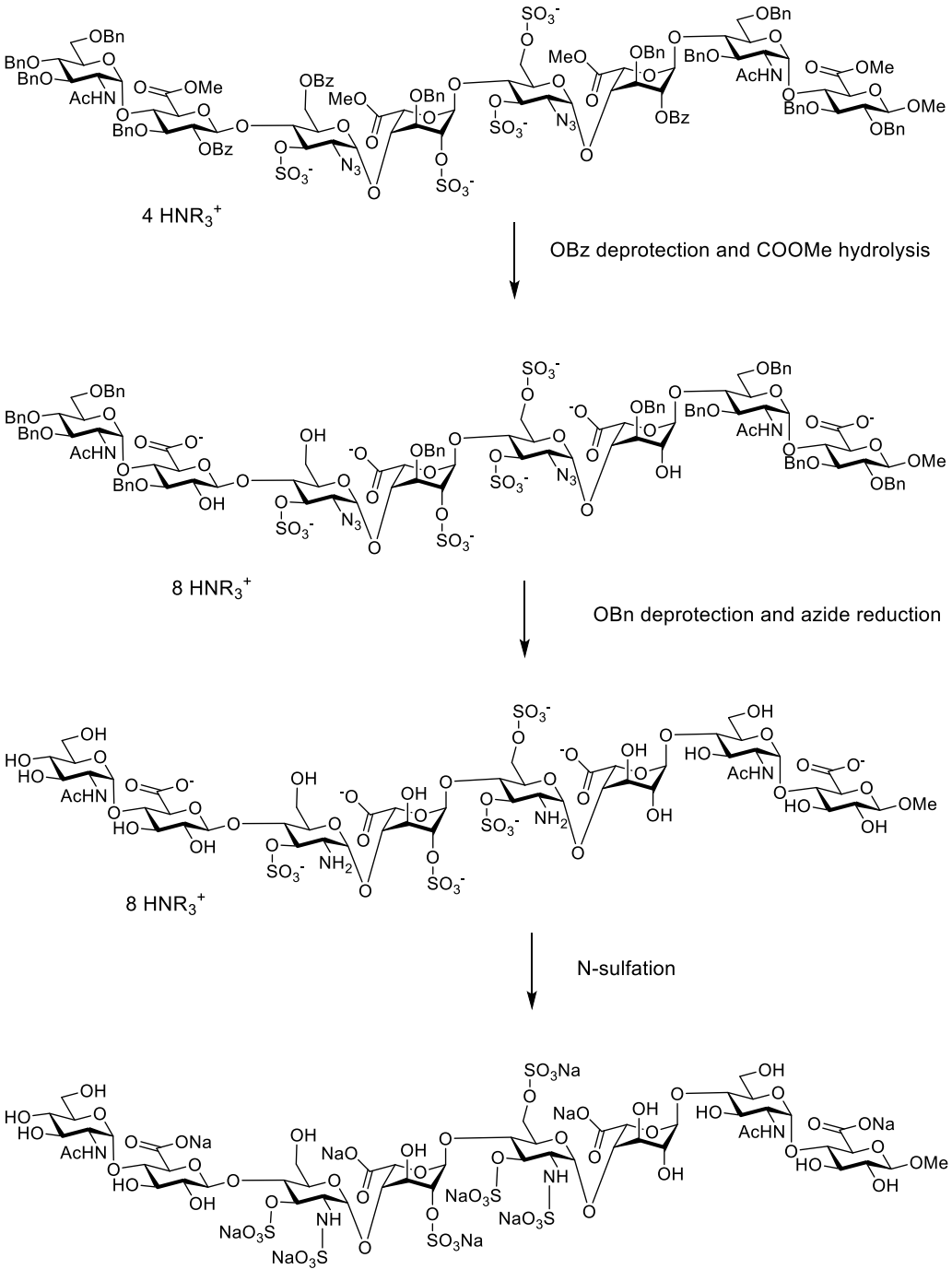

Scheme 67 - Further octasaccharide deprotection and reduction of the azide group followed by N-sulfation.

6. Experimental

All ^{1}H, ^{13}C, DEPT and 2D NMR spectra were acquired on a Bruker 500 MHz spectrometer. Chemical shifts are reported in parts per million (ppm) relative to tetramethylsilane (TMS). NMR data is presented as follows: chemical shift, multiplicity (s = singlet, d = doublet, t = triplet, dd = doublet of doublets, m = multiplet), coupling constant (J) in hertz (Hz), integration. Mass spectra were acquired on a Waters Q-TOF Premier™ Electrospray Mass Spectrometer. Optical rotation measurements were acquired using a Rudolph Research Analytical Autopol IV automatic polarimeter at a wavelength of 589 nm and at a temperature of 20 °C. $[\alpha]_D$ values are given in 10^{-1} deg cm^2 g^{-1}. IR spectra were acquired using a Bruker Optics TENSOR II FT-IR spectrometer. TLC analysis was conducted on silica gel F254 (Merck KGaA) with detection by UV absorption (254 nm) or by dipping in cerium molybdate stain (400 mL 10% sulfuric acid/water, 20 g ammonium molybdate and 0.2 g cerium sulfate) where applicable. Column chromatography was carried out using an automated BÜCHI Pure system and pre-packaged BÜCHI FlashPure EcoFlex silica (50 µm irregular) or FlashPure HP silica (20 µm spherical) columns, or SiliCycle SiliaSep premium silica columns (25 µm spherical). Molecular sieves used were 3 Å beads (sourced from Fisher Scientific) or 4 Å powder (sourced from Sigma-Aldrich), and had been dried for 2 hours under high vacuum at 200 °C and stored on a bench under argon before use. X-ray crystal structures were collected on an Agilent SuperNova diffractometer fitted with an EOS S2 detector.

Crystallographic data:

Compound number	Acceptor **24**	Disaccharide **34**	Monosaccharide **43**
CCDC identifier	1987993	1987991	N/A
Empirical formula	$C_{43}H_{45}N_3O_{14}$	$C_{59}H_{56}ClN_3O_{14}S$	$C_{30}H_{29}N_3O_7S$
Formula weight	827.82	1098.57	575.62
Temperature (K)	120.00(10)	120.00(10)	120.01(10) K
Wavelength (Å)	1.54184	1.54184	1.54184 Å
Crystal system	Orthorhombic	Monoclinic	Orthorhombic
Space group	$P2_12_12_1$	$P2_1$	$P2_12_12_1$
Unit cell dimensions			
a (Å) b (Å) c (Å)	8.0833(2) 18.7876(7) 26.8116(12)	5.23660(10) 35.3229(3) 14.56840(10)	5.12929(5) 22.9252(2) 24.4533(2)
α (°) β (°) γ (°)	90 90 90	90 95.5220(10) 90	90 90 90
Volume ($Å^3$)	4071.8(3)	2682.24(6)	2875.46(5)
Z	4	2	4
Density (calculated) (Mg/m^3)	1.350	1.360	1.330

Absorption coefficient (mm^{-1})	0.852	1.590	1.437
F(000)	1744	1152	1208
Crystal size (mm^3)	0.259 × 0.034 × 0.025	0.484 × 0.098 × 0.055	0.510 × 0.086 × 0.084
Theta range for data collection (°)	4.051 to 74.658	3.944 to 73.534	3.615 to 73.590
Index ranges	-9 <= h <= 9 -22 <= k <= 23 -33 <= l < =31	-5 <= h <= 6 -43 <= k <= 43 -18 <= l <= 18	-6 <= h <= 4 -28 <= k <= 28 -0 <= l <= 30
Reflections collected	64624	48369	23464
Independent reflections	8176 [R(int) = 0.0883]	10328 [R(int) = 0.0367]	5801 [R(int) = 0.0327]
Completeness to theta = 67.684°	100%	98.9%	100.0 %
Absorption correction	Semi-empirical from equivalents	Semi-empirical from equivalents	Semi-empirical from equivalents
Max. and min. transmission	1.000 and 0.575	1.000 and 0.541	1.00000 and 0.66056
Refinement method	Full-matrix least-squares on F^2	Full-matrix least-squares on F^2	Full-matrix least-squares on F^2
Data / restraints / parameters	8176 / 0 / 548	10328 / 68 / 914	5801 / 0 / 372
Goodness-of-fit on F^2	1.054	1.115	1.033
Final R indices [I>2sigma(I)]	R1 = 0.0564 wR2 = 0.1354	R1 = 0.0396 wR2 = 0.1040	R1 = 0.0299 wR2 = 0.0769
R indices (all data)	R1 = 0.0721 wR2 = 0.1464	R1 = 0.0415 wR2 = 0.1051	R1 = 0.0322 wR2 = 0.0781
Absolute structure parameter	-0.06(11)	-0.005(5)	0.008(8)
Largest diff. peak and hole (e.Å-3)	0.292 and -0.217	0.388 and -0.269	0.214 and -0.192

p-Tolyl 2-azido-4,6-*O*-benzylidene-2-deoxy-1-thio-β-D-glucopyranoside **(16)**

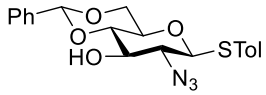

p-Tolyl 2-azido-2-deoxy-1-thio-β-D-glucopyranoside **12** (25.0 g, 80.3 mmol) and (1*S*)-(+)-10-camphorsulfonic acid (0.3 g, 1 mmol, 0.02 equiv.) was dissolved in anhydrous DMF (40 mL) and treated with benzaldehyde dimethyl acetal (30.0 mL, 198 mmol, 2.5 equiv.) under argon. The reaction mixture was stirred at 60 °C under reduced pressure. After 2 hours, TLC analysis showed high level of conversion. The reaction mixture was treated with Et_3N dropwise until a pH of 8 was achieved (1.5 mL), upon which the DMF was removed in vacuo. The resulting brown solid was re-dissolved in CH_2Cl_2. The organic layer was washed with water, then with brine, dried over $MgSO_4$ and evaporated to dryness. Precipitation from a mixture of EtOAc and petroleum ether afforded the title compound as

an off-white powder (22.6 g, 70%), TLC: R_f = 0.6 (EtOAc/toluene, 1/4 *v*/*v*); ^{1}H NMR (500 MHz, $CDCl_3$) δ 7.49 – 7.43 (m, 5H), 7.39 – 7.35 (m, 3H), 7.18 – 7.14 (m, 2H), 5.52 (s, 1H), 4.48 (d, J = 10.2 Hz, 1H), 4.40 – 4.33 (m, 1H), 3.80 – 3.73 (m, 2H), 3.46 – 3.42 (m, 2H), 3.32 (dd, J = 10.1, 9.0 Hz, 1H), 2.37 (s, 3H); ^{13}C NMR (125 MHz, $CDCl_3$) δ 139.1, 136.7, 134.2, 129.9, 129.4, 128.3, 126.8, 126.2, 101.9, 86.8, 80.2, 74.1, 70.2, 68.4, 65.0, 21.2; HRMS (ESI+) calculated for $C_{20}H_{21}N_3O_4SNa$ $[M+Na]^+$ *m*/*z* 422.1150, found 422.1153. Data matches a previous instance of this compound.[194]

p-Tolyl 2-azido-3-*O*-benzyl-4,6-*O*-benzylidene-2-deoxy-1-thio-β-D-glucopyranoside **(17)**

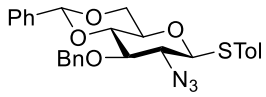

p-Tolyl 2-azido-4,6-*O*-benzylidene-2-deoxy-1-thio-β-D-glucopyranoside **16** (10.7 g, 27.9 mmol) was dissolved in anhydrous DMF (40 mL) and treated with benzyl bromide (6.8 mL, 56 mmol, 2 equiv.) under argon. To the reaction mixture, NaH 60% *w*/*w* dispersion in mineral oil (1.5 g, 45 mmol, 1.6 equiv.) was added in small portions with stirring, while maintaining an overall reaction temperature below 30 °C. The reaction mixture was stirred at room temperature overnight before being quenched with MeOH (5 mL). Upon dilution with water, an off-white precipitate formed. The precipitate was collected by filtration and washed with water and EtOH, and then dried in vacuo, affording the title compound as an off-white powder (13.3 g, 97%), TLC: R_f = 0.7 (EtOAc/toluene, 1/4 *v*/*v*); ^{1}H NMR (500 MHz, $CDCl_3$) δ 7.45 (tt, J = 8.4, 2.4 Hz, 4H), 7.41 – 7.25 (m, 8H), 7.14 (d, J = 7.9 Hz, 2H), 5.55 (s, 1H), 4.90 (d, J = 10.9 Hz, 1H), 4.77 (d, J = 10.9 Hz, 1H), 4.42 (d, J = 10.2 Hz, 1H), 4.38 (dd, J = 10.6, 5.0 Hz, 1H), 3.77 (t, J = 10.3 Hz, 1H), 3.68 – 3.56 (m, 2H), 3.46 – 3.39 (m, 1H), 3.32 (dd, J = 10.2, 8.6 Hz, 1H), 2.35 (s, 3H); ^{13}C NMR (125 MHz, $CDCl_3$) δ 139.1, 137.5, 137.1, 134.5, 129.9, 129.1, 128.4, 128.33, 128.29, 128.0, 126.5, 125.9, 101.2, 86.6, 81.3, 81.0, 75.2, 70.4, 68.5, 64.5, 21.2; HRMS (ESI+) calculated for $C_{27}H_{27}N_3O_4SNa$ $[M+Na]^+$ *m*/*z* 512.1620, found 512.1631. Data matches a previous instance of this compound.[194]

p-Tolyl 2-azido-3-*O*-benzyl-2-deoxy-1-thio-β-D-glucopyranoside **(18)**

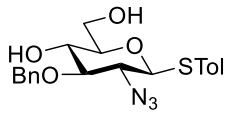

p-Tolyl 2-azido-3-*O*-benzyl-4,6-*O*-benzylidene-2-deoxy-1-thio-β-D-glucopyranoside **17** (10.0 g, 20.5 mmol) was dissolved in 1,4-dioxane (35 mL) and MeOH (16 mL) under argon. In a separate flask, MeOH (20 mL) was cooled to 0 °C and acetyl chloride (0.5 mL, 7 mmol, 0.3 equiv.) was added. The two solutions were combined, and the resulting mixture stirred at room temperature overnight. TLC

analysis showed complete conversion. The reaction was quenched by the addition of Amberlyst A26 (OH) resin, and the pH was found to be neutral after 20 minutes. The resin was filtered off and washed with EtOAc, and the filtrate was concentrated in vacuo. The resulting yellow oily residue was purified by column chromatography to afford the title compound as an off-white foam (5.60 g, 14.0 mmol, 68%), TLC: R_f = 0.35 (EtOAc/toluene, 1/4 *v*/*v*); ^{1}H NMR (500 MHz, $CDCl_3$) δ) 7.46 – 7.41 (m, 2H), 7.40 – 7.29 (m, 5H), 7.14 (d, J = 7.9 Hz, 2H), 4.94 (d, J = 11.3 Hz, 1H), 4.74 (d, J = 11.3 Hz, 1H), 4.41 (d, J = 9.8 Hz, 1H), 3.86 (dt, J = 12.5, 4.0 Hz, 1H), 3.75 (dt, J = 11.5, 5.4 Hz, 1H), 3.51 (td, J = 9.2, 2.8 Hz, 1H), 3.40 – 3.19 (m, 3H), 2.41 (d, J = 3.2 Hz, 1H), 2.34 (s, 3H), 2.06 (t, J = 6.3 Hz, 1H); ^{13}C NMR (125 MHz, $CDCl_3$) δ 138.9, 137.7, 134.0, 129.9, 128.7, 128.3, 128.1, 127.0, 86.4, 84.7, 79.2, 75.5, 70.3, 64.8, 62.5, 21.1; HRMS (ESI+) calculated for $C_{20}H_{23}N_3O_4SNa$ $[M+Na]^+$ *m*/*z* 424.1307, found 424.1303. Data matches a previous instance of this compound.[194]

p-Tolyl 6-*O*-acetyl-2-azido-3-*O*-benzyl-2-deoxy-1-thio-β-D-glucopyranoside (19)

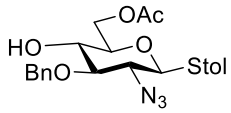

p-Tolyl 2-azido-3-*O*-benzyl-2-deoxy-1-thio-β-D-glucopyranoside **18** (5.0 g, 12 mmol) was dissolved in anhydrous CH_2Cl_2 (50 mL) and treated with pyridine (3.5 mL, 43 mmol, 3.4 equiv.) under argon. The reaction mixture was cooled to -75 °C and treated with acetyl chloride (0.9 mL, 12 mmol, 1 equiv.) dropwise with stirring. The reaction mixture was left to warm to room temperature overnight. The mixture was then washed with HCl (aq), saturated $NaHCO_3$ (aq), and brine, then dried over $MgSO_4$. The salt was filtered off and the solvents removed in vacuo. The resulting yellow oil was purified by column chromatography to yield the title compound as a yellow foam (4.12 g, 9.29 mmol, 75%), TLC: R_f = 0.45 (EtOAc/toluene, 1/4 *v*/*v*); ^{1}H NMR (500 MHz, $CDCl_3$) δ 7.51 – 7.44 (m, 2H), 7.38 – 7.28 (m, 5H), 7.14 – 7.07 (m, 2H), 4.90 (d, J = 11.0 Hz, 1H), 4.79 (d, J = 11.0 Hz, 1H), 4.42 (dd, J = 12.2, 3.9 Hz, 1H), 4.36 (d, J = 10.0 Hz, 1H), 4.29 (dd, J = 12.2, 1.9 Hz, 1H), 3.42 – 3.31 (m, 3H), 3.25 (dd, J = 10.0, 9.0 Hz, 1H), 2.70 (d, J = 2.5 Hz, 1H), 2.34 (s, 3H), 2.09 (s, 3H); ^{13}C NMR (125 MHz, $CDCl_3$) δ 171.65, 171.60, 138.9, 137.7, 134.3, 129.7, 128.7, 128.3, 127.0, 86.2, 84.3, 84.1, 77.8, 77.6, 75.6, 69.8, 64.5, 63.1, 21.2, 20.8; HRMS (ESI+) calculated for $C_{22}H_{25}N_3O_5SNa$ $[M+Na]^+$ *m*/*z* 466.1413, found 466.1411. Data matches a previous instance of this compound.[194]

General Procedure A: Fmoc protection by 'slurry' method

The starting material and DMAP (0.07 equiv.) were dissolved in pyridine (2 mL/g) and CH_2Cl_2 (3 mL/g) under argon, with a large stirrer bar. The solution was cooled to 0 °C and Fmoc-Cl solid (4 equiv.) was added to form a thick slurry. The slurry was stirred vigorously at 0 °C for 20 minutes and then allowed

to warm to room temperature and stirred for 1.5 hours. The slurry was diluted with a large excess of toluene and then filtered through a Celite® pad. The filtrate was concentrated in vacuo and the residue diluted with further toluene and allowed to stand at RT for several hours, during which by-products precipitated. The mixture was filtered through another Celite® pad, the solvent removed in vacuo, and the residue was purified by flash column chromatography (gradient of 0-20% EtOAc in toluene) to give the desired product.

p-Tolyl 6-*O*-acetyl-2-azido-3-*O*-benzyl-2-deoxy-4-*O*-(9-fluorenylmethyloxycarbonyl)-1-thio-β-D-glucopyranoside **(10)**

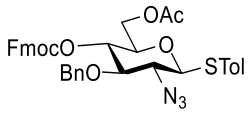

p-Tolyl 6-*O*-acetyl-2-azido-3-*O*-benzyl-2-deoxy-1-thio-β-D-glucopyranoside **19** (3.69 g, 8.32 mmol) was reacted according to General Procedure A to yield the title compound as an off-white foam (4.43 g, 6.65 mmol, 80%), TLC: R_f = 0.7 (EtOAc/toluene, 1/4 *v*/*v*); ^{1}H NMR (500 MHz, $CDCl_3$) δ 7.74 (dd, J = 7.5, 2.7 Hz, 2H), 7.58 (d, J = 7.6 Hz, 1H), 7.54 (d, J = 7.6 Hz, 1H), 7.49 – 7.44 (m, 2H), 7.37 (t, J = 7.5 Hz, 2H), 7.30 – 7.18 (m, 7H), 7.13 (d, J = 7.8 Hz, 2H), 4.81 – 4.69 (m, 2H), 4.61 (d, J = 11.0 Hz, 1H), 4.51 – 4.42 (m, 1H), 4.37 – 4.29 (m, 2H), 4.25 – 4.12 (m, 3H), 3.64 – 3.57 (m, 1H), 3.51 (t, J = 9.3 Hz, 1H), 3.32 (t, J = 9.7 Hz, 1H), 2.35 (s, 3H), 2.06 (s, 3H); ^{13}C NMR (125 MHz, $CDCl_3$) δ 170.5, 154.2, 143.2, 143.0, 141.35, 141.32, 139.2, 137.0, 134.6, 129.8, 128.4, 128.1, 128.04, 128.00, 127.98, 127.2, 126.3, 125.0, 124.9, 120.1, 120.1, 85.9, 82.2, 75.6, 75.5, 74.1, 70.3, 64.4, 62.2, 46.7, 21.2, 20.7; HRMS (ESI+) calculated for $C_{37}H_{35}N_3O_7SNa$ $[M+Na]^+$ *m*/*z* 688.2093, found 688.2091. Data matches a previous instance of this compound.[194]

p-Methoxyphenyl 2-*O*-benzoyl-3-*O*-benzyl-4,6-*O*-benzylidene-β-D-glucopyranoside **(20)**

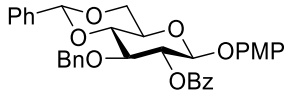

p-Methoxyphenyl 3-*O*-benzyl-4,6-*O*-benzylidene-β-D-glucopyranoside **13** (10.0 g, 21.6 mmol) was dissolved in CH_2Cl_2 (50 mL) and pyridine (25 mL) under argon. The reaction mixture was then cooled to 0 °C, and treated with benzoyl chloride (5.2 mL, 44 mmol, 2.1 equiv.) slowly with stirring. The mixture was then stirred at 0 °C for 30 minutes, after which the reaction flask was left to warm to room temperature and stir for 5 hours. The reaction was quenched with water (2 mL) and then evaporated to dryness. The resulting white solid was re-dissolved in CH_2Cl_2 and washed with HCl (aq), saturated $NaHCO_3$ (aq), and brine, dried over $MgSO_4$, filtered and dried in vacuo. This afforded the

title compound as an off-white foam (11.6 g, 20.4 mmol, 94%), TLC: R_f = 0.8 (EtOAc/toluene, 1/4 *v*/*v*); ^{1}H NMR (500 MHz, $CDCl_3$) δ 8.03 – 7.98 (m, 2H), 7.62 – 7.55 (m, 1H), 7.54 – 7.49 (m, 2H), 7.47 – 7.35 (m, 5H), 7.18 – 7.06 (m, 5H), 6.91 – 6.85 (m, 2H), 6.77 – 6.70 (m, 2H), 5.63 (s, 1H), 5.55 – 5.50 (m, 1H), 5.07 (d, J = 7.8 Hz, 1H), 4.85 (d, J = 12.0 Hz, 1H), 4.72 (d, J = 12.1 Hz, 1H), 4.42 (dd, J = 10.6, 5.0 Hz, 1H), 3.96 – 3.92 (m, 2H), 3.89 (t, J = 10.3 Hz, 1H), 3.72 (s, 3H), 3.66 – 3.50 (m, 1H); ^{13}C NMR (125 MHz, $CDCl_3$) δ 165.0, 155.7, 151.1, 137.7, 137.1, 133.1, 129.8, 129.7, 129.0, 128.3, 128.3, 128.1, 128.0, 127.5, 126.0, 118.9, 114.5, 101.4, 101.3, 81.4, 77.9, 74.0, 73.3, 68.7, 66.5, 55.6; HRMS (ESI+) calculated for $C_{34}H_{32}O_8Na$ $[M+Na]^+$ *m*/*z* 591.1995, found 591.1990. Data matches a previous instance of this compound.[194]

p-Methoxyphenyl 2-*O*-benzoyl-3-*O*-benzyl-β-D-glucopyranoside (21)

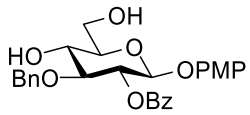

p-Methoxyphenyl 2-*O*-benzoyl-3-*O*-benzyl-4,6-*O*-benzylidene-β-D-glucopyranoside **20** (10.0 g, 17.6 mmol) was dissolved in CH_2Cl_2 (60 mL) and MeOH (40 mL) under argon. In a separate flask, MeOH (20 mL) was cooled to 0 °C and acetyl chloride (0.5 mL, 7 mmol, 0.4 equiv.) added. The two solutions were combined, and the resulting mixture stirred at room temperature overnight. TLC analysis showed complete conversion. The reaction was quenched by the addition of Amberlyst A26 (OH) resin, and the pH was found to be neutral after 20 minutes. The resin was filtered off and washed with EtOAc, and the filtrate was concentrated in vacuo. The white solid formed was recrystallized from EtOAc/petrol to afford the title compound as an off-white foam (5.60 g, 11.7 mmol, 66%), TLC: R_f = 0.35 (EtOAc/toluene, 1/4 *v*/*v*); ^{1}H NMR (500 MHz, $CDCl_3$) δ 8.09 – 7.99 (m, 2H), 7.63 – 7.54 (m, 1H), 7.45 (t, J = 7.8 Hz, 2H), 7.23 – 7.16 (m, 5H), 6.89 – 6.82 (m, 2H), 6.77 – 6.72 (m, 2H), 5.48 (dd, J = 9.4, 7.9 Hz, 1H), 5.04 (d, J = 7.9 Hz, 1H), 4.77 (d, J = 11.5 Hz, 1H), 4.65 (d, J = 11.5 Hz, 1H), 4.00 – 3.91 (m, 1H), 3.89 – 3.81 (m, 2H), 3.76 (t, J = 9.2 Hz, 1H), 3.72 (s, 3H), 3.58 – 3.49 (m, 1H), 2.68 (d, J = 3.3 Hz, 1H), 2.21 (t, J = 6.6 Hz, 1H); ^{13}C NMR (125 MHz, $CDCl_3$) δ 165.2, 155.5, 151.2, 137.7, 133.3, 129.8, 129.7, 128.6, 128.5, 128.1, 128.0, 118.4, 114.5, 100.8, 82.3, 75.5, 74.6, 73.5, 70.3, 62.4, 55.6; HRMS (ESI+) calculated for $C_{27}H_{28}O_8Na$ $[M+Na]^+$ *m*/*z* 503.1682, found 503.1683. Data matches a previous instance of this compound.[194]

p-Methoxyphenyl 2-*O*-benzoyl-3-*O*-benzyl-6-*O*-chloroacetyl-β-D-glucopyranoside (11)

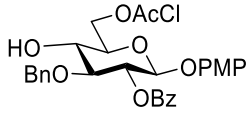

p-Methoxyphenyl 2-*O*-benzoyl-3-*O*-benzyl-β-D-glucopyranoside **21** (5.0 g, 9.9 mmol) was dissolved in CH_2Cl_2 (25 mL) under argon and treated with pyridine (3.4 mL, 42 mmol, 4.2 equiv.). The resulting solution was cooled to -78 °C, and then treated dropwise with chloroacetyl chloride (1 mL, 12 mmol, 1.2 equiv.) and left to stir at room temperature overnight. TLC analysis confirmed the consumption of starting material. The reaction mixture was washed with 1 M HCl (aq) (100 mL) and saturated $NaHCO_3$ (aq) (100 mL), dried over $MgSO_4$ and the solvents removed in vacuo. The material was purified by column chromatography to yield the title compound as an off-white foam (3.25 g, 5.83 mmol, 56%), TLC: R_f = 0.45 (EtOAc/toluene, 1/4 *v*/*v*); ^{1}H NMR (500 MHz, $CDCl_3$) δ 8.09 – 8.03 (m, 2H), 7.63 – 7.56 (m, 1H), 7.49 – 7.41 (m, 2H), 7.24 – 7.19 (m, 5H), 6.91 – 6.85 (m, 2H), 6.78 – 6.70 (m, 2H), 5.53 – 5.45 (m, 1H), 4.99 (d, J = 7.8 Hz, 1H), 4.77 (d, J = 11.4 Hz, 1H), 4.64 (d, J = 11.4 Hz, 1H), 4.54 (dd, J = 11.9, 2.4 Hz, 1H), 4.49 (dd, J = 11.9, 5.3 Hz, 1H), 4.09 (s, 2H), 3.77 – 3.73 (m, 2H), 3.73 (s, 3H), 3.72 – 3.67 (m, 1H), 2.60 (d, J = 2.7 Hz, 1H); ^{13}C NMR (125 MHz, $CDCl_3$) δ 167.4, 165.1, 155.6, 151.2, 137.5, 133.3, 129.8, 129.63, 128.61, 128.55, 128.13, 128.1, 118.8, 114.4, 100.9, 82.1, 74.7, 73.5, 73.3, 69.8, 64.6, 55.6, 40.7; HRMS (ESI+) calculated for $C_{29}H_{29}ClO_9Na$ $[M+Na]^+$ *m*/*z* 579.1398, found 579.1395. Data matches a previous instance of this compound.[194]

_p_-Methoxyphenyl [6-_O_-acetyl-2-azido-3-_O_-benzyl-2-deoxy-4-_O_-(9-fluorenylmethyloxycarbonyl)-α-D-glucopyranosyl (1→4)]-2-_O_-benzoyl-3-_O_-benzyl-6-_O_-chloroacetyl-β-D-glucopyranoside (9)

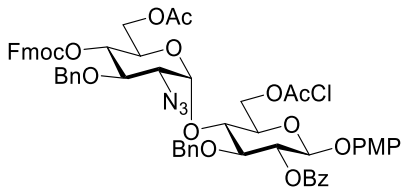

Donor **10** (7.0 g, 11 mmol, 1.3 equiv.) and acceptor **11** (4.5 g, 8.1 mmol) were added to a flask and co-evaporated with toluene. The reactants were then dissolved in toluene (50 mL) and CH_2Cl_2 (50 mL) under argon and cooled to -20 °C. At this point, 4 Å molecular sieves were added to the reaction mixture. After 10 minutes, *N*-iodosuccinimide (3.2 g, 14 mmol, 1.7 equiv.) and silver trifluoromethanesulfonate (0.9 g, 4 mmol, 0.4 equiv.) was added, and the reaction stirred for 15 minutes at -20°C before being allowed to warm to room temperature over an hour. TLC analysis of the reaction mixture indicated the reaction was complete, and the mixture was diluted with EtOAc (200 mL) and filtered through a Celite® pad. The solution was then washed with an equal parts mixture of saturated $NaHCO_3$ (aq) and sodium thiosulfate 10% *w*/*v* (aq) (200 mL), brine (100 mL), dried over $MgSO_4$ and solvents removed in vacuo. The material was purified by column chromatography and recrystallized from toluene to afford the title compound as a light yellow solid (5.9 g, 5.4 mmol, 67%), α/β: ~95:5, α - TLC: R_f = 0.6 (EtOAc/toluene, 1/4 *v*/*v*); mp 120 °C (from toluene); $[\alpha]_D$ 27.2 (c 1 in $CDCl_3$);

IR (ATR): ν_{max}/cm^{-1} 2111 (N_3, s), 1745 and 1729 (C=O, s); ^1H NMR (500 MHz, $CDCl_3$) δ 8.10 – 8.03 (m, 2H), 7.78 – 7.71 (m, 2H), 7.62 – 7.53 (m, 3H), 7.45 (t, J = 7.8 Hz, 2H), 7.40 – 7.35 (m, 2H), 7.32 – 7.18 (m, 12H), 6.94 – 6.87 (m, 2H), 6.81 – 6.74 (m, 2H), 5.61 – 5.53 (m, 2H), 5.12 (d, J = 7.0 Hz, 1H), 4.87 (dd, J = 10.2, 9.1 Hz, 1H), 4.82 – 4.76 (m, 2H), 4.72 (d, J = 10.9 Hz, 1H), 4.66 – 4.60 (m, 2H), 4.49 (dd, J = 10.5, 6.7 Hz, 1H), 4.39 (dd, J = 11.8, 6.1 Hz, 1H), 4.33 (dd, J = 10.5, 7.2 Hz, 1H), 4.27 (dd, J = 12.4, 4.9 Hz, 1H), 4.18 (t, J = 6.9 Hz, 1H), 4.12 – 3.98 (m, 6H), 3.97 – 3.91 (m, 2H), 3.73 (s, 3H), 3.36 (dd, J = 10.3, 3.9 Hz, 1H), 2.05 (s, 3H); ^{13}C NMR (125 MHz, $CDCl_3$) δ 170.5, 166.9, 165.1, 155.7, 154.1, 150.9, 143.2, 143.0, 141.3, 137.2, 137.1, 133.5, 129.8, 129.4, 128.6, 128.47, 128.42, 128.0, 127.9, 127.8, 127.7, 127.2, 125.1, 124.9, 120.1, 118.6, 114.5, 99.9, 97.8, 82.4, 77.4, 75.1, 74.8, 74.7, 74.2, 73.5, 72.3, 70.4, 68.8, 64.9, 62.6, 62.0, 55.6, 46.7, 40.6, 20.7; HRMS (ESI+) calculated for $C_{59}H_{56}ClN_3O_{16}Na$ $[M+Na]^+$ *m/z* 1120.3247, found 1120.3241. The β-anomer was not isolated. Data matches a previous instance of this compound.[194]

General Procedure B: Fmoc deprotection

The starting material (0.2 mmol) was dissolved in CH_2Cl_2 or DMF (20 mL / mmol), and then the resultant solution was treated dropwise with trimethylamine (5 ml per 0.2 mmol) over 5 minutes with vigorous stirring. The reaction was then stirred at room temperature for 1 hour. When TLC analysis of the mixture indicated complete deprotection, the mixture was diluted with CH_2Cl_2 and washed with dilute HCl, water, brine, dried over $MgSO_4$ and solvents removed were in vacuo. The residue was purified by column chromatography.

p-Methoxyphenyl [6-*O*-acetyl-2-azido-3-*O*-benzyl-2-deoxy-α-D-glucopyranosyl (1→4)]-2-*O*-benzoyl-3-*O*-benzyl-6-*O*-chloroacetyl-β-D-glucopyranoside **(22)**

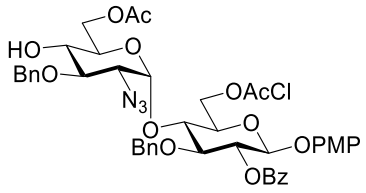

Disaccharide **9** (200 mg, 0.18 mmol) was reacted according to General Procedure B to yield the title compound as a yellow residue (90 mg, 0.10 mmol, 56%), TLC: R_f = 0.35 (EtOAc/toluene, 1/4 *v*/*v*); ^1H NMR (500 MHz, $CDCl_3$) δ 8.10 – 8.04 (m, 2H), 7.62 – 7.54 (m, 1H), 7.49 – 7.42 (m, 2H), 7.45 – 7.33 (m, 4H), 7.37 – 7.27 (m, 1H), 7.28 – 7.16 (m, 4H), 6.93 – 6.86 (m, 2H), 6.80 – 6.73 (m, 2H), 5.59 – 5.52 (m, 2H), 5.09 (d, J = 7.2 Hz, 1H), 4.87 (d, J = 2.1 Hz, 2H), 4.79 (d, J = 1.4 Hz, 2H), 4.62 (dd, J = 11.8, 2.7 Hz, 1H), 4.52 (dd, J = 12.4, 4.1 Hz, 1H), 4.36 (dd, J = 11.7, 6.0 Hz, 1H), 4.18 – 4.10 (m, 1H), 4.09 (t, J = 8.2 Hz, 1H), 4.08 – 3.98 (m, 3H), 3.90 (ddd, J = 9.1, 6.0, 2.7 Hz, 1H), 3.82 – 3.73 (m, 2H), 3.74 (s, 3H), 3.44 (dd, J = 9.9, 8.7 Hz, 1H), 3.25 (dd, J = 10.3, 4.0 Hz, 1H), 2.93 (s, 1H), 2.10 (s, 3H); ^{13}C NMR (126 MHz,

$CDCl_3$) δ 171.8, 166.9, 165.0, 155.6, 151.0, 137.7, 137.3, 133.4, 129.8, 129.4, 128.6, 128.5, 128.3, 128.1, 127.7, 127.6, 118.6, 114.5, 100.0, 98.1, 82.7, 79.1, 75.3, 74.4, 74.1, 73.6, 72.4, 71.3, 70.6, 64.8, 62.8, 62.6, 55.6, 40.5, 20.7; HRMS (ESI+) calculated for $C_{44}H_{46}ClN_3O_{14}Na$ $[M+Na]^+$ 898.2566 *m/z*, found 898.2567.

General procedure C: Selective deprotection of 1-*O*-PMP using CAN hydrolysis

The 1-*O*-PMP protected starting material was dissolved in MeCN (8.5 mL/g), and water (1.5 mL/g) was added dropwise with good stirring to ensure solvent mixing. Then, ceric ammonium nitrate (3 equiv.) was added and the reaction stirred at room temperature for 2 hours. When TLC analysis indicated completion, the mixture was diluted with equal parts toluene and EtOAc, and washed with water, saturated $NaHCO_3$ (aq), and brine, dried over $MgSO_4$ and solvents were removed in vacuo. The residue was purified by column chromatography (gradient of 0-20% EtOAc in toluene or 0-10% of MeCN in CH_2Cl_2) to yield the product as a foam, as a mixture of anomers.

[6-*O*-acetyl-2-azido-3-*O*-benzyl-2-deoxy-4-*O*-(9-fluorenylmethyloxycarbonyl)-α-D-glucopyranosyl (1→4)]-2-*O*-benzoyl-3-*O*-benzyl-6-*O*-chloroacetyl-β-D-glucopyranoside **(23)**

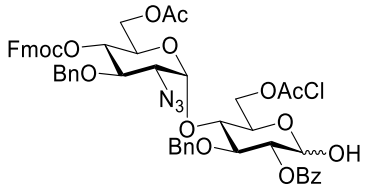

Disaccharide **9** (200 mg, 0.18 mmol) was reacted according to General procedure C to yield the title compound as a mixture of anomers (α/β : 95/5), in the form of a yellow foam (160 mg, 0.16 mmol, 87%); TLC: R_f = 0.45 (EtOAc/toluene, 1/4 *v/v*); ^{1}H NMR (500 MHz, $CDCl_3$) δ 8.22 (d, J = 7.8 Hz, 0.05H), 8.09 – 8.03 (m, 2H), 7.90 (dd, J = 7.6, 3.8 Hz, 0.05H), 7.77 – 7.71 (m, 2H), 7.60 (dd, J = 7.5, 1.0 Hz, 1H), 7.58 – 7.51 (m, 2H), 7.45 – 7.34 (m, 4H), 7.31 – 7.13 (m, 12H), 5.64 (d, J = 3.9 Hz, 1H), 5.56 (d, J = 3.9 Hz, 0.05H), 5.50 (t, J = 3.3 Hz, 1H), 5.25 (s, 0.05H), 5.22 – 5.15 (m, 0.05H), 5.12 (dd, J = 9.7, 3.5 Hz, 1H), 4.93 – 4.85 (m, 3H), 4.76 (d, J = 10.9 Hz, 1H), 4.65 (d, J = 10.9 Hz, 1H), 4.62 (dd, J = 12.0, 2.4 Hz, 1H), 4.47 (dd, J = 10.5, 6.8 Hz, 1H), 4.39 (dd, J = 9.7, 8.5 Hz, 1H), 4.37 – 4.22 (m, 4H), 4.18 (t, J = 7.0 Hz, 1H), 4.13 (s, 2H), 4.07 (dd, J = 12.4, 2.8 Hz, 1H), 3.99 (ddd, J = 10.4, 8.1, 5.2 Hz, 2H), 3.91 (dd, J = 9.8, 8.4 Hz, 1H), 3.78 (ddd, J = 9.8, 5.4, 2.5 Hz, 0.05H), 3.60 (d, J = 3.7 Hz, 1H), 3.51 (t, J = 6.6 Hz, 0.05H), 3.37 (dd, J = 10.3, 3.9 Hz, 1H), 2.34 (s, 0.05H), 2.04 (s, 3H); ^{13}C NMR (126 MHz, $CDCl_3$) δ 168.9, 165.5, 164.0, 152.4, 141.5, 141.2, 139.54, 139.52, 136.0, 135.4, 132.0, 131.8, 128.0, 127.6, 126.8, 126.6, 126.18, 126.13, 125.9, 125.54, 125.46, 123.3, 123.1, 118.33, 118.31, 114.6, 96.3, 93.7, 88.3, 80.7, 77.7, 75.7, 74.5, 73.43, 73.37, 73.1, 72.9, 72.7, 70.7, 68.6, 66.9, 66.2, 63.0, 60.9, 60.1, 44.9, 38.9, 18.9; HRMS (ESI+) calculated for $C_{52}H_{50}ClN_3O_{15}Na$ $[M+Na]^+$ 1014.2828 *m/z*, found 1014.2825.

Methyl (*p*-Methoxyphenyl [6-*O*-acetyl-2-azido-3-*O*-benzyl-2-deoxy-α-D-glucopyranosyl(1→4)]-2-*O*-benzoyl-3-*O*-benzyl-β-D-glucopyranoside) uronate (24)

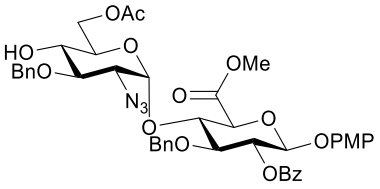

Disaccharide **9** (200 mg, 0.18 mmol) was dissolved in EtOH (10 mL) and MeCN (1 mL), and DABCO (6 equiv., 130 mg, 1.1 mmol) was added. The reaction was stirred at 70 °C for 1.5 hours. The solvents were removed in vacuo, and the residue dissolved in chloroform and filtered through a silica pad. The pad was washed with equal parts EtOAc and petroleum ether, and the filtrate was concentrated in vacuo. The residue was then dissolved in MeCN (10 mL) and water (2 mL), and iodobenzene diacetate (2.5 equiv., 150 mg, 0.46 mmol) and TEMPO (1 equiv., 30 mg, 0.18 mmol) were added. The mixture was stirred at room temperature for 24 hours, and then the solvents were removed in vacuo and the residue was co-evaporated twice with toluene. The residue was then dissolved in MeOH (6 mL) and Et_2O (12 mL) under argon, and trimethylsilyldiazomethane (2 M in hexanes, 2 equiv., 0.2 mL, 0.4 mmol) was added. The reaction was allowed to stir for 1 hour before quenching with 4 drops of glacial acetic acid. The solvents were removed in vacuo and the residue co-evaporated twice with toluene. The residue was then purified by column chromatography (gradient of 0-20% EtOAc in toluene) to yield the title compound as a yellow solid (94 mg, 0.11 mmol, 62%), TLC: R_f = 0.45 (EtOAc/toluene, 1/4 *v*/*v*); mp = 122 °C (from MeOH); ^{1}H NMR (500 MHz, $CDCl_3$) δ 8.08 – 8.02 (m, 2H), 7.61 – 7.53 (m, 1H), 7.48 – 7.28 (m, 7H), 7.31 – 7.16 (m, 5H), 6.93 – 6.86 (m, 2H), 6.79 – 6.73 (m, 2H), 5.59 – 5.51 (m, 2H), 5.15 (d, J = 6.7 Hz, 1H), 4.87 (s, 2H), 4.81 (d, J = 10.6 Hz, 1H), 4.75 (d, J = 10.6 Hz, 1H), 4.55 (dd, J = 12.4, 3.4 Hz, 1H), 4.46 (t, J = 8.8 Hz, 1H), 4.23 – 4.04 (m, 3H), 3.79 – 3.68 (m, 7H), 3.60 – 3.52 (m, 1H), 3.43 (dd, J = 10.1, 8.7 Hz, 1H), 3.25 (dd, J = 10.2, 3.8 Hz, 1H), 2.10 (s, 3H), 0.91 – 0.83 (m, 1H); ^{13}C NMR (126 MHz, $CDCl_3$) δ 172.1, 168.5, 165.0, 155.7, 150.9, 137.9, 137.3, 133.5, 129.8, 129.4, 128.61, 128.57, 128.4, 128.2, 128.1, 127.85, 127.80, 118.7, 114.5, 100.7, 97.8, 82.0, 79.0, 75.3, 74.5, 74.3, 73.9, 70.9, 70.5, 62.8, 62.6, 55.6, 52.7, 20.8; HRMS (ESI+) calculated for $C_{43}H_{45}N_3O_{14}Na$ $[M+Na]^+$ 850.2799 *m*/*z*, found 850.2795.

Methyl (*p*-Methoxyphenyl [6-*O*-acetyl-2-azido-3-*O*-benzyl-2-deoxy-4-*O*-(9-fluorenylmethyloxycarbonyl)-α-D-glucopyranosyl(1→4)]-2-*O*-benzoyl-3-*O*-benzyl-β-D-glucopyranoside) uronate (25)

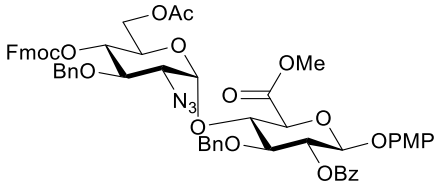

Disaccharide **9** (200 mg, 0.18 mmol) was dissolved in EtOH (10 mL) and MeCN (1 mL), and thiourea (6 equiv., 85 mg, 1.1 mmol) was added. The reaction was stirred at 70 °C for 2 hours, and then left to stir at room temperature for 12 hours. The solvents were removed in vacuo, and the residue dissolved in chloroform and filtered through a silica pad. The pad was washed with equal parts EtOAc and petroleum ether, and the filtrate was concentrated in vacuo. The residue was then dissolved in MeCN (10 mL) and water (2 mL), and iodobenzene diacetate (2.5 equiv., 150 mg, 0.46 mmol) and TEMPO (1 equiv., 30 mg, 0.18 mmol) added. The mixture was stirred at room temperature for 24 hours, and then the solvents were removed in vacuo and the residue was co-evaporated twice with toluene. The residue was then dissolved in MeOH (6 mL) and Et_2O (12 mL) under argon, and trimethylsilyldiazomethane (2 M in hexanes, 2 equiv., 0.2 mL, 0.4 mmol) was added. The reaction was stirred for 1 hour before quenching with 4 drops of glacial acetic acid. The solvents were removed in vacuo and the residue co-evaporated twice with toluene. The residue was then purified by column chromatography (gradient of 0-20% EtOAc in toluene) to yield the title compound as a yellow foam (129 mg, 0.12 mmol, 67%), TLC: R_f = 0.7 (EtOAc/toluene, 1/4 *v*/*v*); $[\alpha]_D$ 24.0 (c 1 in $CDCl_3$); IR (ATR): ν_{max}/cm^{-1} 2108 (N_3, s), 1742 (C=O); ^1H NMR (500 MHz, $CDCl_3$) δ 8.08 – 8.02 (m, 2H), 7.78 – 7.71 (m, 2H), 7.62 – 7.51 (m, 3H), 7.48 – 7.41 (m, 2H), 7.42 – 7.34 (m, 2H), 7.31 – 7.25 (m, 2H), 7.24 – 7.18 (m, 8H), 6.94 – 6.88 (m, 2H), 6.80 – 6.74 (m, 2H), 5.58 – 5.52 (m, 2H), 5.18 (d, J = 6.3 Hz, 1H), 4.89 (dd, J = 10.3, 9.1 Hz, 1H), 4.83 – 4.70 (m, 3H), 4.63 (d, J = 10.9 Hz, 1H), 4.53 – 4.44 (m, 2H), 4.32 (dd, J = 10.5, 7.3 Hz, 1H), 4.27 – 4.20 (m, 2H), 4.20 – 4.06 (m, 3H), 3.93 (dd, J = 10.3, 9.1 Hz, 1H), 3.86 – 3.80 (m, 1H), 3.73 (s, 3H), 3.69 (s, 3H), 3.37 (dd, J = 10.3, 3.7 Hz, 1H), 2.07 (s, 3H), 1.32 – 1.21 (m, 2H); ^{13}C NMR (126 MHz, $CDCl_3$) δ 170.7, 168.4, 165.0, 155.7, 154.2, 150.9, 143.3, 143.1, 141.34, 141.31, 137.23, 137.19, 133.5, 129.8, 129.4, 128.6, 128.39, 128.37, 127.97, 127.94, 127.90, 127.85, 127.79, 127.2, 125.1, 124.9, 120.11, 120.09, 118.5, 114.5, 100.5, 97.6, 81.6, 77.4, 75.0, 74.7, 74.40, 74.35, 74.3, 73.9, 70.3, 68.4, 62.8, 61.5, 60.4, 55.6, 52.7, 46.7, 21.0, 20.7, 14.2; HRMS (ESI+) calculated for $C_{58}H_{55}N_3O_{16}Na$ $[M+Na]^+$ 1072.3480 *m*/*z*, found 1072.3484.

Methyl ([6-*O*-acetyl-2-azido-3-*O*-benzyl-2-deoxy-4-*O*-(9-fluorenylmethyloxycarbonyl)-α-D-glucopyranosyl(1→4)]-2-*O*-benzoyl-3-*O*-benzyl-β-D-glucopyranoside) uronate **(26)**

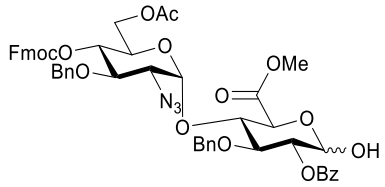

Uronate disaccharide **25** (850 mg, 0.81 mmol) was reacted according to General Procedure C to yield the title compound as a mixture of anomers (α/β : 8/2), appearing as a yellow foam (500 mg, 0.53 mmol, 65%), TLC: R_f = 0.45 (EtOAc/toluene, 1/4 *v*/*v*); ^{1}H NMR (500 MHz, $CDCl_3$) δ 8.12 – 8.06 (m, 1.6H), 8.06 – 8.04 (m, 0.4H), 7.79 – 7.73 (m, 2H), 7.63 – 7.52 (m, 2H), 7.52 – 7.34 (m, 5H), 7.32 – 7.12 (m, 12H), 5.66 (dd, J = 6.6, 3.0 Hz, 0.8H), 5.44 (d, J = 3.7 Hz, 0.2H), 5.37 (d, J = 3.6 Hz, 0.8H), 5.24 – 5.19 (m, 0.2H), 5.13 (dd, J = 7.4, 3.0 Hz, 0.8H), 4.95 (dd, J = 9.2, 6.5 Hz, 0.2H), 4.87 – 4.78 (m, 3H), 4.76 (d, J = 6.9 Hz, 0.8H), 4.63 – 4.59 (m, 0.2H), 4.56 – 4.48 (m, 1H), 4.44 (d, J = 10.9 Hz, 1H), 4.39 – 4.29 (m, 3H), 4.26 – 4.12 (m, 4H), 4.12 – 4.09 (m, 0.2H), 4.06 (d, J = 9.2 Hz, 0.2H), 4.01 (ddd, J = 10.3, 4.7, 2.5 Hz, 1H), 3.89 – 3.83 (m, 0.4H), 3.77 (s, 0.6H), 3.76 (s, 0.2H), 3.74 (d, J = 1.2 Hz, 0.4H), 3.72 (s, 3H), 3.38 – 3.35 (m, 1H), 3.36 – 3.26 (m, 1H), 2.08 (s, 2.4H), 2.07 (s, 0.6H); ^{13}C NMR (126 MHz, $CDCl_3$) δ 171.0, 169.3, 165.7, 154.3, 143.2, 143.1, 141.3, 137.4, 137.2, 133.5, 129.8, 129.3, 128.8, 128.7, 128.4, 128.35, 128.3, 128.0, 127.9, 127.7, 127.6, 127.5, 127.2, 125.0, 124.8, 120.1, 98.6, 95.7, 89.8, 77.4, 77.3, 77.2, 77.0, 76.8, 75.9, 75.0, 74.6, 74.4, 72.1, 71.6, 70.2, 68.4, 62.8, 61.8, 52.6, 46.8, 20.8; HRMS (ESI+) calculated for $C_{51}H_{49}N_3O_{15}Na$ $[M+Na]^+$ 966.3061 *m*/*z*, found 966.3065.

General procedure D: Trichloroacetimidate donor formation

The appropriate hemiacetal was dissolved in anhydrous CH_2Cl_2 (15 mL per 1 mmol hemiacetal) under argon. The reaction mixture was then treated with excess trichloroacetonitrile (10 equiv.), stirred at room temperature briefly, and then catalytic NaH 60% *w*/*w* dispersion in mineral oil (0.3 equiv.) was added. The reaction was stirred at room temperature for approximately 1 hour until TLC analysis indicated completion. The reaction mixture was then filtered through a small silica pad, which was rinsed with EtOAc. The filtrate was then dried over $MgSO_4$ and the solvents removed in vacuo. The crude mixture was purified by column chromatography (gradient of 0-20% EtOAc in toluene or 0-10% of MeCN in CH_2Cl_2) to yield the desired trichloroacetimidate donor as a mixture of anomers.

[6-*O*-acetyl-2-azido-3-*O*-benzyl-2-deoxy-4-*O*-(9-fluorenylmethyloxycarbonyl)-α-D-glucopyranosyl(1→4)]-2-*O*-benzoyl-3-*O*-benzyl-6-*O*-chloroacetyl-α,β-D-glucopyranoside trichloroacetimidate (27)

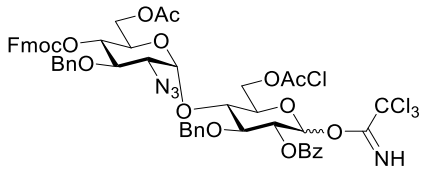

Hemiacetal **23** (300 mg, 0.302 mmol) was reacted according to General procedure D to yield the title compound as a mixture of anomers (α/β: 6/4), as a foam (214 mg, 0.188 mmol, 62%). A sample of each anomer was isolated separately for characterisation.

α - TLC: R_f = 0.65 (EtOAc/toluene, 1/4 *v*/*v*); ^{1}H NMR (500 MHz, $CDCl_3$) δ 8.60 (s, 1H), 8.10 – 7.83 (m, 2H), 7.81 – 7.66 (m, 2H), 7.61 – 7.57 (m, 1H), 7.56 – 7.52 (m, 2H), 7.44 – 7.34 (m, 4H), 7.31 – 7.12 (m, 11H), 6.59 (d, J = 3.6 Hz, 1H), 5.66 (d, J = 3.9 Hz, 1H), 5.40 (dd, J = 9.7, 3.6 Hz, 1H), 4.94 – 4.85 (m, 3H), 4.78 (d, J = 10.9 Hz, 1H), 4.68 (d, J = 10.9 Hz, 1H), 4.62 (dd, J = 12.1, 2.3 Hz, 1H), 4.47 (dd, J = 10.5, 6.8 Hz, 1H), 4.41 (dd, J = 9.7, 8.6 Hz, 1H), 4.37 (dd, J = 12.2, 5.2 Hz, 1H), 4.31 (dd, J = 10.5, 7.3 Hz, 1H), 4.27 (dd, J = 12.5, 4.3 Hz, 1H), 4.25 – 4.20 (m, 1H), 4.18 (t, J = 7.2 Hz, 1H), 4.13 (d, J = 3.0 Hz, 2H), 4.10 – 4.05 (m, 1H), 4.05 – 3.95 (m, 3H), 3.35 (dd, J = 10.3, 4.0 Hz, 1H), 2.05 (s, 3H); ^{13}C NMR (126 MHz, $CDCl_3$) δ 170.5, 167.0, 165.3, 160.5, 154.1, 143.2, 143.0, 141.33, 141.31, 137.5, 137.2, 133.6, 129.8, 129.0, 128.6, 128.41, 128.39, 128.0, 127.9, 127.8, 127.4, 127.2, 125.1, 124.9, 120.1, 98.4, 93.2, 90.9, 79.9, 75.14, 75.08, 74.6, 72.9, 70.6, 70.4, 68.9, 64.4, 62.5, 61.9, 46.7, 40.6, 29.7, 20.7; MS (ESI+) calculated for $C_{54}H_{50}Cl_4N_4O_{15}Na$ $[M+Na]^+$ 1157.1924 *m*/*z*, found 1157.1903.

β - TLC: R_f = 0.70 (EtOAc/toluene, 1/4 *v*/*v*); ^{1}H NMR (500 MHz, $CDCl_3$) δ 8.64 (s, 1H), 8.06 – 7.98 (m, 2H), 7.79 – 7.70 (m, 2H), 7.61 (dd, J = 7.5, 1.0 Hz, 1H), 7.57 – 7.51 (m, 2H), 7.46 – 7.41 (m, 2H), 7.41 – 7.36 (m, 2H), 7.31 – 7.17 (m, 11H), 6.11 (d, J = 5.9 Hz, 1H), 5.59 (t, J = 6.0 Hz, 1H), 5.45 (d, J = 3.9 Hz, 1H), 4.89 – 4.81 (m, 2H), 4.76 (d, J = 10.8 Hz, 1H), 4.65 (dd, J = 11.9, 3.1 Hz, 1H), 4.62 (d, J = 11.0 Hz, 1H), 4.54 – 4.47 (m, 2H), 4.44 (dd, J = 11.9, 5.2 Hz, 1H), 4.34 (dd, J = 10.6, 7.1 Hz, 1H), 4.25 (dd, J = 12.4, 4.6 Hz, 1H), 4.19 (t, J = 6.9 Hz, 1H), 4.15 – 4.06 (m, 6H), 4.03 (ddd, J = 10.2, 4.6, 2.7 Hz, 1H), 3.88 (dd, J = 10.3, 9.1 Hz, 1H), 3.35 (dd, J = 10.3, 3.8 Hz, 1H), 2.06 (s, 3H); ^{13}C NMR (126 MHz, $CDCl_3$) δ 170.5, 167.0, 164.9, 161.0, 154.2, 143.2, 143.0, 141.35, 141.32, 137.16, 137.12, 133.6, 129.8, 129.2, 128.7, 128.43, 128.37, 127.98, 127.95, 127.90, 127.8, 127.7, 127.3, 125.1, 124.9, 120.1, 98.2, 95.7, 90.5, 80.8, 77.4, 75.1, 74.8, 74.7, 73.8, 72.8, 71.1, 70.4, 68.8, 64.8, 62.7, 61.9, 46.7, 40.7, 20.7; MS (ESI+) calculated for $C_{54}H_{50}Cl_4N_4O_{15}Na$ $[M+Na]^+$ 1157.1924 *m*/*z*, found 1157.1947.

Methyl ([6-*O*-acetyl-2-azido-3-*O*-benzyl-2-deoxy-4-*O*-(9-fluorenylmethyloxycarbonyl)-α-D-glucopyranosyl(1→4)]-2-*O*-benzoyl-3-*O*-benzyl-α,β-D-glucopyranoside)uronate trichloroacetimidate **(28)**

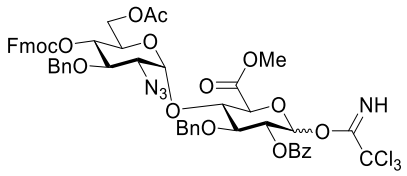

Hemiacetal **26** (300 mg, 0.318 mmol) was reacted according to General procedure D to yield the title compound as a mixture of anomers (α/β: 6/4), as a foam (204 mg, 0.187 mmol, 59%), TLC: R_f = 0.8 (EtOAc/toluene, 1/4 *v*/*v*); ^{1}H NMR (500 MHz, $CDCl_3$) δ 8.83 (s, 0.4H), 8.64 (s, 0.6H), 8.12 – 8.06 (m, 1H), 8.05 – 7.97 (m, 1H), 7.79 – 7.72 (m, 2.6H), 7.65 – 7.45 (m, 5H), 7.46 – 7.35 (m, 4H), 7.33 – 7.15 (m, 11H), 6.67 (d, J = 3.5 Hz, 0.6H), 6.52 (d, J = 3.0 Hz, 0.4H), 5.74 (t, J = 3.1 Hz, 0.4H), 5.60 (d, J = 3.8 Hz, 1H), 5.44 (dd, J = 9.4, 3.5 Hz, 0.6H), 4.93 – 4.85 (m, 2H), 4.85 – 4.80 (m, 0.6H), 4.80 – 4.73 (m, 1H), 4.68 (d, J = 10.8 Hz, 0.4H), 4.63 (d, J = 10.9 Hz, 0.4H), 4.59 (d, J = 10.7 Hz, 0.4H), 4.56 – 4.51 (m, 1H), 4.50 – 4.43 (m, 1H), 4.39 (t, J = 8.9 Hz, 0.6H), 4.34 – 4.28 (m, 2H), 4.27 – 4.22 (m, 1H), 4.20 – 4.15 (m, 1H), 4.15 – 4.07 (m, 1H), 4.01 (dd, J = 10.4, 9.1 Hz, 0.4H), 3.96 (dd, J = 10.4, 9.1 Hz, 0.6H), 3.79 (s, 1.8H), 3.79 (s, 1.2H), 3.37 – 3.28 (m, 1H), 2.08 (s, 1.8H), 2.06 (s, 1.2H); ^{13}C NMR (126 MHz, $CDCl_3$) δ 170.7, 168.5, 168.4, 165.35, 165.25, 160.3, 154.2, 143.3, 143.0, 141.3, 137.3, 137.2, 136.6, 133.6, 130.1, 129.8, 129.1, 128.9, 128.6, 128.45, 128.41, 128.35, 128.31, 127.95, 127.86, 127.82, 127.80, 127.6, 127.2, 125.1, 124.93, 124.87, 120.1, 98.3, 98.1, 94.5, 93.2, 79.2, 75.3, 75.1, 74.3, 73.2, 72.5, 72.1, 72.0, 70.3, 68.5, 68.4, 66.9, 62.6, 61.4, 53.0, 52.9, 46.7, 20.8; HRMS (ESI+) calculated for $C_{53}H_{49}Cl_3N_4O_{15}Na$ $[M+Na]^+$ 1109.216 *m*/*z*, found 1109.217.

General procedure E: *N*-phenyl trifluoroacetimidate donor formation

The appropriate hemiacetal was dissolved in anhydrous CH_2Cl_2 (15 mL per 1 mmol hemiacetal) under argon. The reaction mixture was then treated with 2,2,2-trifluoro-*N*-phenylacetimidoyl chloride (4 equiv.), stirred at room temperature briefly, and then NaH 60% *w*/*w* dispersion in mineral oil (1 equiv.) was added in small portions. The reaction was stirred at room temperature for approximately 30 minutes until TLC analysis indicated completion. The reaction mixture was then filtered through a small silica pad, which was rinsed with EtOAc. The filtrate was then dried over $MgSO_4$ and evaporated to dryness. The crude mixture was purified by column chromatography (gradient of 0-20% EtOAc in toluene or 0-10% of MeCN in CH_2Cl_2) to yield the desired trifluoro-*N*-phenyl trifluoroacetimidate donor as a mixture of anomers.

[6-*O*-acetyl-2-azido-3-*O*-benzyl-2-deoxy-4-*O*-(9-fluorenylmethyloxycarbonyl)-α-D-glucopyranosyl(1→4)]-2-*O*-benzoyl-3-*O*-benzyl-6-*O*-chloroacetyl-α,β-D-glucopyranoside *N*-phenyl trifluoroacetimidate (29)

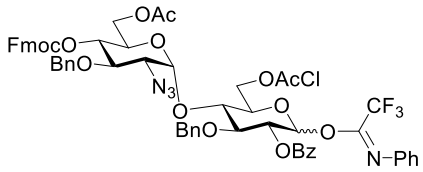

Hemiacetal **23** (100 mg, 0.101 mmol) was reacted according to General procedure E to yield the title compound as a yellow foam (100 mg, 0.085 mmol, 85%), TLC: R_f = 0.8 (EtOAc/toluene, 1/4 *v*/*v*); ^{1}H NMR (500 MHz, $CDCl_3$) δ 8.10 – 8.04 (m, 2H), 8.05 – 8.02 (m, 0.2H), 7.75 (dd, J = 7.7, 3.6 Hz, 2H), 7.63 – 7.52 (m, 4H), 7.47 (t, J = 7.8 Hz, 2H), 7.38 (td, J = 7.6, 1.0 Hz, 2H), 7.32 – 7.16 (m, 15H), 7.14 – 7.07 (m, 1H), 6.76 (d, J = 7.8 Hz, 2H), 6.46 (s, 0.1H), 6.09 (s, 1H), 5.63 (d, J = 3.9 Hz, 0.1H), 5.56 (t, J = 6.1 Hz, 1H), 5.43 (d, J = 3.8 Hz, 1H), 4.89 – 4.82 (m, 2H), 4.78 (d, J = 10.8 Hz, 1H), 4.67 – 4.59 (m, 2H), 4.56 – 4.46 (m, 2H), 4.41 (dd, J = 12.0, 4.8 Hz, 1H), 4.34 (dd, J = 10.6, 7.1 Hz, 1H), 4.26 (dd, J = 12.4, 4.7 Hz, 1H), 4.19 (t, J = 6.9 Hz, 1H), 4.11 – 3.98 (m, 5H), 3.87 (dd, J = 10.3, 9.1 Hz, 1H), 3.40 (dd, J = 10.3, 3.9 Hz, 0.1H), 3.35 (dd, J = 10.3, 3.8 Hz, 1H), 2.06 (s, 3H); ^{13}C NMR (126 MHz, $CDCl_3$) δ 170.5, 167.0, 164.8, 154.2, 143.2, 143.1, 143.0, 141.3, 137.1, 133.7, 129.8, 129.1, 128.8, 128.7, 128.5, 128.4, 127.9, 127.8, 127.6, 127.2, 125.1, 124.9, 124.6, 120.1, 119.3, 98.1, 80.9, 77.4, 75.1, 74.7, 73.8, 73.0, 71.3, 70.3, 68.8, 64.6, 62.7, 61.9, 46.7, 40.5, 20.7; HRMS (ESI+) calculated for $C_{60}H_{54}ClF_3N_3O_{15}Na$ $[M+Na]^+$ 1185.312 *m*/*z*, found 1185.313.

Methyl ([6-*O*-acetyl-2-azido-3-*O*-benzyl-2-deoxy-4-*O*-(9-fluorenylmethyloxycarbonyl)-α-D-glucopyranosyl(1→4)]-2-*O*-benzoyl-3-*O*-benzyl-α,β-D-glucopyranoside) uronate *N*-phenyl trifluoroacetimidate (30)

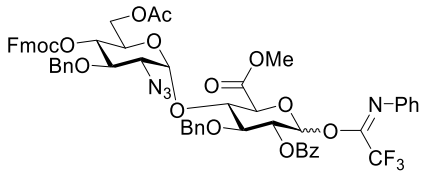

Hemiacetal **26** (50 mg, 0.053 mmol) was reacted according to General procedure E to yield the title compound as a mixture of anomers (α/β: 99/1), asan off-white foam (30 mg, 0.27 mmol, 51%), TLC: R_f = 0.8 (EtOAc/toluene, 1/4 *v*/*v*); α – ^{1}H NMR (500 MHz, $CDCl_3$) δ 8.11 – 8.05 (m, 2H), 7.76 (ddt, J = 7.6, 2.7, 0.9 Hz, 2H), 7.60 (dt, J = 7.5, 0.9 Hz, 1H), 7.61 – 7.49 (m, 2H), 7.48 – 7.41 (m, 2H), 7.39 (tt, J = 7.5, 0.9 Hz, 2H), 7.33 – 7.22 (m, 9H), 7.25 – 7.17 (m, 3H), 7.18 – 7.06 (m, 4H), 6.82 – 6.76 (m, 2H), 5.49 (dd, J = 5.6, 4.3 Hz, 1H), 5.37 (d, J = 3.7 Hz, 1H), 4.86 – 4.78 (m, 2H), 4.77 (d, J = 10.9 Hz, 1H), 4.58 – 4.49

(m, 3H), 4.46 (d, J = 10.9 Hz, 1H), 4.40 – 4.32 (m, 2H), 4.23 – 4.11 (m, 4H), 4.02 – 3.95 (m, 1H), 3.77 (dd, J = 10.3, 9.1 Hz, 1H), 3.74 (s, 3H), 3.31 (dd, J = 10.3, 3.7 Hz, 1H), 2.07 (s, 3H); ^{13}C NMR (126 MHz, $CDCl_3$) δ 170.7, 168.4, 164.9, 154.2, 143.3, 143.2, 143.1, 141.4, 141.3, 137.2, 137.1, 133.7, 129.9, 129.2, 129.1, 128.8, 128.7, 128.4, 128.3, 128.0, 127.8, 127.7, 127.6, 127.2, 125.0, 124.8, 124.4, 120.6, 120.1, 119.3, 98.5, 93.9, 77.4, 75.0, 74.8, 74.5, 73.9, 73.5, 70.7, 70.2, 68.7, 62.7, 61.7, 52.7, 46.8, 29.7, 20.7; HRMS (ESI+) calculated for $C_{59}H_{53}F_3N_4O_{15}Na$ $[M+Na]^+$ 1137.336 *m/z*, found 1137.335. The β-anomer was not observed by NMR.

General procedure F: Disaccharide 1-*O*-acetate formation

Sodium acetate (2 equiv.) and acetic anhydride (2 equiv.) was added to toluene (30 mL per 1 mmol hemiacetal) and heated to reflux. The appropriate hemiacetal was dissolved in a small quantity of toluene (1-5 mL) and injected into the reaction vessel. The reaction was then stirred at reflux for around 2-3 hours, until TLC analysis indicated completion. The reaction mixture was then allowed to cool, and then diluted with EtOAc and washed with saturated $NaHCO_3$ (aq), water, brine, dried over $MgSO_4$ and evaporated to dryness. The crude mixture was purified by column chromatography (gradient of 0-20% EtOAc in toluene), with both anomers of the product eluting as one peak.

[6-*O*-acetyl-2-azido-3-*O*-benzyl-2-deoxy-4-*O*-(9-fluorenylmethyloxycarbonyl)-α-D-glucopyranosyl(1→4)]-1-*O*-acetyl-2-*O*-benzoyl-3-*O*-benzyl-6-*O*-chloroacetyl-β-D-glucopyranoside (31)

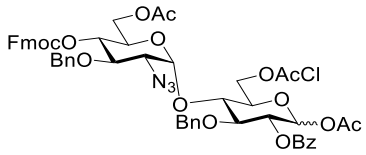

Hemiacetal **23** (675 mg, 0.68 mmol) was reacted according to General procedure F to yield the title compound as a mixture of anomers (α/β: 3/7), appearing as a yellow foam (620 mg, 0.60 mmol, 88%), TLC: R_f = 0.75 (EtOAc/toluene, 1/4 *v*/*v*); ^{1}H NMR (500 MHz, $CDCl_3$) δ 8.05 – 8.01 (m, 1.4H), 8.00 – 7.95 (m, 0.6H), 7.78 – 7.73 (m, 2H), 7.62 – 7.52 (m, 3H), 7.45 (td, J = 8.6, 8.0, 1.4 Hz, 2H), 7.41 – 7.36 (m, 2H), 7.32 – 7.11 (m, 14H), 6.40 (d, J = 3.6 Hz, 0.3H), 5.89 (d, J = 7.4 Hz, 0.7H), 5.64 (d, J = 3.9 Hz, 0.3H), 5.51 (d, J = 3.9 Hz, 0.7H), 5.43 (dd, J = 8.1, 7.5 Hz, 0.7H), 5.33 (dd, J = 9.7, 3.7 Hz, 0.3H), 4.93 – 4.83 (m, 2H), 4.81 – 4.65 (m, 3H), 4.63 – 4.55 (m, 2H), 4.52 – 4.45 (m, 1H), 4.41 – 4.23 (m, 3H), 4.18 (t, J = 7.2 Hz, 1H), 4.14 (s, 2H), 4.12 – 4.04 (m, 2H), 4.02 – 3.89 (m, 4H), 3.39 (dd, J = 10.3, 3.9 Hz, 0.3H), 3.36 (dd, J = 10.3, 3.9 Hz, 0.7H), 2.35 (s, 2H), 2.17 (s, 1H), 2.05 (d, J = 1.1 Hz, 3H), 2.03 (s, 2H); ^{13}C NMR (126 MHz, $CDCl_3$) δ 170.5, 169.2, 168.7, 167.1, 167.0, 165.2, 165.0, 154.2, 143.2, 143.0, 141.34, 141.32, 137.9, 137.5, 137.2, 137.1, 133.7, 133.6, 129.8, 129.7, 129.09, 129.04, 128.69, 128.63, 128.44, 128.39, 128.2,

128.0, 127.9, 127.8, 127.6, 127.29, 127.25, 125.3, 125.1, 124.9, 120.1, 98.1, 98.0, 91.8, 89.2, 82.1, 79.9, 77.6, 77.4, 75.2, 75.0, 74.8, 74.7, 74.4, 73.1, 72.5, 72.3, 70.4, 70.2, 68.9, 64.6, 64.4, 62.69, 62.64, 61.94, 61.88, 46.7, 40.65, 40.61, 21.4, 20.9, 20.7; HRMS (ESI+) calculated for $C_{54}H_{52}ClN_3O_{16}Na$ $[M+NH_4]^+$ 1051.3380 *m*/*z*, found 1051.3383.

Methyl ([6-*O*-acetyl-2-azido-3-*O*-benzyl-2-deoxy-4-*O*-(9-fluorenylmethyloxycarbonyl)-α-D-glucopyranosyl(1→4)]-1-*O*-acetyl-2-*O*-benzoyl-3-*O*-benzyl-β-D-glucopyranosyl) uronate **(32)**

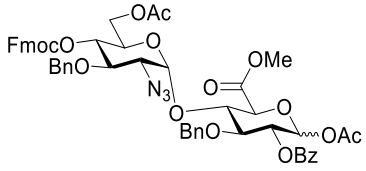

Hemiacetal **26** (150 mg, 0.159 mmol) was reacted according to General procedure F to yield the title compound as a mixture of anomers (α/β: 4/6), appearing as a yellow foam (140 mg, 0.142 mmol, 89%), TLC: R_f = 0.75 (EtOAc/toluene, 1/4 *v*/*v*); ^{1}H NMR (500 MHz, $CDCl_3$) δ 8.07 – 8.02 (m, 1H), 8.02 – 7.99 (m, 1H), 7.79 – 7.73 (m, 2H), 7.62 – 7.52 (m, 3H), 7.49 – 7.33 (m, 5H), 7.32 – 7.16 (m, 10H), 6.50 (d, J = 3.5 Hz, 0.4H), 5.97 (d, J = 6.4 Hz, 0.6H), 5.52 (d, J = 3.8 Hz, 0.4H), 5.46 (d, J = 3.7 Hz, 0.6H), 5.42 (dd, J = 7.4, 6.3 Hz, 0.6H), 5.38 – 5.34 (m, 0.4H), 4.90 – 4.82 (m, 2H), 4.80 – 4.72 (m, 1H), 4.71 – 4.60 (m, 1H), 4.59 – 4.46 (m, 3H), 4.43 – 4.16 (m, 5H), 4.16 – 4.05 (m, 2H), 3.94 – 3.79 (m, 2H), 3.78 (s, 1H), 3.76 (s, 2H), 3.40 – 3.31 (m, 1H), 2.18 (s, 1.2H), 2.08 (s, 1.8H), 2.07 (s, 1.2H), 2.05 (s, 1.8H); 13C NMR (126 MHz, CDCl3) δ 170.71, 170.67, 169.1, 168.54, 168.50, 168.3, 165.2, 165.0, 154.2, 143.3, 143.0, 141.35, 141.31, 137.23, 137.16, 137.1, 133.7, 133.6, 129.9, 129.7, 129.1, 128.7, 128.44, 128.40, 128.37, 128.0, 127.92, 127.85, 127.7, 127.5, 127.2, 125.1, 124.9, 120.1, 98.1, 97.9, 91.6, 89.0, 80.4, 78.9, 77.5, 75.1, 75.1, 74.8, 74.5, 74.4, 74.2, 72.5, 71.8, 71.4, 70.3, 68.6, 68.5, 62.74, 62.69, 61.53, 61.45, 52.90, 52.86, 46.7, 20.86, 20.83, 20.76; HRMS (ESI+) calculated for $C_{53}H_{51}N_3O_{16}Na$ $[M+Na]^+$ 1008.3167 *m*/*z*, found 1008.3170.

General procedure G: Thioglycoside donor formation with an acetate substrate

The appropriate disaccharide acetate and a small quantity of 3 Å molecular sieves was dissolved in anhydrous CH_2Cl_2 (15 mL per 1 mmol hemiacetal) under argon. The reaction mixture was then treated with toluenethiol (solution of 1 g in 10 mL CH_2Cl_2, 1.5 equiv.) followed by boron trifluoride diethyl etherate (0.5 equiv.). The reaction mixture was then stirred at room temperature for around 3 hours, until TLC analysis indicated completion. The reaction mixture was then diluted with EtOAc and washed with saturated $NaHCO_3$ (aq), water, brine, dried over $MgSO_4$ and evaporated to dryness. The crude mixture was purified by column chromatography (gradient of 0-20% EtOAc in toluene) to yield the desired β-thioglycoside.

***p*-Tolyl [6-*O*-acetyl-2-azido-3-*O*-benzyl-2-deoxy-4-*O*-(9-fluorenylmethyloxycarbonyl)-α-D-glucopyranosyl(1→4)]-2-*O*-benzoyl-3-*O*-benzyl-6-*O*-chloroacetyl-1-thiol-β-D-glucopyranoside (33)**

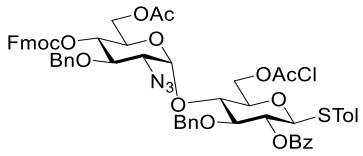

Acetate **31** (120 mg, 0.115 mmol, α/β: 33/67, containing 0.077 mmol β) was reacted according to General procedure G to yield the title compound as an off-white foam (54 mg, 0.049 mmol, 64% based on the amount of β), TLC: R_f = 0.7 (EtOAc/toluene, 1/4 *v*/*v*); mp 124 °C (from MeOH); ^{1}H NMR (500 MHz, $CDCl_3$) δ 8.11 – 8.06 (m, 2H), 7.75 (dd, J = 7.7, 3.9 Hz, 2H), 7.62 – 7.56 (m, 2H), 7.55 (dd, J = 7.5, 1.0 Hz, 1H), 7.49 – 7.43 (m, 2H), 7.41 – 7.33 (m, 5H), 7.28 (tdd, J = 7.5, 3.6, 1.2 Hz, 2H), 7.25 – 7.16 (m, 7H), 7.16 – 7.07 (m, 4H), 5.57 (d, J = 3.9 Hz, 1H), 5.32 – 5.23 (m, 1H), 4.85 (dd, J = 10.2, 9.1 Hz, 1H), 4.79 – 4.63 (m, 6H), 4.47 (dd, J = 10.5, 6.8 Hz, 1H), 4.37 – 4.28 (m, 2H), 4.24 (dd, J = 12.4, 4.7 Hz, 1H), 4.18 (t, J = 6.9 Hz, 1H), 4.09 (s, 1H), 4.08 (s, 1H), 4.07 – 4.00 (m, 2H), 3.97 – 3.90 (m, 2H), 3.87 (dd, J = 9.6, 8.4 Hz, 1H), 3.75 (ddd, J = 9.8, 5.9, 2.5 Hz, 1H), 3.33 (dd, J = 10.3, 4.0 Hz, 1H), 2.34 (s, 3H), 2.04 (s, 3H); ^{13}C NMR (126 MHz, $CDCl_3$) δ 170.5, 166.9, 165.1, 143.2, 143.0, 141.3, 138.6, 137.2, 137.1, 133.7, 133.5, 129.9, 129.62, 128.60, 128.4, 128.0, 127.9, 127.8, 127.6, 127.2, 125.1, 124.9, 120.1, 97.8, 86.1, 84.3, 76.1, 75.1, 74.7, 72.7, 70.4, 68.8, 64.9, 62.5, 62.0, 46.7, 40.6, 21.2, 20.7; HRMS (ESI+) calculated for $C_{59}H_{56}ClN_3O_{14}SNa$ $[M+NH_4]^+$ 1115.3491 *m*/*z*, found 1115.3497.

Methyl (*p*-Tolyl [6-*O*-acetyl-2-azido-3-*O*-benzyl-2-deoxy-4-*O*-(9-fluorenylmethyloxycarbonyl)-α-D-glucopyranosyl(1→4)]-2-*O*-benzoyl-3-*O*-benzyl-1-thiol-β-D-glucopyranoside) uronate (34)

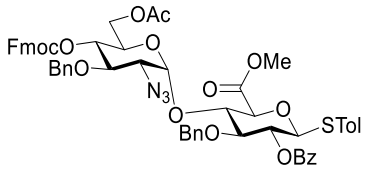

Acetate **32** (120 mg, 0.122 mmol, α/β: 45/55, containing 0.067 mmol β) was reacted according to General procedure G to yield the title compound as an off-white solid (44 mg, 0.041 mmol, 62% based on the amount of β), TLC: R_f = 0.7 (EtOAc/toluene, 1/4 *v*/*v*); mp = 125°C (from MeOH), ^{1}H NMR (500 MHz, $CDCl_3$) δ 8.09 – 8.05 (m, 2H), 7.77 – 7.73 (m, 2H), 7.62 – 7.56 (m, 2H), 7.56 – 7.52 (m, 1H), 7.50 – 7.43 (m, 2H), 7.42 – 7.32 (m, 4H), 7.30 – 7.12 (m, 12H), 7.12 – 7.08 (m, 2H), 5.50 (d, J = 3.7 Hz, 1H), 5.29 (dd, J = 9.7, 8.7 Hz, 1H), 4.86 (dd, J = 10.3, 9.1 Hz, 1H), 4.82 (d, J = 9.7 Hz, 1H), 4.77 – 4.71 (m, 2H), 4.69 – 4.60 (m, 2H), 4.47 (dd, J = 10.5, 6.8 Hz, 1H), 4.33 – 4.28 (m, 1H), 4.26 – 4.20 (m, 2H), 4.18 (t, J = 7.0 Hz, 1H), 4.12 – 4.05 (m, 2H), 4.00 (t, J = 8.6 Hz, 1H), 3.91 (dd, J = 10.3, 9.1 Hz, 1H), 3.81 (s, 3H), 3.73 (ddd, J = 10.2, 3.9, 2.3 Hz, 1H), 3.33 (dd, J = 10.3, 3.8 Hz, 1H), 2.33 (s, 3H), 2.06 (s, 3H); ^{13}C NMR (126

MHz, $CDCl_3$) δ 170.7, 168.1, 164.9, 154.2, 143.3, 143.1, 141.3, 138.6, 137.1, 133.54, 133.45, 129.9, 129.7, 129.6, 129.0, 128.6, 128.4, 128.1, 127.97, 127.94, 127.90, 127.82, 127.79, 127.2, 125.1, 124.9, 120.10, 120.08, 97.5, 87.0, 83.6, 77.9, 75.1, 74.8, 74.3, 72.1, 70.3, 68.4, 62.7, 61.4, 52.8, 46.7, 21.2, 20.7; HRMS (ESI+) calculated for $C_{58}H_{55}N_3O_{14}SNa$ $[M+Na]^+$ 1072.3302 *m*/*z*, found 1072.3311.

Selective anomeric acetate removal to yield hemiacetal **(26)**

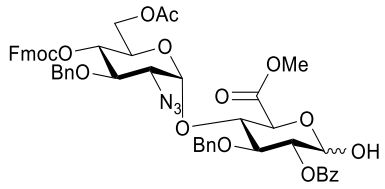

The mixture of anomeric acetates **32** (1.0 g, 1.0 mmol) was dissolved in MeOH (10 mL). Zinc acetate (25 mg, 0.11 mmol, 0.1 equiv.) was added, and the reaction mixture stirred at 50 °C for 6 hours until TLC analysis indicated no further reaction. The solvent was removed in vacuo, and the residue dissolved in EtOAc, washed with water, saturated $NaHCO_3$ (aq), brine, dried over $MgSO_4$ and evaporated to dryness. The mixture was purified by column chromatography to give the desired product as a mixture of anomers (α/β: 6/4), appearing as a yellow foam (700 mg, 0.74 mmol, 73%), TLC: R_f = 0.45 (EtOAc/toluene, 1/4 *v*/*v*); data matches the previous instance of this compound.

[6-*O*-acetyl-2-azido-3-*O*-benzyl-2-deoxy-4-*O*-(9-fluorenylmethyloxycarbonyl)-α-D-glucopyranosyl (1→4)]-2-*O*-benzoyl-3-*O*-benzyl-6-*O*-chloroacetyl-β-D-glucopyranosyl chloride **(35)**

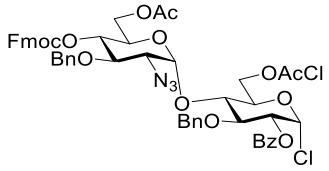

The mixture of anomeric acetates **32** (200 mg, 0.193 mmol) was dissolved in anhydrous CH_2Cl_2 (2 mL) under argon, and then treated with thionyl chloride (28 µL, 2 equiv.) followed by tin tetrachloride (23 µL, 1 equiv.). The reaction mixture was then stirred at room temperature for 2 hours, until TLC analysis indicated completion. The reaction mixture was then quenched with 0.5 mL ice-cold saturated $NaHCO_3$ (aq), and then diluted with CH_2Cl_2. The organic layer was separated and then washed with ice-cold brine, dried over $MgSO_4$ and evaporated to dryness. The mixture was purified by column chromatography to yield the desired α-chloride as an off-white foam (120 mg, 0.119 mmol, 62%), TLC: R_f = 0.7 (EtOAc/toluene, 1/4 *v*/*v*); ^{1}H NMR (500 MHz, $CDCl_3$) δ 8.09 – 8.03 (m, 2H), 7.75 (dd, J = 7.6, 3.6 Hz, 2H), 7.63 – 7.53 (m, 3H), 7.46 (t, J = 7.8 Hz, 2H), 7.39 (t, J = 7.5 Hz, 2H), 7.31 – 7.14 (m, 12H), 6.34 (d, J = 3.9 Hz, 1H), 5.62 (d, J = 3.9 Hz, 1H), 5.29 (dd, J = 9.6, 3.9 Hz, 1H), 4.96 – 4.85 (m, 3H), 4.79 (d, J = 10.9 Hz, 1H), 4.68 (d, J = 10.9 Hz, 1H), 4.64 (dd, J = 12.2, 2.2 Hz, 1H), 4.48 (dd, J = 10.5, 6.7 Hz, 1H), 4.42

– 4.36 (m, 2H), 4.36 – 4.30 (m, 2H), 4.27 (dd, J = 12.5, 4.2 Hz, 1H), 4.18 (t, J = 7.1 Hz, 1H), 4.15 (s, 2H), 4.08 (dd, J = 12.4, 2.8 Hz, 1H), 4.03 – 3.94 (m, 3H), 3.41 (dd, J = 10.3, 3.9 Hz, 1H), 2.05 (s, 3H); ^{13}C NMR (126 MHz, $CDCl_3$) δ 170.5, 167.0, 165.3, 154.2, 143.3, 143.0, 141.3, 137.5, 137.1, 133.8, 129.9, 128.8, 128.7, 128.5, 128.4, 128.00, 127.98, 127.94, 127.8, 127.3, 125.1, 124.9, 120.1, 98.3, 90.7, 79.5, 77.5, 75.3, 75.1, 74.6, 74.4, 73.8, 71.0, 70.4, 68.9, 64.0, 62.7, 61.8, 46.7, 40.6, 20.7; HRMS (ESI+) calculated for $C_{52}H_{49}Cl_2N_3O_{14}Na$ $[M+Na]^+$ 1032.2489 *m/z*, found 1032.2483.

General Procedure H: Glycosylation using a trichloroacetimidate donor

Glycosyl donor (1.3 equiv.) and acceptor (1 equiv.) were dissolved in anhydrous CH_2Cl_2 (3 mL per 0.1 mmol acceptor) under argon, with 3Å molecular sieves (100 mg per 0.1 mmol acceptor). This mixture was cooled to -20 °C using an ice/MeOH bath or -40 °C using a dry ice/MeCN bath, and then treated with trimethylsilyl trifluoromethanesulfonate (0.3 equiv.). The reaction was stirred in the cooling bath for 30 minutes, allowing slow warming to around -10 to 0 °C, until TLC analysis indicated completion, at which point the reaction was quenched with 1 mL aqueous saturated $NaHCO_3$ (aq) whilst still cold. The reaction mixture was then diluted with EtOAc, washed with aqueous saturated $NaHCO_3$ (aq), water, and brine, dried over $MgSO_4$ and evaporated to dryness. The mixture was purified by column chromatography (gradient of 0-20% EtOAc in toluene or 0-10% of MeCN in CH_2Cl_2) to yield the product.

General Procedure I: Glycosylation using a Trifluoro-*N*-phenylacetimidate donor

Glycosyl donor (1.3 equiv.) and acceptor (1 equiv.) were dissolved in anhydrous CH_2Cl_2 (3 mL per 0.1 mmol acceptor) under argon, with 3Å molecular sieves (100 mg per 0.1 mmol acceptor). This mixture was cooled to either -20 °C using an ice/MeOH bath, -40 °C using a dry ice/MeCN bath, or -78 °C using a dry ice/acetone bath, and then treated with trimethylsilyl trifluoromethanesulfonate (0.3 equiv.). The reaction was stirred in the cooling bath for 10-15 minutes, until TLC analysis indicated completion, at which point the reaction was quenched with 1 mL aqueous saturated $NaHCO_3$ (aq) whilst still cold. The reaction mixture was then diluted with EtOAc, washed with aqueous saturated $NaHCO_3$ (aq), water, and brine, dried over $MgSO_4$ and evaporated to dryness. The mixture was purified by column chromatography (gradient of 0-20% EtOAc in toluene or 0-10% of MeCN in CH_2Cl_2) to yield the product as a yellow foam.

General procedure J: Glycosylation using a thioglycoside donor

Glycosyl donor (1.3 equiv.) and acceptor (1 equiv.) were dissolved in anhydrous CH_2Cl_2 (3 mL per 0.1 mmol acceptor) under argon, with 3Å molecular sieves (100 mg per 0.1 mmol acceptor). This mixture was cooled to -20 °C using an ice/MeOH bath, and then treated with *N*-iodosuccinimide (1.7 equiv.) and silver trifluoromethanesulfonate (0.4 equiv.). The reaction was stirred in the cooling bath for 30

minutes, allowing slow warming to around -10 to 0 °C, until TLC analysis indicated completion, at which point the reaction was quenched with 1 mL aqueous saturated $NaHCO_3$ (aq) whilst still cold. The reaction mixture was then diluted with EtOAc, washed with a 1:1 mixture of aqueous saturated $NaHCO_3$ (aq) and sodium thiosulfate 10% *w*/*v* (aq), water, and brine, dried over $MgSO_4$ and evaporated to dryness. The mixture was purified by column chromatography (gradient of 0-20% EtOAc in toluene) to yield the product as a yellow foam.

Hexose tetrasaccharide **(14)**

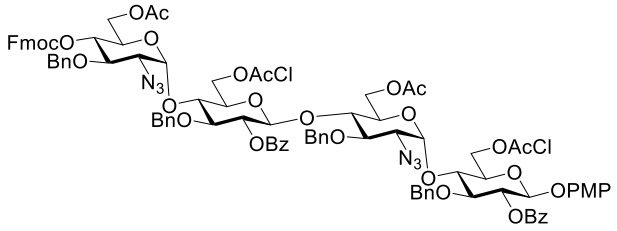

Donor **27** (200 mg, 0.18 mmol, 1.3 equiv.) and acceptor **22** (120 mg, 0.14 mmol) were reacted according to General Procedure H to yield **14** as an off-white foam (230 mg, 0.12 mmol, 90%); donor **29** (200 mg, 0.17 mmol, 1.3 equiv.) and acceptor **22** (120 mg, 0.14 mmol) were reacted according to General Procedure I to yield **14** as an off-white foam (220 mg, 0.12 mmol, 87%); donor **33** (200 mg, 0.18 mmol, 1.3 equiv.) and acceptor **22** (120 mg, 0.14 mmol) were reacted according to General Procedure J to yield **14** as an off-white foam (120 mg, 0.073 mmol, 53%); TLC: R_f = 0.65 (EtOAc/toluene, 1/4 *v*/*v*); $[\alpha]_D$ 42.0 (c 1 in $CDCl_3$); IR (ATR): ν_{max}/cm^{-1} 2108 (N_3, s), 1735 (C=O, s); ^{1}H NMR (500 MHz, $CDCl_3$) δ 8.10 – 8.01 (m, 5H), 7.78 – 7.72 (m, 2H), 7.63 – 7.52 (m, 4H), 7.49 – 7.42 (m, 4H), 7.41 – 7.35 (m, 4H), 7.35 – 7.31 (m, 2H), 7.31 – 7.24 (m, 3H), 7.25 – 7.15 (m, 13H), 7.13 (dd, J = 7.9, 1.8 Hz, 2H), 6.88 – 6.82 (m, 2H), 6.78 – 6.73 (m, 2H), 5.52 – 5.46 (m, 3H), 5.38 (dd, J = 8.8, 7.8 Hz, 1H), 5.10 (d, J = 11.2 Hz, 1H), 5.02 (d, J = 7.1 Hz, 1H), 4.86 (dd, J = 10.2, 9.1 Hz, 1H), 4.80 – 4.67 (m, 7H), 4.67 – 4.62 (m, 2H), 4.48 (dd, J = 10.5, 6.8 Hz, 1H), 4.42 – 4.34 (m, 2H), 4.31 (dd, J = 10.5, 7.3 Hz, 1H), 4.26 – 4.20 (m, 2H), 4.20 – 4.10 (m, 4H), 4.06 – 3.97 (m, 3H), 3.95 – 3.87 (m, 4H), 3.86 (s, 3H), 3.85 – 3.79 (m, 3H), 3.73 (s, 4H), 3.36 (dd, J = 10.3, 3.9 Hz, 1H), 3.25 (dd, J = 10.2, 3.9 Hz, 1H), 2.02 (s, 3H), 2.02 (s, 3H); ^{13}C NMR (126 MHz, $CDCl_3$) δ 170.5, 170.4, 166.9, 166.4, 165.1, 164.9, 155.7, 154.1, 150.9, 143.2, 143.0, 141.34, 141.32, 138.3, 137.3, 137.2, 137.1, 133.8, 133.5, 129.80, 129.76, 129.5, 128.9, 128.8, 128.6, 128.41, 128.36, 128.3, 128.0, 127.9, 127.83, 127.77, 127.73, 127.69, 127.5, 127.4, 127.3, 125.1, 124.9, 120.1, 118.8, 118.7, 114.5, 101.0, 100.1, 97.9, 97.7, 82.74, 82.71, 77.9, 77.7, 77.5, 75.4, 75.2, 75.1, 74.7, 74.63, 74.58, 74.3, 74.2, 73.6, 72.4, 72.3, 70.4, 69.8, 68.8, 64.9, 64.3, 62.7, 62.6, 62.0, 61.8, 55.6, 46.7, 40.4, 20.8, 20.7; HRMS (ESI+) calculated for $C_{96}H_{94}Cl_2N_6O_{28}Na$ $[M+Na]^+$ 1871.5391 *m*/*z*, found 1871.5394.

Uronate tetrasaccharide **(15)**

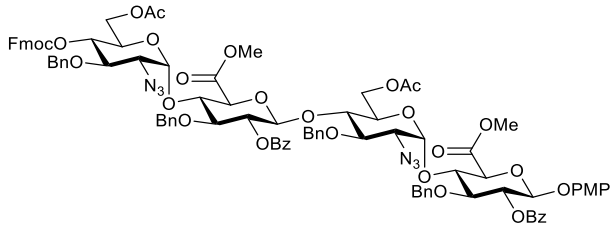

Donor **28** (200 mg, 0.18 mmol, 1.3 equiv.) and acceptor **24** (120 mg, 0.15 mmol) were reacted according to General Procedure H to yield **15** as an off-white foam (120 mg, 0.068 mmol, 47%); donor **30** (200 mg, 0.18 mmol, 1.2 equiv.) and acceptor **24** (120 mg, 0.15 mmol) were reacted according to General Procedure I to yield **15** as an off-white foam (5 mg, 0.007 mmol, 5%); donor **34** (200 mg, 0.19 mmol, 1.3 equiv.) and acceptor **24** (120 mg, 0.15 mmol) were reacted according to General Procedure J to yield **15** as an off-white foam (140 mg, 0.080 mmol, 56%); TLC: R_f = 0.65 (EtOAc/toluene, 1/4 *v*/*v*); $[\alpha]_D$ 30.5 (c 1 in $CDCl_3$); IR (ATR): ν_{max}/cm^{-1} 2108 (N_3, s), 1734 (C=O, s); ^1H NMR (500 MHz, $CDCl_3$) δ 8.14 – 8.07 (m, 2H), 8.05 – 7.99 (m, 2H), 7.75 (dd, J = 7.7, 3.3 Hz, 2H), 7.61 – 7.51 (m, 4H), 7.50 – 7.32 (m, 10H), 7.30 – 7.14 (m, 16H), 7.11 (dd, J = 7.5, 2.1 Hz, 2H), 6.84 (d, J = 9.0 Hz, 2H), 6.73 (d, J = 8.8 Hz, 2H), 5.53 – 5.46 (m, 3H), 5.42 (t, J = 8.4 Hz, 1H), 5.15 (d, J = 10.9 Hz, 1H), 5.06 (d, J = 6.8 Hz, 1H), 4.88 (t, J = 9.7 Hz, 1H), 4.82 – 4.61 (m, 8H), 4.47 (dd, J = 10.6, 6.6 Hz, 1H), 4.35 – 4.26 (m, 4H), 4.23 (dd, J = 12.6, 3.8 Hz, 1H), 4.20 – 4.12 (m, 2H), 4.11 – 3.99 (m, 3H), 3.98 – 3.86 (m, 3H), 3.83 – 3.67 (m, 6H), 3.55 (s, 3H), 3.46 – 3.40 (m, 1H), 3.37 (dd, J = 10.3, 3.8 Hz, 1H), 3.23 (dd, J = 9.9, 3.8 Hz, 1H), 3.17 (s, 3H), 2.09 (s, 3H), 2.05 (s, 3H); ^{13}C NMR (126 MHz, $CDCl_3$) δ 170.70, 170.66, 168.1, 167.8, 165.0, 164.7, 155.7, 154.1, 150.9, 143.3, 143.1, 141.35, 141.32, 138.2, 137.2, 137.13, 137.09, 133.8, 133.5, 129.9, 129.8, 129.4, 128.9, 128.8, 128.6, 128.39, 128.37, 128.34, 127.99, 127.94, 127.86, 127.83, 127.79, 127.63, 127.58, 127.2, 125.1, 124.9, 120.13, 120.10, 118.7, 114.5, 101.1, 100.7, 97.5, 97.3, 82.5, 82.2, 77.7, 77.5, 75.5, 75.4, 75.2, 75.0, 74.8, 74.5, 74.3, 74.2, 74.1, 73.8, 73.5, 70.3, 69.1, 68.4, 62.8, 62.7, 61.6, 61.4, 55.6, 52.7, 52.1, 46.7, 20.9, 20.7.; HRMS (ESI+) calculated for $C_{94}H_{92}N_6O_{28}Na$ $[M+Na]^+$ 1775.5844 *m*/*z*, found 1775.5857.

Tetrasaccharide impurity of TCA glycosylation **(40)**

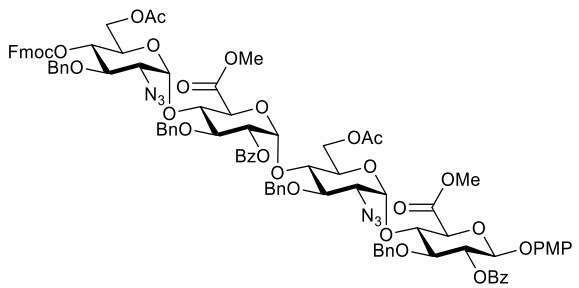

Donor **28** (200 mg, 0.18 mmol, 1.3 equiv.) and acceptor **24** (120 mg, 0.15 mmol) was reacted according to General Procedure H to yield the title compound as an off-white foam (63 mg, 0.038 mmol, 25%); TLC: R_f = 0.55 (EtOAc/toluene, 1/4 *v*/*v*); ^{1}H NMR (500 MHz, CDCl3) δ 8.07 – 8.01 (m, 2H), 7.96 – 7.90 (m, 2H), 7.75 (ddt, J = 7.6, 1.8, 0.9 Hz, 2H), 7.61 (dd, J = 7.5, 0.9 Hz, 1H), 7.59 – 7.52 (m, 3H), 7.48 – 7.40 (m, 2H), 7.42 – 7.32 (m, 6H), 7.28 (ddd, J = 7.5, 3.7, 2.7 Hz, 4H), 7.25 – 7.14 (m, 14H), 7.14 (dd, J = 5.1, 1.9 Hz, 3H), 6.95 – 6.85 (m, 2H), 6.80 – 6.70 (m, 2H), 5.82 (d, J = 5.5 Hz, 1H), 5.59 – 5.51 (m, 3H), 5.31 (s, 1H), 5.15 (d, J = 6.6 Hz, 1H), 4.95 – 4.84 (m, 3H), 4.82 – 4.71 (m, 4H), 4.61 (d, J = 11.1 Hz, 1H), 4.54 – 4.40 (m, 5H), 4.41 – 4.25 (m, 4H), 4.25 – 4.05 (m, 6H), 4.05 – 3.95 (m, 2H), 3.89 – 3.80 (m, 1H), 3.71 (s, 3H), 3.70 (s, 3H), 3.66 (s, 3H), 3.40 – 3.28 (m, 2H), 2.06 (s, 3H), 2.05 (s, 3H); ^{13}C NMR (126 MHz, $CDCl_3$) δ 170.55, 170.51, 168.8, 168.3, 165.1, 165.0, 155.6, 154.2, 151.1, 143.2, 143.0, 141.3, 141.2, 137.4, 137.3, 137.2, 136.8, 133.4, 133.3, 129.85, 129.80, 129.4, 129.3, 128.54, 128.45, 128.40, 128.34, 128.33, 128.30, 128.0, 127.9, 127.8, 127.7, 127.2, 125.1, 124.9, 120.05, 120.03, 118.6, 114.4, 100.6, 98.5, 97.5, 81.7, 79.6, 75.2, 74.8, 74.7, 74.5, 74.4, 74.1, 73.6, 72.5, 70.4, 69.3, 68.6, 63.1, 62.6, 62.5, 61.7, 55.1, 52.8, 52.4, 46.6, 20.8, 20.6; HRMS (ESI+) calculated for $C_{94}H_{92}N_6O_{28}Na$ $[M+Na]^+$ 1775.5844 *m*/*z*, found 1775.5861.

2-(Hydroxymethyl) benzoic acid **(41)**

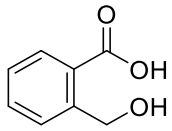

Phthalide (113 g, 843 mmol) and sodium hydroxide (45 g, 1100 mmol, 1.5 equiv.) were suspended in water (1 L). The reaction mixture was then heated with to reflux with stirring, at which point the phthalide dissolved and solution turned a slight yellow colour. The mixture was stirred for 30 minutes at this temperature. The mixture was removed from the heating mantle, and conc. HCl added (92 mL, 1100 mmol, 1.5 equiv.) upon which a white precipitate rapidly formed. This precipitate was immediately collected by filtration whilst the mixture was still hot and washed several times with water and diethyl ether. The solid was dried on a rotary evaporator, co-evaporated with one portion of toluene, and then further dried on the rotary evaporator until a constant mass was achieved. This afforded the product as a white powder, (84 g, 550 mmol, 66%), TLC: R_f = 0.2 (EtOAc/hexanes, 1/1 *v*/*v* with 2% AcOH); ^{1}H NMR (500 MHz, DMSO) δ 7.85 (dd, J = 7.7, 1.4 Hz, 1H), 7.72 (dd, J = 7.8, 1.3 Hz, 1H), 7.57 (td, J = 7.6, 1.5 Hz, 1H), 7.34 (td, J = 7.5, 1.3 Hz, 1H), 4.84 (s, 2H); ^{13}C NMR (126 MHz, DMSO) δ 168.8, 144.7, 132.3, 130.4, 128.8, 127.2, 126.8, 61.6; HRMS (ESI+) calculated for $C_8H_8O_3Na$ $[M+Na]^+$ 175.0371 *m*/*z*, found 175.0371.

2-(Acetoxymethyl) benzoic acid **(42)**

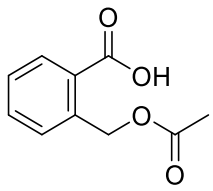

2-(Hydroxymethyl) benzoic acid **41** (35.0 g, 230 mmol) was dissolved in anhydrous DMF (350 mL) under argon and cooled to 0 °C in an ice bath with stirring. To this reaction mixture, 2-chloropyridine (41 mL, 430 mmol, 1.9 equiv.) was added, and the reaction mixture stirred for one minute to ensure good mixing and consistent temperature. Then, acetyl chloride (35 mL, 490 mmol, 2.1 equiv.) was added dropwise over a period of 10 minutes using a dropping funnel. The reaction mixture was stirred for a further 30 minutes at 0 °C. Then, a single portion of 1 M HCl (aq) (50 mL) was added to the mixture whilst still in the ice bath, which raised the internal temperature of the mixture to RT. The mixture was diluted with EtOAc, washed with 1 M HCl (aq) (500 mL) three times, filtered and the filtrate was dried over $MgSO_4$. The filtrate was concentrated to an oil, which was then dissolved in a small amount of EtOAc, and then a large excess of petroleum ether was added with stirring. A white precipitate formed over 30 seconds, which was immediately collected by filtration and washed with a small quantity of petroleum ether to afford the product as a white powder (11.5 g, 95% purity, 57.1 mmol, 26% yield, contains 5% phthalide by NMR integration), TLC: R_f = 0.4 (EtOAc/hexanes, 1/1 *v*/*v* with 2% AcOH); ^{1}H NMR (500 MHz, $CDCl_3$) δ 8.14 (dd, J = 7.9, 1.4 Hz, 1H), 7.60 (td, J = 7.6, 1.4 Hz, 1H), 7.54 (dd, J = 7.9, 1.3 Hz, 1H), 7.42 (td, J = 7.6, 1.4 Hz, 1H), 5.59 (s, 2H), 2.17 (s, 3H); ^{13}C NMR (126 MHz, $CDCl_3$) δ 172.2, 170.8, 138.8, 133.4, 131.8, 128.1, 127.8, 127.3, 64.5, 20.9; HRMS (ESI+) calculated for $C_{10}H_{10}O_4Na$ $[M+Na]^+$ 217.0477 *m*/*z*, found 217.0487.

p-Tolyl 2-azido-3-*O*-(2-(acetoxymethyl) benzoyl)-4,6-*O*-benzylidene-2-deoxy-1-thio-β-D-glucopyranoside **(43)**

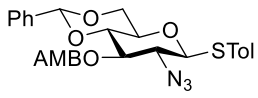

p-Tolyl 2-azido-4,6-*O*-benzylidene-2-deoxy-1-thio-β-D-glucopyranoside **16** (1.0 g, 2.5 mmol), AMB (0.6 g, 3 mmol, 1.2 equiv.), DCC (1.0 g, 4.8 mmol, 2 equiv.) and DMAP (7 mg, 0.06 mmol, 0.2 equiv.) were dissolved in anhydrous CH_2Cl_2 (10 mL) and stirred at RT. The R_f of the starting material and product proved to be nearly identical by TLC in all eluent systems, so after four hours, the reaction was presumed finished and the mixture was diluted with EtOAc. The mixture was then filtered through a Celite® pad, removing a large amount of solid DCU precipitate, the filtrate was evaporated to an oil.

The oil was then redissolved in toluene and left overnight to form any further DCU precipitate. The mixture was again filtered through a Celite® pad, evaporated to dryness, and the mixture recrystallized from EtOAc and petrol to yield the product as a white solid (1.05 g, 1.82 mmol, 73%); TLC: R_f = 0.6 (EtOAc/toluene, 1/4 *v*/*v*); mp 128 °C (from hexanes); $[\alpha]_D$ -88.4 (c 1 in $CDCl_3$); IR (ATR): ν_{max}/cm^{-1} 2111 (N_3, s), 1742 and 1717 (C=O, s); ^{1}H NMR (500 MHz, $CDCl_3$) δ 7.98 – 7.86 (m, 1H), 7.63 – 7.51 (m, 1H), 7.51 – 7.45 (m, 3H), 7.42 – 7.35 (m, 3H), 7.33 – 7.26 (m, 3H), 7.21 – 7.15 (m, 2H), 5.52 (s, 1H), 5.49 – 5.40 (m, 3H), 4.63 (d, J = 10.0 Hz, 1H), 4.41 (dd, J = 10.6, 5.0 Hz, 1H), 3.81 (t, J = 10.3 Hz, 1H), 3.69 (t, J = 9.5 Hz, 1H), 3.62 – 3.55 (m, 1H), 3.51 (t, J = 9.8 Hz, 1H), 2.38 (s, 3H), 2.00 (s, 3H); ^{13}C NMR (126 MHz, $CDCl_3$) δ 170.6, 165.4, 139.2, 137.7, 136.6, 134.3, 132.7, 130.6, 130.0, 129.1, 128.7, 128.3, 128.2, 127.9, 126.6, 126.1, 101.5, 87.2, 78.3, 73.6, 70.7, 68.4, 64.2, 63.6, 21.2, 20.7; HRMS (ESI+) calculated for $C_{30}H_{29}N_3O_7SNa$ $[M+Na]^+$ 598.1624 *m*/*z*, found 598.1633.

p-Tolyl 2-azido-3-*O*-(2-(acetoxymethyl) benzoyl)-2-deoxy-1-thio-β-D-glucopyranoside **(44)**

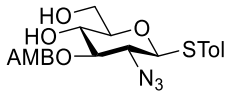

p-Tolyl 2-azido-3-*O*-(2-(acetoxymethyl) benzoyl)-4,6-*O*-benzylidene-2-deoxy-1-thio-β-D-glucopyranoside **43** (350 mg, 0.61 mmol) was dissolved in AcOH/H_2O (3:2, 5 mL) and heated to reflux. The reaction was stirred at this temperature for 1 hour until TLC analysis indicated completion. The reaction mixture was diluted with toluene and evaporated to dryness, and then the mixture was purified by column chromatography to yield the product as an off-white foam, (237 mg, 0.49 mmol, 80%); TLC: R_f = 0.4 (EtOAc/toluene, 1/4 *v*/*v*); ^{1}H NMR (500 MHz, $CDCl_3$) δ 7.89 (dd, J = 7.9, 1.4 Hz, 1H), 7.56 (td, J = 7.5, 1.4 Hz, 1H), 7.51 (dd, J = 7.8, 1.4 Hz, 1H), 7.50 – 7.44 (m, 2H), 7.40 (td, J = 7.6, 1.5 Hz, 1H), 7.19 – 7.14 (m, 2H), 5.57 (d, J = 13.5 Hz, 1H), 5.35 (d, J = 13.5 Hz, 1H), 5.18 (t, J = 9.5 Hz, 1H), 4.57 (d, J = 10.1 Hz, 1H), 3.99 – 3.91 (m, 1H), 3.87 – 3.79 (m, 1H), 3.74 (td, J = 9.4, 4.3 Hz, 1H), 3.54 (d, J = 4.7 Hz, 1H), 3.50 – 3.43 (m, 2H), 2.36 (s, 3H), 2.07 (s, 3H), 1.67 (s, 2H); ^{13}C NMR (126 MHz, $CDCl_3$) δ 171.1, 167.1, 139.1, 137.2, 134.1, 132.7, 130.2, 130.0, 129.4, 129.0, 128.1, 126.9, 86.4, 79.8, 78.2, 69.3, 64.2, 63.1, 62.3, 21.2, 20.9; HRMS (ESI+) calculated for $C_{23}H_{25}N_3O_7SNa$ $[M+Na]^+$ 510.1311 *m*/*z*, found 510.1308.

p-Tolyl 6-*O*-acetyl-2-azido-3-*O*(2-(acetoxymethyl) benzoyl)-2-deoxy-4-*O*-(9-fluorenylmethyloxycarbonyl)-1-thio-β-D-glucopyranoside **(47)**

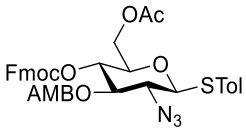

p-Tolyl 2-azido-3-*O*-(2-(acetoxymethyl) benzoyl)-2-deoxy-1-thio-β-D-glucopyranoside (17.5 g, 35.9 mmol) was dissolved in anhydrous CH_2Cl_2 (150 mL) under argon and cooled to -78 °C. To this mixture, pyridine (18 mL, 220 mmol, 6 equiv.) was added, and the mixture stirred briefly to ensure good mixing and consistent temperature. The mixture was then treated dropwise with acetyl chloride (2.5 mL, 35 mmol, 1 equiv.) through a dropping funnel, and stirred for a further 30 minutes after addition was complete. Following this, Fmoc-Cl solid (11.5 g, 43.6 mmol, 1.2 equiv.) was added and the reaction mixture was then stirred for a further hour, until TLC analysis indicated the reaction was complete. The reaction mixture was then washed with saturated $NaHCO_3$ (aq) and brine, dried over $MgSO_4$ and evaporated to dryness. The mixture was purified by column chromatography to yield the desired product as an off-white foam (19.9 g, 26.5 mmol, 74%); TLC: R_f = 0.65 (EtOAc/toluene, 1/4 *v*/*v*); $[\alpha]_D$ -74.7 (c 1 in $CDCl_3$); IR (ATR): ν_{max}/cm^{-1} 2110 (N_3, s), 1741 (C=O); ^{1}H NMR (500 MHz, $CDCl_3$) δ 7.89 (dd, J = 7.9, 1.4 Hz, 1H), 7.72 – 7.63 (m, 2H), 7.55 – 7.49 (m, 2H), 7.48 – 7.40 (m, 4H), 7.39 – 7.26 (m, 3H), 7.24 – 7.19 (m, 1H), 7.19 – 7.13 (m, 3H), 5.52 (d, J = 14.2 Hz, 1H), 5.46 – 5.31 (m, 2H), 4.94 (t, J = 9.8 Hz, 1H), 4.55 (d, J = 10.0 Hz, 1H), 4.32 – 4.19 (m, 4H), 4.01 (t, J = 7.4 Hz, 1H), 3.88 – 3.75 (m, 1H), 3.51 (t, J = 9.9 Hz, 1H), 2.38 (s, 3H), 2.10 (s, 3H), 2.07 (s, 3H); ^{13}C NMR (126 MHz, $CDCl_3$) δ 170.5, 165.0, 143.0, 141.1, 139.3, 138.6, 134.6, 133.0, 130.8, 129.9, 128.5, 127.9, 127.8, 127.2, 127.1, 125.0, 124.9, 119.9, 86.3, 75.6, 74.2, 72.1, 70.6, 64.2, 62.8, 62.0, 46.4, 21.2, 20.8, 20.7; HRMS (ESI+) calculated for $C_{40}H_{37}N_3O_{10}SNa$ $[M+Na]^+$ 774.2097 *m*/*z*, found 774.2097.

p-Tolyl 6-*O*-benzoyl-2-azido-3-*O*-(2-(acetoxymethyl) benzoyl)-2-deoxy-4-*O*-(9-fluorenylmethyloxycarbonyl)-1-thio-β-D-glucopyranoside **(48)**

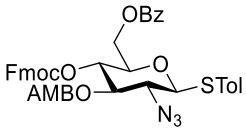

p-Tolyl 2-azido-3-*O*-(2-(acetoxymethyl) benzoyl)-2-deoxy-1-thio-β-D-glucopyranoside (50.0 g, 103 mmol) was dissolved in anhydrous CH_2Cl_2 (250 mL) under argon and cooled to -78 °C with stirring. To this mixture, pyridine (50 mL, 610 mmol, 6 equiv.) was added, and the mixture stirred briefly to ensure good mixing and consistent temperature. The mixture was then treated slowly and dropwise with benzoyl chloride (12.0 mL, 102 mmol, 1 equiv.) through a dropping funnel, and stirred for a further 30

minutes after addition was complete. Following this, Fmoc-Cl solid (32.0 g, 121 mmol, 1.2 equiv.) was added and stirred for a further hour, until TLC analysis indicated completion. The reaction mixture was then washed with saturated $NaHCO_3$ (aq), followed by brine, dried over $MgSO_4$ and evaporated to dryness. The mixture was recrystallized from EtOAc and petroleum ether to yield the desired product as an off-white foam (72.3 g, 88.8 mmol, 87%), TLC: R_f = 0.65 (EtOAc/toluene, 1/4 *v*/*v*); $[\alpha]_D$ -36.1 (c 1 in $CDCl_3$); IR (ATR): ν_{max}/cm^{-1} 2113 (N_3, s), 1749 and 1719 (C=O, s); ^1H NMR (500 MHz, $CDCl_3$) δ 8.17 – 8.01 (m, 2H), 7.89 (dd, J = 7.8, 1.3 Hz, 1H), 7.76 – 7.63 (m, 2H), 7.63 – 7.55 (m, 1H), 7.50 – 7.38 (m, 8H), 7.37 – 7.23 (m, 3H), 7.20 (td, J = 7.5, 1.2 Hz, 1H), 7.13 (td, J = 7.5, 1.1 Hz, 1H), 7.04 – 6.94 (m, 2H), 5.53 (d, J = 14.1 Hz, 1H), 5.45 (t, J = 9.7 Hz, 1H), 5.38 (d, J = 14.1 Hz, 1H), 5.03 (t, J = 9.8 Hz, 1H), 4.67 (dd, J = 12.3, 2.7 Hz, 1H), 4.58 (d, J = 10.0 Hz, 1H), 4.42 (dd, J = 12.3, 4.6 Hz, 1H), 4.23 (d, J = 7.4 Hz, 2H), 4.02 – 3.92 (m, 2H), 3.51 (t, J = 9.9 Hz, 1H), 2.30 (s, 3H), 2.06 (s, 3H); ^{13}C NMR (126 MHz, $CDCl_3$) δ 170.5, 165.9, 165.1, 154.1, 143.0, 142.9, 141.1, 139.2, 138.6, 134.8, 133.3, 133.0, 130.8, 129.9, 129.7, 128.6, 128.5, 127.8, 127.8, 127.2, 127.1, 127.1, 126.0, 125.0, 124.9, 120.0, 119.9, 86.1, 77.3, 77.0, 76.7, 75.6, 74.2, 72.3, 70.5, 64.2, 62.7, 62.3, 46.4, 21.2, 20.8; HRMS (ESI+) calculated for $C_{45}H_{39}N_3O_{10}SNa$ $[M+Na]^+$ 836.2254 *m*/*z*, found 836.2256.

p-Methoxyphenyl [6-*O*-acetyl-2-azido-3-*O*-(2-(acetoxymethyl) benzoyl)-2-deoxy-4-*O*-(9-fluorenylmethyloxycarbonyl)-α-D-glucopyranosyl (1→4)]-2-*O*-benzoyl-3-*O*-benzyl-6-*O*-chloroacetyl-1-*O*-β-L-idopyranoside **(6)**

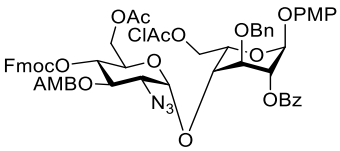

p-Tolyl 6-*O*-acetyl-2-azido-3-*O*-(2-(acetoxymethyl) benzoyl)-2-deoxy-4-*O*-(9-fluorenylmethyloxycarbonyl)-1-thio-β-D-glucopyranoside **47** (19.9 g, 26.5 mmol, 1.2 equiv.) and idose acceptor **49** (12.0 g, 21.5 mmol) were reacted according to General Procedure J to yield the title compound as an off-white foam (20.8 g, 17.6 mmol, 81%); TLC: R_f = 0.5 (EtOAc/toluene, 1/4 *v*/*v*); $[\alpha]_D$ -16.9 (c 1 in $CDCl_3$); IR (ATR): ν_{max}/cm^{-1} 2109 (N_3, s), 1726 (C=O); ^1H NMR (500 MHz, CDCl3) δ 8.14 – 8.09 (m, 2H), 7.83 (dd, J = 7.9, 1.4 Hz, 1H), 7.73 – 7.67 (m, 2H), 7.49 – 7.39 (m, 9H), 7.39 – 7.18 (m, 8H), 7.08 – 7.00 (m, 2H), 6.89 – 6.81 (m, 2H), 5.63 (dd, J = 10.6, 9.3 Hz, 1H), 5.60 (d, J = 2.1 Hz, 1H), 5.49 (d, J = 14.5 Hz, 1H), 5.43 (dd, J = 3.5, 2.2 Hz, 1H), 5.38 (d, J = 14.4 Hz, 1H), 5.02 – 4.90 (m, 3H), 4.78 (d, J = 11.4 Hz, 1H), 4.66 – 4.55 (m, 2H), 4.47 (dd, J = 10.7, 3.2 Hz, 1H), 4.31 (dd, J = 12.2, 4.9 Hz, 1H), 4.29 – 4.25 (m, 2H), 4.25 – 4.15 (m, 3H), 4.04 (t, J = 7.3 Hz, 1H), 3.98 – 3.87 (m, 3H), 3.78 (s, 3H), 3.51 (dd, J = 10.6, 3.7 Hz, 1H), 2.09 (s, 3H), 2.05 (s, 3H); ^{13}C NMR (126 MHz, CDCl3) δ 170.4, 170.4, 166.9, 165.8, 164.8, 155.3, 154.1, 150.2, 143.0, 142.9, 141.1, 141.1, 138.7, 137.4, 133.3, 133.1, 130.9, 129.8, 129.2,

128.5, 128.4, 128.1, 128.0, 127.9, 127.8, 127.6, 127.2, 127.1, 126.7, 125.0, 119.9, 119.9, 118.3, 114.5, 97.7, 77.3, 77.0, 76.8, 74.1, 73.2, 72.7, 72.5, 70.9, 70.6, 69.2, 68.4, 66.4, 64.7, 64.2, 61.9, 61.2, 55.6, 46.4, 40.5, 20.9, 20.6; HRMS (ESI+) calculated for $C_{62}H_{58}ClN_3O_{19}Na$ $[M+Na]^+$ 1206.3251 *m*/*z*, found 1206.3241.

6'-*O*-Bz protected disaccharide **(7)**

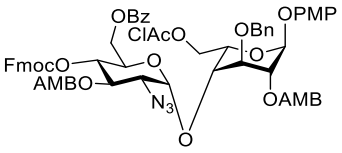

p-Tolyl 6-*O*-benzoyl-2-azido-3-*O*-(2-(acetoxymethyl) benzoyl)-2-deoxy-4-*O*-(9-fluorenylmethyloxycarbonyl)-1-thio-β-D-glucopyranoside **48** (10.0 g, 12.3 mmol, 1.2 equiv.) and acceptor **50** (6.3 g, 10 mmol) were reacted according to General Procedure J to yield the title compound as an off-yellow foam (10.9 g, 8.3 mmol, 83%); TLC: R_f = 0.5 (EtOAc/toluene, 1/4 *v*/*v*); $[\alpha]_D$ -1.9 (c 1 in $CDCl_3$); IR (ATR): ν_{max}/cm^{-1} 2109 (N_3, s), 1722 (C=O); ^{1}H NMR (500 MHz, $CDCl_3$) δ 8.11 (dd, J = 7.7, 1.5 Hz, 1H), 8.06 – 8.01 (m, 2H), 7.84 (dd, J = 7.8, 1.3 Hz, 1H), 7.69 (t, J = 7.0 Hz, 2H), 7.56 – 7.51 (m, 1H), 7.51 – 7.19 (m, 18H), 7.16 (td, J = 7.5, 1.1 Hz, 1H), 7.07 – 7.01 (m, 2H), 6.88 – 6.82 (m, 2H), 5.66 – 5.53 (m, 4H), 5.50 – 5.36 (m, 3H), 5.06 (t, J = 9.8 Hz, 1H), 4.97 – 4.91 (m, 2H), 4.76 (d, J = 11.6 Hz, 1H), 4.68 – 4.59 (m, 2H), 4.55 (dd, J = 12.3, 2.6 Hz, 1H), 4.48 (dd, J = 10.4, 3.1 Hz, 1H), 4.42 (dd, J = 12.3, 4.9 Hz, 1H), 4.38 – 4.31 (m, 1H), 4.29 – 4.21 (m, 2H), 4.15 (t, J = 3.6 Hz, 1H), 4.00 (t, J = 7.2 Hz, 1H), 3.96 (t, J = 3.2 Hz, 1H), 3.93 – 3.83 (m, 2H), 3.79 (s, 3H), 3.50 (dd, J = 10.6, 3.7 Hz, 1H), 2.10 (s, 3H), 2.08 (s, 3H); ^{13}C NMR (126 MHz, $CDCl_3$) δ 170.6, 170.4, 166.8, 165.9, 165.6, 164.7, 155.3, 154.2, 150.2, 143.0, 142.8, 141.1, 138.7, 138.3, 137.3, 133.2, 133.0, 132.9, 131.1, 130.9, 129.7, 129.5, 128.5, 128.4, 128.1, 128.0, 127.8, 127.6, 127.5, 127.1, 127.1, 126.7, 125.0, 124.9, 119.9, 119.9, 118.4, 114.6, 97.5, 97.3, 77.2, 73.7, 72.8, 72.7, 72.6, 70.9, 70.5, 68.9, 68.6, 66.1, 64.6, 64.1, 62.4, 61.3, 55.6, 46.5, 40.5, 20.9, 20.8; HRMS (ESI+) calculated for $C_{70}H_{64}ClN_3O_{21}Na$ $[M+Na]^+$ 1340.3619 *m*/*z*, found 1340.3627.

6'-*O*-Ac protected disaccharide hemiacetal **(51)**

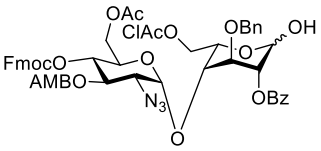

Disaccharide **6** (9.2 g, 7.8 mmol) was reacted according to General Procedure C to yield the title compound as a mixture of anomers, as a yellow foam (6.2 g, 5.7 mmol, 74%), TLC: R_f = 0.4 (EtOAc/toluene, 1/4 *v*/*v*); ^{1}H NMR (500 MHz, $CDCl_3$) δ 8.12 – 8.05 (m, 2H), 7.81 (d, J = 7.8 Hz, 1H), 7.71 (dd, J = 7.6, 5.2 Hz, 2H), 7.49 – 7.17 (m, 18H), 5.60 – 5.52 (m, 1H), 5.47 (d, J = 14.5 Hz, 1H), 5.37 (d, J =

14.5 Hz, 1.5H), 5.30 (d, J = 5.4 Hz, 0.5H), 5.14 (t, J = 3.9 Hz, 0.5H), 5.11 (dd, J = 5.4, 2.5 Hz, 0.5H), 5.00 (d, J = 3.7 Hz, 0.5H), 4.98 – 4.92 (m, 1.5H), 4.89 (dd, J = 11.3, 8.0 Hz, 1H), 4.78 (dd, J = 11.3, 2.7 Hz, 1H), 4.74 (dd, J = 11.7, 6.7 Hz, 0.5H), 4.63 (dd, J = 11.0, 6.7 Hz, 0.5H), 4.58 – 4.48 (m, 1.5H), 4.36 (t, J = 5.3 Hz, 0.5H), 4.34 – 4.13 (m, 7H), 4.10 – 3.99 (m, 1.5H), 3.93 – 3.82 (m, 1H), 3.70 (d, J = 8.4 Hz, 0.5H), 3.53 – 3.42 (m, 1H), 2.10 – 2.08 (m, 3H), 2.08 (s, 3H); ^{13}C NMR (126 MHz, $CDCl_3$) δ 170.5, 170.4, 167.3, 167.0, 166.2, 166.2, 164.8, 164.7, 154.1, 143.0, 142.8, 141.1, 141.1, 138.7, 137.1, 136.5, 133.4, 133.1, 130.9, 129.7, 129.7, 129.2, 129.2, 128.6, 128.5, 128.5, 128.4, 128.3, 128.2, 128.1, 128.0, 127.9, 127.8, 127.6, 127.2, 127.1, 126.6, 125.0, 125.0, 119.9, 119.9, 98.1, 98.1, 93.0, 91.9, 74.3, 74.0, 73.9, 73.8, 73.6, 73.5, 72.5, 72.4, 70.9, 70.8, 70.6, 70.0, 68.5, 68.4, 66.0, 65.8, 64.6, 64.2, 61.9, 61.8, 61.2, 61.1, 46.4, 40.8, 40.7, 29.7, 20.9, 20.7; HRMS (ESI+) calculated for $C_{55}H_{52}ClN_3O_{18}Na$ $[M+Na]^+$ 1100.2832 *m/z*, found 1100.2841.

6'-*O*-Bz protected disaccharide hemiacetal **(54)**

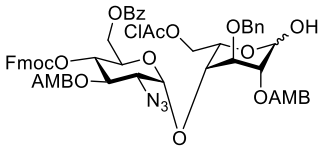

Disaccharide **7** (10.0 g, 7.6 mmol) was reacted according to General Procedure C to yield the title compound as a mixture of anomers, as a yellow foam (6.2 g, 5.1 mmol, 67%), TLC: R_f = 0.4 (EtOAc/toluene, 1/4 *v*/*v*); ^{1}H NMR (500 MHz, $CDCl_3$) δ 8.13 (dd, J = 7.8, 1.5 Hz, 0.6H), 8.09 – 8.01 (m, 2.4H), 7.81 (dd, J = 14.7, 7.8 Hz, 1H), 7.69 (t, J = 7.1 Hz, 2H), 7.58 – 7.52 (m, 1.6H), 7.50 (d, J = 7.7 Hz, 0.4H), 7.47 – 7.39 (m, 7H), 7.39 – 7.26 (m, 8H), 7.26 – 7.20 (m, 2H), 7.18 – 7.13 (m, 1H), 5.65 (s, 1H), 5.63 – 5.50 (m, 2H), 5.46 (d, J = 6.2 Hz, 0.4H), 5.43 (d, J = 6.2 Hz, 1H), 5.38 (d, J = 14.5 Hz, 1H), 5.32 – 5.25 (m, 1H), 5.14 – 5.09 (m, 1H), 5.09 – 5.01 (m, 1H), 4.89 (d, J = 3.8 Hz, 0.4H), 4.88 – 4.80 (m, 2H), 4.74 (d, J = 11.5 Hz, 1H), 4.71 – 4.64 (m, 1H), 4.61 – 4.45 (m, 3H), 4.44 – 4.37 (m, 1H), 4.36 – 4.30 (m, 2H), 4.29 – 4.21 (m, 3H), 4.21 – 4.08 (m, 2.4H), 3.99 (t, J = 7.2 Hz, 1H), 3.90 (t, J = 3.9 Hz, 0.4H), 3.77 (t, J = 3.6 Hz, 0.6H), 3.53 (dd, J = 10.6, 3.8 Hz, 0.6H), 3.49 (dd, J = 10.6, 3.8 Hz, 0.4H), 2.12 (s, 1H), 2.10 (s, 2H), 2.10 (s, 2H), 2.09 (s, 1H); ^{13}C NMR (126 MHz, $CDCl_3$) δ 170.7, 170.5, 167.3, 167.0, 166.4, 166.0, 165.9, 164.7, 154.1, 154.1, 143.0, 142.8, 141.1, 138.8, 138.7, 138.2, 137.3, 137.0, 136.4, 133.3, 133.1, 133.1, 133.0, 133.0, 131.5, 131.1, 131.0, 130.9, 129.7, 129.5, 128.6, 128.5, 128.5, 128.5, 128.4, 128.3, 128.2, 128.1, 127.9, 127.9, 127.9, 127.8, 127.8, 127.6, 127.5, 127.5, 127.2, 127.1, 126.6, 126.5, 125.0, 124.9, 124.9, 124.9, 119.9, 119.9, 97.6, 97.5, 92.8, 92.1, 73.8, 73.8, 73.5, 73.2, 72.9, 72.8, 72.6, 72.3, 71.0, 70.8, 70.5, 70.4, 69.4, 68.6, 68.6, 65.6, 65.5, 64.6, 64.5, 64.1, 64.1, 62.3, 62.2, 61.3, 61.2, 46.5, 46.4, 40.8, 40.7, 21.0, 21.0, 20.9; HRMS (ESI+) calculated for $C_{63}H_{58}ClN_3O_{20}Na$ $[M+Na]^+$ 1234.3200 *m/z*, found 1234.3204.

6'-*O*-Ac protected disaccharide TCA donor **(52)**

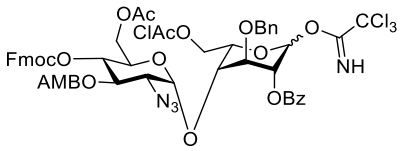

Hemiacetal **51** (1.0 g, 0.93 mmol) was reacted according to General Procedure D to yield the title compound as a mixture of anomers (α/β : 6/4), as a yellow foam (900 mg, 0.74 mmol, 79%). A sample of each anomer was isolated separately for characterisation.

α – TLC: R_f = 0.75 (EtOAc/toluene, 1/4 *v*/*v*); ^{1}H NMR (500 MHz, $CDCl_3$) δ 8.71 (s, 1H), 8.18 – 8.04 (m, 2H), 7.81 (dd, J = 7.9, 1.4 Hz, 1H), 7.71 (dd, J = 7.6, 4.4 Hz, 2H), 7.50 – 7.16 (m, 17H), 6.45 (s, 1H), 5.59 (dd, J = 10.6, 9.3 Hz, 1H), 5.47 (d, J = 14.5 Hz, 1H), 5.42 (t, J = 2.3 Hz, 1H), 5.37 (d, J = 14.5 Hz, 1H), 5.01 – 4.91 (m, 3H), 4.75 (d, J = 11.5 Hz, 1H), 4.72 – 4.68 (m, 1H), 4.62 (dd, J = 11.5, 7.5 Hz, 1H), 4.51 (dd, J = 11.5, 4.5 Hz, 1H), 4.33 – 4.21 (m, 5H), 4.19 (dd, J = 12.2, 2.3 Hz, 1H), 4.11 (d, J = 2.4 Hz, 2H), 4.05 (t, J = 7.3 Hz, 1H), 3.94 (t, J = 3.1 Hz, 1H), 3.53 (dd, J = 10.6, 3.7 Hz, 1H), 2.09 (s, 3H), 2.06 (s, 3H); ^{13}C NMR (126 MHz, $CDCl_3$) δ 170.5, 170.4, 166.9, 165.8, 164.7, 160.4, 154.2, 143.1, 142.9, 141.2, 141.1, 138.8, 137.1, 133.4, 133.1, 130.9, 129.8, 129.0, 128.6, 128.4, 128.0, 128.0, 127.9, 127.8, 127.6, 127.2, 127.1, 126.7, 125.1, 125.00, 120.0, 119.9, 97.8, 95.4, 90.9, 77.3, 77.0, 76.8, 73.9, 72.6, 72.5, 72.1, 71.0, 70.6, 68.6, 67.5, 67.1, 64.7, 64.2, 61.9, 61.3, 46.5, 40.6, 20.9, 20.7; HRMS (ESI+) calculated for $C_{57}H_{52}Cl_4N_4O_{18}Na$ $[M+Na]^+$ 1243.1928 *m*/*z*, found 1243.1921.

β – TLC: R_f = 0.65 (EtOAc/toluene, 1/4 *v*/*v*); ^{1}H NMR (500 MHz, $CDCl_3$) δ 8.56 (s, 1H), 8.02 – 7.95 (m, 2H), 7.91 (dd, J = 7.9, 1.4 Hz, 1H), 7.70 (t, J = 7.1 Hz, 2H), 7.56 – 7.50 (m, 1H), 7.51 – 7.14 (m, 16H), 6.64 (d, J = 3.5 Hz, 1H), 5.77 (dd, J = 10.8, 9.4 Hz, 1H), 5.55 – 5.50 (m, 2H), 5.43 (d, J = 14.2 Hz, 1H), 5.38 (dd, J = 9.1, 3.5 Hz, 1H), 5.09 – 5.00 (m, 1H), 4.94 – 4.82 (m, 2H), 4.79 – 4.70 (m, 2H), 4.55 (td, J = 6.6, 5.2 Hz, 1H), 4.47 (t, J = 9.1 Hz, 1H), 4.36 – 4.20 (m, 8H), 4.02 (t, J = 7.4 Hz, 1H), 3.42 (dd, J = 10.7, 3.6 Hz, 1H), 2.10 (s, 3H), 2.09 (s, 3H); ^{13}C NMR (126 MHz, $CDCl_3$) δ 170.5, 170.4, 167.1, 165.5, 165.2, 160.8, 154.1, 143.0, 142.8, 141.2, 141.1, 138.7, 137.1, 133.6, 133.1, 131.0, 129.8, 128.9, 128.5, 128.5, 128.4, 128.0, 127.9, 127.8, 127.7, 127.2, 127.1, 127.0, 125.0, 120.0, 119.9, 99.0, 94.6, 90.6, 77.3, 77.0, 76.8, 75.4, 75.4, 74.2, 73.6, 72.6, 72.4, 70.7, 70.1, 68.4, 66.4, 64.2, 62.0, 60.9, 46.4, 40.7, 20.9, 20.7; HRMS (ESI+) calculated for $C_{57}H_{52}Cl_4N_4O_{18}Na$ $[M+Na]^+$ 1243.1928 *m*/*z*, found 1243.1925.

6'-*O*-Bz protected disaccharide TCA donor **(55)**

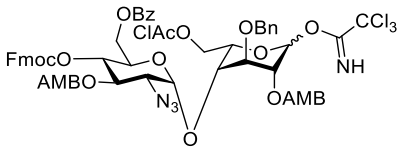

Hemiacetal **54** (820 mg, 0.68 mmol) was reacted according to General Procedure D to yield the title compound as a mixture of anomers (α/β : 6/4), as a yellow foam (700 mg, 0.52 mmol, 76%). A sample of each anomer was isolated separately for characterisation.

α - TLC: R_f = 0.75 (EtOAc/toluene, 1/4 *v*/*v*); ^{1}H NMR (500 MHz, $CDCl_3$) δ 8.71 (s, 1H), 8.13 (dd, J = 7.6, 1.7 Hz, 1H), 8.05 (dd, J = 8.3, 1.4 Hz, 2H), 7.82 (dd, J = 7.8, 1.4 Hz, 1H), 7.74 – 7.64 (m, 2H), 7.57 – 7.50 (m, 1H), 7.51 – 7.20 (m, 18H), 7.18 – 7.14 (m, 1H), 6.46 (s, 1H), 5.62 – 5.56 (m, 3H), 5.46 (d, J = 14.6 Hz, 1H), 5.41 (d, J = 2.4 Hz, 1H), 5.38 (d, J = 14.5 Hz, 1H), 5.07 (t, J = 9.7 Hz, 1H), 4.95 (d, J = 3.8 Hz, 1H), 4.90 (d, J = 11.7 Hz, 1H), 4.74 – 4.69 (m, 2H), 4.65 (dd, J = 11.4, 7.4 Hz, 1H), 4.56 (dd, J = 12.3, 2.5 Hz, 1H), 4.51 (dd, J = 11.4, 4.6 Hz, 1H), 4.42 (dd, J = 12.3, 4.6 Hz, 1H), 4.39 – 4.33 (m, 1H), 4.31 – 4.21 (m, 2H), 4.20 – 4.15 (m, 1H), 4.06 (s, 2H), 4.01 (t, J = 7.3 Hz, 1H), 3.96 (t, J = 3.0 Hz, 1H), 3.51 (dd, J = 10.6, 3.8 Hz, 1H), 2.13 (s, 3H), 2.09 (s, 3H); ^{13}C NMR (126 MHz, $CDCl_3$) δ 170.7, 170.4, 166.9, 165.9, 165.5, 164.7, 160.4, 154.2, 143.0, 142.9, 141.2, 138.8, 138.4, 137.0, 133.3, 133.1, 133.1, 131.3, 130.9, 129.8, 129.5, 128.6, 128.5, 128.4, 128.1, 128.0, 128.0, 128.0, 127.9, 127.8, 127.6, 127.3, 127.2, 127.1, 126.7, 125.0, 124.9, 120.0, 119.9, 97.5, 95.1, 90.9, 73.3, 72.7, 72.5, 71.6, 70.9, 70.5, 68.7, 67.3, 66.8, 64.7, 64.6, 64.1, 62.3, 61.3, 46.5, 40.6, 21.0, 20.9; HRMS (ESI+) calculated for $C_{65}H_{58}Cl_4N_4O_{20}Na$ $[M+Na]^+$ 1377.2296 *m*/*z*, found 1377.2294.

β - TLC: R_f = 0.65 (EtOAc/toluene, 1/4 *v*/*v*); ^{1}H NMR (500 MHz, $CDCl_3$) δ 8.61 (s, 1H), 8.10 – 8.02 (m, 2H), 7.96 – 7.83 (m, 2H), 7.73 – 7.63 (m, 2H), 7.61 – 7.55 (m, 1H), 7.53 – 7.39 (m, 8H), 7.37 – 7.13 (m, 11H), 6.62 (d, J = 3.2 Hz, 1H), 5.78 (dd, J = 10.7, 9.3 Hz, 1H), 5.59 (d, J = 14.8 Hz, 1H), 5.54 – 5.49 (m, 2H), 5.46 (d, J = 3.8 Hz, 1H), 5.43 (d, J = 14.2 Hz, 1H), 5.32 (dd, J = 8.7, 3.3 Hz, 1H), 5.12 (t, J = 9.3 Hz, 1H), 4.86 (s, 2H), 4.80 – 4.68 (m, 2H), 4.61 – 4.54 (m, 2H), 4.50 – 4.40 (m, 3H), 4.33 (d, J = 15.1 Hz, 1H), 4.30 – 4.21 (m, 4H), 3.99 (t, J = 7.3 Hz, 1H), 3.46 (dd, J = 10.7, 3.6 Hz, 1H), 2.13 (s, 3H), 2.08 (s, 3H); ^{13}C NMR (126 MHz, $CDCl_3$) δ 170.6, 170.5, 167.2, 166.0, 165.2, 165.0, 160.7, 154.2, 143.0, 142.8, 141.2, 141.1, 139.2, 138.7, 137.1, 133.4, 133.1, 133.1, 131.0, 130.8, 129.7, 129.5, 128.6, 128.5, 128.0, 127.9, 127.8, 127.7, 127.5, 127.2, 127.1, 127.0, 126.7, 125.0, 124.9, 120.0, 119.9, 98.7, 94.6, 90.6, 77.2, 75.2, 75.1, 73.9, 73.7, 73.0, 71.7, 70.6, 70.2, 68.5, 66.3, 64.3, 64.2, 62.6, 61.0, 46.5, 40.7, 20.9, 20.8; HRMS (ESI+) calculated for $C_{65}H_{58}Cl_4N_4O_{20}Na$ $[M+Na]^+$ 1377.2296 *m*/*z*, found 1377.2299.

6'-*O*-Ac protected disaccharide *N*-PTFA donor **(53)**

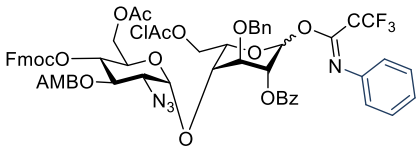

Hemiacetal **51** (1.4 g, 1.3 mmol) was reacted according to General Procedure E to yield the title compound as a yellow foam (1.2 g, 0.96 mmol, 74%); TLC: R_f = 0.75 (EtOAc/toluene, 1/4 *v*/*v*); ^{1}H NMR (500 MHz, $CDCl_3$) δ 8.14 – 8.01 (m, 2H), 7.90 (dd, J = 7.9, 1.3 Hz, 0.3H), 7.81 (dd, J = 7.9, 1.4 Hz, 0.7H), 7.73 – 7.65 (m, 2H), 7.58 – 7.53 (m, 0.3H), 7.49 – 7.14 (m, 19H), 7.12 – 7.01 (m, 1H), 6.85 (d, J = 7.9 Hz, 1.4H), 6.59 (s, 0.3H), 6.54 (d, J = 7.8 Hz, 0.6H), 6.38 (s, 1H), 5.78 – 5.68 (m, 0.3H), 5.57 (dd, J = 10.6, 9.3 Hz, 0.7H), 5.49 (dd, J = 27.5, 14.4 Hz, 1H), 5.44 – 5.33 (m, 2H), 5.04 (t, J = 9.7 Hz, 0.3H), 4.98 – 4.93 (m, 1.3H), 4.92 – 4.83 (m, 1.3H), 4.76 (d, J = 11.5 Hz, 1H), 4.75 – 4.66 (m, 0.3H), 4.66 – 4.57 (m, 1.4H), 4.54 – 4.47 (m, 1H), 4.44 (t, J = 8.0 Hz, 0.3H), 4.37 – 4.16 (m, 7H), 4.13 (s, 1.4H), 4.04 (dd, J = 8.6, 6.2 Hz, 1H), 3.90 (t, J = 2.8 Hz, 0.7H), 3.52 (dd, J = 10.6, 3.6 Hz, 0.7H), 3.46 (dd, J = 10.6, 3.7 Hz, 0.3H), 2.09 (s, 1H), 2.09 (s, 2H), 2.08 (s, 2H), 2.07 (s, 2H); ^{13}C NMR (126 MHz, $CDCl_3$) δ 170.5, 170.5, 170.4, 167.1, 166.9, 165.7, 165.6, 165.1, 164.7, 154.2, 143.3, 143.1, 143.0, 142.9, 142.9, 141.2, 141.2, 138.8, 138.7, 137.1, 133.7, 133.5, 133.1, 131.0, 130.9, 129.8, 129.0, 128.9, 128.8, 128.7, 128.7, 128.6, 128.5, 128.4, 128.1, 128.1, 128.0, 127.9, 127.9, 127.9, 127.8, 127.6, 127.2, 127.2, 127.1, 126.9, 126.7, 125.0, 124.7, 124.6, 124.4, 120.0, 119.9, 119.5, 119.2, 98.9, 97.8, 94.9, 93.1, 77.3, 75.1, 74.2, 73.8, 73.6, 72.8, 72.6, 72.5, 72.0, 71.0, 70.7, 70.7, 70.4, 68.7, 68.5, 67.5, 66.9, 65.3, 64.7, 64.3, 64.2, 62.0, 61.9, 61.3, 61.0, 46.5, 46.5, 40.7, 40.6, 20.9, 20.7, 20.7; HRMS (ESI+) calculated for $C_{63}H_{56}ClF_3N_4O_{18}Na$ $[M+Na]^+$ 1271.3128 *m*/*z*, found 1271.3130.

6'-*O*-Bz protected disaccharide *N*-PTFA donor **(56)**

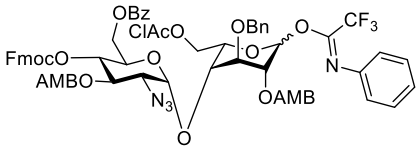

Hemiacetal **54** (10.0 g, 12.3 mmol, 1.2 equiv.) was reacted according to General Procedure E to yield the title compound as a yellow foam (10.9 g, 8.27 mmol, 83%), TLC: R_f = 0.75 (EtOAc/toluene, 1/4 *v*/*v*); ^{1}H NMR (500 MHz, $CDCl_3$) δ 8.13 – 7.98 (m, 3H), 7.89 (dd, J = 7.9, 1.3 Hz, 0.6H), 7.82 (dd, J = 7.9, 1.3 Hz, 0.4H), 7.69 (t, J = 7.3 Hz, 2H), 7.61 – 7.50 (m, 2.4H), 7.49 – 7.19 (m, 19H), 7.18 – 7.13 (m, 1H), 7.12 – 7.02 (m, 1H), 6.85 (d, J = 7.8 Hz, 1H), 6.61 (d, J = 7.7 Hz, 1H), 6.51 (s, 0.6H), 5.72 (t, J = 10.0 Hz, 0.6H), 5.61 – 5.48 (m, 3H), 5.48 – 5.34 (m, 2.4H), 5.30 – 5.26 (m, 0.6H), 5.15 – 5.02 (m, 1H), 4.93 – 4.88 (m, 1H), 4.84 (s, 1H), 4.79 – 4.61 (m, 2.4H), 4.58 (ddd, J = 12.4, 5.5, 2.5 Hz, 1H), 4.53 – 4.40 (m, 2.6H), 4.36

(dt, J = 13.1, 7.5 Hz, 1H), 4.30 – 4.23 (m, 2H), 4.22 (d, J = 1.6 Hz, 1H), 4.14 (dd, J = 13.9, 5.4 Hz, 1H), 4.09 (s, 1H), 4.00 (t, J = 7.3 Hz, 1H), 3.93 (d, J = 3.4 Hz, 0.4H), 3.54 – 3.45 (m, 1H), 2.10 – 2.06 (m, 6H); ^{13}C NMR (126 MHz, $CDCl_3$) δ 170.6, 170.5, 170.5, 170.4, 167.1, 166.8, 166.0, 165.9, 165.5, 165.3, 165.0, 164.7, 154.2, 143.0, 142.9, 142.8, 141.2, 141.1, 139.0, 138.8, 138.7, 138.4, 137.0, 133.4, 133.3, 133.2, 133.1, 131.2, 131.0, 130.9, 130.9, 129.8, 129.7, 129.5, 129.5, 128.8, 128.7, 128.6, 128.5, 128.3, 128.1, 128.0, 128.0, 127.9, 127.8, 127.7, 127.6, 127.2, 127.1, 126.9, 126.6, 125.0, 124.9, 124.4, 120.0, 119.9, 119.4, 119.2, 98.4, 97.4, 93.2, 74.7, 74.5, 73.7, 73.6, 73.2, 72.9, 72.7, 71.4, 70.9, 70.6, 70.5, 70.4, 68.7, 68.6, 67.3, 66.6, 65.2, 64.7, 64.5, 64.3, 64.2, 64.1, 62.5, 62.3, 61.4, 61.1, 46.5, 40.7, 40.5, 20.9, 20.9; HRMS (ESI+) calculated for $C_{71}H_{62}ClF_3N_4O_{20}Na$ [M+Na]+ 1405.3496 *m*/*z*, found 1405.3501.

Terminal disaccharide TCA donor **(57)**

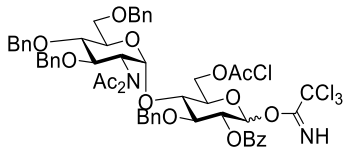

Hemiacetal **58** (1.4 g, 1.3 mmol) was reacted according to General Procedure D to yield the title compound as a mixture of anomers (α/β : 7/3), as a yellow foam (1.2 g, 0.96 mmol, 74%). A sample of each anomer was isolated separately for characterisation.

α - TLC: R_f = 0.75 ($MeCN/CH_2Cl_2$, 1/9 *v*/*v*); ^{1}H NMR (500 MHz, $CDCl_3$) δ 8.56 (s, 1H), 7.97 (dd, J = 8.3, 1.4 Hz, 2H), 7.59 – 7.49 (m, 1H), 7.40 (t, J = 7.8 Hz, 2H), 7.35 – 7.32 (m, 3H), 7.31 – 7.23 (m, 6H), 7.22 – 7.14 (m, 8H), 7.15 – 7.09 (m, 2H), 6.53 (d, J = 3.4 Hz, 1H), 5.74 (d, J = 4.5 Hz, 1H), 5.37 (dd, J = 9.8, 3.5 Hz, 1H), 4.81 (dd, J = 11.2, 1.5 Hz, 2H), 4.77 (d, J = 11.0 Hz, 1H), 4.72 (dd, J = 11.0, 8.4 Hz, 1H), 4.67 (d, J = 11.3 Hz, 1H), 4.62 – 4.56 (m, 5H), 4.54 (d, J = 12.0 Hz, 1H), 4.33 – 4.24 (m, 3H), 4.16 (dd, J = 10.1, 8.5 Hz, 1H), 4.12 – 4.06 (m, 1H), 4.01 (s, 2H), 3.79 – 3.61 (m, 4H), 2.20 (s, 6H); ^{13}C NMR (126 MHz, $CDCl_3$) δ 175.6, 166.9, 165.2, 160.2, 138.5, 137.8, 137.5, 137.1, 133.6, 129.7, 128.9, 128.6, 128.5, 128.5, 128.4, 128.0, 127.9, 127.8, 127.8, 127.7, 127.6, 127.5, 127.2, 97.8, 93.2, 90.8, 79.8, 79.4, 78.8, 77.3, 77.0, 76.8, 74.8, 73.9, 73.8, 73.6, 72.5, 72.1, 70.6, 70.5, 68.1, 64.1, 59.6, 40.6, 26.7; HRMS (ESI+) calculated for $C_{55}H_{56}Cl_4N_2O_{14}Na$ $[M+Na]^+$ 1131.2383 *m*/*z*, found 1131.2378.

β - TLC: R_f = 0.6 ($MeCN/CH_2Cl_2$, 1/9 *v*/*v*); ^{1}H NMR (500 MHz, $CDCl_3$) δ 8.61 (s, 1H), 7.99 (dd, J = 8.4, 1.4 Hz, 2H), 7.58 – 7.50 (m, 1H), 7.39 (t, J = 7.8 Hz, 2H), 7.35 – 7.12 (m, 20H), 6.03 (d, J = 6.1 Hz, 1H), 5.60 (t, J = 6.5 Hz, 1H), 5.52 (d, J = 4.3 Hz, 1H), 4.78 – 4.73 (m, 3H), 4.70 – 4.58 (m, 3H), 4.57 (d, J = 2.8 Hz, 1H), 4.55 (d, J = 2.7 Hz, 2H), 4.52 (d, J = 3.3 Hz, 1H), 4.36 (dd, J = 11.9, 4.9 Hz, 1H), 4.23 – 4.15 (m, 2H), 4.04 (d, J = 2.4 Hz, 2H), 4.01 – 3.96 (m, 1H), 3.90 (t, J = 7.2 Hz, 1H), 3.81 – 3.73 (m, 2H), 3.69 – 3.61 (m, 2H), 2.12 (s, 6H); ^{13}C NMR (126 MHz, $CDCl_3$) δ 175.3, 166.9, 164.8, 160.9, 138.5, 137.8, 137.5, 136.9,

133.5, 129.7, 129.1, 128.6, 128.5, 128.4, 128.3, 128.0, 127.9, 127.8, 127.8, 127.6, 127.6, 127.4, 97.9, 95.7, 90.4, 81.3, 79.5, 78.4, 77.3, 77.0, 76.7, 74.8, 73.9, 73.7, 72.7, 72.1, 72.0, 71.4, 70.7, 68.1, 64.4, 59.9, 40.7, 26.6; HRMS (ESI+) calculated for $C_{55}H_{56}Cl_4N_2O_{14}Na$ $[M+Na]^+$ 1131.2383 *m/z*, found 1131.2371.

Terminal disaccharide *N*-PTFA donor **(59)**

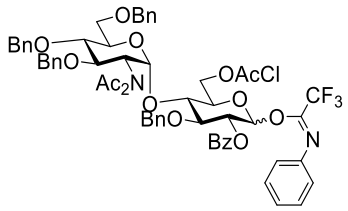

Hemiacetal **58** (270 mg, 0.28 mmol) was reacted according to General Procedure E to yield the title compound as a mixture of anomers, as a yellow foam (300 mg, 0.26 mmol, 94%); TLC: R_f = 0.7 (MeCN/CH_2Cl_2, 1/9 *v*/*v*); ^{1}H NMR (500 MHz, $CDCl_3$) δ 8.05 – 7.98 (m, 2.3H), 7.63 – 7.54 (m, 1.3H), 7.49 – 7.38 (m, 2.5H), 7.37 – 7.06 (m, 23.7H), 7.02 (q, J = 8.0, 7.3 Hz, 0.15H), 6.72 (d, J = 7.8 Hz, 2.0H), 6.41 (s, 0.2H), 6.02 (s, 0.9H), 5.72 (d, J = 4.4 Hz, 0.15H), 5.56 (t, J = 6.6 Hz, 1.0H), 5.51 (d, J = 4.2 Hz, 1.0H), 5.35 (d, J = 9.6 Hz, 0.15H), 4.86 – 4.80 (m, 0.3H), 4.79 – 4.71 (m, 3.15H), 4.70 – 4.51 (m, 7.6H), 4.33 (dd, J = 12.0, 4.9 Hz, 1H), 4.29 – 4.22 (m, 0.2H), 4.21 – 4.13 (m, 2.0H), 4.02 (s, 0.3H), 4.01 (s, 1.8H), 3.88 (t, J = 7.3 Hz, 1.5H), 3.80 – 3.70 (m, 2.0H), 3.68 – 3.62 (m, 2.3H), 2.21 (s, 0.8H), 2.12 (s, 5.7H); ^{13}C NMR (126 MHz, $CDCl_3$) δ 175.3, 166.9, 164.8, 143.1, 138.5, 137.8, 137.6, 136.9, 133.7, 129.8, 129.4, 129.0, 128.8, 128.7, 128.6, 128.5, 128.3, 128.0, 127.9, 127.9, 127.8, 127.6, 127.6, 127.5, 127.5, 127.2, 124.5, 120.4, 119.2, 97.8, 94.5, 81.6, 79.5, 78.9, 78.5, 74.9, 74.0, 73.9, 73.8, 73.8, 73.7, 72.9, 72.3, 72.2, 72.1, 71.2, 71.1, 70.8, 68.2, 64.3, 59.9, 59.9, 40.6, 26.6; HRMS (ESI+) calculated for $C_{61}H_{60}ClF_3N_2O_{14}Na$ $[M+Na]^+$ 1159.3583 *m/z*, found 1159.3582.

General Procedure K: Benzylidene selective opening to 6-*O*-Bn protection

The 4,6-benzylidene protected monosaccharide starting material was dissolved in anhydrous CH_2Cl_2 (10 mL/g) under argon and cooled to 0 °C in an ice bath. The reaction mixture was then treated with triethylsilane (5 equiv.), stirred briefly to ensure good mixing and consistent temperature, and then treated with triflic acid (5 equiv.) dropwise. The mixture was stirred for a further 30 minutes in the ice bath, and then allowed to warm to RT. The reaction mixture was then diluted with CH_2Cl_2 and washed with saturated $NaHCO_3$ (aq), followed by brine, dried over $MgSO_4$ and evaporated to dryness. The mixture was purified by column chromatography to give the desired product.

p-Tolyl 2-azido-3,6-*O*-benzyl-2-deoxy-1-thio-β-D-glucopyranoside **(63)**

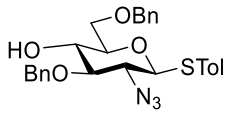

p-Tolyl 2-azido-3-*O*-benzyl-4,6-*O*-benzylidene-2-deoxy-1-thio-β-D-glucopyranoside **17** (1.0 g, 2.0 mmol) was reacted according to General Procedure K to yield the desired product as a yellow oil (700 mg, 1.4 mmol, 70%), TLC: R_f = 0.45 (EtOAc/toluene, 1/4 *v*/*v*); ^{1}H NMR (500 MHz, $CDCl_3$) δ 7.48 – 7.44 (m, 2H), 7.39 – 7.27 (m, 10H), 7.09 – 7.05 (m, 2H), 4.88 (d, J = 11.1 Hz, 1H), 4.81 (d, J = 11.0 Hz, 1H), 4.56 (q, J = 11.9 Hz, 2H), 4.36 (d, J = 10.0 Hz, 1H), 3.80 – 3.70 (m, 2H), 3.60 (td, J = 9.2, 2.4 Hz, 1H), 3.42 (dt, J = 9.4, 4.6 Hz, 1H), 3.35 (t, J = 9.0 Hz, 1H), 3.27 (t, 1H), 2.76 – 2.60 (m, 1H), 2.31 (s, 3H); ^{13}C NMR (126 MHz, $CDCl_3$) δ 138.7, 137.8, 137.7, 134.2, 129.8, 128.6, 128.5, 128.2, 128.1, 127.8, 127.7, 127.1, 86.2, 84.6, 77.9, 77.3, 77.0, 76.8, 75.5, 73.8, 72.0, 70.3, 64.4, 21.2; HRMS (ESI+) calculated for $C_{27}H_{29}N_3O_4SNa$ $[M+Na]^+$ 514.1776 *m*/*z*, found 514.1780.

p-Tolyl 3-*O*-(acetoxy-2-methylbenzoate)-2-azido-6-*O*-benzyl-2-deoxy-1-thio-β-D-glucopyranoside **(65)**

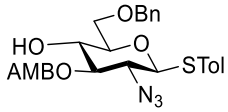

p-Tolyl 3-*O*-(acetoxy-2-methylbenzoate)-2-azido-4,6-*O*-benzylidene-2-deoxy-1-thio-β-D-glucopyranoside **43** (1.0 g, 1.7 mmol) was reacted according to General Procedure K to yield the desired product as a yellow oil (900 mg, 1.6 mmol, 90%), TLC: R_f = 0.45 (EtOAc/toluene, 1/4 *v*/*v*); ^{1}H NMR (500 MHz, $CDCl_3$) δ 7.91 (dd, J = 7.7, 1.4 Hz, 1H), 7.54 (td, J = 7.5, 1.4 Hz, 1H), 7.52 – 7.47 (m, 3H), 7.39 (td, J = 7.6, 1.5 Hz, 1H), 7.36 – 7.32 (m, 4H), 7.32 – 7.27 (m, 1H), 7.10 (d, J = 7.8 Hz, 2H), 5.55 (d, J = 13.6 Hz, 1H), 5.39 (d, J = 13.6 Hz, 1H), 5.19 (t, J = 9.5 Hz, 1H), 4.64 – 4.56 (m, 2H), 4.53 (d, J = 10.1 Hz, 1H), 3.84 – 3.80 (m, 2H), 3.76 (td, J = 9.5, 3.7 Hz, 1H), 3.62 – 3.53 (m, 1H), 3.45 (t, J = 9.9 Hz, 1H), 3.35 (d, J = 4.0 Hz, 1H), 2.34 (s, 3H), 2.06 (s, 3H); ^{13}C NMR (126 MHz, $CDCl_3$) δ 170.9, 166.8, 138.8, 137.9, 137.4, 134.1, 132.7, 130.4, 129.8, 129.2, 128.8, 128.4, 128.1, 127.7, 127.6, 127.1, 86.4, 78.8, 77.9, 77.3, 77.0, 76.8, 73.6, 69.9, 69.7, 64.3, 62.9, 21.2, 20.9; HRMS (ESI+) calculated for $C_{30}H_{31}N_3O_7SNa$ $[M+Na]^+$ 600.1780 *m*/*z*, found 600.1778.

p-Tolyl 2-azido-3,6-*O*-benzyl-2-deoxy-4-*O*-(9-fluorenylmethyloxycarbonyl)-1-thio-β-D-glucopyranoside **(64)**

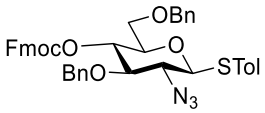

p-Tolyl 2-azido-3,6-*O*-benzyl-2-deoxy-1-thio-β-D-glucopyranoside **63** (700 mg, 1.4 mmol) was reacted according to General Procedure A to yield the desired product as a yellow oil (700 mg, 0.98 mmol, 69%), TLC: R_f = 0.7 (EtOAc/toluene, 1/4 *v*/*v*); ^{1}H NMR (500 MHz, $CDCl_3$) δ 7.74 (d, J = 7.6 Hz, 2H), 7.56 (d, J = 7.5 Hz, 1H), 7.51 (d, J = 7.5 Hz, 1H), 7.48 – 7.44 (m, 2H), 7.41 – 7.35 (m, 2H), 7.34 – 7.27 (m, 4H), 7.27 – 7.20 (m, 8H), 7.06 (d, J = 7.9 Hz, 2H), 4.81 – 4.73 (m, 2H), 4.65 (d, J = 10.9 Hz, 1H), 4.52 (d, J = 3.0 Hz, 2H), 4.37 (d, J = 10.2 Hz, 1H), 4.35 – 4.31 (m, 1H), 4.28 (dd, J = 10.5, 7.3 Hz, 1H), 4.11 (t, J = 7.1 Hz, 1H), 3.67 – 3.59 (m, 3H), 3.54 (t, J = 9.4 Hz, 1H), 3.33 (t, J = 9.8 Hz, 1H), 2.32 (s, 3H); ^{13}C NMR (126 MHz, $CDCl_3$) δ 154.2, 143.2, 143.0, 141.3, 141.2, 138.9, 137.9, 137.2, 134.3, 129.8, 128.3, 128.3, 128.0, 127.9, 127.9, 127.6, 127.5, 127.1, 126.6, 125.0, 124.9, 120.1, 85.9, 82.4, 75.5, 75.1, 73.5, 70.1, 69.3, 64.4, 46.6, 21.1; HRMS (ESI+) calculated for $C_{42}H_{39}N_3O_6SNa$ $[M+Na]^+$ 736.2457 *m*/*z*, found 736.2452.

p-Tolyl 3-*O*-(acetoxy-2-methylbenzoate)-2-azido-6-*O*-benzyl-2-deoxy-4-*O*-(9-fluorenylmethyloxycarbonyl)-1-thio-β-D-glucopyranoside **(66)**

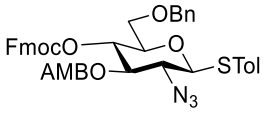

p-Tolyl 3-*O*-(acetoxy-2-methylbenzoate)-2-azido-6-*O*-benzyl-2-deoxy-1-thio-β-D-glucopyranoside **65** (900 mg, 1.6 mmol) was reacted according to General Procedure A to yield the desired product as a yellow foam (1.0 g, 1.3 mmol, 80%), TLC: R_f = 0.7 (EtOAc/toluene, 1/4 *v*/*v*); $[\alpha]_D$ -35.8 (c 1 in $CDCl_3$); IR (ATR): ν_{max}/cm^{-1} 2109 (N_3, s), 1744 and 1730 (C=O); ^{1}H NMR (500 MHz, $CDCl_3$) δ 7.91 (dd, J = 7.9, 1.4 Hz, 1H), 7.72 – 7.64 (m, 2H), 7.53 – 7.49 (m, 2H), 7.49 – 7.39 (m, 4H), 7.37 – 7.26 (m, 8H), 7.23 – 7.19 (m, 1H), 7.18 – 7.13 (m, 1H), 7.12 – 7.07 (m, 2H), 5.53 (d, J = 14.1 Hz, 1H), 5.45 – 5.32 (m, 2H), 5.01 (t, J = 9.8 Hz, 1H), 4.61 – 4.48 (m, 3H), 4.24 (dd, J = 10.4, 7.3 Hz, 1H), 4.14 (dd, J = 10.4, 7.7 Hz, 1H), 3.97 (t, J = 7.4 Hz, 1H), 3.82 – 3.76 (m, 1H), 3.73 – 3.62 (m, 2H), 3.52 (t, J = 9.9 Hz, 1H), 2.35 (s, 3H), 2.06 (s, 3H); ^{13}C NMR (126 MHz, $CDCl_3$) δ 170.5, 165.2, 154.1, 143.1, 142.9, 141.1, 139.1, 138.5, 137.8, 134.3, 132.9, 130.8, 129.9, 128.5, 128.3, 127.85, 127.8, 127.7, 127.6, 127.3, 127.1, 126.6, 125.0, 124.9, 119.9, 119.9, 86.4, 77.3, 74.5, 73.6, 72.7, 70.4, 68.7, 64.2, 62.9, 46.4, 21.2, 20.8; HRMS (ESI+) calculated for $C_{45}H_{41}N_3O_9SNa$ $[M+Na]^+$ 822.2461 *m*/*z*, found 822.2457.

Starting disaccharide acceptor **(70)**

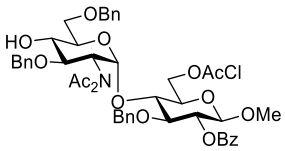

Disaccharide **8** (2.0 g, 1.8 mmol) was reacted according to General Procedure B to yield the product **70** as a foam, (1.2 g, 1.3 mmol, 75%), TLC: R_f = 0.4 (EtOAc/toluene, 1/4 *v*/*v*); ^{1}H NMR (500 MHz, $CDCl_3$) δ 8.10 – 7.94 (m, 2H), 7.59 – 7.54 (m, 1H), 7.44 (t, J = 7.7 Hz, 2H), 7.38 – 7.29 (m, 7H), 7.28 – 7.22 (m, 3H), 7.22 – 7.14 (m, 3H), 7.13 – 7.09 (m, 2H), 5.58 (d, J = 4.1 Hz, 1H), 5.31 (dd, J = 8.7, 7.3 Hz, 1H), 4.78 (d, J = 11.7 Hz, 1H), 4.69 – 4.46 (m, 8H), 4.32 (dd, J = 11.8, 4.7 Hz, 1H), 4.19 (dd, J = 11.0, 4.1 Hz, 1H), 4.11 – 4.04 (m, 3H), 3.85 (t, J = 8.6 Hz, 1H), 3.77 – 3.62 (m, 5H), 3.44 (s, 3H), 2.58 (d, J = 2.6 Hz, 1H), 2.17 (s, 6H); ^{13}C NMR (126 MHz, $CDCl_3$) δ 175.4, 167.0, 165.0, 138.6, 137.4, 137.0, 133.3, 129.8, 129.5, 128.5, 128.5, 128.4, 128.2, 128.0, 127.8, 127.8, 127.7, 127.6, 127.5, 101.6, 97.4, 82.7, 77.9, 73.9, 73.6, 73.3, 72.9, 72.3, 72.1, 71.2, 70.8, 69.9, 64.5, 59.0, 56.8, 40.7, 26.6; HRMS (ESI+) calculated for $C_{47}H_{52}ClNO_{14}Na$ [M+Na]+ 912.2974 *m*/*z*, found 912.2976.

Tetrasaccharide **(71)**

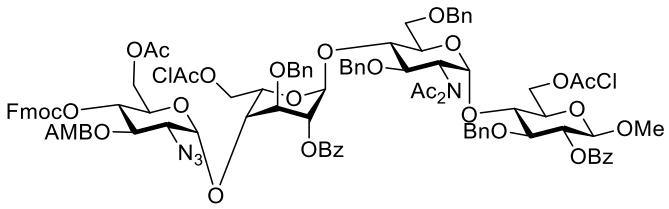

Donor **52** (5.9 g, 4.8 mmol, 1.3 equiv.) and acceptor **70** (3.2 g, 3.6 mmol) was reacted according to General Procedure H to yield **71** as a foam (6.7 g, 3.5 mmol, 96%), TLC: R_f = 0.6 (EtOAc/toluene, 1/4 *v*/*v*); $[\alpha]_D$ 77.4 (c 1 in $CDCl_3$); IR (ATR): ν_{max}/cm^{-1} 2109 (N_3, s), 1727 (C=O); ^{1}H NMR (500 MHz, $CDCl_3$) δ 8.05 – 7.99 (m, 4H), 7.87 (dd, J = 7.8, 1.3 Hz, 1H), 7.73 – 7.65 (m, 2H), 7.60 – 7.53 (m, 1H), 7.53 – 7.38 (m, 10H), 7.39 – 7.16 (m, 20H), 7.12 (ddd, J = 9.7, 7.9, 1.7 Hz, 4H), 5.66 (dd, J = 10.6, 9.3 Hz, 1H), 5.60 (d, J = 4.5 Hz, 1H), 5.50 (d, J = 14.4 Hz, 1H), 5.40 (d, J = 14.4 Hz, 1H), 5.32 – 5.23 (m, 2H), 5.18 (d, J = 4.0 Hz, 1H), 5.11 (d, J = 3.7 Hz, 1H), 5.00 (t, J = 9.8 Hz, 1H), 4.89 (d, J = 11.4 Hz, 1H), 4.81 (d, J = 11.0 Hz, 1H), 4.72 (d, J = 11.0 Hz, 1H), 4.68 – 4.49 (m, 6H), 4.50 – 4.44 (m, 2H), 4.45 – 4.31 (m, 3H), 4.33 – 4.23 (m, 4H), 4.19 (dd, J = 11.8, 4.5 Hz, 1H), 4.17 – 4.09 (m, 3H), 4.08 – 3.93 (m, 5H), 3.94 – 3.85 (m, 3H), 3.82 (t, J = 8.6 Hz, 1H), 3.73 (dd, J = 11.0, 3.3 Hz, 1H), 3.66 (dt, J = 10.0, 2.6 Hz, 1H), 3.58 (tt, J = 7.5, 3.3 Hz, 2H), 3.42 (s, 4H), 2.14 (s, 6H), 2.08 (s, 3H), 2.01 (s, 3H); ^{13}C NMR (126 MHz, $CDCl_3$) δ 175.4, 170.4, 170.4, 166.8, 166.7, 165.5, 165.1, 165.0, 154.1, 143.0, 142.9, 141.2, 141.1, 138.7, 138.7, 137.6, 137.1, 137.0, 133.5, 133.3, 133.1, 131.0, 129.8, 129.7, 129.5, 129.2, 128.6, 128.5, 128.4, 128.3, 128.1, 127.9,

127.8, 127.7, 127.5, 127.4, 127.3, 127.2, 127.1, 126.9, 125.0, 119.9, 119.9, 101.6, 98.2, 97.3, 97.3, 82.8, 77.3, 77.0, 76.8, 76.1, 75.2, 74.4, 73.7, 73.7, 73.4, 73.0, 72.4, 72.3, 72.3, 71.9, 70.9, 70.6, 68.3, 67.9, 67.4, 64.2, 64.0, 61.7, 61.1, 59.6, 56.7, 46.4, 40.7, 40.5, 29.7, 26.7, 20.8, 20.6; HRMS (ESI+) calculated for $C_{102}H_{102}Cl_2N_4O_{31}Na$ $[M+Na]^+$ 1971.5803 *m*/*z*, found 1971.5790.

Tetrasaccharide acceptor **(72)**

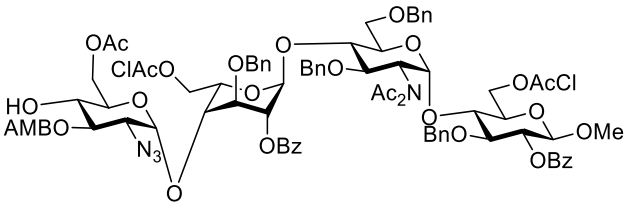

Tetrasaccharide **71** (5.9 g, 3.0 mmol) was reacted according to General procedure B to yield tetrasaccharide acceptor **72** as an off-white foam (3.7 g, 2.1 mmol, 71%), TLC: R_f = 0.4 (EtOAc/toluene, 1/4 *v*/*v*); $[\alpha]_D$ 96.3 (c 1 in $CDCl_3$); IR (ATR): ν_{max}/cm^{-1} 2108 (N_3, s), 1724 (C=O); ^1H NMR (500 MHz, $CDCl_3$) δ 8.04 – 7.98 (m, 4H), 7.83 (dd, J = 7.9, 1.4 Hz, 1H), 7.59 – 7.53 (m, 2H), 7.52 – 7.49 (m, 1H), 7.49 – 7.41 (m, 3H), 7.41 – 7.36 (m, 3H), 7.32 – 7.22 (m, 14H), 7.21 – 7.16 (m, 2H), 7.14 – 7.08 (m, 4H), 5.61 – 5.53 (m, 2H), 5.47 – 5.35 (m, 2H), 5.28 (dd, J = 8.8, 7.4 Hz, 1H), 5.23 (dd, J = 5.2, 4.0 Hz, 1H), 5.17 (d, J = 4.0 Hz, 1H), 5.05 (d, J = 3.7 Hz, 1H), 4.89 (d, J = 11.4 Hz, 1H), 4.80 (d, J = 11.0 Hz, 1H), 4.73 (d, J = 11.1 Hz, 1H), 4.67 – 4.45 (m, 8H), 4.43 – 4.38 (m, 2H), 4.35 (d, J = 5.8 Hz, 2H), 4.29 – 4.23 (m, 2H), 4.19 (dd, J = 11.8, 4.5 Hz, 1H), 4.08 (t, J = 5.4 Hz, 1H), 4.04 – 3.85 (m, 8H), 3.82 (t, J = 8.6 Hz, 1H), 3.72 (dd, J = 10.9, 3.3 Hz, 1H), 3.69 – 3.55 (m, 4H), 3.49 (d, J = 4.9 Hz, 1H), 3.41 (s, 3H), 3.35 (dd, J = 10.7, 3.7 Hz, 1H), 2.13 (s, 6H), 2.09 (s, 3H), 2.02 (s, 3H); ^{13}C NMR (126 MHz, $CDCl_3$) δ 175.4, 171.2, 171.0, 166.9, 166.8, 166.7, 165.5, 165.0, 138.7, 137.5, 137.4, 137.1, 137.0, 133.4, 133.3, 132.7, 130.4, 129.8, 129.6, 129.5, 129.35, 129.3, 128.7, 128.6, 128.55, 128.5, 128.4, 128.3, 128.2, 128.05, 128.0, 127.95, 127.9, 127.8, 127.5, 127.4, 127.3, 101.6, 98.3, 97.3, 82.7, 76.1, 75.0, 74.1, 73.8, 73.7, 73.6, 73.5, 72.9, 72.3, 72.3, 71.9, 71.1, 71.0, 70.9, 69.2, 67.9, 67.5, 64.3, 64.2, 64.0, 62.8, 61.2, 59.6, 56.7, 40.7, 40.6, 26.7, 20.9, 20.7; HRMS (ESI+) calculated for $C_{87}H_{92}Cl_2N_4O_{29}Na$ $[M+Na]^+$ 1749.5122 *m*/*z*, found 1749.5177.

Hexasaccharide (73)

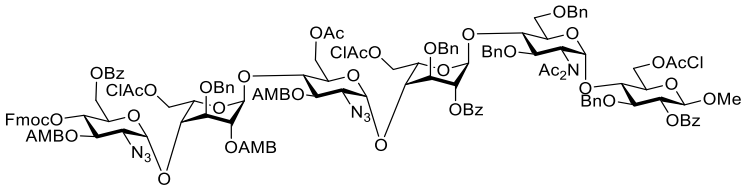

Disaccharide donor **56** (500 mg, 0.36 mmol, 1.4 equiv.) and tetrasaccharide acceptor **72** (450 mg, 0.26 mmol) was reacted according to General Procedure I to yield **73** as a foam (490 mg, 0.17 mmol, 64%). Additionally, the by-product glycal **78** was isolated as a foam (180 mg).

Data for hexasaccharide (73)

TLC: R_f = 0.55 ($MeCN/CH_2Cl_2$, 1/9 *v*/*v*); $[\alpha]_D$ 55.9 (c 1 in $CDCl_3$); IR (ATR): ν_{max}/cm^{-1} 2108 (N_3, s), 1724 (C=O); ^1H NMR (500 MHz, $CDCl_3$) δ 8.08 – 7.94 (m, 9H), 7.90 – 7.84 (m, 1H), 7.69 (t, J = 6.7 Hz, 3H), 7.61 – 7.06 (m, 49H), 5.64 – 5.33 (m, 9H), 5.30 – 5.21 (m, 2H), 5.18 – 5.07 (m, 5H), 5.02 (d, J = 4.9 Hz, 1H), 4.87 (d, J = 11.5 Hz, 1H), 4.77 – 4.37 (m, 14H), 4.36 – 4.10 (m, 12H), 4.10 – 3.78 (m, 13H), 3.69 (dd, J = 11.0, 3.3 Hz, 1H), 3.65 – 3.59 (m, 1H), 3.59 – 3.50 (m, 2H), 3.41 (s, 3H), 3.36 (dd, J = 10.7, 3.7 Hz, 1H), 2.13 (s, 6H), 2.12 (s, 7H), 2.08 (s, 2H), 2.06 (s, 3H), 2.00 (s, 3H); ^{13}C NMR (126 MHz, $CDCl_3$) δ 175.3, 170.6, 170.5, 166.9, 166.7, 165.9, 165.4, 165.0, 164.8, 154.1, 142.9, 142.8, 141.1, 139.1, 138.9, 138.7, 138.6, 137.5, 137.1, 136.9, 133.3, 133.1, 131.0, 130.6, 129.8, 129.7, 129.5, 129.1, 128.6, 128.5, 128.5, 128.4, 128.4, 128.2, 128.1, 128.0, 128.0, 127.9, 127.8, 127.7, 127.6, 127.5, 127.3, 127.2, 127.1, 126.8, 124.9, 124.8, 119.9, 119.9, 101.5, 98.6, 97.8, 97.3, 97.1, 82.8, 77.2, 76.3, 75.5, 73.9, 73.7, 73.7, 73.5, 73.4, 73.3, 73.0, 72.5, 72.3, 72.3, 71.8, 71.5, 70.9, 70.4, 69.6, 68.8, 68.1, 67.8, 67.7, 64.2, 64.2, 63.7, 63.0, 62.0, 61.6, 61.1, 61.0, 59.5, 56.7, 46.4, 40.8, 40.7, 40.5, 26.6, 20.9, 20.9, 20.8, 20.6; HRMS (ESI+) calculated for $C_{150}H_{148}Cl_3N_7O_{48}Na$ $[M+Na]^+$ 2942.8319 *m*/*z*, found 2942.8325.

Data for glycal by-product (78)

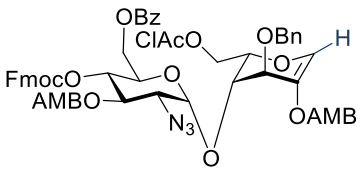

TLC: R_f = 0.75 ($MeCN/CH_2Cl_2$, 1/9 *v*/*v*); ^1H NMR (500 MHz, $CDCl_3$) δ 8.11 – 8.06 (m, 2H), 7.99 (dd, J = 7.9, 1.4 Hz, 1H), 7.94 (dd, J = 7.9, 1.4 Hz, 1H), 7.72 – 7.66 (m, 2H), 7.60 – 7.53 (m, 2H), 7.52 – 7.18 (m, 15H), 7.19 – 7.12 (m, 3H), 6.85 (s, 1H), 5.83 (dd, J = 10.8, 9.3 Hz, 1H), 5.53 (d, J = 14.0 Hz, 1H), 5.48 (d, J = 14.4 Hz, 1H), 5.42 (dd, J = 14.2, 3.5 Hz, 2H), 5.30 (d, J = 3.8 Hz, 1H), 5.16 (dd, J = 10.2, 9.3 Hz, 1H), 4.66 (dd, J = 6.2, 2.2 Hz, 2H), 4.60 (dd, J = 12.3, 2.8 Hz, 1H), 4.56 (s, 2H), 4.49 (dd, J = 12.3, 4.9 Hz, 1H),

4.41 (d, J = 2.6 Hz, 1H), 4.40 – 4.33 (m, 2H), 4.28 (d, J = 7.3 Hz, 2H), 4.14 (s, 2H), 4.13 (dd, J = 2.6, 1.5 Hz, 1H), 4.02 (t, J = 7.3 Hz, 1H), 3.45 (dd, J = 10.8, 3.6 Hz, 1H), 2.10 (s, 3H), 2.06 (s, 3H); ^{13}C NMR (126 MHz, $CDCl_3$) δ 170.5, 170.4, 166.9, 165.9, 165.2, 165.0, 154.2, 143.0, 142.9, 141.1, 140.0, 138.8, 138.4, 137.2, 133.3, 133.0, 132.9, 131.3, 131.0, 129.7, 129.5, 128.6, 128.5, 128.5, 128.2, 128.0, 127.9, 127.8, 127.8, 127.7, 127.3, 127.2, 127.1, 125.0, 124.9, 119.9, 119.8, 95.8, 73.0, 71.7, 71.2, 70.5, 70.0, 68.5, 67.4, 64.3, 64.3, 63.7, 62.5, 60.8, 46.5, 40.6, 20.8, 20.8; HRMS (ESI+) calculated for $C_{63}H_{56}ClN_3O_{19}Na$ $[M+Na]^+$ 1216.3094 *m*/*z*, found 1216.3142.

Hexasaccharide (76)

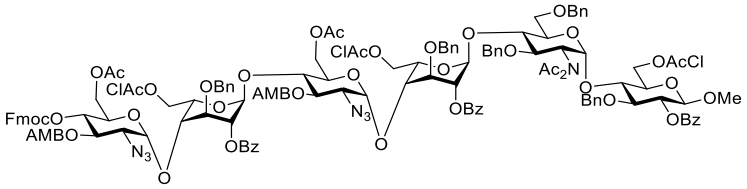

Disaccharide donor **53** (500 mg, 0.36 mmol, 1.4 equiv.) and tetrasaccharide acceptor **72** (450 mg, 0.26 mmol) was reacted according to General Procedure I to yield **76** as a foam (550 mg, 0.20 mmol, 76%), TLC: R_f = 0.55 (MeCN/CH_2Cl_2, 1/9 *v*/*v*); $[\alpha]_D$ 54.8 (c 1 in $CDCl_3$); IR (ATR): ν_{max}/cm^{-1} 2108 (N_3, s), 1728 (C=O); ^{1}H NMR (500 MHz, $CDCl_3$) δ 8.09 – 7.95 (m, 8H), 7.88 (d, J = 7.9 Hz, 1H), 7.71 (dd, J = 7.6, 5.0 Hz, 3H), 7.61 – 7.48 (m, 5H), 7.49 – 7.07 (m, 41H), 5.66 – 5.53 (m, 5H), 5.50 (d, J = 14.3 Hz, 1H), 5.40 (d, J = 14.3 Hz, 1H), 5.27 (dd, J = 8.8, 7.4 Hz, 1H), 5.24 – 5.20 (m, 2H), 5.19 – 5.13 (m, 1H), 5.09 (d, J = 4.5 Hz, 1H), 5.05 – 4.99 (m, 2H), 4.84 (d, J = 11.6 Hz, 1H), 4.77 – 4.39 (m, 13H), 4.37 – 3.75 (m, 27H), 3.68 (dd, J = 11.0, 3.3 Hz, 1H), 3.65 – 3.60 (m, 1H), 3.60 – 3.49 (m, 2H), 3.44 – 3.38 (m, 4H), 3.34 (dd, J = 10.7, 3.7 Hz, 1H), 2.14 (s, 5H), 2.13 (s, 6H), 2.08 (s, 3H), 2.06 (s, 3H), 1.97 (s, 3H); ^{13}C NMR (126 MHz, $CDCl_3$) δ 175.4, 170.6, 170.5, 166.9, 166.7, 166.7, 165.4, 165.1, 165.0, 154.1, 143.0, 142.8, 141.1, 138.9, 138.7, 138.6, 137.5, 137.1, 136.9, 133.5, 133.5, 133.3, 133.1, 132.9, 131.0, 130.6, 129.8, 129.7, 129.5, 129.1, 129.0, 128.6, 128.6, 128.5, 128.5, 128.4, 128.3, 128.3, 128.1, 128.1, 128.0, 128.0, 127.9, 127.8, 127.7, 127.6, 127.5, 127.4, 127.3, 127.2, 127.1, 126.8, 124.9, 120.0, 119.9, 101.5, 98.7, 98.2, 97.8, 97.3, 97.1, 82.8, 77.2, 76.9, 76.2, 75.5, 74.1, 73.7, 73.3, 73.0, 72.3, 72.0, 71.8, 71.5, 70.9, 70.5, 70.3, 69.6, 69.4, 68.0, 67.8, 67.7, 64.2, 64.1, 63.7, 62.9, 61.6, 61.3, 61.0, 60.9, 59.5, 56.7, 46.4, 40.8, 40.7, 40.5, 26.7, 20.9, 20.8, 20.6; HRMS (ESI+) calculated for $C_{142}H_{142}Cl_3N_7O_{46}Na$ $[M+Na]^+$ 2808.7951 *m*/*z*, found 2808.8018.

Hexasaccharide acceptor **(74)**

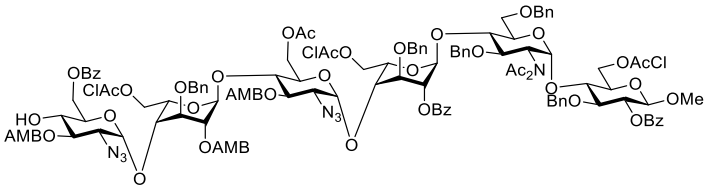

Hexasaccharide **73** (1.5 g, 0.51 mmol) was reacted according to General procedure B to yield hexasaccharide acceptor **74** as a yellow foam (900 mg, 0.33 mmol, 65%); TLC: R_f = 0.4 (EtOAc/toluene, 1/4 *v*/*v*); $[\alpha]_D$ 67.9 (c 1 in $CDCl_3$); IR (ATR): ν_{max}/cm^{-1} 2108 (N_3, s), 1721 (C=O); ^1H NMR (500 MHz, $CDCl_3$) δ 8.06 – 7.97 (m, 7H), 7.93 (t, J = 7.0 Hz, 2H), 7.88 – 7.82 (m, 1H), 7.60 – 7.49 (m, 8H), 7.48 – 7.39 (m, 9H), 7.39 – 7.13 (m, 24H), 7.13 – 7.07 (m, 4H), 5.65 – 5.47 (m, 6H), 5.45 – 5.36 (m, 3H), 5.32 – 5.21 (m, 2H), 5.17 (d, J = 3.7 Hz, 1H), 5.14 (d, J = 4.4 Hz, 1H), 5.10 (q, J = 4.7 Hz, 1H), 5.02 (d, J = 4.2 Hz, 1H), 4.97 (d, J = 3.7 Hz, 1H), 4.87 (d, J = 11.6 Hz, 1H), 4.77 (d, J = 10.9 Hz, 1H), 4.75 – 4.42 (m, 14H), 4.38 – 4.27 (m, 4H), 4.27 – 4.22 (m, 3H), 4.21 – 4.11 (m, 3H), 4.09 (t, J = 5.9 Hz, 1H), 4.05 – 3.77 (m, 12H), 3.72 – 3.61 (m, 3H), 3.60 – 3.51 (m, 2H), 3.41 (s, 4H), 3.34 – 3.24 (m, 2H), 2.17 (s, 3H), 2.13 (s, 5H), 2.10 (s, 3H), 2.08 (s, 3H), 1.97 (s, 3H); ^{13}C NMR (126 MHz, $CDCl_3$) δ 175.3, 171.4, 170.9, 170.5, 170.4, 167.2, 166.7, 166.2, 165.5, 165.0, 164.9, 138.9, 138.7, 138.5, 137.5, 137.5, 137.1, 137.0, 136.9, 133.5, 133.3, 132.9, 132.9, 132.7, 130.9, 130.5, 130.4, 129.8, 129.7, 129.7, 129.6, 129.5, 129.1, 128.9, 128.6, 128.5, 128.5, 128.4, 128.4, 128.1, 128.0, 127.9, 127.8, 127.7, 127.6, 127.5, 127.4, 127.3, 127.1, 126.8, 101.5, 98.6, 97.8, 97.4, 97.3, 97.1, 82.8, 77.1, 76.2, 75.5, 75.1, 74.9, 73.8, 73.7, 73.5, 73.4, 73.2, 72.9, 72.6, 72.3, 71.9, 71.2, 71.2, 70.9, 70.8, 69.4, 69.3, 68.4, 67.7, 67.5, 64.3, 64.2, 64.1, 63.8, 63.6, 63.0, 61.8, 61.3, 61.2, 59.5, 56.7, 41.0, 40.8, 40.5, 26.7, 21.0, 20.9, 20.9, 20.6; HRMS (ESI+) calculated for $C_{135}H_{138}Cl_3N_7O_{46}Na$ $[M+Na]^+$ 2720.7638 *m*/*z*, found 2720.7649.

Hexasaccharide acceptor **(77)**

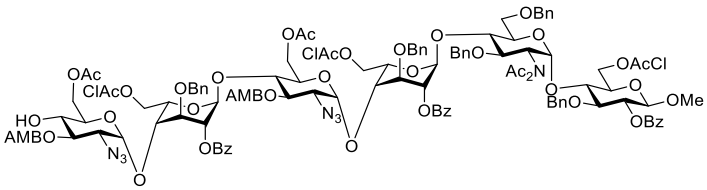

Hexasaccharide **76** (500 mg, 0.18 mmol) was reacted according to General procedure B to yield hexasaccharide acceptor **77** as a yellow foam (350 mg, 0.14 mmol, 76%); TLC: R_f = 0.4 ($MeCN/CH_2Cl_2$, 1/9 *v*/*v*); $[\alpha]_D$ 66.5 (c 1 in $CDCl_3$); IR (ATR): ν_{max}/cm^{-1} 2108 (N_3, s), 1726 (C=O); ^1H NMR (500 MHz, $CDCl_3$) δ 8.11 – 7.96 (m, 6H), 7.94 (d, J = 7.8 Hz, 1H), 7.88 (d, J = 7.7 Hz, 1H), 7.66 – 7.50 (m, 7H), 7.50 – 7.34 (m, 9H), 7.34 – 7.12 (m, 23H), 7.12 – 7.04 (m, 4H), 5.67 – 5.50 (m, 5H), 5.45 – 5.37 (m, 2H), 5.28 (dd, J = 8.7, 7.5 Hz, 1H), 5.23 (t, J = 5.1 Hz, 1H), 5.17 – 5.10 (m, 2H), 5.08 (d, J = 3.7 Hz, 1H), 4.99 (d, J = 4.9

Hz, 1H), 4.84 (d, J = 11.7 Hz, 1H), 4.76 (d, J = 10.9 Hz, 1H), 4.73 – 4.67 (m, 2H), 4.67 – 4.62 (m, 2H), 4.61 – 4.41 (m, 9H), 4.33 – 4.09 (m, 9H), 4.08 – 3.74 (m, 15H), 3.69 (dd, J = 11.0, 3.3 Hz, 1H), 3.66 – 3.52 (m, 3H), 3.41 (s, 4H), 3.28 (dd, J = 10.6, 3.7 Hz, 2H), 2.17 (s, 3H), 2.13 (s, 6H), 2.12 (s, 4H), 2.08 (s, 3H), 1.93 (s, 3H); ^{13}C NMR (126 MHz, $CDCl_3$) δ 175.4, 171.4, 171.2, 170.9, 170.4, 167.2, 166.7, 166.4, 165.5, 165.1, 165.0, 164.9, 138.7, 138.5, 137.5, 137.4, 137.1, 137.0, 136.9, 133.5, 133.4, 133.3, 132.9, 132.7, 130.5, 130.4, 129.8, 129.7, 129.5, 129.1, 129.0, 128.6, 128.6, 128.5, 128.5, 128.4, 128.4, 128.3, 128.1, 128.1, 128.0, 127.9, 127.8, 127.7, 127.5, 127.4, 127.3, 127.1, 101.5, 98.8, 98.1, 97.3, 97.3, 97.1, 82.8, 76.4, 76.1, 75.8, 74.9, 73.9, 73.8, 73.7, 73.3, 73.2, 72.9, 72.6, 72.3, 71.9, 71.8, 71.2, 70.9, 70.8, 69.3, 69.1, 69.0, 67.8, 67.5, 64.3, 64.1, 63.6, 63.5, 62.5, 61.7, 61.2, 61.0, 59.5, 56.7, 40.9, 40.7, 40.5, 29.7, 26.7, 21.0, 20.9, 20.8, 20.6; HRMS (ESI+) calculated for $C_{127}H_{132}Cl_3N_7O_{44}Na$ $[M+Na]^+$ 2586.7270 *m/z*, found 2586.7329.

6'-*O*-Bz disaccharide acceptor **(79)**

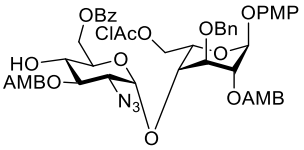

Disaccharide **7** (1.5 g, 1.1 mmol) was reacted according to General Procedure B to yield **79** as a foam (840 mg, 0.76 mmol, 67%), TLC: R_f = 0.4 (MeCN/CH_2Cl_2, 1/4 *v/v*); $[\alpha]_D$ -7.2 (c 1 in $CDCl_3$); IR (ATR): ν_{max}/cm^{-1} 2108 (N_3, s), 1716 (C=O); ^{1}H NMR (500 MHz, $CDCl_3$) δ 8.10 (dd, J = 7.7, 1.5 Hz, 1H), 8.05 – 7.97 (m, 2H), 7.78 (dd, J = 7.9, 1.4 Hz, 1H), 7.57 – 7.52 (m, 2H), 7.50 (dd, J = 7.8, 1.4 Hz, 1H), 7.47 (dd, J = 7.7, 1.3 Hz, 1H), 7.43 – 7.25 (m, 10H), 7.06 – 6.99 (m, 2H), 6.89 – 6.77 (m, 2H), 5.68 (d, J = 14.5 Hz, 1H), 5.60 – 5.46 (m, 3H), 5.42 – 5.35 (m, 3H), 4.94 (d, J = 11.6 Hz, 1H), 4.84 (d, J = 3.8 Hz, 1H), 4.76 (d, J = 11.6 Hz, 1H), 4.66 – 4.61 (m, 3H), 4.58 (dd, J = 11.3, 8.0 Hz, 1H), 4.46 (dd, J = 11.3, 3.6 Hz, 1H), 4.15 – 4.07 (m, 2H), 3.90 – 3.80 (m, 3H), 3.78 (s, 3H), 3.69 – 3.58 (m, 1H), 3.54 (d, J = 5.8 Hz, 1H), 3.44 (dd, J = 10.5, 3.8 Hz, 1H), 2.12 (s, 3H), 2.10 (s, 3H); ^{13}C NMR (126 MHz, $CDCl_3$) δ 170.9, 170.8, 166.9, 166.6, 166.5, 165.6, 155.3, 150.1, 138.2, 137.7, 137.3, 133.2, 132.8, 132.8, 131.2, 130.4, 129.7, 129.6, 128.9, 128.4, 128.4, 128.3, 128.2, 128.1, 128.0, 127.9, 127.8, 127.5, 118.4, 114.5, 97.8, 97.4, 74.3, 74.1, 72.5, 72.4, 71.5, 69.7, 68.6, 66.2, 64.9, 64.6, 64.3, 63.4, 61.5, 55.6, 40.5, 21.0, 20.9; HRMS (ESI+) calculated for $C_{55}H_{54}ClN_3O_{19}Na$ $[M+Na]^+$ 1118.2938 *m/z*, found 1118.2922.

6'-*O*-Ac disaccharide acceptor **(84)**

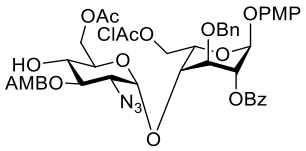

Disaccharide **6** (800 mg, 0.68 mmol) was reacted according to General Procedure B to yield **84** as a foam (600 mg, 0.620 mmol, 92%), TLC: R_f = 0.4 (MeCN/CH_2Cl_2, 1/9 *v*/*v*); $[\alpha]_D$ -11.7 (c 1 in $CDCl_3$); IR (ATR): ν_{max}/cm^{-1} 2108 (N_3, s), 1720 (C=O); ^1H NMR (500 MHz, $CDCl_3$) δ 8.16 – 8.04 (m, 2H), 7.77 (dd, J = 7.8, 1.4 Hz, 1H), 7.58 – 7.53 (m, 1H), 7.53 – 7.49 (m, 1H), 7.45 – 7.27 (m, 10H), 7.07 – 6.98 (m, 2H), 6.88 – 6.79 (m, 2H), 5.62 – 5.51 (m, 2H), 5.43 – 5.31 (m, 3H), 4.97 (d, J = 11.5 Hz, 1H), 4.89 (d, J = 3.7 Hz, 1H), 4.78 (d, J = 11.5 Hz, 1H), 4.64 – 4.58 (m, 1H), 4.54 (dd, J = 11.4, 7.8 Hz, 1H), 4.47 (dd, J = 11.4, 3.8 Hz, 1H), 4.39 (dd, J = 12.2, 5.2 Hz, 1H), 4.34 (dd, J = 12.2, 2.4 Hz, 1H), 4.18 (t, J = 3.8 Hz, 1H), 3.96 – 3.92 (m, 1H), 3.91 – 3.86 (m, 2H), 3.78 (s, 3H), 3.58 (t, J = 9.5 Hz, 1H), 3.53 (s, 1H), 3.43 (dd, J = 10.5, 3.7 Hz, 1H), 2.11 (s, 3H), 2.06 (s, 3H); ^{13}C NMR (126 MHz, $CDCl_3$) δ 171.1, 170.9, 166.9, 166.9, 165.8, 155.2, 150.2, 137.6, 137.4, 133.2, 132.8, 130.4, 129.7, 129.4, 129.1, 128.4, 128.4, 128.1, 128.0, 118.3, 114.5, 97.9, 97.6, 74.5, 74.0, 72.9, 72.6, 71.3, 69.5, 69.0, 66.4, 64.8, 64.3, 62.9, 61.3, 55.6, 40.5, 20.9, 20.7; HRMS (ESI+) calculated for $C_{47}H_{48}ClN_3O_{17}Na$ $[M+Na]^+$ 984.2570 *m*/*z*, found 984.2559.

Terminal tetrasaccharide **(80)**

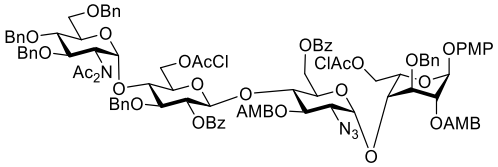

Disaccharide donor **57** (250 mg, 0.23 mmol, 1.2 equiv.) and disaccharide acceptor **79** (200 mg, 0.18 mmol) was reacted according to General Procedure H (at -30 °C) to yield **80** as a foam (240 mg, 0.12 mmol, 65%), TLC: R_f = 0.6 (MeCN/CH_2Cl_2, 1/9 *v*/*v*); $[\alpha]_D$ 88.6 (c 1 in $CDCl_3$); IR (ATR): ν_{max}/cm^{-1} 2109 (N_3, s), 1722 (C=O); ^1H NMR (500 MHz, $CDCl_3$) δ 8.07 – 7.97 (m, 3H), 7.87 – 7.75 (m, 3H), 7.59 – 7.36 (m, 9H), 7.36 – 7.19 (m, 17H), 7.19 – 7.09 (m, 8H), 7.05 – 7.01 (m, 2H), 7.00 – 6.94 (m, 2H), 6.85 – 6.81 (m, 2H), 5.56 (d, J = 4.4 Hz, 1H), 5.55 – 5.49 (m, 3H), 5.44 (dd, J = 8.9, 5.1 Hz, 2H), 5.40 (dd, J = 4.2, 2.7 Hz, 1H), 5.31 (d, J = 14.8 Hz, 1H), 5.10 (d, J = 14.7 Hz, 1H), 5.06 (d, J = 3.8 Hz, 1H), 5.03 (dd, J = 9.4, 3.8 Hz, 1H), 4.88 – 4.80 (m, 2H), 4.78 – 4.70 (m, 3H), 4.68 (d, J = 9.5 Hz, 1H), 4.67 – 4.42 (m, 12H), 4.36 (dd, J = 11.2, 4.4 Hz, 1H), 4.24 – 4.16 (m, 2H), 4.14 (t, J = 4.4 Hz, 1H), 4.10 – 4.00 (m, 5H), 3.98 (d, J = 2.4 Hz, 2H), 3.91 (d, J = 2.9 Hz, 2H), 3.77 (s, 3H), 3.74 – 3.67 (m, 2H), 3.67 – 3.63 (m, 1H), 3.61 – 3.57 (m, 1H), 3.27 (dd, J = 9.9, 3.8 Hz, 1H), 2.17 (s, 6H), 2.08 (s, 3H), 2.04 (s, 3H); ^{13}C NMR (126 MHz, $CDCl_3$) δ 175.4, 170.5, 170.3, 166.9, 166.8, 166.0, 165.6, 165.5, 164.2, 155.3, 150.3, 139.1, 138.5, 138.2, 137.9, 137.6,

137.3, 137.2, 133.4, 133.3, 133.2, 132.9, 131.0, 129.8, 129.7, 129.4, 128.8, 128.8, 128.6, 128.4, 128.4, 128.3, 128.2, 128.0, 127.9, 127.8, 127.7, 127.6, 127.5, 127.5, 127.4, 127.1, 126.3, 118.5, 114.5, 97.9, 97.6, 96.1, 96.0, 79.4, 78.7, 78.5, 77.3, 77.2, 77.0, 76.8, 74.7, 73.7, 73.5, 73.4, 73.3, 73.0, 72.8, 72.5, 72.3, 72.1, 72.0, 71.7, 69.9, 69.8, 68.1, 66.8, 64.6, 64.3, 64.2, 63.3, 61.0, 58.9, 55.6, 40.6, 40.5, 26.7, 20.9; HRMS (ESI+) calculated for $C_{108}H_{108}Cl_2N_4O_{32}Na$ $[M+Na]^+$ 2065.6221 *m/z*, found 2065.6240.

Terminal tetrasaccharide (85)

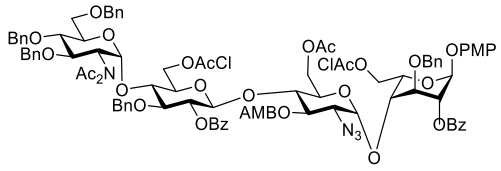

Disaccharide donor **57** (270 mg, 0.24 mmol, 1.2 equiv.) and disaccharide acceptor **84** (190 mg, 0.20 mmol) was reacted according to General Procedure H to yield **85** as a foam (80 mg, 0.04 mmol, 21%), TLC: R_f = 0.6 (MeCN/CH_2Cl_2, 1/9 *v/v*); $[\alpha]_D$ 106.6 (c 1 in $CDCl_3$); IR (ATR): ν_{max}/cm^{-1} 2109 (N_3, s), 1725 (C=O); ^1H NMR (500 MHz, $CDCl_3$) δ 8.08 – 8.02 (m, 2H), 7.85 – 7.78 (m, 2H), 7.77 (dd, J = 7.9, 1.4 Hz, 1H), 7.56 – 7.45 (m, 3H), 7.42 (dd, J = 7.9, 1.3 Hz, 1H), 7.41 – 7.20 (m, 22H), 7.20 – 7.14 (m, 4H), 7.14 – 7.09 (m, 3H), 7.07 – 7.01 (m, 2H), 7.00 – 6.94 (m, 2H), 6.86 – 6.79 (m, 2H), 5.58 (d, J = 4.3 Hz, 1H), 5.55 (d, J = 2.7 Hz, 1H), 5.48 (dd, J = 9.9, 8.1 Hz, 1H), 5.44 (dd, J = 4.4, 2.7 Hz, 1H), 5.39 (d, J = 3.8 Hz, 1H), 5.31 (d, J = 14.7 Hz, 1H), 5.11 – 5.05 (m, 2H), 5.03 (dd, J = 9.5, 3.8 Hz, 1H), 4.91 (d, J = 11.4 Hz, 1H), 4.79 – 4.71 (m, 3H), 4.69 – 4.45 (m, 12H), 4.33 – 4.21 (m, 3H), 4.19 (t, J = 4.7 Hz, 1H), 4.09 (dd, J = 5.0, 3.5 Hz, 1H), 4.07 – 3.90 (m, 8H), 3.77 (s, 3H), 3.75 – 3.68 (m, 2H), 3.68 – 3.60 (m, 2H), 3.24 (dd, J = 9.9, 3.8 Hz, 1H), 2.17 (s, 6H), 2.09 (s, 6H); ^{13}C NMR (126 MHz, $CDCl_3$) δ 175.5, 170.4, 170.4, 166.9, 166.9, 165.7, 165.4, 164.2, 155.3, 150.3, 139.0, 138.5, 137.8, 137.6, 137.3, 137.1, 133.4, 133.4, 133.2, 131.0, 129.8, 129.1, 128.7, 128.5, 128.4, 128.4, 128.3, 128.3, 128.0, 127.9, 127.9, 127.8, 127.8, 127.6, 127.6, 127.6, 127.4, 127.0, 126.3, 118.3, 114.5, 97.8, 97.7, 96.3, 96.1, 79.4, 78.9, 78.6, 77.3, 77.0, 76.8, 74.8, 73.7, 73.7, 73.5, 73.3, 72.9, 72.4, 72.4, 72.1, 72.0, 71.3, 70.3, 69.7, 69.6, 68.1, 67.1, 64.4, 64.2, 64.1, 62.8, 60.9, 59.2, 55.6, 40.7, 40.6, 26.7, 20.9, 20.7; HRMS (ESI+) calculated for $C_{100}H_{102}Cl_2N_4O_{30}Na$ $[M+Na]^+$ 1931.5854 *m/z*, found 1931.5844.

Terminal tetrasaccharide hemiacetal (81)

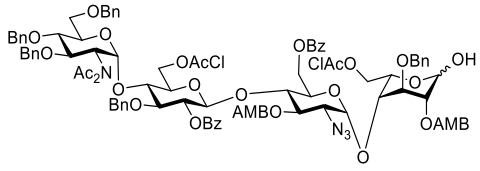

Tetrasaccharide **80** (135 mg, 0.066 mmol) was reacted according to General Procedure C to yield **81** as a mixture of anomers, as a foam (90 mg, 0.046 mmol, 70%), TLC: R_f = 0.4 (MeCN/CH_2Cl_2, 1/9 *v*/*v*); ^{1}H NMR (500 MHz, $CDCl_3$) δ 8.12 – 8.05 (m, 2H), 8.03 (dd, J = 7.9, 1.4 Hz, 0.7H), 7.97 (dd, J = 7.9, 1.4 Hz, 0.3H), 7.89 – 7.82 (m, 2H), 7.79 (dd, J = 7.9, 1.4 Hz, 0.3H), 7.75 (dd, J = 7.9, 1.4 Hz, 0.7H), 7.62 – 7.56 (m, 1H), 7.56 – 7.22 (m, 26H), 7.19 – 7.12 (m, 4H), 7.13 – 7.08 (m, 3H), 7.01 – 6.95 (m, 2H), 5.62 – 5.56 (m, 1.7H), 5.54 – 5.40 (m, 3.3H), 5.29 (d, J = 14.7 Hz, 0.3H), 5.27 – 5.23 (m, 1H), 5.21 (d, J = 15.0 Hz, 0.7H), 5.11 – 4.98 (m, 3.3H), 4.90 – 4.63 (m, 8H), 4.63 – 4.41 (m, 10H), 4.39 – 4.34 (m, 1H), 4.33 – 4.29 (m, 0.7H), 4.26 – 4.17 (m, 3H), 4.15 (d, J = 4.7 Hz, 2H), 4.10 – 3.99 (m, 4.6H), 3.98 – 3.91 (m, 3.3H), 3.79 (t, J = 3.8 Hz, 0.7H), 3.76 – 3.55 (m, 4H), 3.32 (dd, J = 10.1, 3.9 Hz, 0.7H), 3.24 (dd, J = 9.9, 3.8 Hz, 0.3H), 2.19 (s, 3.7H), 2.18 (s, 2H), 2.12 (s, 2H), 2.08 (s, 1H), 2.07 (s, 2H), 2.06 (s, 1.3H); ^{13}C NMR (126 MHz, $CDCl_3$) δ 175.5, 170.7, 170.4, 170.4, 170.3, 167.2, 167.0, 166.9, 166.5, 166.1, 166.0, 166.0, 165.5, 165.5, 164.2, 164.1, 139.3, 139.1, 138.6, 138.1, 137.9, 137.7, 137.2, 137.0, 136.5, 133.5, 133.5, 133.4, 133.3, 133.3, 133.0, 131.5, 131.4, 131.0, 129.9, 129.8, 129.8, 129.5, 129.5, 128.9, 128.7, 128.7, 128.6, 128.6, 128.5, 128.4, 128.4, 128.3, 128.3, 128.2, 128.1, 128.1, 128.0, 128.0, 127.9, 127.8, 127.7, 127.6, 127.6, 127.4, 127.1, 126.3, 125.9, 97.9, 97.9, 96.5, 96.4, 96.2, 96.0, 92.7, 92.0, 79.4, 78.8, 78.7, 78.6, 78.6, 74.8, 73.9, 73.7, 73.6, 73.6, 73.5, 73.3, 73.1, 72.9, 72.7, 72.6, 72.5, 72.4, 72.2, 72.1, 71.8, 71.7, 71.6, 70.9, 70.8, 69.9, 69.9, 68.2, 66.6, 65.6, 64.6, 64.4, 64.3, 64.2, 64.1, 63.2, 63.0, 61.6, 61.0, 59.0, 59.0, 40.8, 40.8, 40.7, 29.7, 26.7, 21.1, 20.9, 20.9; HRMS (ESI+) calculated for $C_{101}H_{102}Cl_2N_4O_{31}Na$ $[M+Na]^+$ 1959.5803 *m*/*z*, found 1959.5764.

Terminal tetrasaccharide hemiacetal **(86)**

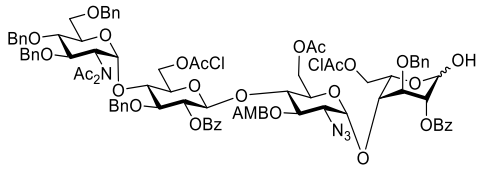

Tetrasaccharide **85** (80 mg, 0.042 mmol) was reacted according to General Procedure C to yield **86** as a mixture of anomers, as a film (45 mg, 0.025 mmol, 59%), TLC: R_f = 0.4 (MeCN/CH_2Cl_2, 1/9 *v*/*v*); ^{1}H NMR (500 MHz, $CDCl_3$) δ 8.08 – 7.99 (m, 2H), 7.84 – 7.71 (m, 3H), 7.57 – 7.45 (m, 3H), 7.41 (dd, J = 8.0, 2.3 Hz, 1H), 7.40 – 7.20 (m, 18H), 7.20 – 7.14 (m, 4H), 7.14 – 7.08 (m, 3H), 6.98 (dd, J = 6.6, 3.0 Hz, 2H), 5.61 – 5.53 (m, 1H), 5.50 – 5.40 (m, 1H), 5.40 – 5.30 (m, 2H), 5.27 (dd, J = 9.0, 3.9 Hz, 1H), 5.14 – 4.97 (m, 4H), 4.85 (dd, J = 16.7, 11.1 Hz, 1H), 4.80 – 4.71 (m, 4H), 4.69 – 4.44 (m, 12H), 4.39 – 4.17 (m, 7H), 4.13 – 3.90 (m, 8H), 3.86 (d, J = 8.8 Hz, 1H), 3.75 – 3.68 (m, 2H), 3.68 – 3.57 (m, 2H), 3.49 (d, J = 7.7 Hz, 1H), 3.20 (dt, J = 10.0, 4.2 Hz, 1H), 2.18 (s, 6H), 2.14 (s, 3H), 2.10 (s, 1H), 2.09 (s, 2H); ^{13}C NMR (126 MHz, $CDCl_3$) δ 175.4, 170.4, 167.3, 167.0, 166.9, 166.3, 166.1, 165.4, 164.2, 164.2, 139.1, 139.0, 138.5, 137.8, 137.6, 137.1, 136.6, 133.5, 133.5, 133.4, 133.2, 131.0, 129.8, 129.7, 129.0, 128.7, 128.6, 128.5,

128.5, 128.4, 128.4, 128.4, 128.3, 128.3, 128.1, 128.0, 127.9, 127.9, 127.8, 127.8, 127.6, 127.6, 127.6, 127.4, 127.0, 126.3, 126.2, 97.8, 97.8, 96.9, 96.7, 96.2, 96.1, 92.9, 91.9, 79.4, 78.9, 78.9, 78.6, 74.8, 74.1, 73.7, 73.5, 73.3, 73.2, 72.7, 72.4, 72.4, 72.3, 72.2, 72.0, 71.5, 71.4, 71.3, 69.7, 69.7, 69.6, 68.1, 67.1, 65.7, 64.5, 64.2, 64.1, 62.7, 61.0, 60.8, 59.2, 59.2, 40.9, 40.8, 40.7, 26.7, 20.9, 20.8; HRMS (ESI+) calculated for $C_{93}H_{96}Cl_2N_4O_{29}Na$ $[M+Na]^+$ 1825.5435 *m*/*z*, found 1825.5427.

Terminal tetrasaccharide *N*-PTFA donor (82)

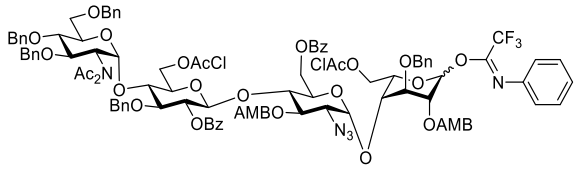

Tetrasaccharide hemiacetal **81** (110 mg, 0.057 mmol) was reacted according to General Procedure E to yield **82** as a mixture of anomers, appearing as a film (99 mg, 0.047 mmol, 83%), TLC: R_f = 0.7 (MeCN/CH_2Cl_2, 1/9 *v*/*v*); ^{1}H NMR (500 MHz, $CDCl_3$) δ 8.11 – 8.02 (m, 2.25H), 8.00 – 7.94 (m, 1H), 7.88 – 7.81 (m, 1.25H), 7.80 – 7.76 (m, 2H), 7.63 – 7.57 (m, 1H), 7.56 – 7.51 (m, 2.5H), 7.50 – 7.45 (m, 4H), 7.45 – 7.39 (m, 2.25H), 7.38 – 7.19 (m, 19H), 7.20 – 7.14 (m, 10H), 7.13 – 7.09 (m, 3.75H), 7.07 – 7.02 (m, 1H), 7.01 – 6.93 (m, 2H), 6.83 (d, J = 7.8 Hz, 0.5H), 6.56 (d, J = 8.0 Hz, 2H), 5.43 (d, J = 3.7 Hz, 0.25H), 5.12 – 4.99 (m, 2H), 4.99 (d, J = 3.9 Hz, 0.25H), 4.88 (dd, J = 11.9, 2.1 Hz, 0.75H), 4.84 (d, J = 11.6 Hz, 0.5H), 4.80 – 4.71 (m, 3H), 4.68 (d, J = 10.9 Hz, 1H), 4.66 – 4.47 (m, 10H), 4.45 (dd, J = 12.0, 2.7 Hz, 0.5H), 4.41 – 4.30 (m, 3H), 4.30 – 4.23 (m, 1H), 4.23 – 4.16 (m, 3H), 4.13 (t, J = 3.7 Hz, 0.25H), 4.11 – 4.05 (m, 3.5H), 4.04 – 3.90 (m, 4H), 3.76 – 3.55 (m, 4H), 3.28 (dd, J = 9.8, 3.7 Hz, 0.25H), 3.25 (dd, J = 10.1, 3.8 Hz, 0.75H), 2.19 (s, 4.5H), 2.18 (s, 1.5H), 2.08 (s, 3H), 2.04 (s, 2.25H), 2.03 (s, 0.75H); ^{13}C NMR (126 MHz, $CDCl_3$) δ 175.5, 170.6, 170.5, 170.4, 167.0, 166.9, 166.9, 166.8, 166.1, 166.0, 165.5, 165.1, 164.4, 164.1, 143.3, 143.0, 139.1, 139.0, 138.6, 138.2, 137.9, 137.7, 137.2, 137.1, 137.0, 133.6, 133.5, 133.4, 133.3, 133.01, 131.0, 130.8, 129.85, 129.8, 129.7, 129.55, 129.5, 129.5, 129.4, 129.35, 129.3, 129.1, 128.9, 128.85, 128.8, 128.7, 128.55, 128.5, 128.45, 128.4, 128.35, 128.3, 128.25, 128.2, 128.2, 128.15, 128.1, 128.05, 128.0, 127.95, 127.8, 127.75, 127.65, 127.6, 127.45, 127.4, 127.35, 127.3, 127.25, 127.2, 127.1, 127.0, 126.4, 126.3, 124.4, 119.4, 119.2, 117.0, 114.7, 98.0, 97.9, 96.4, 96.0, 95.8, 93.1, 79.4, 78.8, 78.7, 78.6, 77.2, 76.9, 75.0, 74.8, 74.5, 73.7, 73.6, 73.5, 73.3, 73.0, 72.9, 72.6, 72.5, 72.4, 72.2, 72.0, 71.8, 71.3, 71.2, 70.9, 70.0, 69.9, 69.8, 68.2, 67.6, 67.2, 65.0, 64.7, 64.5, 64.4, 64.2, 63.3, 63.1, 61.1, 61.0, 59.0, 40.8, 40.7, 40.6, 29.7, 26.7, 20.9, 20.8; HRMS (ESI+) calculated for $C_{109}H_{106}Cl_2F_3N_5O_{31}Na$ $[M+Na]^+$ 2130.6099 *m*/*z*, found 2130.6106.

Terminal tetrasaccharide *N*-PTFA donor (87)

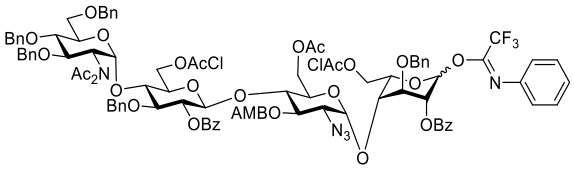

Tetrasaccharide hemiacetal **86** (45 mg, 0.025 mmol) was reacted according to General Procedure E to yield **87** as a mixture of anomers, appearing as a film (35 mg, 0.018 mmol, 71%), TLC: R_f = 0.7 (MeCN/CH_2Cl_2, 1/9 *v*/*v*); ^{1}H NMR (500 MHz, $CDCl_3$) δ 8.05 – 7.96 (m, 2H), 7.86 – 7.79 (m, 1.6H), 7.77 – 7.70 (m, 1.4H), 7.59 (t, J = 7.5 Hz, 0.4H), 7.56 – 7.39 (m, 5H), 7.38 – 7.21 (m, 20H), 7.20 – 7.14 (m, 7H), 7.14 – 7.11 (m, 3H), 7.11 – 7.01 (m, 1H), 7.00 – 6.96 (m, 2H), 6.83 (d, J = 7.8 Hz, 1.4H), 6.63 (s, 0.4H), 6.49 (d, J = 7.8 Hz, 0.8H), 5.63 – 5.53 (m, 1.4H), 5.48 – 5.35 (m, 3H), 5.31 (dd, J = 14.6, 12.4 Hz, 1H), 5.09 – 4.99 (m, 2.6H), 4.93 – 4.71 (m, 4.4H), 4.70 – 4.46 (m, 11.6H), 4.40 (t, J = 8.7 Hz, 0.4H), 4.34 – 4.17 (m, 5H), 4.15 (s, 1H), 4.09 – 3.86 (m, 6.4H), 3.76 – 3.68 (m, 2H), 3.68 – 3.55 (m, 2H), 3.25 (dd, J = 9.9, 3.8 Hz, 0.6H), 3.20 (dd, J = 10.1, 3.9 Hz, 0.4H), 2.18 (s, 2.6H), 2.17 (s, 3.6H), 2.16 (s, 1.4H), 2.12 (s, 2H), 2.09 (s, 3H); ^{13}C NMR (126 MHz, $CDCl_3$) δ 175.5, 170.4, 170.4, 167.0, 167.0, 166.9, 165.6, 165.5, 165.5, 165.4, 164.4, 164.1, 143.2, 142.9, 139.1, 138.5, 138.5, 137.9, 137.8, 137.6, 137.2, 137.1, 133.7, 133.6, 133.4, 133.2, 131.0, 129.8, 129.7, 128.85, 128.8, 128.7, 128.6, 128.55, 128.5, 128.45, 128.4, 128.35, 128.3, 128.1, 128.05, 128.0, 128.0, 127.9, 127.85, 127.8, 127.8, 127.7, 127.6, 127.6, 127.5, 127.4, 127.1, 127.0, 126.4, 126.3, 124.5, 124.4, 119.4, 119.1, 98.5, 97.8, 97.8, 96.6, 96.0, 95.9, 93.1, 79.4, 79.0, 78.9, 78.6, 75.2, 74.9, 74.8, 73.7, 73.5, 73.5, 73.1, 73.0, 72.6, 72.4, 72.1, 72.0, 72.0, 71.6, 71.4, 71.3, 69.8, 69.7, 69.6, 68.1, 67.9, 67.7, 65.1, 64.6, 64.2, 64.1, 62.8, 62.7, 61.1, 60.9, 59.3, 59.2, 40.8, 40.7, 40.6, 29.7, 26.7, 20.9, 20.85, 20.8; HRMS (ESI+) calculated for $C_{101}H_{100}Cl_2F_3N_5O_{29}Na$ $[M+Na]^+$ 1996.5731 *m*/*z*, found 1996.5697.

Octasaccharide (3)

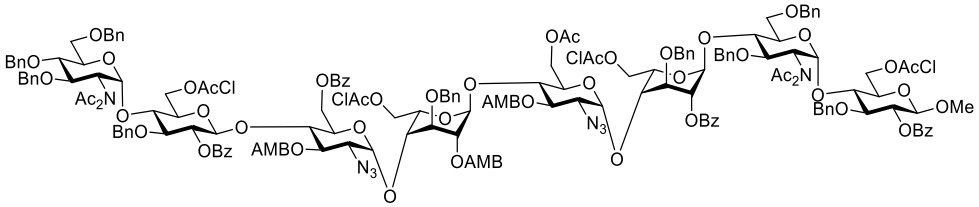

Donor **82** (99 mg, 0.047 mmol, 1.2 equiv.) and acceptor **72** (65 mg, 0.038 mmol) was reacted according to General Procedure I to yield **3** as a film (59 mg, 0.043 mmol, 43%). Additionally, the glycal **83** was isolated as a by-product (25 mg).

Data for octasaccharide **(3)**

TLC: R_f = 0.55 (MeCN/CH_2Cl_2, 1/9 *v*/*v*); $[\alpha]_D$ 107.6 (c 1 in $CDCl_3$); IR (ATR): ν_{max}/cm^{-1} 2109 (N_3, s), 1723 (C=O); ^{1}H NMR (500 MHz, $CDCl_3$) δ 8.07 – 8.04 (m, 2H), 8.03 – 8.00 (m, 2H), 8.00 – 7.96 (m, 2H), 7.96 – 7.93 (m, 2H), 7.81 – 7.78 (m, 1H), 7.77 – 7.72 (m, 2H), 7.62 – 7.50 (m, 7H), 7.51 – 7.38 (m, 13H), 7.39 – 7.36 (m, 1H), 7.36 – 7.08 (m, 48H), 7.00 – 6.92 (m, 3H), 5.60 – 5.56 (m, 3H), 5.54 – 5.51 (m, 2H), 5.50 – 5.40 (m, 5H), 5.33 – 5.24 (m, 2H), 5.23 (dd, J = 6.0, 4.8 Hz, 1H), 5.16 (d, J = 3.8 Hz, 1H), 5.14 (d, J = 3.8 Hz, 1H), 5.10 (dd, J = 8.0, 3.3 Hz, 2H), 5.05 – 4.99 (m, 2H), 4.98 (d, J = 5.0 Hz, 1H), 4.87 (d, J = 11.5 Hz, 1H), 4.82 – 4.77 (m, 1H), 4.77 – 4.68 (m, 5H), 4.67 – 4.53 (m, 9H), 4.53 – 4.43 (m, 8H), 4.41 – 4.37 (m, 1H), 4.36 – 4.26 (m, 4H), 4.25 – 4.19 (m, 2H), 4.19 – 4.10 (m, 5H), 4.08 – 4.02 (m, 3H), 4.01 – 3.83 (m, 13H), 3.82 – 3.78 (m, 1H), 3.72 – 3.64 (m, 4H), 3.64 – 3.60 (m, 1H), 3.56 (dd, J = 11.7, 4.9 Hz, 1H), 3.52 (dd, J = 11.0, 1.9 Hz, 1H), 3.41 (s, 3H), 3.37 – 3.30 (m, 1H), 3.13 (dd, J = 10.1, 3.7 Hz, 1H), 2.21 (s, 6H), 2.12 (s, 6H), 2.11 (s, 3H), 2.04 (s, 6H), 1.97 (s, 3H); ^{13}C NMR (126 MHz, $CDCl_3$) δ 13C NMR (126 MHz, CDCl3) δ 175.5, 175.4, 170.7, 170.5, 170.4, 166.8, 166.8, 166.7, 165.9, 165.5, 165.4, 165.2, 165.1, 164.8, 164.3, 139.0, 138.8, 138.5, 137.9, 137.6, 137.5, 137.2, 137.0, 133.6, 133.4, 133.3, 133.1, 132.9, 131.0, 130.7, 130.6, 129.8, 129.7, 129.5, 129.3, 129.2, 128.74, 128.72, 128.6, 128.5, 128.4, 128.4, 128.3, 128.2, 128.2, 128.1, 128.0, 127.9, 127.8, 127.8, 127.6, 127.5, 127.4, 127.4, 127.3, 127.1, 126.9, 126.4, 101.6, 98.3, 98.0, 97.7, 97.3, 97.2, 96.7, 96.3, 82.8, 79.4, 78.7, 78.6, 76.3, 75.8, 74.8, 74.0, 73.8, 73.7, 73.6, 73.5, 73.3, 73.0, 72.4, 72.3, 72.2, 72.0, 71.9, 71.6, 71.3, 71.0, 69.8, 69.7, 69.6, 68.7, 68.1, 67.9, 67.7, 64.3, 64.2, 64.1, 63.8, 62.7, 61.7, 61.2, 61.0, 59.5, 59.2, 56.7, 40.8, 40.7, 40.7, 40.6, 40.5, 29.7, 29.3, 26.7, 20.9, 20.9, 20.7; HRMS (ESI+) calculated for $C_{188}H_{192}Cl_4N_8O_{59}Na$ $[M+Na]^+$ 3668.0921 *m*/*z*, found 3668.0891.

Tetrasaccharide glycal by-product **(83)**

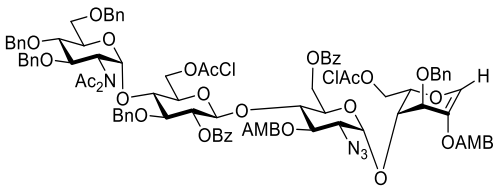

TLC: R_f = 0.7 (MeCN/CH_2Cl_2, 1/9 *v*/*v*); ^{1}H NMR (500 MHz, $CDCl_3$) δ 8.12 – 8.07 (m, 2H), 7.95 (dd, J = 7.9, 1.4 Hz, 1H), 7.88 – 7.78 (m, 3H), 7.61 – 7.39 (m, 8H), 7.40 – 7.20 (m, 14H), 7.21 – 7.13 (m, 6H), 7.14 – 7.07 (m, 6H), 7.04 – 6.95 (m, 2H), 6.78 (s, 1H), 5.64 – 5.57 (m, 2H), 5.51 (d, J = 3.8 Hz, 1H), 5.42 (d, J = 14.4 Hz, 1H), 5.36 (d, J = 9.2 Hz, 1H), 5.33 (d, J = 9.1 Hz, 1H), 5.30 (d, J = 3.7 Hz, 1H), 5.10 (d, J = 14.0 Hz, 1H), 5.07 (dd, J = 8.9, 3.1 Hz, 1H), 4.88 (dd, J = 12.0, 2.0 Hz, 1H), 4.77 (d, J = 11.4 Hz, 1H), 4.73 (d, J = 11.0 Hz, 1H), 4.70 (d, J = 11.2 Hz, 1H), 4.65 – 4.45 (m, 13H), 4.40 – 4.34 (m, 3H), 4.26 – 4.20 (m, 2H), 4.19 – 4.13 (m, 3H), 4.12 (dd, J = 2.8, 1.4 Hz, 1H), 4.08 (dd, J = 9.5, 8.1 Hz, 1H), 4.05 – 4.01 (m, 1H), 3.99

(d, J = 3.1 Hz, 2H), 3.95 (dd, J = 9.4, 8.3 Hz, 1H), 3.76 – 3.71 (m, 1H), 3.71 – 3.63 (m, 2H), 3.60 (dd, J = 10.4, 1.4 Hz, 1H), 3.29 (dd, J = 10.1, 3.6 Hz, 1H), 2.19 (s, 6H), 2.07 (s, 6H).; ^{13}C NMR (126 MHz, $CDCl_3$) δ 175.5, 170.5, 167.0, 166.9, 166.0, 165.5, 165.1, 164.5, 139.9, 138.8, 138.5, 137.8, 137.6, 137.3, 137.2, 133.5, 133.4, 133.1, 131.4, 131.1, 129.8, 129.7, 129.7, 129.4, 128.7, 128.5, 128.4, 128.4, 128.3, 128.3, 128.1, 128.0, 127.9, 127.8, 127.8, 127.7, 127.6, 127.4, 127.3, 127.1, 126.9, 97.9, 96.1, 94.9, 79.4, 78.9, 78.5, 74.8, 73.7, 73.6, 73.4, 72.4, 72.2, 72.0, 71.7, 71.6, 71.1, 69.8, 69.7, 69.5, 68.1, 66.8, 64.3, 64.3, 63.7, 63.4, 60.6, 59.0, 40.7, 26.7, 20.9; HRMS (ESI+) calculated for $C_{101}H_{100}Cl_2N_4O_{30}Na$ $[M+Na]^+$ 1941.5697 *m*/*z*, found 1941.5691.

Octasaccharide **(4)**

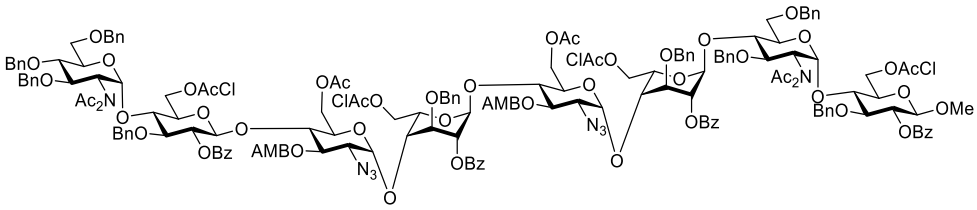

Donor **87** (35 mg, 0.018 mmol, 1.2 equiv.) and acceptor **72** (25 mg, 0.014 mmol) was reacted according to General Procedure I to yield **4** as a film (20 mg, 0.006 mmol, 39%), TLC: R_f = 0.55 ($MeCN/CH_2Cl_2$, 1/9 *v*/*v*); $[\alpha]_D$ 72.1 (c 1 in $CDCl_3$); IR (ATR): ν_{max}/cm^{-1} 2109 (N_3, s), 1728 (C=O); ^{1}H NMR (500 MHz, $CDCl_3$) δ 8.04 – 7.99 (m, 5H), 7.99 – 7.93 (m, 3H), 7.83 – 7.76 (m, 2H), 7.74 (dd, J = 8.4, 1.3 Hz, 2H), 7.64 – 7.47 (m, 7H), 7.47 – 7.06 (m, 52H), 7.01 – 6.93 (m, 3H), 5.60 (d, J = 4.4 Hz, 1H), 5.57 (d, J = 4.4 Hz, 1H), 5.53 (s, 2H), 5.47 – 5.40 (m, 1H), 5.40 – 5.33 (m, 2H), 5.34 – 5.23 (m, 3H), 5.23 – 5.19 (m, 1H), 5.19 – 5.15 (m, 1H), 5.14 (d, J = 3.9 Hz, 1H), 5.12 – 5.00 (m, 4H), 4.96 (d, J = 5.7 Hz, 1H), 4.89 – 4.35 (m, 29H), 4.35 – 4.11 (m, 9H), 4.09 – 3.87 (m, 15H), 3.86 (d, J = 9.3 Hz, 2H), 3.81 (d, J = 8.0 Hz, 1H), 3.75 – 3.47 (m, 7H), 3.41 (s, 3H), 3.36 – 3.29 (m, 1H), 3.10 (dd, J = 10.0, 3.8 Hz, 1H), 2.19 (s, 6H), 2.18 – 2.15 (m, 3H), 2.13 (s, 3H), 2.12 (s, 6H), 2.10 (s, 2H), 2.05 (s, 3H), 1.94 (s, 3H); ^{13}C NMR (Data from HSQC, 126 MHz, $CDCl_3$) δ 133.4, 133.3, 130.9, 130.3, 129.8, 129.7, 128.6, 128.5, 128.4, 128.3, 128.2, 128.0, 127.9, 127.8, 127.5, 127.1, 101.5, 98.5, 97.8, 97.5, 97.2, 97.1, 96.2, 82.8, 79.4, 78.9, 78.7, 77.0, 76.2, 76.1, 76.0, 74.7, 74.0, 73.9, 73.8, 73.7, 73.6, 73.5, 73.4, 73.2, 73.0, 72.4, 72.2, 72.1, 72.0, 71.9, 71.5, 70.9, 69.5, 69.4, 68.3, 68.1, 68.0, 67.9, 67.8, 64.3, 64.2, 64.1, 64.0, 63.8, 63.7, 62.7, 62.6, 62.5, 61.0, 60.9, 59.5, 56.7, 40.6, 40.5, 40.4, 26.7, 26.6, 20.9, 20.8, 20.7, 20.6; HRMS (ESI+) calculated for $C_{180}H_{186}Cl_4N_3O_{57}Na$ $[M+Na]^+$ 3534.0554 *m*/*z*, found 3534.0535.

7. NMR spectra

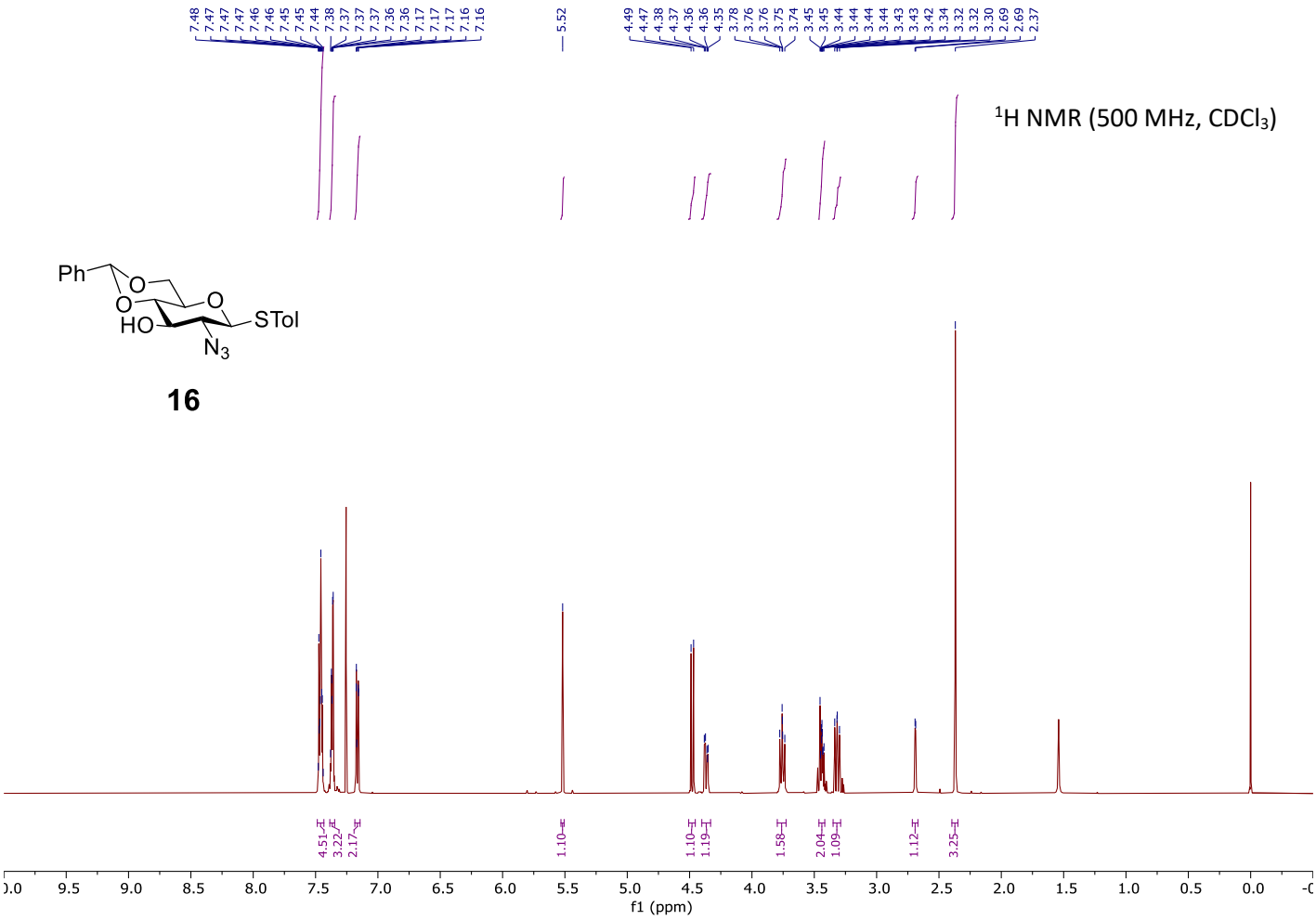

^{1}H NMR (500 MHz, $CDCl_3$)

16

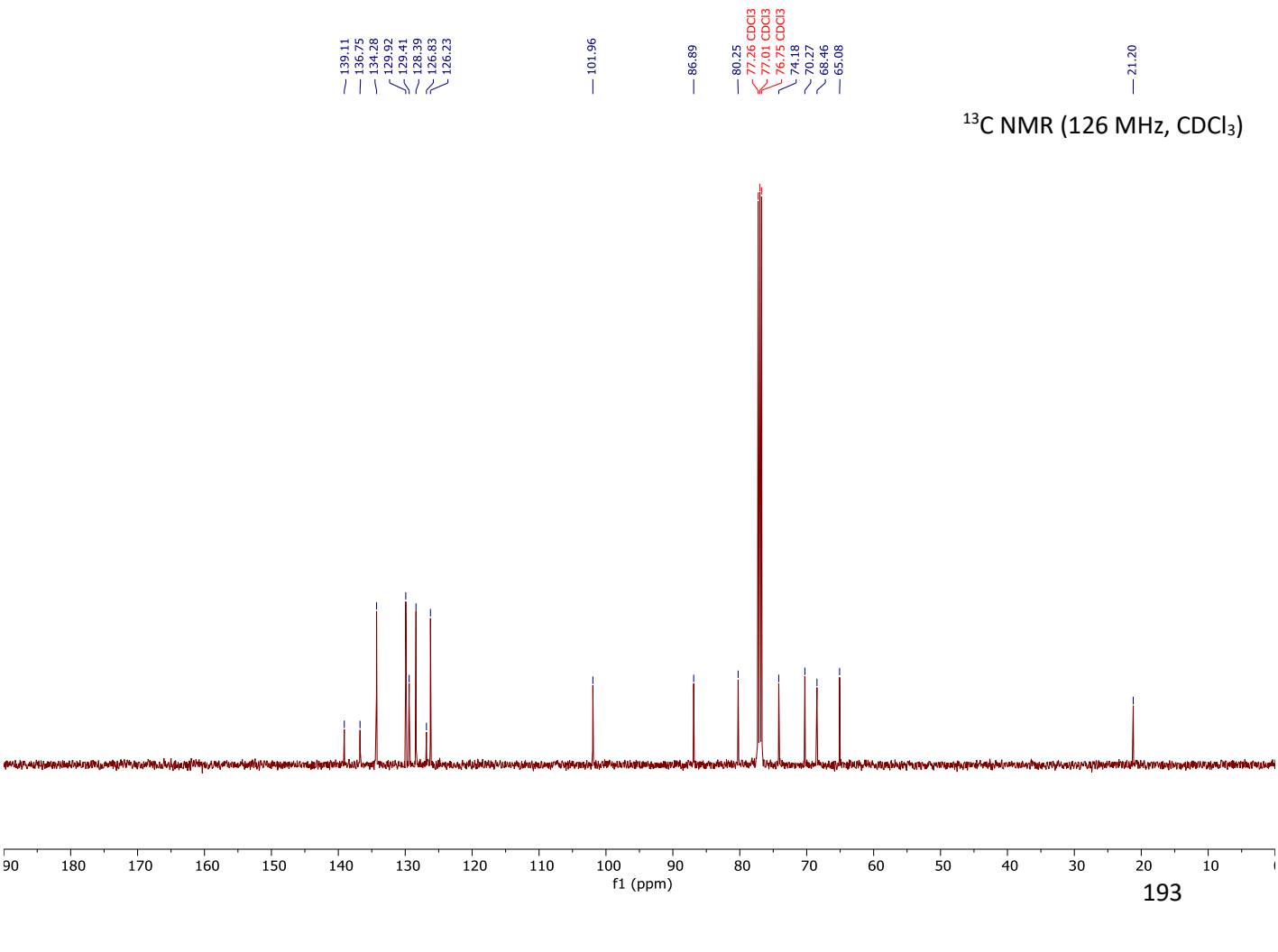

^{13}C NMR (126 MHz, $CDCl_3$)

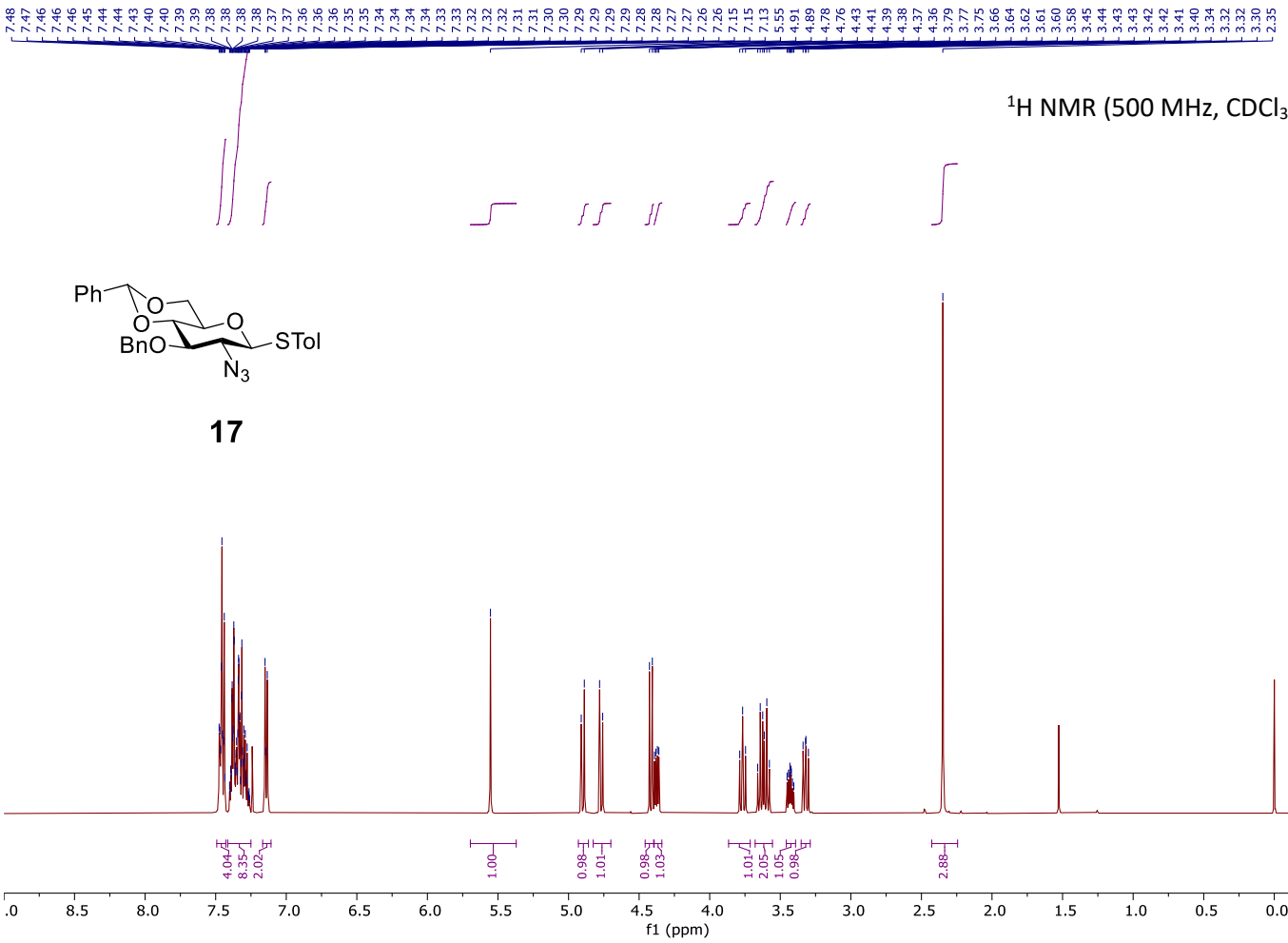

17

^{1}H NMR (500 MHz, $CDCl_3$)

^{13}C NMR (126 MHz, $CDCl_3$)

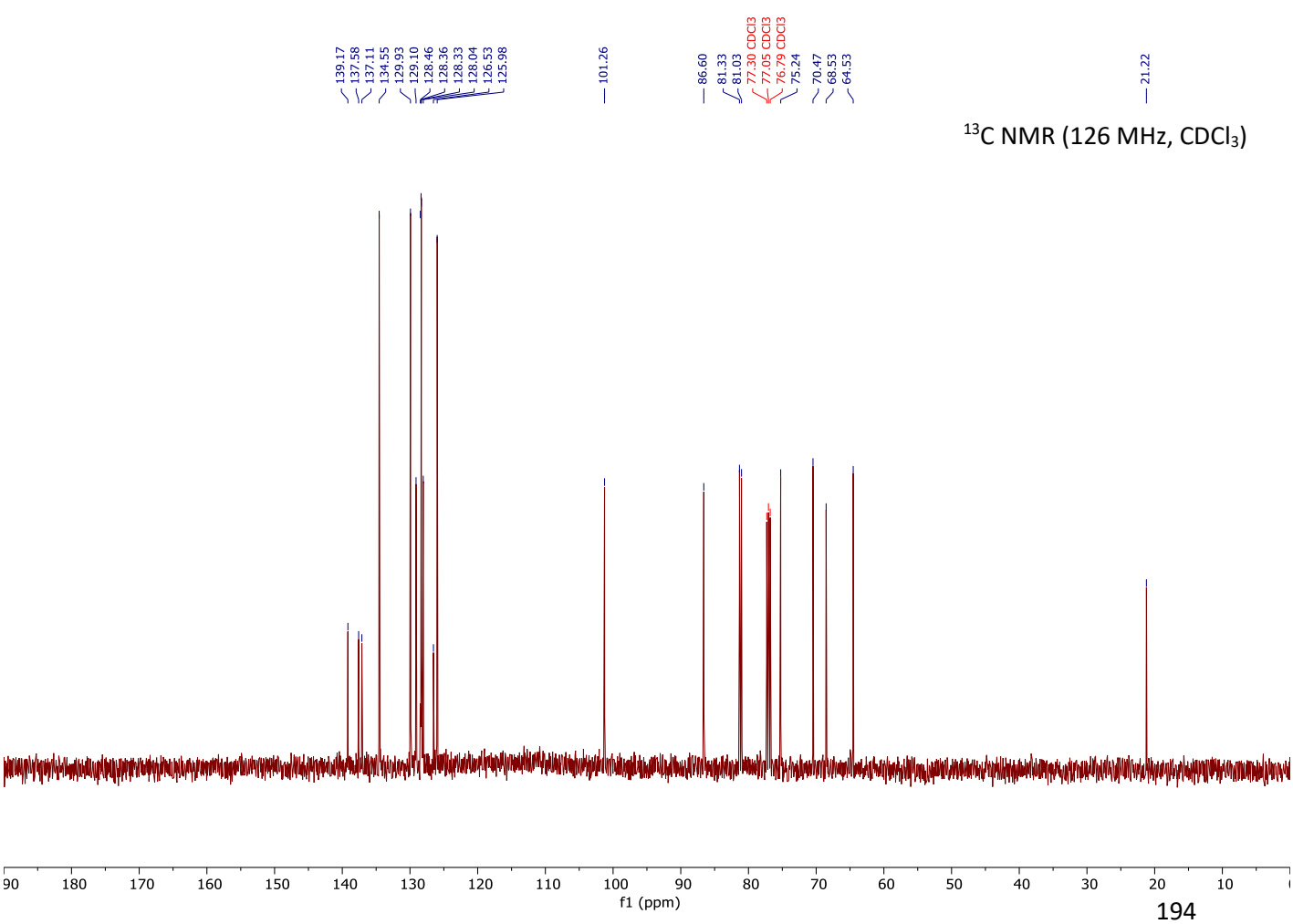

^{1}H NMR (500 MHz, $CDCl_3$)

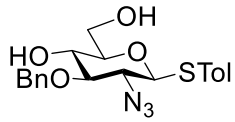

18

f1 (ppm)

^{13}C NMR (126 MHz, $CDCl_3$)

f1 (ppm)

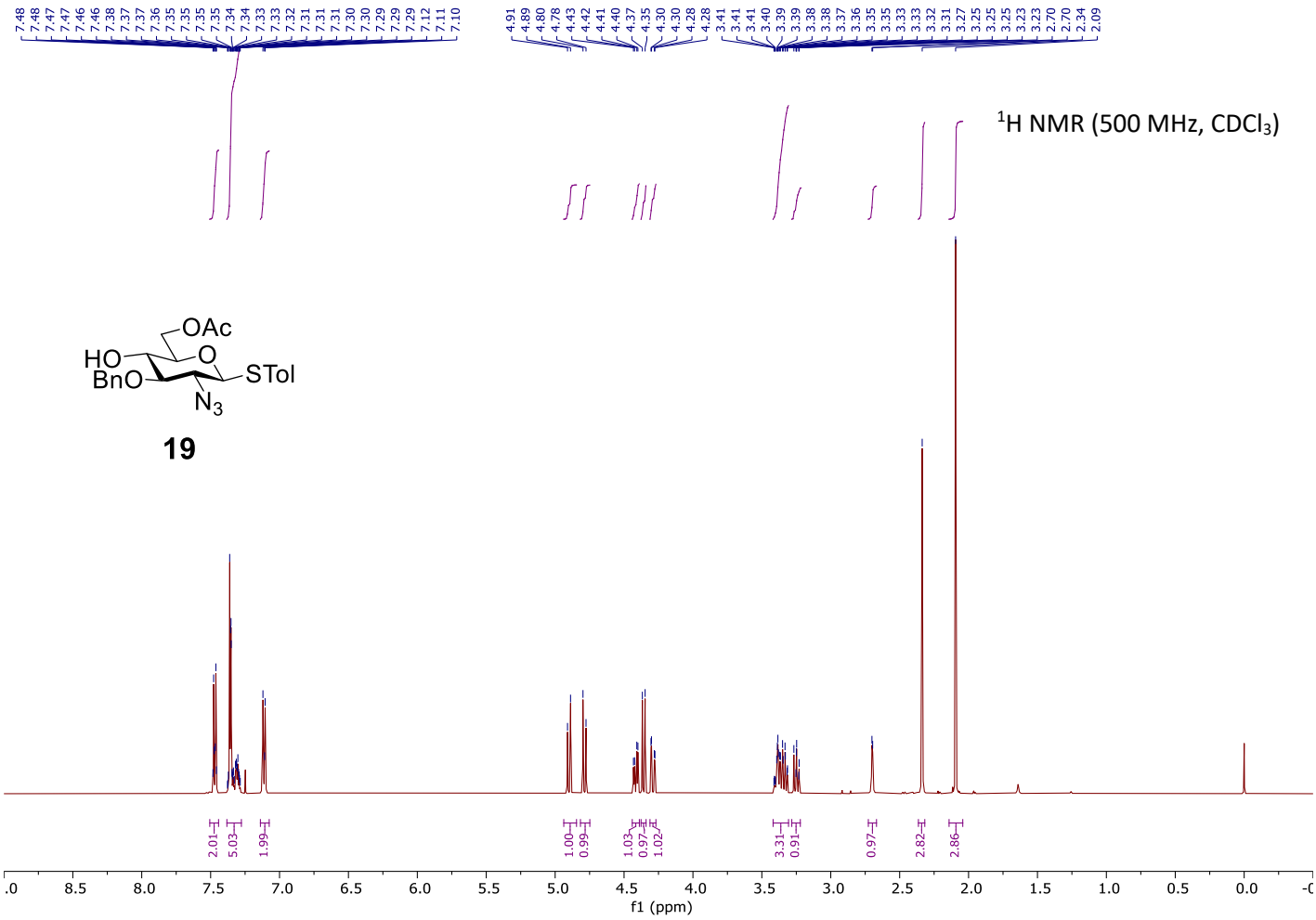

^{1}H NMR (500 MHz, $CDCl_3$)

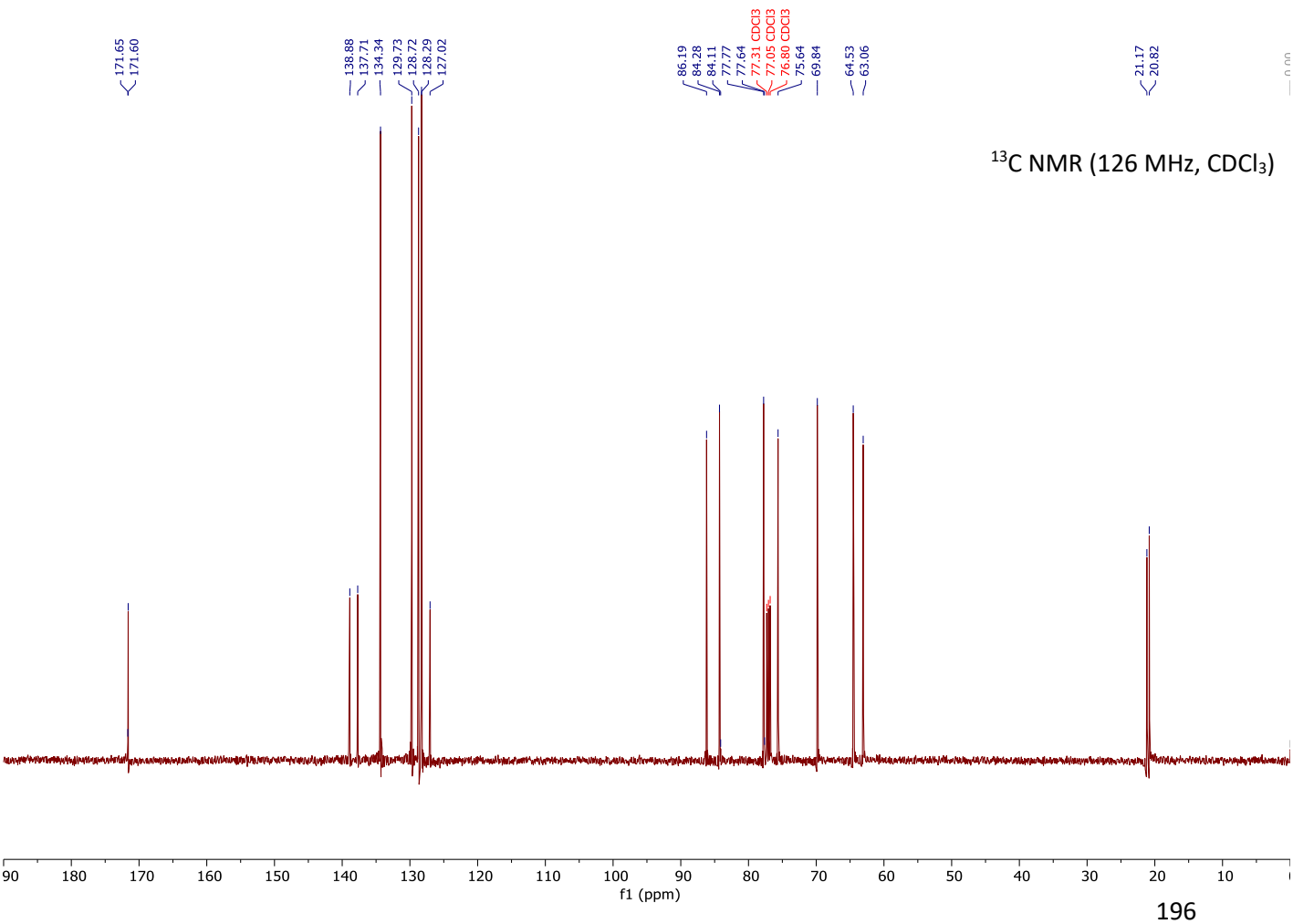

^{13}C NMR (126 MHz, $CDCl_3$)

^{1}H NMR (500 MHz, $CDCl_3$)

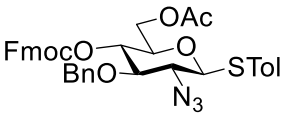

10

f1 (ppm)

^{13}C NMR (126 MHz, $CDCl_3$)

f1 (ppm)

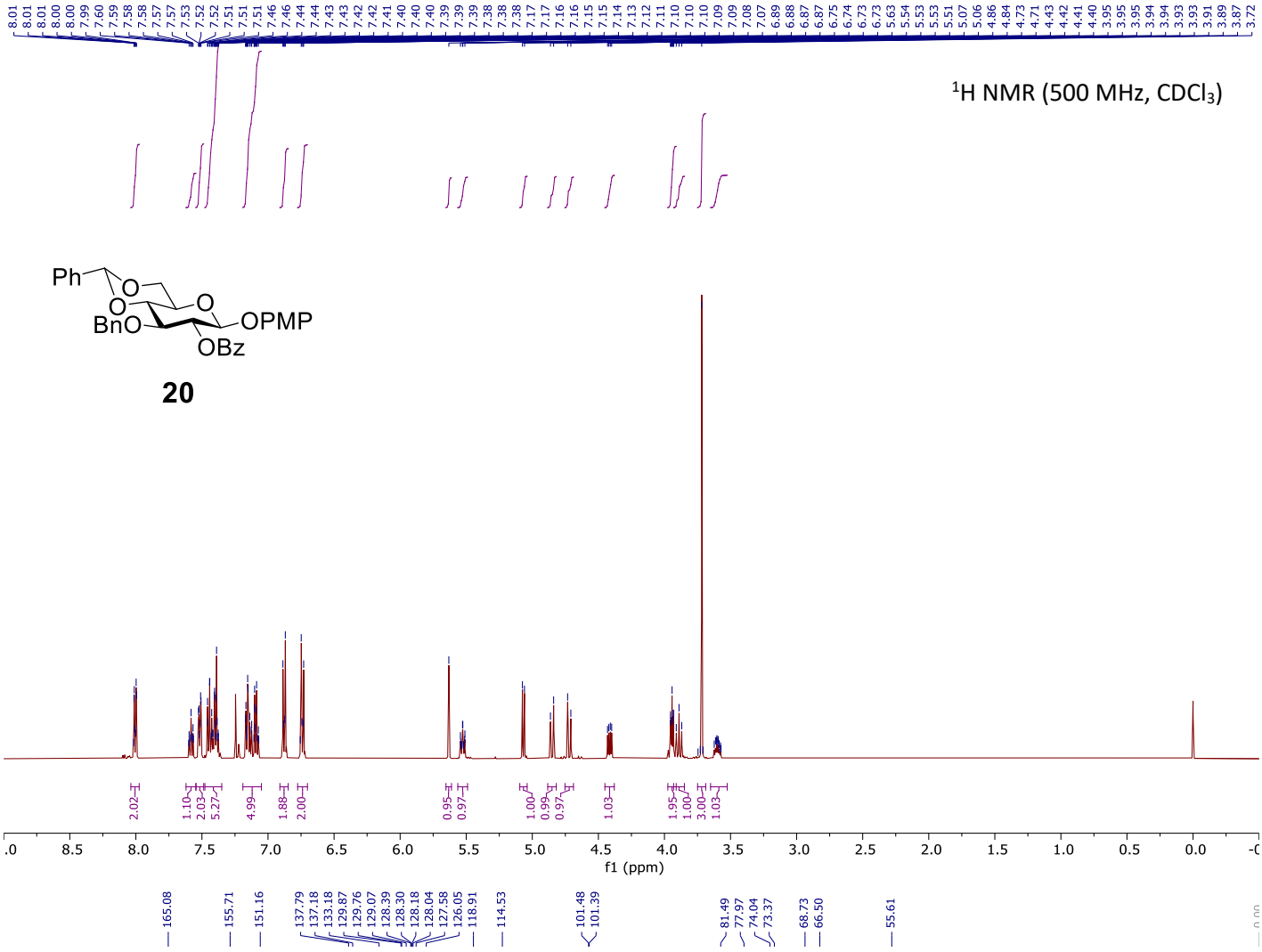

20

^{1}H NMR (500 MHz, $CDCl_3$)

^{13}C NMR (126 MHz, $CDCl_3$)

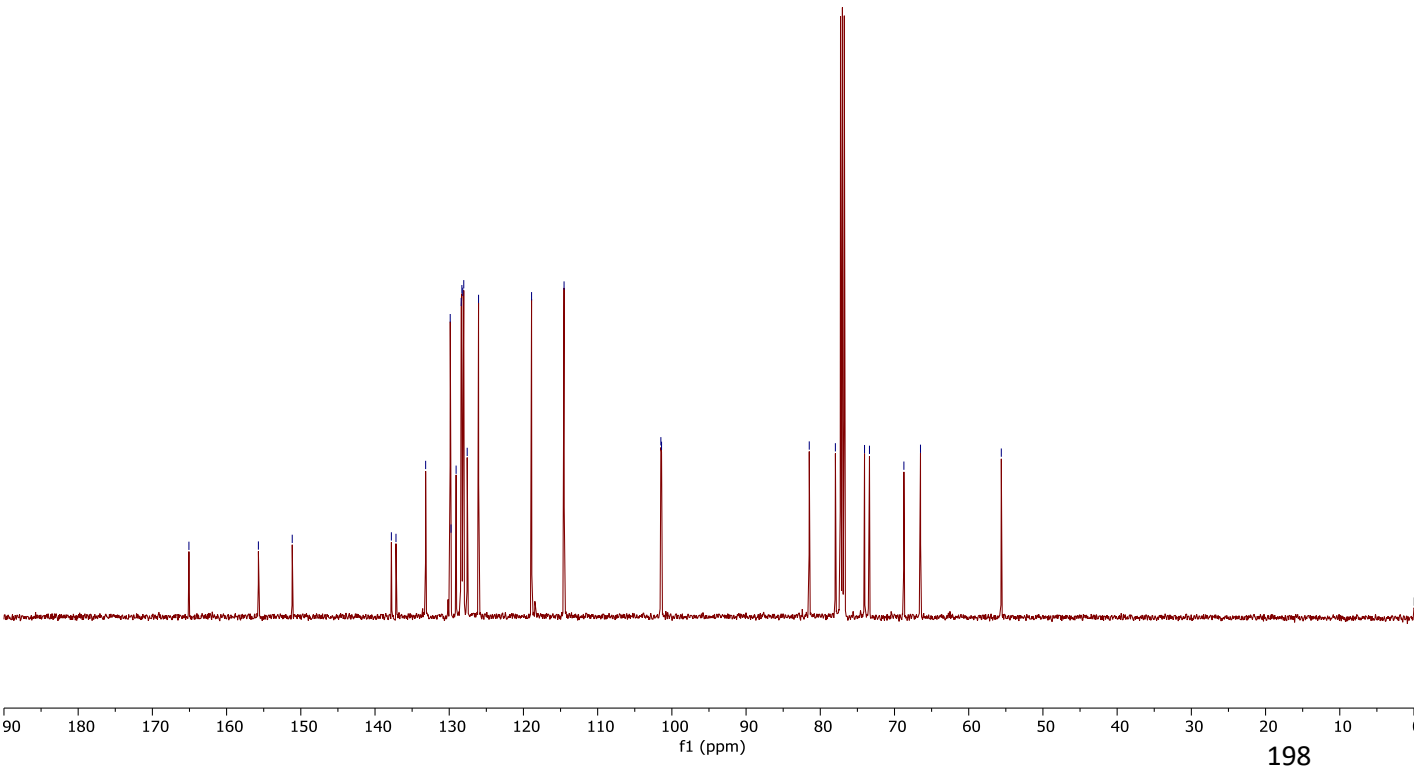

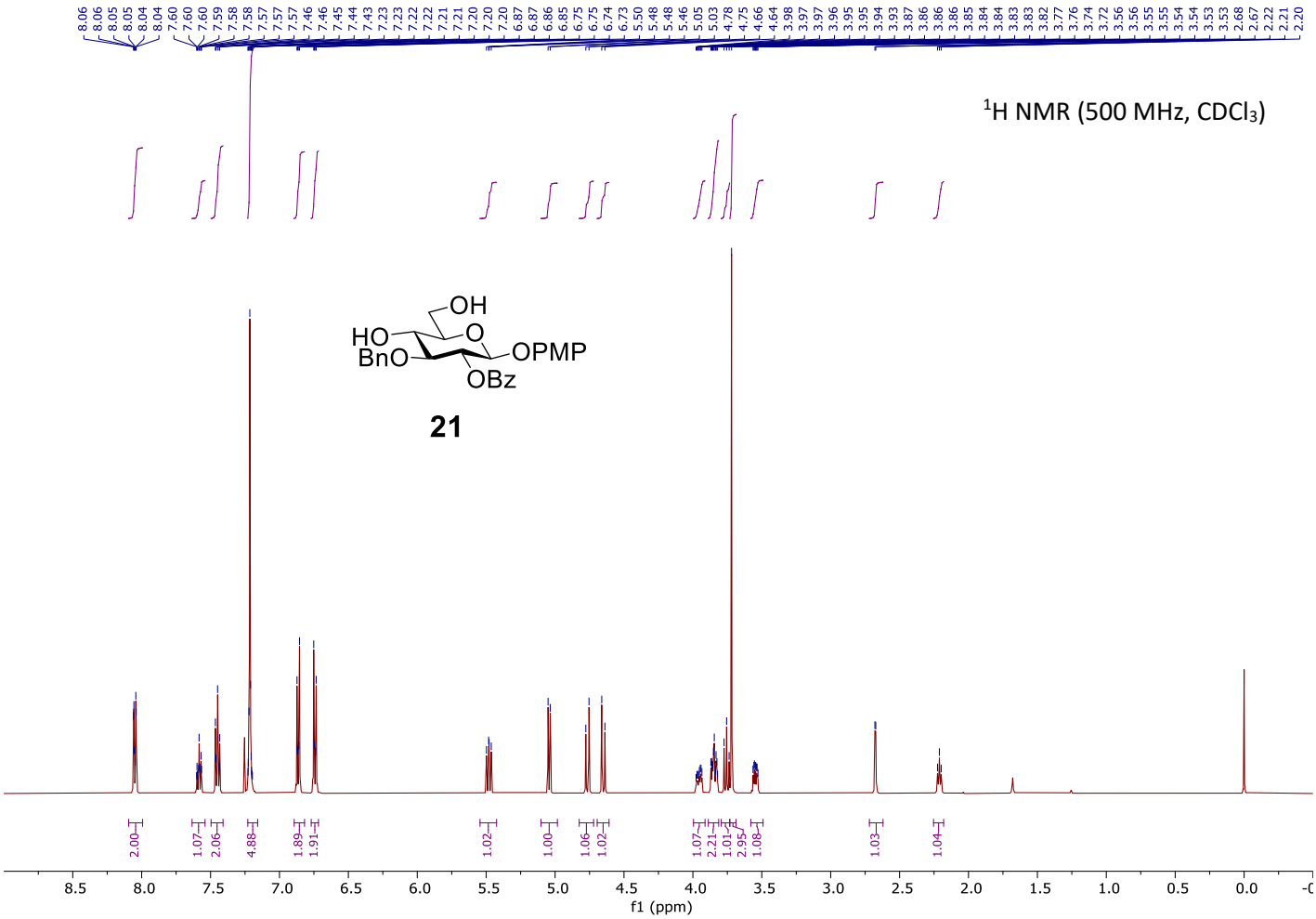

^{1}H NMR (500 MHz, $CDCl_3$)

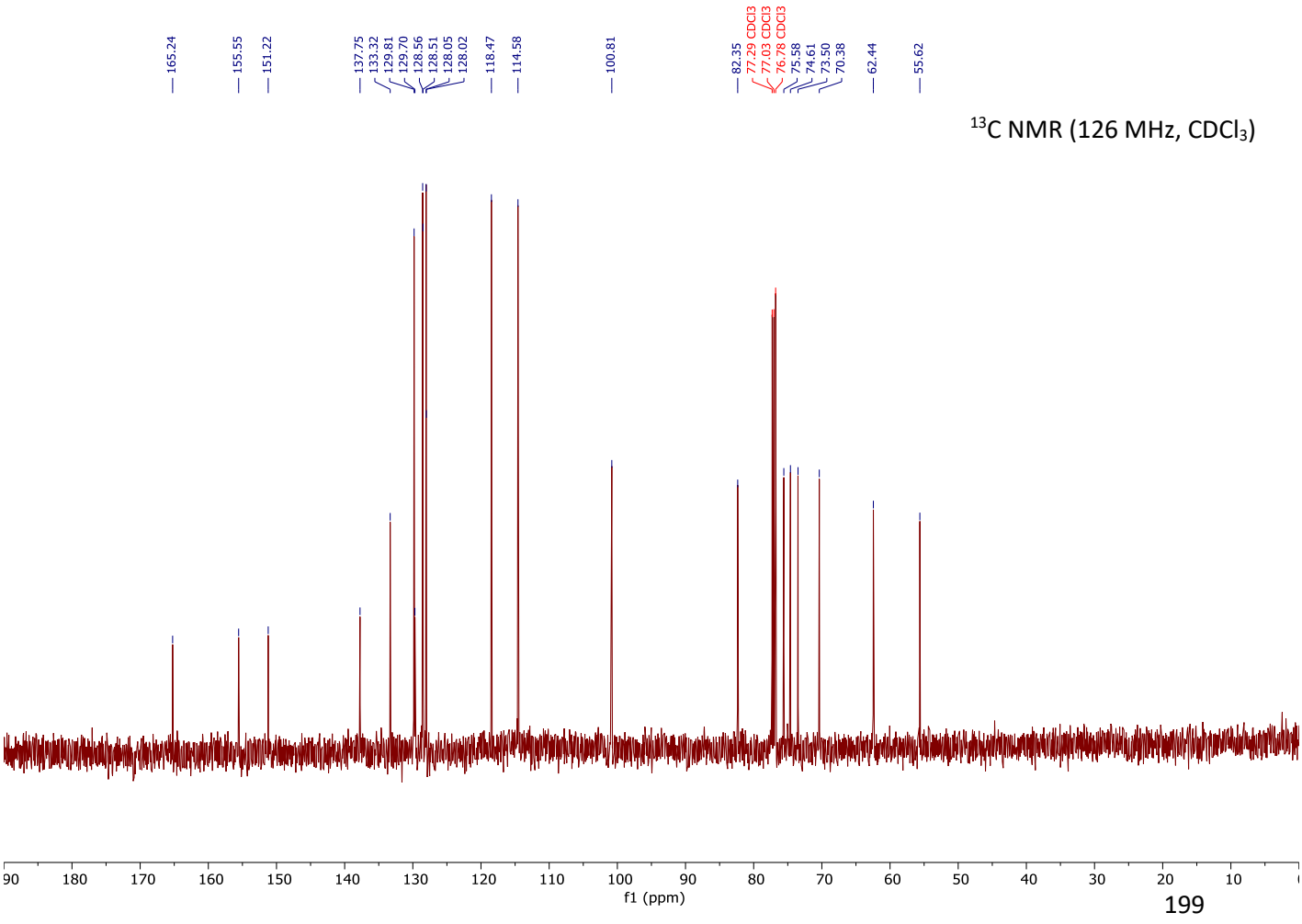

^{13}C NMR (126 MHz, $CDCl_3$)

^{1}H NMR (500 MHz, $CDCl_3$)

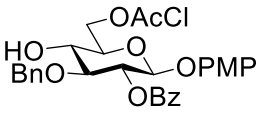

11

f1 (ppm)

^{13}C NMR (126 MHz, $CDCl_3$)

f1 (ppm)

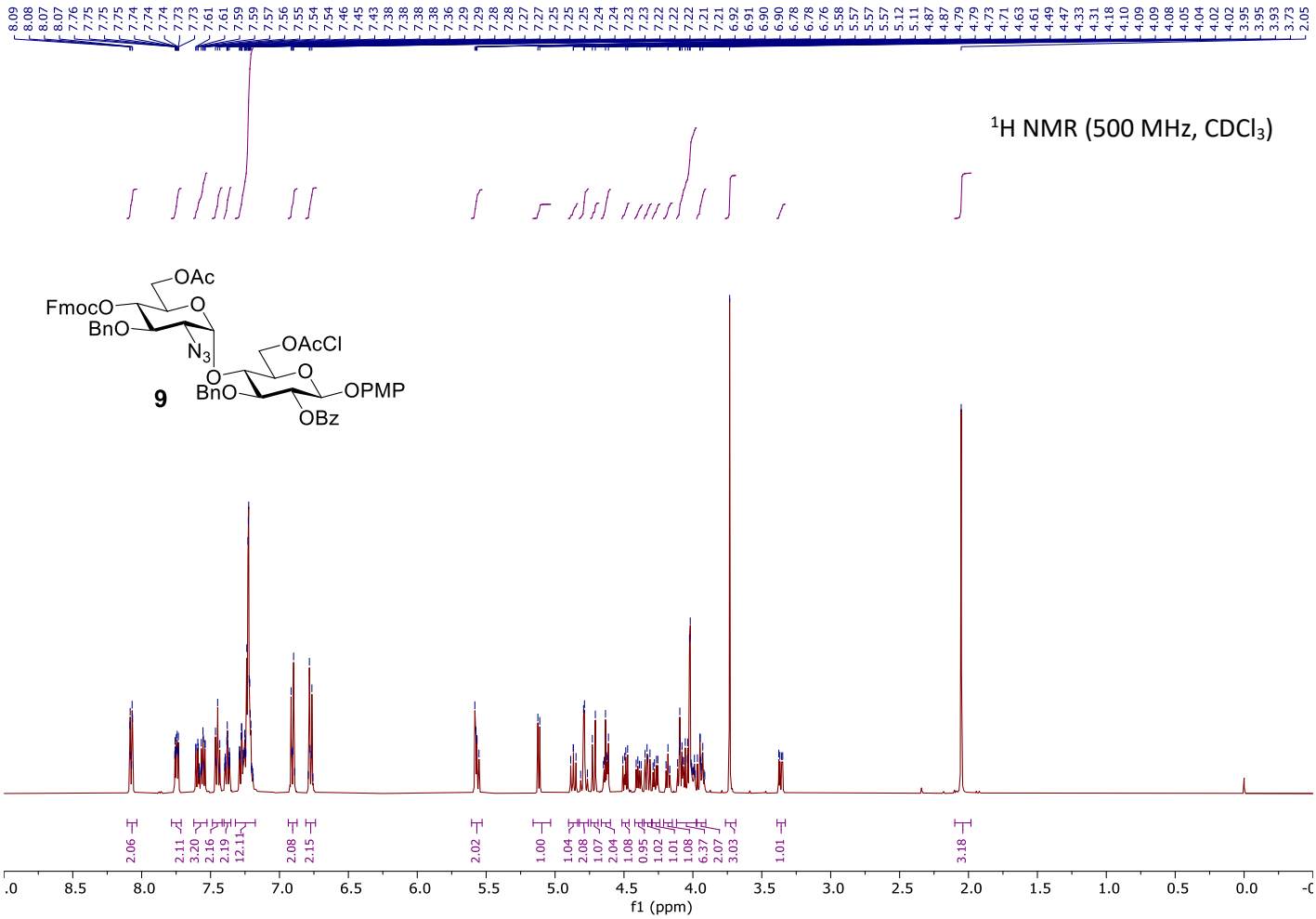
^{1}H NMR (500 MHz, $CDCl_3$)
OAc
FmocO
O
BnO
N_3
OAcCl
O
O
BnO
OPMP
OBz
9
f1 (ppm)

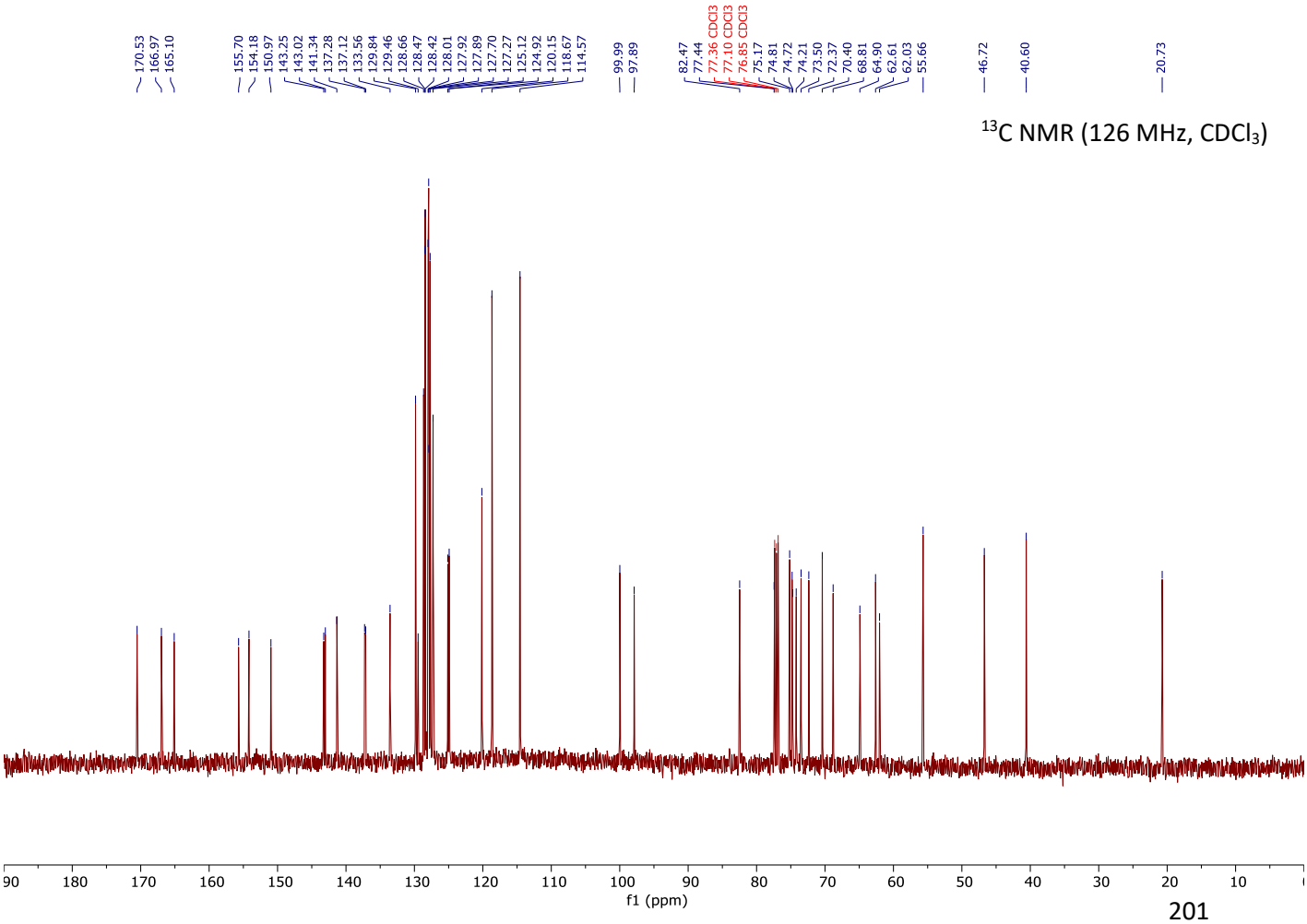
^{13}C NMR (126 MHz, $CDCl_3$)
f1 (ppm)

^{1}H NMR (500 MHz, $CDCl_3$)

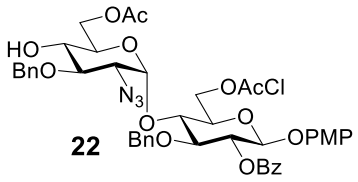

22

f1 (ppm)

^{13}C NMR (126 MHz, $CDCl_3$)

f1 (ppm)

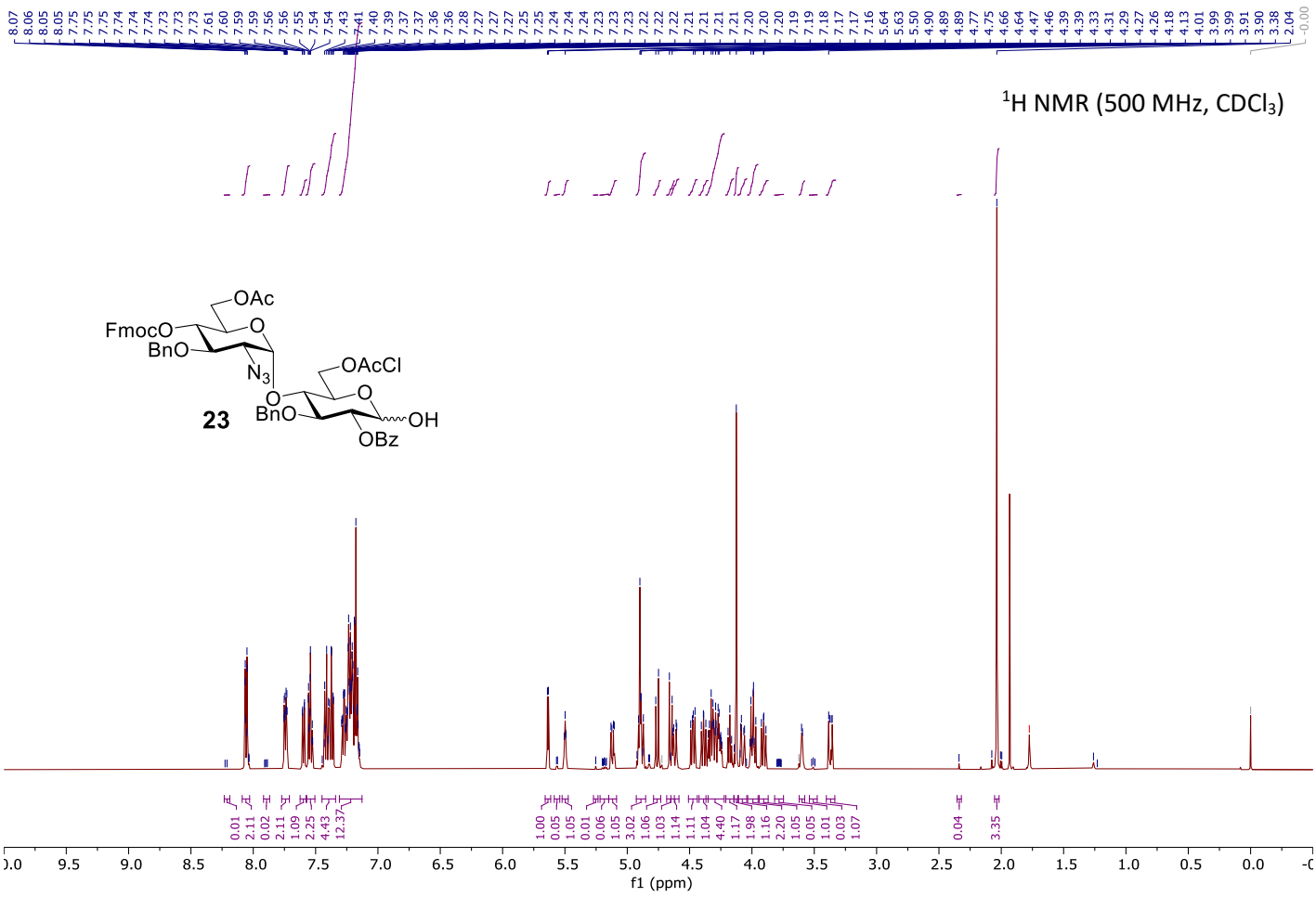
^{1}H NMR (500 MHz, $CDCl_3$)
OAc
FmocO
BnO
N_3
OAcCl
O
BnO
OH
OBz
23
f1 (ppm)

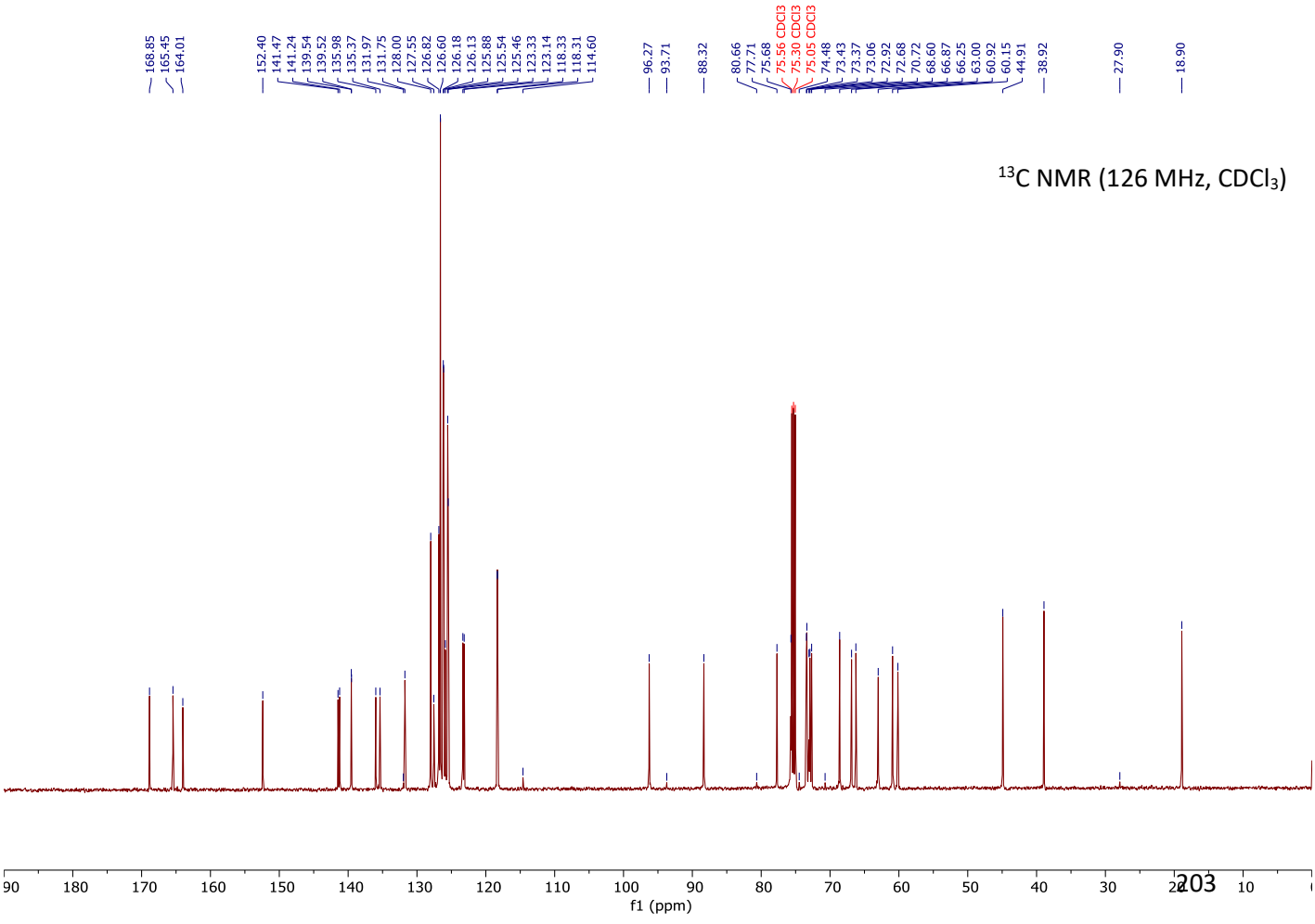
^{13}C NMR (126 MHz, $CDCl_3$)
f1 (ppm)

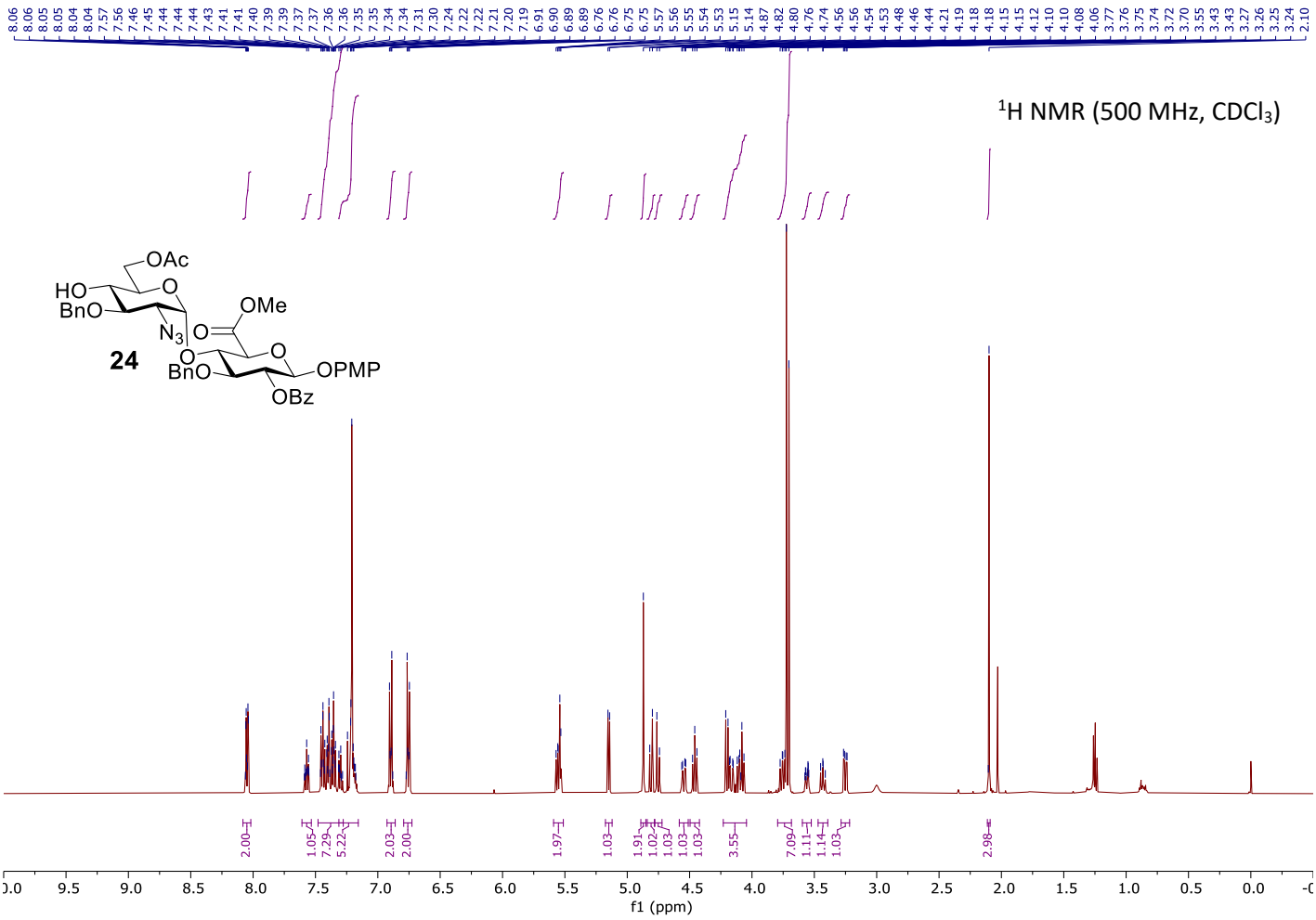

^{1}H NMR (500 MHz, $CDCl_3$)

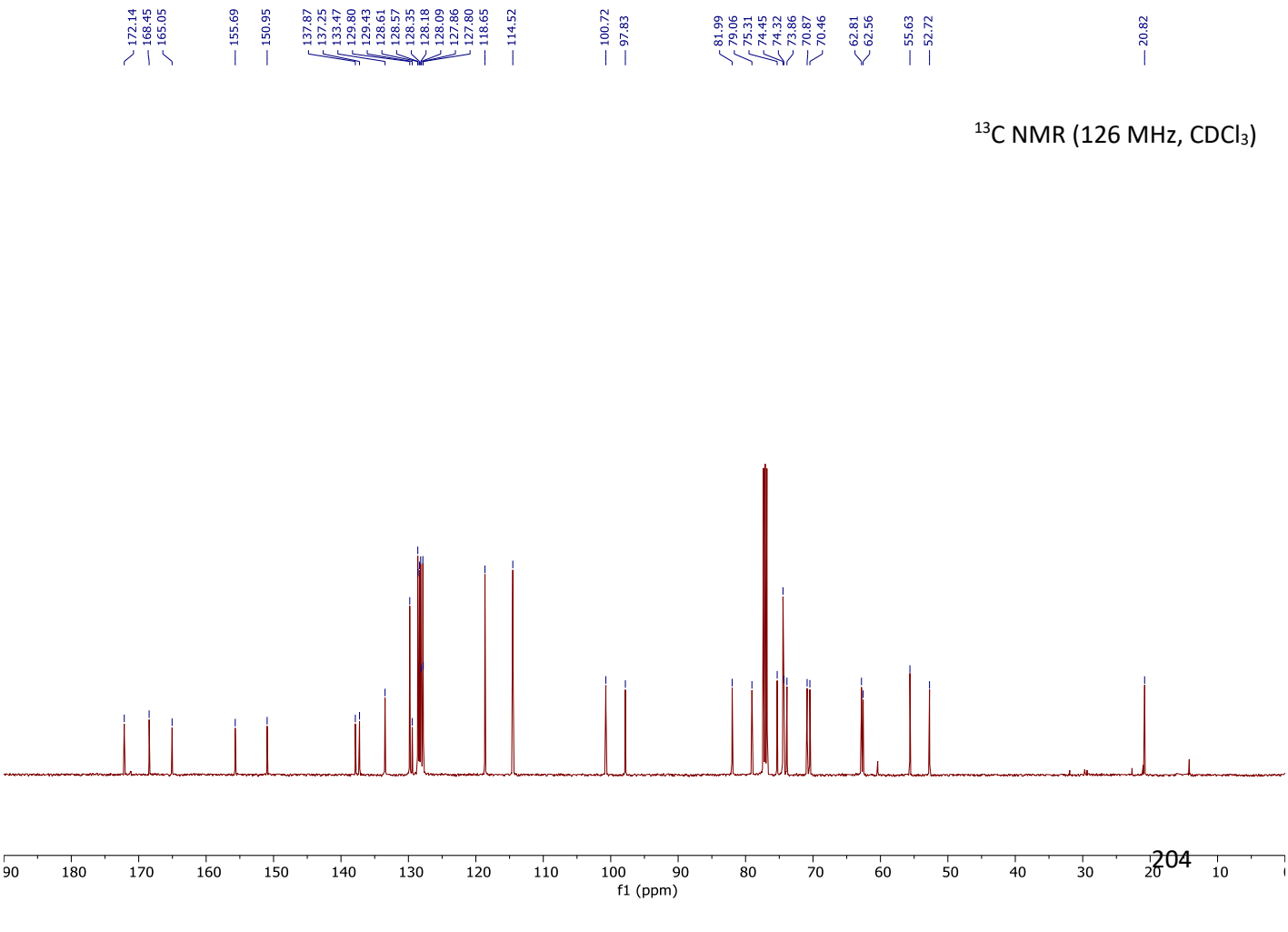

^{13}C NMR (126 MHz, $CDCl_3$)

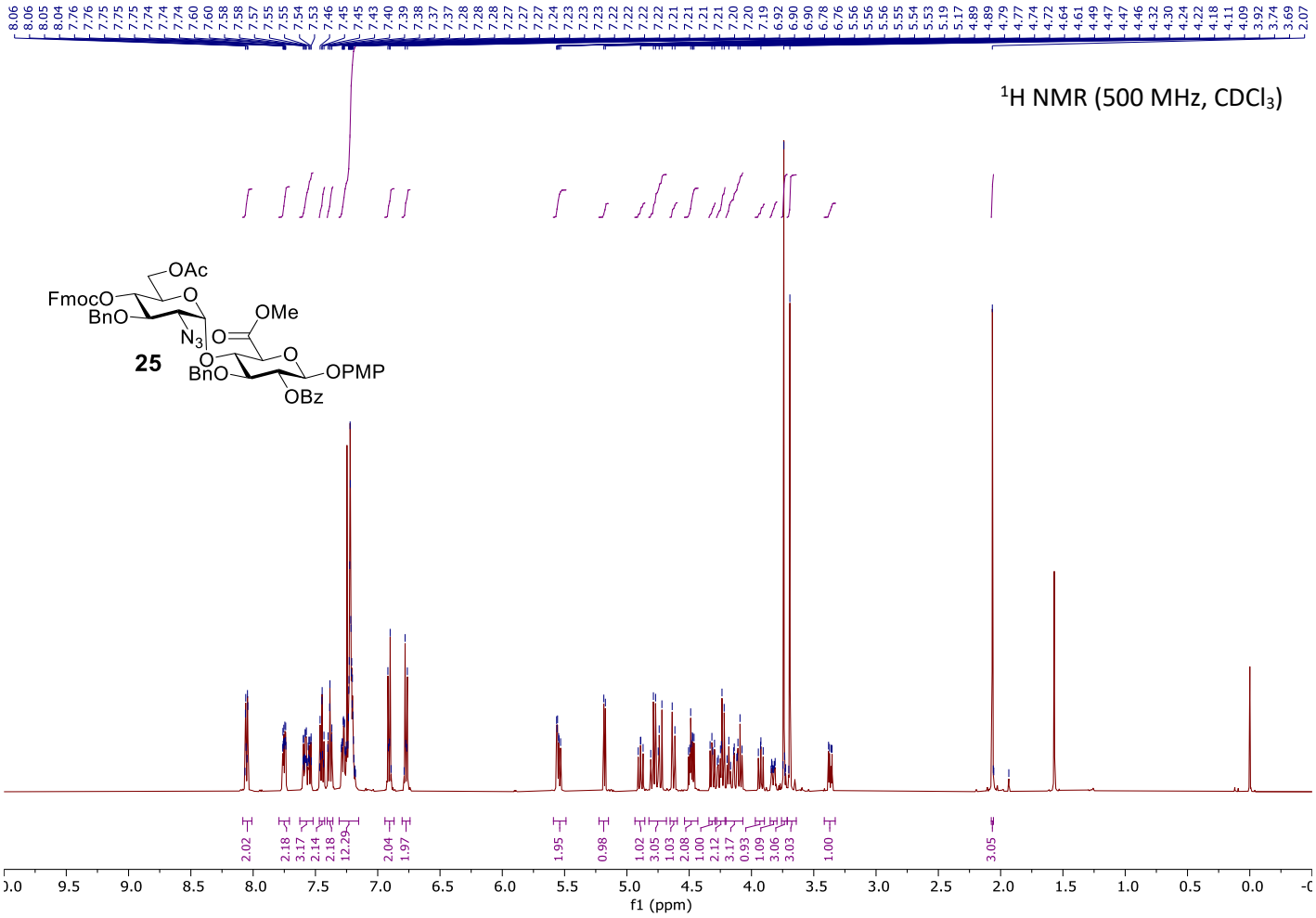
^{1}H NMR (500 MHz, $CDCl_3$)
OAc
FmocO
BnO
O
OMe
N_3
O
O
O
BnO
OPMP
OBz
25
f1 (ppm)

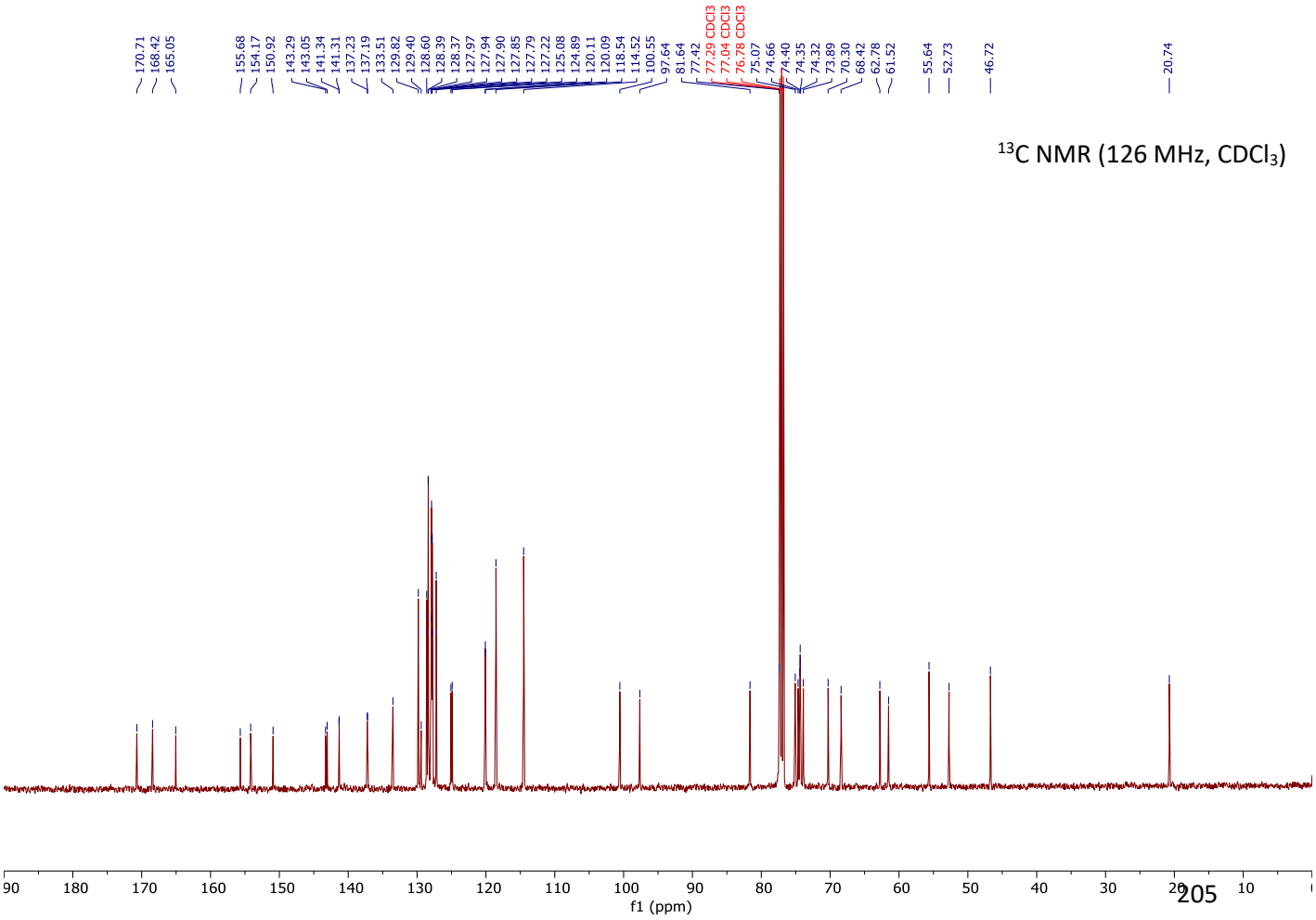
^{13}C NMR (126 MHz, $CDCl_3$)
f1 (ppm)

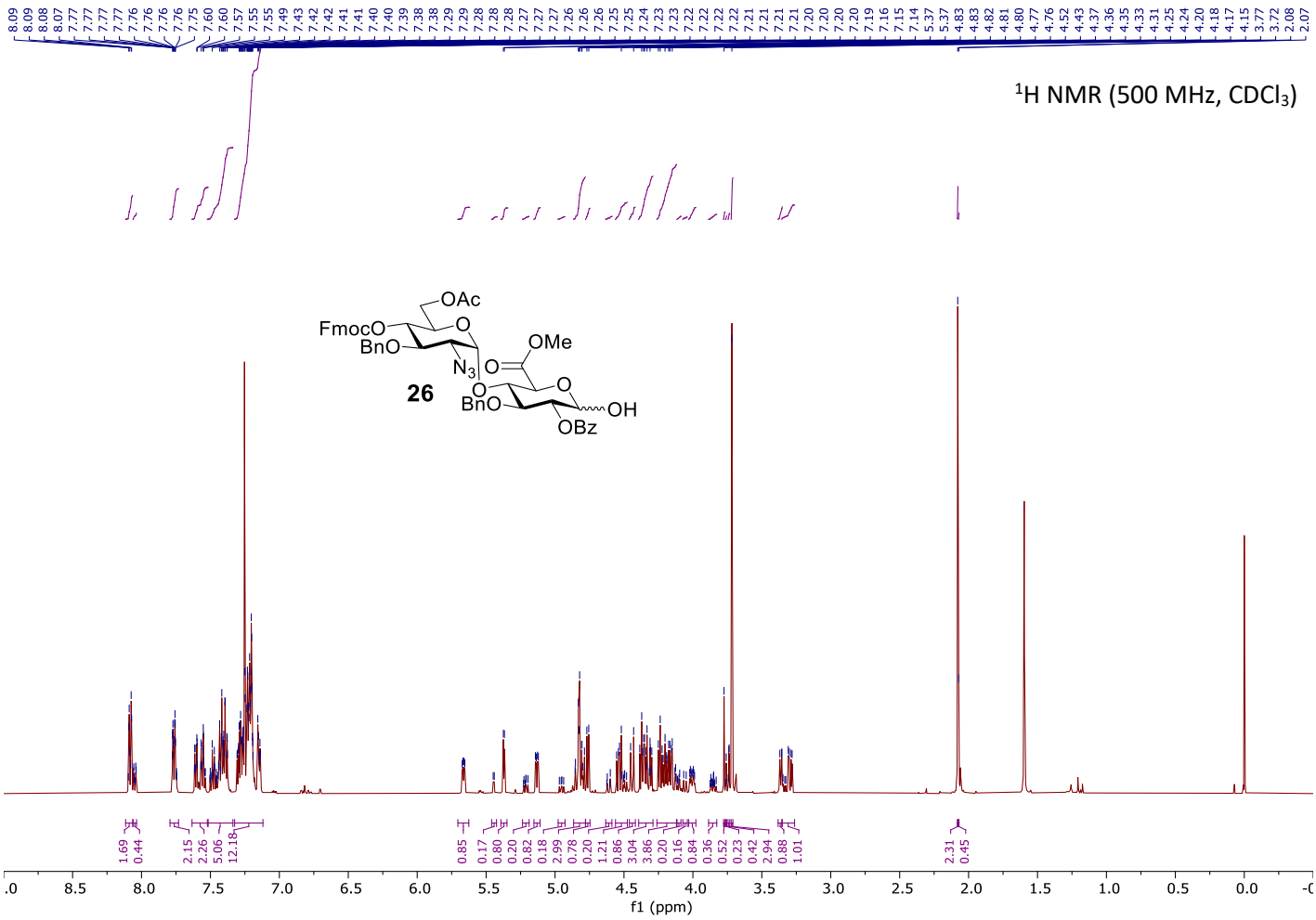

^{1}H NMR (500 MHz, $CDCl_3$)

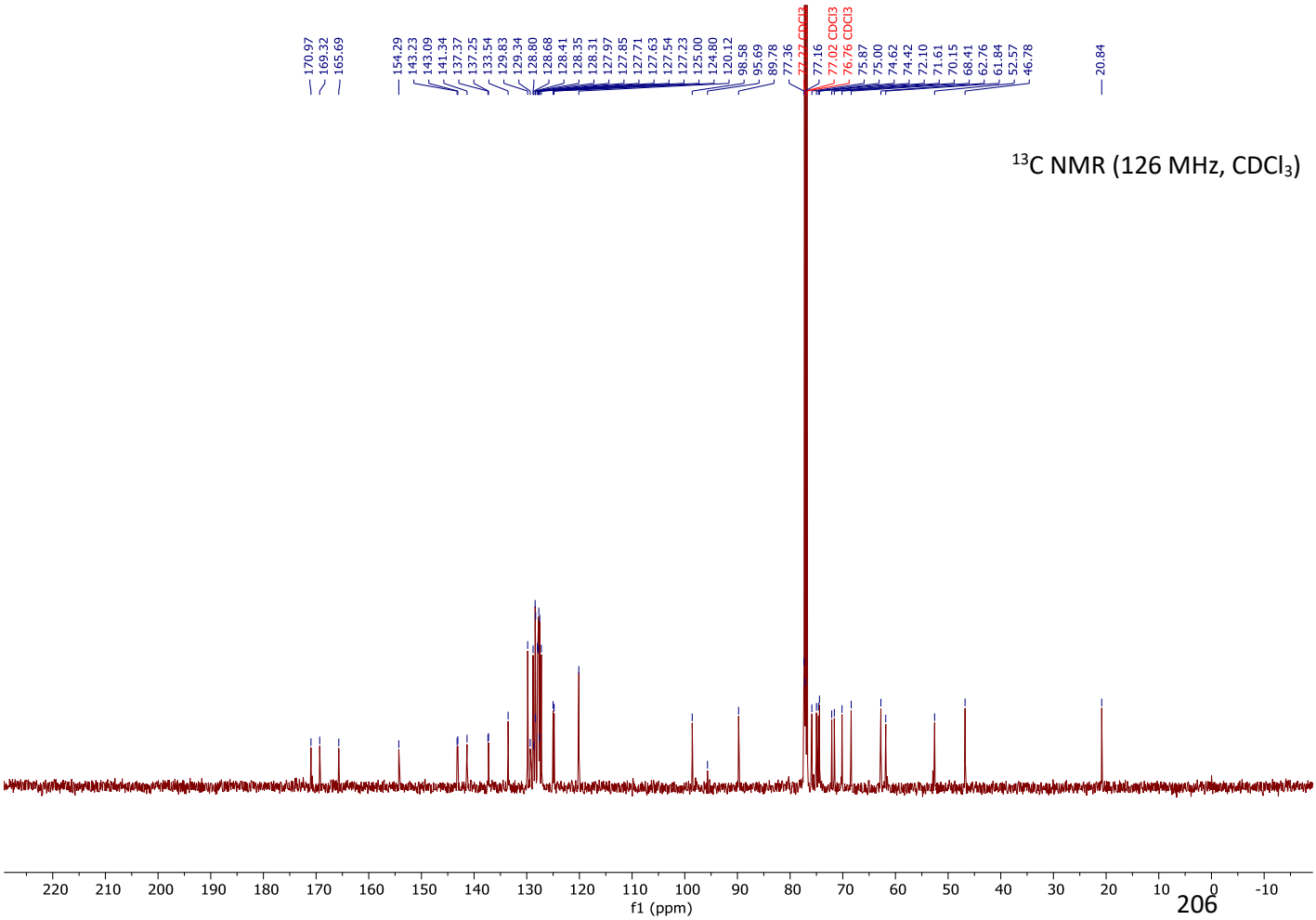

^{13}C NMR (126 MHz, $CDCl_3$)

^{1}H NMR (500 MHz, $CDCl_3$)

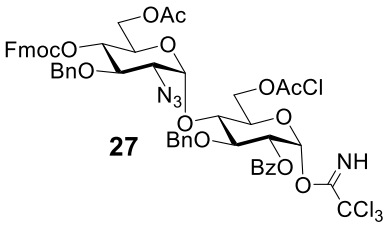

27

^{13}C NMR (126 MHz, $CDCl_3$)

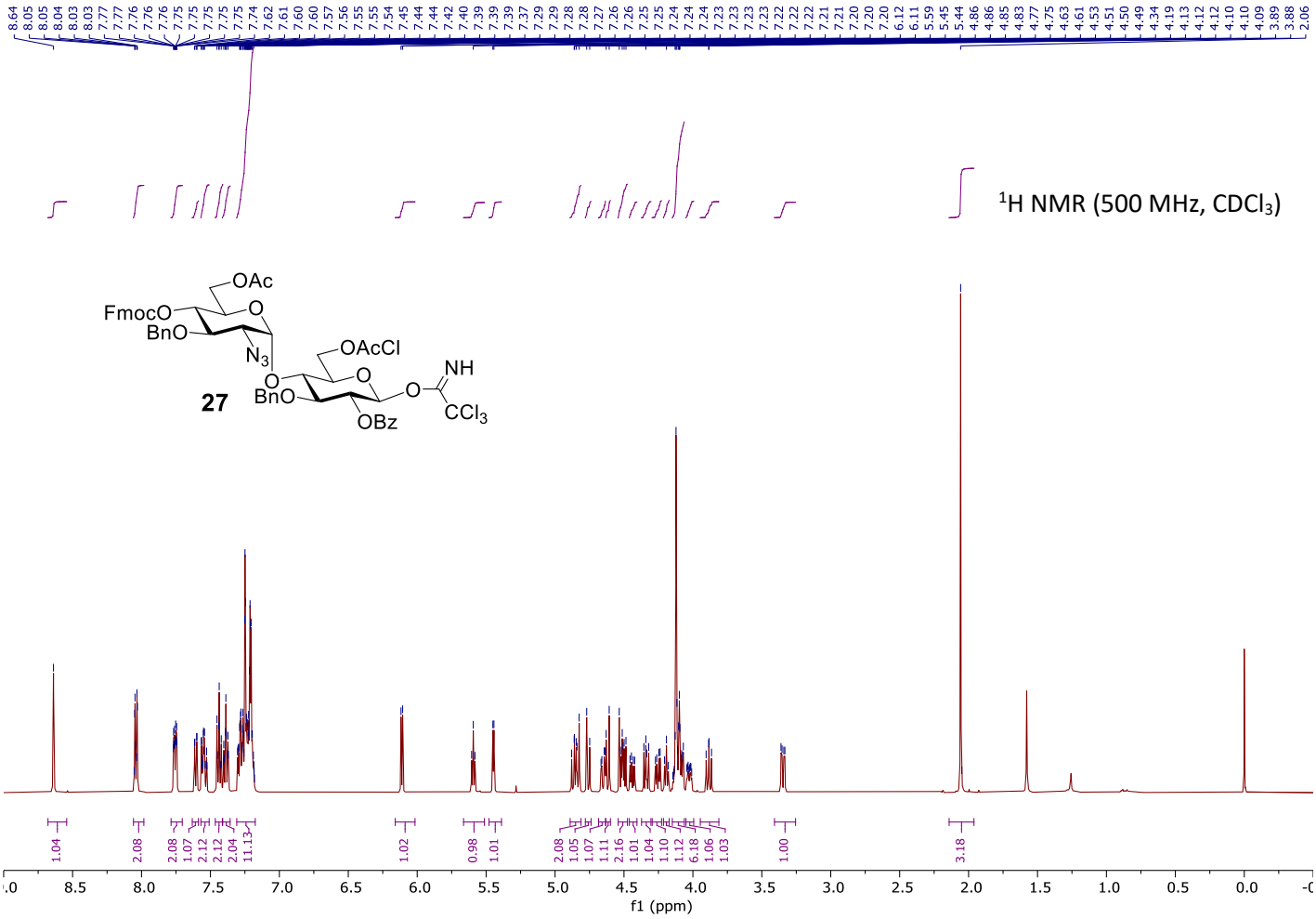

^{1}H NMR (500 MHz, $CDCl_3$)

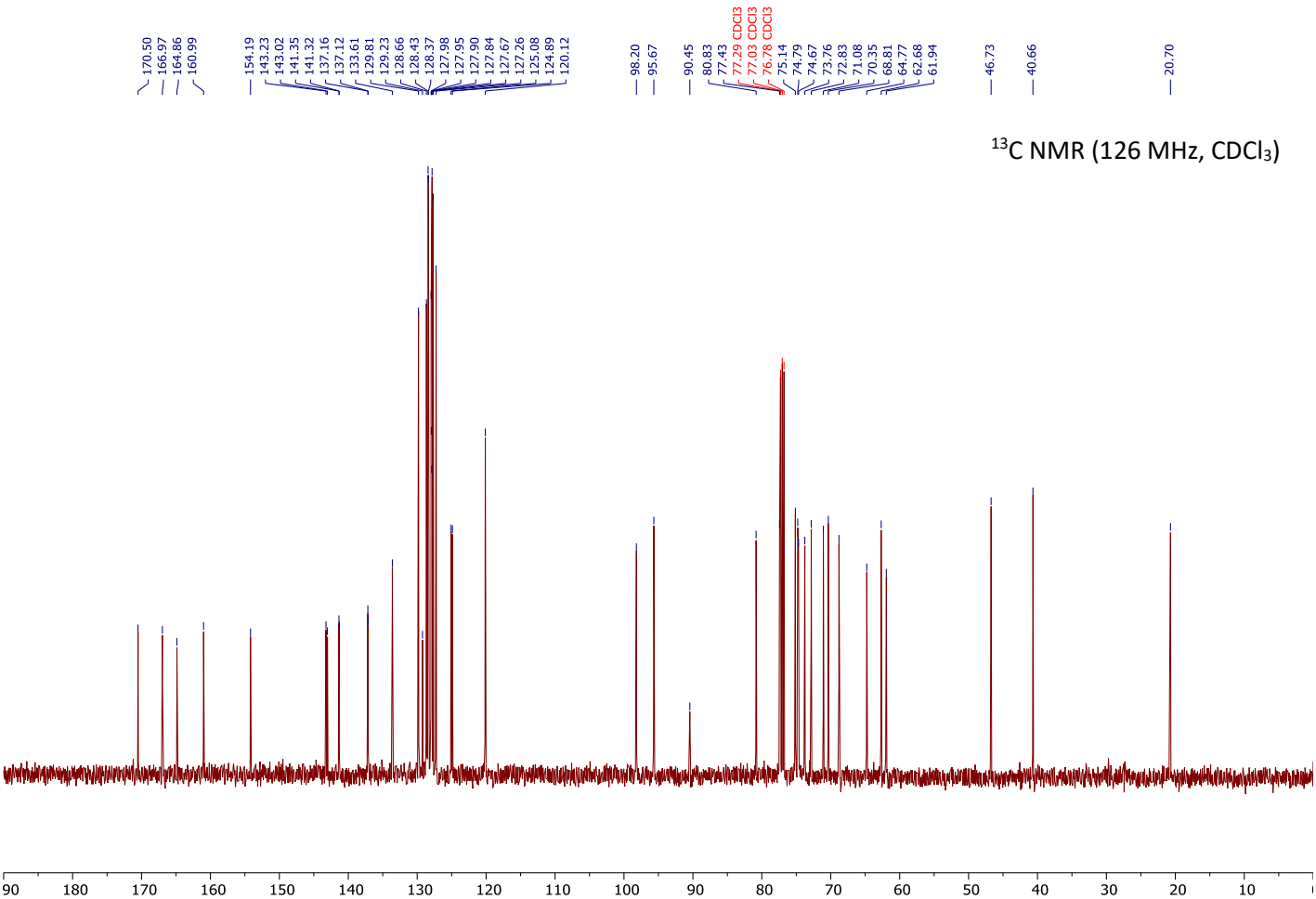

^{13}C NMR (126 MHz, $CDCl_3$)

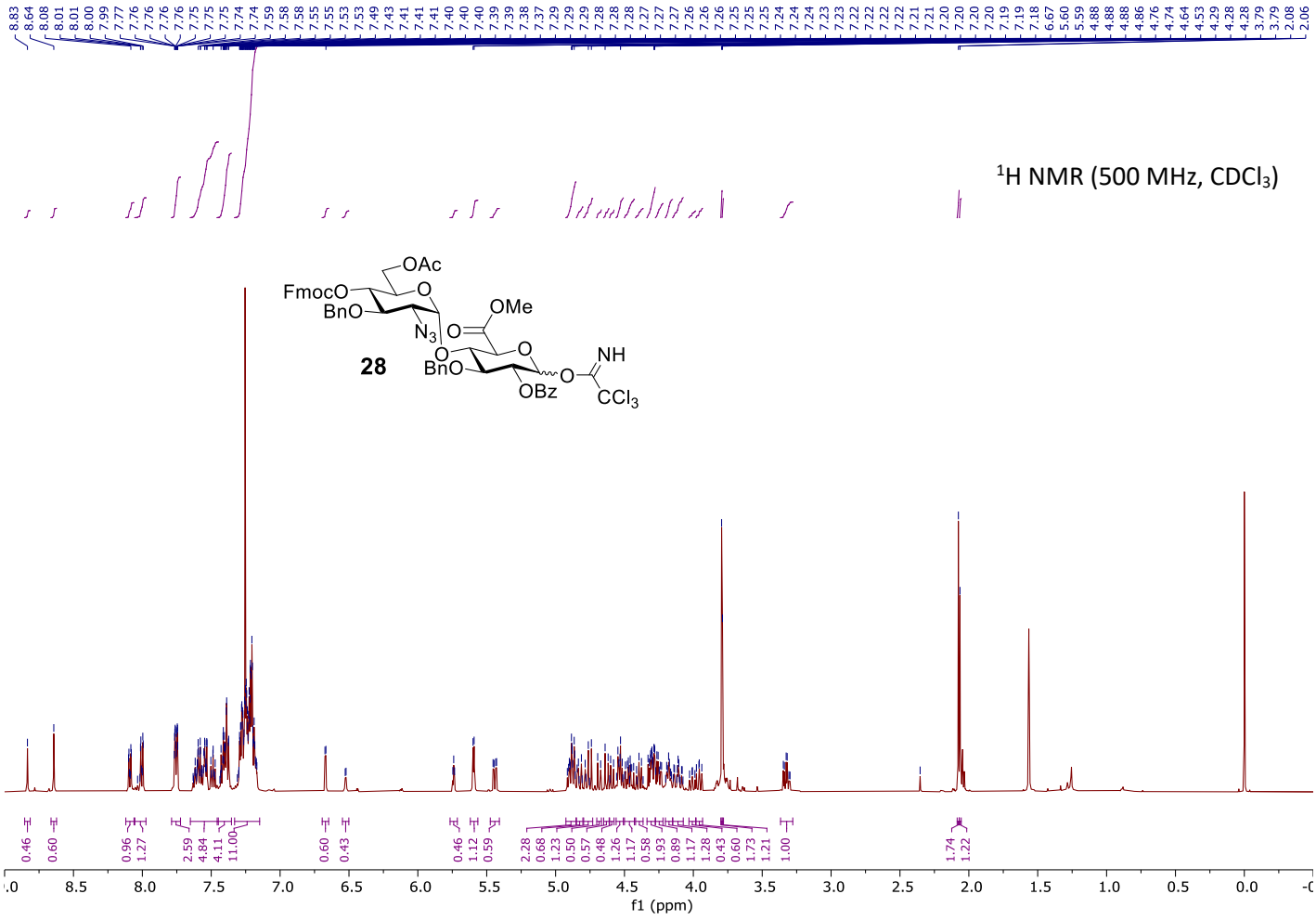

^{1}H NMR (500 MHz, $CDCl_3$)

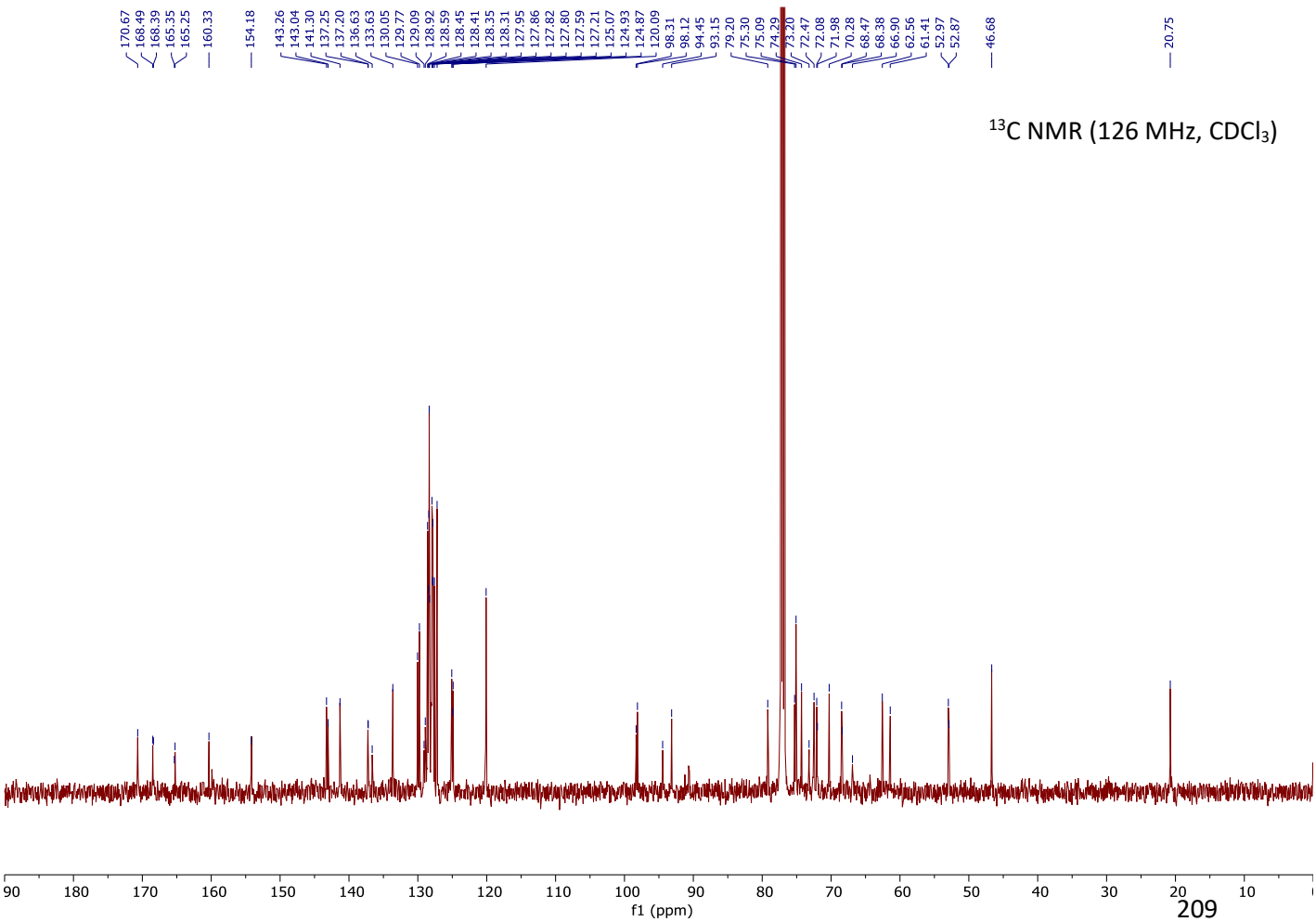

^{13}C NMR (126 MHz, $CDCl_3$)

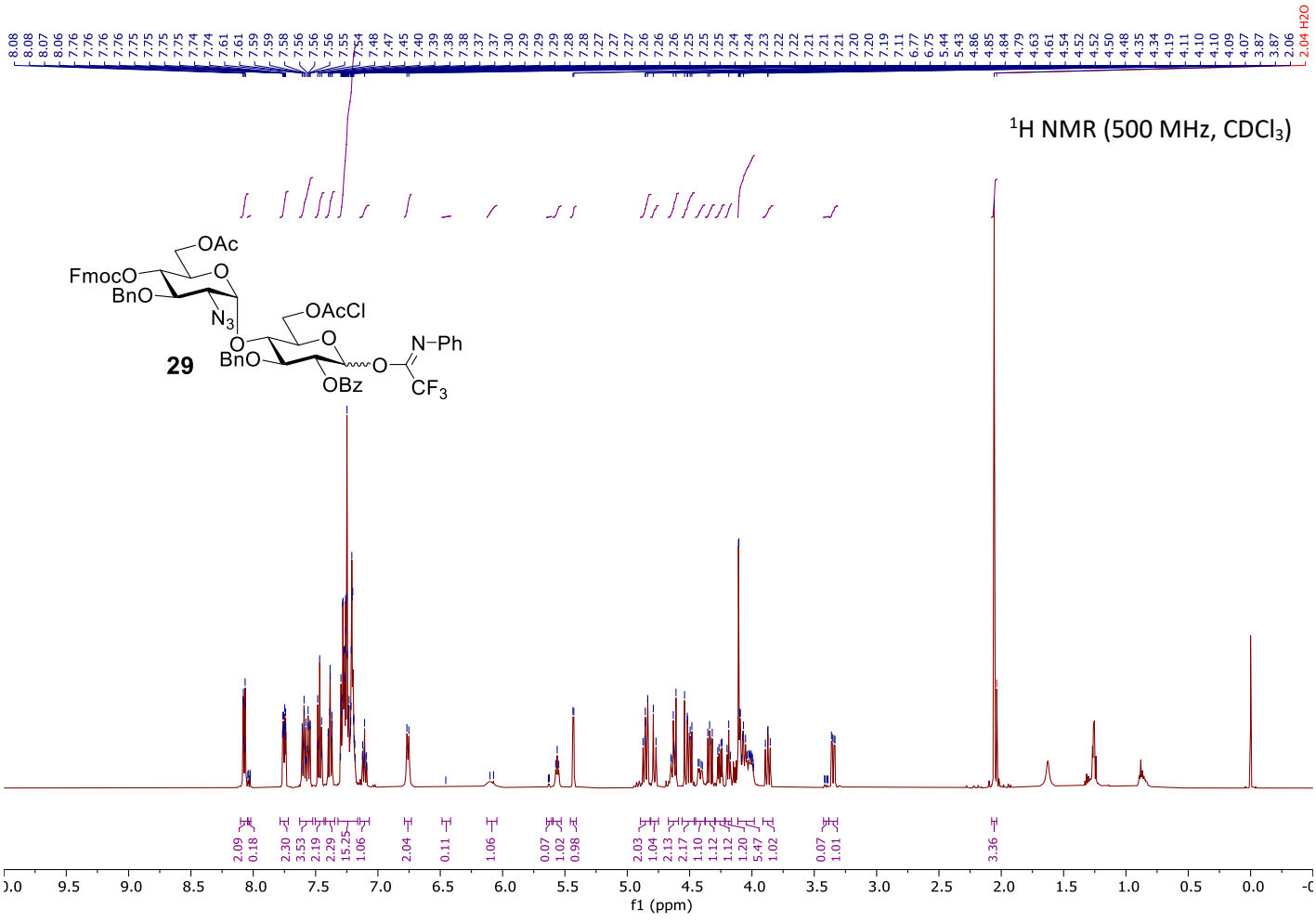
^{1}H NMR (500 MHz, $CDCl_3$)
OAc
FmocO
BnO
N_3
OAcCl
O
BnO
N–Ph
O
OBz
CF_3
29
f1 (ppm)

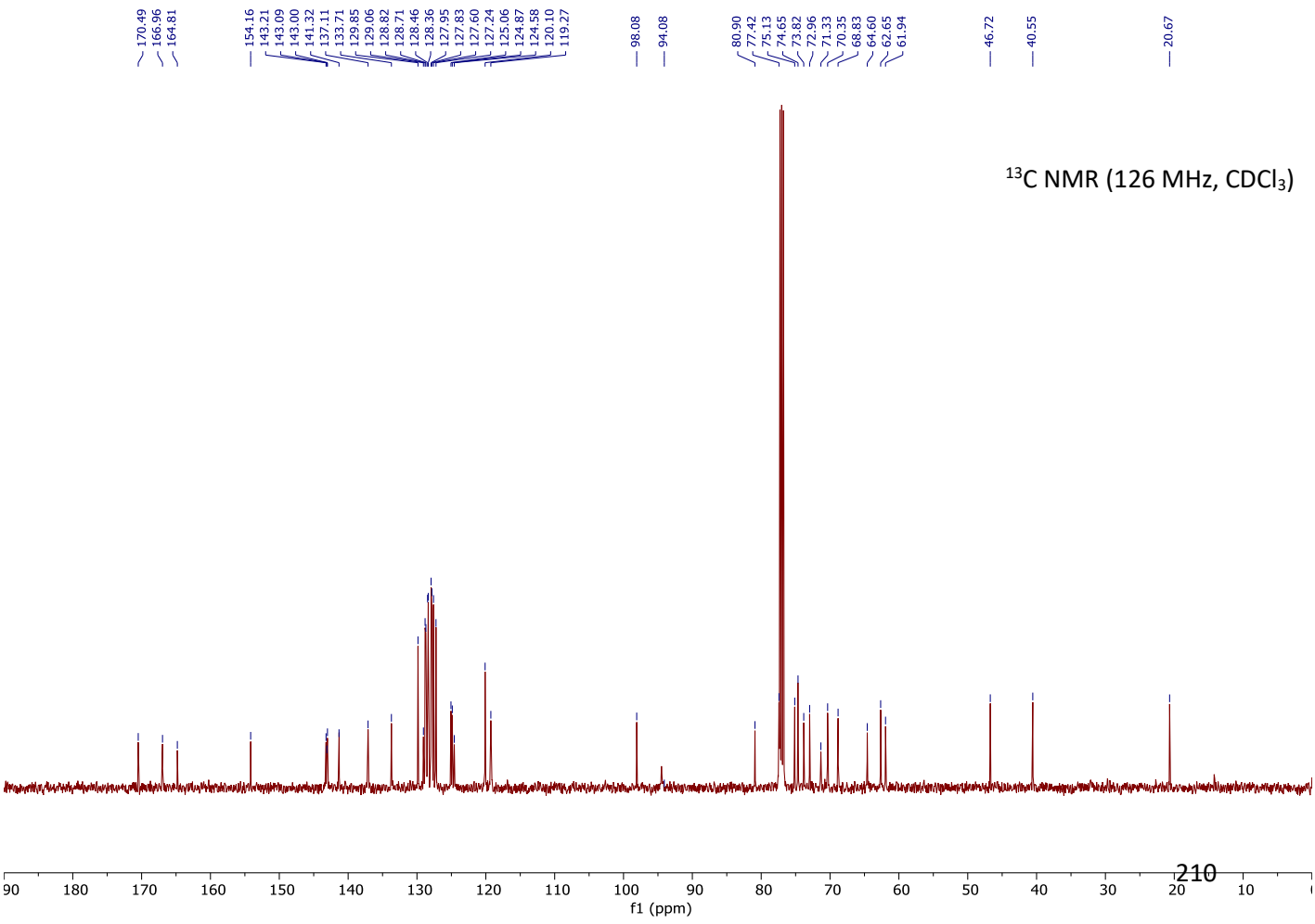
^{13}C NMR (126 MHz, $CDCl_3$)
f1 (ppm)

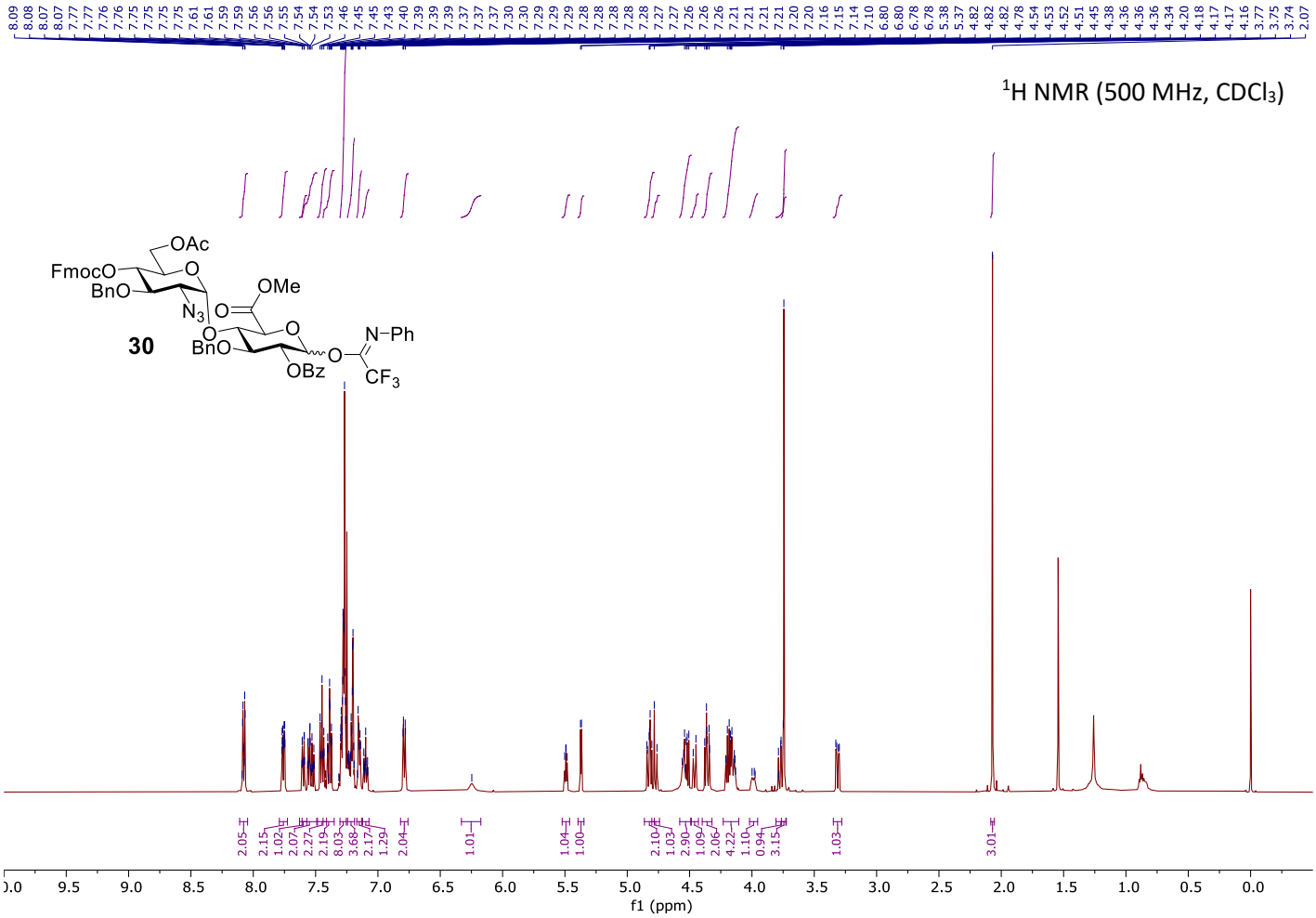

^{1}H NMR (500 MHz, $CDCl_3$)

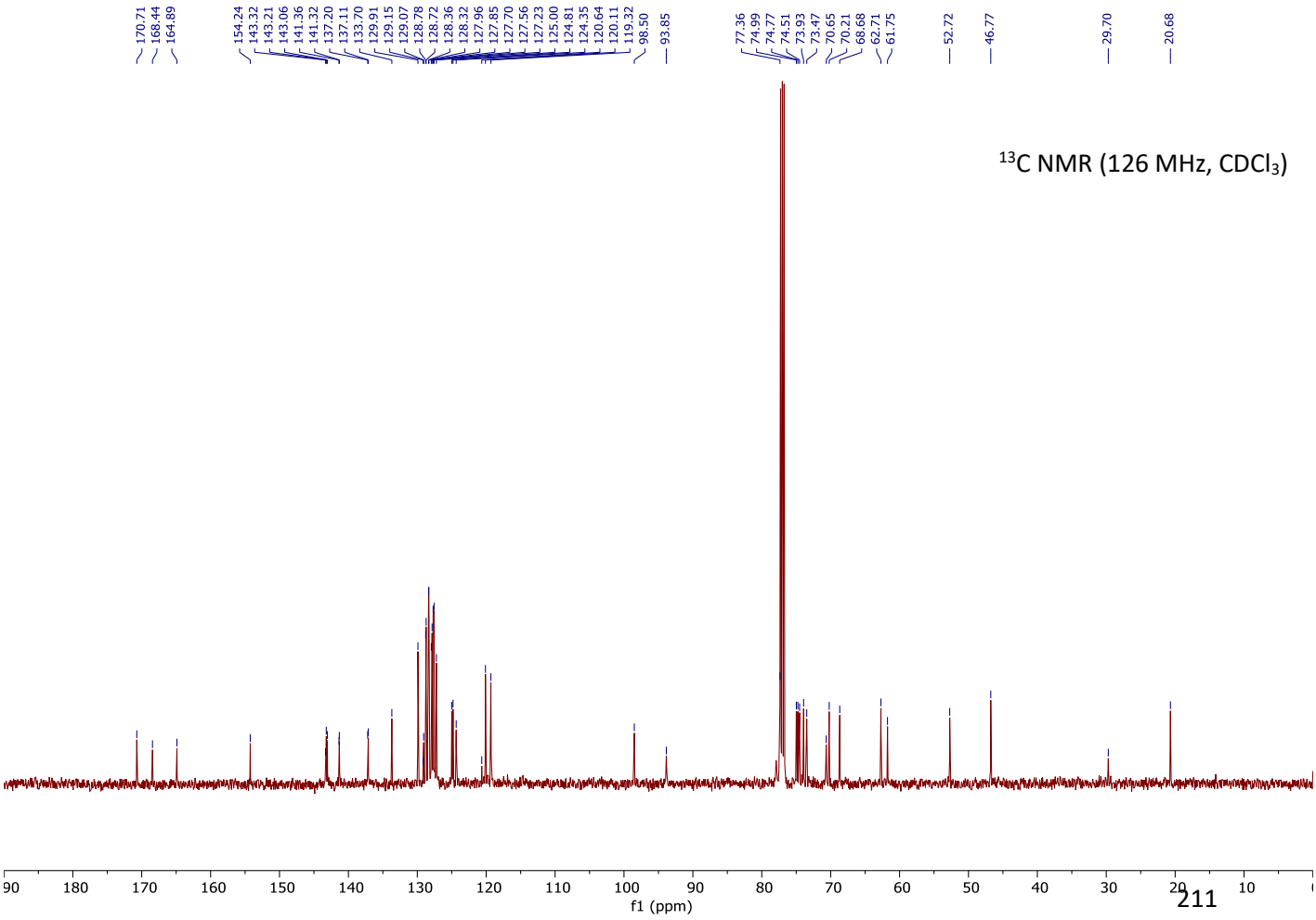

^{13}C NMR (126 MHz, $CDCl_3$)

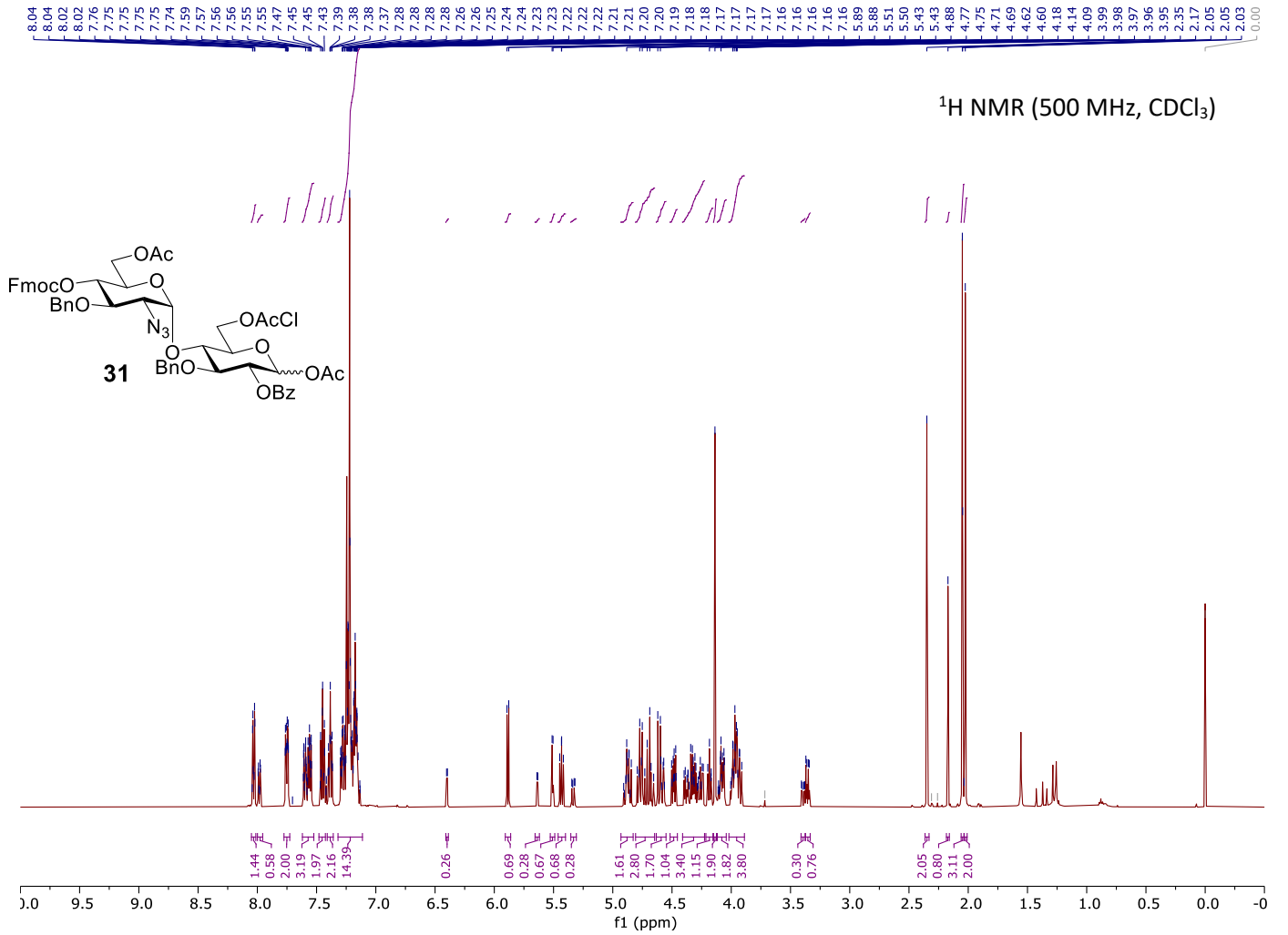
^{1}H NMR (500 MHz, $CDCl_3$)
OAc
FmocO
O
BnO
N_3
OAcCl
O
O
BnO
OAc
OBz
31
f1 (ppm)

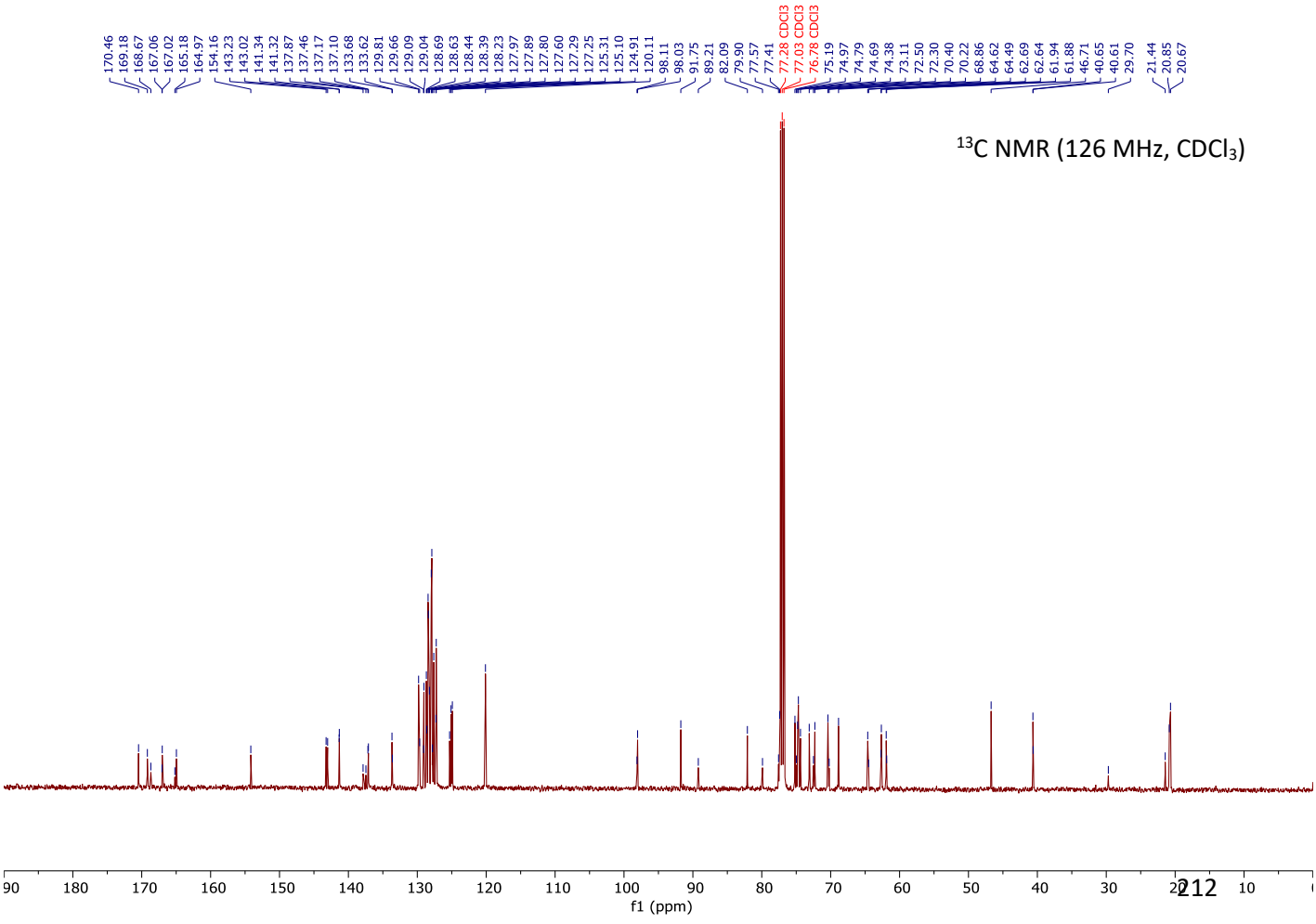
^{13}C NMR (126 MHz, $CDCl_3$)
77.28 CDCl3
77.03 CDCl3
76.78 CDCl3
f1 (ppm)

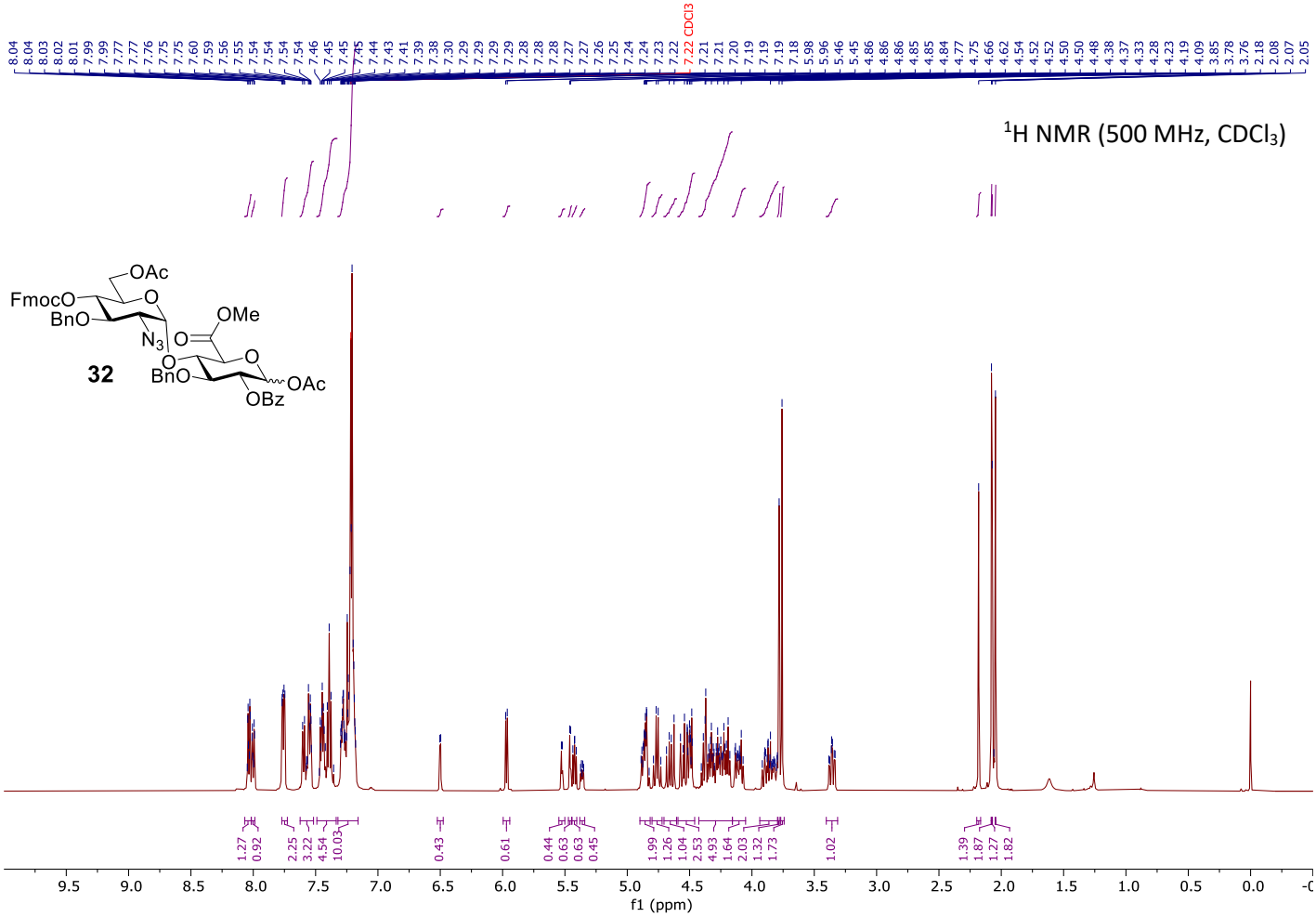

^{1}H NMR (500 MHz, $CDCl_3$)

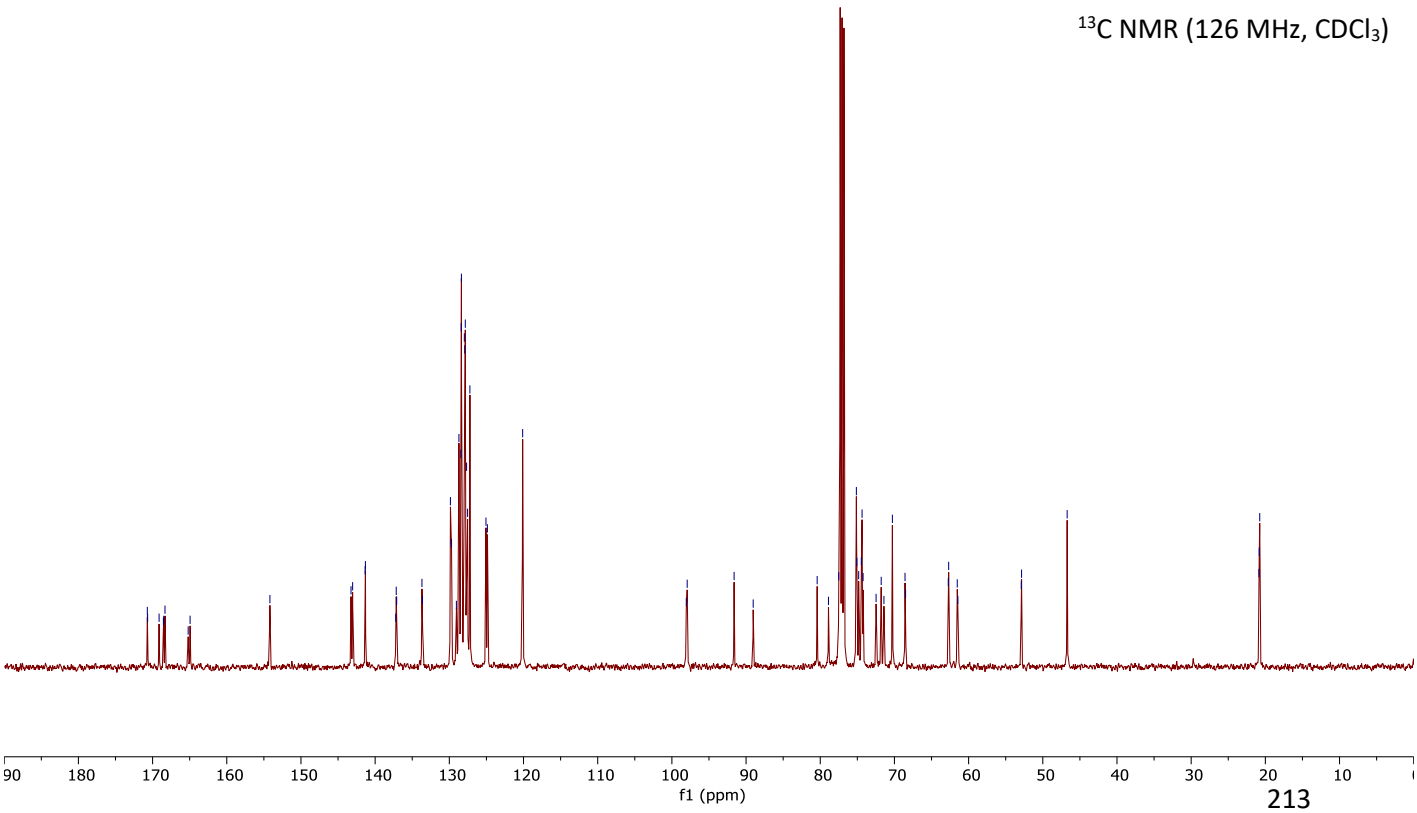

^{13}C NMR (126 MHz, $CDCl_3$)

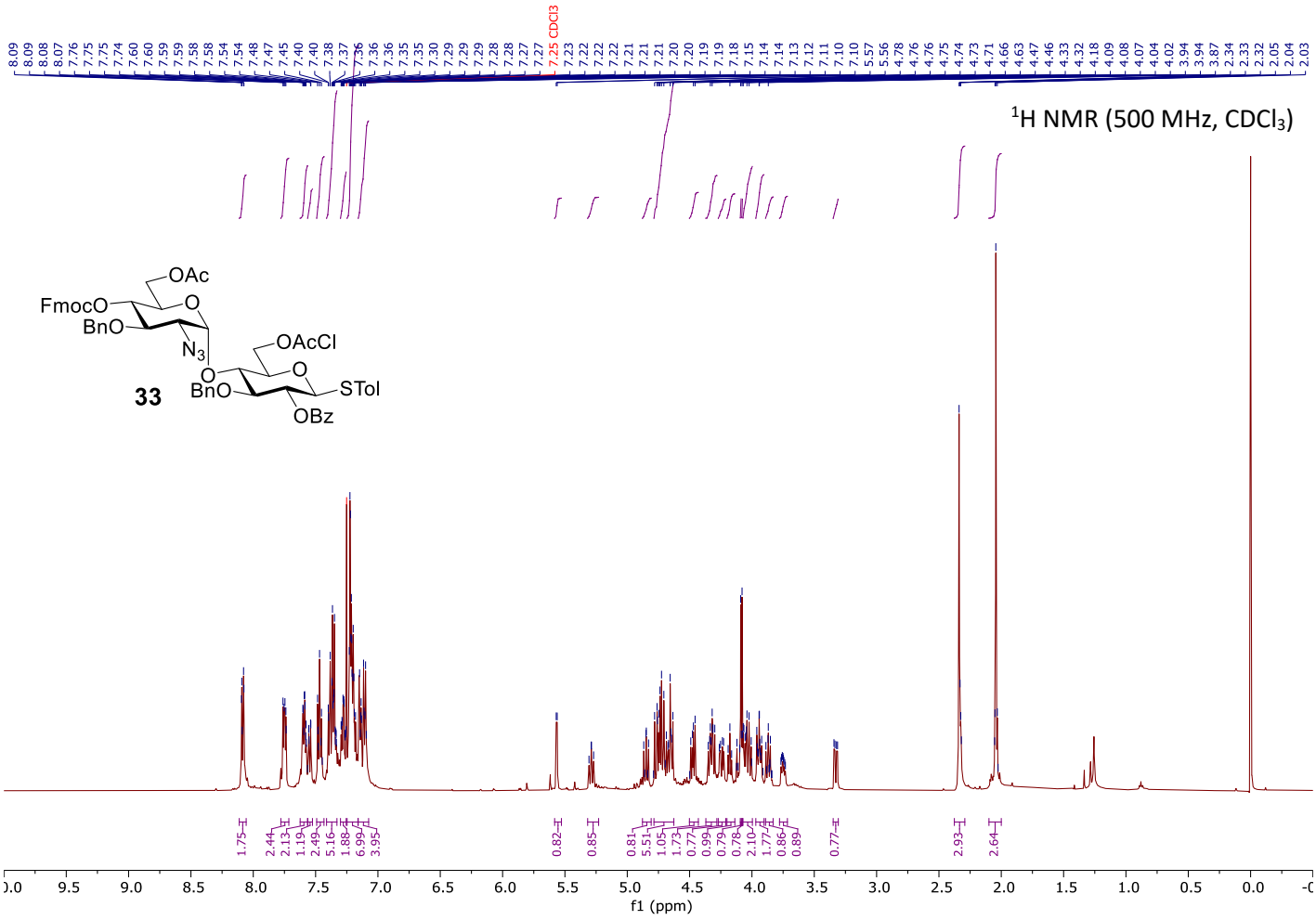
^{1}H NMR (500 MHz, $CDCl_3$)
OAc
FmocO
O
BnO
N_3
OAcCl
O
O
BnO
STol
OBz
33
f1 (ppm)

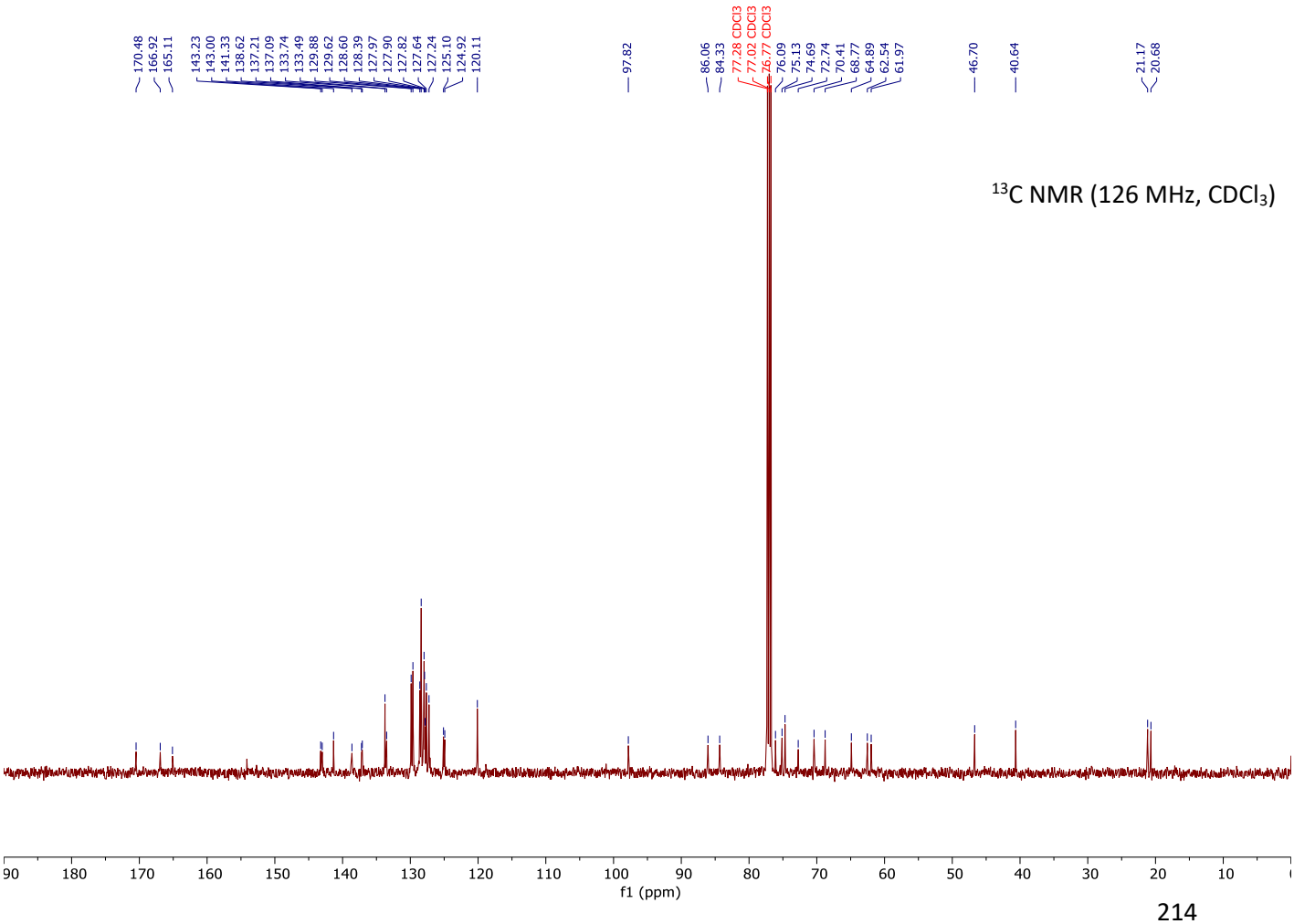
^{13}C NMR (126 MHz, $CDCl_3$)
f1 (ppm)

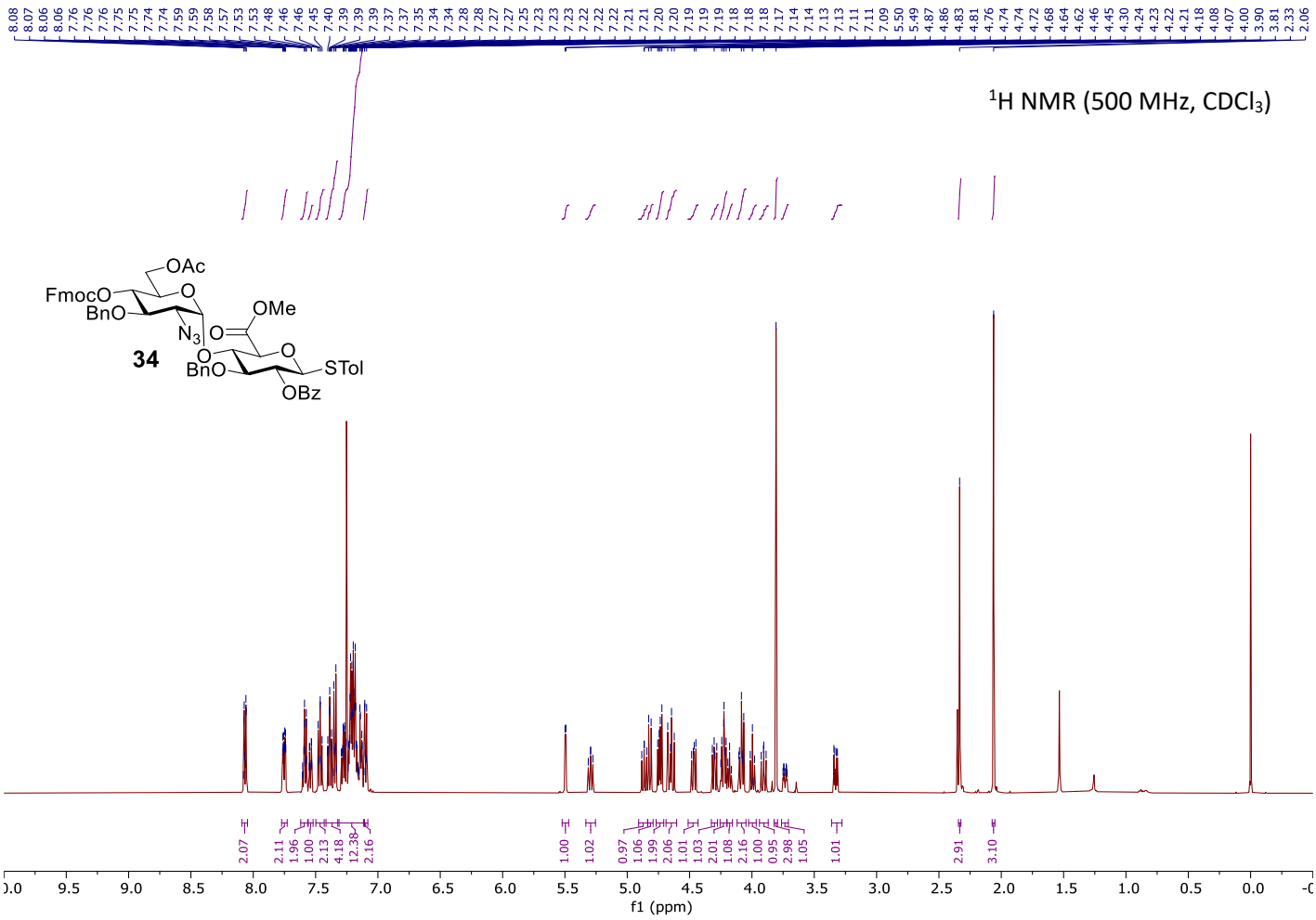

^{1}H NMR (500 MHz, $CDCl_3$)

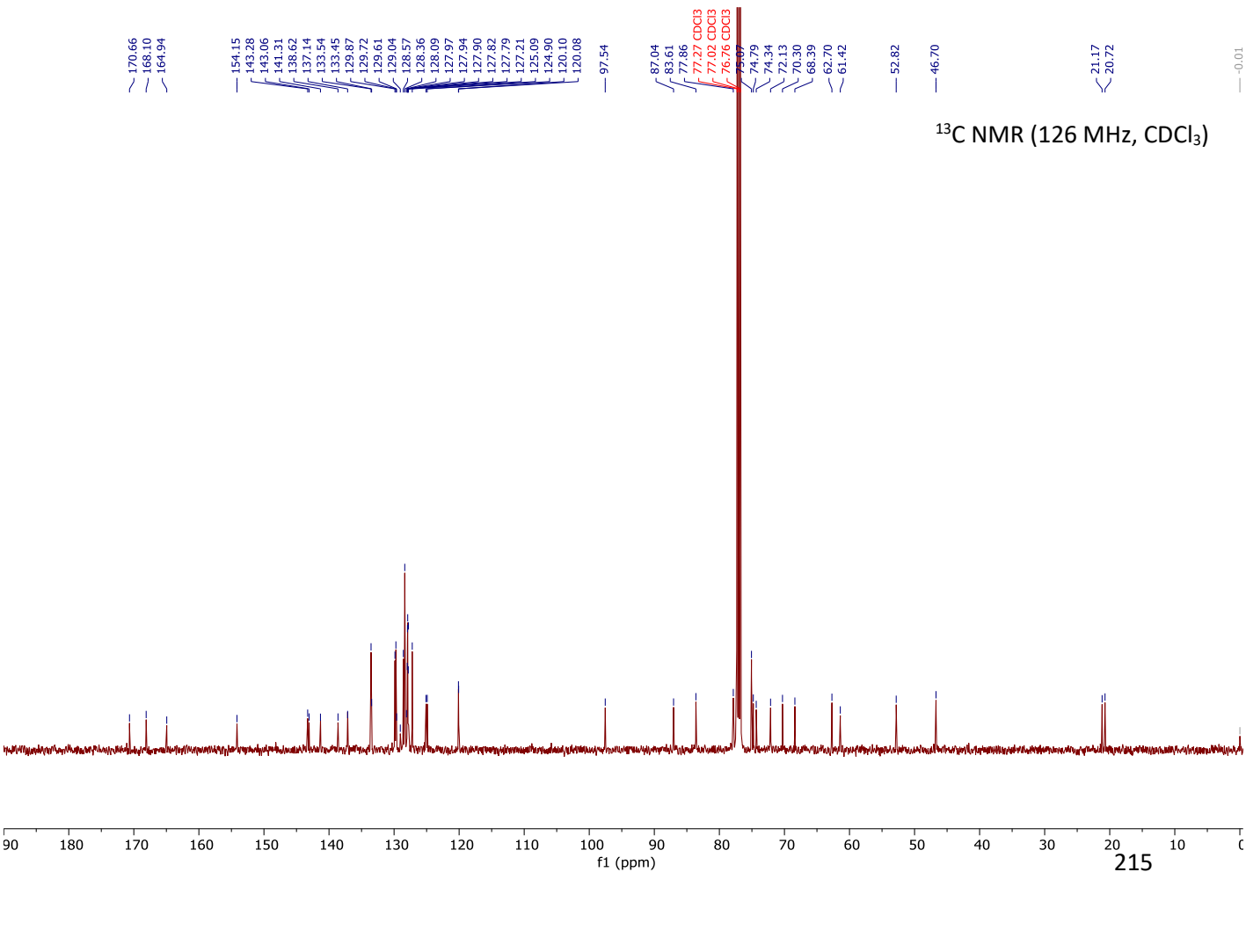

^{13}C NMR (126 MHz, $CDCl_3$)

^{1}H NMR (500 MHz, $CDCl_3$)

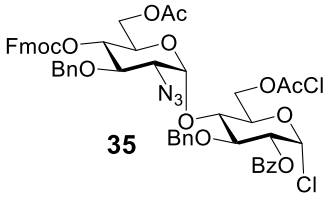

35

f1 (ppm)

^{13}C NMR (126 MHz, $CDCl_3$)

f1 (ppm)

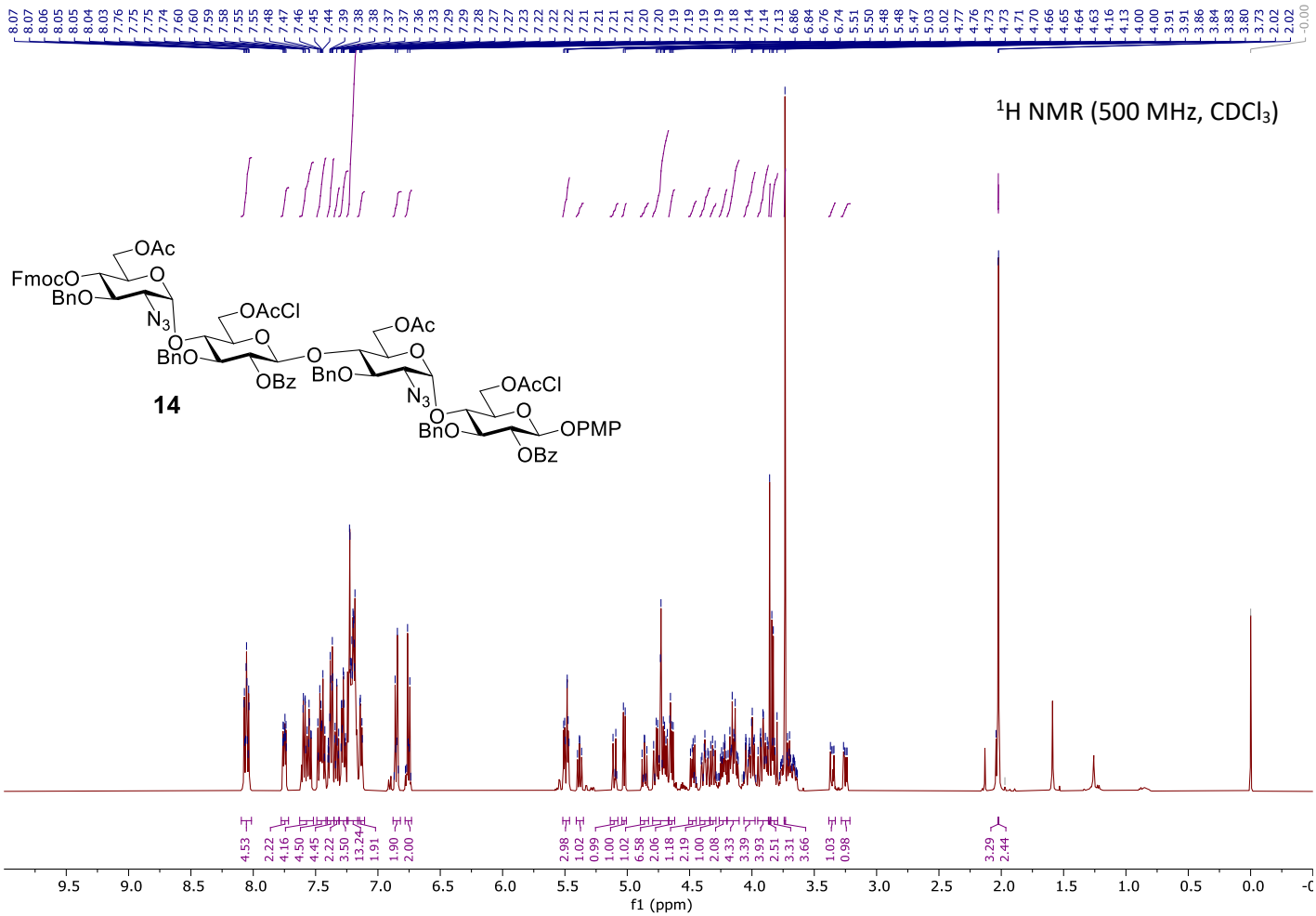
^{1}H NMR (500 MHz, $CDCl_3$)
OAc
FmocO
O
BnO
N_3
OAcCl
O
BnO
OBz
OAc
O
BnO
O
BnO
N_3
OAcCl
O
BnO
OPMP
OBz
14
f1 (ppm)

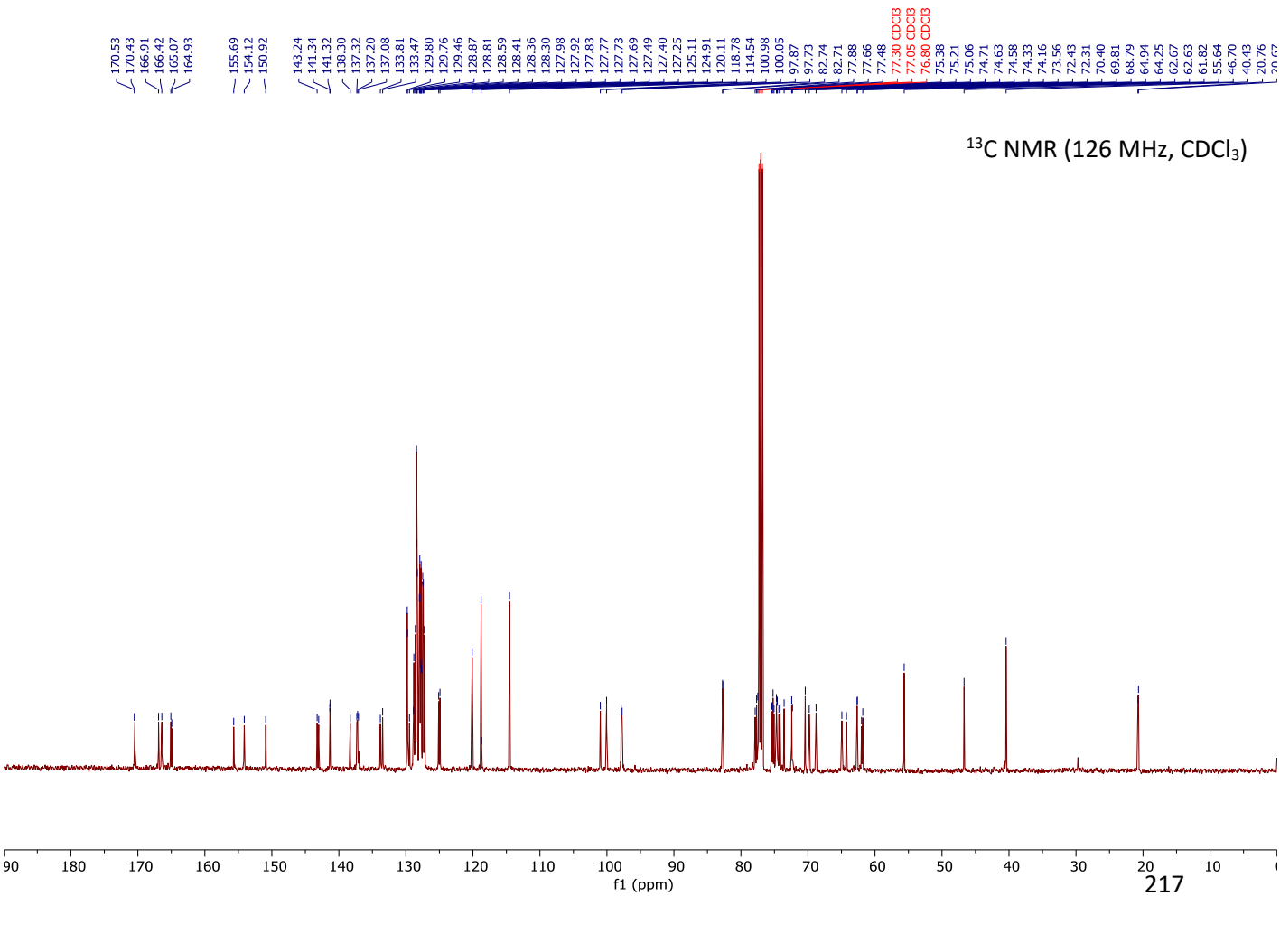
^{13}C NMR (126 MHz, $CDCl_3$)
f1 (ppm)

^{1}H NMR (500 MHz, $CDCl_3$)

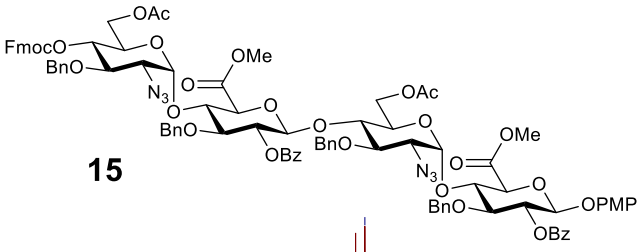

15

f1 (ppm)

^{13}C NMR (126 MHz, $CDCl_3$)

f1 (ppm)

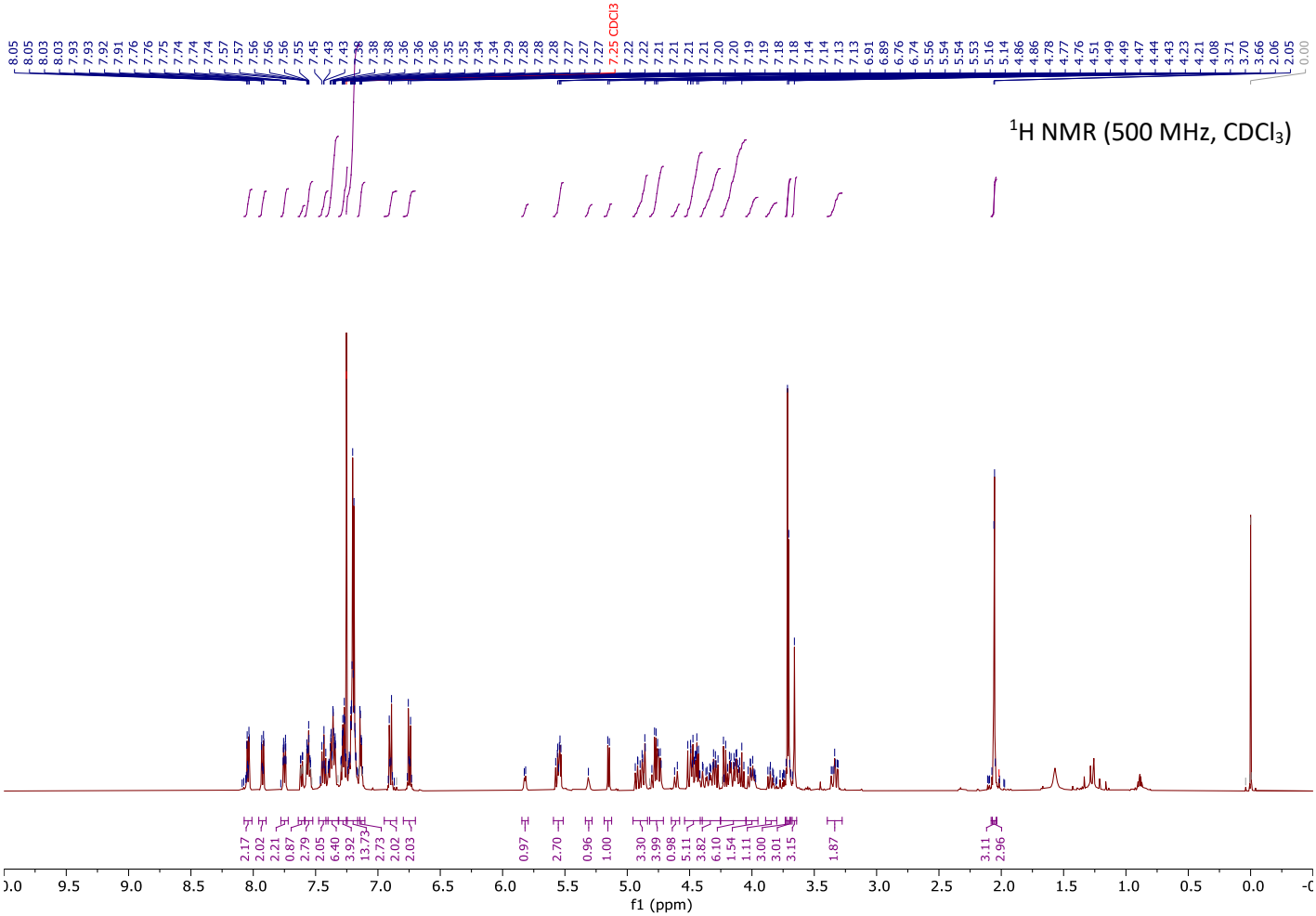
^{1}H NMR (500 MHz, $CDCl_3$)
f1 (ppm)

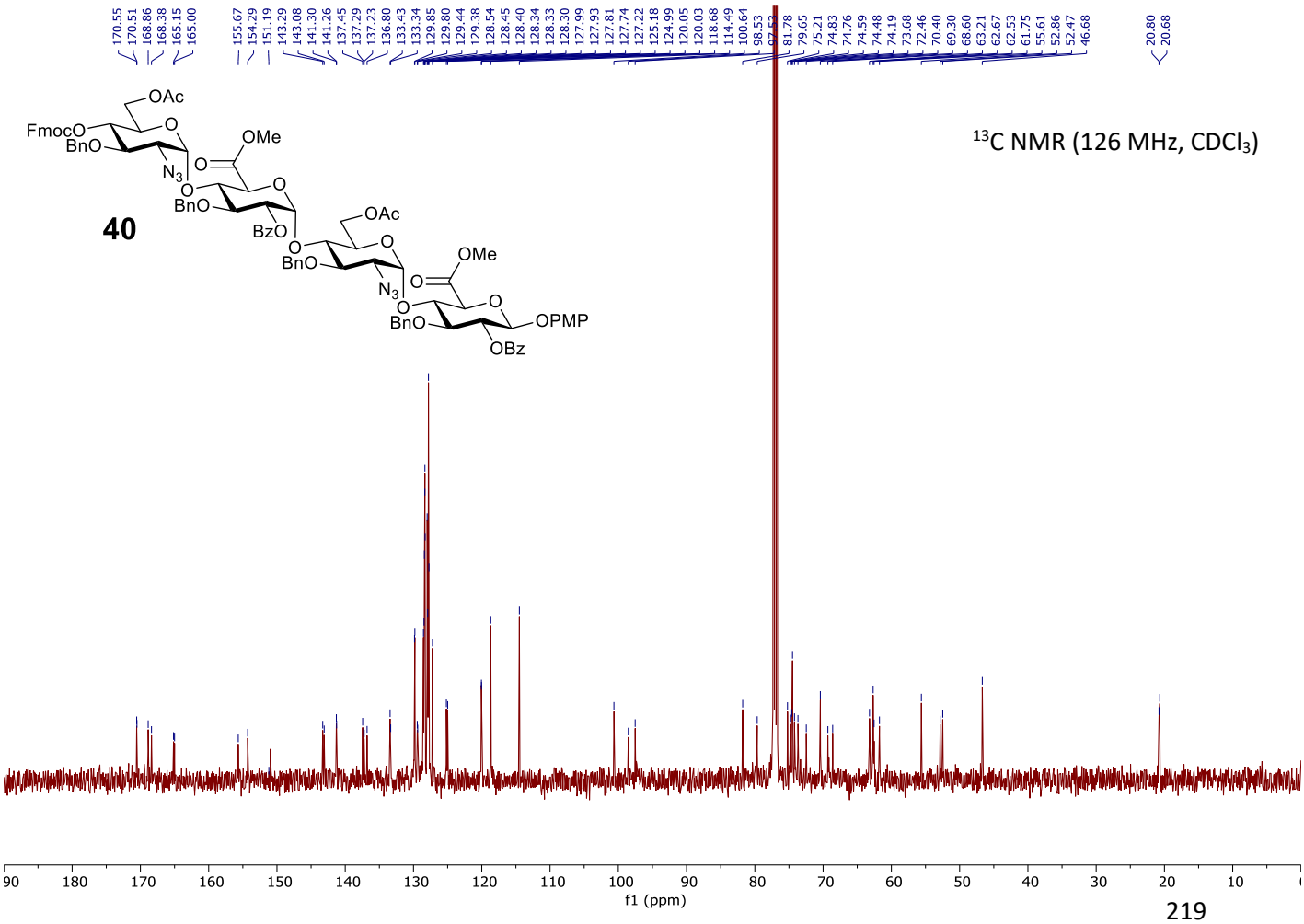
^{13}C NMR (126 MHz, $CDCl_3$)
f1 (ppm)

OAc
FmocO
BnO
O
OMe
N3
BnO
BzO
OAc
BnO
OMe
N3
BnO
OPMP
OBz

40

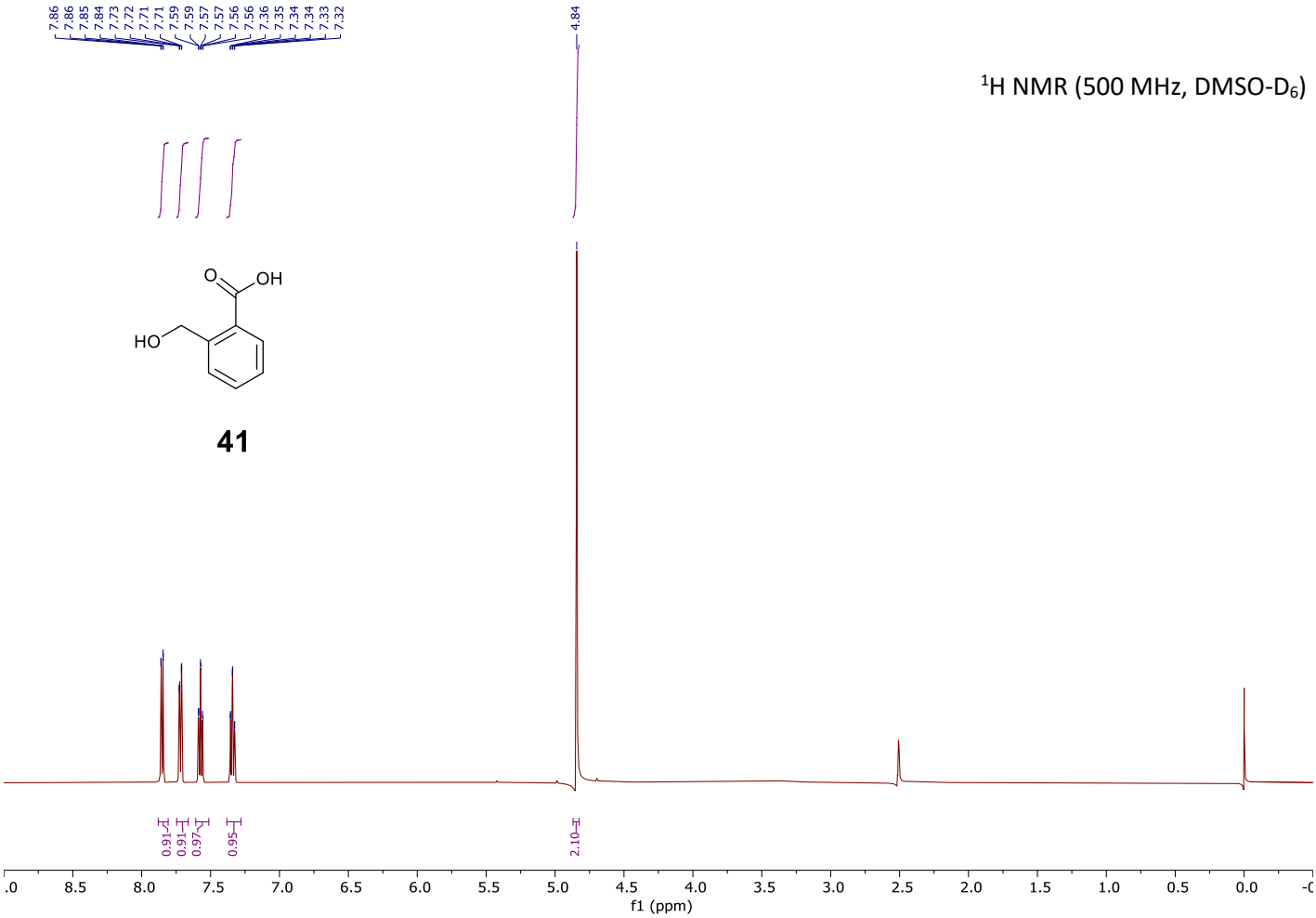

^{1}H NMR (500 MHz, DMSO-D_6)

41

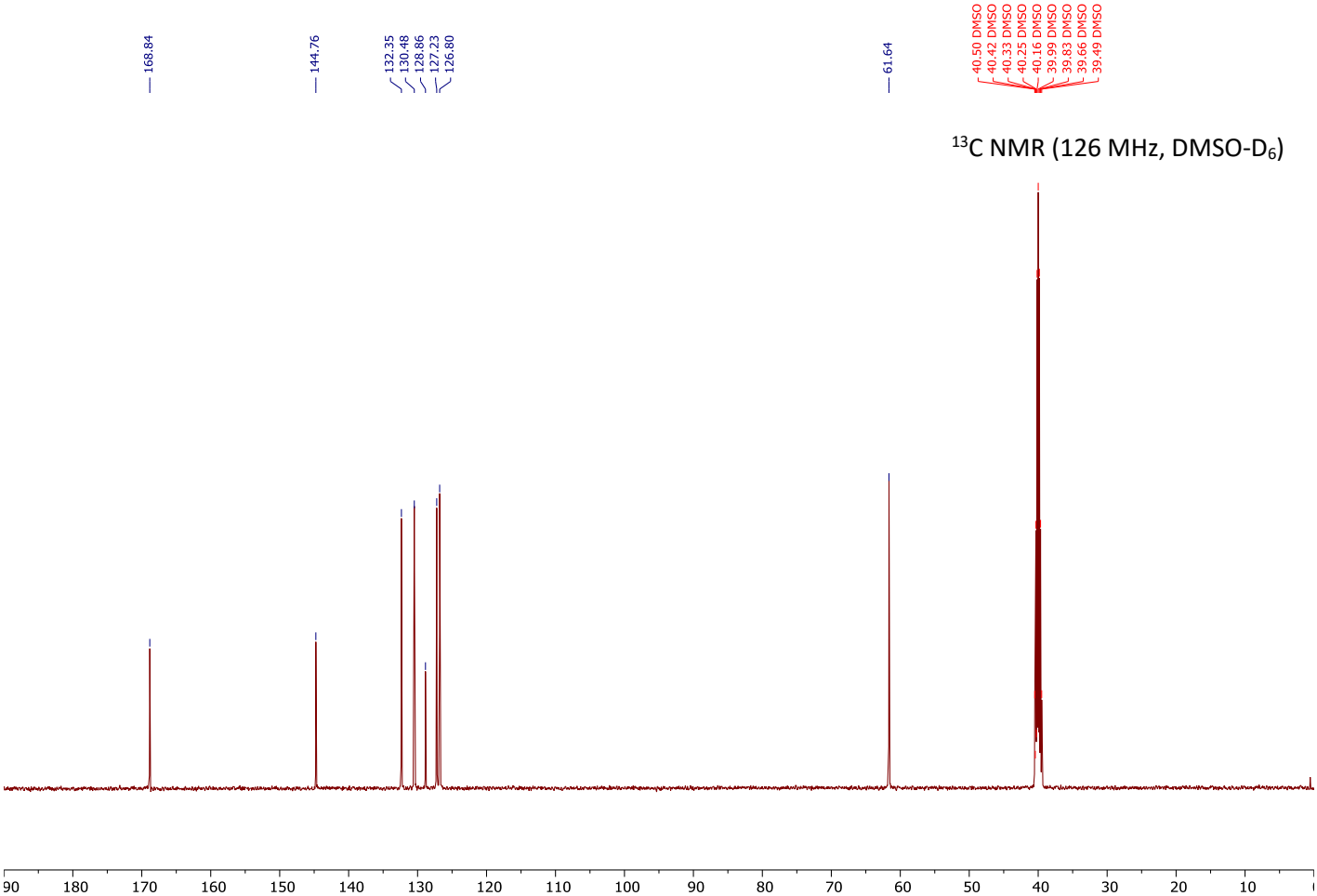

^{13}C NMR (126 MHz, DMSO-D_6)

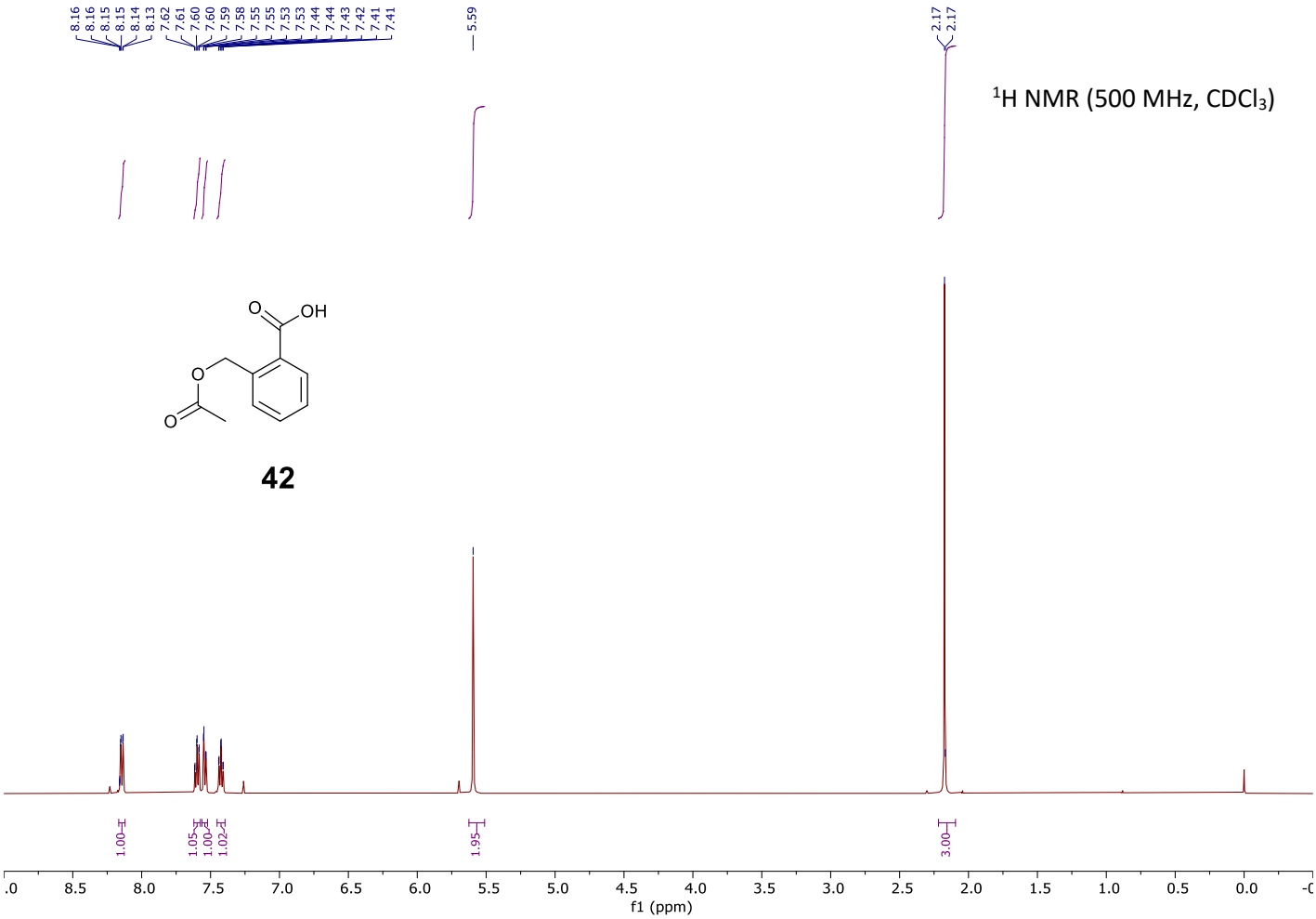

^{1}H NMR (500 MHz, $CDCl_3$)

42

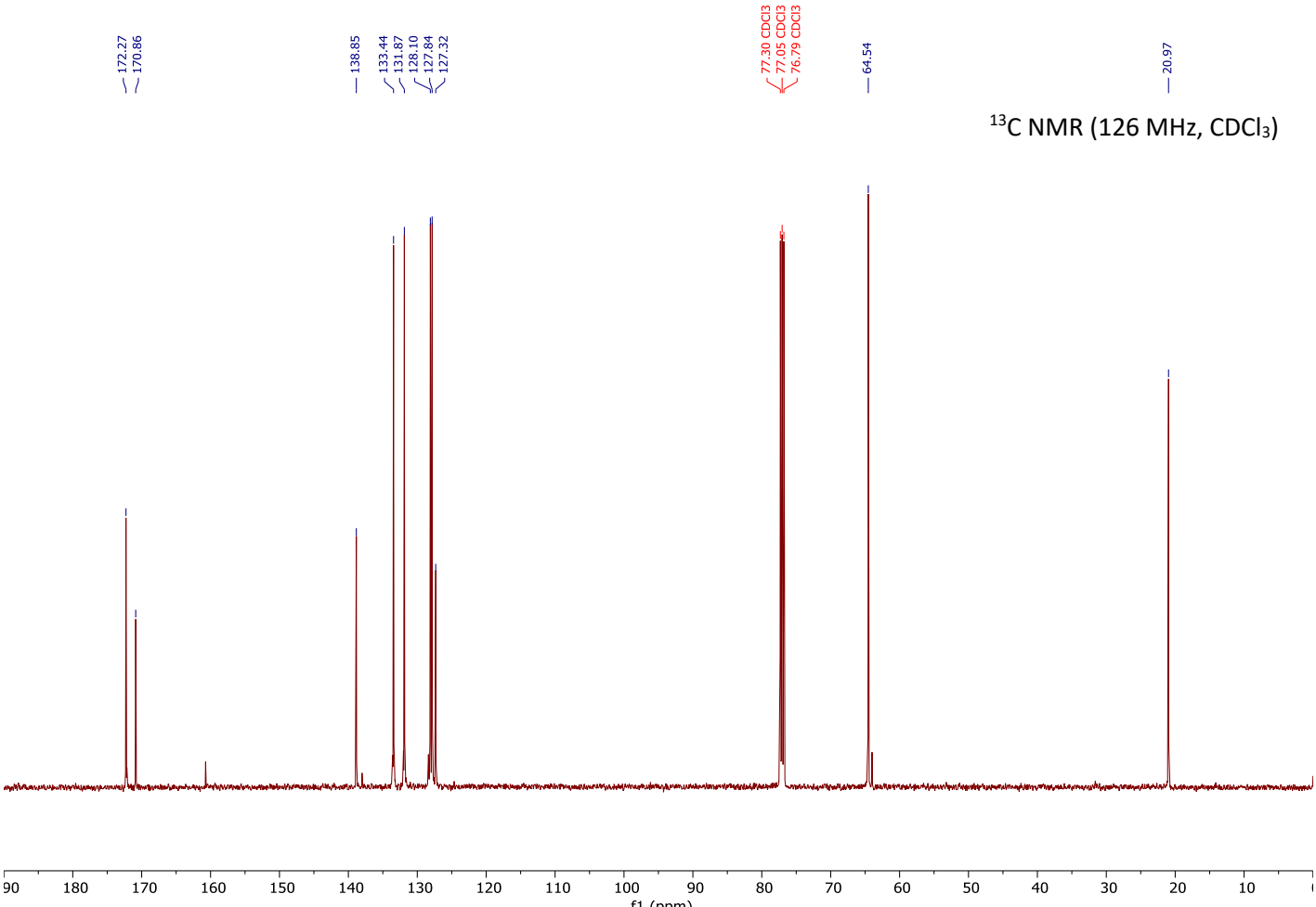

^{13}C NMR (126 MHz, $CDCl_3$)

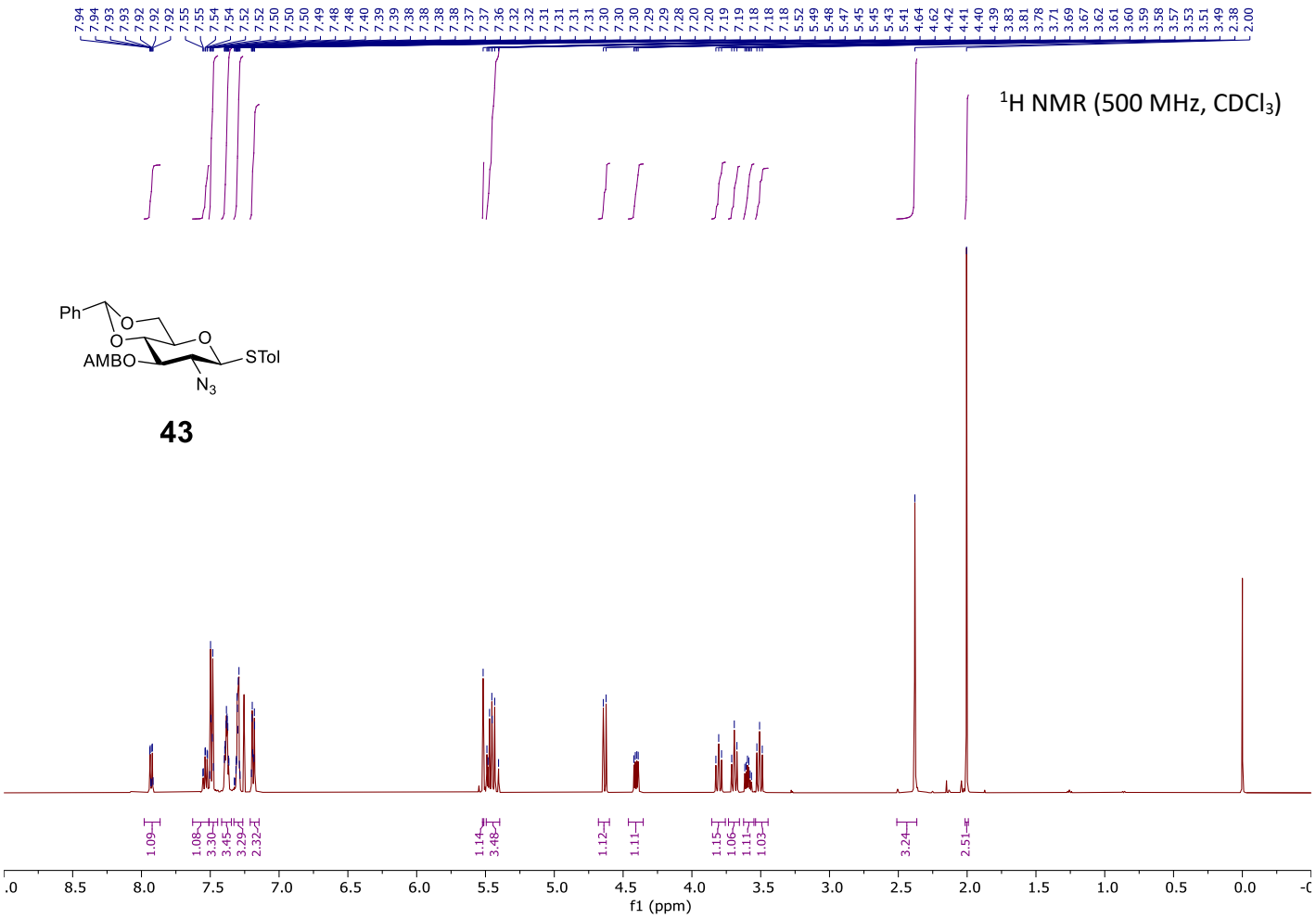

43

^{1}H NMR (500 MHz, $CDCl_3$)

^{13}C NMR (126 MHz, $CDCl_3$)

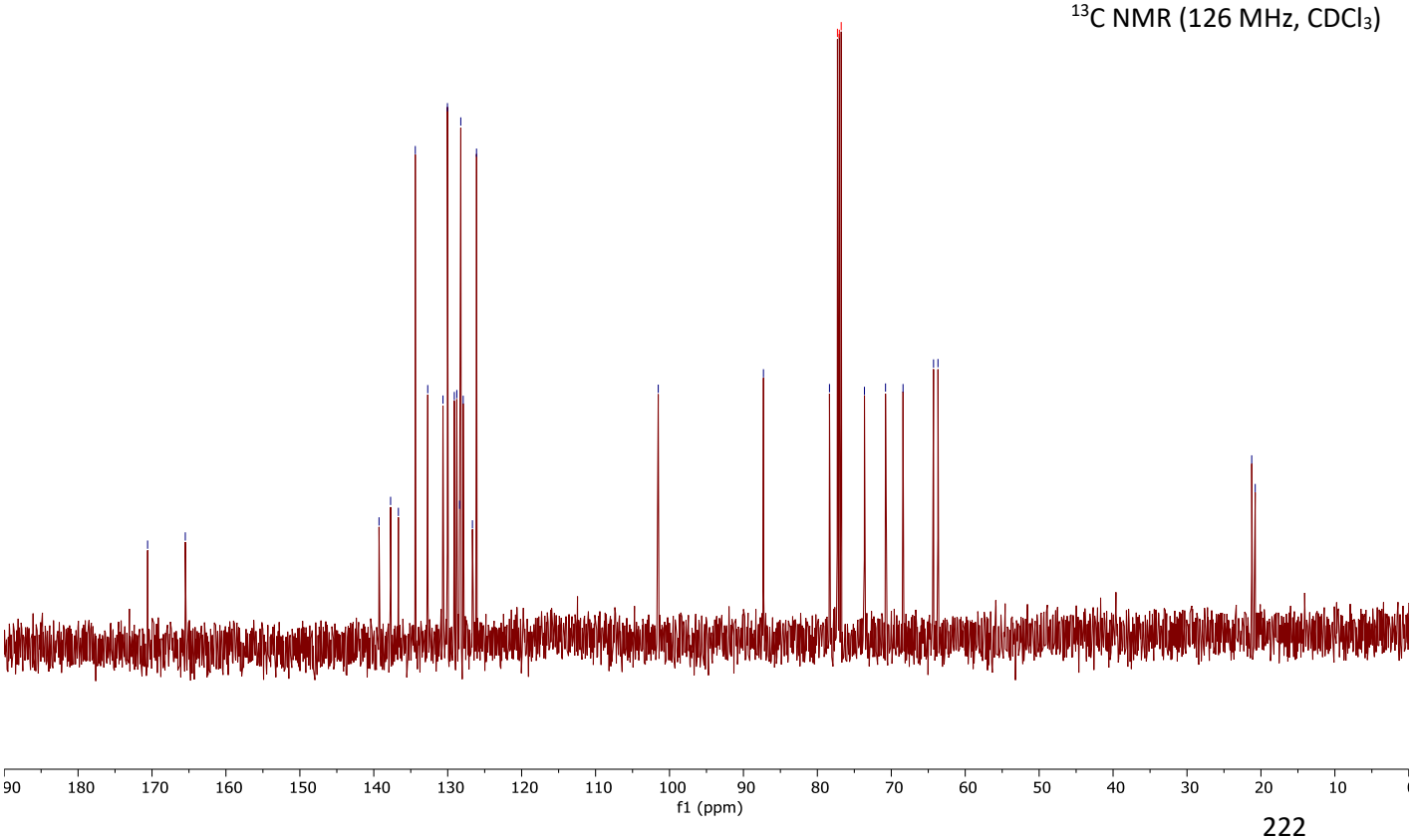

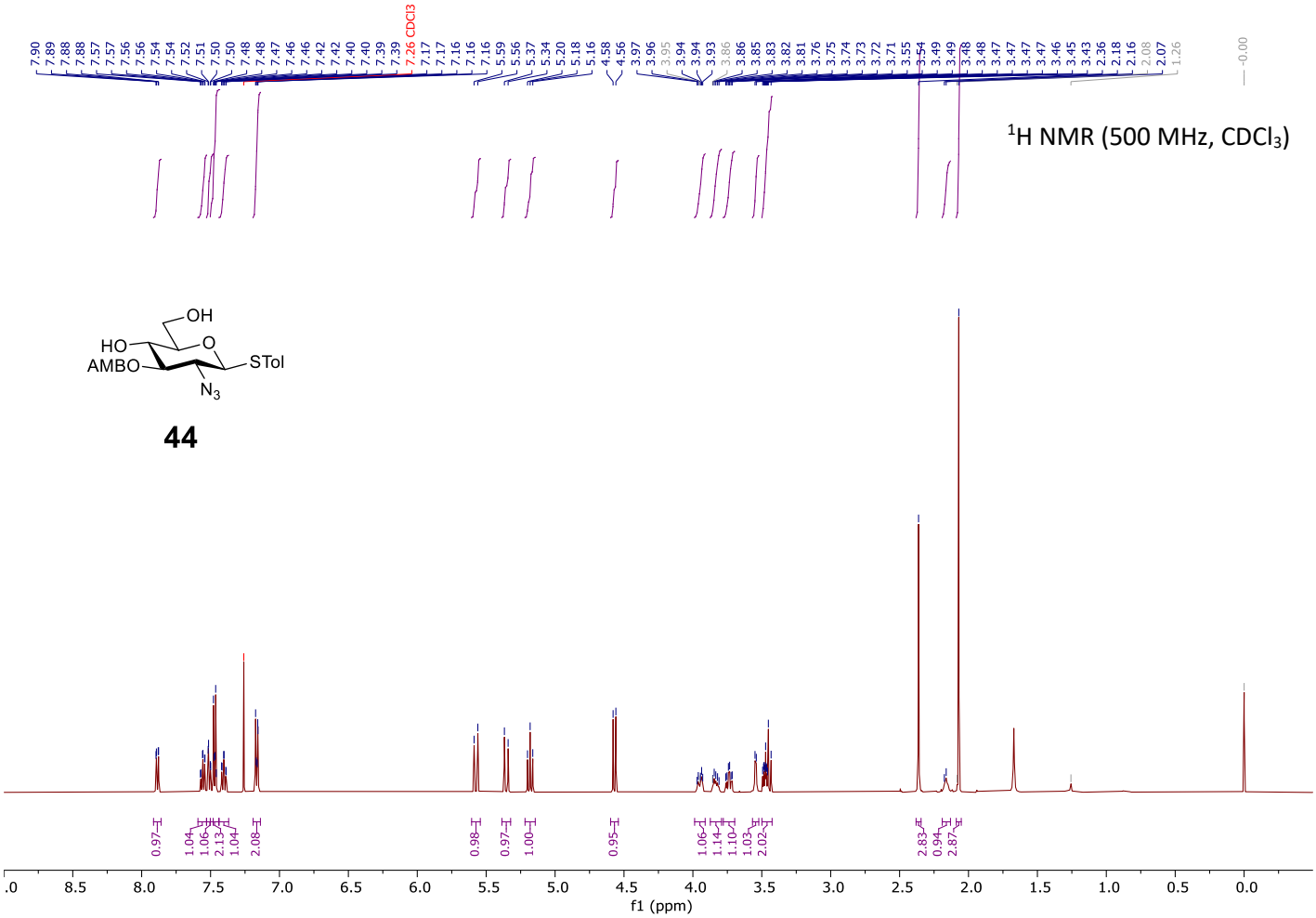

^{1}H NMR (500 MHz, $CDCl_3$)

44

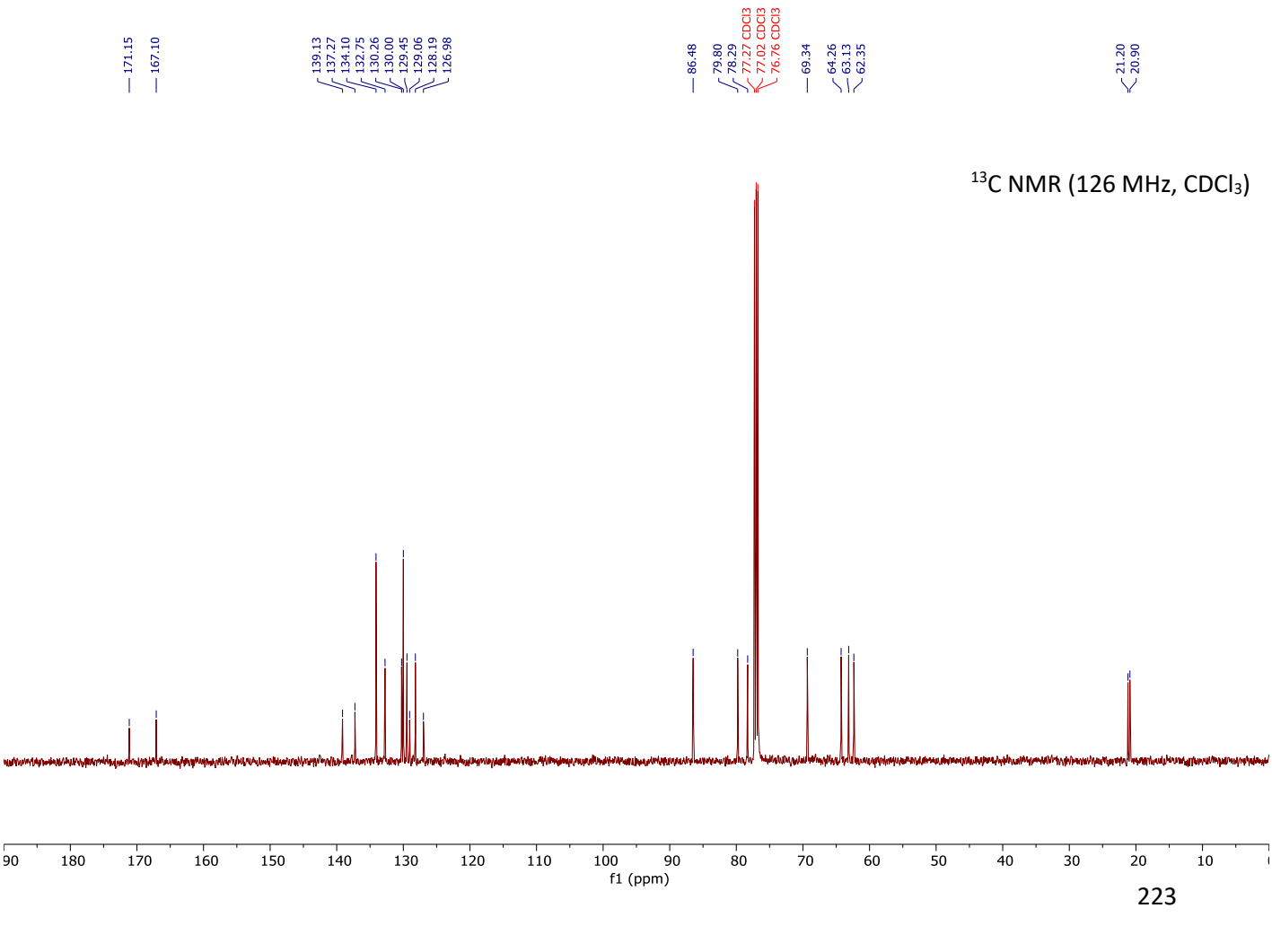

^{13}C NMR (126 MHz, $CDCl_3$)

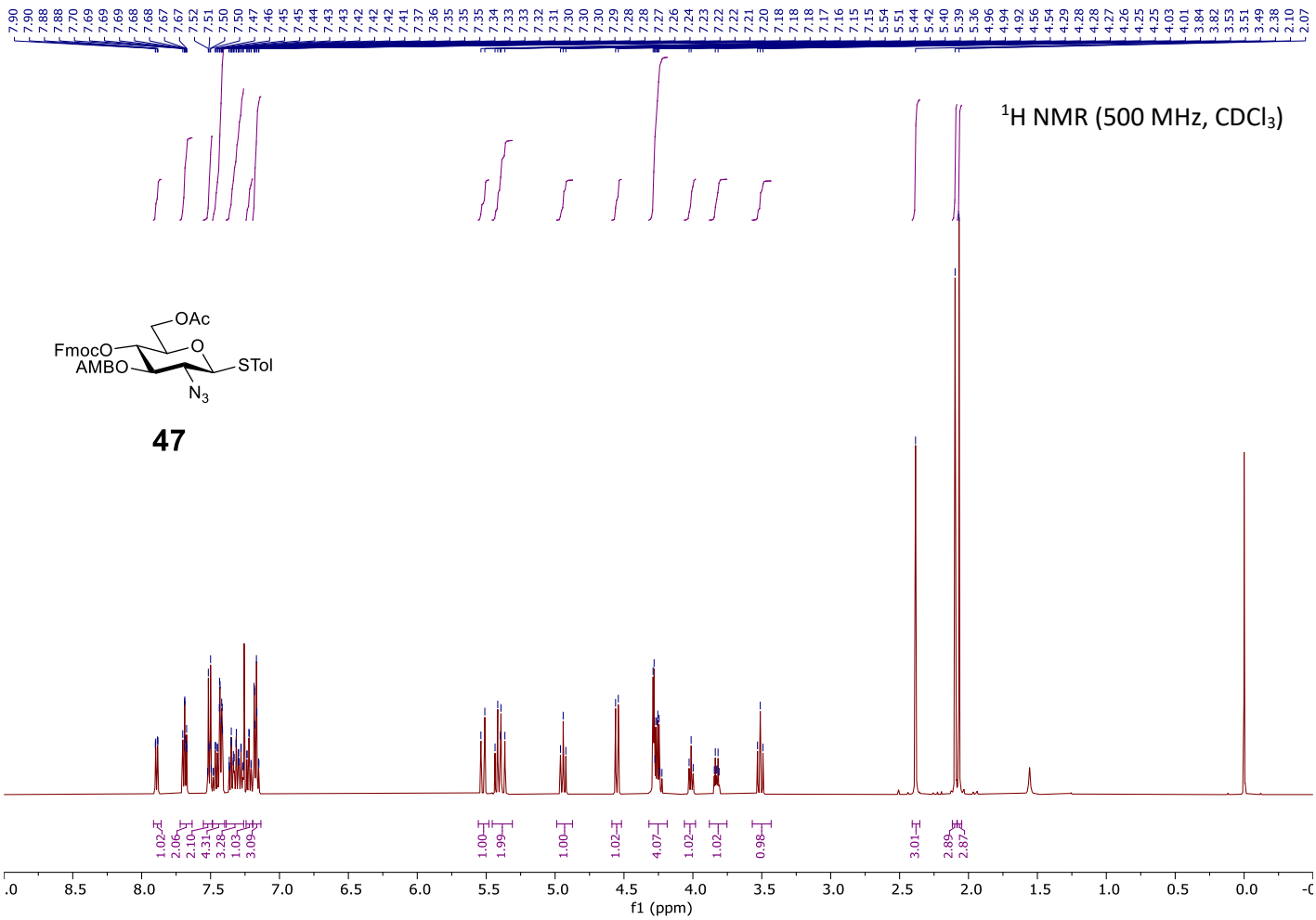
^{1}H NMR (500 MHz, $CDCl_3$)
OAc
FmocO
AMBO
O
STol
N_3
47
f1 (ppm)

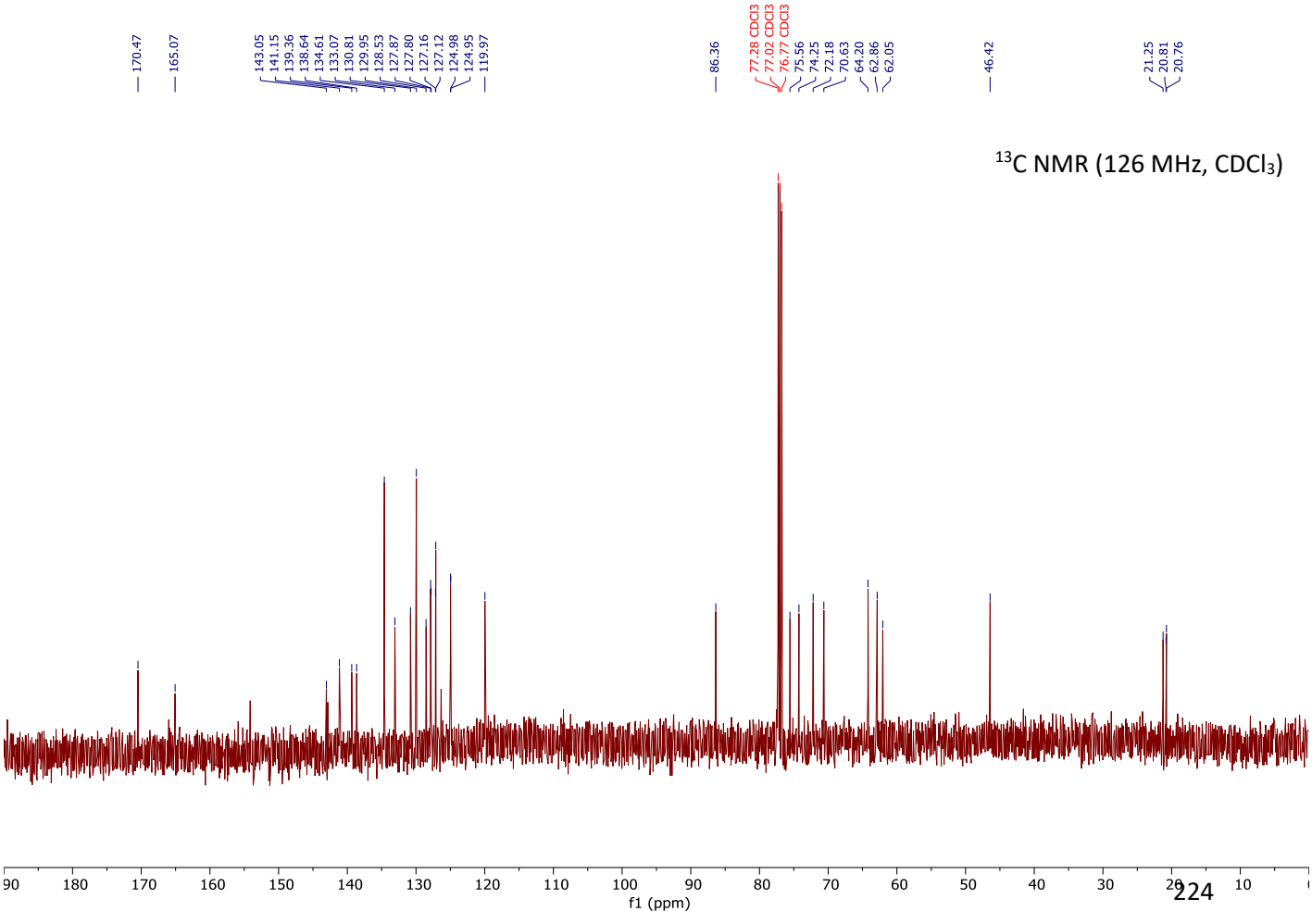
^{13}C NMR (126 MHz, $CDCl_3$)
f1 (ppm)

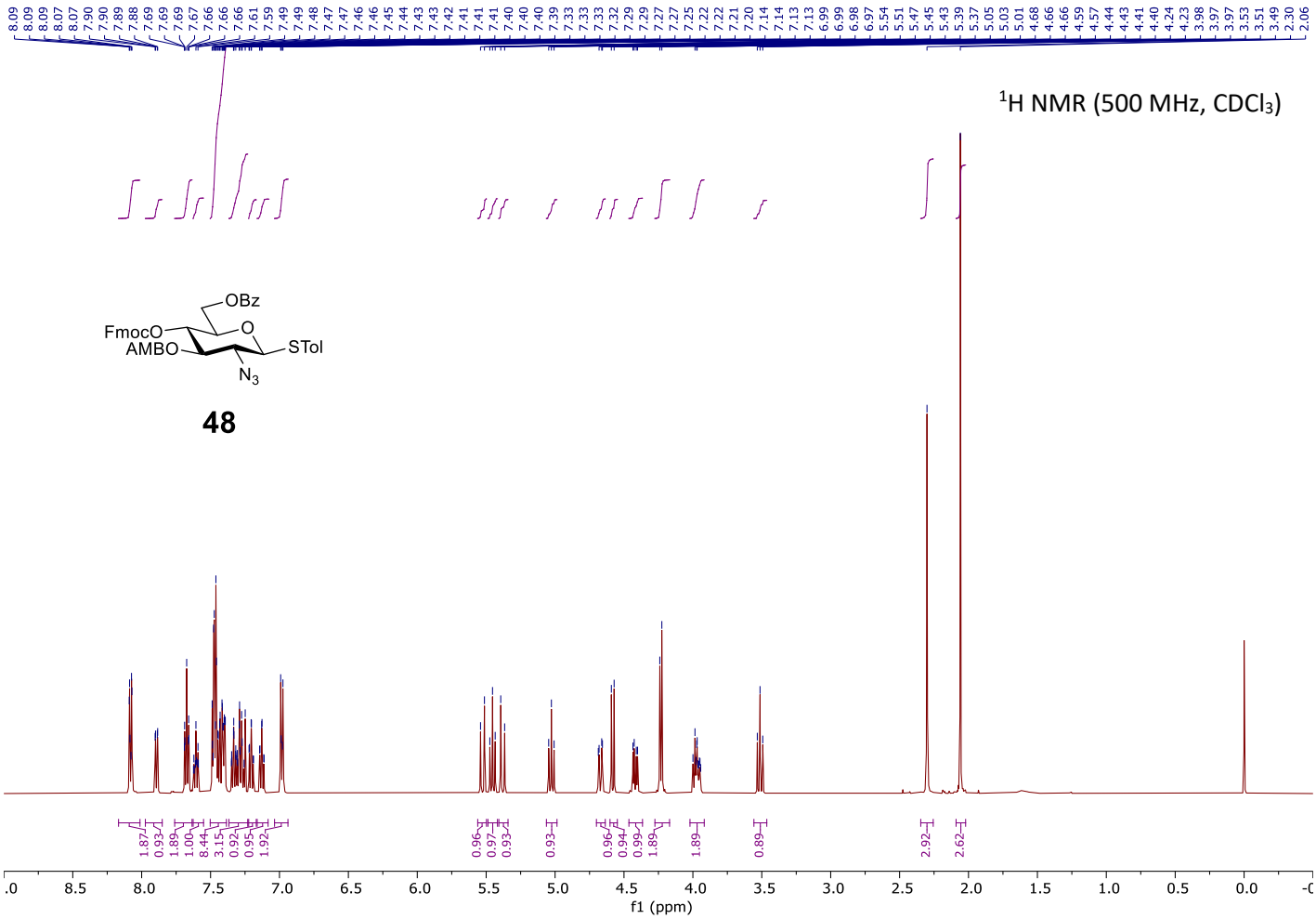
8.09 8.09 8.09 8.07 8.07 7.90 7.90 7.89 7.88 7.69 7.69 7.69 7.67 7.66 7.66 7.66 7.61 7.59 7.49 7.49 7.48 7.47 7.47 7.46 7.46 7.45 7.44 7.43 7.43 7.42 7.41 7.41 7.41 7.40 7.40 7.40 7.39 7.33 7.33 7.32 7.29 7.29 7.27 7.27 7.25 7.22 7.22 7.21 7.20 7.14 7.14 7.13 7.13 6.99 6.99 6.98 6.97 5.54 5.51 5.47 5.45 5.43 5.39 5.37 5.05 5.03 5.01 4.68 4.66 4.66 4.59 4.57 4.44 4.43 4.41 4.40 4.24 4.23 3.98 3.97 3.97 3.53 3.51 3.49 2.30 2.06
1H NMR (500 MHz, CDCl3)
OBz
FmocO
AMBO
O
STol
N3
48
1.87 0.93 1.89 1.00 8.44 3.15 0.92 0.95 1.92 0.96 0.97 0.93 0.93 0.96 0.94 0.99 1.89 1.89 0.89 2.92 2.62
f1 (ppm)

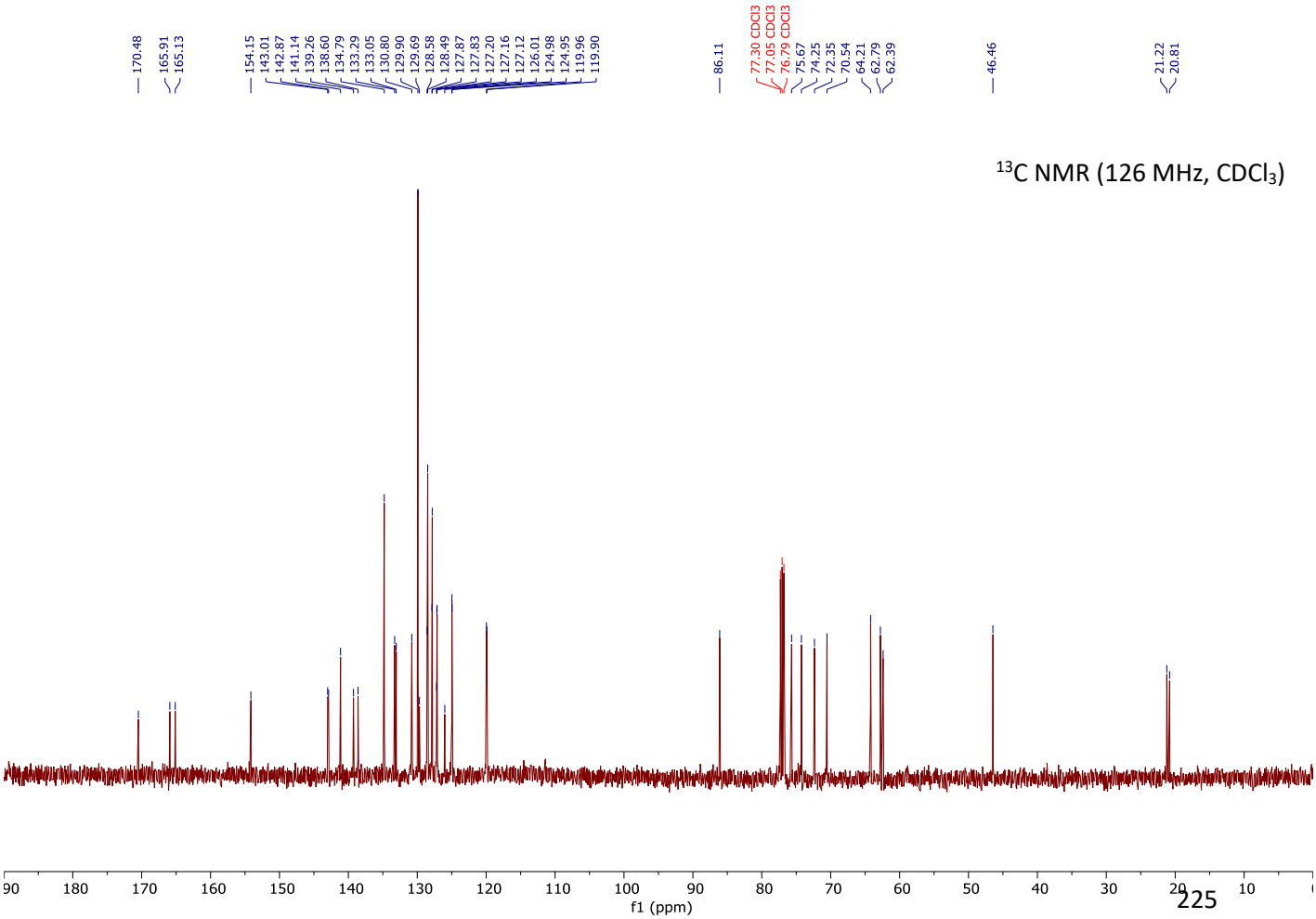
170.48 165.91 165.13 154.15 143.01 142.87 141.14 139.26 138.60 134.79 133.29 133.05 130.80 129.90 129.69 128.58 128.49 127.87 127.83 127.20 127.16 127.12 126.01 124.98 124.95 119.96 119.90 86.11 77.30 CDCl3 77.05 CDCl3 76.79 CDCl3 75.67 74.25 72.35 70.54 64.21 62.79 62.39 46.46 21.22 20.81
13C NMR (126 MHz, CDCl3)
f1 (ppm)

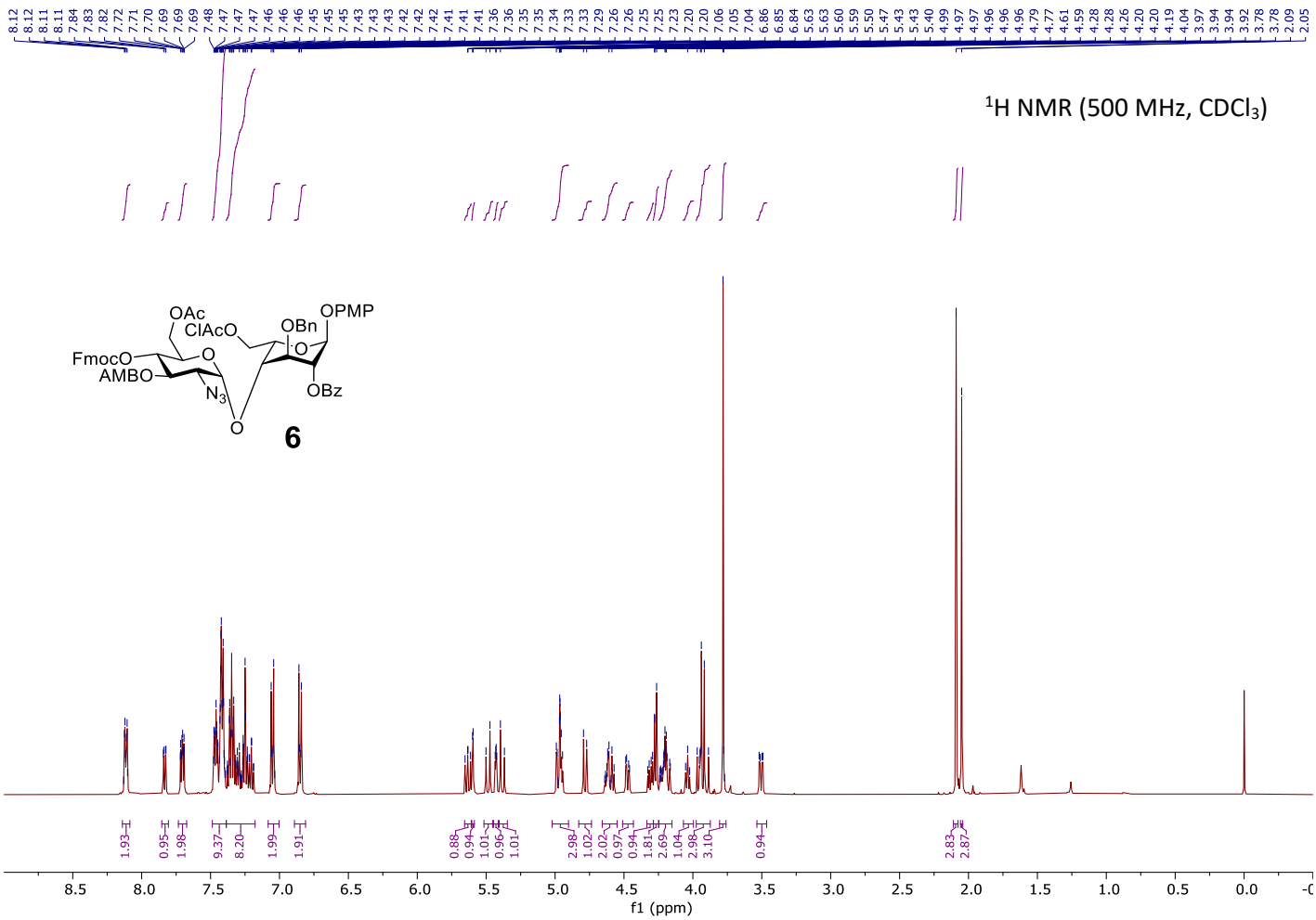

^{1}H NMR (500 MHz, $CDCl_3$)

6

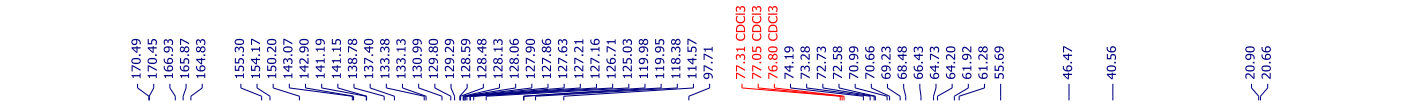

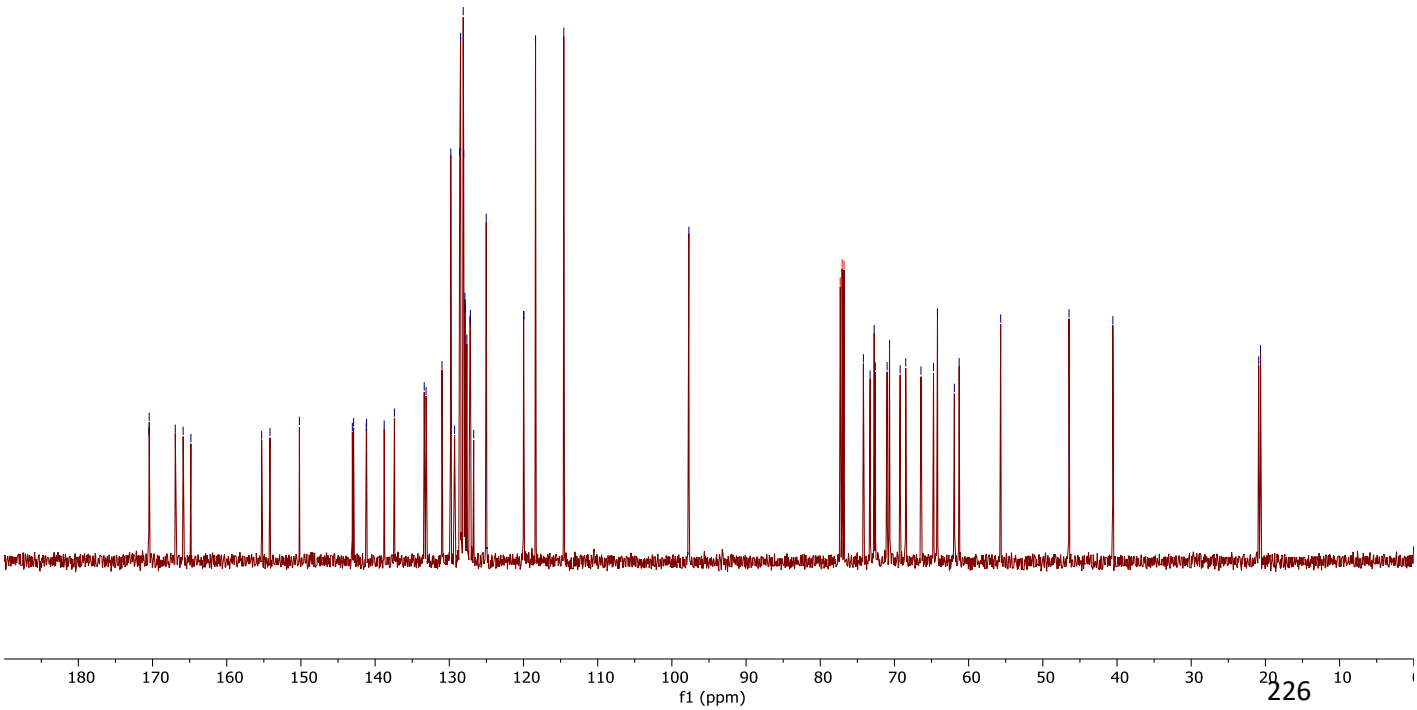

^{13}C NMR (126 MHz, $CDCl_3$)

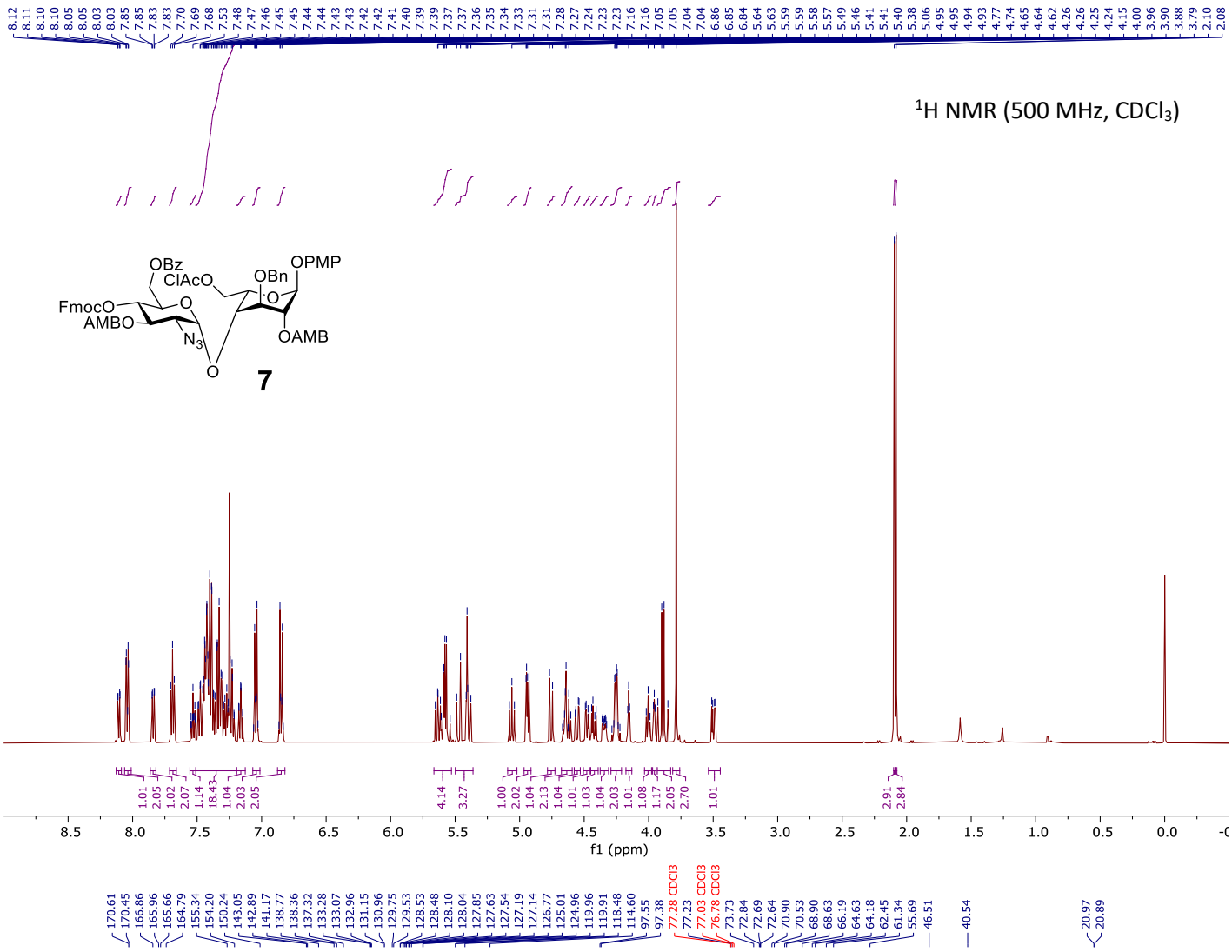
^{1}H NMR (500 MHz, CDCl$_3$)
OBz
ClAcO
OBn
OPMP
FmocO
AMBO
N$_3$
OAMB
7
f1 (ppm)

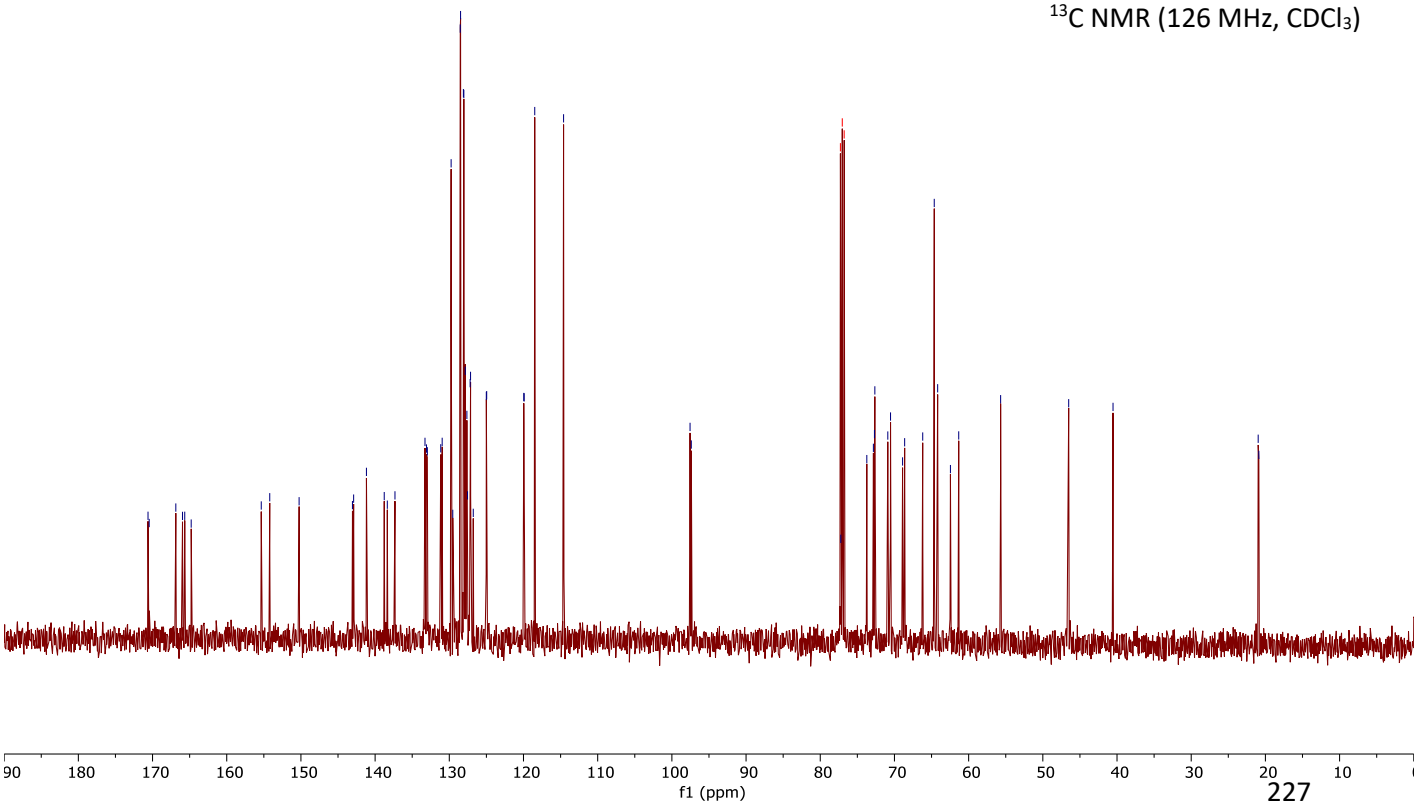
^{13}C NMR (126 MHz, CDCl$_3$)
f1 (ppm)

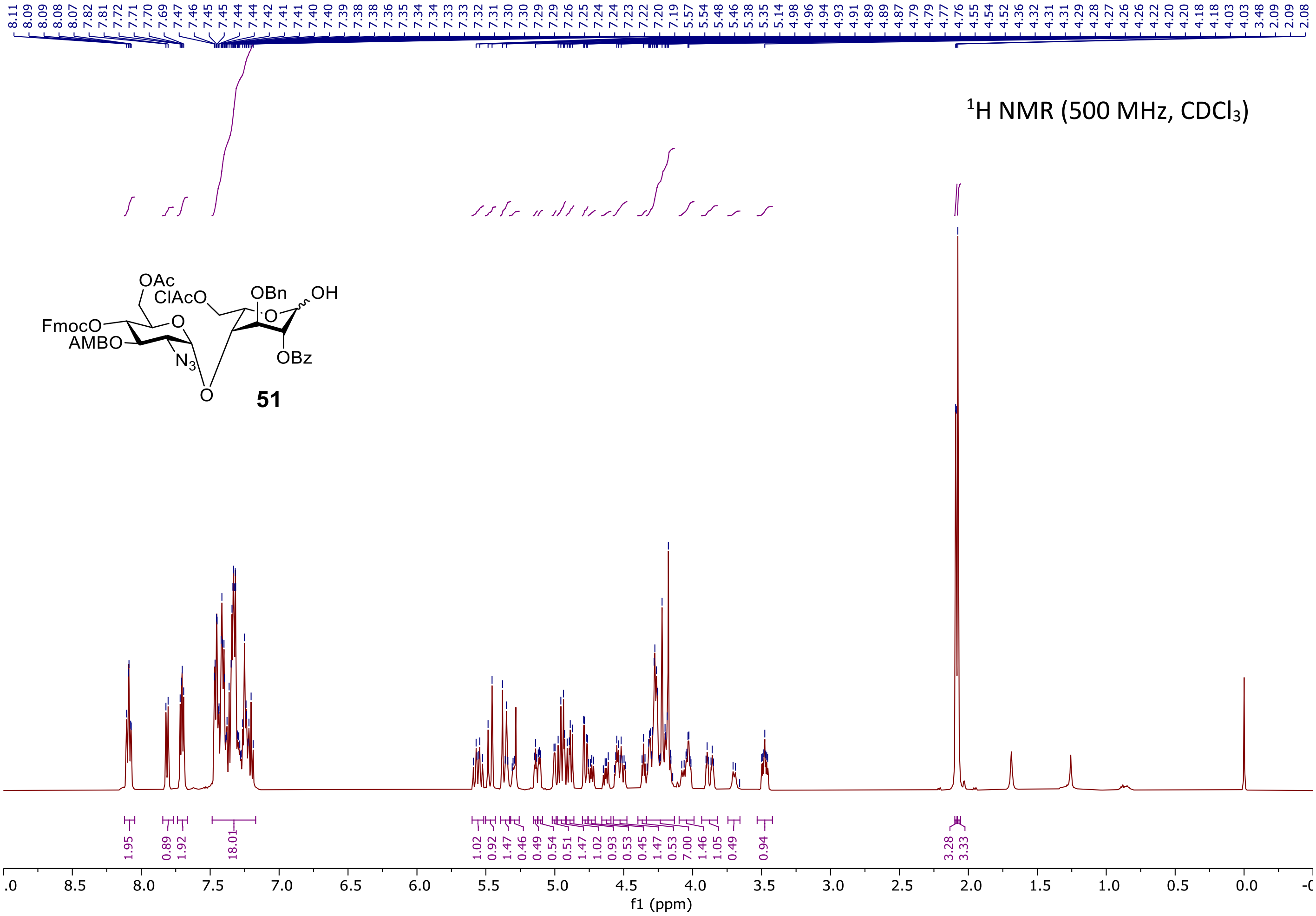
^{1}H NMR (500 MHz, CDCl$_3$)
OAc
ClAcO
OBn
OH
FmocO
AMBO
O
O
N3
OBz
O
51
8.11 8.09 8.09 8.08 8.07 7.82 7.81 7.72 7.71 7.70 7.69 7.47 7.46 7.45 7.45 7.44 7.44 7.42 7.41 7.41 7.40 7.40 7.39 7.38 7.38 7.36 7.35 7.34 7.34 7.33 7.33 7.32 7.31 7.30 7.30 7.29 7.29 7.26 7.25 7.24 7.24 7.23 7.22 7.20 7.19 5.57 5.54 5.48 5.46 5.38 5.35 5.14 4.98 4.96 4.94 4.93 4.91 4.89 4.89 4.87 4.79 4.79 4.77 4.76 4.55 4.54 4.52 4.36 4.32 4.31 4.31 4.29 4.28 4.27 4.26 4.26 4.22 4.20 4.20 4.18 4.18 4.03 4.03 3.48 2.09 2.09 2.08
1.95 0.89 1.92 18.01 1.02 0.92 1.47 0.46 0.49 0.54 0.51 1.47 1.02 0.93 0.53 0.45 1.47 0.53 7.00 1.46 1.05 0.49 0.94 3.28 3.33
f1 (ppm)

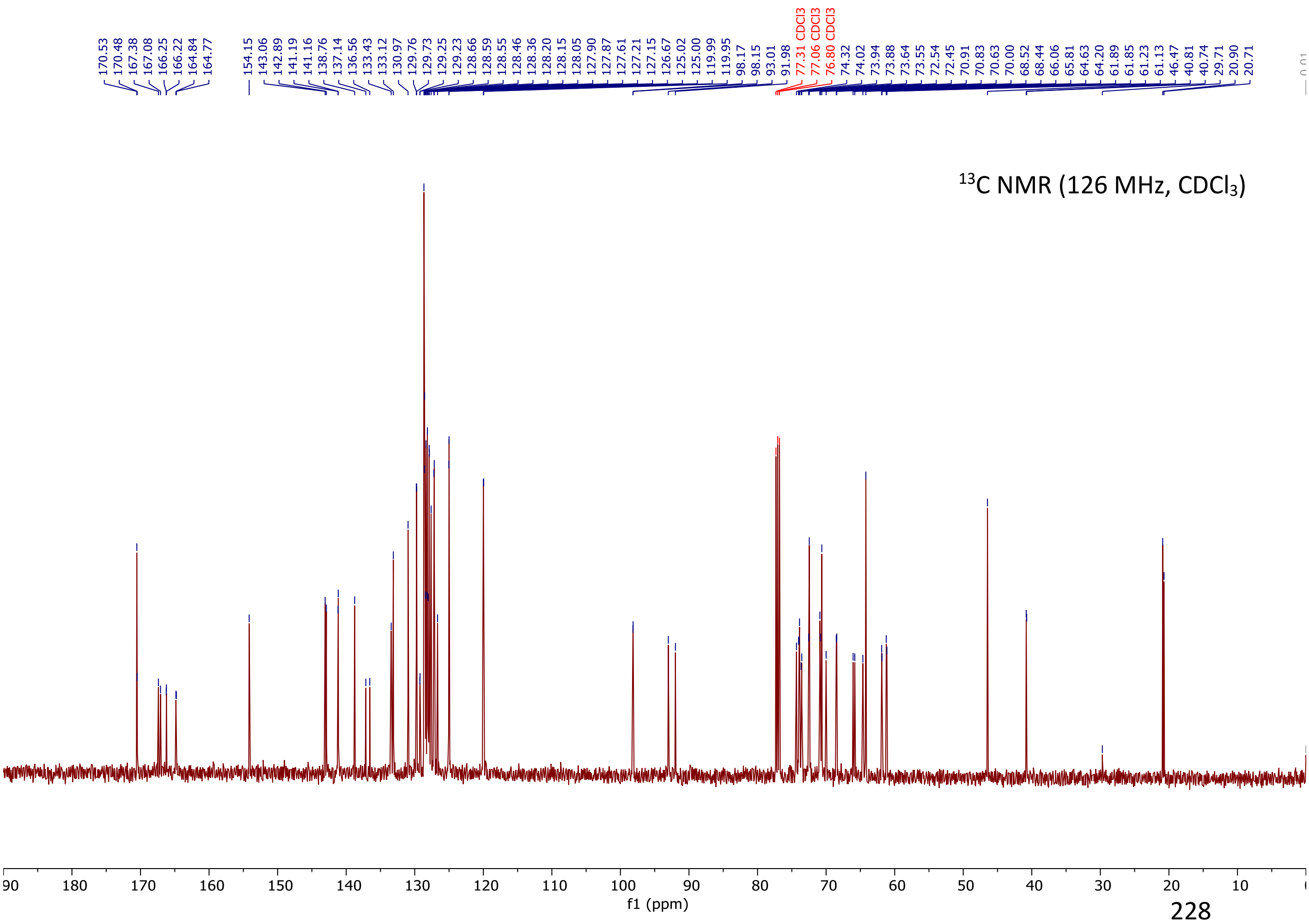
^{13}C NMR (126 MHz, CDCl$_3$)
170.53 170.48 167.38 167.08 166.25 166.22 164.84 164.77 154.15 143.06 142.89 141.19 141.16 138.76 137.14 136.56 133.43 133.12 130.97 129.76 129.73 129.25 129.23 128.66 128.59 128.55 128.46 128.36 128.20 128.15 128.05 127.90 127.87 127.61 127.21 127.15 126.67 125.02 125.00 119.99 119.95 98.17 98.15 93.01 91.98 77.31 CDCl3 77.06 CDCl3 76.80 CDCl3 74.32 74.02 73.94 73.88 73.64 73.55 72.54 72.45 70.91 70.83 70.63 70.00 68.52 68.44 66.06 65.81 64.63 64.20 61.89 61.85 61.23 61.13 46.47 40.81 40.74 29.71 20.90 20.71
f1 (ppm)

^{1}H NMR (500 MHz, $CDCl_3$)

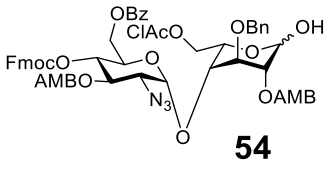

54

f1 (ppm)

^{13}C NMR (126 MHz, $CDCl_3$)

f1 (ppm)

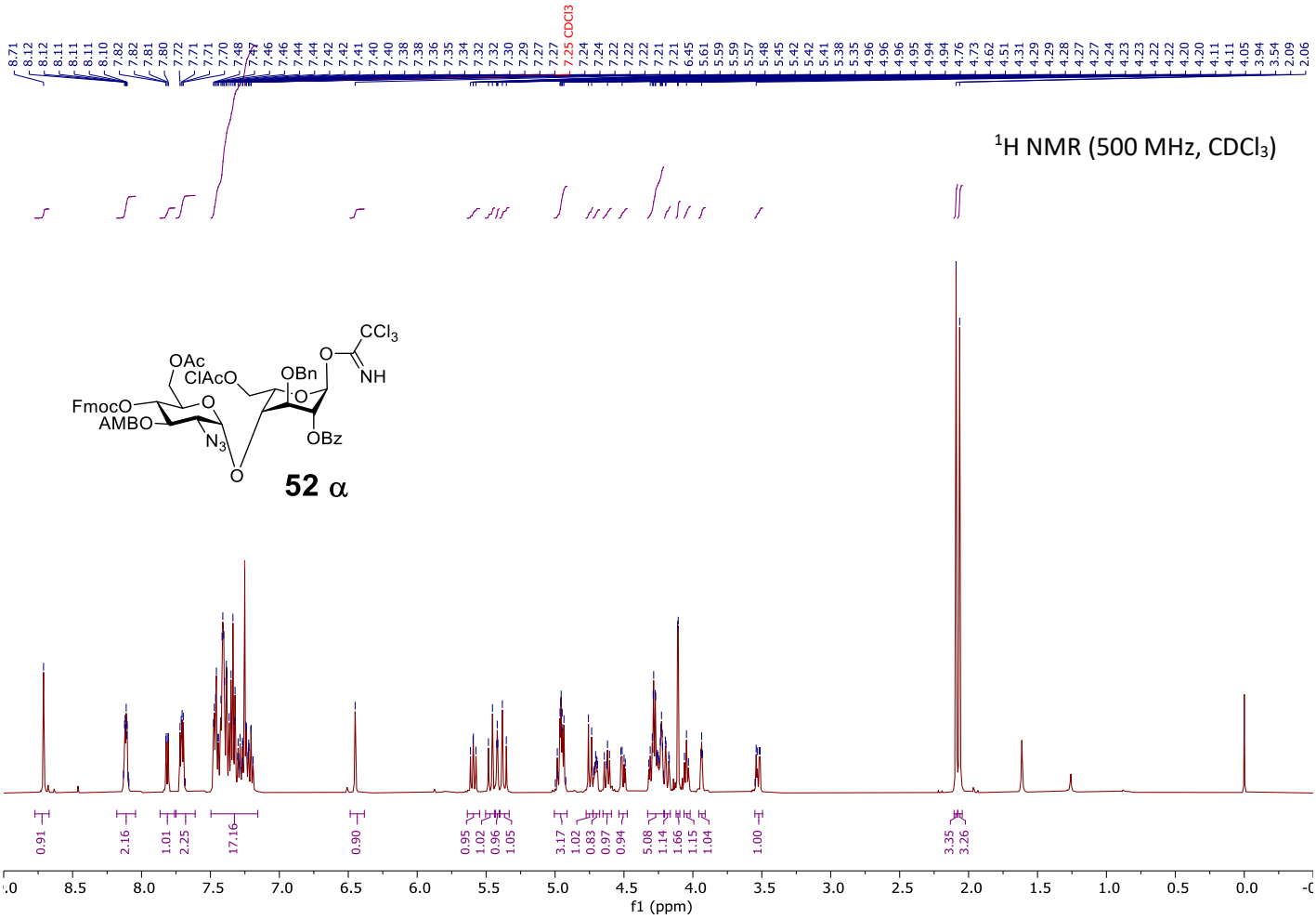

^{1}H NMR (500 MHz, $CDCl_3$)

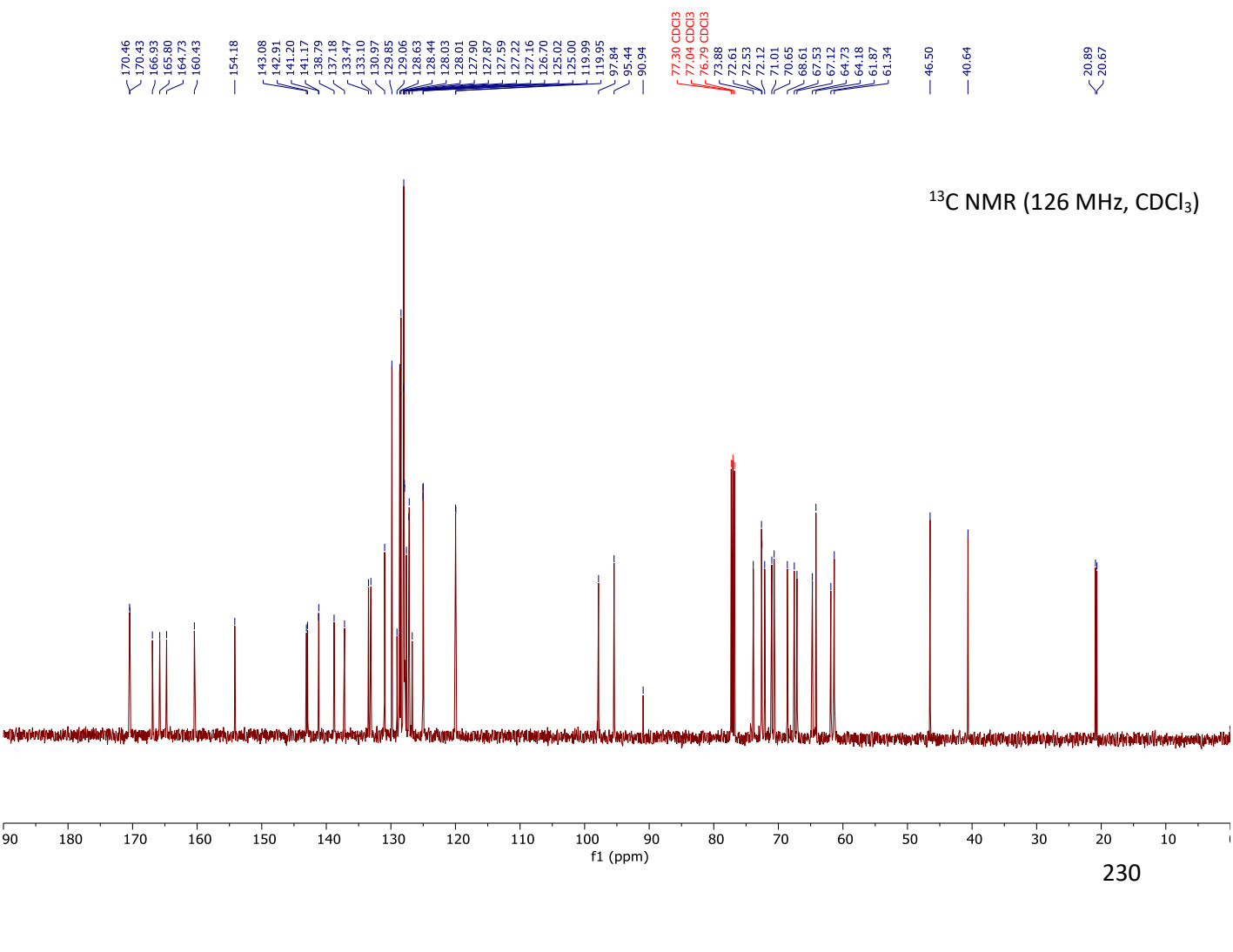

^{13}C NMR (126 MHz, $CDCl_3$)

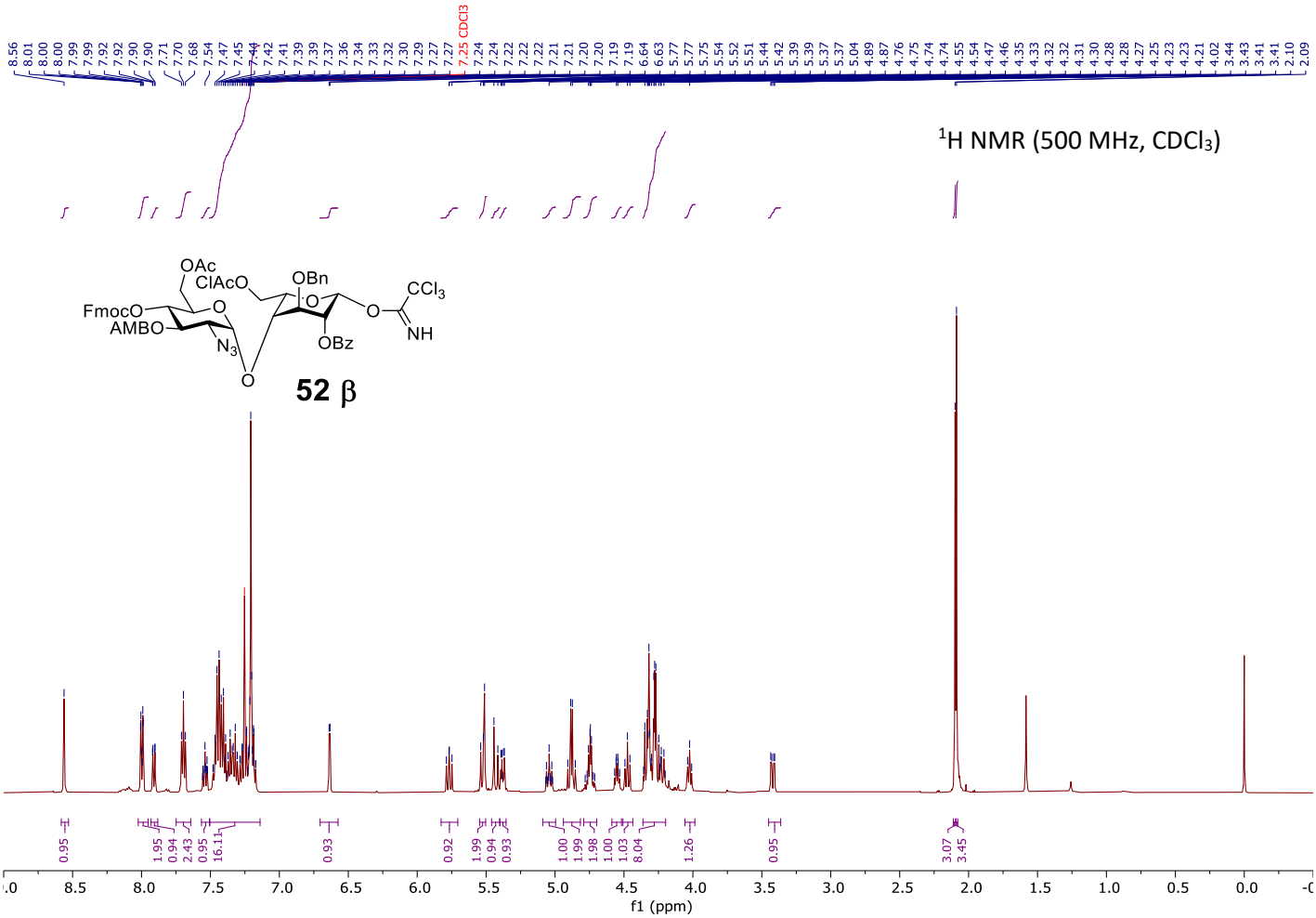

^{1}H NMR (500 MHz, $CDCl_3$)

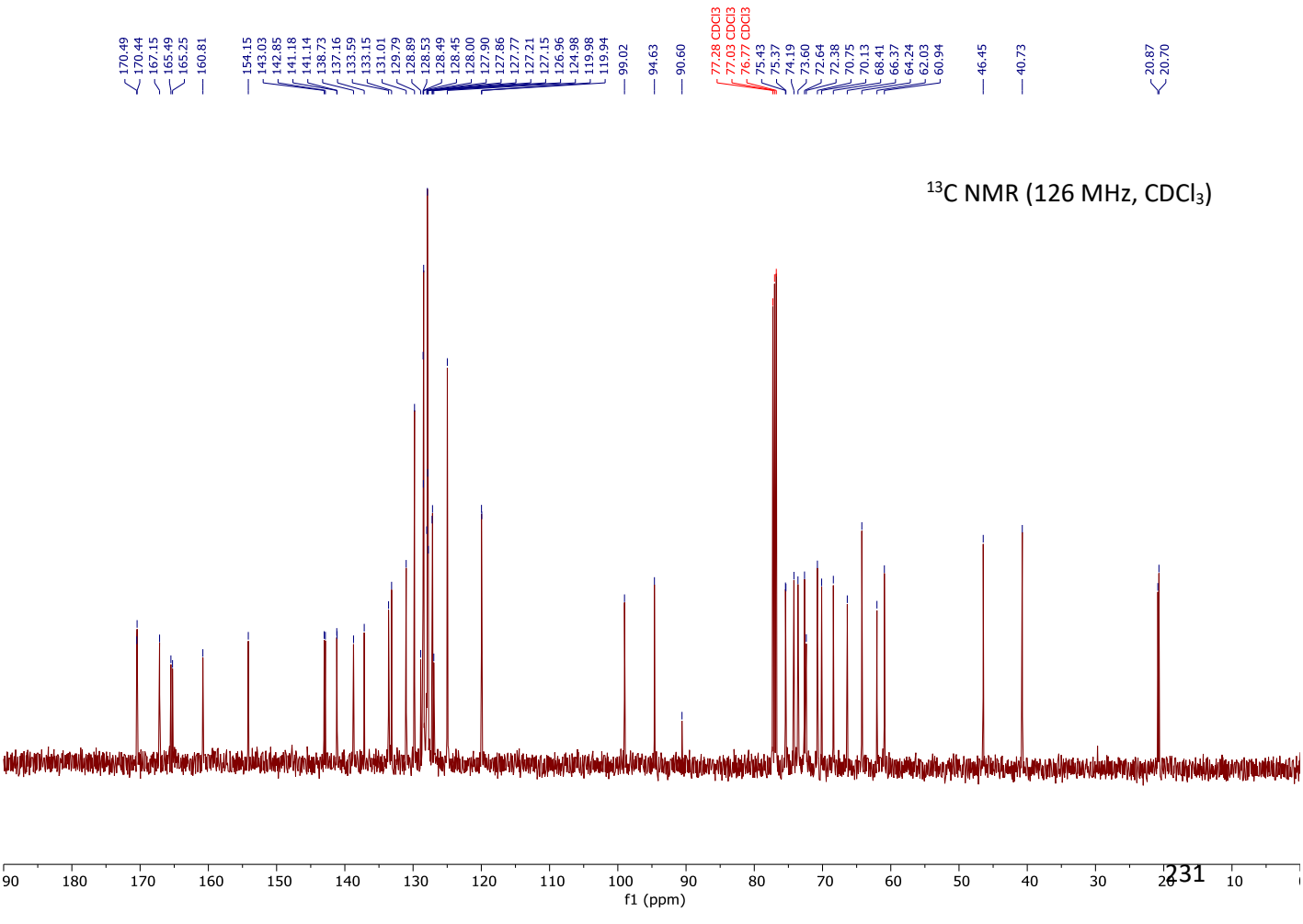

^{13}C NMR (126 MHz, $CDCl_3$)

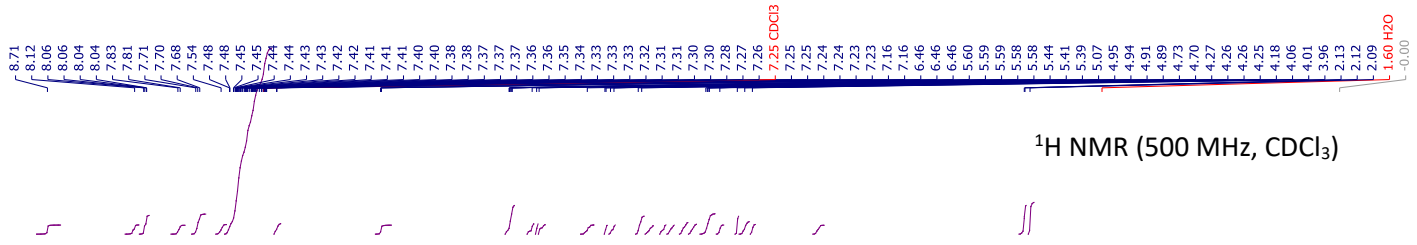

^{1}H NMR (500 MHz, $CDCl_3$)

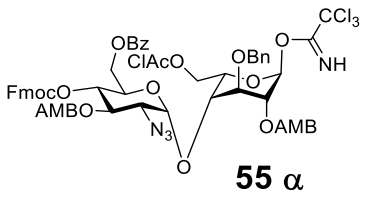

55 α

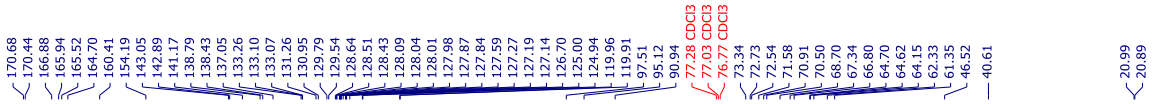

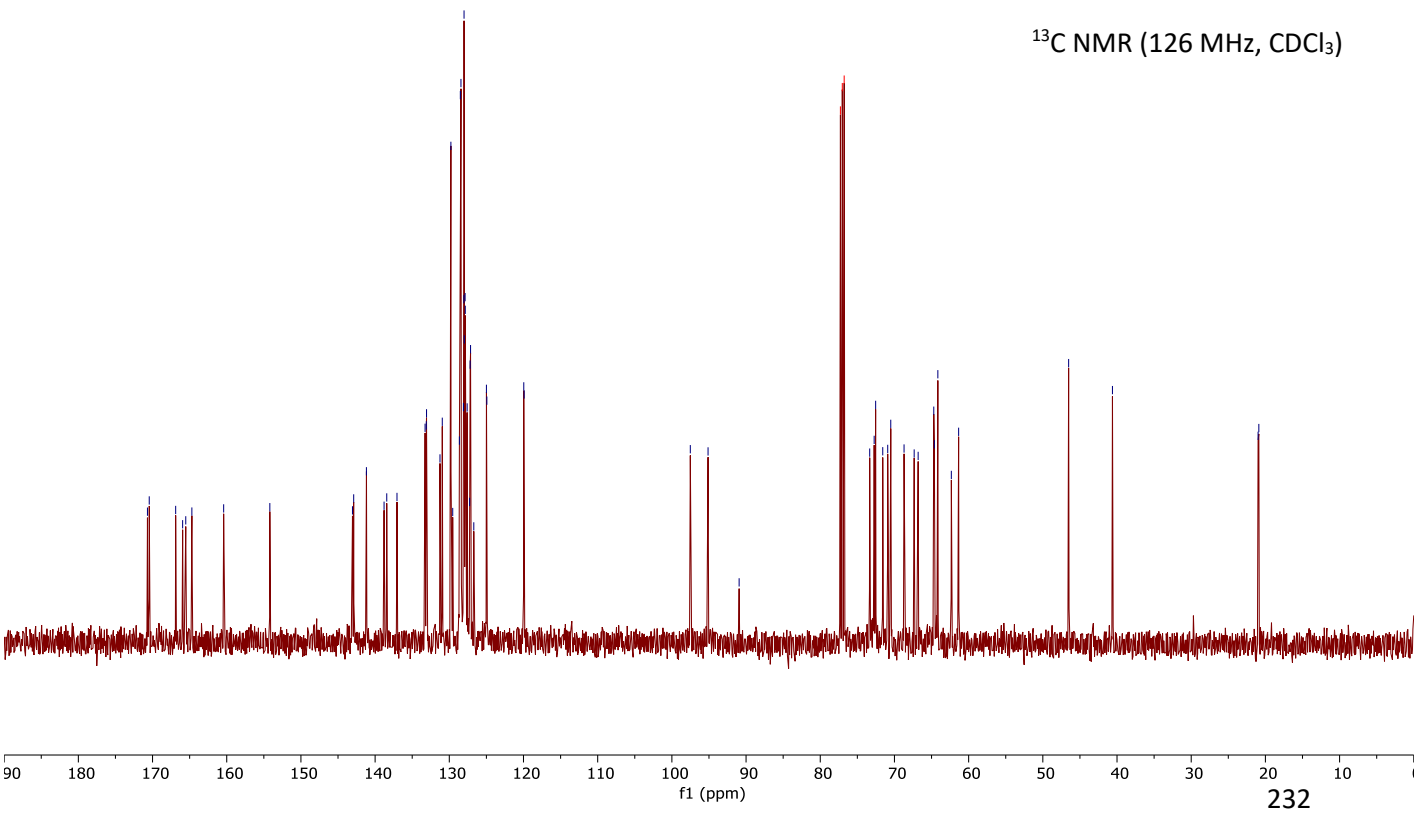

^{13}C NMR (126 MHz, $CDCl_3$)

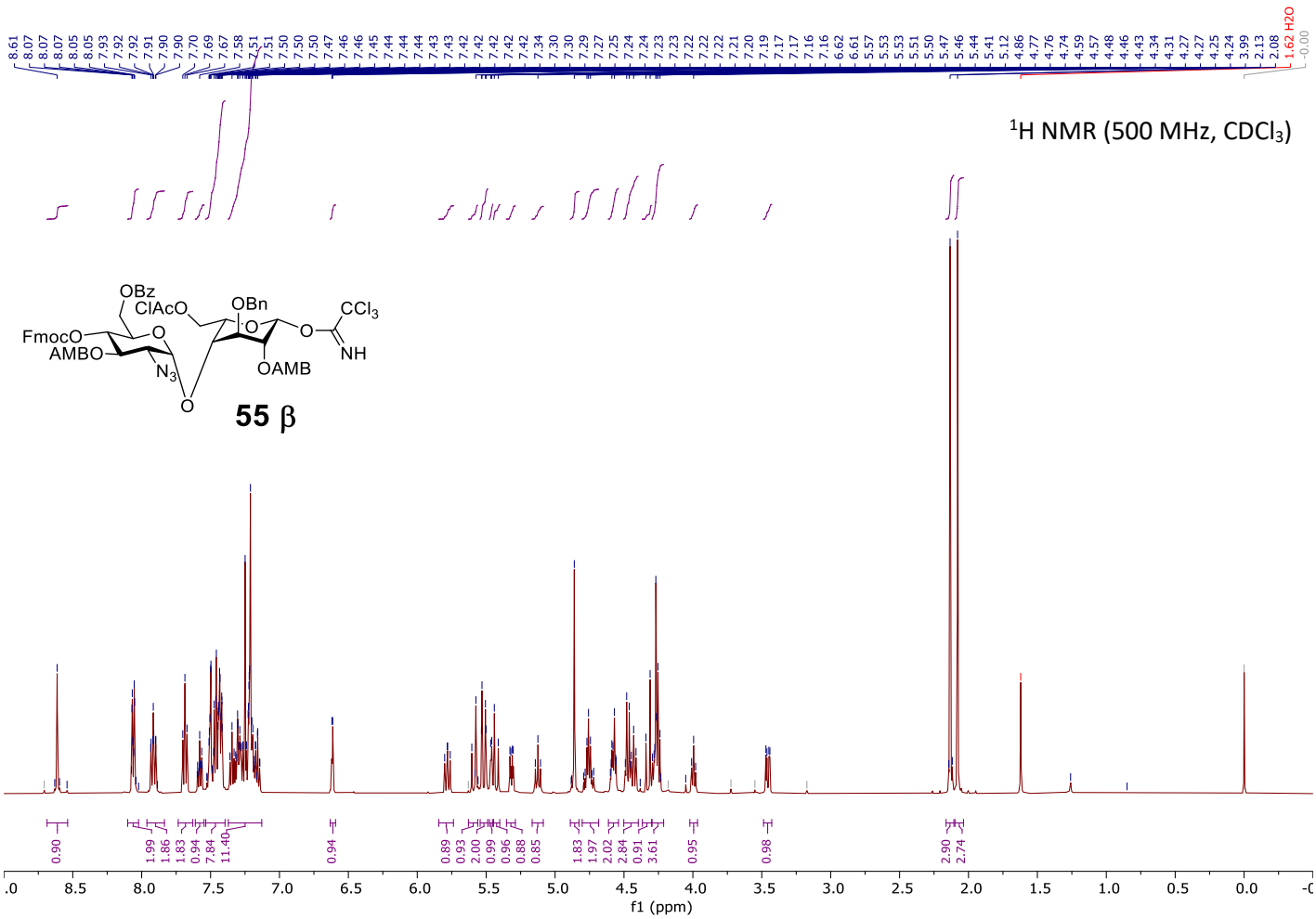

^{1}H NMR (500 MHz, $CDCl_3$)

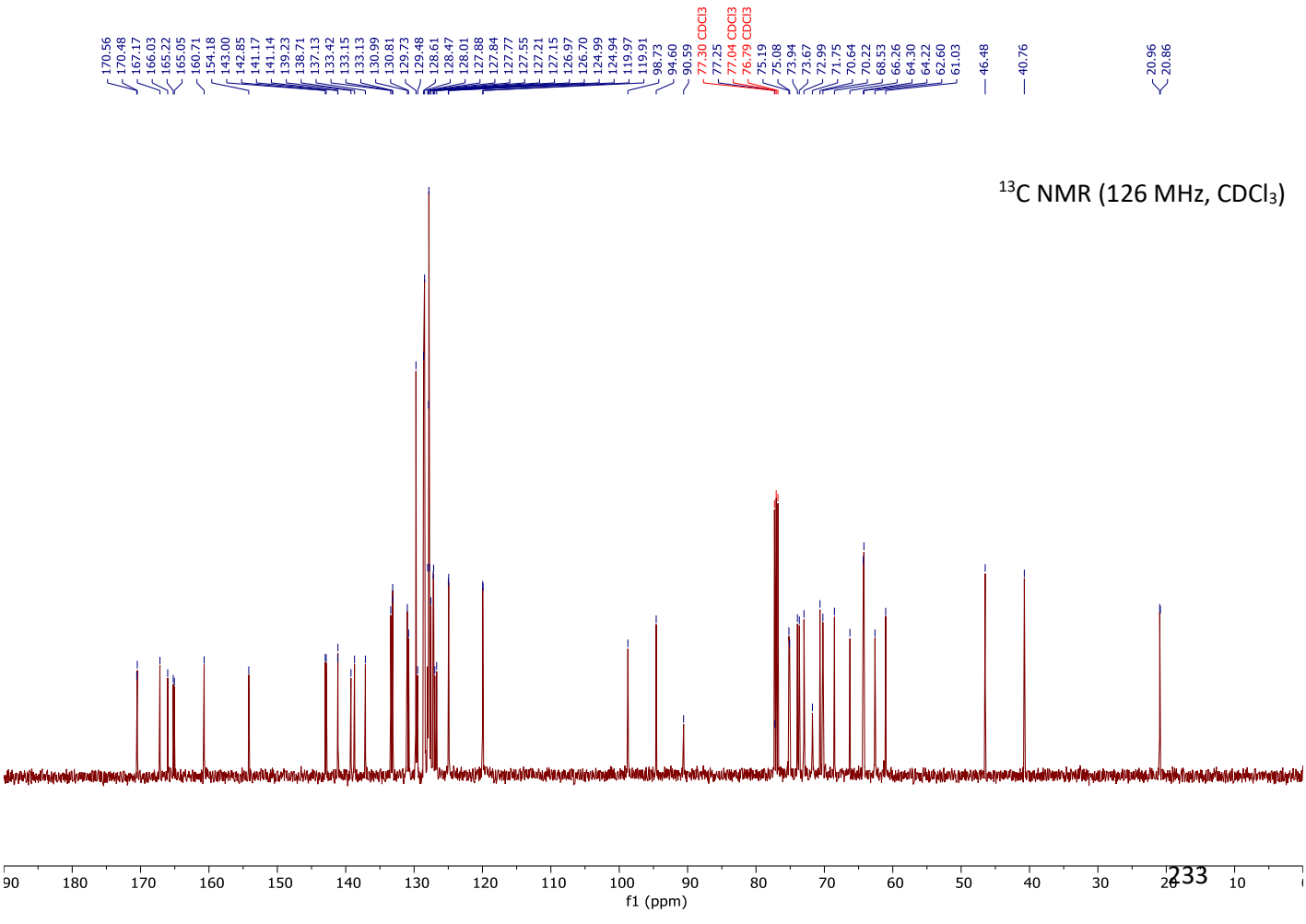

^{13}C NMR (126 MHz, $CDCl_3$)

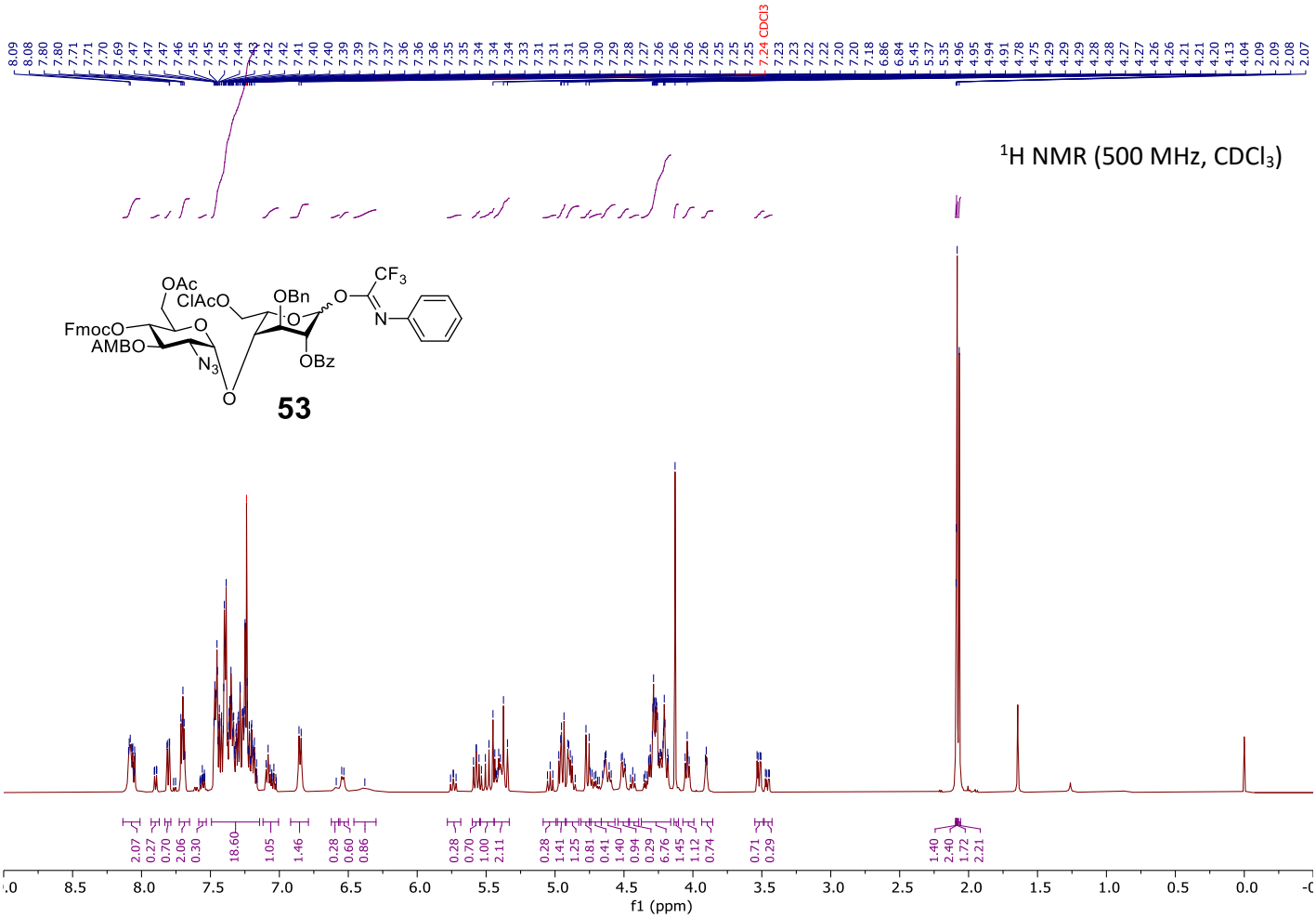

^{1}H NMR (500 MHz, $CDCl_3$)

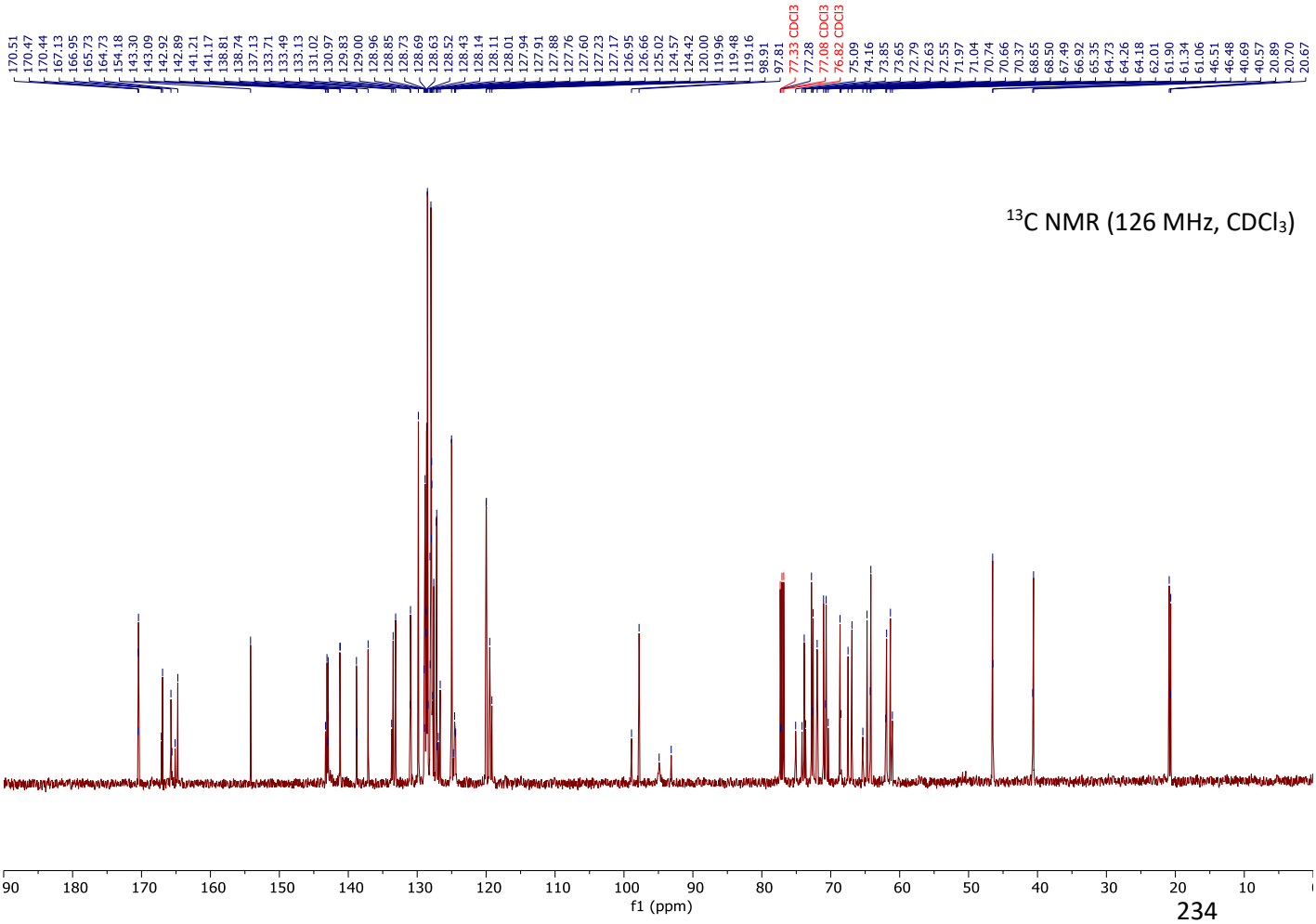

^{13}C NMR (126 MHz, $CDCl_3$)

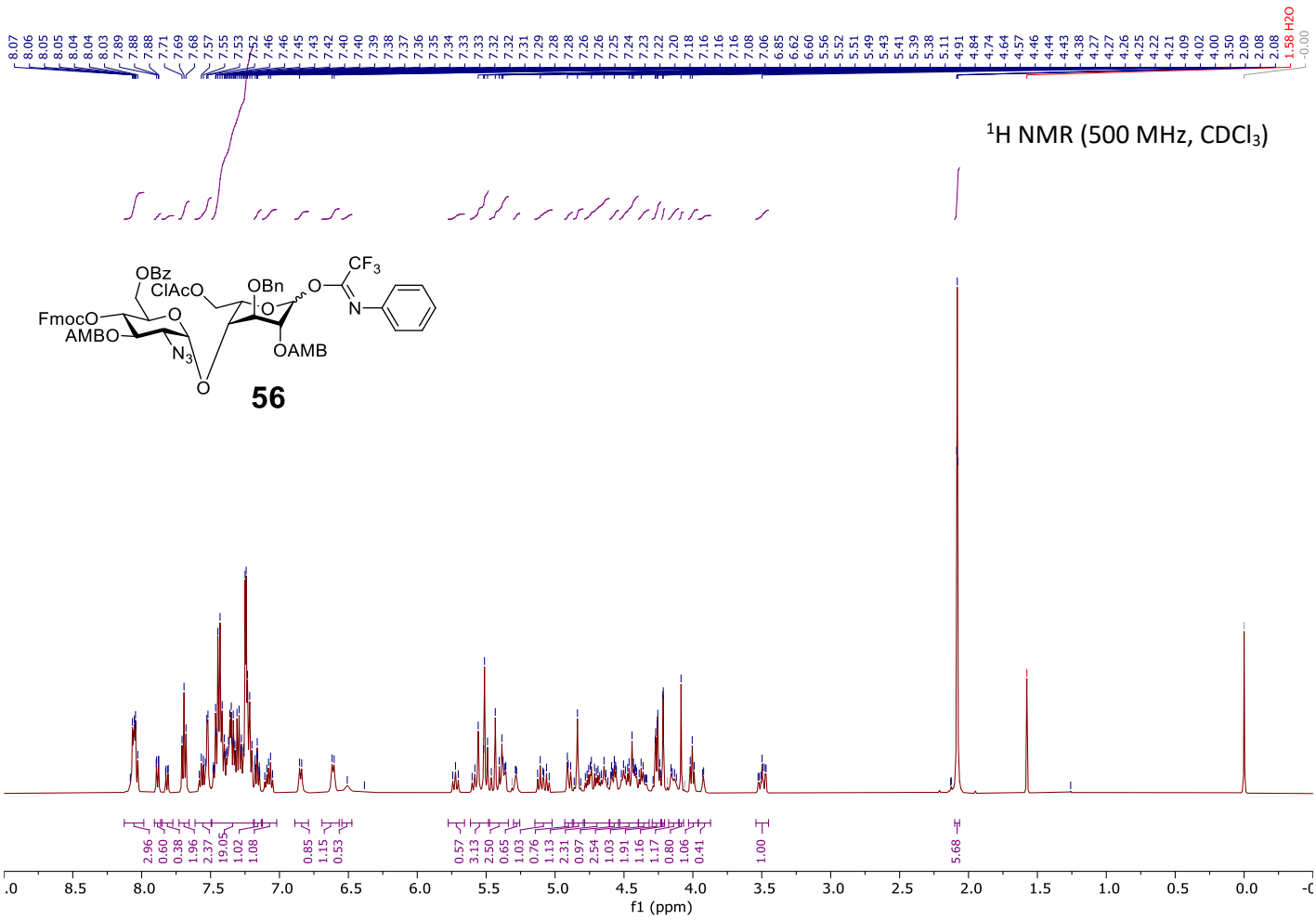
OBz
ClAcO
OBn
O
CF3
FmocO
AMBO
O
N3
O
N
OAMB
O
56
1H NMR (500 MHz, CDCl3)
f1 (ppm)

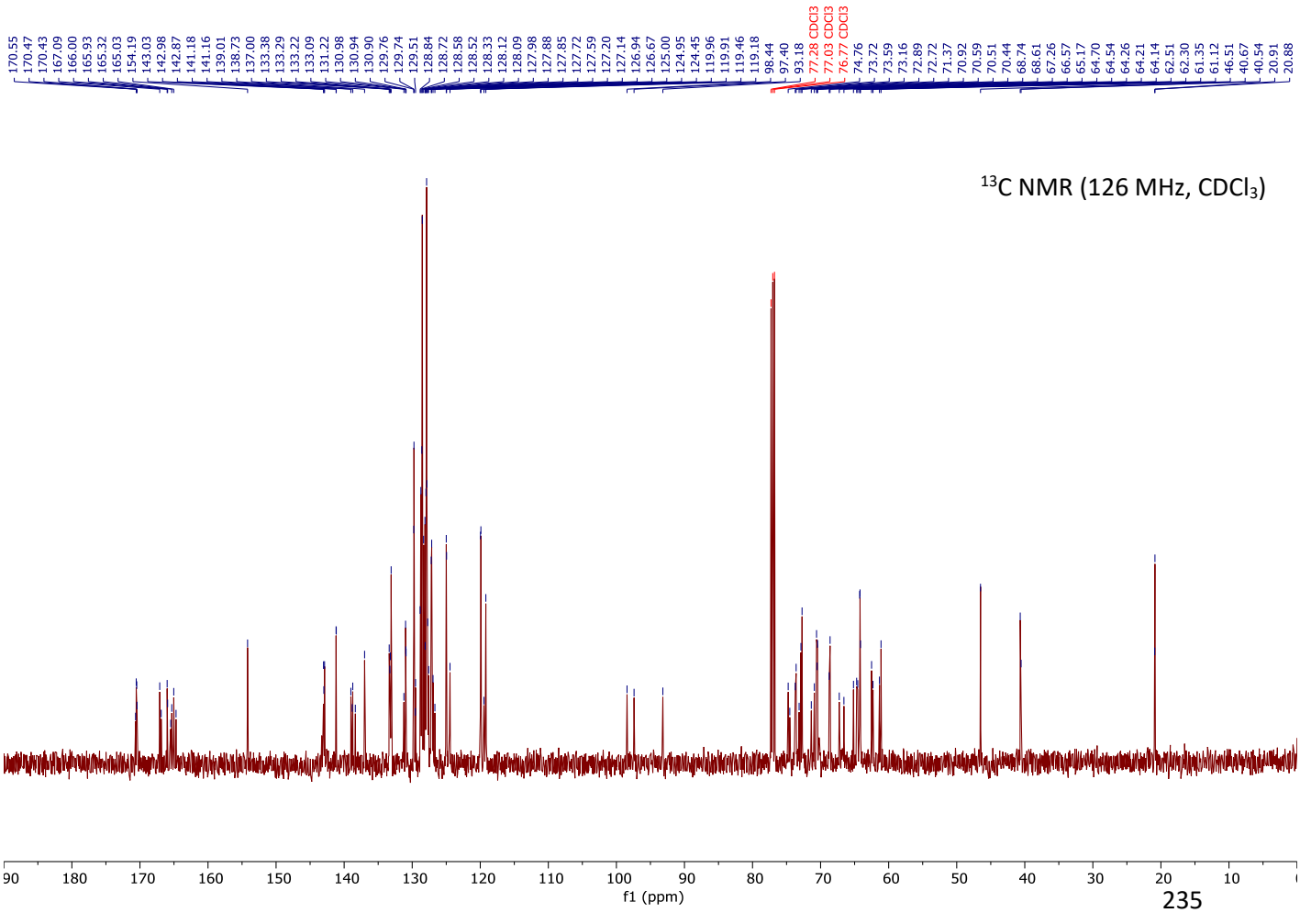
13C NMR (126 MHz, CDCl3)
f1 (ppm)

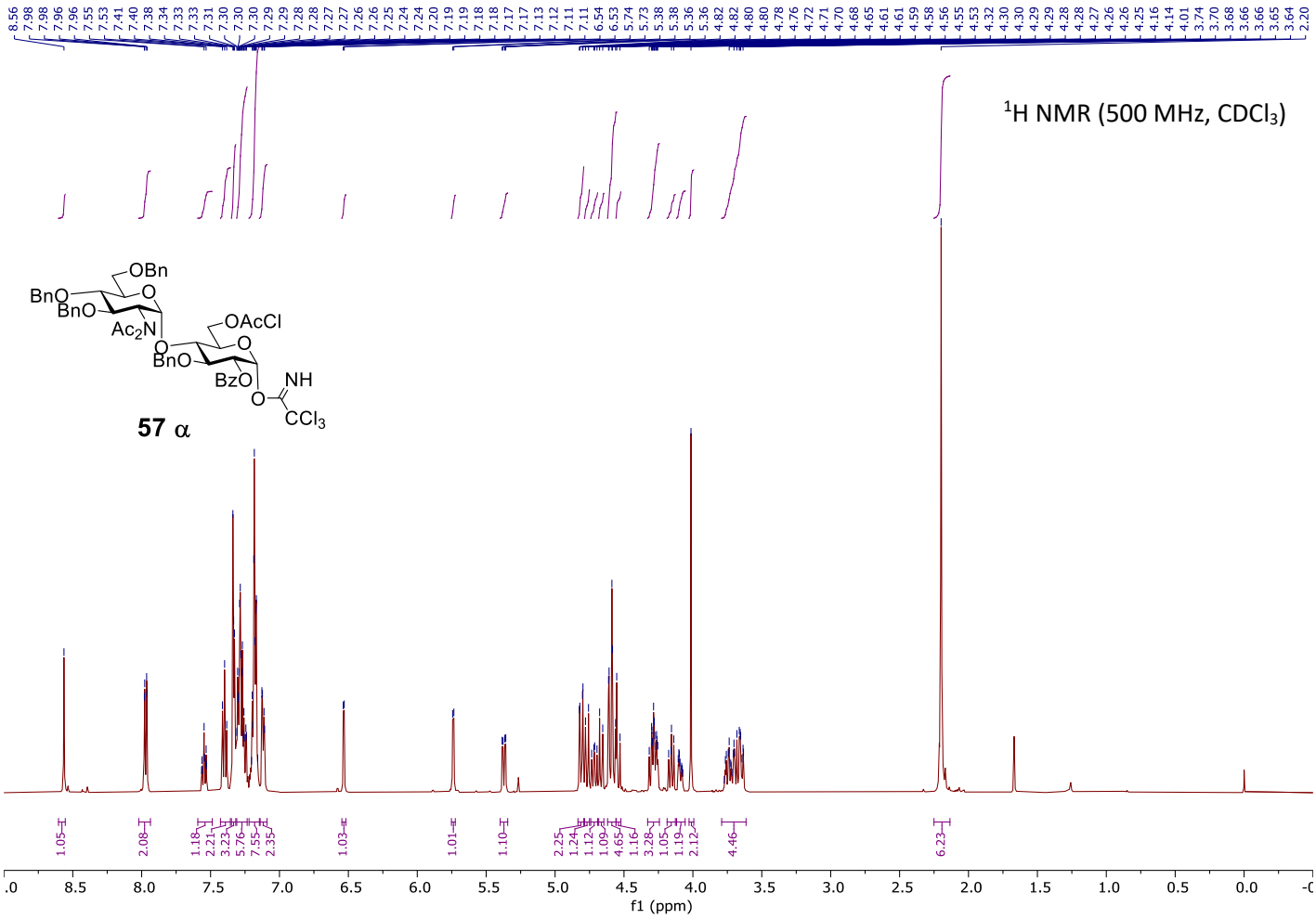
^{1}H NMR (500 MHz, $CDCl_3$)
OBn
BnO
BnO
Ac_2N
O
OAcCl
O
BnO
BzO
NH
O
CCl_3
57 α
f1 (ppm)

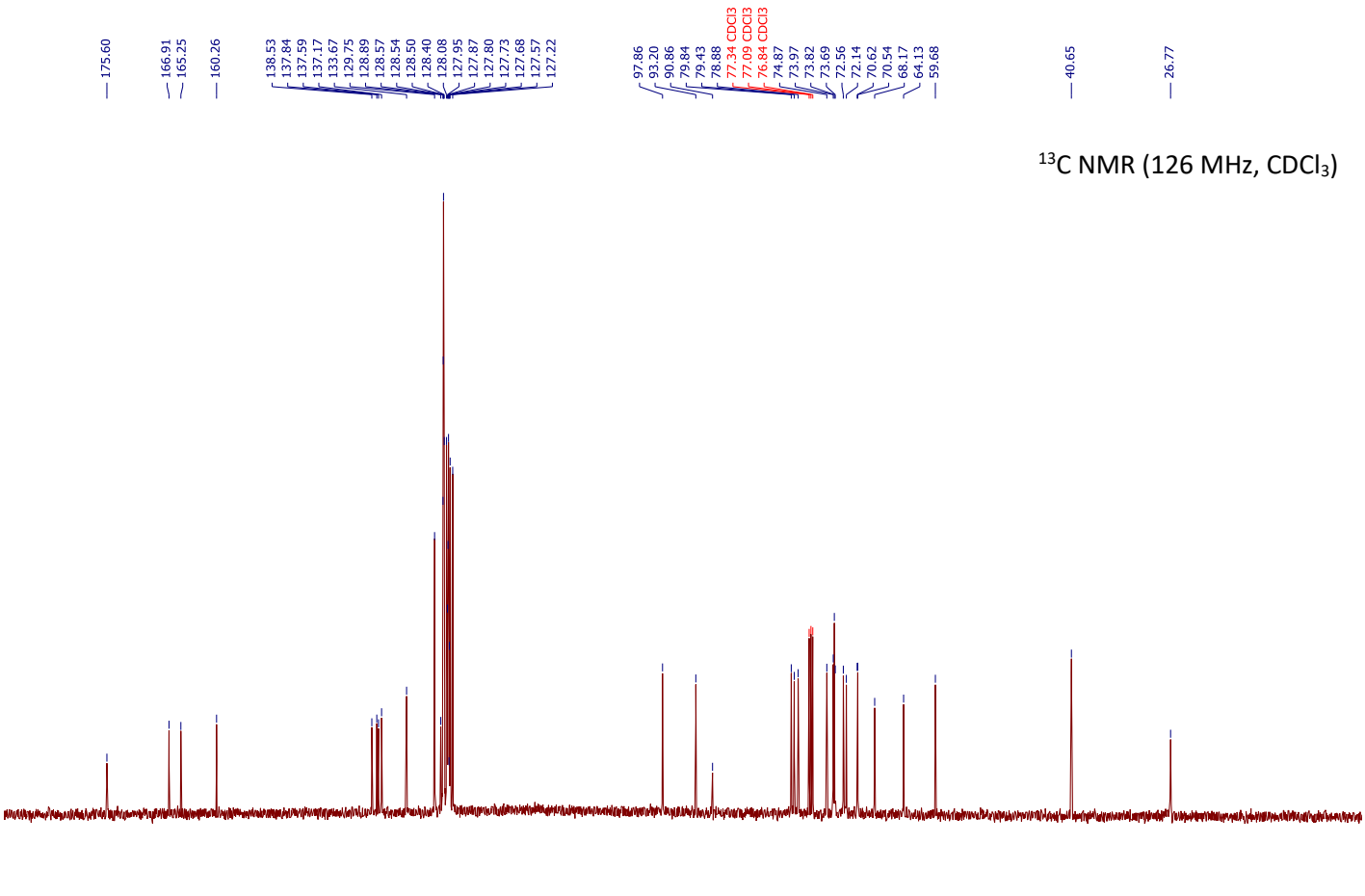
^{13}C NMR (126 MHz, $CDCl_3$)
f1 (ppm)

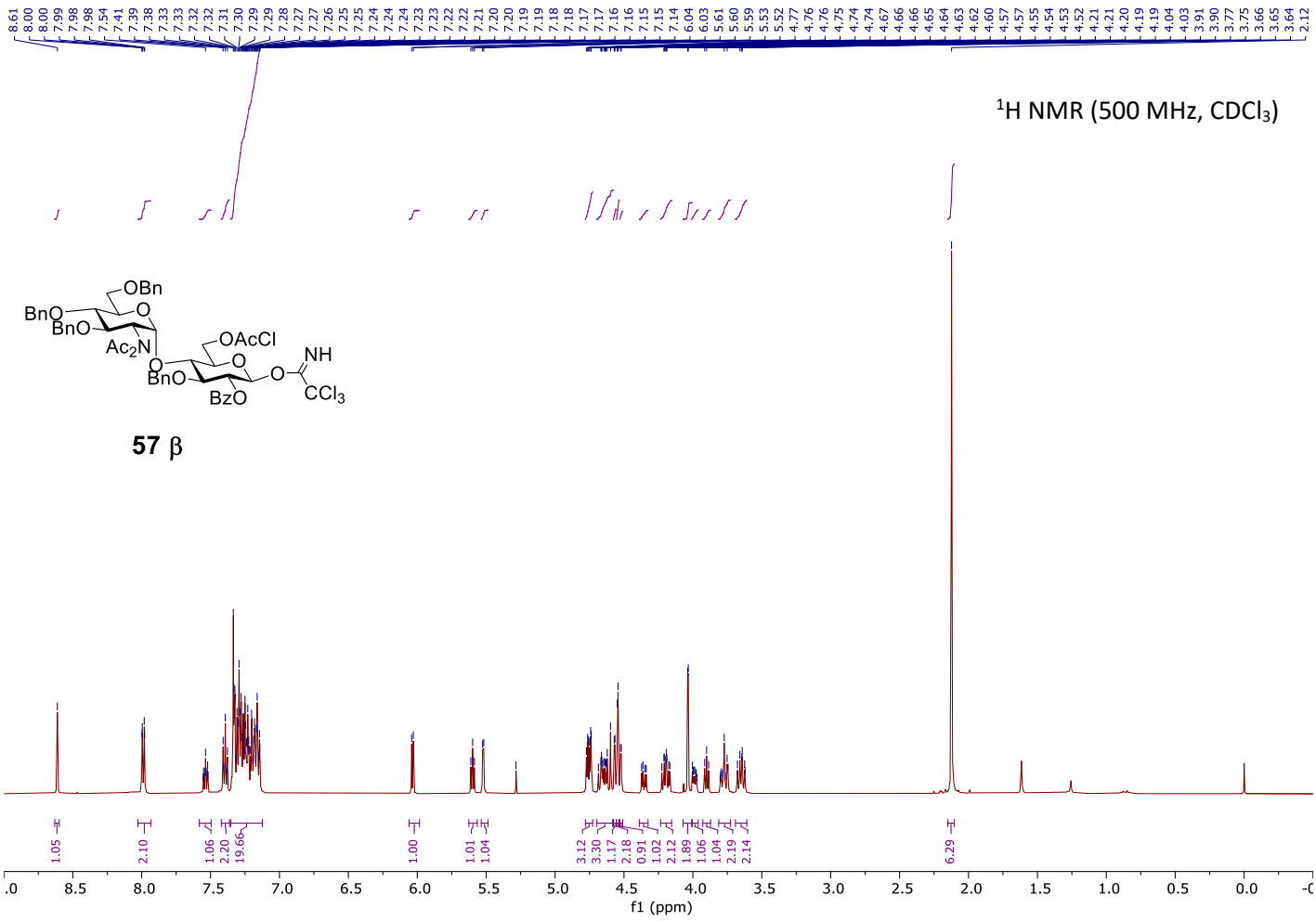

^{1}H NMR (500 MHz, $CDCl_3$)

57 β

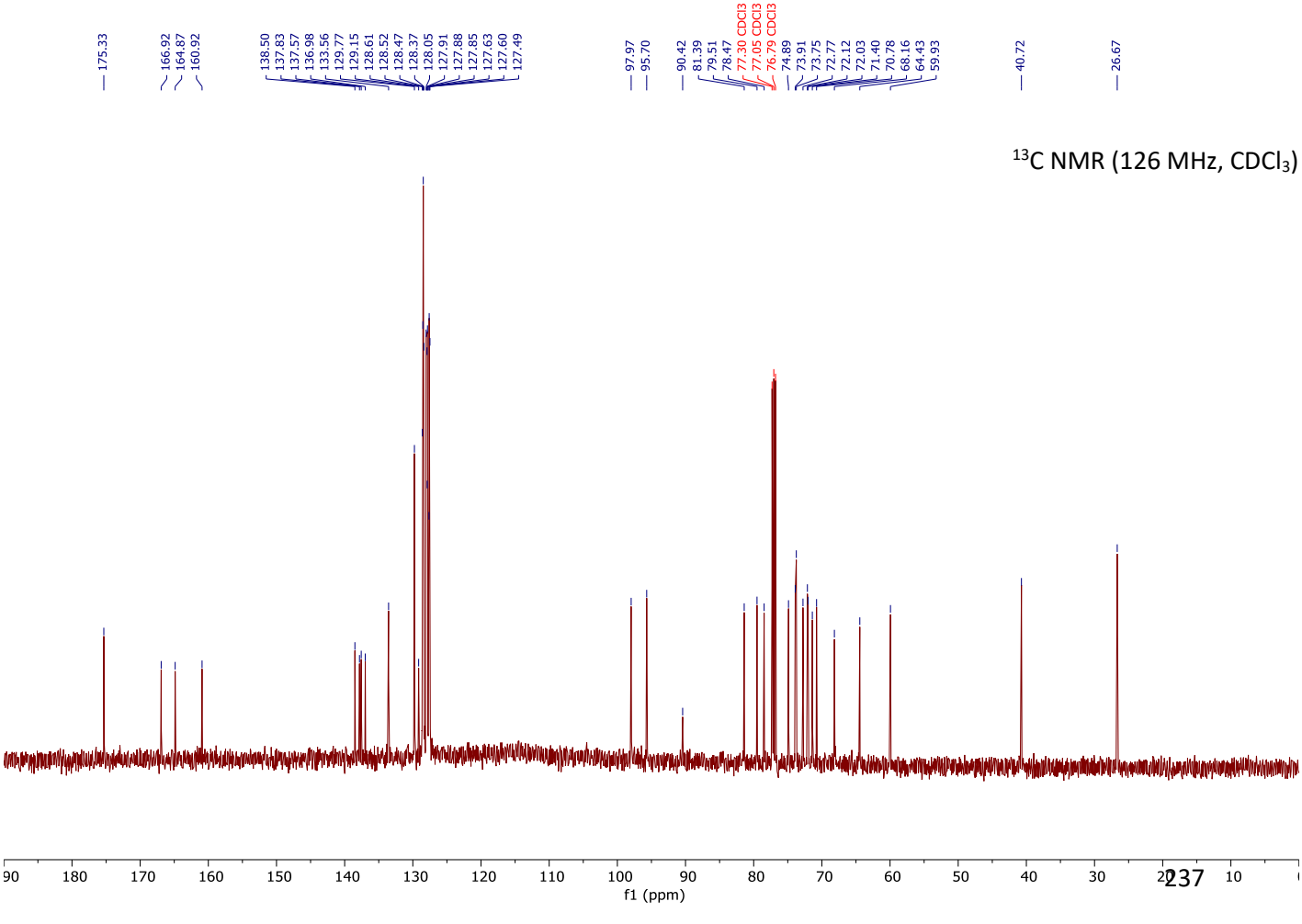

^{13}C NMR (126 MHz, $CDCl_3$)

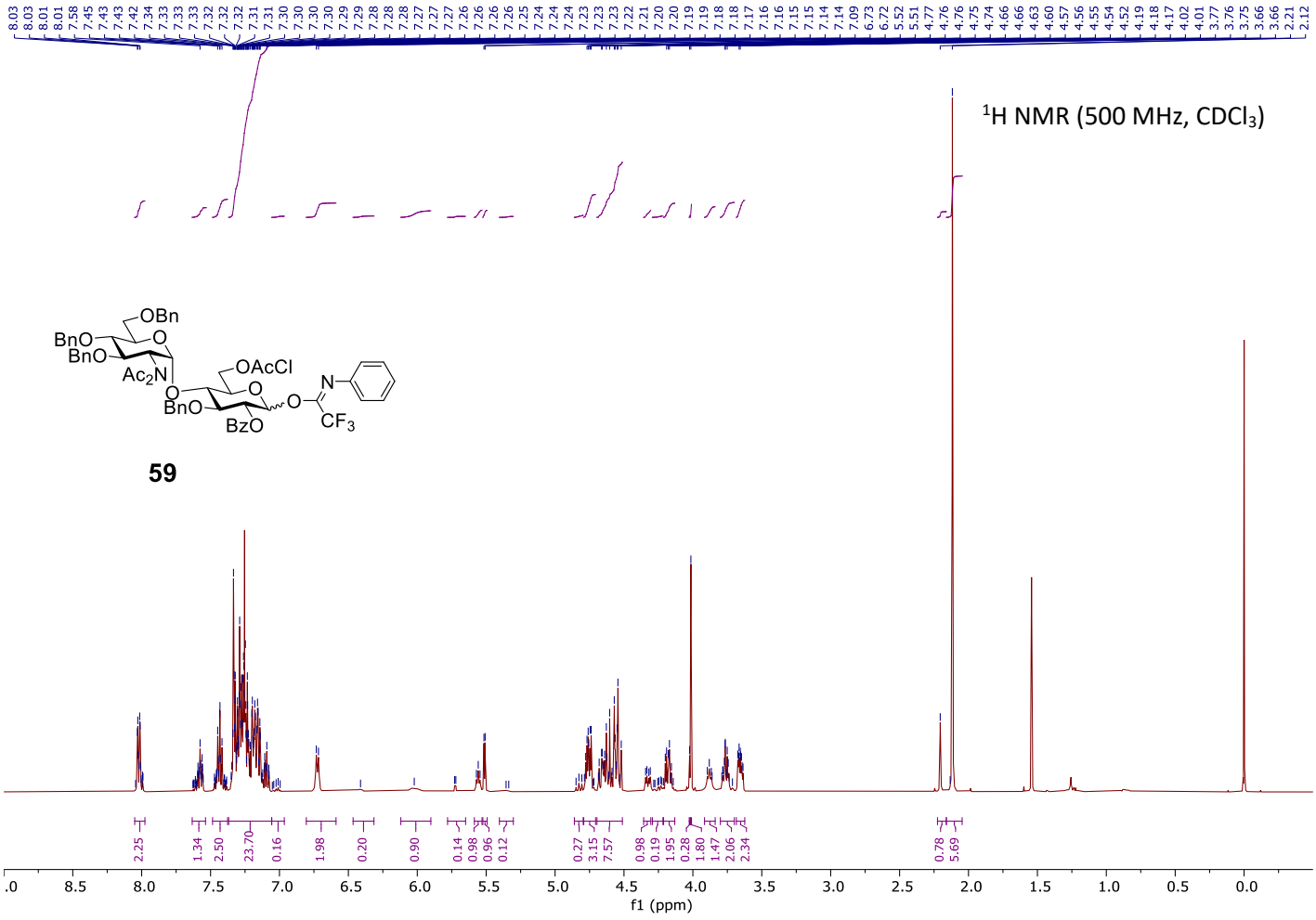
^{1}H NMR (500 MHz, $CDCl_3$)
OBn
BnO
BnO
Ac_2N
OAcCl
O
BnO
BzO
N
CF_3
59
f1 (ppm)

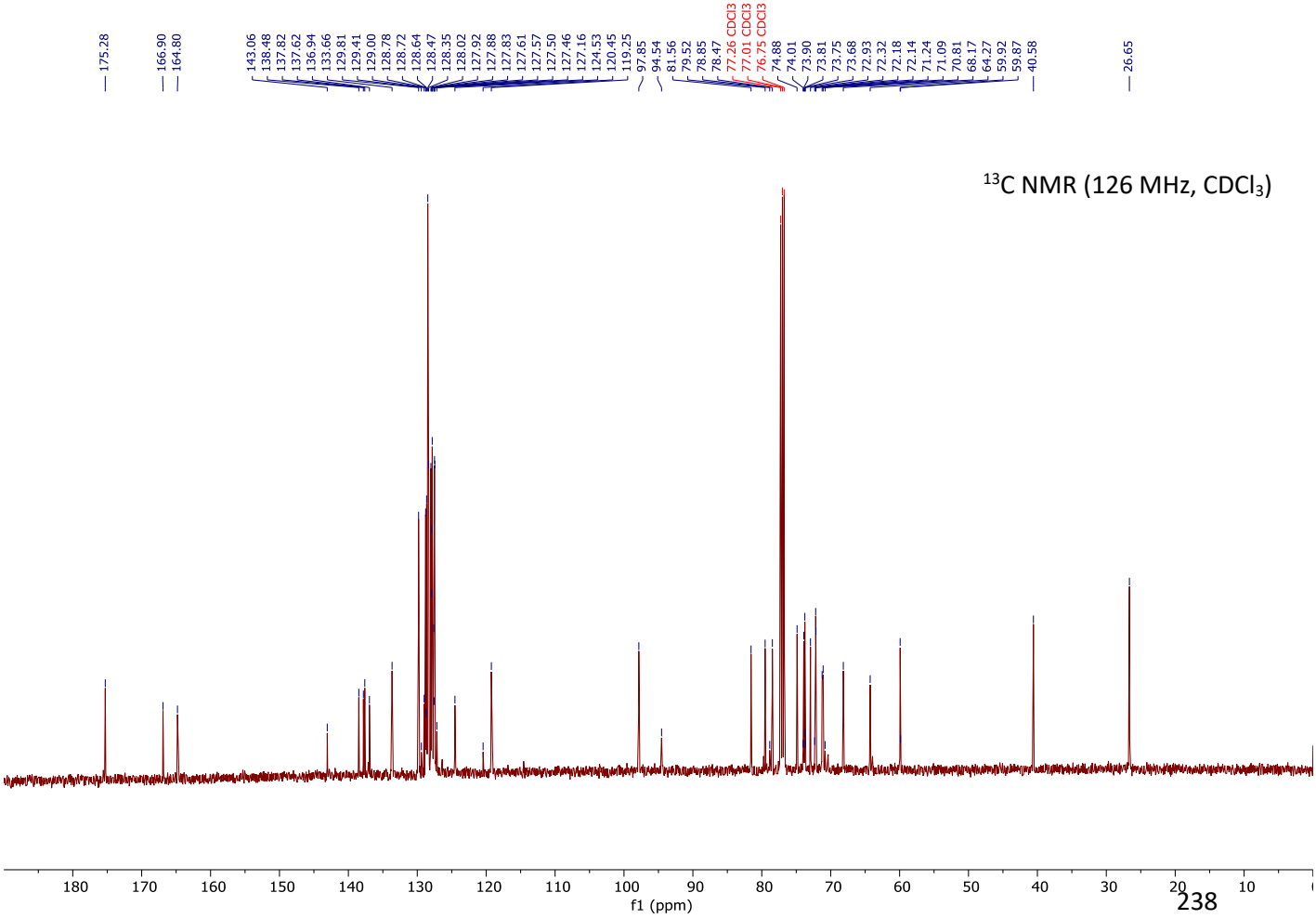
^{13}C NMR (126 MHz, $CDCl_3$)
f1 (ppm)

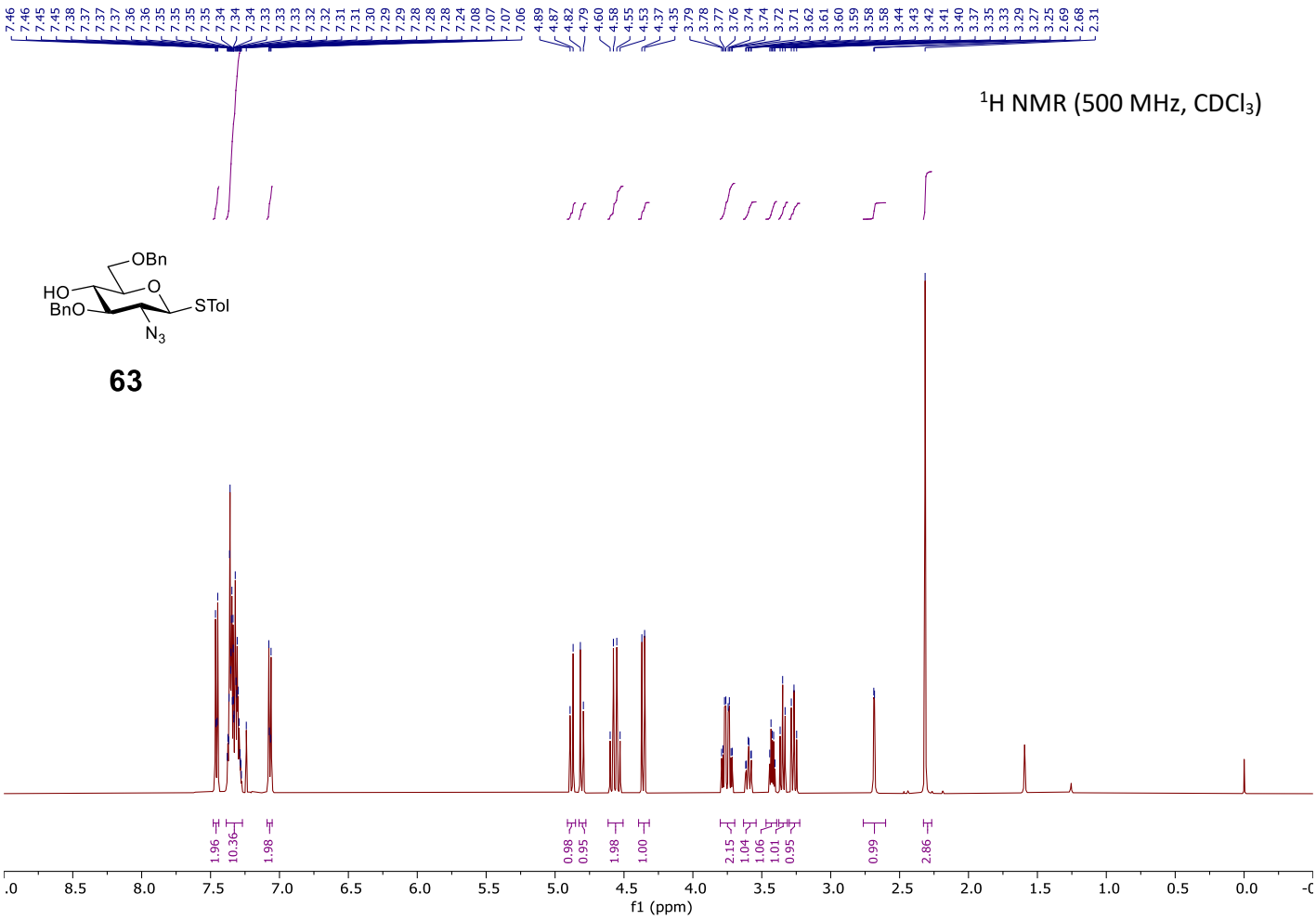

63

^{1}H NMR (500 MHz, $CDCl_3$)

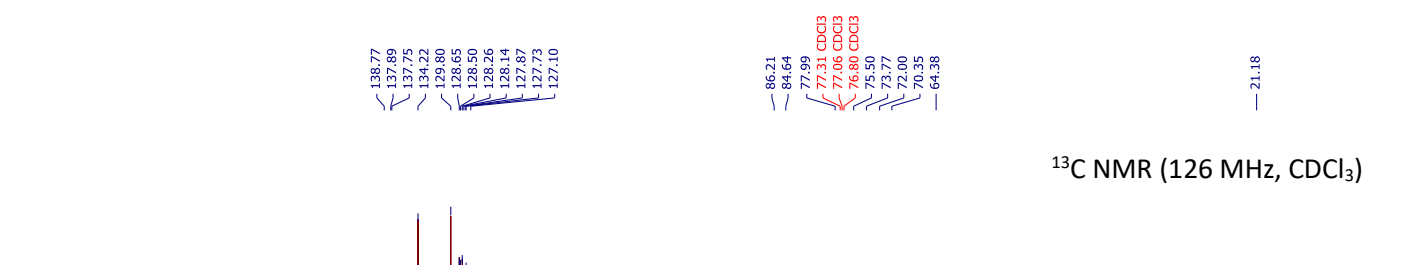

^{13}C NMR (126 MHz, $CDCl_3$)

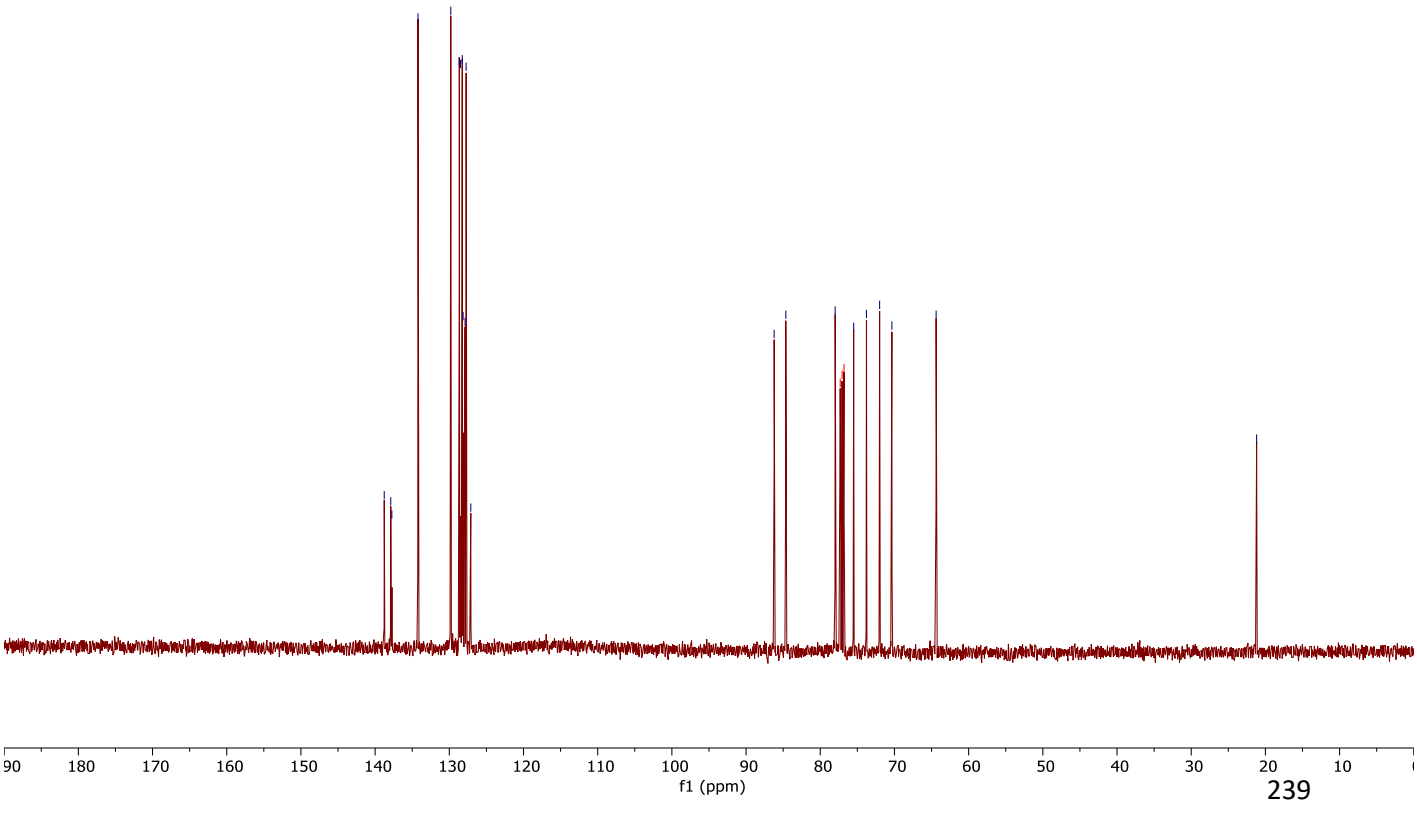

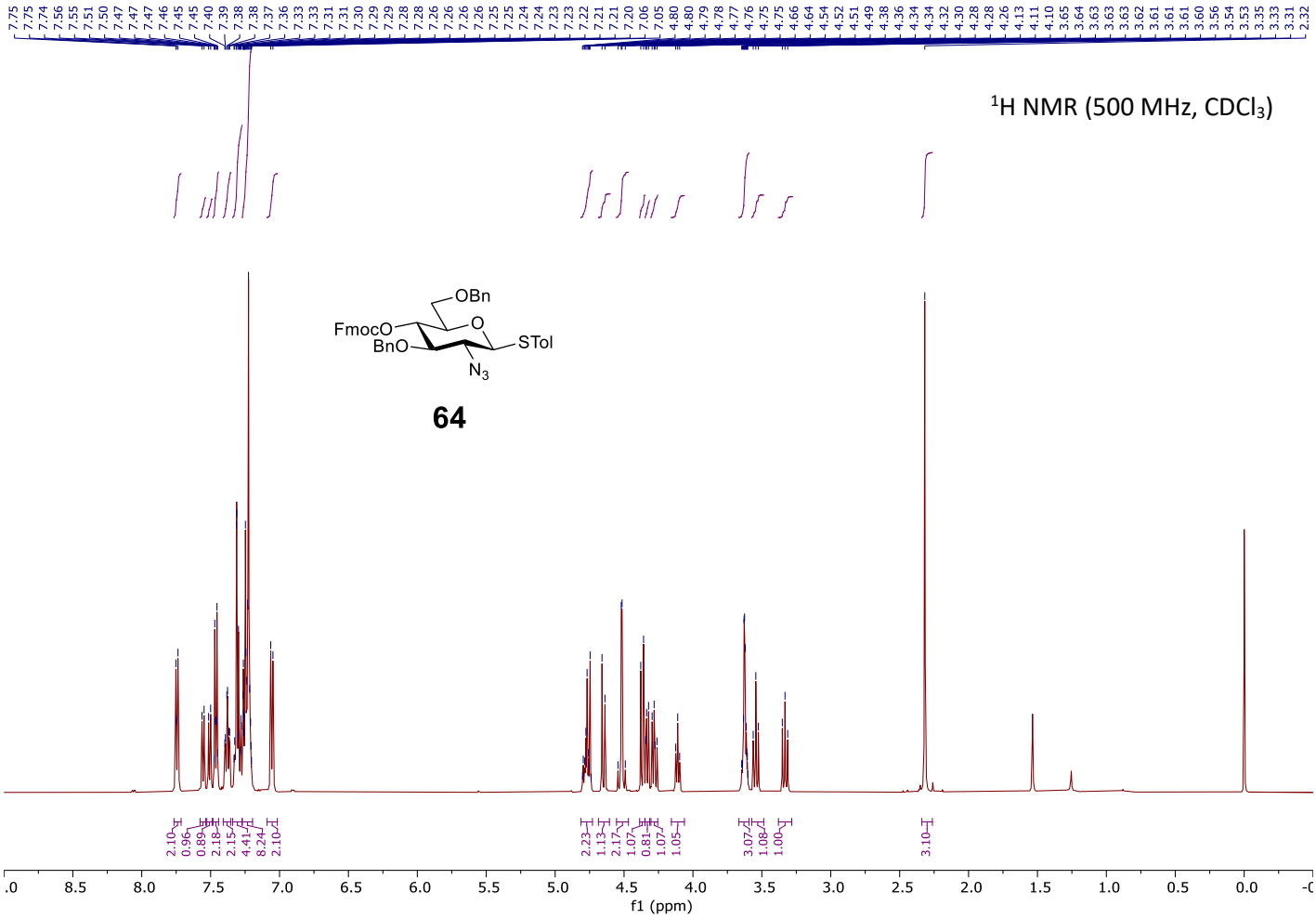

64

^{1}H NMR (500 MHz, $CDCl_3$)

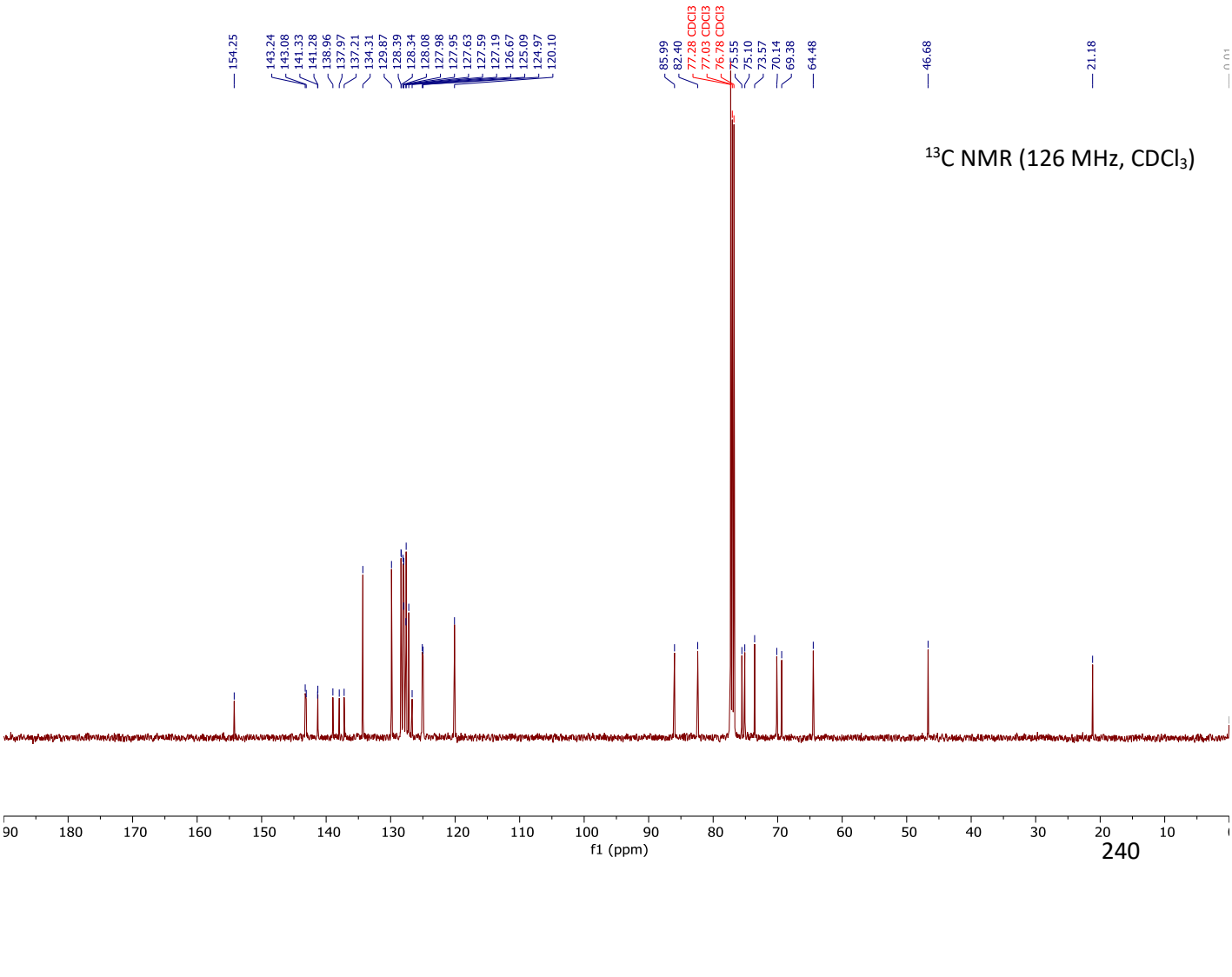

^{13}C NMR (126 MHz, $CDCl_3$)

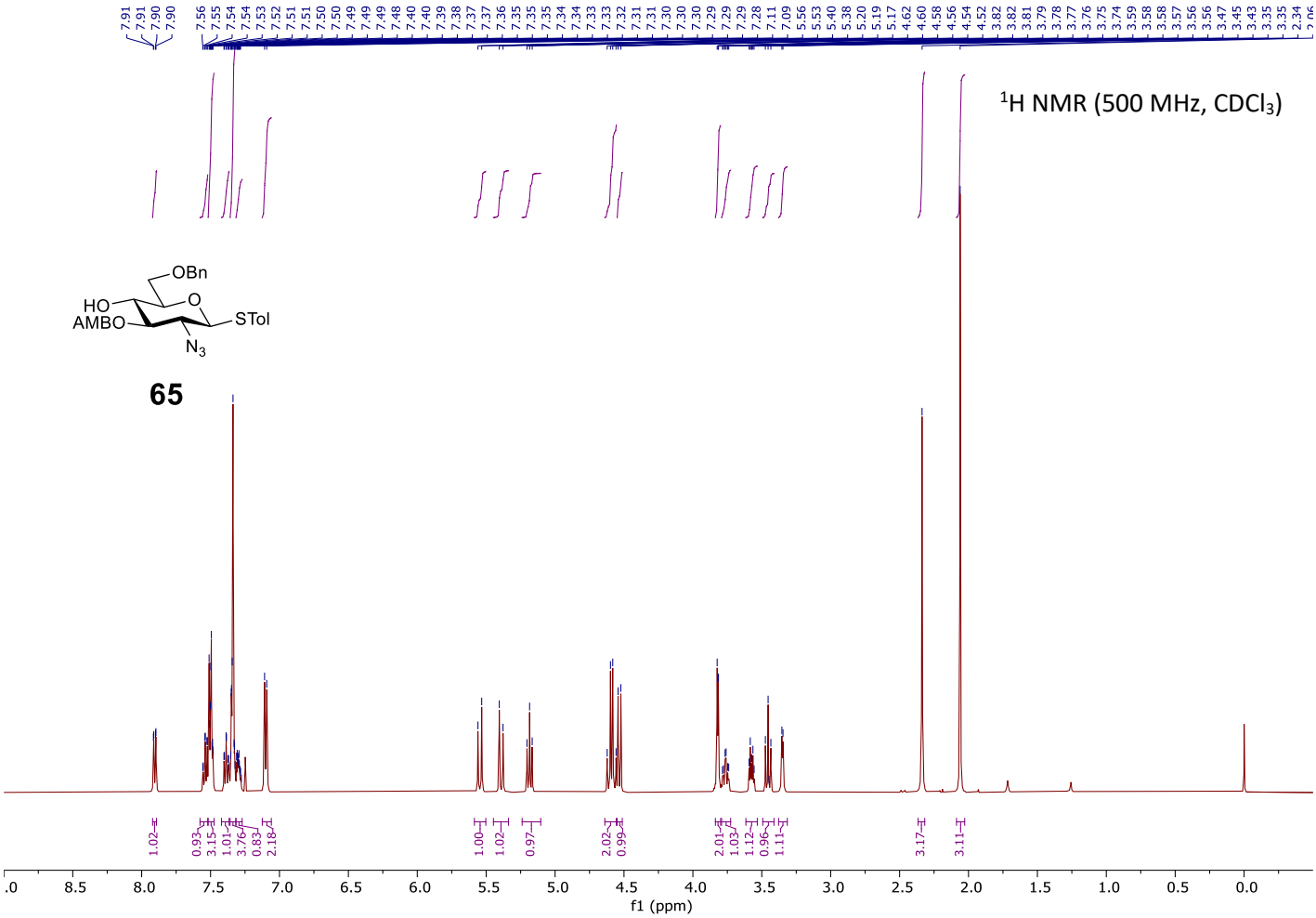
^{1}H NMR (500 MHz, $CDCl_3$)
OBn
HO
AMBO
O
STol
N_3
65
f1 (ppm)

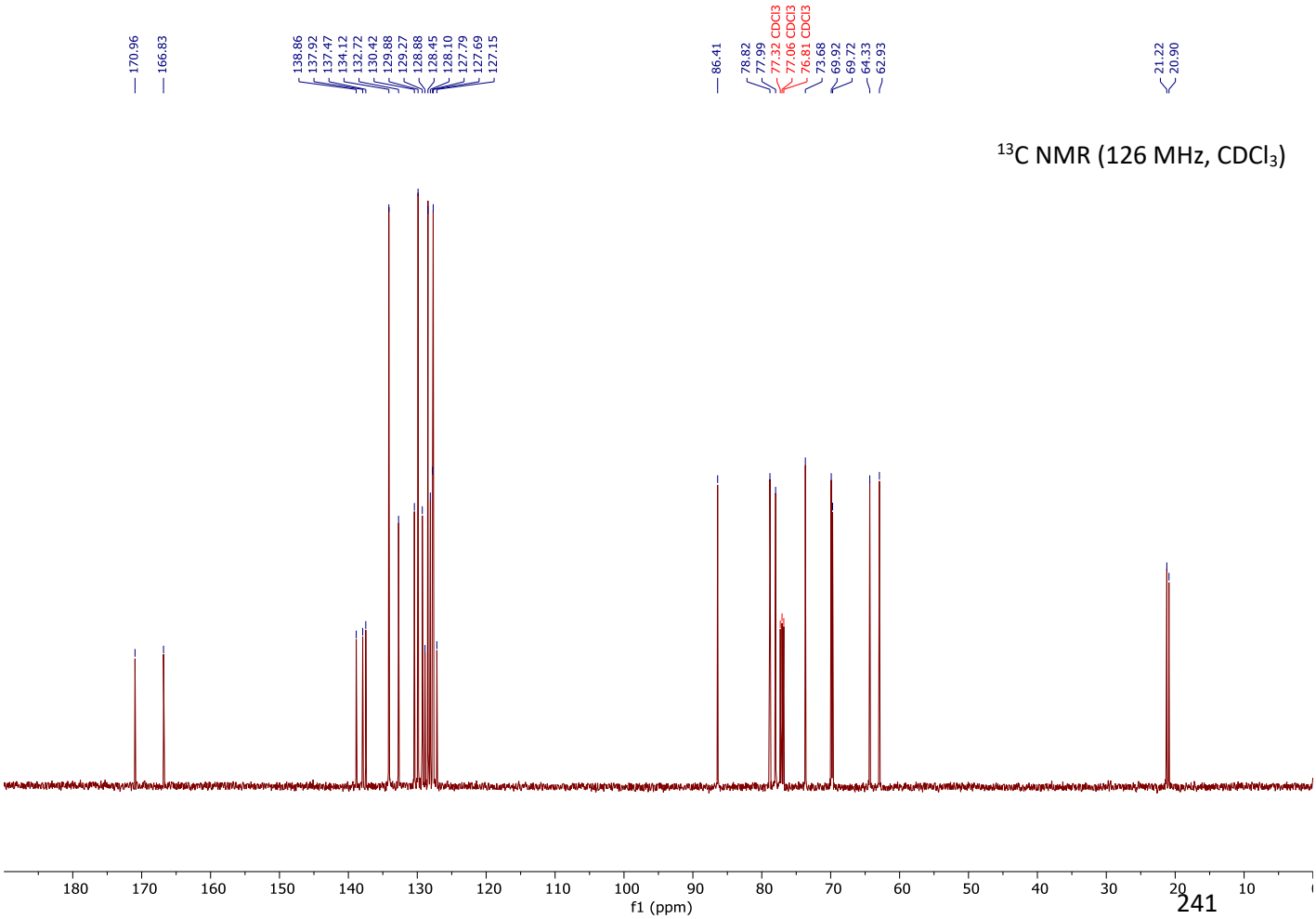
^{13}C NMR (126 MHz, $CDCl_3$)
f1 (ppm)

^{1}H NMR (500 MHz, $CDCl_3$)

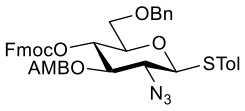

66

f1 (ppm)

^{13}C NMR (126 MHz, $CDCl_3$)

f1 (ppm)

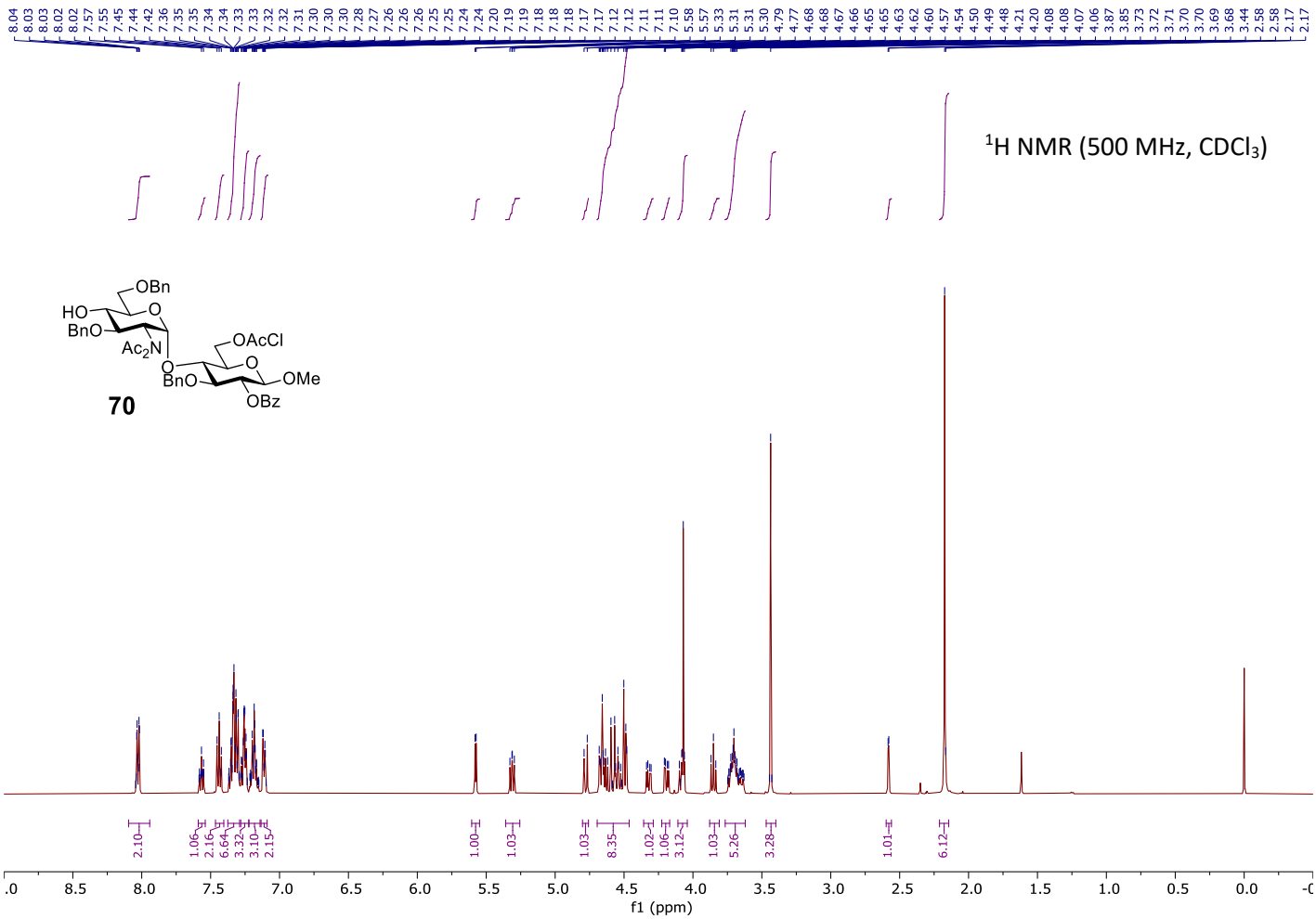
^{1}H NMR (500 MHz, $CDCl_3$)
OBn
HO
O
BnO
Ac_2N
OAcCl
O
O
BnO
OMe
OBz
70
f1 (ppm)

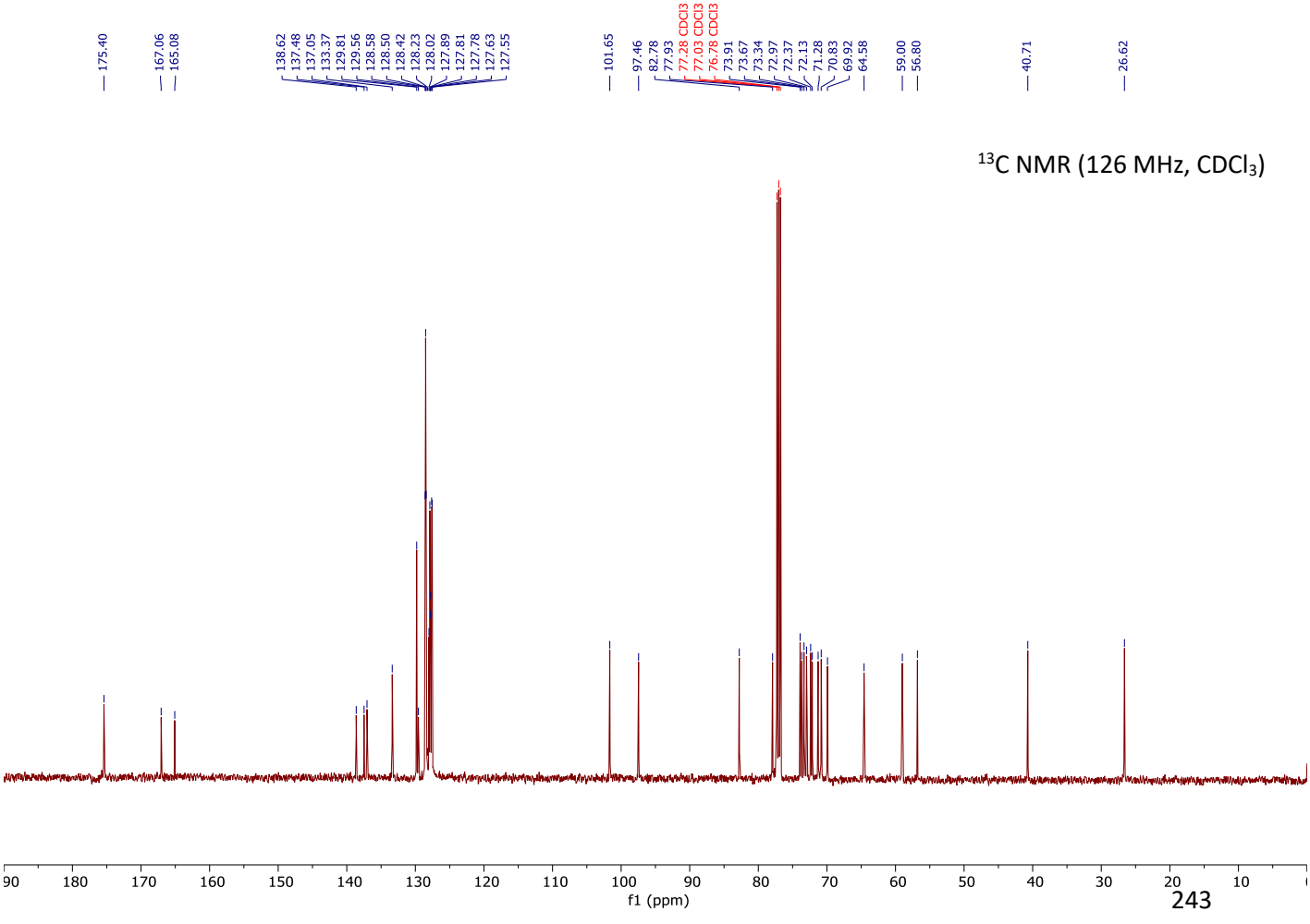
^{13}C NMR (126 MHz, $CDCl_3$)
f1 (ppm)

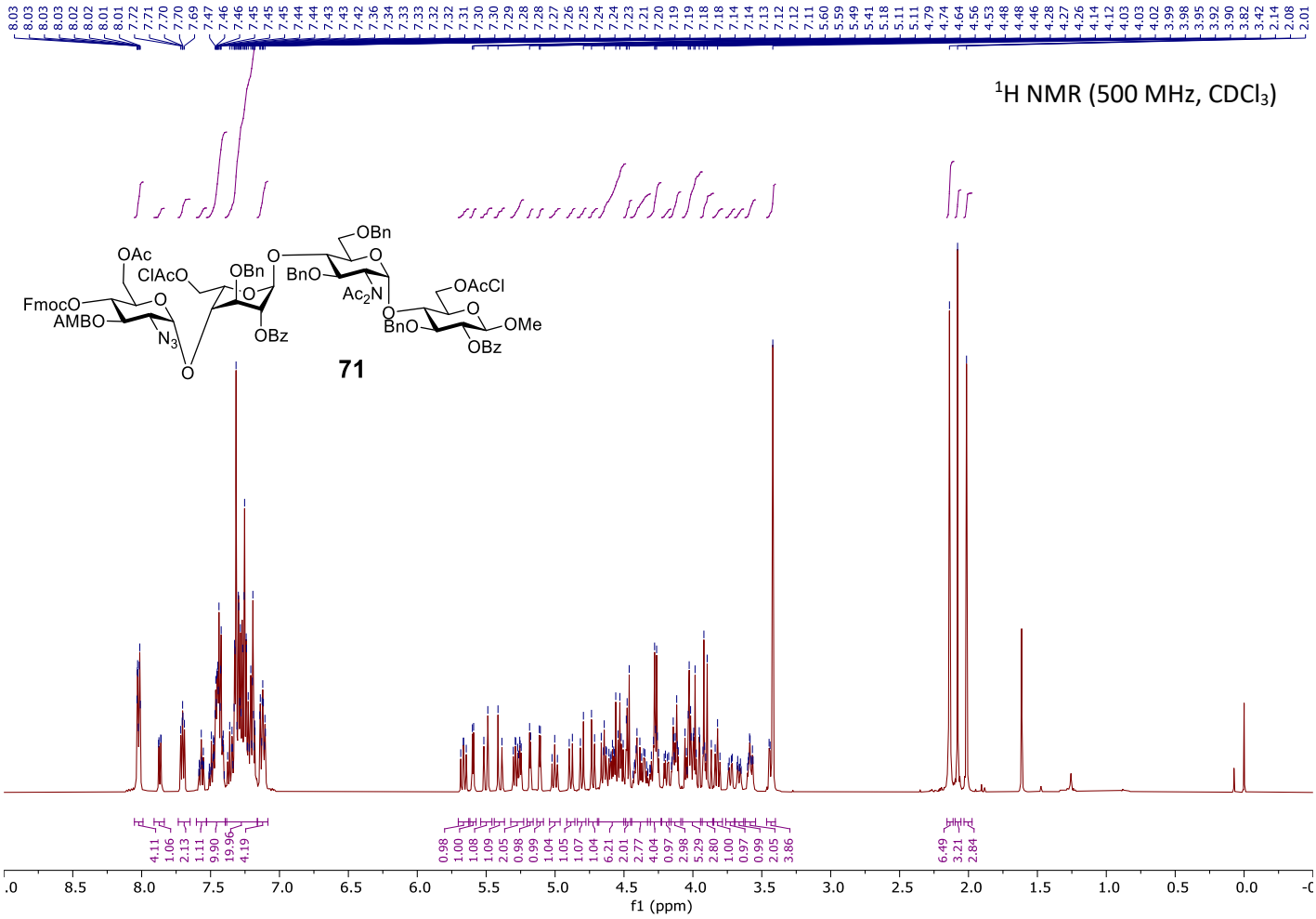

^{1}H NMR (500 MHz, $CDCl_3$)

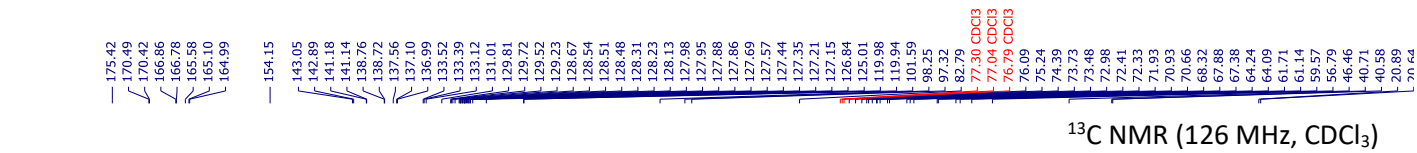

^{13}C NMR (126 MHz, $CDCl_3$)

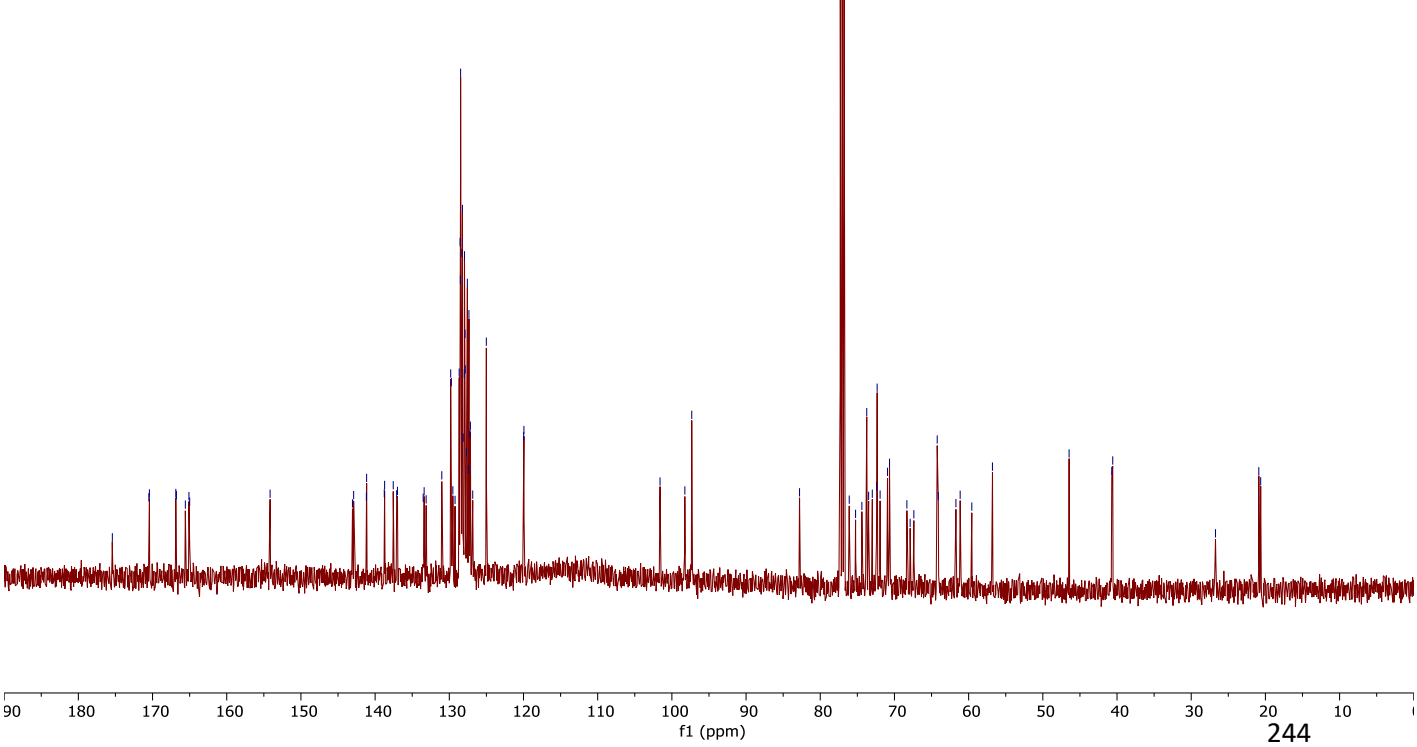

^{1}H NMR (500 MHz, $CDCl_3$)

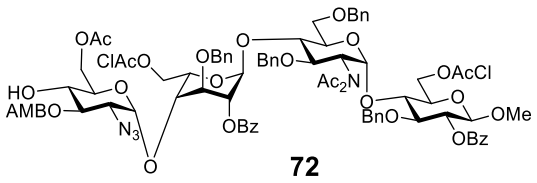

72

f1 (ppm)

^{13}C NMR (126 MHz, $CDCl_3$)

f1 (ppm)

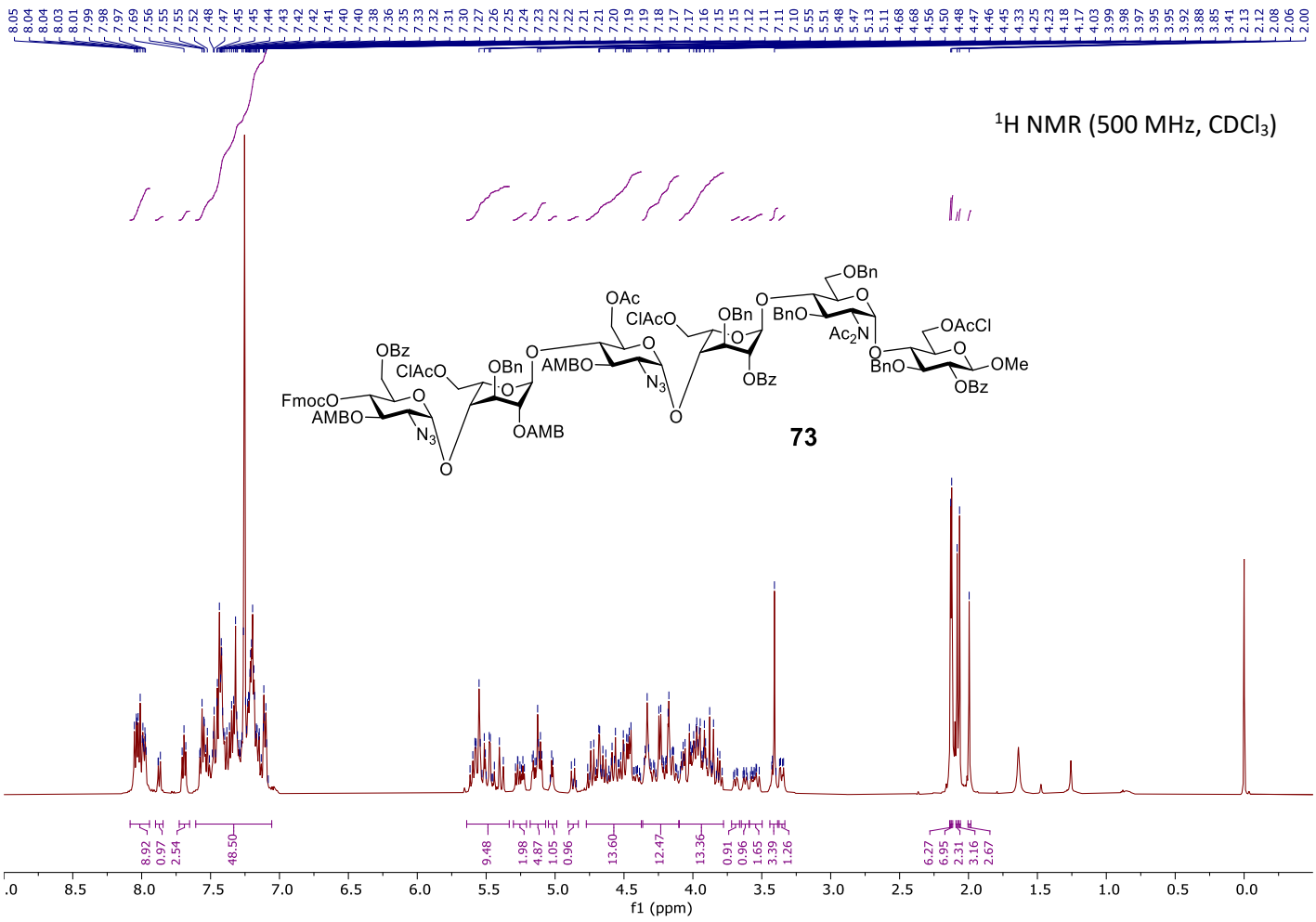
^{1}H NMR (500 MHz, $CDCl_3$)
73
f1 (ppm)

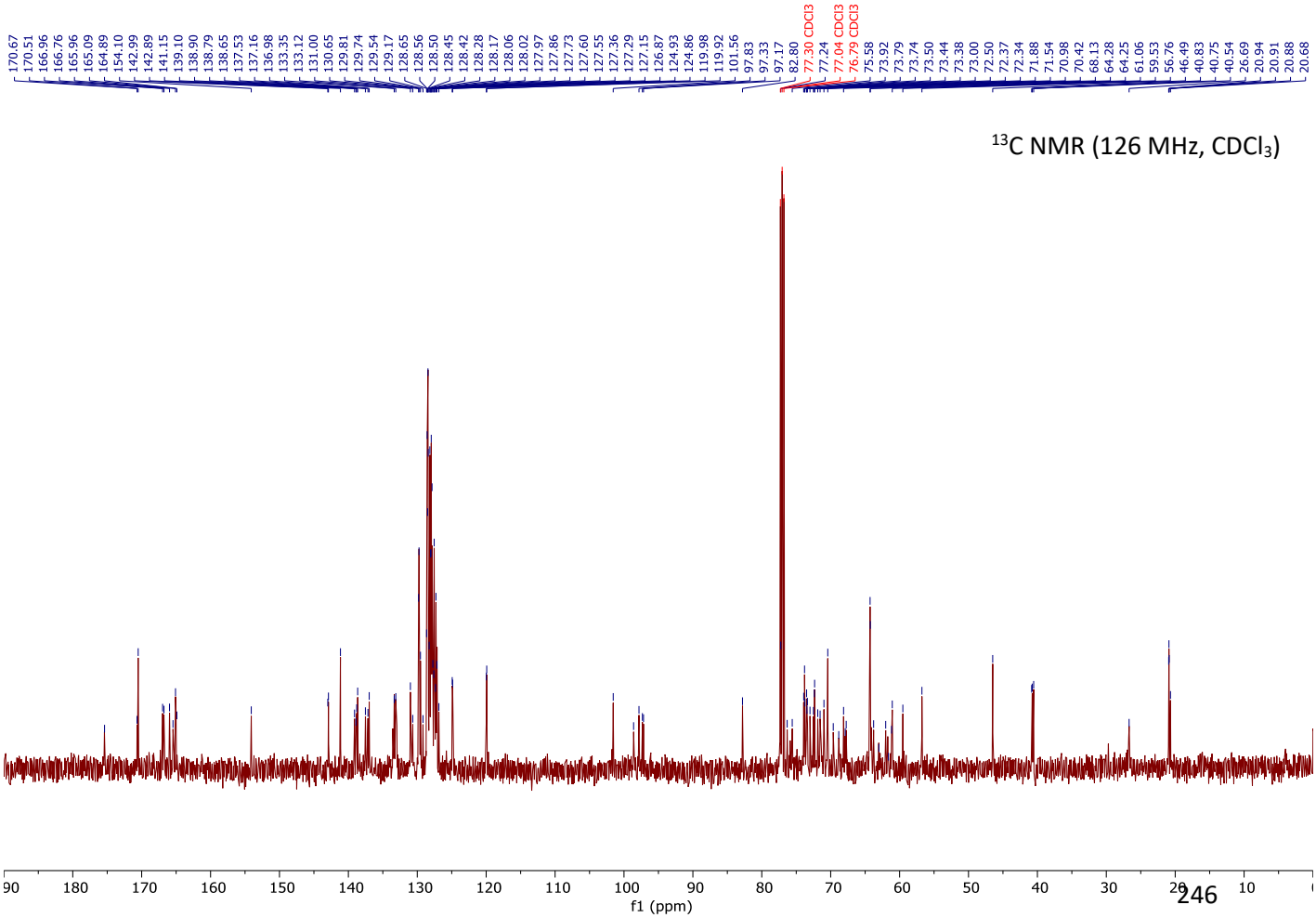
^{13}C NMR (126 MHz, $CDCl_3$)
f1 (ppm)

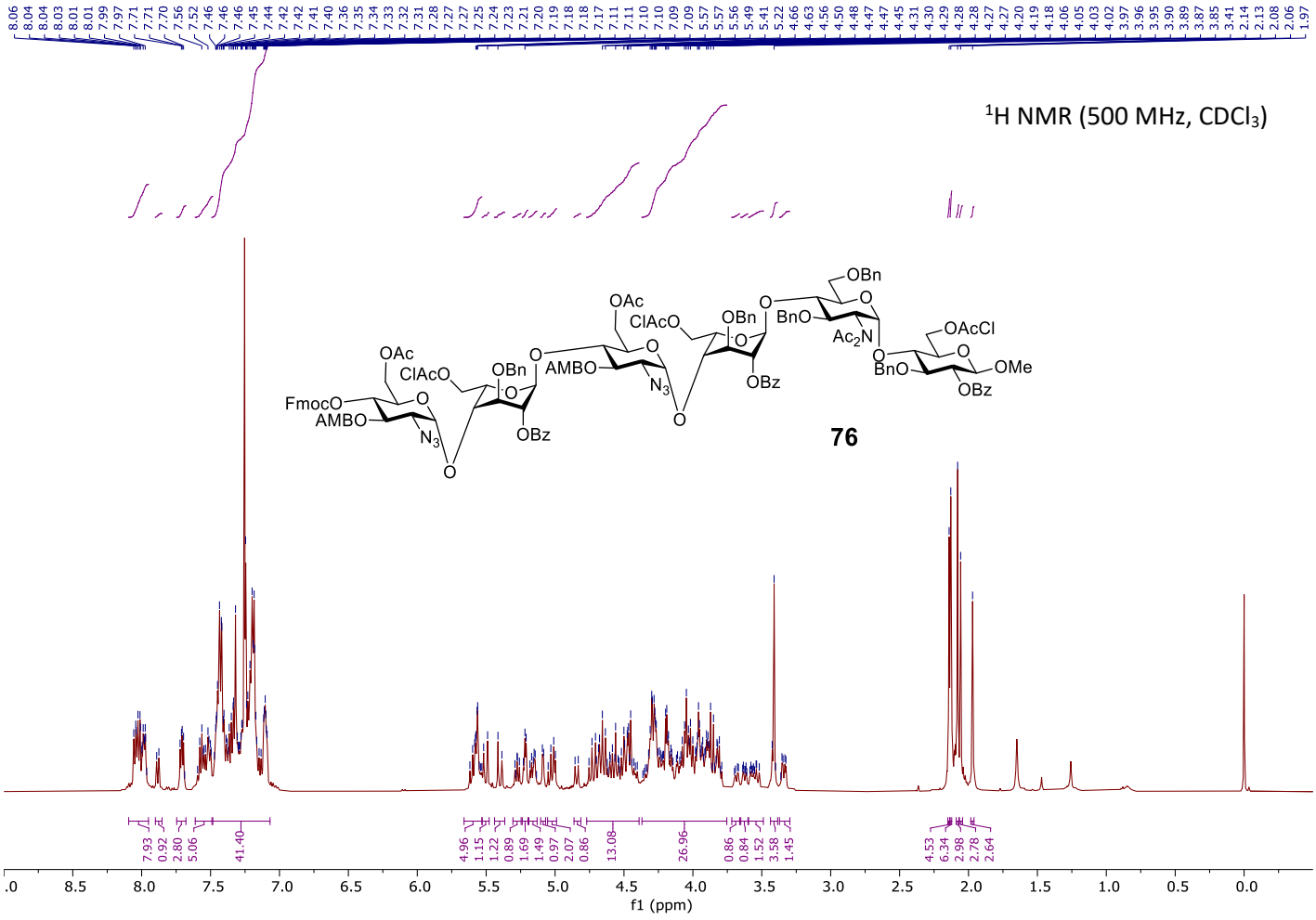
^{1}H NMR (500 MHz, $CDCl_3$)
76
f1 (ppm)

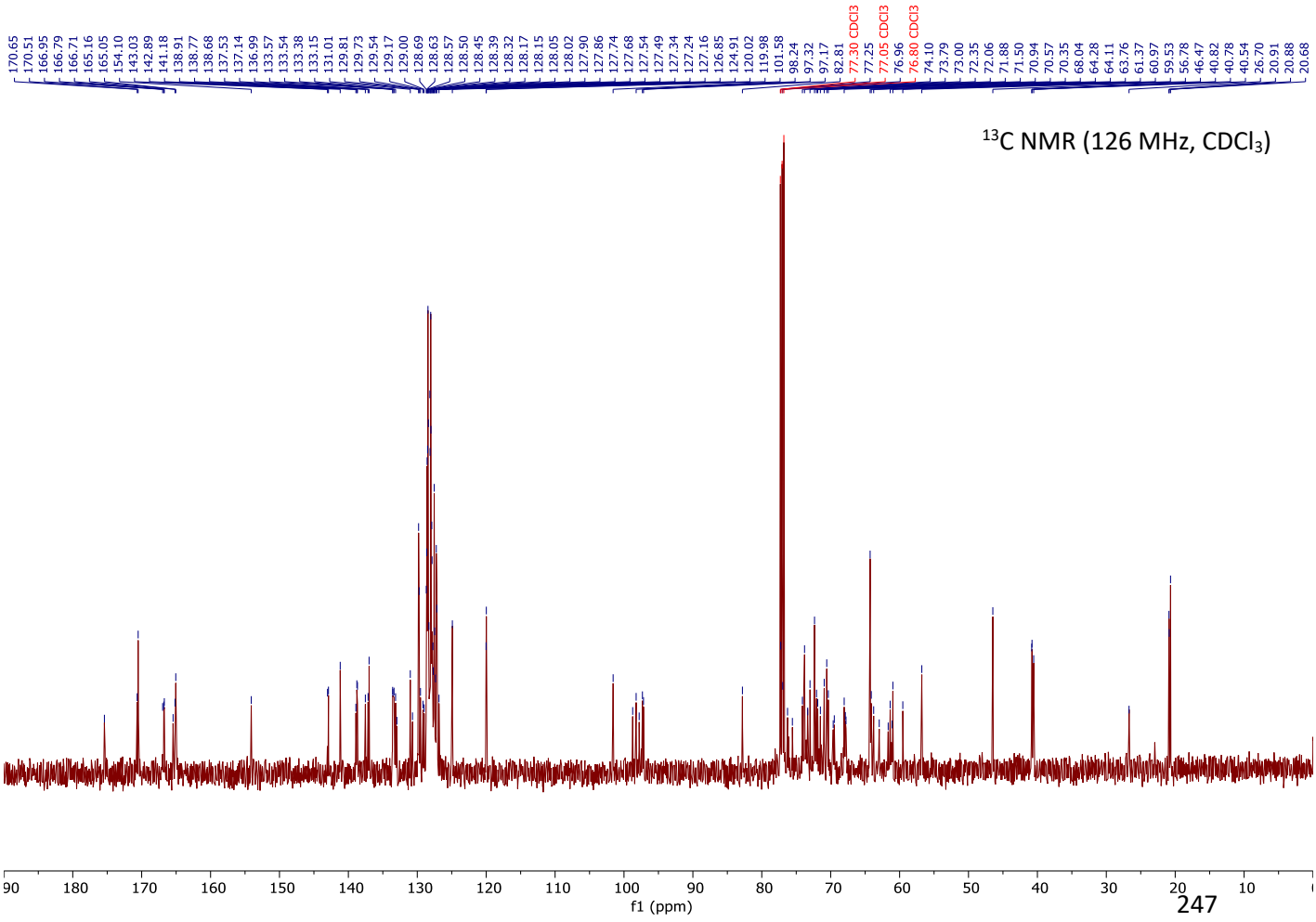
^{13}C NMR (126 MHz, $CDCl_3$)
f1 (ppm)

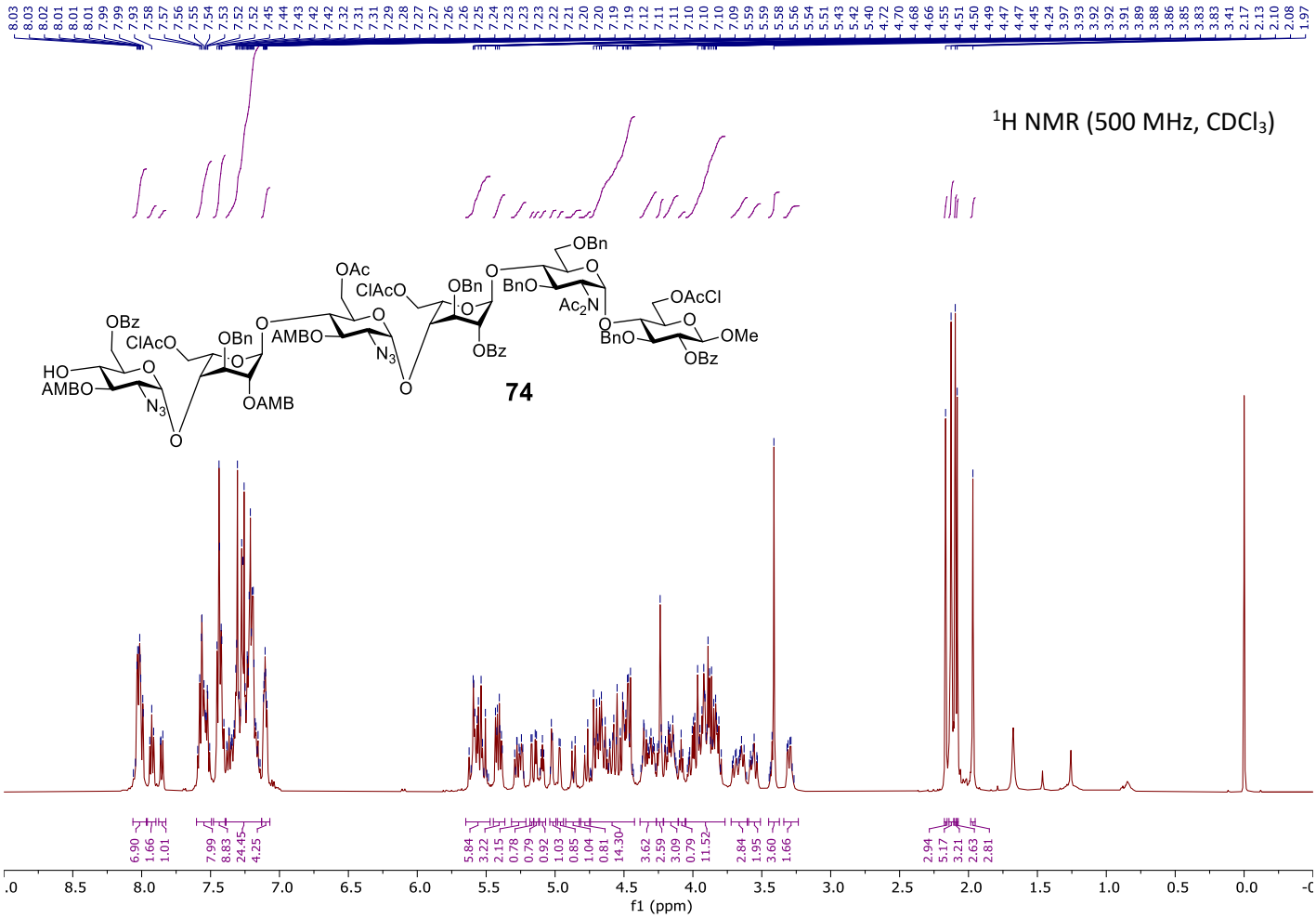

^{1}H NMR (500 MHz, $CDCl_3$)

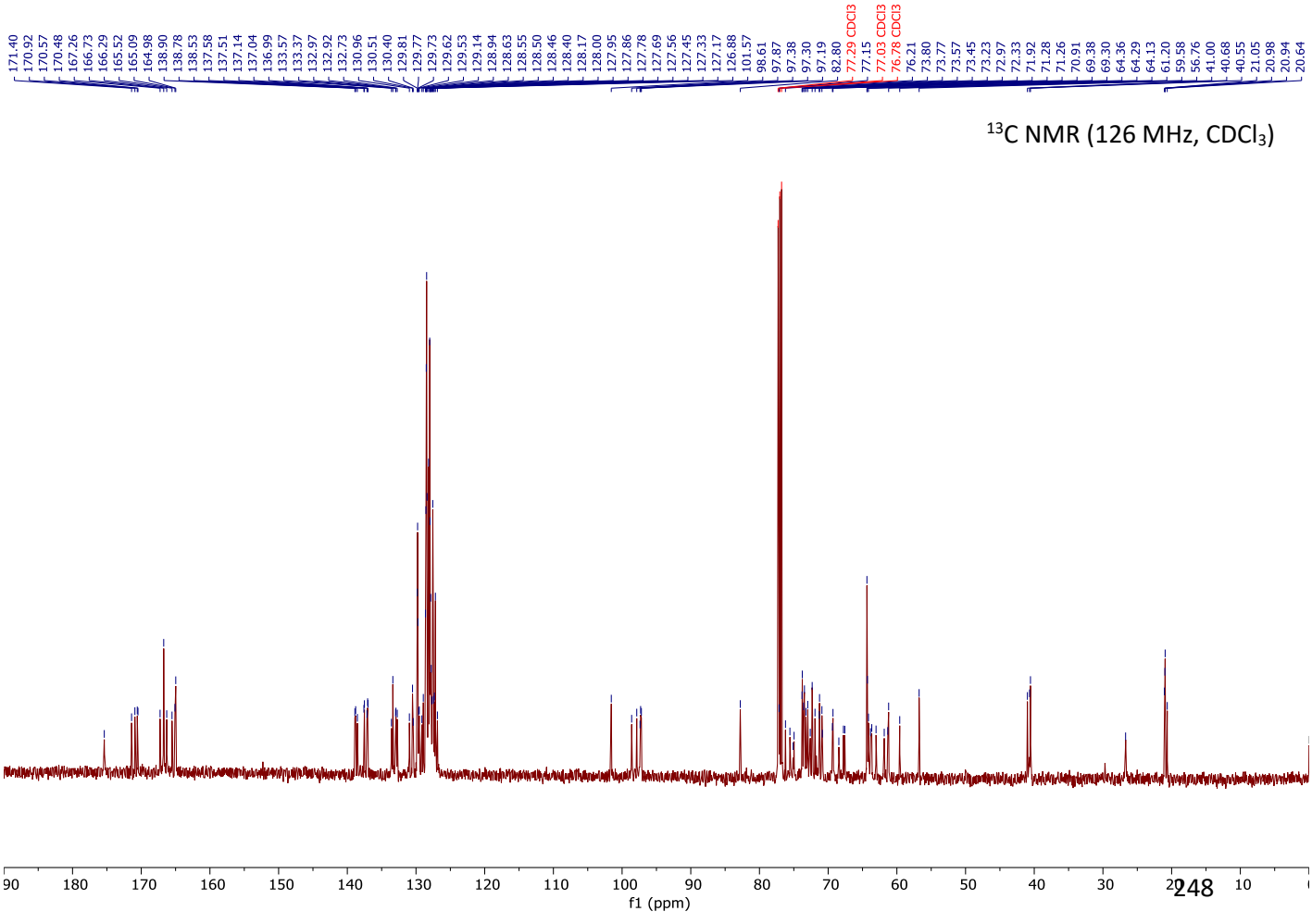

^{13}C NMR (126 MHz, $CDCl_3$)

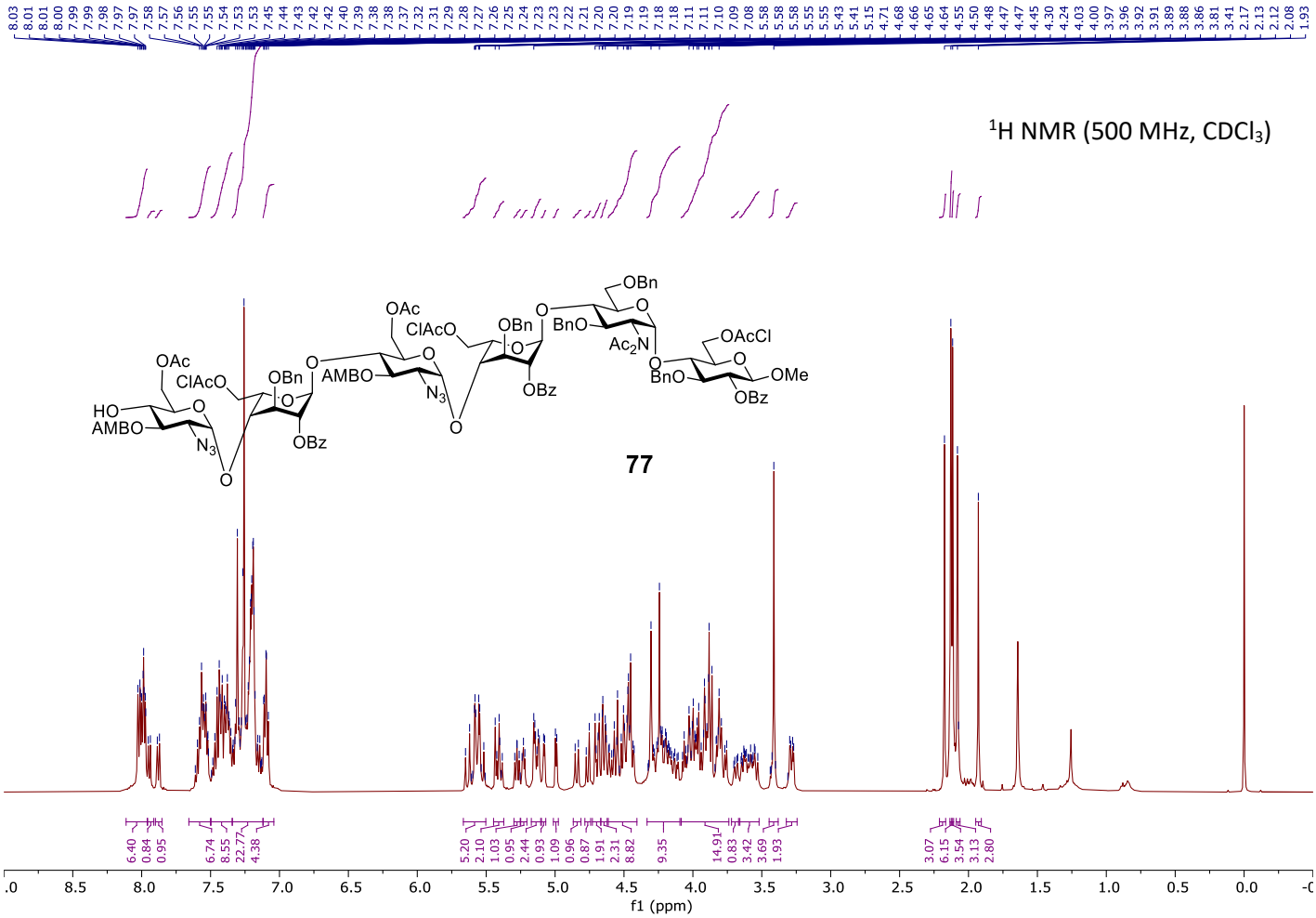
^{1}H NMR (500 MHz, $CDCl_3$)
77
f1 (ppm)

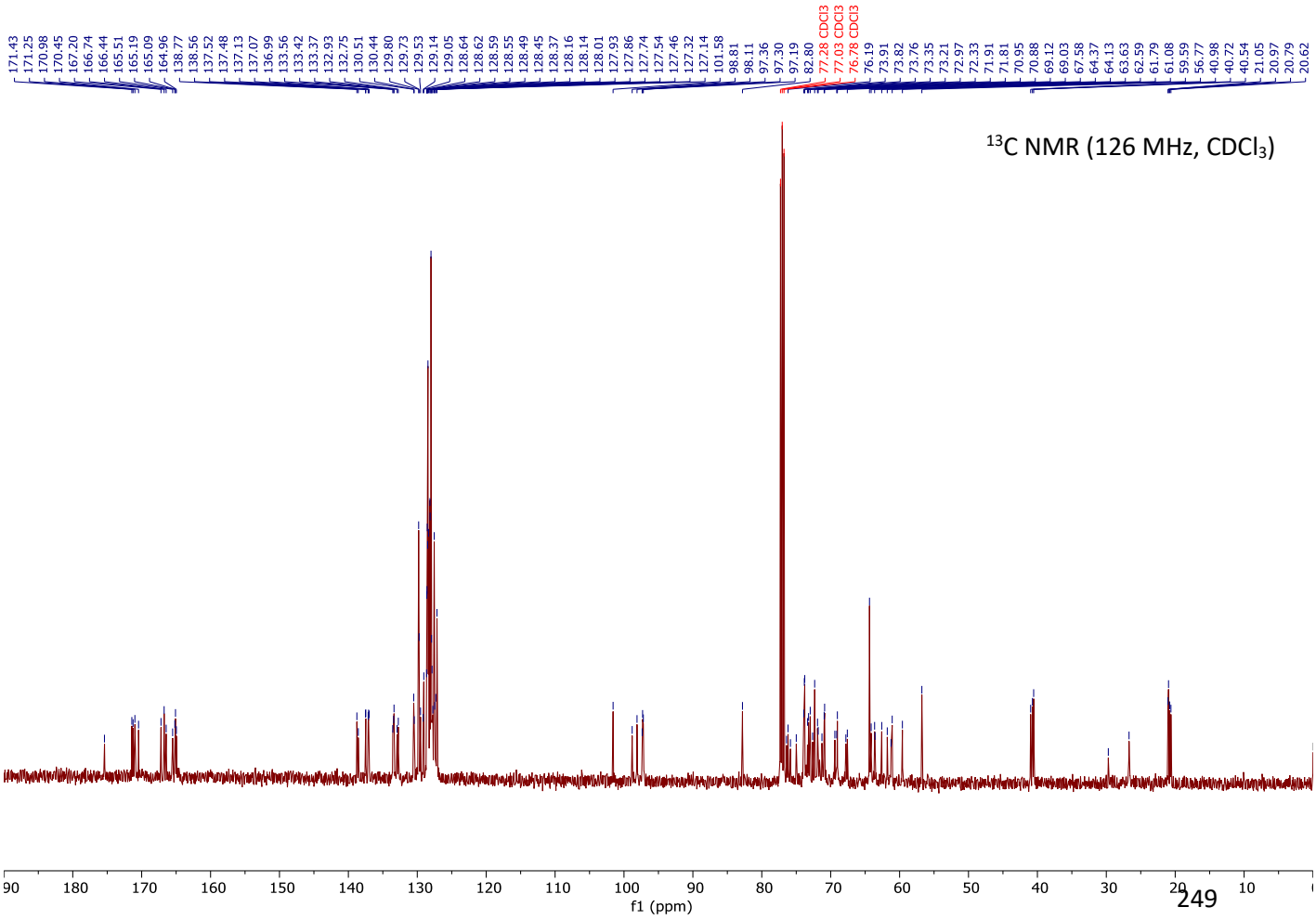
^{13}C NMR (126 MHz, $CDCl_3$)
f1 (ppm)

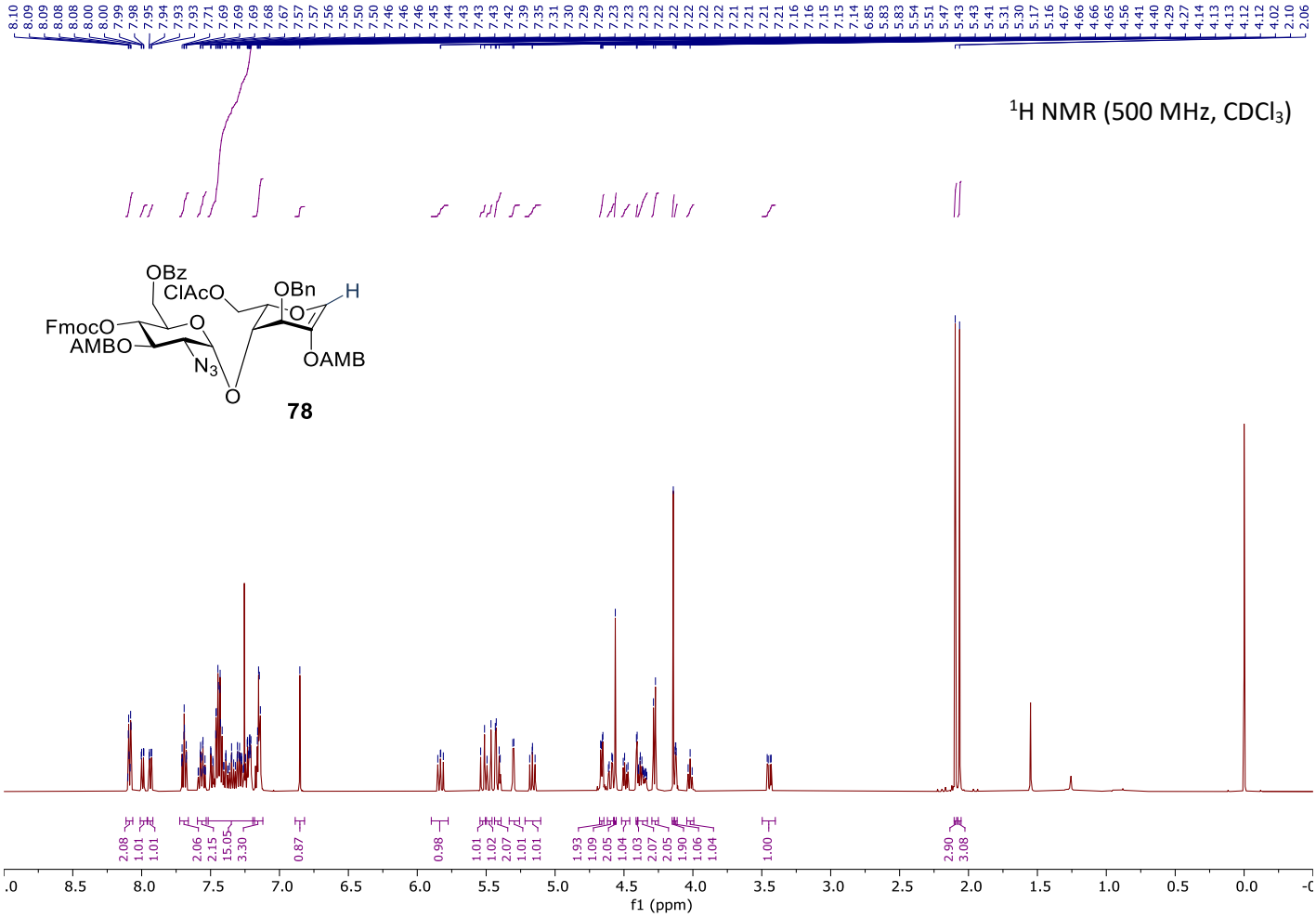

^{1}H NMR (500 MHz, $CDCl_3$)

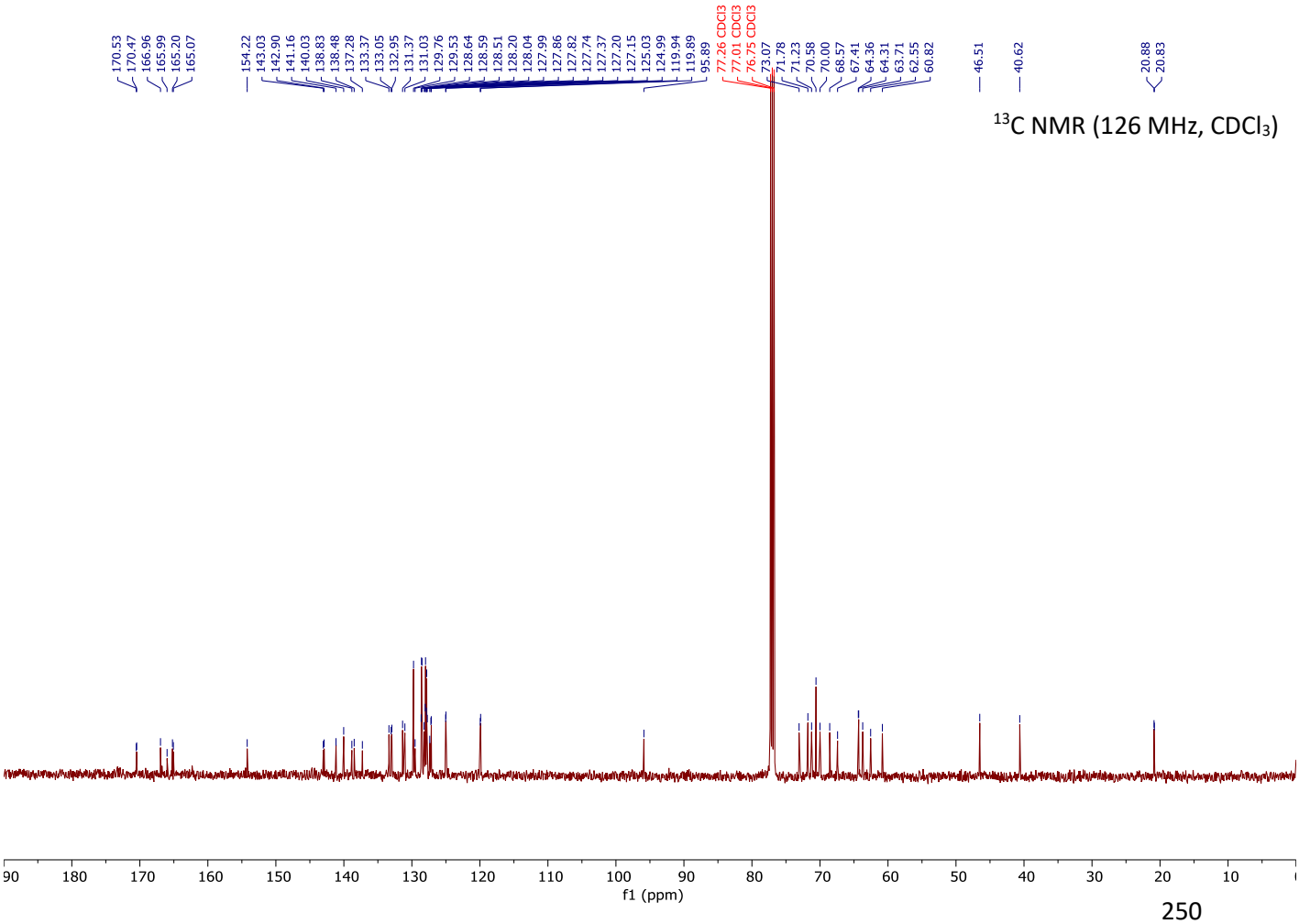

^{13}C NMR (126 MHz, $CDCl_3$)

^{1}H NMR (500 MHz, $CDCl_3$)

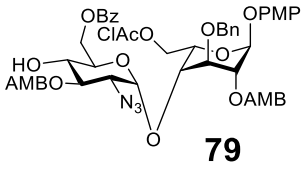

79

f1 (ppm)

^{13}C NMR (126 MHz, $CDCl_3$)

f1 (ppm)

^{1}H NMR (500 MHz, $CDCl_3$)

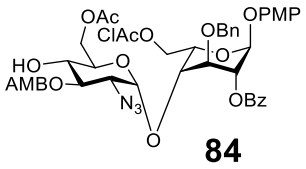

84

f1 (ppm)

^{13}C NMR (126 MHz, $CDCl_3$)

f1 (ppm)

^{1}H NMR (500 MHz, $CDCl_3$)

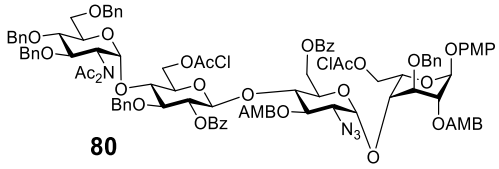

80

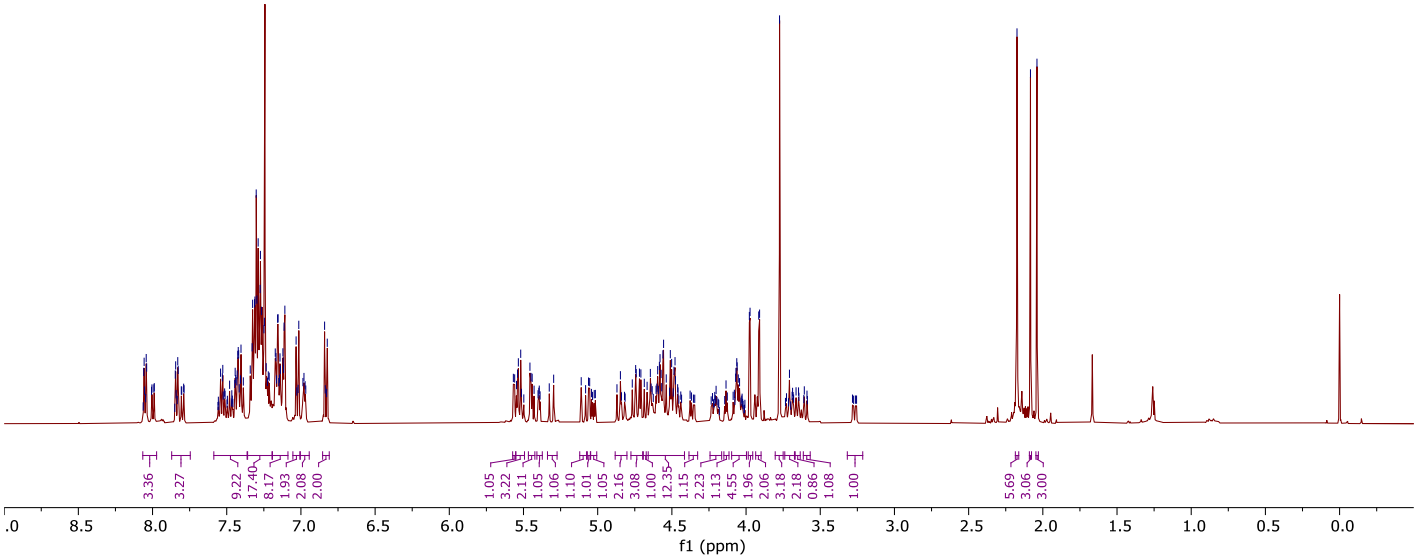

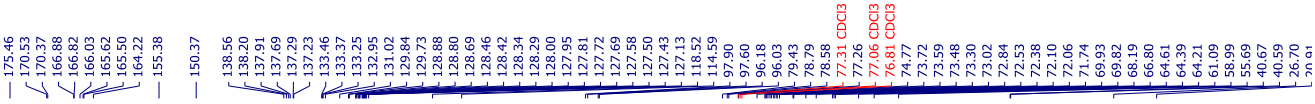

^{13}C NMR (126 MHz, $CDCl_3$)

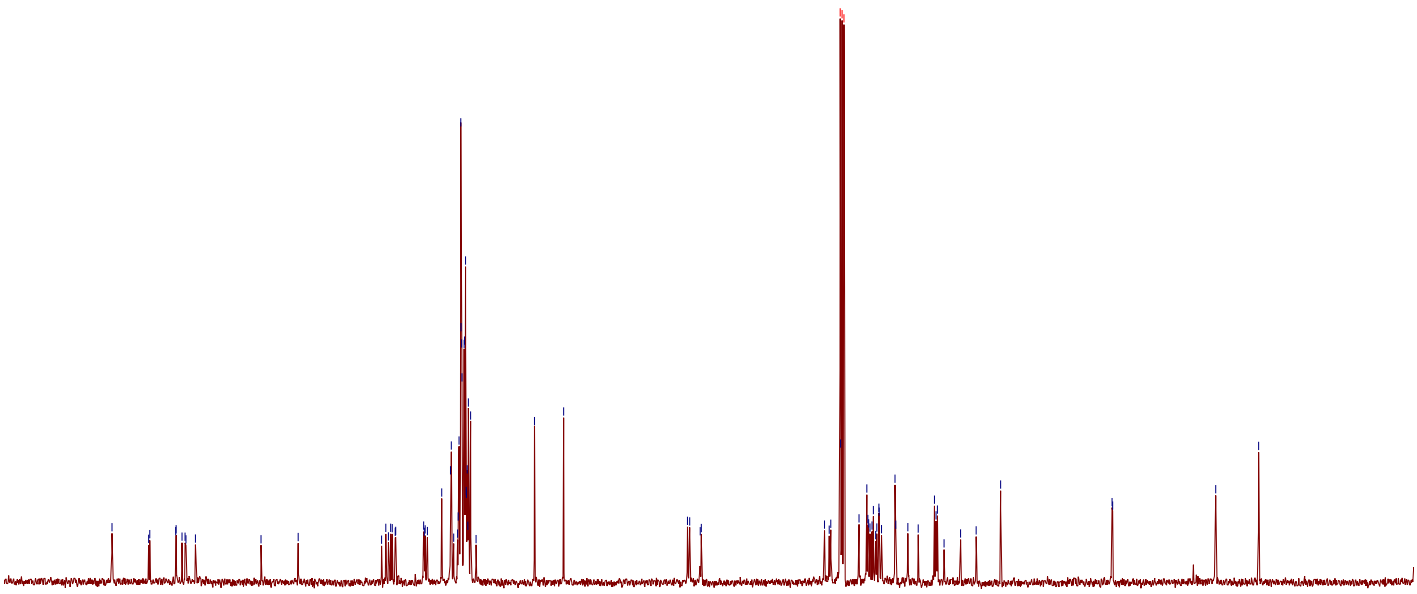

^{1}H NMR (500 MHz, $CDCl_3$)

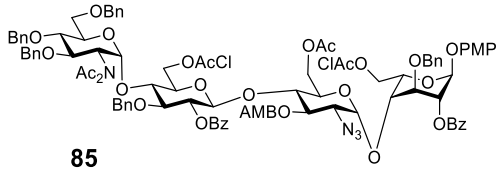

85

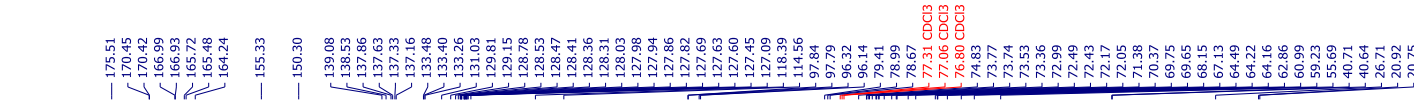

^{13}C NMR (126 MHz, $CDCl_3$)

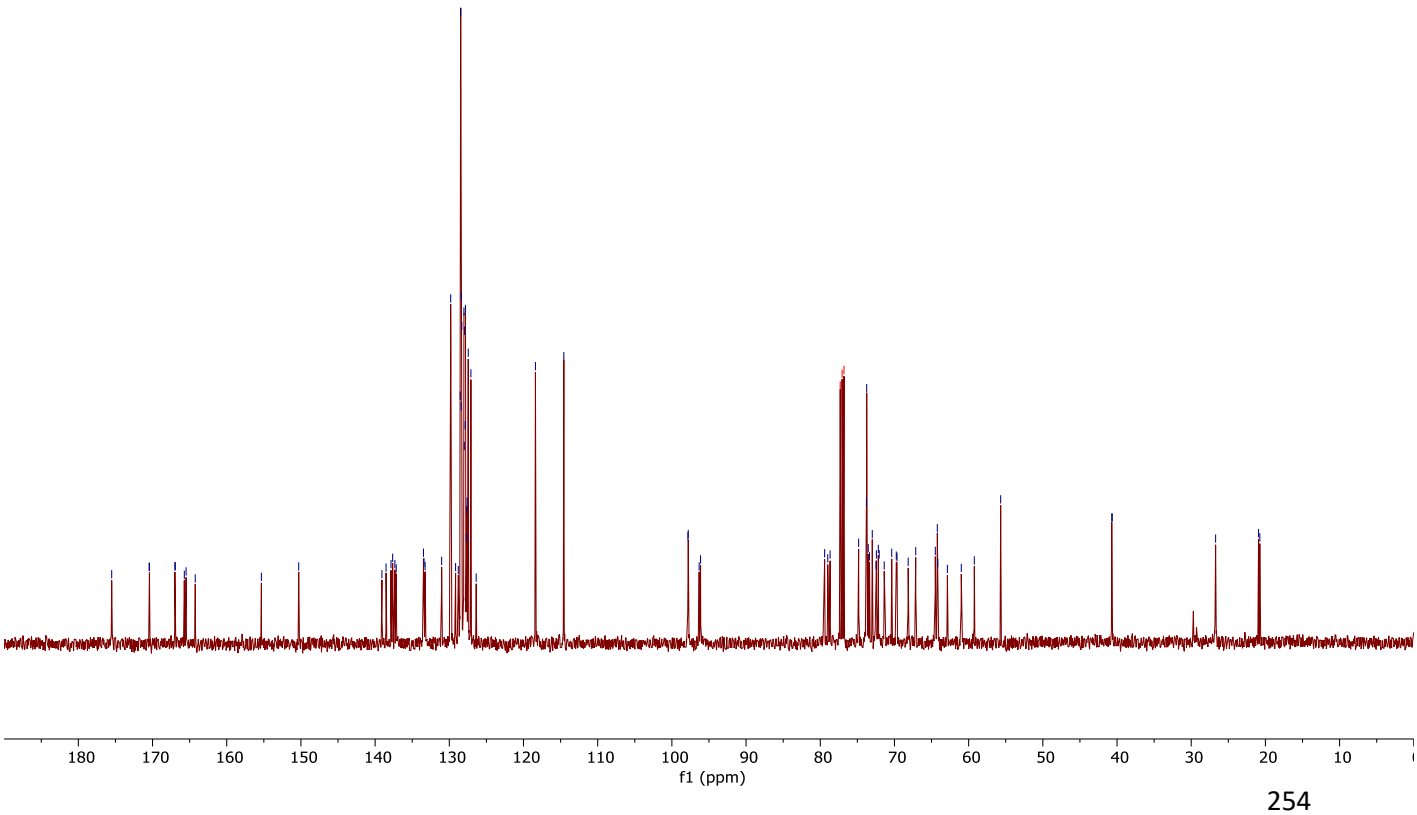

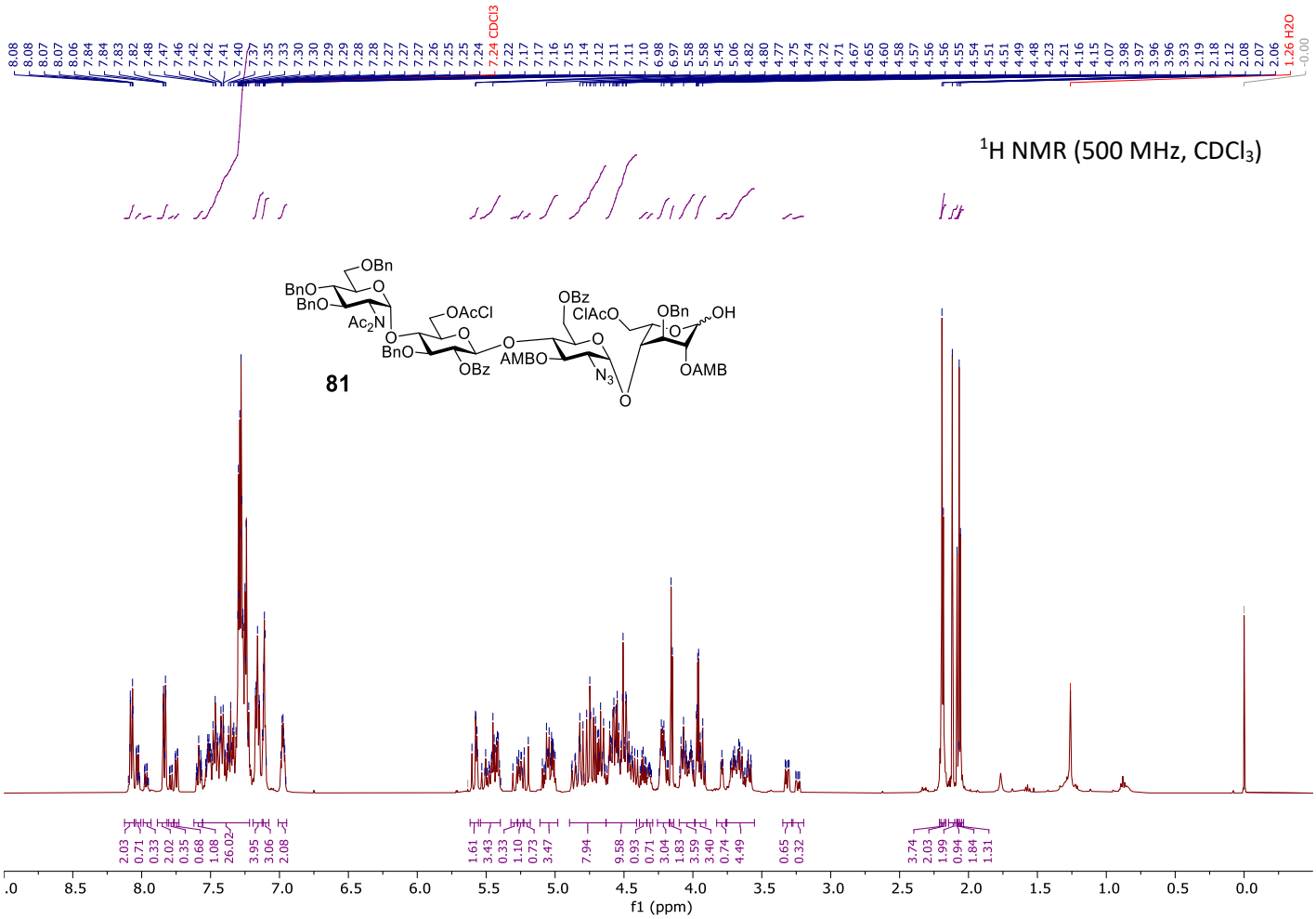
^{1}H NMR (500 MHz, $CDCl_3$)
81
f1 (ppm)

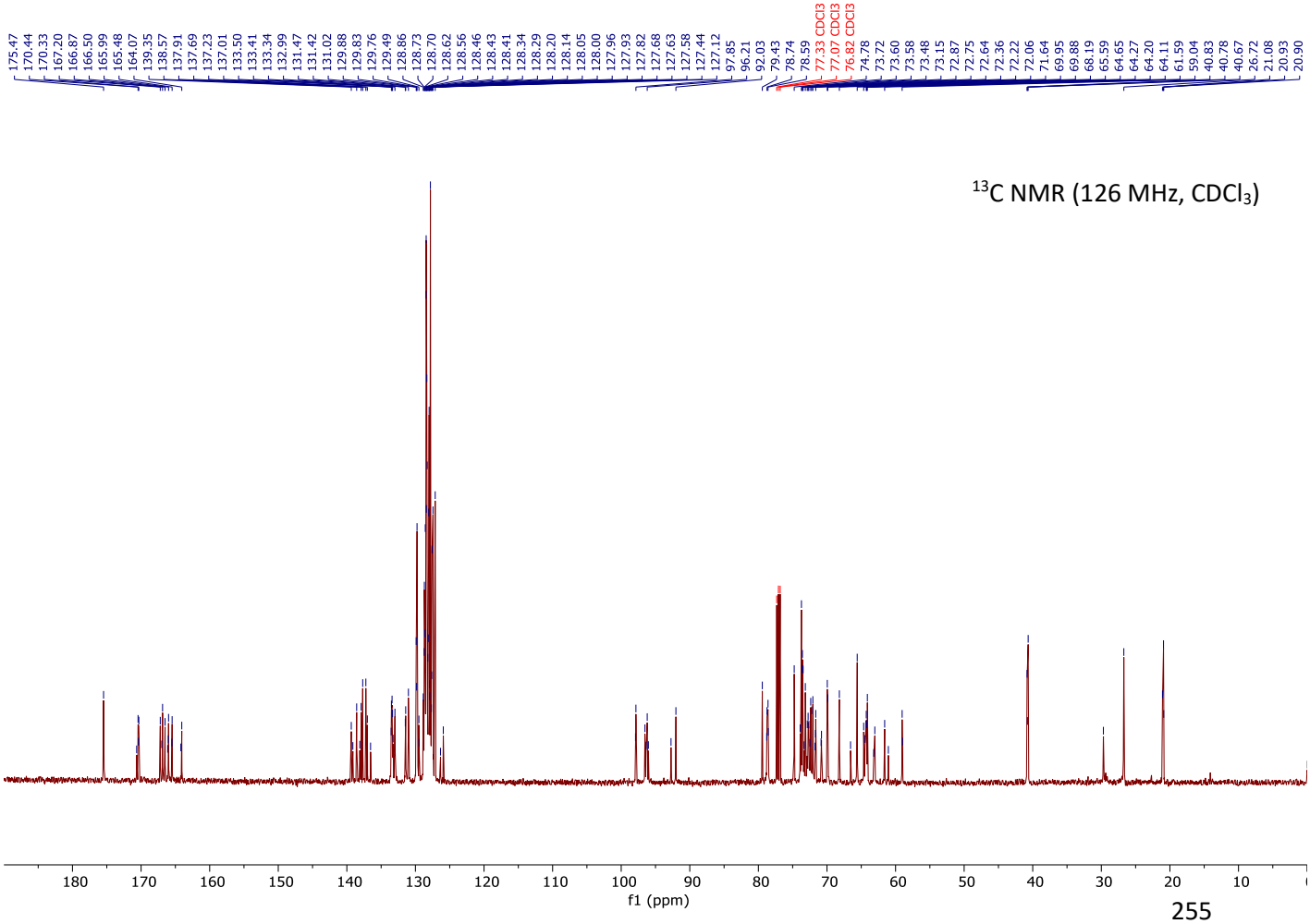
^{13}C NMR (126 MHz, $CDCl_3$)
f1 (ppm)

^{1}H NMR (500 MHz, $CDCl_3$)

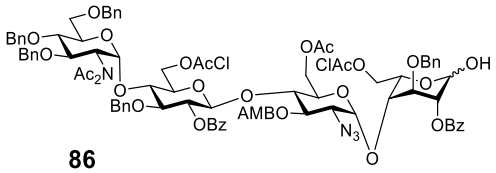

86

^{13}C NMR (126 MHz, $CDCl_3$)

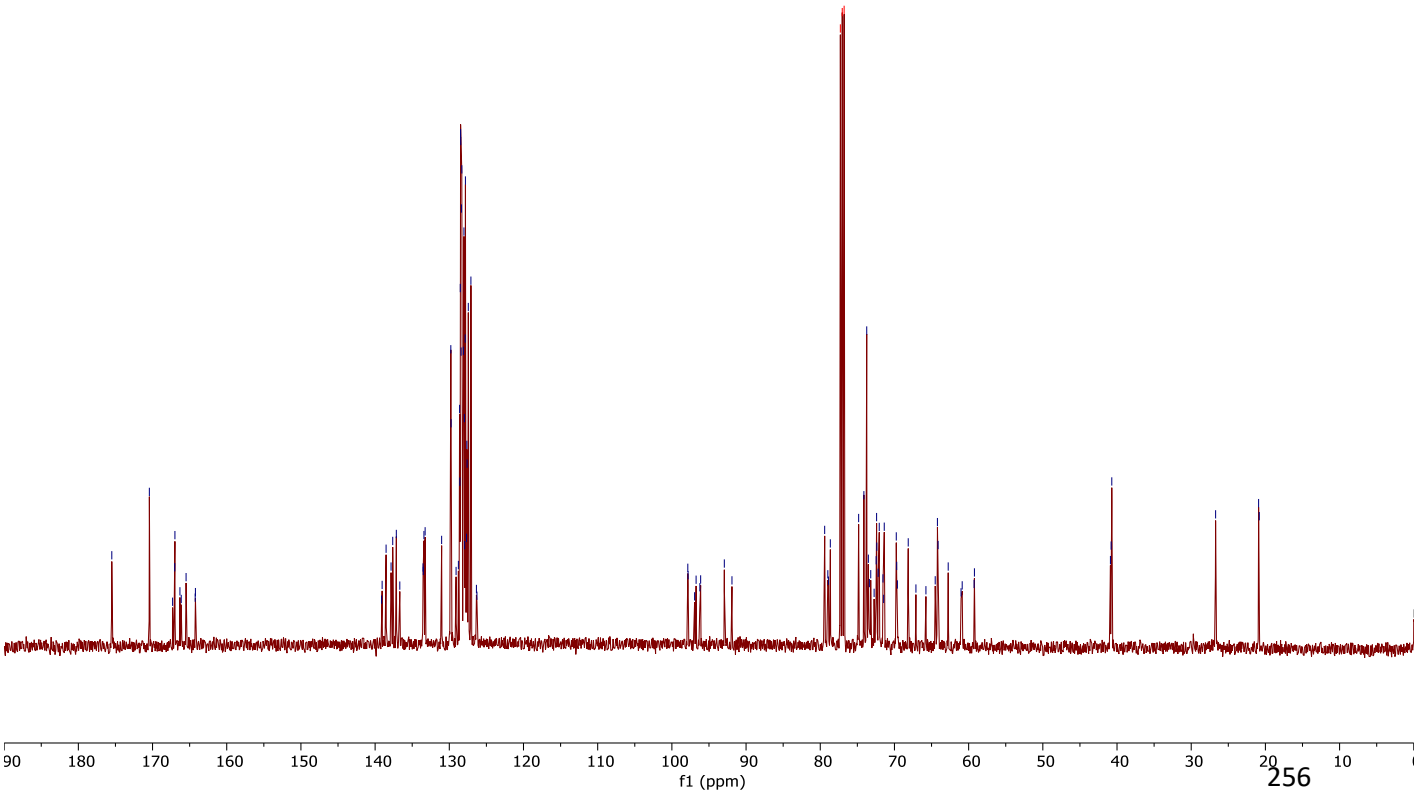

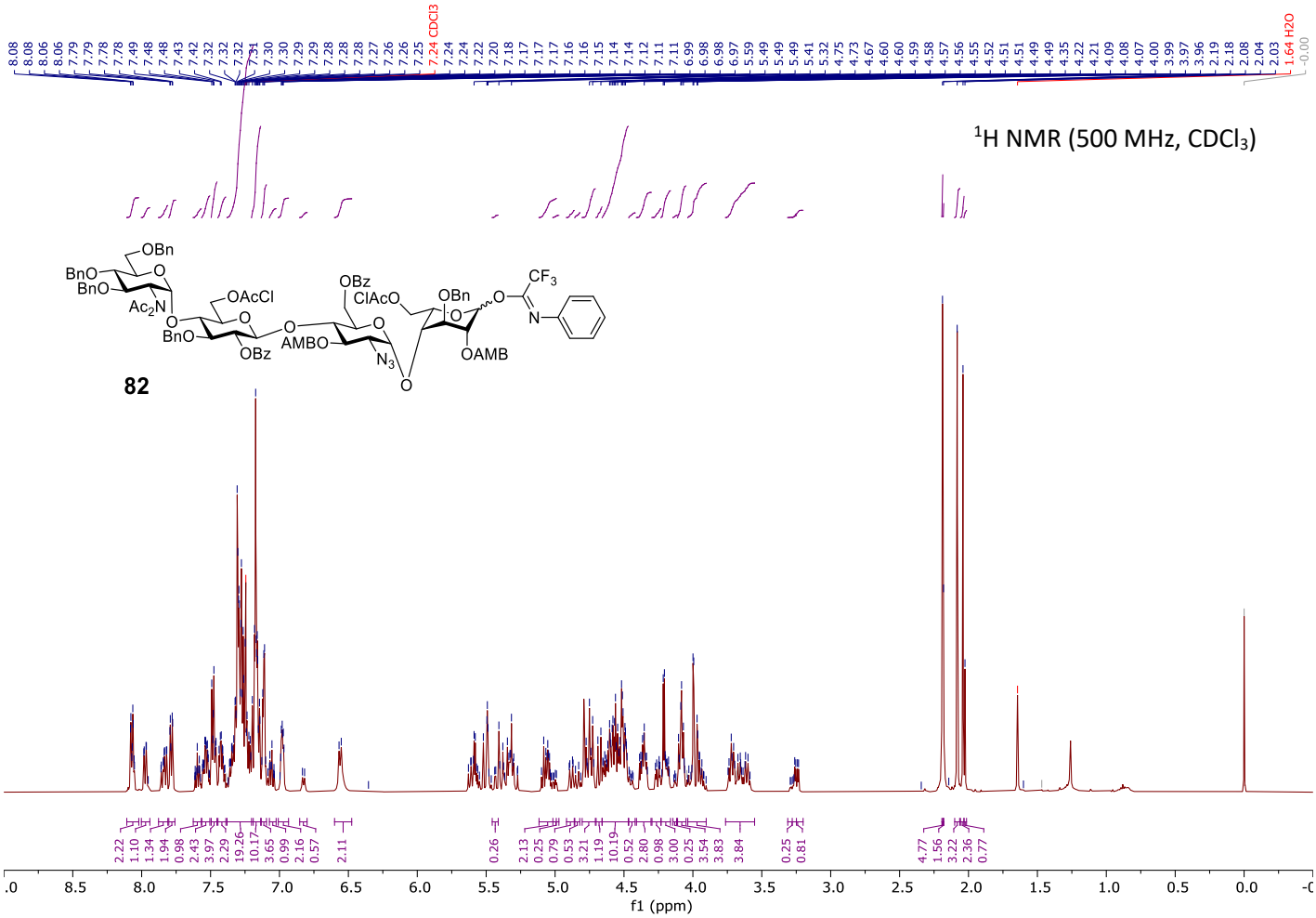
^{1}H NMR (500 MHz, $CDCl_3$)
82
f1 (ppm)

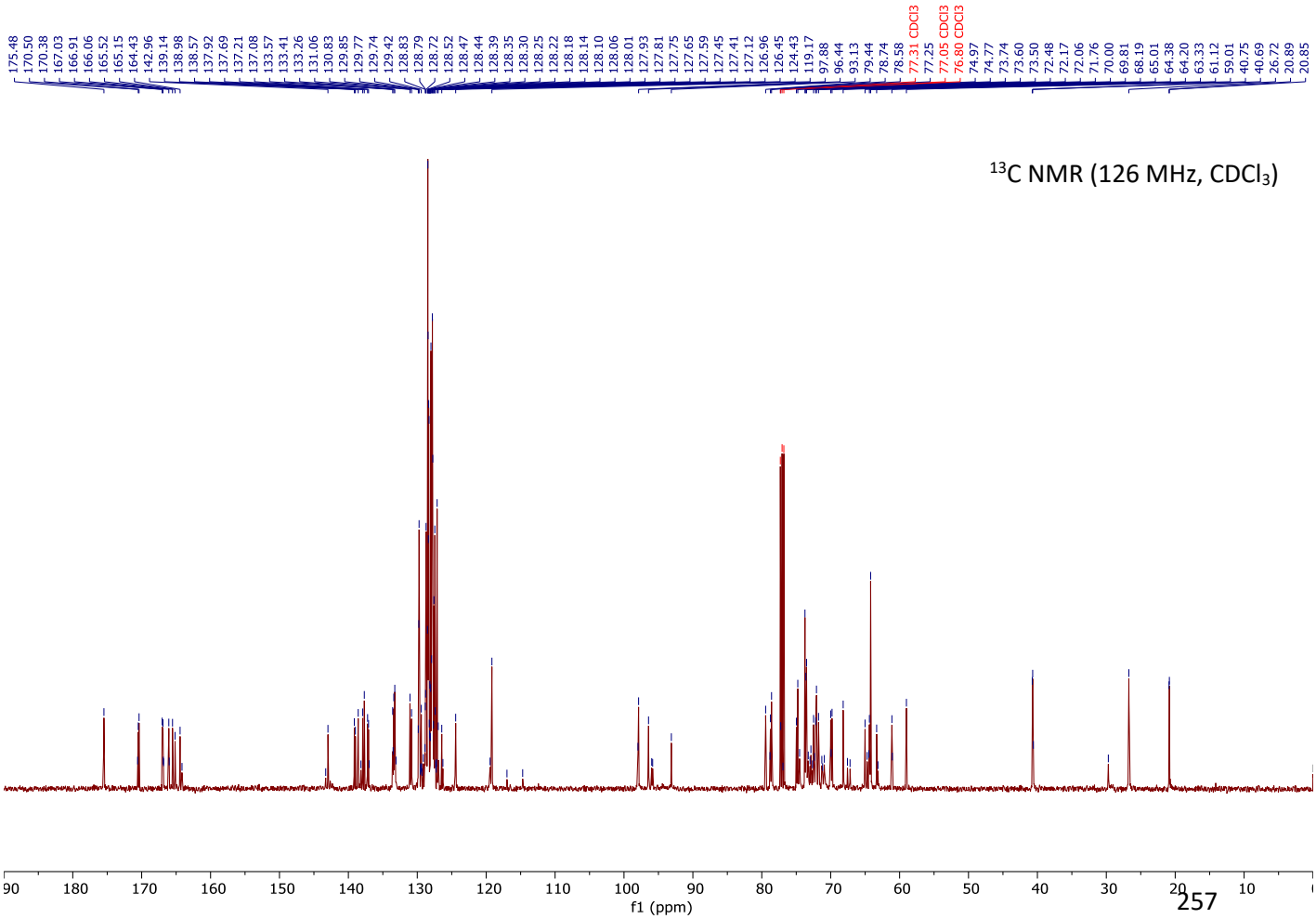
^{13}C NMR (126 MHz, $CDCl_3$)
f1 (ppm)

^{1}H NMR (500 MHz, $CDCl_3$)

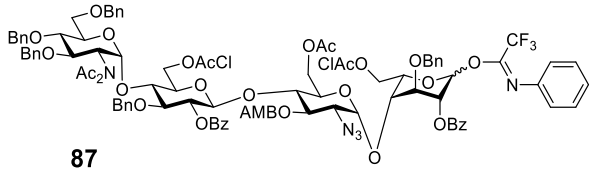

87

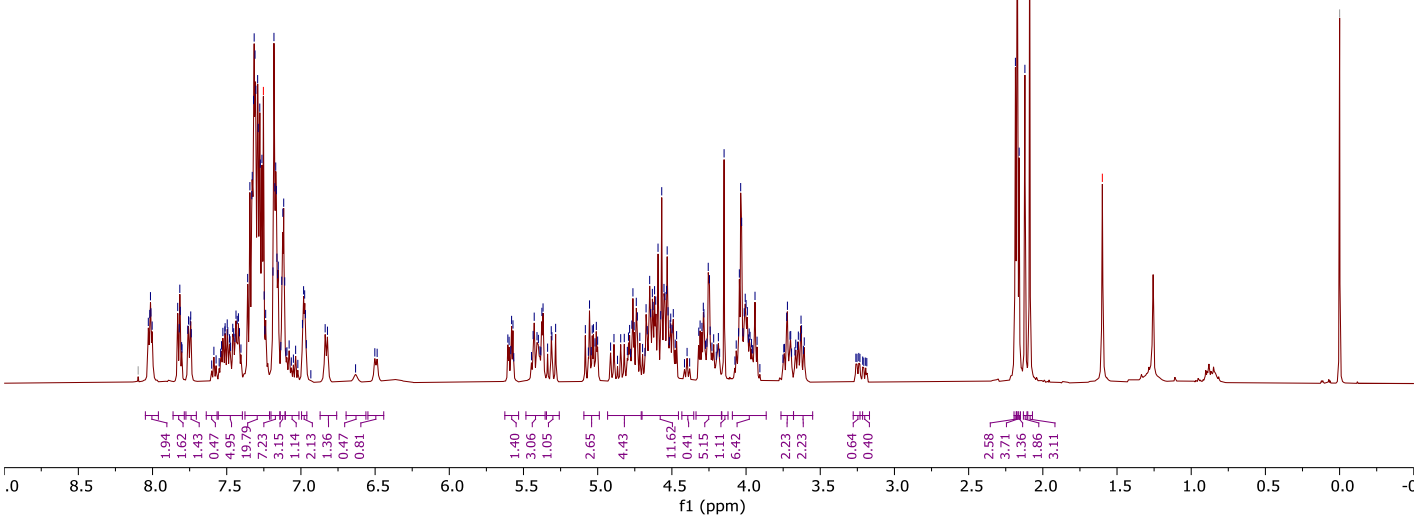

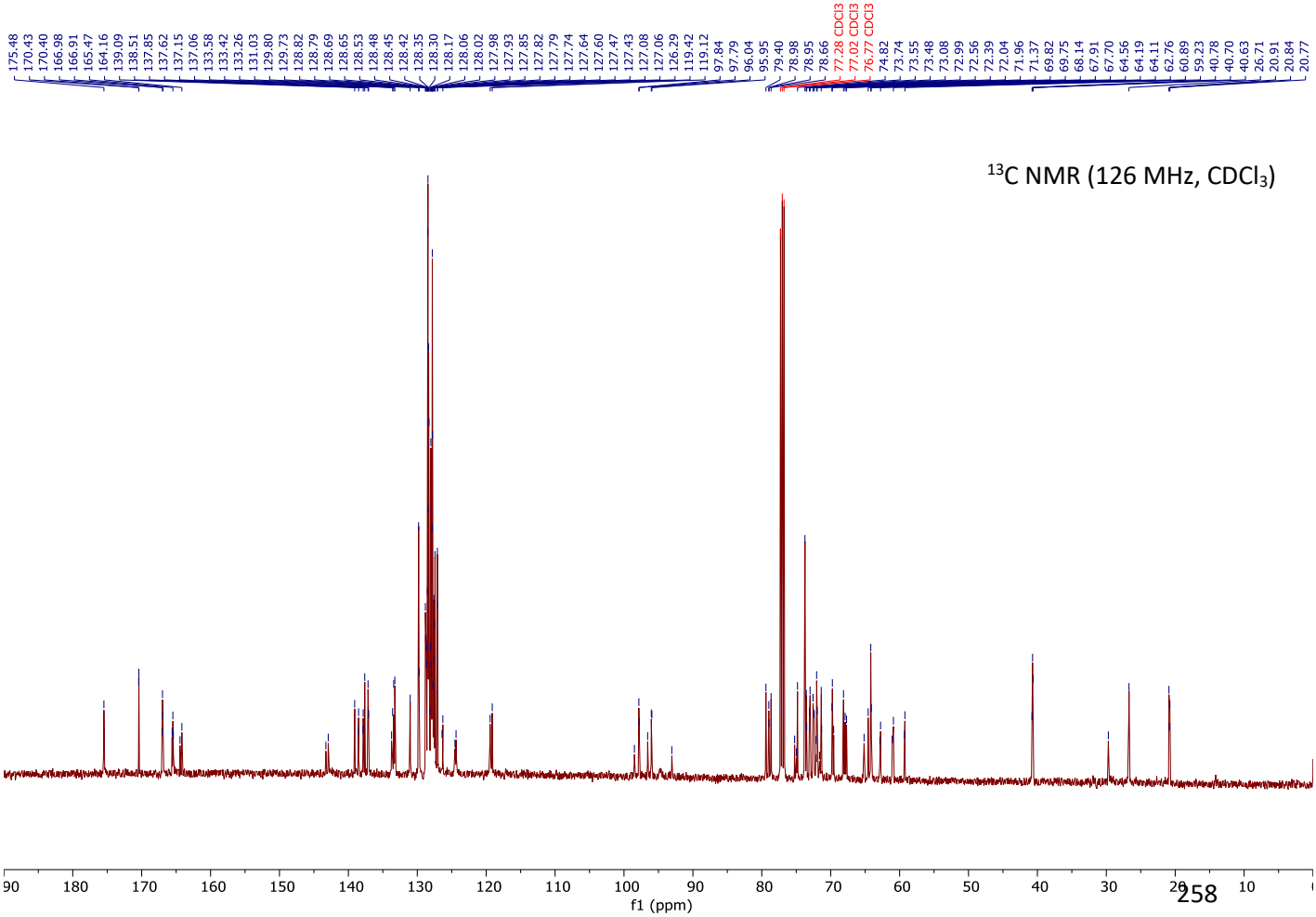

^{13}C NMR (126 MHz, $CDCl_3$)

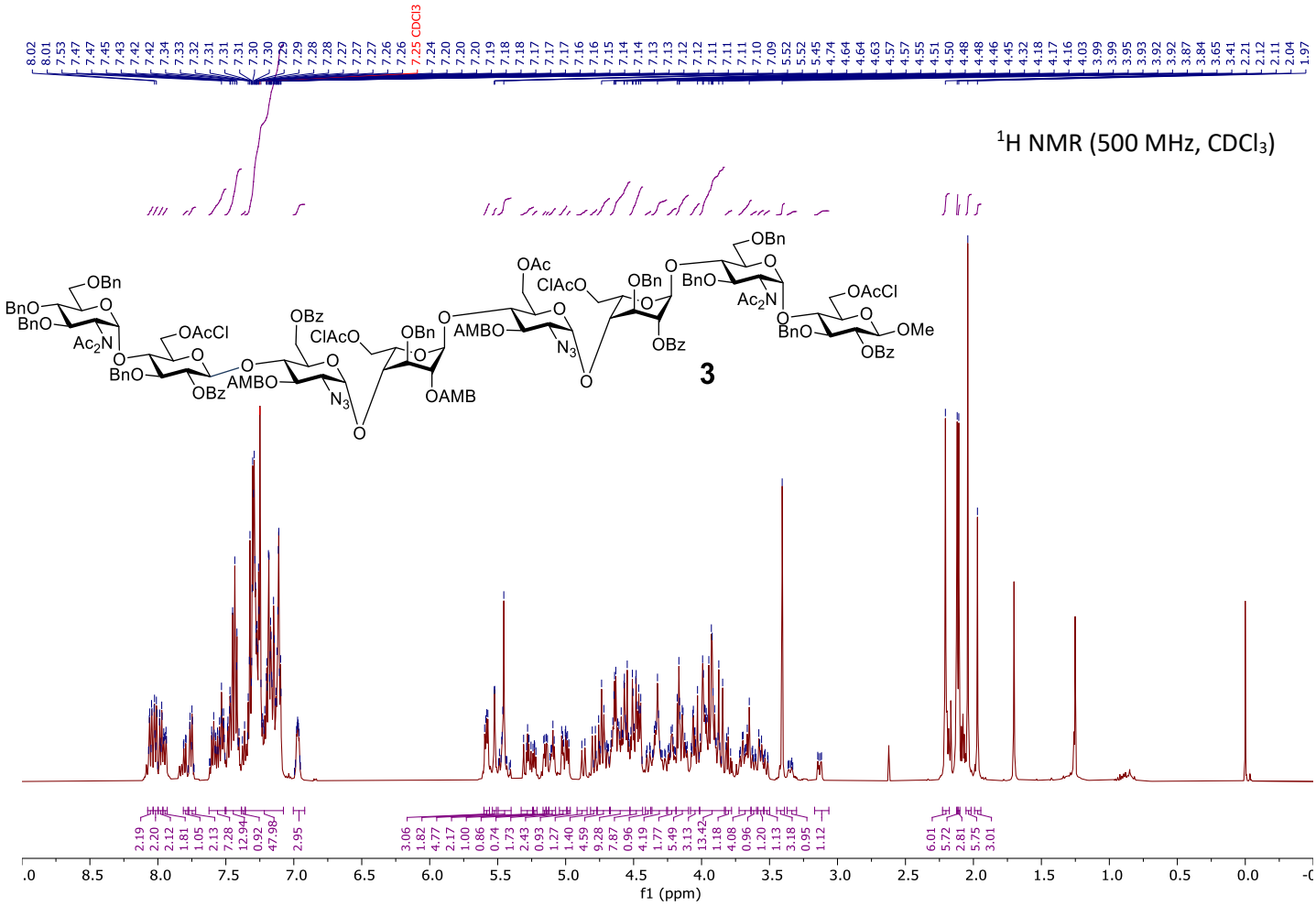

^{1}H NMR (500 MHz, $CDCl_3$)

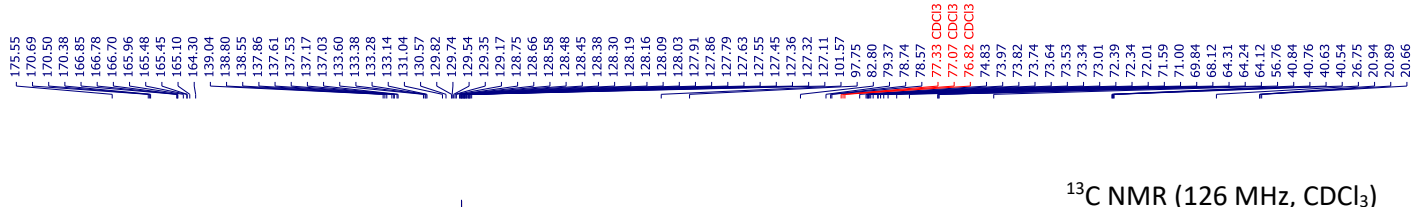

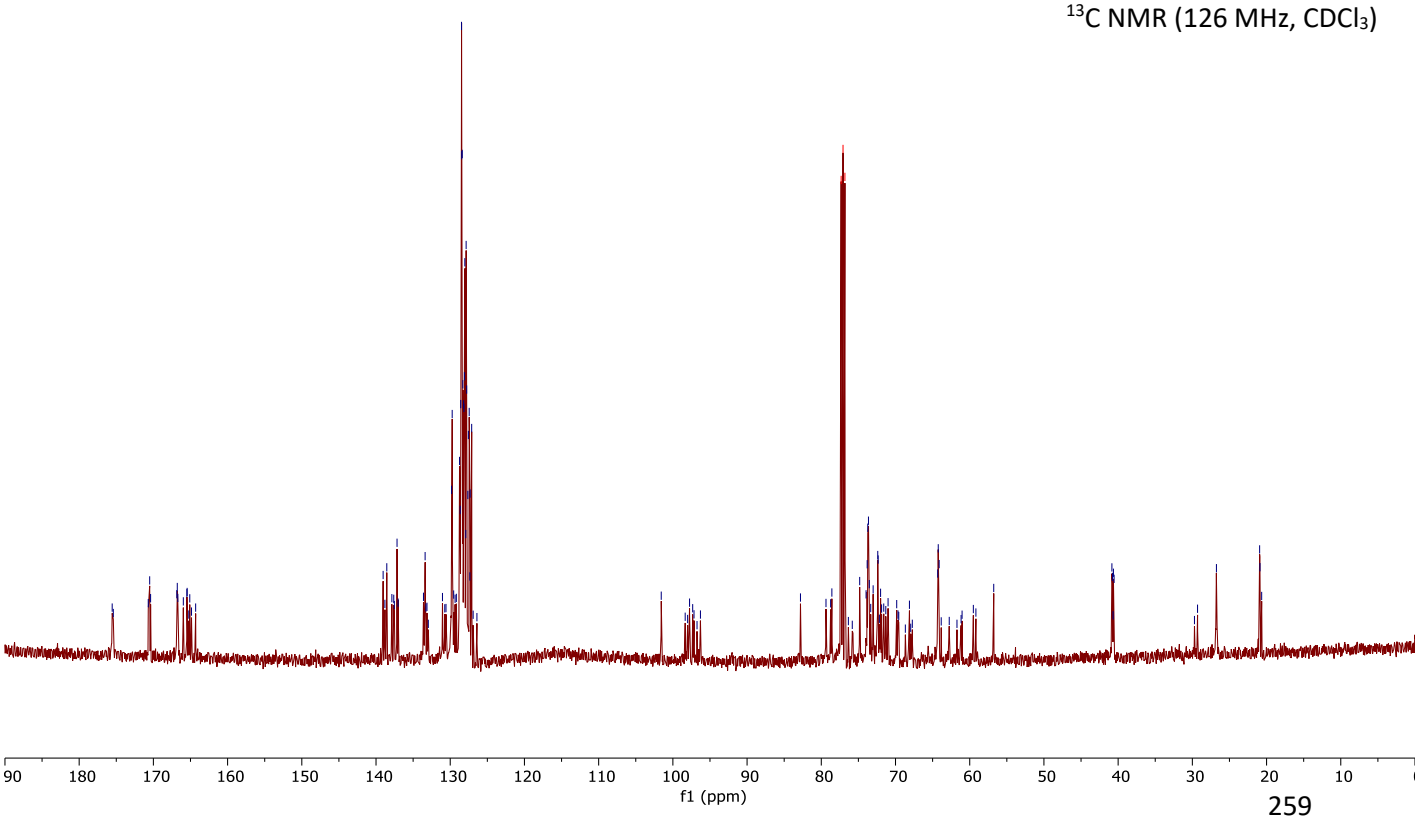

^{13}C NMR (126 MHz, $CDCl_3$)

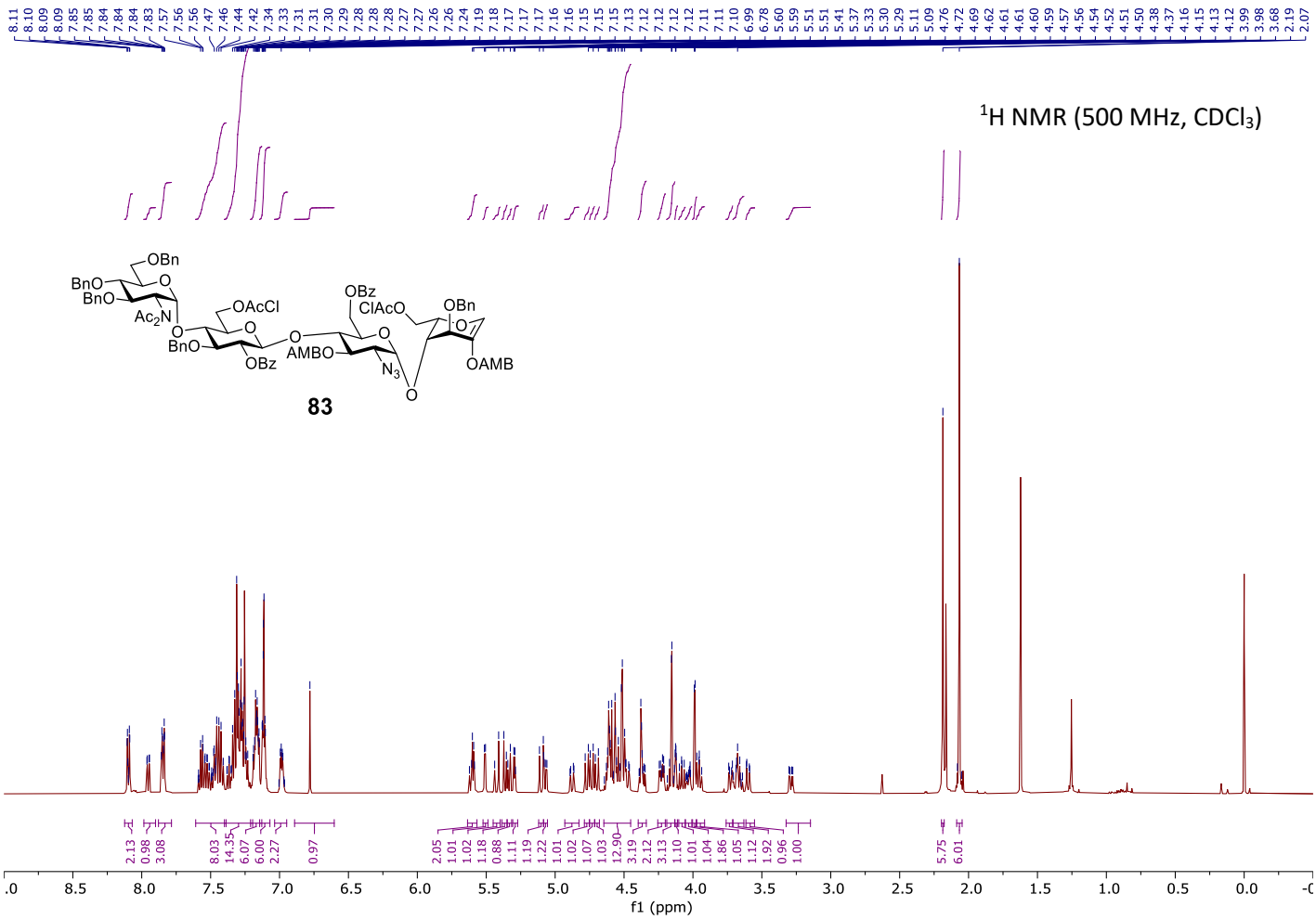
^{1}H NMR (500 MHz, $CDCl_3$)
f1 (ppm)

OBn
BnO
BnO
Ac2N
OAcCl
BnO
OBz
AMBO
OBz
ClAcO
OBn
N3
OAMB

83

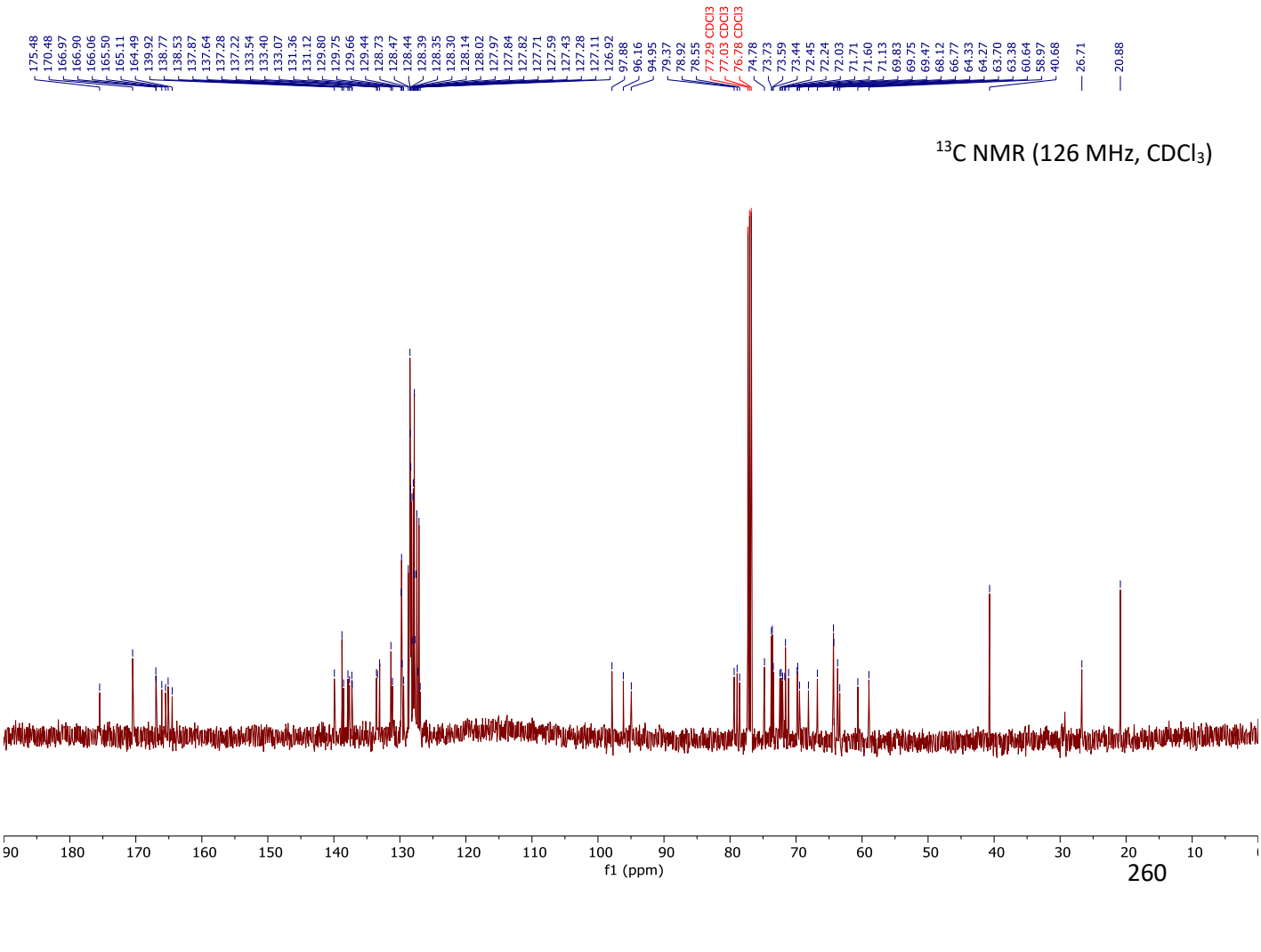
^{13}C NMR (126 MHz, $CDCl_3$)
f1 (ppm)

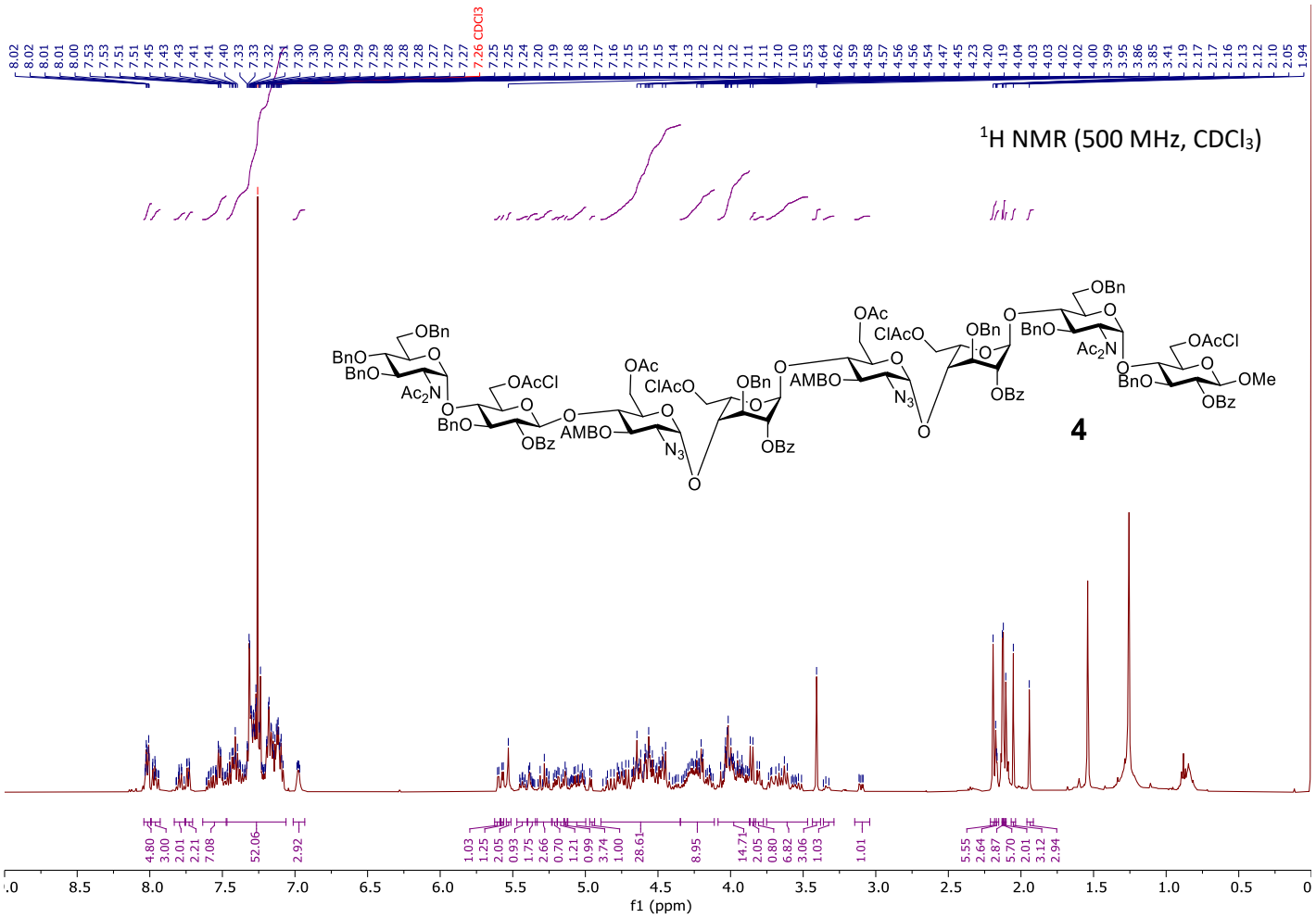
^{1}H NMR (500 MHz, $CDCl_3$)
4
f1 (ppm)

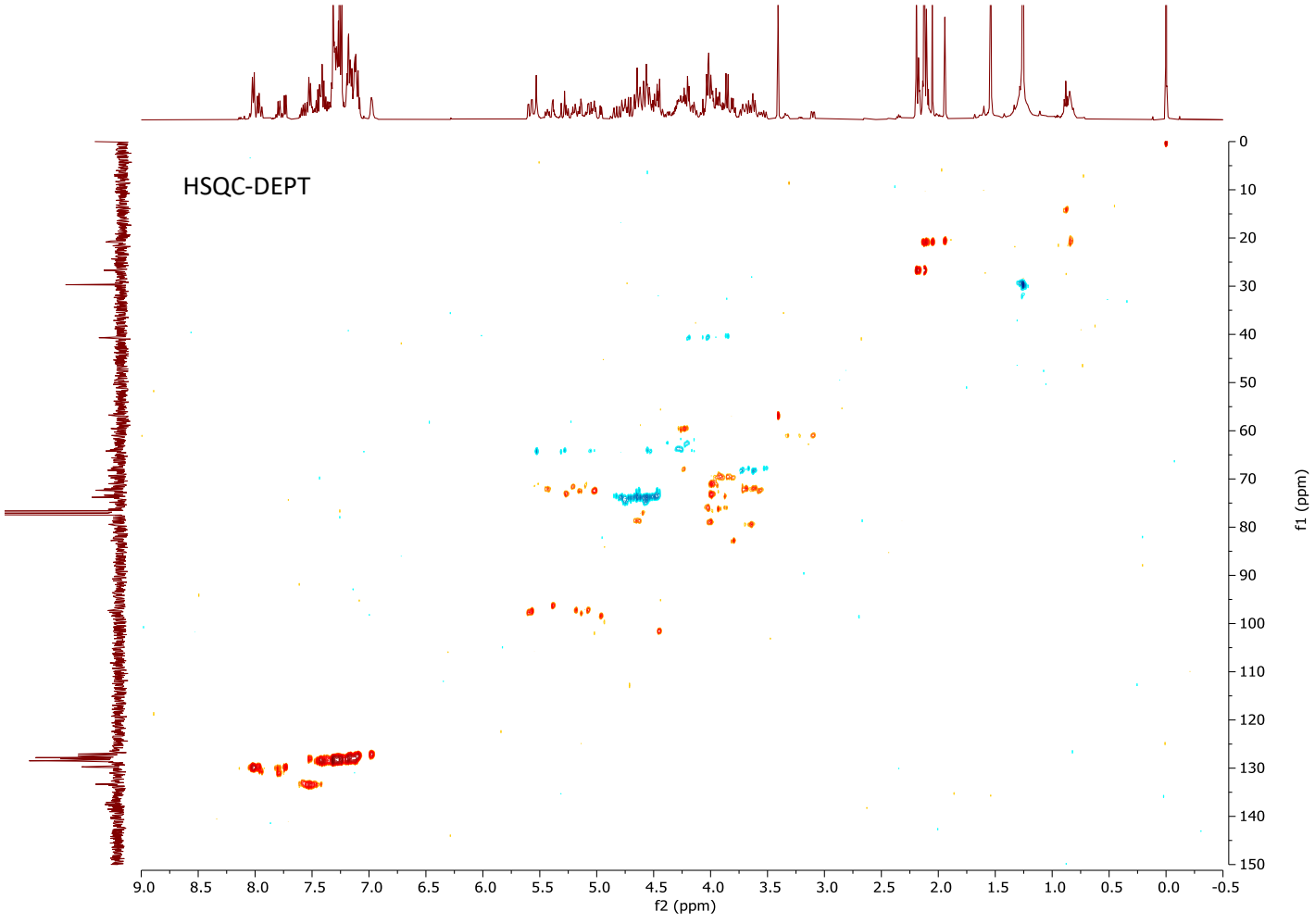
HSQC-DEPT
f2 (ppm)
f1 (ppm)

8. References

(1) Hassan, N.; Greve, B.; Espinoza-Sánchez, N. A.; Götte, M. *Cellular Signalling* **2021**, *77*, 109822.

(2) Payrastre, B.; Missy, K.; Giuriato, S.; Bodin, S.; Plantavid, M.; Gratacap, M.-P. *Cellular Signalling* **2001**, *13*, 377.

(3) Soo-Hyun, K.; Jeremy, T.; Scott, G. *Journal of Endocrinology* **2011**, *209*, 139.

(4) Kawashima, K.; Fujii, T.; Moriwaki, Y.; Misawa, H.; Horiguchi, K. *International Immunopharmacology* **2015**, *29*, 127.

(5) Adeva-Andany, M. M.; Funcasta-Calderon, R.; Fernandez-Fernandez, C.; Castro-Quintela, E.; Carneiro-Freire, N. *Journal of Clinical & Translational Endocrinology* **2019**, *15*, 45.

(6) van Niekerk, G.; Christowitz, C.; Conradie, D.; Engelbrecht, A. M. *Cytokine and Growth Factor Reviews* **2020**, *52*, 34.

(7) Akhtar, A.; Sah, S. P. *Neurochemistry International* **2020**, *135*, 104707.

(8) Dubey, S. K.; Lakshmi, K. K.; Krishna, K. V.; Agrawal, M.; Singhvi, G.; Saha, R. N.; Saraf, S.; Saraf, S.; Shukla, R.; Alexander, A. *Life Sciences* **2020**, 117540.

(9) Rabenstein, D. L. *Natural Product Reports* **2002**, *19*, 312.

(10) Turnbull, J. E.; Powell, A.; Guimond, S. *Trends in Cell Biology* **2001**, *11*, 75.

(11) Bernfield, M.; Götte, M.; Park, P. W.; Reizes, O.; Fitzgerald, M. L.; Lincecum, J.; Zako, M. *Annual Review of Biochemistry* **1999**, *68*, 729.

(12) Gallagher, J. T.; Walker, A. *Biochemistry* **1985**, *230*, 665.

(13) Hacker, U.; Nybakken, K.; Perrimon, N. *Nature Reviews Molecular Cell Biology* **2005**, *6*, 530.

(14) Kjellen, L.; Lindahl, U. *Current Opinion in Structural Biology* **2018**, *50*, 101.

(15) Christianson, H. C.; Belting, M. *Matrix Biology* **2014**, *35*, 51.

(16) Sasisekharan, R.; Raman, R.; Prabhakar, V. *Annual Review of Biomedical Engineering* **2006**, *8*, 181.

(17) Peter-Katalinić, J. In *Mass Spectrometry: Modified Proteins and Glycoconjugates* 2005, p 139.

(18) Schwarz, F.; Aebi, M. *Current Opinion in Structural Biology* **2011**, *21*, 576.

(19) Kreuger, J.; Kjellén, L. *Journal of Histochemistry & Cytochemistry* **2012**, *60*, 898.

(20) Multhaupt, H. A. B.; Couchman, J. R. *Journal of Histochemistry & Cytochemistry* **2012**, *60*, 908.

(21) Li, J. P.; Kusche-Gullberg, M. In *International Review of Cell and Molecular Biology*; Jeon, K. W., Ed.; Academic Press: 2016; Vol. 325, p 215.

(22) Annaval, T.; Wild, R.; Crétinon, Y.; Sadir, R.; Vivès, R. R.; Lortat-Jacob, H. *Molecules* **2020**, *25*, 4215.

(23) Neelamegham, S.; Aoki-Kinoshita, K.; Bolton, E.; Frank, M.; Lisacek, F.; Lütteke, T.; O'Boyle, N.; Packer, N. H.; Stanley, P.; Toukach, P.; Varki, A.; Woods, R. J.; The, S. D. G. *Glycobiology* **2019**, *29*, 620.

(24) Varki, A.; Cummings, R. D.; Aebi, M.; Packer, N. H.; Seeberger, P. H.; Esko, J. D.; Stanley, P.; Hart, G.; Darvill, A.; Kinoshita, T.; Prestegard, J. J.; Schnaar, R. L.; Freeze, H. H.; Marth, J. D.; Bertozzi, C. R.; Etzler, M. E.; Frank, M.; Vliegenthart, J. F. G.; Lütteke, T.; Perez, S.; Bolton, E.; Rudd, P.; Paulson, J.; Kanehisa, M.; Toukach, P.; Aoki-Kinoshita, K. F.; Dell, A.; Narimatsu, H.; York, W.; Taniguchi, N.; Kornfeld, S. *Glycobiology* **2015**, *25*, 1323.

(25) Thacker, B. E.; Xu, D.; Lawrence, R.; Esko, J. D. *Matrix Biology* **2014**, *35*, 60.

(26) Chopra, P.; Joshi, A.; Wu, J.; Lu, W.; Yadavalli, T.; Wolfert, M. A.; Shukla, D.; Zaia, J.; Boons, G.-J. *Proceedings of the National Academy of Sciences of the United States of America* **2021**, *118*, e2012935118.

(27) Huang, Y.; Mao, Y.; Zong, C.; Lin, C.; Boons, G.-J.; Zaia, J. *Analyltical Chemistry* **2015**, *87*, 592.

(28) Lamanna, W. C.; Kalus, I.; Padva, M.; Baldwin, R. J.; Merry, C. L.; Dierks, T. *Journal of Biotechnology* **2007**, *129*, 290.

(29) Busse, M.; Kusche-Gullberg, M. *Journal of Biological Chemistry* **2003**, *278*, 41333.

(30) Kim, B. T.; Kitagawa, H.; Tanaka, J.; Tamura, J.; Sugahara, K. *Journal of Biological Chemistry* **2003**, *278*, 41618.

(31) Busse, M.; Feta, A.; Presto, J.; Wilen, M.; Gronning, M.; Kjellen, L.; Kusche-Gullberg, M. *Journal of Biological Chemistry* **2007**, *282*, 32802.

(32) Gill, R. M.; Michael, A.; Westley, L.; Kocher, H. M.; Murphy, J. I.; Dhoot, G. K. *Experimental Cell Research* **2014**, *324*, 157.

(33) Joy, M. T.; Vrbova, G.; Dhoot, G. K.; Anderson, P. N. *Experimental Neurology* **2015**, *263*, 150.

(34) Krishnakumar, K.; Chakravorty, I.; Foy, W.; Allen, S.; Justo, T.; Mukherjee, A.; Dhoot, G. K. *Experimental Cell Research* **2018**, *364*, 16.

(35) Ricard-Blum, S. *Perspectives in Science* **2017**, *11*, 62.

(36) Iozzo, R. V.; Schaefer, L. *Matrix Biology* **2015**, *42*, 11.

(37) Weiss, R. J.; Esko, J. D.; Tor, Y. *Organic & biomolecular chemistry* **2017**, *15*, 5656.

(38) Gordts, P.; Esko, J. D. *Matrix Biology* **2018**, *71-72*, 262.

(39) Casu, B.; Naggi, A.; Torri, G. *Matrix Biology* **2010**, *29*, 442.

(40) Mulloy, B.; Hogwood, J.; Gray, E.; Lever, R.; Page, C. P. *Pharmacological Reviews* **2016**, *68*, 76.

(41) Filmus, J.; Capurro, M.; Rast, J. *Genome Biology* **2008**, *9*, 224.

(42) van Wijk, X. M.; van Kuppevelt, T. H. *Angiogenesis* **2014**, *17*, 443.

(43) Piecewicz, S.; Sengupta, S. *Stem Cells and Development* **2011**, *20*.

(44) Roudsari, L. C.; West, J. L. *Advanced Drug Delivery Reviews* **2016**, *97*, 250.

(45) Peysselon, F.; Ricard-Blum, S. *Matrix Biology* **2014**, *35*, 73.

(46) Stewart, M. D.; Sanderson, R. D. *Matrix Biology* **2014**, *35*, 56.

(47) Avizienyte, E.; Cole, C. L.; Rushton, G.; Miller, G. J.; Bugatti, A.; Presta, M.; Gardiner, J. M.; Jayson, G. C. *PLOS One* **2016**, *11*, e0159739.

(48) Kreuger, J.; Spillmann, D.; Li, J. P.; Lindahl, U. *Journal of Cell Biology* **2006**, *174*, 323.

(49) Xu, D.; Esko, J. D. *Annual Review of Biochemistry* **2014**, *83*, 129.

(50) Powell, A. K.; Yates, E. A.; Fernig, D. G.; Turnbull, J. E. *Glycobiology* **2004**, *14*, 17R.

(51) Xu, D.; Arnold, K.; Liu, J. *Current Opinion in Structural Biology* **2018**, *50*, 155.

(52) Schievano, E.; Tonoli, M.; Rastrelli, F. *Analyltical Chemistry* **2017**, *89*, 13405.

(53) Mulloy, B.; Johnson, E. A. *Carbohydrate research* **1987**, *170*, 151.

(54) Kailemia, M. J.; Ruhaak, L. R.; Lebrilla, C. B.; Amster, I. J. *Analyltical Chemistry* **2014**, *86*, 196.

(55) Hu, H.; Mao, Y.; Huang, Y.; Lin, C.; Zaia, J. *Perspectives in Science* **2017**, *11*, 40.

(56) Miller, R. L.; Guimond, S. E.; Schworer, R.; Zubkova, O. V.; Tyler, P. C.; Xu, Y.; Liu, J.; Chopra, P.; Boons, G. J.; Grabarics, M.; Manz, C.; Hofmann, J.; Karlsson, N. G.; Turnbull, J. E.; Struwe, W. B.; Pagel, K. *Nature communications* **2020**, *11*, 1481.

(57) Turnbull, J. E.; Fernig, D. G.; Ke, Y.; Wilkinson, M. C.; Gallagher, J. T. *Journal of Biological Chemistry* **1992**, *267*, 10337.

(58) Walker, A.; Turnbull, J. E.; Gallagher, J. T. *Journal of Biological Chemistry* **1994**, *269*, 931.

(59) Zhu, Z.; Zhu, B.; Ai, C.; Lu, J.; Wu, S.; Liu, Y.; Wang, L.; Yang, J.; Song, S.; Liu, X. *Carbohydrate research* **2018**, *466*, 11.

(60) Liang, Q.; Chopra, P.; Boons, G. J.; Sharp, J. S. *Carbohydrate research* **2018**, *465*, 16.
(61) Lakshminarayanan, A.; Richard, M.; Davis, B. G. *Nature Reviews Chemistry* **2018**, *2*, 148.
(62) Niu, C.; Zhao, Y.; Bobst, C. E.; Savinov, S. N.; Kaltashov, I. A. *Analytical Chemistry* **2020**, *92*, 7565.
(63) Ernst, S.; Langer, R.; Cooney, C. L.; Sasisekharan, R. *Critical reviews in biochemistry and molecular biology* **1995**, *30*, 387.
(64) Morimoto-Tomita, M.; Uchimura, K.; Werb, Z.; Hemmerich, S.; Rosen, S. D. *Journal of Biological Chemistry* **2002**, *277*, 49175.
(65) WuDunn, D.; Spear, P. G. *Journal of Virology* **1989**, *63*, 52.
(66) Barth, H.; Schnober, E. K.; Zhang, F.; Linhardt, R. J.; Depla, E.; Boson, B.; Cosset, F. L.; Patel, A. H.; Blum, H. E.; Baumert, T. F. *Journal of Virology* **2006**, *80*, 10579.
(67) Chang, H. C.; Samaniego, F.; Nair, B. C.; Buonaguro, L.; Ensoli, B. *AIDS* **1997**, *11*, 1421.
(68) Chen, Y.; Maguire, T.; Hileman, R. E.; Fromm, J. R.; Esko, J. D.; Linhardt, R. J.; Marks, R. M. *Nature Medicine* **1997**, *3*, 866.
(69) Vanheule, V.; Vervaeke, P.; Mortier, A.; Noppen, S.; Gouwy, M.; Snoeck, R.; Andrei, G.; Van Damme, J.; Liekens, S.; Proost, P. *Biochemical Pharmacology* **2016**, *100*, 73.
(70) Wardrop, D.; Keeling, D. *The British Journal of Haematology* **2008**, *141*, 757.
(71) Mohamed, S.; Coombe, D. R. *Pharmaceuticals* **2017**, *10*.
(72) Hedlund, K. D.; Coyne, D. P.; Sanford, D. M.; Huddelson, J. *Perfusion* **2013**, *28*, 61.
(73) Fu, L.; Suflita, M.; Linhardt, R. J. *Advanced Drug Delivery Reviews* **2016**, *97*, 237.
(74) Robert D Rosenberg, P. S. D. *Journal of Biological Chemistry* **1973**, *248*, 6490.
(75) Petitou, M.; van Boeckel, C. A. *Angewandte Chemie International Edition in English* **2004**, *43*, 3118.
(76) Capila, I.; Linhardt, R. J. *Angewandte Chemie International Edition in English* **2002**, *41*, 390.
(77) Lever, R.; Page, C. P. *Nature Reviews Drug Discovery* **2002**, *1*, 140.
(78) Zhao, D.; Sang, Q.; Cui, H. *Biomedicine & Pharmacotherapy* **2016**, *79*, 194.
(79) Bounameaux, H.; Goldhaber, S. Z. *Blood Reviews* **1995**, *9*, 213.
(80) Samama, M. M.; Cohen, A. T.; Darmon, J.-Y.; Desjardins, L.; Eldor, A.; Janbon, C.; Leizorovicz, A.; Nguyen, H.; Olsson, C.-G.; Turpie, A. G.; Weisslinger, N. *New England Journal of Medicine* **1999**, *341*, 793.
(81) Ingle, R. G.; Agarwal, A. S. *Carbohydrate Polymers* **2014**, *106*, 148.
(82) Bauer, K. A.; Eriksson, B. I.; Lassen, M. R.; Turpie, A. G. G. *New England Journal of Medicine* **2001**, *345*, 1305.
(83) Dey, S.; Lo, H.-J.; Wong, C.-H. *Journal of the American Chemical Society* **2019**, *141*, 10309.
(84) Manikowski, A.; Koziol, A.; Czajkowska-Wojciechowska, E. *Carbohydrate research* **2012**, *361*, 155.
(85) Lin, F.; Lian, G.; Zhou, Y. *Carbohydrate research* **2013**, *371*, 32.
(86) Ding, Y.; Vara Prasad, C.; Bai, H.; Wang, B. *Bioorganic & Medicinal Chemistry Letters* **2017**, *27*, 2424.
(87) Vetter, A.; Perera, G.; Leithner, K.; Klima, G.; Bernkop-Schnurch, A. *European Journal of Pharmaceutical Sciences* **2010**, *41*, 489.
(88) Ralay-Ranaivo, B.; Desmaele, D.; Bianchini, E. P.; Lepeltier, E.; Bourgaux, C.; Borgel, D.; Pouget, T.; Tranchant, J. F.; Couvreur, P.; Gref, R. *Journal of Controlled Release* **2014**, *194*, 323.
(89) Ni Ainle, F.; Preston, R. J.; Jenkins, P. V.; Nel, H. J.; Johnson, J. A.; Smith, O. P.; White, B.; Fallon, P. G.; O'Donnell, J. S. *Blood* **2009**, *114*, 1658.
(90) Kalaska, B.; Kaminski, K.; Miklosz, J.; Yusa, S.-i.; Sokolowska, E.; Blazejczyk, A.; Wietrzyk, J.; Kasacka, I.; Szczubialka, K.; Pawlak, D.; Nowakowska, M.; Mogielnicki, A. *Translational Research* **2016**, *177*, 98.

(91) Zhang, G. Q.; Jin, H.; Zhao, Y.; Guo, L.; Gao, X.; Wang, X.; Tie, S.; Shen, J.; Wang, P. G.; Gan, H.; Cui, H.; Zhao, W. *European Journal of Medicinal Chemistry* **2017**, *126*, 1039.

(92) Minsky, B. B.; Abzalimov, R. R.; Niu, C.; Zhao, Y.; Kirsch, Z.; Dubin, P. L.; Savinov, S. N.; Kaltashov, I. A. *Biochemistry* **2018**, *57*, 4880.

(93) Scholefield, Z.; Yates, E. A.; Wayne, G.; Amour, A.; McDowell, W.; Turnbull, J. E. *Journal of Cell Biology* **2003**, *163*, 97.

(94) Karran, E.; Mercken, M.; De Strooper, B. *Nature Reviews Drug Discovery* **2011**, *10*, 698.

(95) Qiu, C.; Kivipelto, M.; von Strauss, E. *Dialogues in Clinical Neuroscience* **2009**, *11*, 111.

(96) Stopschinski, B. E.; Holmes, B. B.; Miller, G. M.; Manon, V. A.; Vaquer-Alicea, J.; Prueitt, W. L.; Hsieh-Wilson, L. C.; Diamond, M. I. *Journal of Biological Chemistry* **2018**, *293*, 10826.

(97) Yamada, M.; Hamaguchi, T. *Journal of Biological Chemistry* **2018**, *293*, 10841.

(98) Long, J. M.; Holtzman, D. M. *Cell* **2019**.

(99) Fraser, P. E.; Darabie, A. A.; McLaurin, J. A. *Journal of Biological Chemistry* **2001**, *276*, 6412.

(100) Torres-Bugeau, C. M.; Avila, C. L.; Raisman-Vozari, R.; Papy-Garcia, D.; Itri, R.; Barbosa, L. R.; Cortez, L. M.; Sim, V. L.; Chehin, R. N. *Journal of Biological Chemistry* **2012**, *287*, 2398.

(101) Schultz, V.; Suflita, M.; Liu, X.; Zhang, X.; Yu, Y.; Li, L.; Green, D. E.; Xu, Y.; Zhang, F.; DeAngelis, P. L.; Liu, J.; Linhardt, R. J. *Journal of Biological Chemistry* **2017**, *292*, 2495.

(102) Zulueta, M. M. L.; Chyan, C. L.; Hung, S. C. *Current Opinion in Structural Biology* **2018**, *50*, 126.

(103) Ghadiali, R. S.; Guimond, S. E.; Turnbull, J. E.; Pisconti, A. *Matrix Biology* **2017**, *59*, 54.

(104) Ornitz, D. M. *BioEssays* **2000**, *22*, 108.

(105) Smock, R. G.; Meijers, R. *Open Biol* **2018**, *8*, 180026.

(106) Lin, X.; Buff, E. M.; Perrimon, N.; Michelson, A. M. *Development* **1999**, *126*, 3715.

(107) Faham, S.; Linhardt, R. J.; Rees, D. C. *Current Opinion in Structural Biology* **1998**, *8*, 578.

(108) Benington, L.; Rajan, G.; Locher, C.; Lim, L. Y. *Pharmaceutics* **2020**, *12*.

(109) Schlessinger., J.; Plotnikov., A. N.; Ibrahimi, O. A.; Eliseenkova, A. V.; Yeh, B. K.; Yayon, A.; Linhardt, R. J.; Mohammadi, M. *Molecular Cell* **2000**, *6*, 743.

(110) Theocharis, A. D.; Karamanos, N. K. *Matrix Biology* **2019**, *75-76*, 220.

(111) Melrose, J. *Bone and Tissue Regeneration Insights* **2016**, *7*, BTRI.S38670.

(112) Ravikumar, M.; Smith, R. A. A.; Nurcombe, V.; Cool, S. M. *Front Cell Dev Biol* **2020**, *8*, 581213.

(113) Turner, N.; Grose, R. *Nature Reviews Cancer* **2010**, *10*, 116.

(114) Knelson, E. H.; Nee, J. C.; Blobe, G. C. *Trends in Biochemical Sciences* **2014**, *39*, 277.

(115) Kuhnast, B.; El Hadri, A.; Boisgard, R.; Hinnen, F.; Richard, S.; Caravano, A.; Nancy-Portebois, V.; Petitou, M.; Tavitian, B.; Dolle, F. *Organic & biomolecular chemistry* **2016**, *14*, 1915.

(116) Lortat-Jacob, H. *Current Opinion in Structural Biology* **2009**, *19*, 543.

(117) Lazennec, G.; Richmond, A. *Trends in Molecular Medicine* **2010**, *16*, 133.

(118) Mackay, C. R. *Current Biology* **1997**, *7*, 384.

(119) Bazan, J. F.; Bacon, K. B.; Hardiman, G.; Wang, W.; Soo, K.; Rossi, D.; Greaves, D. R.; Zlotnik, A.; Schall, T. J. *Nature* **1997**, *385*, 640.

(120) Jayson, G. C.; Hansen, S. U.; Miller, G. J.; Cole, C. L.; Rushton, G.; Avizienyte, E.; Gardiner, J. M. *Chemical communications* **2015**, *51*, 13846.

(121) Xie, M.; Li, J. P. *Cellular Signalling* **2019**, *54*, 115.

(122) Sankarayanarayanan, N. V.; Strebel, T. R.; Boothello, R. S.; Sheerin, K.; Raghuraman, A.; Sallas, F.; Mosier, P. D.; Watermeyer, N. D.; Oscarson, S.; Desai, U. R. *Angewandte Chemie International Edition in English* **2017**, *56*, 2312.

(123) Pratt, C. W.; Tobin, R. B.; Church, F. C. *Journal of Biological Chemistry* **1990**, *265*, 6092.

(124) Baglin, T. P.; Carrell, R. W.; Church, F. C.; Esmon, C. T.; Huntington, J. A. *Proceedings of the National Academy of Sciences of the United States of America* **2002**, *99*, 11079.

(125) Tsai, C. T.; Zulueta, M. M. L.; Hung, S. C. *Current Opinion in Biotechnology* **2017**, *40*, 152.

(126) Fernández, C.; Hattan, C. M.; Kerns, R. J. *Carbohydrate research* **2006**, *341*, 1253.

(127) Zong, C.; Huang, R.; Condac, E.; Chiu, Y.; Xiao, W.; Li, X.; Lu, W.; Ishihara, M.; Wang, S.; Ramiah, A.; Stickney, M.; Azadi, P.; Amster, I. J.; Moremen, K. W.; Wang, L.; Sharp, J. S.; Boons, G. J. *Journal of the American Chemical Society* **2016**, *138*, 13059.

(128) Badri, A.; Williams, A.; Linhardt, R. J.; Koffas, M. A. *Current Opinion in Biotechnology* **2018**, *53*, 85.

(129) Pomin, V. H. *Medicinal Research Reviews* **2015**, *35*, 1195.

(130) Zhang, X.; Wang, Y. *Journal of Molecular Biology* **2016**, *428*, 3183.

(131) Kovalszky, I.; Hjerpe, A.; Dobra, K. *Biochimica et Biophysica Acta* **2014**, *1840*, 2491.

(132) Laremore, T. N.; Zhang, F.; Dordick, J. S.; Liu, J.; Linhardt, R. J. *Current Opinion in Biotechnology* **2009**, *13*, 633.

(133) He, W.; Fu, L.; Li, G.; Andrew Jones, J.; Linhardt, R. J.; Koffas, M. *Metabolic Engineering* **2015**, *27*, 92.

(134) Baik, J. Y.; Gasimli, L.; Yang, B.; Datta, P.; Zhang, F.; Glass, C. A.; Esko, J. D.; Linhardt, R. J.; Sharfstein, S. T. *Metabolic Engineering* **2012**, *14*, 81.

(135) Jin, P.; Zhang, L.; Yuan, P.; Kang, Z.; Du, G.; Chen, J. *Carbohydrate Polymers* **2016**, *140*, 424.

(136) Kang, Z.; Zhou, Z.; Wang, Y.; Huang, H.; Du, G.; Chen, J. *Trends in Biochemical Sciences* **2018**, *36*, 806.

(137) Davis, B. G. *Chemical Reviews* **2002**, *102*, 579.

(138) Gamblin, D. P.; Scanlan, E. M.; Davis, B. G. *Chemical Reviews* **2009**, *109*, 131.

(139) Dutta, D.; Mandal, C.; Mandal, C. *Biochimica et Biophysica Acta General Subjects* **2017**, *1861*, 3096.

(140) Kogan, G.; Soltes, L.; Stern, R.; Gemeiner, P. *Biotechnology Letters* **2007**, *29*, 17.

(141) Lord, M. S.; Cheng, B.; Tang, F.; Lyons, J. G.; Rnjak-Kovacina, J.; Whitelock, J. M. *Metabolic Engineering* **2016**, *38*, 105.

(142) Dulaney, S. B.; Xu, Y.; Wang, P.; Tiruchinapally, G.; Wang, Z.; Kathawa, J.; El-Dakdouki, M. H.; Yang, B.; Liu, J.; Huang, X. *Journal of Organic Chemistry* **2015**, *80*, 12265.

(143) Gagarinov, I. A.; Li, T.; Torano, J. S.; Caval, T.; Srivastava, A. D.; Kruijtzer, J. A.; Heck, A. J.; Boons, G. J. *Journal of the American Chemical Society* **2017**, *139*, 1011.

(144) Liu, Y.; Wen, L.; Li, L.; Gadi, M. R.; Guan, W.; Huang, K.; Xiao, Z.; Wei, M.; Ma, C.; Zhang, Q.; Yu, H.; Chen, X.; Wang, P. G.; Fang, J. *European Journal of Organic Chemistry* **2016**, *2016*, 4315.

(145) Davis, B. G.; Boyer, V. *Natural Product Reports* **2001**, *18*, 618.

(146) Paulson, J. C.; Colley, K. J. *Journal of Biological Chemistry* **1989**, *264*, 17615.

(147) Lairson, L. L.; Henrissat, B.; Davies, G. J.; Withers, S. G. *Annual Review of Biochemistry* **2008**, *77*, 521.

(148) Gamage, N.; Barnett, A.; Hempel, N.; Duggleby, R. G.; Windmill, K. F.; Martin, J. L.; McManus, M. E. *Toxicological Sciences* **2006**, *90*, 5.

(149) Delos, M.; Foulquier, F.; Hellec, C.; Vicogne, D.; Fifre, A.; Carpentier, M.; Papy-Garcia, D.; Allain, F.; Denys, A. *Biochimica et Biophysica Acta General Subjects* **2018**, *1862*, 1644.

(150) Jin, W.; Li, S.; Chen, J.; Liu, B.; Li, J.; Li, X.; Zhang, F.; Linhardt, R. J.; Zhong, W. *Protein Expression and Purification* **2018**, *151*, 23.

(151) Gesteira, T. F.; Coulson-Thomas, V. J. *Glycobiology* **2018**, *28*, 885.

(152) DeAngelis, P. L.; Liu, J.; Linhardt, R. J. *Glycobiology* **2013**, *23*, 764.

(153) Adrio, J. L.; Demain, A. L. *Biomolecules* **2014**, *4*, 117.

(154) Gurung, N.; Ray, S.; Bose, S.; Rai, V. *BioMed Research International* **2013**, *2013*, 329121.

(155) Sterner, E.; Li, L.; Paul, P.; Beaudet, J. M.; Liu, J.; Linhardt, R. J.; Dordick, J. S. *Anal Bioanal Chem* **2014**, *406*, 525.

(156) Moon, A. F.; Xu, Y.; Woody, S. M.; Krahn, J. M.; Linhardt, R. J.; Liu, J.; Pedersen, L. C. *Proceedings of the National Academy of Sciences of the United States of America* **2012**, *109*, 5265.

(157) Zhang, L.; Beeler, D. L.; Lawrence, R.; Lech, M.; Liu, J.; Davis, J. C.; Shriver, Z.; Sasisekharan, R.; Rosenberg, R. D. *Journal of Biological Chemistry* **2001**, *276*, 42311.

(158) Doncel-Perez, E.; Aranaz, I.; Bastida, A.; Revuelta, J.; Camacho, C.; Acosta, N.; Garrido, L.; Civera, C.; Garcia-Junceda, E.; Heras, A.; Fernandez-Mayoralas, A. *Carbohydrate Polymers* **2018**, *191*, 225.

(159) Zulueta, M. M.; Lin, S. Y.; Hu, Y. P.; Hung, S. C. *Current Opinion in Biotechnology* **2013**, *17*, 1023.

(160) Revuelta, J.; Fuentes, R.; Lagartera, L.; Hernaiz, M. J.; Bastida, A.; Garcia-Junceda, E.; Fernandez-Mayoralas, A. *Chemical communications* **2018**, *54*, 13455.

(161) Liu, H.; Zhang, X.; Wu, M.; Li, Z. *Carbohydrate research* **2018**, *467*, 45.

(162) Barroca, N.; Jacquinet, J.-C. *Carbohydrate research* **2000**, *329*, 667.

(163) Ojeda, R.; de Paz, J.; Martín-Lomas, M.; Lassaletta, J. *Synlett* **1999**, *1999*, 1316.

(164) Crich, D. *Journal of the American Chemical Society* **2021**, *143*, 17.

(165) Phan, T. B.; Nolte, C.; Kobayashi, S.; Ofial, A. R.; Mayr, H. *Journal of the American Chemical Society* **2009**, *131*, 11392.

(166) Hansen, T.; Lebedel, L.; Remmerswaal, W. A.; van der Vorm, S.; Wander, D. P. A.; Somers, M.; Overkleeft, H. S.; Filippov, D. V.; Desire, J.; Mingot, A.; Bleriot, Y.; van der Marel, G. A.; Thibaudeau, S.; Codée, J. D. C. *ACS Central Science* **2019**, *5*, 781.

(167) van der Vorm, S.; Hansen, T.; Overkleeft, H. S.; van der Marel, G. A.; Codée, J. D. C. *Chemical science* **2017**, *8*, 1867.

(168) Chang, C.-W.; Wu, C.-H.; Lin, M.-H.; Liao, P.-H.; Chang, C.-C.; Chuang, H.-H.; Lin, S.-C.; Lam, S.; Verma, V. P.; Hsu, C.-P.; Wang, C.-C. *Angewandte Chemie International Edition in English* **2019**, *58*, 16775.

(169) Das, R.; Mukhopadhyay, B. *ChemistryOpen* **2016**, *5*, 401.

(170) Freitas, M. P. *Organic & biomolecular chemistry* **2013**, *11*, 2885.

(171) Juaristi, E.; Cuevas, G. *Tetrahedron* **1992**, *48*, 5019.

(172) Zhou, X.; Yu, D.; Rong, C.; Lu, T.; Liu, S. *Chemical Physics Letters* **2017**, *684*, 97.

(173) Martins, F. A.; Silla, J. M.; Freitas, M. P. *Carbohydrate research* **2017**, *451*, 29.

(174) Wiberg, K. B.; Bailey, W. F.; Lambert, K. M.; Stempel, Z. D. *Journal of Organic Chemistry* **2018**, *83*, 5242.

(175) Karst, N.; Jacquinet, J.-C. *European Journal of Organic Chemistry* **2002**, 815.

(176) Mannino, M. P.; Yasomanee, J. P.; Demchenko, A. V. *Carbohydrate research* **2018**, *470*, 1.

(177) Guo, J.; Ye, X. S. *Molecules* **2010**, *15*, 7235.

(178) de Kleijne, F. F. J.; Moons, S. J.; White, P. B.; Boltje, T. J. *Organic & biomolecular chemistry* **2020**, *18*, 1165.

(179) Farrell, M. P.; Doyle, L. M.; Murphy, P. V. *Tetrahedron Letters* **2018**, *59*, 2726.

(180) Ning, J.; Zhang, W.; Yi, Y.; Yang, G.; Wu, Z.; Yi, J.; Kong, F. *Bioorganic & Medicinal Chemistry* **2003**, *11*, 2193.

(181) Forman, A.; Auzanneau, F. I. *Carbohydrate research* **2016**, *425*, 10.

(182) Sau, A.; Panchadhayee, R.; Ghosh, D.; Misra, A. K. *Carbohydrate research* **2012**, *352*, 18.

(183) Crich, D.; Patel, M. *Carbohydrate research* **2006**, *341*, 1467.

(184) Leng, W.-L.; Yao, H.; He, J.-X.; Liu, X.-W. *Accounts of Chemical Research* **2018**, *51*, 628.

(185) Chatterjee, S.; Moon, S.; Hentschel, F.; Gilmore, K.; Seeberger, P. H. *Journal of the American Chemical Society* **2018**, *140*, 11942.

(186) Squillacote, M.; Sheridan, R. S.; Chapman, O. L.; Anet, F. A. L. *Journal of the American Chemical Society* **1975**, *97*, 3244.

(187) Maruyama, T.; Toida, T.; Imanari, T.; Yu, G.; Linhardt, R. J. *Carbohydrate research* **1997**, *306*, 35.

(188) Ronnols, J.; Walvoort, M. T.; van der Marel, G. A.; Codée, J. D.; Widmalm, G. *Organic & biomolecular chemistry* **2013**, *11*, 8127.

(189) Mulloy, B.; Forster, M. J. *Glycobiology* **2000**, *10*, 1147.

(190) Marszalek, P. E.; Oberhauser, A. F.; Li, H.; Fernandez, J. M. *Biophys J* **2003**, *85*, 2696.

(191) Codée, J. D. C.; Ali, A.; Overkleeft, H. S.; van der Marel, G. A. *Comptes Rendus Chimie* **2011**, *14*, 178.

(192) Kaeothip, S.; Demchenko, A. V. *Carbohydrate research* **2011**, *346*, 1371.

(193) Wang, T.; Demchenko, A. V. *Organic & biomolecular chemistry* **2019**, *17*, 4934.

(194) Schwörer, R.; Zubkova, O. V.; Turnbull, J. E.; Tyler, P. C. *Chemistry – A European Journal* **2013**, *19*, 6817.

(195) Daragics, K.; Fügedi, P. *Organic Letters* **2010**, *12*, 2076.

(196) Ágoston, K.; Watt, G. M.; Fügedi, P. *Tetrahedron Letters* **2015**, *56*, 5010.

(197) Boltje, T. J.; Li, C.; Boons, G.-J. *Organic Letters* **2010**, *12*, 4636.

(198) Ágoston, K.; Streicher, H.; Fügedi, P. *Tetrahedron: Asymmetry* **2016**, *27*, 707.

(199) Serna, S.; Kardak, B.; Reichardt, N.-C.; Martin-Lomas, M. *Tetrahedron: Asymmetry* **2009**, *20*, 851.

(200) Dhamale, O. P.; Zong, C.; Al-Mafraji, K.; Boons, G. J. *Organic & biomolecular chemistry* **2014**, *12*, 2087.

(201) Hansen, S. U.; Dalton, C. E.; Barath, M.; Kwan, G.; Raftery, J.; Jayson, G. C.; Miller, G. J.; Gardiner, J. M. *Journal of Organic Chemistry* **2015**, *80*, 3777.

(202) Fraser-Reid, B.; Udodong, U. E.; Wu, Z.; Ottosson, H.; Merritt, J. R.; Rao, C. S.; Roberts, C.; Madsen, R. *Synlett* **1992**, *1992*, 927.

(203) Spijker, N. M.; van Boeckel, C. A. A. *Angewandte Chemie International Edition in English* **1991**, *30*, 180.

(204) Fraser-Reid, B.; López, J. C.; Gómez, Ana M.; Uriel, C. *European Journal of Organic Chemistry* **2004**, *2004*, 1387.

(205) van der Vorm, S.; van Hengst, J. M. A.; Bakker, M.; Overkleeft, H. S.; van der Marel, G. A.; Codée, J. D. C. *Angewandte Chemie International Edition in English* **2018**, *57*, 8240.

(206) Zhang, Z.; Ollmann, I. R.; Ye, X.-S.; Wischnat, R.; Baasov, T.; Wong, C.-H. *Journal of the American Chemical Society* **1999**, *121*, 734.

(207) Cheng, C.-W.; Zhou, Y.; Pan, W.-H.; Dey, S.; Wu, C.-Y.; Hsu, W.-L.; Wong, C.-H. *Nature communications* **2018**, *9*, 5202.

(208) Mong, K.-K. T.; Wong, C.-H. *Angewandte Chemie International Edition in English* **2002**, *41*, 4087.

(209) Ritter, T. K.; Mong, K.-K. T.; Liu, H.; Nakatani, T.; Wong, C.-H. *Angewandte Chemie International Edition in English* **2003**, *42*, 4657.

(210) Ye, X.-S.; Wong, C.-H. *Journal of Organic Chemistry* **2000**, *65*, 2410.

(211) Cheng, A.; Hendel, J. L.; Colangelo, K.; Bonin, M.; Auzanneau, F.-I. *Journal of Organic Chemistry* **2008**, *73*, 7574.

(212) Yao, H.; Vu, M. D.; Liu, X. W. *Carbohydrate research* **2018**, *473*, 72.

(213) Tanaka, H.; Tateno, Y.; Takahashi, T. *Organic & biomolecular chemistry* **2012**, *10*, 9570.

(214) Karst, N.; Jacquinet, J.-C. *Journal of the Chemical Society, Perkin Transactions 1* **2000**, 2709.

(215) Tsabedze, S. B.; Kabotso, D. E. K.; Pohl, N. L. B. *Tetrahedron Letters* **2013**, *54*, 6983.

(216) Barroca-Aubry, N.; Benchekroun, M.; Gomes, F.; Bonnaffé, D. *Tetrahedron Letters* **2013**, *54*, 5118.

(217) Wang, L.; Overkleeft, H. S.; van der Marel, G. A.; Codée, J. D. C. *Journal of the American Chemical Society* **2018**, *140*, 4632.

(218) Hasegawa, J. Y.; Hamada, M.; Miyamoto, T.; Nishide, K.; Kajimoto, T.; Uenishi, J.; Node, M. *Carbohydrate research* **2005**, *340*, 2360.

(219) Lian, G.; Zhang, X.; Yu, B. *Carbohydrate research* **2015**, *403*, 13.

(220) Tatai, J.; Osztrovszky, G.; Kajtar-Peredy, M.; Fügedi, P. *Carbohydrate research* **2008**, *343*, 596.

(221) Wang, Z.; Xu, Y.; Yang, B.; Tiruchinapally, G.; Sun, B.; Liu, R.; Dulaney, S.; Liu, J.; Huang, X. *Chemistry – A European Journal* **2010**, *16*, 8365.

(222) Wang, Q.; Fu, J.; Zhang, J. *Carbohydrate research* **2008**, *343*, 2989.

(223) Ghosh, R.; Chakraborty, A.; Maiti, S. *Tetrahedron Letters* **2004**, *45*, 9631.

(224) Nigudkar, S. S.; Wang, T.; Pistorio, S. G.; Yasomanee, J. P.; Stine, K. J.; Demchenko, A. V. *Organic & biomolecular chemistry* **2017**, *15*, 348.

(225) Lazar, L.; Borbas, A.; Somsak, L. *Carbohydrate research* **2018**, *470*, 8.

(226) Zheng, Z.; Zhang, L. *Carbohydrate research* **2019**, *471*, 56.

(227) Yang, T.; Zhu, F.; Walczak, M. A. *Nature communications* **2018**, *9*, 3650.

(228) Christensen, H. M.; Oscarson, S.; Jensen, H. H. *Carbohydrate research* **2015**, *408*, 51.

(229) Heuckendorff, M.; Jensen, H. H. *Carbohydrate research* **2017**, *439*, 50.

(230) Nielsen, M. M.; Pedersen, C. M. *Chemical Reviews* **2018**, *118*, 8285.

(231) Sawant, R. C.; Lih, Y.-H.; Yang, S.-A.; Yeh, C.-H.; Tai, H.-J.; Huang, C.-L.; Lin, H.-S.; Badsara, S. S.; Luo, S.-Y. *RSC Advances* **2014**, *4*, 26524.

(232) Dar, A. R.; Aga, M. A.; Kumar, B.; Yousuf, S. K.; Taneja, S. C. *Organic & biomolecular chemistry* **2013**, *11*, 6195.

(233) Verdelet, T.; Benmahdjoub, S.; Benmerad, B.; Alami, M.; Messaoudi, S. *Journal of Organic Chemistry* **2019**, *84*, 9226.

(234) Lin, S.; Lowary, T. L. *Organic Letters* **2020**, *22*, 7645.

(235) Jana, M.; Bennett, C. S. *Organic Letters* **2018**, *20*, 7598.

(236) Ashmus, R. A.; Jayasuriya, A. B.; Lim, Y.-J.; O'Doherty, G. A.; Lowary, T. L. *Journal of Organic Chemistry* **2016**, *81*, 3058.

(237) Hanessian, S.; Mascitti, V.; Rogel, O. *Journal of Organic Chemistry* **2002**, *67*, 3346.

(238) Hansen, S. U.; Miller, G. J.; Cliff, M. J.; Jayson, G. C.; Gardiner, J. M. *Chemical science* **2015**, *6*, 6158.

(239) Hansen, S. U.; Miller, G. J.; Cole, C.; Rushton, G.; Avizienyte, E.; Jayson, G. C.; Gardiner, J. M. *Nature communications* **2013**, *4*, 2016.

(240) Hansen, S. U.; Miller, G. J.; Jayson, G. C.; Gardiner, J. M. *Organic Letters* **2013**, *15*, 88.

(241) Hu, Y.-P.; Lin, S.-Y.; Huang, C.-Y.; Zulueta, M. M. L.; Liu, J.-Y.; Chang, W.; Hung, S.-C. *Nature Chemistry* **2011**, *3*, 557.

(242) Jacquinet, J.-C.; Petitou, M.; Duchaussoy, P.; Lederman, I.; Choay, J.; Torri, G.; Sinaÿ, P. *Carbohydrate research* **1984**, *130*, 221.

(243) Lei, P.-S.; Duchaussoy, P.; Sizun, P.; Mallet, J.-M.; Petitou, M.; Sinay, P. *Bioorganic & Medicinal Chemistry Letters* **1998**, *6*, 1337.

(244) Norsikian, S.; Tresse, C.; François-Eude, M.; Jeanne-Julien, L.; Masson, G.; Servajean, V.; Genta-Jouve, G.; Beau, J.-M.; Roulland, E. *Angewandte Chemie International Edition in English* **2020**, *59*, 6612.

(245) Lloyd, D.; Bennett, C. S. *Chemistry – A European Journal* **2018**, *24*, 7610.

(246) Paulsen, H. *Angewandte Chemie International Edition in English* **1982**, *21*, 155.

(247) Codée, J. D. C.; Overkleeft, H. S.; van der Marel, G. A.; van Boeckel, C. A. A. *Drug Discovery Today: Technologies* **2004**, *1*, 317.

(248) Zhou, J.; Manabe, Y.; Tanaka, K.; Fukase, K. *Chemistry – An Asian Journal* **2016**, *11*, 1436.

(249) Lázár, L.; Mező, E.; Herczeg, M.; Lipták, A.; Antus, S.; Borbás, A. *Tetrahedron* **2012**, *68*, 7386.

(250) Mende, M.; Bednarek, C.; Wawryszyn, M.; Sauter, P.; Biskup, M. B.; Schepers, U.; Brase, S. *Chemical Reviews* **2016**, *116*, 8193.

(251) Paz, J.-Luis d.; Ojeda, R.; Reichardt, N.; Martín-Lomas, M. *European Journal of Organic Chemistry* **2003**, *2003*, 3308.

(252) Mensink, R. A.; Elferink, H.; White, P. B.; Pers, N.; Rutjes, F. P. J. T.; Boltje, T. J. *European Journal of Organic Chemistry* **2016**, *2016*, 4656.

(253) Zulueta, M. M. L.; Lin, S.-Y.; Hung, S.-C. *Trends in Glycoscience and Glycotechnology* **2013**, *25*, 141.

(254) Wu, Y.; Xiong, D. C.; Chen, S. C.; Wang, Y. S.; Ye, X. S. *Nature communications* **2017**, *8*, 14851.

(255) Sun, L.; Chopra, P.; Boons, G.-J. *The Journal of organic chemistry* **2020**, *85*, 16082.

(256) Seeberger, P. H.; Haase, W.-C. *Chemical Reviews* **2000**, *100*, 4349.

(257) Seeberger, P. H.; Werz, D. B. *Nature* **2007**, *446*, 1046.

(258) Seeberger, P. H.; Plante, O. J.; Palmacci, E. R. *Science* **2001**, *291*, 1523

(259) Seeberger, P. H. *Accounts of Chemical Research* **2015**, *48*, 1450.

(260) Yu, Y.; Kononov, A.; Delbianco, M.; Seeberger, P. H. *Chemistry – A European Journal* **2018**, *24*, 6075.

(261) Guedes, N.; Czechura, P.; Echeverria, B.; Ruiz, A.; Michelena, O.; Martin-Lomas, M.; Reichardt, N.-C. *The Journal of organic chemistry* **2013**, *78*, 6911.

(262) Guedes, N.; Kopitzki, S.; Echeverria, B.; Pazos, R.; Elosegui, E.; Calvo, J.; Reichardt, N.-C. *RSC Advances* **2015**, *5*, 9325.

(263) Codée, J. D.; Krock, L.; Castagner, B.; Seeberger, P. H. *Chemistry – A European Journal* **2008**, *14*, 3987.

(264) Walvoort, M. T. C.; Volbeda, A. G.; Reintjens, N. R. M.; Elst, H. v. d.; Plante, O. J.; Overkleeft, H. S.; Marel, G. A. v. d.; Codée, J. D. C. *Organic Letters* **2012**, *14*, 3776.

(265) Hahm, H. S.; Schlegel, M. K.; Hurevich, M.; Eller, S.; Schuhmacher, F.; Hofmann, J.; Pagel, K.; Seeberger, P. H. *Proceedings of the National Academy of Sciences of the United States of America* **2017**, *114*, E3385.

(266) Budhadev, D.; Saxby, K.; Walton, J.; Davies, G.; Tyler, P. C.; Schwörer, R.; Fascione, M. A. *Organic & biomolecular chemistry* **2019**, *17*, 1817.

(267) Czechura, P.; Guedes, N.; Kopitzki, S.; Vazquez, N.; Martin-Lomas, M.; Reichardt, N.-C. *Chemical communications* **2011**, *47*, 2390.

(268) Schumann, B.; Parameswarappa, S. G.; Lisboa, M. P.; Kottari, N.; Guidetti, F.; Pereira, C. L.; Seeberger, P. H. *Angewandte Chemie International Edition in English* **2016**, *55*, 14431.

(269) Saliba, R. C.; Wooke, Z. J.; Nieves, G. A.; Chu, A. A.; Bennett, C. S.; Pohl, N. L. B. *Organic Letters* **2018**, *20*, 800.

(270) Plutschack, M. B.; Pieber, B.; Gilmore, K.; Seeberger, P. H. *Chemical Reviews* **2017**, *117*, 11796.

(271) Marion, K. C.; Wooke, Z.; Pohl, N. L. B. *Carbohydrate research* **2018**, *468*, 23.

(272) Codée, J. D.; Christina, A. E.; Walvoort, M. T.; Overkleeft, H. S.; van der Marel, G. A. *Topics in Current Chemistry* **2011**, *301*, 253.

(273) Kuijpers, W. H. A.; Kuyl-Yeheskiely, E.; Boom, J. H. v.; Boeckel, C. A. A. v. *Nucleic Acids Research* **1993**, *21*, 3493.

(274) Kuijpers, W. H. A.; van Boeckel, C. A. A. *Tetrahedron* **1993**, *49*, 10931.

(275) Turnbull, J. Unpublished results.

(276) Wadouachi, A.; Kovensky, J. *Molecules* **2011**, *16*, 3933.

(277) Lu, H.; Drelich, A.; Omri, M.; Pezron, I.; Wadouachi, A.; Pourceau, G. *Molecules* **2016**, *21*.

(278) van den Bos, L. J.; Codée, J. D. C.; Litjens, R. E. J. N.; Dinkelaar, J.; Overkleeft, H. S.; van der Marel, G. A. *European Journal of Organic Chemistry* **2007**, *2007*, 3963.

(279) Pews-Davtyan, A.; Pirojan, A.; Shaljyan, I.; Awetissjan, A. A.; Reinke, H.; Vogel, C. *Journal of Carbohydrate Chemistry* **2003**, *22*, 939.

(280) Walvoort, M. T.; Lodder, G.; Overkleeft, H. S.; Codée, J. D.; van der Marel, G. A. *Journal of Organic Chemistry* **2010**, *75*, 7990.

(281) Seifert, J.; Singh, L.; Ramsdale, T. E.; West, M. L.; Drinnan, N. B.; Patent, Alchemia Pty Ltd, WO2003022860A1: 2003.

(282) Gainsford, G. J.; Schworer, R.; Tyler, P. C. *Acta Crystallographica Section C* **2013**, *69*, 679.

(283) Lim, D.; Fairbanks, A. J. *Chemical science* **2017**, *8*, 1896.

(284) Mojtahedi, M. M.; Samadian, S. *Journal of Chemistry* **2013**, *2013*, 1.

(285) Lemieux, R. U. *Canadian Journal of Chemistry* **1951**, *29*, 1079.

(286) Ferrier, R. J.; Furneaux, R. H. *Carbohydrate research* **1976**, *52*, 63.

(287) Pilgrim, W.; Murphy, P. V. *Journal of Organic Chemistry* **2010**, *75*, 6747.

(288) Kaya, E.; Sonmez, F.; Kucukislamoglu, M.; Nebioglu, M. *Chemical Papers* **2012**, *66*.

(289) O'Brien, C.; Polakova, M.; Pitt, N.; Tosin, M.; Murphy, P. V. *Chemistry – A European Journal* **2007**, *13*, 902.

(290) Wagner, D.; Verheyden, J. P. H.; Moffatt, J. G. *Journal of Organic Chemistry* **1974**, *39*, 24.

(291) Kartha, K. P. R.; Kiso, M.; Hasegawa, A.; Jennings, H. J. *Journal of Carbohydrate Chemistry* **1998**, *17*, 811.

(292) Hori, H.; Nishida, Y.; Ohrui, H.; Meguro, H. *Journal of Organic Chemistry* **1989**, *54*, 1346.

(293) Nilsson, U.; Ray, A. K.; Magnusson, G. *Carbohydrate research* **1990**, *208*, 260.

(294) Montero, J.-L.; Winum, J.-Y.; Leydet, A.; Kamal, M.; Pavia, A. A.; Roque, J.-P. *Carbohydrate research* **1997**, *297*, 175.

(295) Sugiyama, S.; Diakur, J. M. *Organic Letters* **2000**, *2*, 2713.

(296) Ernst, B.; Winkler, T. *Tetrahedron Letters* **1989**, *30*, 3081.

(297) Chang, C.-W.; Chang, S.-S.; Chao, C.-S.; Mong, K.-K. T. *Tetrahedron Letters* **2009**, *50*, 4536.

(298) Kong, F. *Carbohydrate research* **2007**, *342*, 345.

(299) Tamura, J.-i.; Nakada, Y.; Taniguchi, K.; Yamane, M. *Carbohydrate research* **2008**, *343*, 39.

(300) Reddy Vakiti, J.; Hanessian, S. *Organic Letters* **2020**, *22*, 3345.

(301) Crich, D.; Smith, M. *Journal of the American Chemical Society* **2001**, *123*, 9015.

(302) Tatai, J.; Fügedi, P. *Organic Letters* **2007**, *9*.

(303) Codee, J. D. C.; Litjens, R. E. J. N.; Heeten, R.; Overkleeft, H. S.; Boom, J. H. v.; Marel, G. A. v. d. *Organic Letters* **2003**, *5*, 1519.

(304) Crich, D.; Li, W. *Organic Letters* **2006**, *8*, 959.

(305) Crich, D.; Cai, F.; Yang, F. *Carbohydrate research* **2008**, *343*, 1858.

(306) Demchenko, A. V.; Boons, G.-J. *Tetrahedron Letters* **1998**, *39*, 3065.

(307) Heuckendorff, M.; Jensen, H. H. *Carbohydrate research* **2018**, *455*, 86.

(308) Sheppard, D. J.; Cameron, S. A.; Tyler, P. C.; Schwörer, R. *Organic & biomolecular chemistry* **2020**, 4728

(309) Wada, T.; Ohkubo, A.; Mochizuki, A.; Sekine, M. *Tetrahedron Letters* **2001**, *42*, 1069.

(310) Love, K. R.; Andrade, R. B.; Seeberger, P. H. *Journal of Organic Chemistry* **2001**, *66*, 8165.

(311) Ziegler, T.; Pantkowski, G. *European Journal of Organic Chemistry* **1994**, *1994*, 659.

(312) Miller, C. M.; Xu, Y.; Kudrna, K. M.; Hass, B. E.; Kellar, B. M.; Egger, A. W.; Liu, J.; Harris, E. N. *Thrombosis Research* **2018**, *167*, 80.

(313) Gainsford, G. J.; Schwörer, R. *Acta Crystallographica Section E* **2013**, *69*, 259.

(314) Cain, B. F. *Journal of Organic Chemistry* **1976**, *41*, 2029.

(315) Nakano, T.; Takewaki, K.; Yade, T.; Okamoto, Y. *Journal of the American Chemical Society* **2001**, *123*, 9182.
(316) Ferrari, V.; Serpi, M.; McGuigan, C.; Pertusati, F. *Nucleosides, Nucleotides and Nucleic Acids* **2015**, *34*, 799.
(317) Neumann, J.; Thiem, J. *European Journal of Organic Chemistry* **2010**, *2010*, 900.
(318) Ghosh, T.; Santra, A.; Misra, A. K. *Beilstein Journal of Organic Chemistry* **2013**, *9*, 974.
(319) Castro-Palomino, J. C.; Schmidt, R. R. *Tetrahedron Letters* **1995**, *36*, 6871.
(320) Agnihotri, G.; Tiwari, P.; Misra, A. K. *Carbohydrate research* **2005**, *340*, 1393.
(321) Hain, J.; Rollin, P.; Klaffke, W.; Lindhorst, T. K. *Beilstein Journal of Organic Chemistry* **2018**, *14*, 1619.
(322) Camp, D.; Jenkins, I. *Australian Journal of Chemistry* **1990**, *43*, 161.
(323) Takeuchi, H.; Fujimori, Y.; Ueda, Y.; Shibayama, H.; Nagaishi, M.; Yoshimura, T.; Sasamori, T.; Tokitoh, N.; Furuta, T.; Kawabata, T. *Organic Letters* **2020**, *22*, 4754.
(324) Fürstner, A. *Liebigs Annalen der Chemie* **1993**, *1993*, 1211.
(325) Tadashi, E.; Shinichi, I.; Teruaki, M. *Bulletin of the Chemical Society of Japan* **1970**, *43*, 2632.
(326) Smith, R.; Müller-Bunz, H.; Zhu, X. *Organic Letters* **2016**, *18*, 3578.
(327) Heuckendorff, M.; Poulsen, L. T.; Hedberg, C.; Jensen, H. H. *Organic & biomolecular chemistry* **2018**, *16*, 2277.
(328) Tomonari, T.; Takeshi, M.; Masato, N.; Atsushi, K.; Shin-ichiro, S. *Chemistry Letters* **2009**, *38*, 458.
(329) Fairbanks, A. J. *Carbohydrate research* **2021**, *499*, 108197.
(330) Seeberger, P. H.; Lohman, G. J. S. *Journal of Organic Chemistry* **2004**, *69*, 4081.
(331) Schmidt, R. R.; Toepfer, A. *Tetrahedron Letters* **1991**, *32*, 3353.
(332) Ferrier, R. J.; Overend, W. G.; Ryan, A. E. *Journal of the Chemical Society (Resumed)* **1962**, 3667.
(333) Ferrier, R. J.; Zubkov, O. A. In *Organic Reactions* 2004, p 569.
(334) Choutka, J.; Kratochvíl, M.; Zýka, J.; Pohl, R.; Parkan, K. *Carbohydrate research* **2020**, *496*, 108086.
(335) Wulff, G.; Röhle, G. *Angewandte Chemie International Edition in English* **1974**, *13*, 157.
(336) Yamada, H.; Harada, T.; Miyazaki, H.; Takahashi, T. *Tetrahedron Letters* **1994**, *35*, 3979.
(337) Singh, Y.; Demchenko, A. V. *Chemistry – A European Journal* **2019**, *25*, 1461.
(338) Kim, K. S.; Fulse, D. B.; Baek, J. Y.; Lee, B.-Y.; Jeon, H. B. *Journal of the American Chemical Society* **2008**, *130*, 8537.
(339) Garcia, B. A.; Gin, D. Y. *Journal of the American Chemical Society* **2000**, *122*, 4269.
(340) D'Angelo, K. A.; Taylor, M. S. *Journal of the American Chemical Society* **2016**, *138*, 11058.
(341) Leroux, J.; Perlin, A. S. *Carbohydrate research* **1978**, *67*, 163.
(342) Lee, J. C.; Chang, S. W.; Liao, C. C.; Chi, F. C.; Chen, C. S.; Wen, Y. S.; Wang, C. C.; Kulkarni, S. S.; Puranik, R.; Liu, Y. H.; Hung, S. C. *Chemistry – A European Journal* **2004**, *10*, 399.
(343) van der Vorm, S.; Hansen, T.; van Hengst, J. M. A.; Overkleeft, H. S.; van der Marel, G. A.; Codée, J. D. C. *Chemical Society Reviews* **2019**, *48*, 4688.
(344) Magaud, D.; Dolmazon, R.; Anker, D.; Doutheau, A.; Dory, Y. L.; Deslongchamps, P. *Organic Letters* **2000**, *2*, 2275.
(345) Crich, D.; Dudkin, V. *Journal of the American Chemical Society* **2001**, *123*, 6819.
(346) Crich, D.; Vinod, A. U. *Journal of Organic Chemistry* **2005**, *70*, 1291.
(347) Mannino, M. P.; Demchenko, A. V. *Chemistry – A European Journal* **2020**, *26*, 2927.
(348) Mannino, M. P.; Demchenko, A. V. *Chemistry – A European Journal* **2020**, *26*, 2938.
(349) Pornsuriyasak, P.; Demchenko, A. V. *Chemistry – A European Journal* **2006**, *12*, 6630.
(350) Hasty, S. J.; Demchenko, A. V. *Chemistry of Heterocyclic Compounds* **2012**, *48*, 220.

(351) Caputo, R.; Kunz, H.; Mastroianni, D.; Palumbo, G.; Pedatella, S.; Solla, F. *European Journal of Organic Chemistry* **1999**, *1999*, 3147.

(352) Mukhopadhyay, B.; Kartha, K. P. R.; Russell, D. A.; Field, R. A. *Journal of Organic Chemistry* **2004**, *69*, 7758.

(353) Gervay-Hague, J. *Accounts of Chemical Research* **2016**, *49*, 35.

(354) Ravidà, A.; Liu, X.; Kovacs, L.; Seeberger, P. H. *Organic Letters* **2006**, *8*, 1815.

(355) Plante, O. J.; Palmacci, E. R.; Andrade, R. B.; Seeberger, P. H. *Journal of the American Chemical Society* **2001**, *123*, 9545.

(356) Arihara, R.; Kakita, K.; Suzuki, N.; Nakamura, S.; Hashimoto, S. *Journal of Organic Chemistry* **2015**, *80*, 4259.

(357) Garcia, B. A.; Gin, D. Y. *Organic Letters* **2000**, *2*, 2135.